

Bioprospecting of antibacterial metabolites in seaweed associated bacterial flora along the southeast coast of India

Thesis submitted to

COCHIN UNIVERSITY OF SCIENCE AND TECHNOLOGY

In partial fulfillment of the requirements for the degree of

DOCTOR OF PHILOSOPHY

in

MARINE SCIENCES

By

BINI THILAKAN

(Reg. No.3782)



CENTRAL MARINE FISHERIES RESEARCH INSTITUTE

(Indian council of Agricultural Research)

Post Box No. 1603, Cochin-682018, INDIA



October 2015

Declaration

I do hereby declare that the thesis entitled “**Bioprospecting of antibacterial metabolites in seaweed associated bacterial flora along the southeast coast of India**” is the authentic and bonafide record of the research work carried out by me under the guidance of Dr. Kajal Chakraborty, Senior Scientist, Central Marine Fisheries Research Institute, Cochin, in partial fulfilment for the award of Ph.D. degree under the Faculty of Marine Sciences of Cochin University of Science and Technology, Cochin and no part thereof has been previously formed the basis for the award of any degree, diploma, associate ship, fellowship or other similar titles or recognition.

Place: Cochin

Date: 16/10/2015

BINI THILAKAN

Dedicated to my family

Acknowledgement

On this occasion of completing my doctoral degree dissertation, I realize that this work was not completed in a vacuum. I am thankful to many people who have helped me through the completion of this dissertation. Without thanking them my work will be incomplete.

The first and foremost I wish to thank my supervisor, Dr.Kajal Chakraborty, Senior Scientist, Marine Biotechnology Division, CMFRI. who has been supportive since the days i joined CMFRI as a project assistant. He helped me come up with the thesis topic and guided me through the rough road to finish this thesis. Thanks to him for supporting me academically over almost a year of development and for the encouragement and the freedom i needed to move on.

I feel extremely privileged to thank Dr. A. Gopalakrishnan, Director, Central Marine Fisheries Research Institute for being kind enough to extend all the necessary facilities and support required to carry out my research work. I record my deep sense of respect and gratitude to him for providing me with the

absolute freedom to successfully complete this thesis. I extend my deep sense of gratitude and respect to Dr. G. Syda Rao, former Director of Central Marine Fisheries Research Institute for being kind enough to permit me to register for the Ph.D. programme and providing me with all the necessary facilities required to carry out this work.

I express my heartfelt gratitude to Dr. Bobby Ignatius, Principal Scientist, HRD Cell for kindly facilitating my Ph.D. programme. I feel privileged to place on record my sincere gratitude to Dr. P.C. Thomas for facilitating my doctoral work during his tenure as Scientist-in-Charge, HRD cell of CMFRI.

I express my deep sense of gratitude to Dr. P. Vijayagopal, HOD, Marine Biotechnology Division, CMFRI for his consistent help, guidance and encouragement during the research work. I extend my deep sense of gratitude and respect to Dr. K.K.Vijayan, former HOD, Marine Biotechnology Division, CMFRI for his consistent help, guidance, subjective criticism and encouragement during the research work.

I extend my sincere thanks to Dr. Rekhadevi Chakraborty, Mr. N.K Sanil, Dr. V. Srinivasa Raghavan, Dr. Pradeep M.A and Dr. Sandhya Sukumaran for all the encouragement and support.

I wish to express my heartfelt thanks to Dr. M.P. Paulton (Senior Technical Officer), Mr. Nandakumar Rao, Mr. K.K Surendran (Technical officers, CMFRI), and Mrs. P. Vineetha, of Marine Biotechnology Division, CMFRI for their cooperation and help.

I express my deepest sense of gratitude to Mr. Edwin Joseph, OIC library, library support staff, the canteen, security personnel and employees of CMFRI, Cochin, for their sincere help and cooperation extended during the tenure.

I acknowledge the staffs of SAIF, IIT Chennai and staffs of STIC, Cochin University of Science and Technology (CUSAT) for their help and support extended towards the spectroscopic studies.

I express my heart felt gratitude to my colleagues Dr. N. K. Praveen, Mr. Deepu Joseph and Mrs. Selsa Chakkalakkal for bouncing ideas with me. I am grateful to Vamsi Krishna Raola for

his help extended towards compiling my spectroscopic studies. I express my deep sense of gratitude to Dr. Anju Antony, Dr. Vikas P.A and Mrs. Vidya Susan Philip for their support and help. I remember Mr. Jackson K.V, Mrs. Anijo, Mr. Neil, Mrs. Anusree, , Mr. Reynold Peter, Mr. Renjith Kumar, Mr. Sajesh Kumar, Mrs. Preetha, Mrs. Suja, Mr. Subin, Mr. Raja, Mrs Sreedevi, Mrs Keerthi, Mrs Githa, Mrs Sajeela and all my junior research scholars of MBTD for their timely help.

I also thank Central Marine Fisheries Research institute and organization, ICAR; under which I completed my research.

Last but not the least I thank my entire family for their support and encouragement. I express my love towards my little ones Avishai and Upasana who sacrificed the most during my research work. I am indebted to my loving husband Mr. Sreenesh N.S for his care, cooperation, endless patience and encouragement throughout the period of my work. I remember my heavenly father MR. P.K. Thilakan and mother Baby K.P with profound sense of gratitude whose selfless sacrifice and their great efforts with pain and tears and unceasing prayers has enabled me to successfully complete the research work. My

special gratitude is due to my Sisters Nidhi, Nila and brother-in-law 'Sreejith N.S' for their loving support. I am forever indebted to my parents-in-law for their help and support which made my task much easier.

Finally, I thank all those who have helped me directly or indirectly in the successful completion of my thesis. Above all I humbly bow before the almighty God for showering his blessings upon me and giving me the strength, wisdom, health and luck to accomplish this endeavor.

Abbreviation

1HNMR	-	Proton Nuclear Magnetic Resonance
BLAST	-	Basic local alignment search tool
COSY	-	Correlation Spectroscopy
DEPT	-	Distortionless Enhancement By Polarization Transfer
DNA	-	deoxyribonucleic acid
EMBL	-	European Molecular Biology Laboratory
EtOAc	-	Ethyl Acetate
FAME	-	Fatty Acid Methyl Esters
HMBC	-	Heteronuclear Multiple Bond Correlation
HPLC	-	High-Performance Liquid Chromatography
HRMS	-	High Resolution Mass Spectroscopy
HSQC	-	Heteronuclear Single Quantum Coherence
Min	-	minutes
NCBI	-	National centre for biotechnology information
NMR	-	Nuclear Magnetic Resonance
NOESY	-	Nuclear Overhauser Effect Spectroscopy
NRPS	-	Nonribosomal peptide synthetase
PCR	-	polymerase chain reaction
PKS	-	Polyketide synthetase
P-TLC	-	Preparative Thin Layer Chromatography
R _f	-	Retardation Factor
R _t	-	Retention Time
TBE	-	Tris boric acid Ethylene diamine tetra acetic acid
TLC	-	Thin Layer Chromatography
UV-VIS	-	Ultra Violet-Visible
NA	-	Nutrient agar
ZMA	-	Zobell Marine agar
SWA	-	Sea water agar

Contents

	<i>Page No:</i>
<i>Chapter 1 Introduction</i>	<i>1-13</i>
<i>1.1 Background</i>	
<i>1.2 Seaweed resistance to microbial attack</i>	
<i>1.3 The symbiotic role of marine microbes on living surfaces</i>	
<i>1.4 Bacterial communities coexisting with the seaweeds as a source of novel natural compounds</i>	
<i>1.5 Functional genes associated with the seaweed-associated bacteria and their relation to the bioactivity</i>	
<i>1.6 Objectives of the proposed work</i>	
<i>1.7 Thesis outline</i>	
<i>Chapter 2 Review of literature</i>	<i>14-47</i>
<i>2.1 Background</i>	
<i>2.2 Marine Microorganisms as a Source of Bioactive Metabolites</i>	
<i>2.3 Microbial natural products</i>	
<i>2.4 Natural product derived drug molecules</i>	
<i>2.5 Bioactivities of molecules from microbial flora</i>	
<i>2.5.1 Immunosuppressant molecules from marine microbial flora</i>	
<i>2.5.2 Antitumor drugs from microbial sources</i>	
<i>2.5.3 Microbial products in agriculture</i>	

2.5.4 *Aquaculture grade chemicals from marine microbes*

2.6 *New molecules from marine bacteria as a solution towards
multiresistant antibiotic and drug molecules*

2.7 *Symbiotic role of marine microbes and bioactive compound
production*

2.8 *Why seaweed associated bacteria?*

2.8.1 *Seaweed associated bioactive bacterial isolates*

2.8.2 *Protective role of seaweed associated bacteria against fouling*

2.8.3 *Seaweed associated bacteria against fish pathogens*

2.9 *Seaweed associated bacterial as a source of antimicrobial
compounds*

2.10 *Diversity of seaweed associated antibiotic producers*

2.11 *Antibiotic Compounds from Bacillus: Why are they so amazing?*

2.12 *Functional genes related to the antimicrobial activity of the
seaweed associated bacteria*

2.13 *Conclusions*

Chapter 3 *Isolation of antagonistic bacterial flora associated with seaweeds* 48-81

3.1 *Background*

3.2 *Materials and Methods*

3.2.1 *Seaweed sample collection*

3.2.2 *Isolation of Seaweed-Associated Bacteria*

3.2.3 *Purification of Seaweed-Associated Bacterial isolates*

3.2.3.1 *The streak-plate method for isolation of pure cultures*

3.2.4 *Pathogenic test organisms used for the study*

3.2.4.1 *Vibrio parahaemolyticus*

3.2.4.1.1 *Vibrio parahaemolyticus (ATCC® 17802™)*

3.2.4.1.2 *Vibrio parahaemolyticus* MTCC451

3.2.4.2 *Vibrio vulnificus* MTCC1145

3.2.4.3 *Vibrio harveyi*

3.2.4.4 *Aeromonas hydrophilla*

3.2.4.5 *Vibrio alginolyticus*

3.2.4.6 *Vibrio anguillarum*

3.2.5 Screening of isolated strains for their antibacterial activity against the pathogens

3.2.6 Preservation of isolated strains with antibacterial activity against the tested pathogens

3.2.6.1 Serial sub culture on agar slants

3.2.6.2 Oil sealing

3.2.6.3 Storage at low temperature

3.2.6.4 Preservation by Lyophilization

3.2.6.5 Preservation using Seaweed Extract Agar

3.2.7 Identification of isolated strains with antibacterial activity

3.2.7.1 Biochemical identification

3.2.7.2 Molecular identification based on 16S rna genes

3.2.7.2.1 DNA isolation

3.2.7.2.2 PCR

3.2.7.2.3 BLAST

3.2.7.2.4 Phylogenetic tree construction

3.2.7.2.5 Nucleotide Accession numbers

3.2.7.3 Chemotaxonomy based on analysis of fatty acid profiles

3.2.7.3.1 Analysis of cellular fatty acids

3.2.7.3.2 Gas liquid chromatography

3.2.7.3.3 Reproducibility of FAME analysis

3.3 Results and discussion

3.3.1 Algal samples

	3.3.2 Isolation and antimicrobial screening	
	3.3.3 Preservation of candidate strains	
	3.3.4 Identification	
	3.3.4.1 Biochemical Identification	
	3.3.4.2 16S rRNA based Phylogeny	
	3.3.4.3 Identification by Fattyacid profiles	
	3.4 Conclusions	
Chapter 4	<i>Characterization of antagonistic potential of seaweed associated bacterial isolates</i>	82-95
	4.1 Background	
	4.2 Materials and methods	
	4.2.1 Release of Antibiotic Substances to the Culture Medium	
	4.2.2 Antagonism assays among the isolated marine bacteria and their auto inhibition	
	4.2.3 Plasmid profiling	
	4.2.4 Plasmid curing	
	4.2.5 Identification and analysis of PKS and NRPS gene fragments	
	4.2.6 Sequence analysis	
	4.3 Results and Discussion	
	4.3.1 Release of Antibiotic Substances to the Culture Medium	
	4.3.2 Antagonism assays among the isolated marine bacteria and their autoinhibition	
	4.3.4 Identification and analysis of PKS and NRPS gene fragments	
	4.4 Conclusions	
Chapter 5	<i>Bioprospecting of antagonistic bacteria associated with seaweeds for antibacterial metabolites</i>	96-102
	5.1 Background of the study	
	5.2 General Materials and Methods	
	5.2.1 Microbial strains used in the study	
	5.2.2 Antibiotic resistance and Abiotic stress tolerance	

5.2.3 *Optimization of growth conditions for optimized compound production*

5.2.3.1 *Optimization of Time*

5.2.3.2 *Optimization of Temperature*

5.2.3.3 *Optimization of pH*

5.2.4 *Chemicals and Reagents*

5.2.5 *Preparation of Crude Extracts from Cultures*

5.2.6 *Determination of Antibacterial Activities by Agar Diffusion Method*

5.2.7 *Analysis*

5.2.7.1 *Chromatographic Analyses*

5.2.7.1A *Preparative Thin Layer Chromatography*

5.2.7.1B *Flash column chromatography*

5.2.7.1C *Vacuum Column Chromatography*

5.2.7.1D *High Performance Liquid Chromatography*

5.2.7.2 *Spectroscopic Analyses*

5.2.7.2A *Fourier Transform Infra Red spectrometer*

5.2.7.2B *Mass Spectrometry and Elemental Analysis*

5.2.7.2C *Nuclear Magnetic Resonance Spectroscopy*

5.3 *Isolation and Purification of Secondary Metabolites*

Chapter 5A *Bioprospecting of Bacillus subtilis MTCC 10403 associated with Anthophycus longifolium (SWI 2) for antibacterial metabolites*

103-156

5A.1 *Materials and Methods*

5A.1.1 *Microbial strain under the study*

5A.1.2 *Antibiotic resistance and abiotic stress tolerance*

5A.1.3 *Optimization of Time*

5A.1.4 *Optimization of Temperature*

5A.1.5 *Optimization of pH*

5A.1.6 *Preparation of crude extract for purification of secondary metabolites*

5A.1.7 Purification of secondary metabolites

5A.1.8 Analysis of pure fractions

5A.2 Results and Discussion

5A.2.1 Antibiotic resistance and abiotic stress tolerance

5A.2.2 Optimization of Time, Temperature and pH

5A.2.3 Yield

5A.2.4 Antibacterial activities of the crude extracts by agar diffusion Method.

5A.2.5 Secondary Metabolites from *B. Subtilis* MTCC 10403 associated with *Anthophycus longifolium*(SWI2)

5A.2.6 Structural Characterization of secondary metabolites with antibacterial activity

5A.2.6.1 Structural Characterization of Compound 1

5A.2.6.2 Structural Characterization of Compound 2

5A.2.6.3 Structural Characterization of Compound 3

5A.2.6.4 Structural Characterization of Compound 4

5A.2.6.5 Structural Characterization of Compound 5

5A.2.6.6 Structural Characterization of Compound 6

5A.3 Conclusions

Chapter 5B *Bioprospecting of antagonistic bacteria B. amyloliquefacens* MTCC 10456 associated with seaweed *laurenciae papillosa* (SWI4B) for antibacterial metabolites

157-186

5B.1 Materials and Methods

5B.1.1 Microbial strain under the study

5B.1.2 Antibiotic resistance and abiotic stress tolerance

5B.1.3 Optimization of Time

5B.1.4 Optimization of Temperature

5B.1.5 Optimization of pH

5B.1.6 Preparation of crude extract for purification of secondary metabolites

5B.1.7 Purification of secondary metabolites

5B.1.8 Analysis of pure fractions

5B.2 Results and Discussion

5B.2.1 Antibiotic resistance and abiotic stress tolerance

5B.2.2 Optimization of Time, Temperature and pH

5B.2.3 Yield

5B.2.4 Antibacterial activities of the crude extracts by agar diffusion Method.

5B.2.5 Secondary Metabolites from B. Amylolyticus MTCC 10456 associated with Laurentia papillosa(SWI4B)

5B.2.6 Structural Characterization of antibacterial metabolites from B. Amylolyticus MTCC 10456

5B.2.6.1 Structural characterization of compound 7

5B.2.6.2 Structural characterization of compound 8

5B.3 Conclusions

Chapter 5C Bioprospecting of antagonistic bacteria B.subtilisMTCC10407 associated with seaweed sargassum myriocystum (SWI 19) for antibacterial metabolites

187-204

5C.1 Materials and Methods

5C.1.1 Microbial strain under the study

5C.1.2 Antibiotic resistance and abiotic stress tolerance

5C.1.3 Optimization of Time

5C.1.4 Optimization of Temperature

5C.1.5 Optimization of pH

5C.1.6 Preparation of crude extract for purification of secondary metabolites

5C.1.7 Bioassay guided purification of antibacterial compound from B. Subtilis MTCC 10407 associated with seaweed Sargassum myriocystum

5C.2 Results and Discussion:

5C.2.1 Antibiotic resistance and abiotic stress tolerance

5C.2.2 Optimization of Time, Temperature and pH

5C.2.3 Yield

5C.2.4 *Antibacterial activities of the crude extracts by agar diffusion method.*

5C.2.5 *Secondary Metabolites from B. Subtilis MTCC 10407 associated with Sargassum myriocystum (SWI19)*

5C.2.6 *Structural Characterization of Antibacterial O-heterocycle pyran derivatives from B. Subtilis MTCC 10407.*

5C.2.6.1 *Structural Characterization of Compound 9*

5C.2.6.2 *Structural Characterization of Compound 10*

5C.3 *Conclusions*

Chapter 5D *Bioprospecting of antagonistic bacteria B. amyloliquefacens associated with seaweed Padina gymnospora(SWI 7)for antibacterial metabolites* 205-233

5D.1 *Materials and Methods*

5D.1.1 *Microbial strain under the study*

5D.1.2 *Antibiotic resistance and abiotic stress tolerance*

5D.1.3 *Optimization of Time*

5D.1.4 *Optimization of Temperature*

5D.1.5 *Optimization of pH*

5D.1.6 *Preparation of crude extract for purification of secondary metabolites*

5D.1.7 *Purification of secondary metabolites*

5D.2 *Results and Discussion*

5D.2.1 *Antibiotic resistance, abiotic stress tolerance and growth conditions of the culture*

5D.2.2 *Yield*

5D.2.3 *Antibacterial activities of the crude extracts by Agar Diffusion Method.*

5D.2.4 *Secondary Metabolites from B. Amyloliquefacens MTCC 10456^B associated with Padina gymnospora(SWI7)*

5D.2.4.1 *Structural characterization of the compound 11*

5D.2.4.2 *Structural characterization of the compound 12*

5D.2.4.3. *Structural characterization of the compound 13*

5D.2.4.4 Structural characterization of the compound 14

5D.3 Conclusions

Chapter 6 *Secondary metabolites and seaweed-bacterial interactions* 234-235

6.1 *Background of the study*

Chapter 6A *Antibacterial secondary metabolites and seaweed bacterial interactions* 236-266

6A.1 *Background of the study*

6A.2 *Materials and methods*

6A.2.1 *General*

6A.2.2 *Seaweed samples and associated antibacterial isolates*

6A.2.3 *Bioassay guided purification of antibacterial compound from B. Subtilis MTCC 10407 associated with seaweed Sargassum myriocystum*

6A.2.4 *Bioassay guided chromatographic purification of the ethyl acetate extract of Sargassum myriocystum*

6A.2.5 *Antimicrobial assay*

6A.3 *Results*

6A.3.1 *Isolation and antibacterial activities of Bacillus subtilis MTCC 10407 associated with intertidal seaweed Sargassum myriocystum*

6A.3.2 *Antibacterial activities of chromatographic fractions of Sargassum myriocystum and its associated B. Subtilis MTCC 10407 by agar diffusion method*

6A.3.3 *Structural characterization of antibacterial O-heterocycle pyrans from B. Subtilis MTCC 10407*

6A.3.4 *Structural characterization of secondary metabolites from Sargassum myriocystum*

6A.3.4.1 *Structural characterization of compound 15*

6A.3.4.2 *Structural characterization of compound 16*

6A.4 *Discussion*

6A.5 *Conclusions*

Chapter 6B *Chemical ecology of seaweed-associated antagonistic bacillus sp based on differential membrane fatty acid composition* 267-291

6B.1 *Background of the study*

6B.2 Materials and methods

6B.2.1 Isolation and molecular identification of the seaweed associated antagonistic bacteria

6B.2.2 Preservation of bacterial strains on seaweed extract agar

6B.2.3 Chemistry

6B.2.4 Fatty acid analyses and gas chromatography

6B.2.5 Seaweed material and preparation of crude extracts

6B.2.6 Chromatographic purification of substituted vinylphenanthrenyl-2-methylbutanoate from *Anthophycus longifolium*

6B.2.7 Structural characterization of compound 13

6B.3 Results

6B.3.1 Isolation, Molecular Identification and Preservation of the Seaweed Associated Antagonistic Bacteria

6B.3.2 Analysis of Cellular Fatty Acid of *Bacillus* sp isolated from seaweeds

6B.3.3 Structural Characterization of Vinylphenanthrenyl-2-Methylbutanoate from *Anthophycus longifolium*

6B.3.4 Correlations between Fatty Acids and Antibacterial Activity

6B.4 Discussion

6B.5 Conclusions

Chapter 7	summary and conclusion	292-298
References		299-319
Publications		320

List of Figures

Figure No.	Figure Captions	Page No:
1.1	<i>seaweed collection area in Gulf of Mannar (Mandapam) (Inset: seaweed and their associated bacteria (Bacillus subtilis)</i>	6
2.1	<i>Share of different classes of marine organisms to produce bioactive molecules</i>	19
2.2	<i>The brominated antibiotic 2,4-dibromo-6-(3,4,5-tribromo-1H-pyrrol-2-yl) phenol</i>	20
2.3	<i>Antibiotics from marine bacteria</i>	20
2.4	<i>Planer structure of Korormicin</i>	21
2.5	<i>Structure of 1, 4-dihydro-1-methylquinoline</i>	21
2.6	<i>Schematic representation of bioprospecting antibacterial molecules from microbial flora</i>	23
2.7	<i>The antifungal compounds (A) isatin and (B) 2, 3-indolinedione produced by symbiotic Alteromonas sp.</i>	31
2.8	<i>The antibiotic harman isolated from the tunicate-associated bacterium Enterococcus faecium</i>	32
2.9	<i>(A) The seaweeds and the bacterial flora associated with them; (B) Different parts of seaweed</i>	33
2.10	<i>Different seaweed species (A) Sargassum sp; (B) Gracillaria sp, (C) Padina sp., (D) A seaweed collection site</i>	35
2.11	<i>Chemical structure of Haliangicin</i>	37
2.12	<i>Chemical structure of lobophorolide and related macrolides</i>	38
2.13	<i>Collection site of seaweeds at Gulf of Mannar region of South East coast of India</i>	40
2.14	<i>Difficidin and oxydifficidin (macrocyclic polyene lactone phosphate esters) from Bacillus subtilis ATCC 39320 and B. subtilis ATCC 39374, respectively.</i>	41
3.1	<i>Indicative pictures showing (A) sample collecion site (B) Padina gymnospora (C) Sargassum myriocystum (D) Sargassum wightii</i>	49
3.2	<i>Indicative pictures showing (A) Antibiotic susceptibility testing for A.hydrophilla used for the study (B) Pathogen challenging via injection of the pathogenic bacteria in shrimp.</i>	51
3.3	<i>Indicative pictures showing preliminary screening (spot over lawn assay)of seaweed associated bacterial isolates (A)Bacterial</i>	55

	<i>isolates of brown seaweed Dictyota dichotoma are spotted against V.vulnificus (B) Bacterial isolates of brown seaweed Anthophycus longifolium against V.parahaemolyticus MTCC451. Live cells are stained in blue with MTT solution and the bactericidal zones are visualized as yellowish clear zone around the spotted seaweed associated bacterial isolates.</i>	
3.4	<i>Preservation techniques used(A) Cultures preserved with oil sealing (B) Cultures preserved with Lypphillization (C) Seaweed Extract used for preservation media enrichment (D) Cultures preserved with oil sealing in Seaweed extract agar.</i>	57
3.5	<i>Indicative pictures of the algal samples screened for antagonistic activity and their isolates.(A)Seaweed sample Bacterial isolates of brown seaweed Anthophycus longifolium (5) and inset shows antibacterial activity assay of its isolates against V.parahaemolyticus MTCC451(55 and 510 are with inhibitory zones) (B) Seaweed sample Halimeda sp. and its isolates Isolate 33 inhibiting V.parahaemolyticus ATCC17802</i>	63
3.6	<i>Indicative pictures showing the Gram staining of the isolates (a) Gram negative strains (S. algae) (b) Gram positive strains (B. subtilis)</i>	76
3.7	<i>Phylogenetic tree derived from nearly complete 16S rRNA gene sequences</i>	78
4.1	<i>Indicative pictures showing the release of the compound (A) disc diffusion assay of the broth and (B) spot over lawn assay of the culture pellet against V.parahaemolyticus MTCC 451</i>	87
4.2	<i>Indicative pictures for autoinhibition and mutual inhibition of seaweed associated isolates (A) SW IMTCC10404 (B) SWI 4b MTCC 10456</i>	88
4.3	<i>Plasmid profiles of the antagonistic isolates before and after curing.</i>	90
4.4	<i>Molecular phylogeny analysis of ketosynthase regions with respect to diverse range of ketosynthase domains</i>	94
4.5	<i>Amino acid sequence alignments of active sites of Type I KS domains</i>	95
5A.1	<i>Antagonistic spectrum of seaweed isolates SWI2</i>	103
5A.2	<i>Schematic representaion of bioprospecting of Bacillus subtilis MTCC 10403</i>	106
5A.3	<i>Antibiotic sensitivity profile of MTCC10403</i>	107
5A.4	<i>Graphical representation of antibacterial compound production at different incubation time,temperature and pH</i>	107
5A.5	<i>Graphical presentation showing antibacterial activities of solvent extracts of B. subtilis MTCC10403 against the pathogenic strains</i>	108

5A.6	(A) ¹ H, (B) ¹³ C NMR spectrum of compound 1	119
5A.7	2D NMR correlations as observed in 7-O-methyl-5'-hydroxy-3'-heptenoate-macrolactin.	120
5A.8	Mass fragmentation pattern of 7-O-methyl-5'-hydroxy-3'-heptenoate-macrolactin	121
5A.9	(A) Sketch model of 7-O-methyl-5'-hydroxy-3'-heptenoate-macrolactin	123
5A.9	(B) Antibacterial activity of 7-O-methyl-5'-hydroxy-3'-heptenoate-macrolactin against <i>V. parahemolyticus</i>	123
5A.10	Hypothetical pathways for biosynthesis of the bacterial metabolite 7-O-methyl-5'-hydroxy-3'-heptenoate-macrolactin	126-128
5A.11	HPLC Chromatogram of B2E56(Compound 2)	133
5A.12	(A) ¹ H, (B) ¹³ C NMR spectrum of Compound 2	134
5A.13	HPLC Chromatogram of B2E56 (Compound 3)	136
5A.14	(A) ¹ H, (B) ¹³ C NMR spectrum of B2E25(Compound 3)	137
5A.15	(A) HMBC correlation spectrum of B2E25 (B) Prominent HSQC correlation spectrum of B2E25 (Compound 3)	138
5A.16	HPLC chromatogram of B2E29 (Compound 4)	144
5A.17	NMR spectroscopic studies of compound 4	144-146
5A.18	HPLC chromatogram of (B2E35) (Compound 5)	148
5A.19	¹ H and ¹³ C NMR of compound 5	149
5A.20	¹ H- ¹ H COSY and HMBC couplings of compound 5	149
5A.21	HPLC chromatogram of Compound 6	153
5A.22	¹ H and ¹³ C NMR spectrum of Compound 6	154
5B.1	(A) <i>Laurenciae pappilosa</i> at harvest location (9° 17' 0" North, 79° 7' 0" East). (B) Spot over lawn assay of <i>B. amyloliquefaciens</i> MTCC 10456 culture against pathogenic <i>Vibrio vulnificus</i> MTCC 1145. The clearance zones realized by the isolates signify the antibacterial activity. (C) Bioautographic plate showing inhibitory activity of the column fraction B4E3 from crude culture extract	159
5B.2	Schematic representaion of bioprospecting of <i>B. amyloliquefaciens</i> MTCC 10456	160
5B.3	Graphical representation of antibacterial activity of cultures incubated at different pH, temperature and time	161
5B.4	Graphical representation of antibacterial activity of different crude solvent extracts to the tested pathogens	162
5B.5	HPLC Chromatogram of compound 7	166

5B.6	<i>HPLC Chromatogram of compound 8</i>	168
5B.7	<i>(A) ¹H, (B) DEPT135 and (C) ¹³C NMR spectrum of 7.</i>	173
5B.8	<i>(A) ¹H–¹H COSY - NMR spectrum of 7. The key ¹H-¹H COSY couplings have been represented by the bold face bonds. (B) Prominent HSQC correlation spectrum of 7</i>	174
5B.9	<i>(A) HMBC and (B) NOESY spectra of 7. The key HMBC couplings have been indicated as double barbed arrow. The NOESY spectrum have been indicated as two sided arrows.</i>	175
5B.10	<i>Mass fragmentation pattern of 3- (Octahydro-9-isopropyl-2H-benzo [h] chromen-4-yl) - 2- methylpropyl benzoate</i>	176
5B.11	<i>(A) ¹H, (B) DEPT135 and (C) ¹³C NMR spectrum of 8</i>	179
5B.12	<i>(A) ¹H–¹H COSY - NMR spectrum of 8. The key ¹H-¹H COSY couplings have been represented by the bold face bonds. (B) Prominent HSQC correlation spectrum of 8</i>	180
5B.13	<i>(A) HMBC and (B) NOESY spectra of 8. The key HMBC couplings have been indicated as double barbed arrow. The NOESY spectrum have been indicated as two sided arrows</i>	181
5B.14	<i>Mass fragmentation pattern of Methyl 8- (2- (benzoyloxy) ethyl) – hexahydro -4- ((E) – pent - 2- enyl) - 2H-chromene-6-carboxylate.</i>	182
5C.1	<i>Purification scheme for bioactive secondary metabolites from MTCC 10407.</i>	189
5C.2	<i>Graphical representation of antibacterial compound production at different incubation time,temperature and pH</i>	190
5C.3	<i>Graphical representation of antibacterial activity of different solvent extracts to test pathogens</i>	191
5C.4	<i>HPLC Chromatogram of compound 9</i>	194
5C.5	<i>¹H, (B) ¹³C and (C) ¹H–¹H COSY - NMR spectrum of 9.</i>	197
5C.6	<i>Mass fragmentation pattern of O-heterocycle pyran derivative compound 9</i>	198
5C.7	<i>HPLC chromatogram of compound 10</i>	199
5C.8	<i>(A) ¹H, (B) ¹³C and (C) DEPT135 - NMR spectrum of 10.</i>	202
5C.9	<i>(A) ¹H–¹H COSY and (B) prominent HSQC correlation spectra of 10.</i>	202
5C.10	<i>(A)HMBC and (B) NOESY spectra of 10.</i>	203
5C.11	<i>Mass fragmentation pattern of O-heterocycle pyran derivative compound 10 from B. subtilis MTCC 10407.</i>	203

5D.1	<i>Schematic representation showing the purification scheme for bioprospecting of antibacterial metabolites in B. amyloliquefaciens associated with Padina gymnospora</i>	207
5D.2	<i>Graphical representation of antibacterial activity of solvent extracts of bacterial metabolites against test pathogens.</i>	208
5D.3	<i>HPLC Chromatogram of compound11</i>	215
5D.4	<i>(A) 1H–1H COSY - NMR spectrum of compound11 (B) Prominent HSQC correlation spectrum of compound11</i>	215
5D.4	<i>(C) HMBC and (D) NOESY spectra of compound11</i>	216
5D.5	<i>HPLC Chromatogram of compound 12</i>	219
5D.6	<i>(A) 1H, (B) 13C NMR spectrum of compound12</i>	220
5D.7	<i>(A)1H–1H COSY - NMR spectrum of compound12 (B) Prominent HSQC correlation spectrum of compound12</i>	220
5D.8	<i>(A) HMBC and (B) NOESY spectra of compound12. The key HMBC couplings have been indicated as double barbed arrow. The NOESY spectrum have been indicated as two sided arrows.</i>	221
5D.9	<i>HPLC Chromatogram of compound 13</i>	225
5D.10	<i>(A) 1H, (B) 13C NMR (Inset DEPT)spectrum of compound13</i>	225
5D.11	<i>A) 1H–1H COSY - NMR spectrum of compound13 (B) Prominent HSQC correlation spectrum of compound13</i>	226
5D.12	<i>A) HMBC and (B) NOESY spectra of compound13.</i>	226
5D.13	<i>HPLC Chromatogram of compound 14</i>	230
5D.14	<i>(A) 1H, (B) 13C NMR (Inset DEPT)spectrum of compound14</i>	231
5D.15	<i>A) 1H–1H COSY - NMR spectrum of compound14 (B) Prominent HSQC correlation spectrum of compound14</i>	232
5D.16	<i>A) HMBC and (B) NOESY spectra of compound14</i>	232
6A.1	<i>(A) The Gram stained B. subtilis MTCC 10407. The antibacterial activities of ethyl acetate extract of B. subtilis MTCC 10407 and the compounds purified (B) Antibacterial activities of the purified compounds (1-4) against Aeromonas hydrophilla (C) Inhibitory activities of the purified compounds (1-4) against Vibrio alginolyticus MTCC 4439</i>	240
6A.2	<i>(A) 1H and (B) DEPT135 - NMR spectrum of 15.</i>	245
6A.3	<i>Comparison of 13C-NMR between the compounds (A) 9 isolated from B. subtilis MTCC 10407 and (B) 15 from seaweed Sargassum myriocystum</i>	246
6A.4	<i>(A) 1H–1H COSY and (B) prominent HSQC correlation spectra of 15.</i>	247

6A.5	(A) <i>HMBC</i> and (B) <i>NOESY</i> spectra of 15.	247
6A.6	(A) Mass fragmentation pattern of 15 from seaweed <i>Sargassum myriocystum</i> ; (B) Mass fragmentation pattern of 16 from seaweed <i>Sargassum myriocystum</i>	250
6A.7	(A) <i>1H</i> , (B) <i>13C</i> and (C) <i>DEPT135</i> - <i>NMR</i> spectra of 16.	251
6A.8	(A) <i>1H–1H COSY</i> and (B) prominent <i>HSQC</i> correlation spectra of 16.	252
6A.9	(A) Prominent <i>HMBC</i> and (B) <i>NOESY</i> spectra of 16.	252
6A.10	Hypothetical biosynthetic transformation of 9 in the seaweed metabolic pool	260
6A.11	Hypothetical biosynthetic pathways of 1	261- 265
6B.1	(A) <i>FAME</i> profile of <i>Bacillus</i> sp. (B) Comparison of specific group of fatty acids in different bacterial isolates and the ratio of different <i>FAMEs</i> .	276
6B.2	Representative <i>FAME</i> profile of (A) <i>Bacillus subtilis</i> MTCC 10403B, (B) <i>Bacillus subtilis</i> MTCC 10403, (C) <i>Bacillus amyloliquefaciens</i> MTCC 10456B, and (D) <i>Bacillus amyloliquefaciens</i> MTCC 10456C.	277
6B.3	(A) <i>13C-NMR</i> and (B) <i>1H-NMR</i> spectra of 1,2,3,4,4a,4b,5,6,7,8,10,10a-dodecahydro-3-methoxy-4a-methyl-2-vinylphenanthren-7-yl -2-methylbutanoate.	280
6B.4	2D <i>NMR</i> correlations in 1,2,3,4,4a,4b,5,6,7,8,10,10a-dodecahydro-3-methoxy-4a-methyl-2-vinylphenanthren-7-yl -2-methylbutanoate. (A) Key <i>1H–1H COSY</i> couplings; (B) the key <i>1H–1H COSY</i> couplings have been represented by the bold face bonds; (C) key <i>HSQC</i> correlations.	280
6B.5	2D <i>NMR</i> correlations in 1,2,3,4,4a,4b,5,6,7,8,10,10a-dodecahydro-3-methoxy-4a-methyl-2-vinylphenanthren-7-yl -2-methylbutanoate. (A) Key <i>HMBC</i> couplings; (B) the key <i>HMBC</i> couplings are indicated as double barbed arrow; (C) key <i>NOESY</i> correlations; (D) The <i>NOE</i> couplings are indicated as double barbed arrow	281
6B.6	Correlation between antibacterial activities activity to fatty acid content of the seaweed associated <i>Bacillus</i> spp by scatterplot analyses.	282
6B.7	Hypothetical sequence of events for biosynthesis of the bacterial fatty acids anteisoC15:0 and anteisoC17:0 fatty acids from the precursor 2-keto-3-methyl valerate	289

List of Tables

<i>Table No.</i>	<i>Title</i>	<i>Page No:</i>
2.1	<i>Various classes of antibiotics/drugs from microbial flora (upto 2000)</i>	25
2.2	<i>Metabolite production of B. amyloliquefaciens GA1 detected by HPLC-ESI mass spectrometry</i>	43
2.3	<i>Survey of the types of PKSs.</i>	45
3.1	<i>Active isolates of preliminary screening</i>	64
3.2	<i>Antimicrobial spectrum of candidate strains</i>	65
3.3	<i>(A)Morphological tests of the test bacteria</i>	67-68
	<i>(B)Physiological tests of the test bacteria</i>	69-72
	<i>(C)Biochemical tests of the test bacteria</i>	72-76
3.4	<i>Comparison of the fatty acids present in Bacillus sp</i>	79
3.5	<i>Comparison of the fatty acids present in Shewanella alga isolated from the seaweeds</i>	80
4.1	<i>Autoinhibition and mutual inhibition pattern (expressed in mm) of antagonistic isolates associated with seaweed</i>	88-89
5A.1	<i>Yield, activity Rt and Rf values of the fractions at different purification stages</i>	110-112
5A.2	<i>NMR spectroscopic data of 17-O-methyl-5'-hydroxy-3'-heptenoate-macrolactin in CDCl₃.a</i>	117-118
5A.3	<i>NMR spectroscopic data of 6-(4-acetylphenyl)-5-hydroxyhexanoic macrolactin in CDCl₃.a</i>	129-130
5A.4	<i>NMR spectroscopic data of 6-(4-acetylphenyl)-5-hydroxyhexanoic macrolactin in CDCl₃.a</i>	135-136
5A.5	<i>NMR spectroscopic data of Methyl3-(2-((E)-2-(2-(furan-2-yl)ethyl)-1-hydroxy-6-methylhept-4-en-3-yl)-1,2,3,4,4a, 5,6,8a-octahydronaphthalen-7-yl)propanoate in CDCl₃.a</i>	142
5A.6	<i>NMR spectroscopic data of 5a,6,7,8,9,9a-hexahydro-7-isopentyl-8-methoxynaphtho[2,1-b]furan in CDCl₃.</i>	147-148
5A.7	<i>NMR spectroscopic data of methyl 3-(4a,5,6,8,8a,9-</i>	152-153

	<i>hexahydro-4-((E)-3-methylpent-1-enyl)-4H-furo[3,2-g]iso chromen-6-yl)propanoate in CDCl₃</i>	
5B.1	<i>Yield, activity Rt and Rf values of the fractions at different purification stages</i>	163-164
5B.2	<i>NMR spectroscopic data of 7 in CDCl₃</i>	164-165
5B.3	<i>NMR spectroscopic data of 8 in CDCl₃</i>	168-169
5C.1	<i>Yield, activity Rt and Rf values of the fractions at different purification stages</i>	192-193
5C.2	<i>¹H and, ¹³C-NMR spectroscopic data of compound 9</i>	195
5C.3	<i>¹H and, ¹³C-NMR spectroscopic data of compound 10</i>	201
5D.1	<i>Yield, activity ,Rt and Rf values of the fractions at different purification stages</i>	210
5D.2	<i>NMR spectroscopic data of compound 11 in CDCl₃.a</i>	212
5D.3	<i>NMR spectroscopic data of compound 11 in CDCl₃</i>	217
5D.4	<i>NMR spectroscopic data of compound 13 in CDCl₃</i>	222
5D.5	<i>NMR spectroscopic data of compound 14 in CDCl₃</i>	227
6A.1	<i>Antibacterial activity of the crude ethyl acetate extracts purified compounds from B. subtilis MTCC 10407 and seaweed host Sargassum myriocystum</i>	241
6A.2	<i>NMR spectroscopic data of 15 in CDCl₃a</i>	243
6A.3	<i>NMR spectroscopic data of 16 in CDCl₃a</i>	248
6A.4	<i>Physicochemical descriptor variables of 9 and 15 derived from B. subtilis MTCC 10407 vis-à-vis 10 and 16 isolated from brown seaweed Sargassum myriocystum</i>	257
6B.1	<i>NMR spectroscopic data of 1,2,3,4,4a,4b, 5,6,7,8,10, 10a-dodecahydro-3-methoxy-4a-methyl-2-vinylphenanthren-7-yl 2-methylbutanoate in CDCl₃</i>	273

CHAPTER 1

INTRODUCTION

1.1 Background

Control of the unwanted microorganisms is essential in all aspects of life, and microbial diseases must be treated in humans, animals, and plants. Emergence of antibiotic resistant bacteria and the need for novel, antimicrobial compounds led to the exploration of new habitats to screen the production of bioactive substances (Gram et al. 2010). Nature provides a treasure-trove of chemicals that can be used in chemical manufacturing processes, or developed into drugs for the treatment of human disease. New environmental niches provide a new source of microbes and potential for novel compound production (Sfanos et al. 2005).

Advances in natural product chemistry are expected to rely ever more on interdisciplinary research, and this is particularly important for marine microbial products. The marine environment contains over 80% of world's plant and animal species (Jha et al. 2004). Marine natural products from the microbes have lagged behind those from macroorganisms. Therefore, marine microorganisms deserve more and more organized attention by the natural products chemists (Pietra 1997). Marine microorganisms are valuable resources due to the production of a wide range of natural products with potential biotechnological and pharmaceutical application (Gram et al. 2010). Antibiotic production by marine bacteria has been documented for a long time. However, there is a paucity of information dealing with the isolation and purification of the active inhibitory substances (Barja et al. 1989).

1.2 Seaweed resistance to microbial attack

Seaweeds are potential sources of high biotechnological interest due to the production of a great diversity of compounds exhibiting a broad spectrum of biological activities. Several species of seaweed have the capacity to produce a diverse array of secondary metabolites, which exhibit important and vital ecological roles as defense and/or signal compounds, and are also of biotechnological interest (Pereira 2011). More than 2500 secondary metabolites have been isolated from the seaweeds (Chakraborty et al. 2010, 2008, 2009). A typical milliliter of seawater contains 10^3 fungal cells, 10^6 bacteria, and 10^7 viruses, including pathogens that cause widespread mortalities and microbes that initiate fouling of host surfaces. Thus, marine plants and animals are continually exposed to greater concentrations of potentially harmful microbes. Yet, many sessile organisms, such as, seaweeds and sponges suffer remarkably low levels of microbial infection, despite lacking cell-based immune systems. Antimicrobial defenses of marine organisms are largely uncharacterized, although from a small number of studies it appeared that chemical defenses might improve host resistance (Kubaneck et al. 2003). In order to survive in a highly competitive environment, seaweeds have to develop defense strategies that result in a tremendous diversity of compounds derived from different metabolic pathways (Cardozo et al. 2007).

1.3 The symbiotic role of marine microbes on living surfaces

Every surface immersed in the sea, including those of organisms, provide an organic material rich habitat to the microorganisms to thrive. Bacteria associated with live or inert surfaces are more likely to display antibacterial activity (Gram et al. 2010, Armstrong et al. 2001). In order to survive in a highly competitive environment, freshwater or marine algae have to develop defense strategies that result in a tremendous diversity of compounds from different metabolic pathways (Cardozo et al. 2007; Gram et al. 2010). Various novel compounds with antibiotic activity from seaweeds are found to have structural

similarities to microbial compounds (Kubaneck et al. 2003). It is interesting to note that the bacteria associated with live or inert surfaces are more likely to display antibacterial activity (Amstrong et al. 2001).

The surfaces of marine eukaryotes provide a unique habitat for colonizing microorganisms where competition between members of these communities and chemically mediated interactions with their host are thought to influence both microbial diversity and function. For example, it is believed that marine eukaryotes may use their surface-associated bacteria to produce bioactive compounds in defense against competition and to protect the host against further colonization. With the increasing need for novel drug discovery, marine epibiotic bacteria may thus represent a largely underexplored source of new antimicrobial compounds. A greater percentage of epiphytic isolates possessing antimicrobial activities also highlights the biotechnological potential for targeted isolation of marine eukaryote-associated bacteria. Products from such microorganisms may prove to be a valuable source of future novel drugs (Penesyan et al. 2009).

Chemically driven interactions are important in the establishment of cross relationships between marine surface-associated microorganisms and their eukaryotic host (Imhoff et al. 2011). Marine microbial symbionts are possibly the true producers or take part in the biosynthesis of some bioactive marine natural products isolated from the eukaryotic hosts as reported in an array of similar studies (Kubaneck et al. 2003; Zhang et al. 2009; Li 2009). Plurality of culture dependent and independent studies on sponges and their associated microbiota validated this hypothesis. The alkaloid harman, previously reported from some marine invertebrates, was identified as the antibiotic substance of the tunicate-associated bacterium *Enterococcus faecium*. It exhibited antibacterial activity (MIC, 0.017 mM) against the ichthyopathogenic strain *Vibrio anguillarum* (Aassila et al. 2003).

1.4 Bacterial communities coexisting with the seaweeds as a source of novel natural compounds

Seaweeds are prolific natural product synthesizers. The colonization of sessile eukaryotic host surfaces by bacteria is common in the marine environment, and seaweeds have been known to support the bacterial populations (Rao et al. 2005). Seaweed associated bacterial population comprises a major share of their biomass. The majority of marine organisms including seaweeds remain relatively free from macrofouling, although some may be covered in a thin film of epibiotic bacteria. The role of these bacteria in maintaining the health of the host has received little attention. It is likely that many marine plants use chemical defenses against the microbial pathogens, epiphytes, and saprophytes, but this hypothesis has rarely been tested. Seaweed epibionts may play a protective role, releasing compounds into the surrounding seawater that help prevent extensive fouling of the surface. Secondary metabolites from these bacteria associated with seaweeds were reported to use targeted antimicrobial chemical defense strategies to deter microbial infection. These compounds may also have industrial and medical applications.

Weinberger and Friedlander (2000) found that rhodophytan seaweed *Gracilaria conferta* exhibited an antagonistic response to the deleterious bacterial populations. Gil-Turnes et al. (1989) discovered that shrimp embryos are covered by a bacterium, *Alteromonas* sp that produces the broad-spectrum antifungal compound isatin, and that this compound was found to protect the embryos from a pathogenic fungus *Lagenidium callinectes*. *Pseudomonas* and *Bacillus* are common beneficial bacterial candidates in marine environments, and are known to produce a wide range of secondary metabolites inhibiting a wide range of pathogenic bacteria (Raaijmakers et al. 1997). Amphiphilic phenols from marine *Pseudomonas* sp isolated from seaweed have been demonstrated to inhibit several marine bacteria and fungi (Kozubek et al. 1991). Torrento and Torres (1996) reported *in vitro* inhibition of *V. harveyi* by a *Pseudomonas* species isolated from the aquatic environment. Probiotic activity of *Bacillus* sp has been shown to improve survival of penaeid adults in ponds and larvae in hatchery (Moriarty et al.

1997). The relative ease of culturing these microbes, compared to other bacteria that produce active compounds, suggests that the seaweed-associated bacteria may be useful in bioprocess applications, such as the production of antimicrobial or antifouling compounds (Armstrong et al. 2001).

The proportion of active bacteria associated with invertebrates (20%) and seaweeds (11%) was reported to be higher than those isolated from seawater (7%) and sediments (5%) (Li 2009). Chemically driven interactions are important in the establishment of cross relationships between the marine surface-associated microorganisms and their eukaryotic host (Imhoff et al. 2011). Marine microbial symbionts are possibly the true producers or take part in the biosynthesis of some bioactive marine natural products isolated from the eukaryotic hosts as reported in an array of similar studies (Li 2009; Kubanek et al. 2003). Pluralities of culture dependent and independent studies on sponges and their associated microbiota validated this hypothesis. Investigations of the pharmaceutical metabolites revealed the biosynthesis mechanisms of related natural products and solve the current problem of supply limitation in marine drug development (Li 2009).

Despite the fact that the seaweeds like their terrestrial counterparts, are potential sources of novel secondary metabolites. However the number of seaweed species studied and identified corresponds to a meager 2% of the 150,000 known species reported worldwide (Gómez et al. 2010). A preliminary study was conducted by Lemose et al. (1985), where he reported the seaweed-associated bacteria as sources of bioactive metabolites. Further diversity of the antibiotic producing bacteria was studied by Wiese et al. (2009), and in terms of chemical ecology; the protective role of epibiotic bacteria was proposed (Armstrong et al. 2001). Even though such interesting reports are there in relation to the seaweed-associated bacteria, no detailed study concerning the characterization of seaweed-associated bacteria exploring antibiotic effects is available (Wiese et al. 2009).

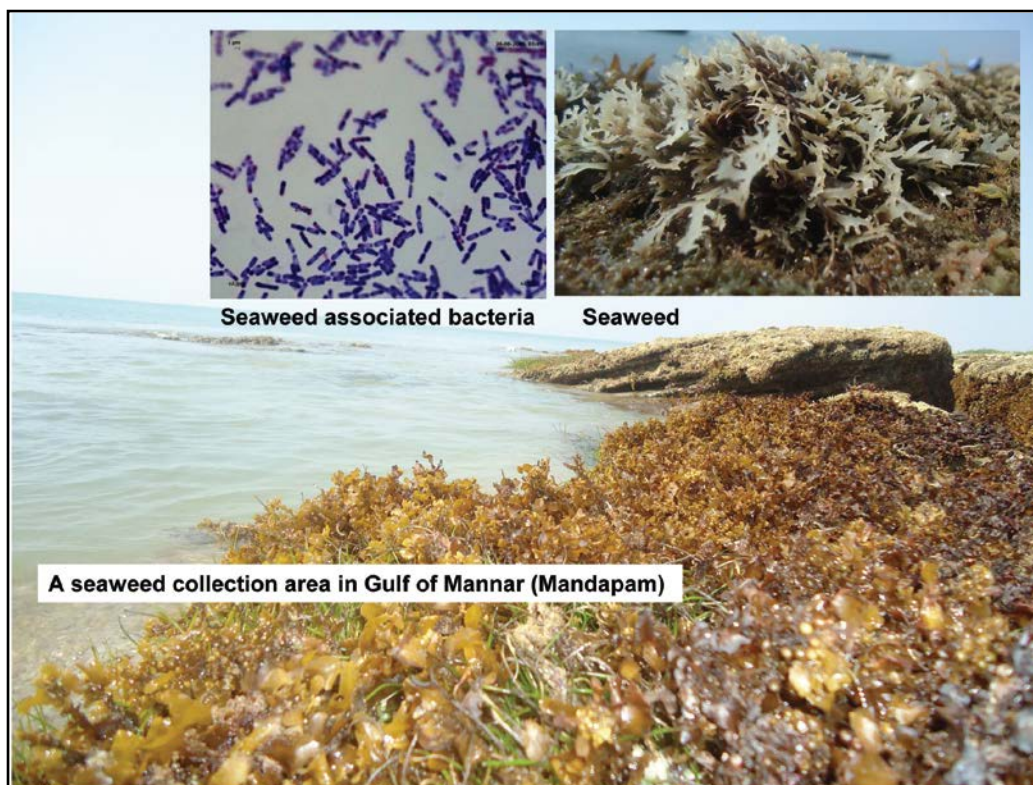


Figure 1.1

**A seaweed collection area in Gulf of Mannar (Mandapam)
(Inset: seaweed and their associated bacteria (*Bacillus subtilis*))**

Positive seaweed–bacterial interactions include phytohormone production, morphogenesis of seaweed triggered by bacterial products, specific antibiotic activities affecting epibionts and elicitation of oxidative burst mechanisms. Some bacteria are able to prevent biofouling or pathogen invasion, or extend the defense mechanisms of the seaweed itself. Deleterious seaweed–bacterial interactions induce or generate algal diseases. To inhibit settlement, growth and biofilm formation by bacteria, seaweeds influence bacterial metabolism and quorum sensing, and produce antibiotic compounds. There is a strong need to investigate the bacterial communities living on different seaweeds. Based on this background, it is imperative to investigate the bacterial communities living on seaweeds using new technologies, and also to investigate the production, localization and secretion

of the biologically active metabolites involved in those possible ecological interactions (Goecke et al. 2010).

Considering that so far virtually all macroorganisms collected and extracted for chemical studies include the associated microorganisms, questions about the true biosynthetic origin of molecules isolated from seaweeds need to be addressed. In several cases, it has already been proven that metabolites initially assigned to the basibionts are in fact of microbial origin. Chlorophyll *d*, for example, is not a constituent of red algae as was described for more than 60 years. In fact, it does not even occur in eukaryotes at all, but is produced by the cyanobacterium *Acaryochloris* spp (Goecke et al. 2010).

In support of this, Kubanek et al. (2003) isolated and characterized a 22-membered cyclic lactone, lobophorolide, of presumed polyketide origin. Lobophorolide is structurally unprecedented, yet parts of the molecule are related to tolytoxin, scytophycins, and the swinholides. These macrolides were previously isolated from the terrestrial cyanobacteria and marine sponges. The structural similarity of Lobophorolide to bacterial metabolites suggests that the polyketide analogue could be the product of a microbial symbiont of *L. variegata*, although no such symbiont has yet been identified.

Based on these we hypothesized that the chemical defense could be a widespread strategy used by the marine macroorganisms to deter microbial infection. Antimicrobial activity is widespread among seaweed associated bacteria (Wiese et al. 2009, Burgess et al. 1999; Kanagasabhapathy et al. 2008; Penesyan et al. 2009). Bacteria producing antibiotic substances reflect an important part of bacterial communities on surfaces of marine organisms as compared to the free-living bacterial communities. However, we still have a long way to go in understanding how bacteria really protect their hosts, and the structural information of the antimicrobial compounds they may produce under multifactorial natural conditions *in situ* (Goecke et al. 2010).

In this study, we have adopted a culture dependent method to assess the diversity of cultivable antagonistic heterotrophic bacterial communities associated

with seven species of intertidal seaweeds at the Gulf of Mannar in the South-East Coast of India bordering the Bay of Bengal to explore them as a source for potentially useful antimicrobial substances. Only a minor fraction of the marine microbiota is culturable, and assessing the complete potential of bioactivity of the entire marine microbial population would require inclusion of both culturable and non-culturable organisms. In principle, (meta)genomic data can be used to determine the presence of genes encoding possible antibiotic activity, however, it requires that the mechanisms (and the genetic background) of antagonistic activity are known. Also, if genes encoding antagonistic activity are only present in specific niches, they may not be detected in metagenomic data. For instance, luminous genes in *Vibrio fischeri* were not found in data from the GOS expedition. Despite the limitations of cultivation-based studies, cultivation remains essential as it provides opportunities to study and understand microbial ecology and physiology and design antibiotic screening assays (Gram et al. 2010).

1.5 Functional genes associated with the seaweed-associated bacteria and their relation to the bioactivity

As the activity-based analysis for the bioactive compounds possesses the limitation that the culture conditions may not be suitable for the growth of the isolates for the production of the bioactive metabolites, and so there is a trend towards a functional gene based molecular screening strategy (Zhou et al. 2009). Polyketide synthetases (PKS) and non-ribosomal peptide synthetases (NRPS) are multifunctional enzymes catalyzing the biosynthesis of structurally diverse bioactive natural products (Hutchinson 2003), which has been commonly employed for designing molecular tools to assess metabolically active bacterial groups (Kennedy et al. 2009; Zhang et al. 2009). It is thought that the modular nature of type I PKS and NRPS has facilitated the diversity of the polyketide/nonribosomal peptide natural product families through genetic recombination events, which generate pluralities of novel biologically active molecules (Ayuso-Sacido and Genilloud 2005). PKSs catalyze the biosynthesis of polyketide chain from simple molecular building blocks, such as, carboxylic acid CoA esters (e.g., acetate and propionate units) through a series of decarboxylative condensation reactions (Jez et al. 2002). On the basis of the architecture and mode

of action of the enzymatic assembly lines, PKSs are classified into type I, type II and type III. The type I PKSs refers to linearly arranged and covalently fused catalytic domains within large multifunctional enzymes, whereas the term type II indicates a dissociable complex of discrete and usually monofunctional enzymes. Furthermore, a third group of multifunctional enzymes of the chalcone synthase type is denoted as type III PKSs (Hertweck et al. 2009). Polyketides and nonribosomal peptides have been immensely concerned over the past few decades, and numbers of various novel polyketide and non-ribosomal peptide compounds have been found from marine-derived microbes, most of which showed different biological activities and ecological functions (Zhou et al. 2011). There is evidence that the presence of biosynthesis genes encoding PKSs and NRPSs in marine sponge-derived actinomycetes are useful indicators for the selection of strains to isolate new natural products (Xi et al. 2012).

Polyketides, nonribosomal peptides, and PKS/NRPS hybrid compounds are important classes of natural products, and include many important drugs. There are several reports regarding the filtration and screening of polyketide synthetase (*pks*) and nonribosomal peptide synthetase (*nrps*) genes from bacteria and fungi isolated from sponges and soil showing bioactivity (Zhou et al. 2011). Despite being very important marker gene systems, little is known about the presence of *nrps* and *pks-I* in the diverse seaweed-associated microbiota. Phytochemical studies showed the ability of seaweeds to produce and store polyketide as polycyclic ether macrolides and open chain polyketides. Although macrolides produced by the terrestrial microorganisms have been used for long in human therapeutics, microlides from marine algae is a recent citation (Cardozo et al. 2007). Compounds of polyketide origin, with bioactivity have been isolated from seaweeds, and have reported to have structural similarity to the known compounds of terrestrial cyanobacteria. It is apparent that seaweeds use targeted antimicrobial chemical defense strategies and that secondary metabolites important in the ecological interactions between marine macroorganisms and microorganisms could be a promising source of novel bioactive compounds, but this hypothesis has rarely been tested (Kubanek et al. 2003). In support, it was found that the deduced amino acid sequence of type III PKS (SbPKS) from a brown seaweed, *Sargassum binderi*, shared a greater

sequence similarity with bacterial PKSs (38% identity) than plant PKSs (Baharum et al. 2011). This further strengthens the hypothesis of ecological interactions between the seaweed host and their associated bacterial flora.

Bacillus subtilis has been extensively studied to isolate several antibiotics belonging to surfactins, subtilosin, lantibiotics, subtilin, mersacidin, ericins, etc. (Ongena et al. 2005). The gene clusters of these products and biosynthetic routes have been studied earlier. Other than the peptides, the polyketides form the dominant group of secondary metabolites with pluralities of bioactivities. However, only a few have been isolated and characterized from the genus *Bacillus*. With the help of extensive spectroscopic studies, the polyketides, such as, bacillaene, difficidin, and oxydifficidin, encoded by gene clusters *pks1* and *pks3*, were isolated and characterized from *B. subtilis*. This group of compounds realized tremendous commercial potential in human health and development of pharmaceutical leads with an international market share of about \$10 billion per annum. The macrolactin family of bacterial secondary metabolites, such as, macrolactins A–F and their open chain variants macrolactinic and isomacrolactinic acid belong to the polyketide family of compounds was originally isolated from a deep-sea bacterium. The macrolactin antibiotics are the biosynthetic products of *pks* gene cluster. Other macrolactin include macrolactins G–N, 7-*O*-malonyl/succinyl derivatives of macrolactin A (Romero-Tabarez et al. 2006). Macrolactin A showed selective antibacterial activities, whereas 7-*O*-malonyl macrolactin demonstrated to be active against Gram-positive pathogenic bacterial strains. Over the years, a total of eighteen macrolactins have been characterized from a total of about thirty *Bacillus* strains, in particular *Bacillus amyloliquefaciens*.

There are several reports regarding the filtration and screening of *pks* and *nrps* genes from bacteria and fungi isolated from sponges and soil showing bioactivity (Melkat et al. 2011; Zhou et al. 2011). Despite being very important marker gene systems, little is known about the presence of *nrps* and *pks-I* in the diverse seaweed-associated microbiota. It is therefore imperative to assay the potential of the seaweed-associated microbiota to produce secondary metabolites

and analyze them by polymerase chain reaction employing degenerate primers of polyketide synthetase (*pks-I*) and nonribosomal peptide synthetase (*nrps*) genes exploiting their conserved nature.

1.6 Objectives of the proposed work

Seaweeds and their associated microorganisms were reported to use the targeted antimicrobial chemical defense strategies, and that secondary metabolites produced by them could be a promising source of novel bioactive compounds. Marine plants and animals are continually exposed to high concentrations of potentially harmful microbes. These pathogenic microbes can devastate populations of marine plants and animals. Yet many sessile organisms like seaweeds suffer remarkably low levels of microbial infection, despite lacking cell-based immune systems (Chakraborty et al. 2008; 2009; 2010). We hypothesize that chemical defense could be a widespread strategy used by marine macroorganisms to deter microbial infection, and this might be a product of associated microorganism. Although examples are rare, symbionts may be an important source of antimicrobial chemical defenses for plants and animals (Kubaneck et al. 2003).

In this study, we have adopted a culture dependent method to assess the diversity of cultivable antagonistic heterotrophic bacterial communities associated with seven species of intertidal seaweeds at the Gulf of Mannar in the South-East Coast of India bordering the Bay of Bengal. The potential of the seaweed-associated microbiota to produce secondary metabolites was analyzed by polymerase chain reaction employing degenerate primers of polyketide synthetase (*pks-I*) and nonribosomal peptide synthetase (*nrps*) genes exploiting their conserved nature. We extended the analysis to understand the biosynthetic product of the functional gene cluster of seaweed-associated bacteria, and reported the isolation and structural characterization of antibacterial secondary metabolites from the bacterial flora.

Based on this background the objectives of the thesis are as follows:

- (1) To screen seaweeds associated bacterial flora with greater antibacterial potential.
- (2) To identify the microbial diversity of bioactive seaweed-associated microbial populations using classical microbiological methods supported by molecular techniques.
- (3) To develop an optimized protocol at laboratory for extraction and isolation of antibacterial substances from seaweeds and bacterial populations associated with seaweeds.
- (4) To Analyze the extracts from seaweed-associated bacteria for their antagonistic potential by *in vitro* antibacterial assay. Bioactivity-guided chromatographic purification of the lead molecules having potential antibacterial activities from crude extracts.
- (5) To elucidate structures of purified molecules by different spectroscopic techniques to explore the diversity of antibacterial substances in the seaweed-associated bacterial flora.
- (6) To study the ecological interactions of seaweeds and their associated bacteria based on the structural similarities between the antimicrobial metabolites derived from the seaweed-associated bacterial flora and seaweed host.

1.7 Thesis outline

Based on the above objectives the present thesis have been crystallized into a total of six chapters. The background and importance of the study with objectives were discussed and explained in the Introduction under the Chapter 1. Chapter 2 dealt with the detailed review of the works carried out regarding the significance of seaweed-associated bacteria, detailed review of the works carried out on the seaweed and its associated bacteria and their bioactivities. Subsequently, the isolation and identification of seaweed-associated bacteria with antibacterial

activity described in Chapter 3. Chapter 4 described the characterization of the antagonistic potential of the seaweed-associated bacteria. Chapter 5 summarized the bioprospecting of promising isolates for their bioactive secondary metabolites. An attempt to explain the ecological interactions of seaweeds with its associated bacteria has been carried out under Chapter 6. Chapter 7 summarized the entire work carried out in the present study.

CHAPTER 2

REVIEW OF LITERATURE

2.1 Background

The sea offers an enormous resource for novel compounds, and it has been classified as the largest reservoir of natural molecules for drug discovery (Nunez et al. 2006). Although the marine environment covers about 70% of the planet's surface and holds high biodiversity, very few species have been explored or used for biotechnological purposes (Pereira et al. 2011). Environments such as the deep sea floor, once thought barren, are now known to be equally or more biologically diverse than tropical rainforests. It has been known for at least 40 years that microorganisms could be recovered from the sea. An impressive number of modern drugs have been isolated from microorganisms, mainly based on their use in traditional medicine. In the past century, however, an increasing role has been played by microorganisms in the production of antibiotics and other drugs (Fenical 1993). The importance of terrestrial bacteria and fungi as sources of valuable bioactive metabolites is very well established for more than half a century. As a result, over 120 of the most important medicines (penicillins, cyclosporin A, adriamycine, etc.) in use today are obtained from terrestrial microorganisms (Alanis 2005). For more than two decades, there has been an ongoing quest to discover new drugs from the sea. Most efforts have been directed towards chemical studies of marine invertebrates. Although these studies have indeed proven that marine invertebrates are an important source of new biomedical leads, a fact well demonstrated by the number of compounds currently in clinical trials, it has proven notoriously difficult to obtain adequate, reliable supplies of these compounds from nature. Because of these problems, a new avenue of study focusing on marine

microorganisms has been gaining considerable attention (Faulkner 2001). At first sight thus, the expectable enormous biodiversity of marine microorganisms might have been the reason for the interest in their study. Although marine microorganisms are not well defined taxonomically, preliminary studies indicate that the wealth of microbial diversity in the world's oceans, make this a promising frontier for the discovery of new medicines (Blunt et al. 2009). Marine bacteria are most generally defined by their requirements of seawater, or more specifically sodium for growth. In the case of marine fungi, which in general do not display specific ion requirements, obligate marine species are generally considered to be those that grow and sporulate exclusively in a marine habitat. Although such definitions can prove useful, they tend to select for a subset of the microorganisms that can be isolated from any one environment. This problem is compounded in the case of near - shore or estuarine samples where a large percentage of the resident microbes are adapted to varying degrees of marine exposure. For the purpose of microbial drug discovery, it seems only logical to study all microbes that can be isolated from the marine environment. Based on the species studied, most of the new compounds reported from marine microorganisms were obtained from species that can, in principle, be isolated from both land and sea. Although these facultative marine species are clearly a good source of novel metabolites, their ecological roles and degrees of adaptation to the marine environment is largely unknown. Screening of marine bacteria isolated from the surface of marine algae and invertebrates has shown that a high percentage produce antimicrobial metabolites. Marine microbial floras have an unrivalled capacity to synthesize bioactive secondary metabolites with a wide spectrum of bioactivities. Historically, microorganisms have provided the source for the majority of the drugs in use today. As new chemical entities are likely to be discovered from novel microbes, marine microorganisms are a likely target for improved technological platforms in the search and discovery of novel bioactive compounds. The first antibiotic from marine bacterium was identified and characterized in 1966 (Burkholder et al. 1966). In addition, bacteria in biofilms formed on the surface of marine organisms have been documented to contain a high proportion of antibiotic producing bacteria than some other marine environment (Lemos et al. 1985; Anand et al. 2006).

Marine epiphytic bacteria, associated with nutrient rich algal surfaces and invertebrates, have also been shown to produce antibacterial secondary metabolites, which inhibit the settlement of potential competitors (Bernan et al. 1997). A number of surface associated marine bacteria have also been found to produce antibiotics. A *Bacillus* sp. isolated from a marine worm in Papua New Guinea produced a novel cyclic decapeptide antibiotic, loloatin B, which inhibit growth of MRSA (methicillin resistant *Staphylococcus aureus*) and VRE (Vancomycin resistant *Enterococcus*) (Gerard et al. 1999). The marine bacterium *Alteromonas rava* was found to produce a new antibiotic thiomarinol (Shiozawa et al. 1993). Antibiotics from marine microorganisms have been reported, including loloatins from *Bacillus*. Agrochelin and sesbanimides from *Agrobacterium* (Acebal et al. 1999), pelagiomicins from *Pelagibacter variabilis* (Imamura 1997), pyrones from *Pseudomonas* (Singh et al. 2003). Screening of seaweed and invertebrate-associated bacteria has shown their bioactivities (Chakraborty et al. 2010), and that over 25% of these isolates can produce compounds capable of killing methicillin resistant *Staphylococcus aureus* (MRSA) and vancomycin resistant *Enterococcus* (VRE) (Mearns-Spragg et al. 1997). This is a much higher proportion than found with free-living or soil-associated bacteria.

There is a general call for new antibiotics, chemotherapeutic agents, and agrochemicals that are highly effective, possess low toxicity, and have a minor environmental impact. The natural products are valuable lead molecules whose activity can be enhanced by manipulation through combinatorial and synthetic chemistry. Natural products have been the traditional pathfinder compounds, offering an untold diversity of chemical structures unparalleled by even the largest combinatorial databases (Strobel and Daisy 2003). Marine organisms have become source of great interest to natural product chemistry, since they provide a large proportion of bioactive metabolites with different biological activities (Radjasa et al. 2007). The marine environment may contain over 80% of world's plant and animal species. In recent years, many bioactive compounds have been extracted from various marine animals and plants like tunicates, sponges, soft corals, sea hares, nudibranchs, bryozoans, sea slugs, seaweeds and marine organisms. The search for new metabolites from marine flora and fauna has resulted in the

isolation of more than 10,000 metabolites, many of which are endowed with interesting pharmacodynamic properties (Jha et al. 2004).

2.2 Marine microorganisms as a source of bioactive metabolites

Marine environment supports the unexplored diversity of life and represents a vast untapped resource with potential benefits in many different areas such as medicine, aquaculture and fisheries, industry, research tools and environmental applications. By an estimate only 7% of the oceans and 1% of the oceans' floor has been sampled till date and over 93% of the ocean still remains unexplored. The magnitude of the Indian ocean with its distribution of over 74×10^6 square kilometers, an average depth of 4000 meters and an 8129 kilometers perimeter with India's coastline supports abundant resources for exploration. The potential economic and public health benefits of pharmaceuticals, pesticides, hormones, enzymes and polymers derived from marine organisms are high, yet unexploited. Bioprospecting, in order to identify and collect a variety of organisms or genes of potential use with desirable characteristics, is the need of the hour. Microbial flora made a phenomenal contribution to the health and well-being of people throughout the world. In addition to producing many primary metabolites, such as fatty acids, amino acids, and vitamins and enzymes, they are capable of making secondary metabolites, which constitute half of the pharmaceuticals on the market today and provide agriculture and aquaculture with many essential products. Marine microbial flora have an unrivalled capacity to synthesize bioactive secondary metabolites with a wide spectrum of bioactivities. As new chemical entities are likely to be discovered from novel microbes, marine microorganisms are a likely target for improved technological platforms in the search and discovery of novel bioactive compounds. Microorganisms are a prolific source of structurally diverse bioactive metabolites and have yielded some of the most important products of the pharmaceutical and aquaculture industry.

It has been argued that because of the high dilution effect of seawater, marine-derived bioactive compounds may have evolved great potency. This theory was supported in 2004 with the report of a first-in-class antimicrobial compound,

was described from a marine isolate *Verrucosispora*. Renewed interest in marine microorganisms and their ability to produce antimicrobials has resulted in numerous reports of novel antimicrobial compounds. The period of antimicrobial drug discovery from the early 1940s to the 1960s is referred to as the Golden Age. During this time, the industrialization of penicillin production created the expertise and facilities to make significant quantities of antimicrobial compounds by fermentation. The clinical use of antibiotics heralded a health care miracle; deaths due to bacterial infections were significantly reduced, resulting in increases in life expectancy. The majority of compounds that were discovered during this period were isolated from soil bacteria, most notably the filamentous *Actinobacteria*. Microorganisms are a prolific source of structurally diverse bioactive metabolites and have yielded some of the most important products of the pharmaceutical industry. Microbial secondary metabolites are now being used for applications other than antibacterial, antifungal and antiviral infections. It was during the 1928s when Alexander Fleming (Fleming 1929) began the microbial drug era when he discovered in a Petri dish seeded with *Staphylococcus aureus*, that a compound (penicillin) produced by a fungus/mold killed the bacteria. Later, penicillin was isolated as a yellow powder and used as a potent antibacterial compound during the Second World War. Following this extraordinary discovery by Flemming, the antibiotics chloramphenicol and streptomycin, were isolated from microbes. Naturally occurring antibiotics are produced by fermentation, an old technique that can be traced back almost 8000 years. Owing to technical improvements in screening programs, and separation and isolation techniques, the number of natural compounds discovered exceeds 1 million (Ecker et al. 2005). Among them, 50–60% are produced by plants (alkaloids, flavonoids, terpenoids, steroids, carbohydrates, etc.) and 5% have a microbial origin. Of all the reported natural products, approximately 20–25% show biological activity, and of these approximately 10% have been obtained from microbes. Furthermore, from the 22 500 biologically active compounds that have been obtained so far from microbes, 45% are produced by bacteria or bacteria-like microbes, 38% by fungi and 17% by others (Berdy 2005). However, the development of resistance in microbes to

various life-threatening diseases and in aquaculture has become a major problem and requires much research effort to combat it.

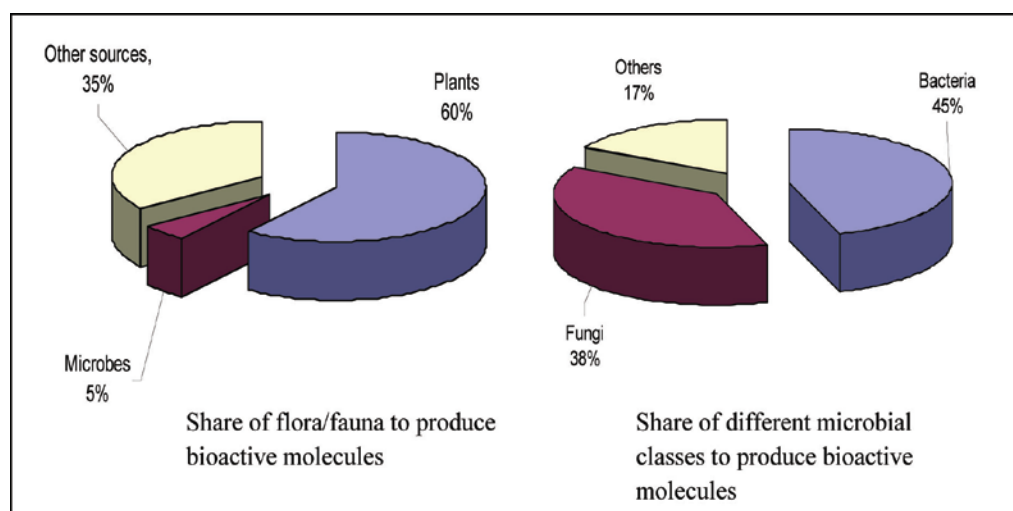


Figure 2.1

Share of different classes of marine organisms to produce bioactive molecules

Marine natural products from microbes have lagged behind those from macroorganisms (Pietra 1997). The marine environment should be considered as a potential source of antibiotics and the sea may represent a reservoir of microbial antagonists. The bactericidal activity of seawater is due to the presence of antibiotic producing antagonistic cultures were proposed (Rosenfeld 1947). Marine organisms may have novel biochemical activities, which are quite different from terrestrial ones (Okami 1986). Marine bacteria can be subdivided into Actinobacteria, Cyanobacteria and all other Eubacteria may be detailed enough to allow some understanding of the patterns (Pietra 1997) of natural products chemistry.

The first antibiotic from a marine bacterium was identified and characterized in 1966. The bacterium was isolated upon several occasions from *Thalassia* located near La Parguera, Puerto Rico (Burkholder et al. 1966). Evidence is presented for the isolation and identification of bacteria able to synthesize an unusual antibiotic containing five bromine atoms per molecule. Bacterium, a pseudomonad, has been given the name *Pseudomonas bromoutilis* because of its

distinctive capability. The antibiotic has been extracted, purified, and obtained in crystal form, and its structure has been determined (Burkholder et al. 1966; Lovell 1966).

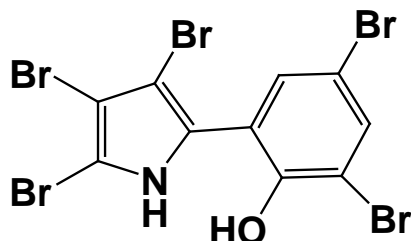


Figure 2.2
The brominated antibiotic 2,4-dibromo-6-(3,4,5-tribromo-1H-pyrrol-2-yl) phenol

Three distinct classes of pharmaceutical compounds, antibiotics, antiviral compounds and antitumour drugs, have been associated with marine bacteria. Antibiotic compounds from marine bacteria published may be summarized as brominated antibiotics, quinolinols, low molecular weight inhibitors, aminoglycoside antibiotics and other complex antibiotics such as aplasmomycin B (Austin 1989).

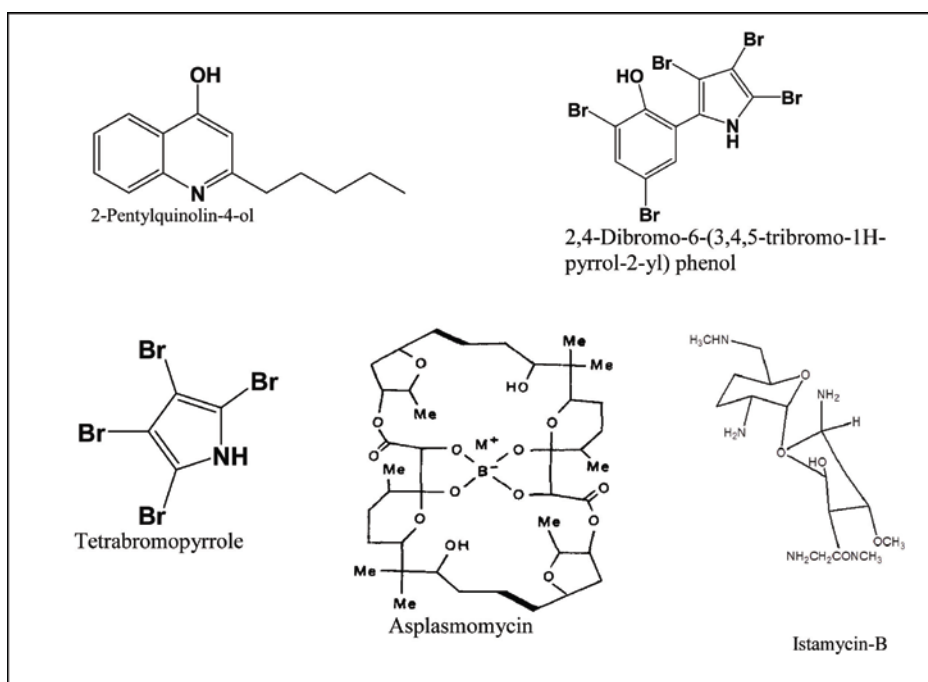


Figure 2.3
Antibiotics from marine bacteria

Novel antibiotic named korormicin was isolated from the marine bacterium, *Pseudoalteromonas* sp. F-420. This strain was isolated from the surface of a macroalga *Halimeda* sp. collected from Palau (the Republic of Belau). The planar structure of Korormicin was determined by the result of 2D NMR studies and mass spectral data. Korormicin had specific inhibitory activity against marine Gram-negative bacteria, but was inactive against terrestrial microorganisms. (Yoshikawa et al. 1997)

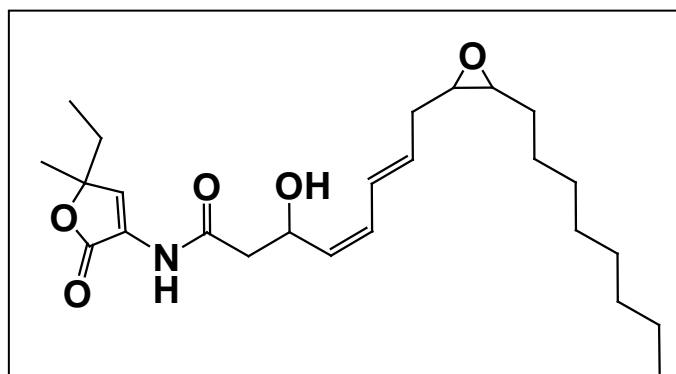


Figure 2.4
Planer structure of Korormicin

A marine bacterium *Pseudomonas aeruginosa* was isolated from Eal fish of Baluchistan coast of Pakistan. This strain produced a bactericidal antibiotic against environmental and clinical isolates. Bactericidal antibiotic from the ethyl acetate extract of the cells of *P. aeruginosa* were purified and chemically characterized as 1-methyl-1,4 dihydroquinoline (Uzair et al. 2006).

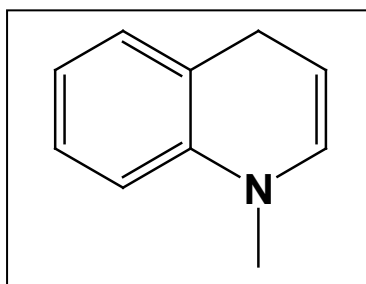


Figure 2.5
Structure of 1, 4-dihydro-1-methylquinoline

2.3 Microbial natural products

Microbial natural products that have reached the market without any chemical modifications are a testimony to the remarkable ability of microorganisms to produce drug-like small molecules. Although still in clinical trials, a feature example of this is salinosporamide A (NPI-0052), a novel anticancer agent found in the exploration of new marine environments (Fenical et al. 2009). In 2008, over 1000 marine natural products were reported (Blunt et al. 2009). However, out of the 19 microbial-derived drugs reported in 2008, no natural products from marine microbes were present, signifying the novelty of their systematic exploration. Currently, more than 30 compounds of marine microbial origin are in clinical or preclinical studies for the treatment of different types of cancer (Simmons et al. 2005) clearly demonstrating that marine microorganisms have become an essential resource in the discovery of new antibiotic leads. The evolution of marine microbial natural product collections and development of high-throughput screening methods have attracted researchers to the use of natural product libraries in drug discovery. These libraries include subsections of crude extracts, pre-fractionated extracts (automated HPLC-MS fractionation) and purified natural products. A research group in Ireland has developed a two-dimensional chromatographic strategy that include a protocol to generate purified marine natural product libraries that are accurately characterized by mass during production to expedite dereplication of known compounds and identification of novel chemotypes. Although the biosynthetic and regulative crosstalk of secondary metabolite biosynthesis is complex within and between microorganisms, all levels can be influenced by imitating natural environmental changes.

The schematic diagram illustrating the development of microbial natural products library (MNPL) is shown below.

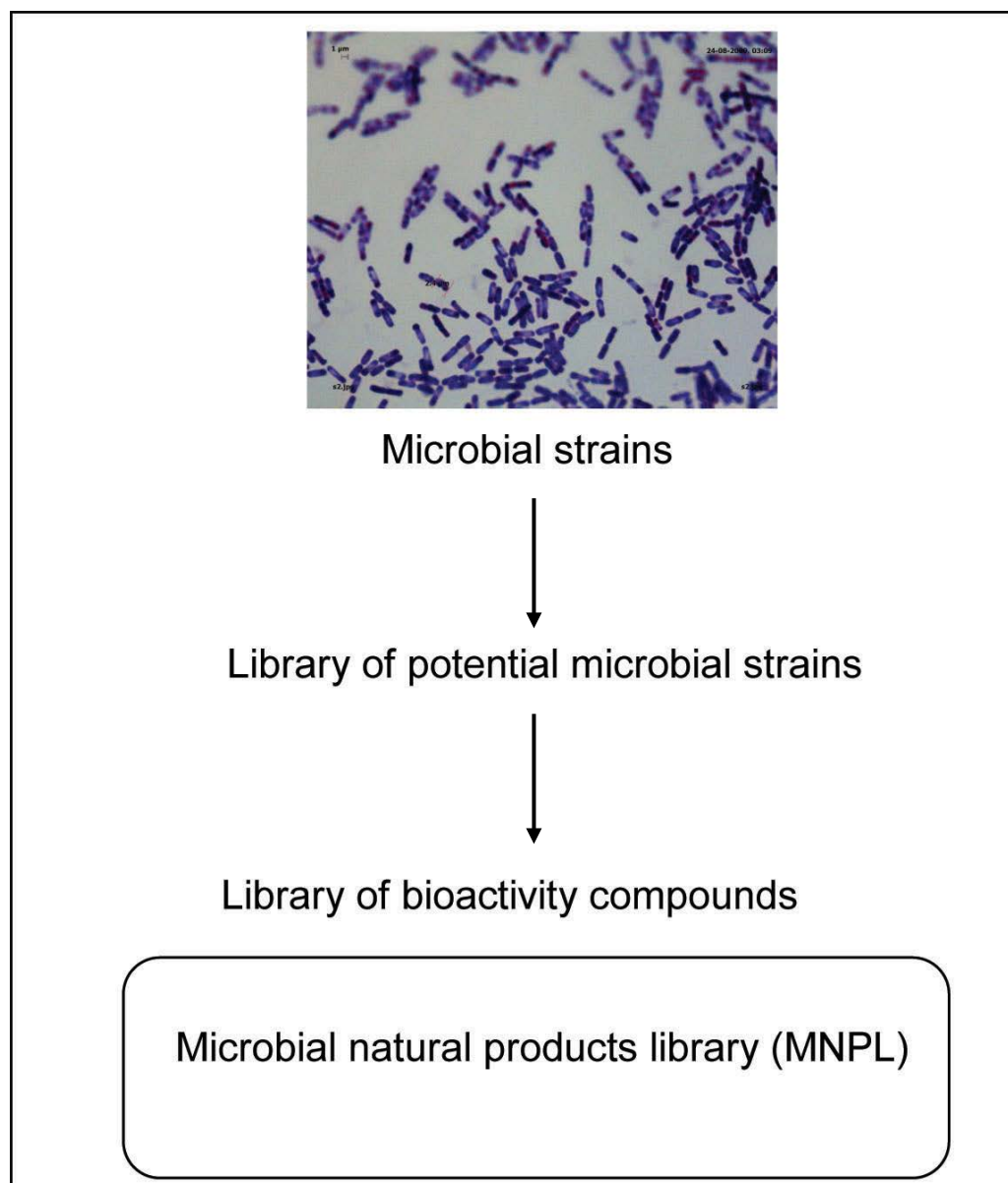


Figure 2.6

Schematic representation of bioprospecting antibacterial molecules from microbial flora

An optimization of ‘one strain, many active compounds’ can be used together with ‘fingerprint’ methods (HPLC and NMR) including tandem analytical techniques, such as, MS/MS, GC-EI/MS, HPLC-SPE-NMR, LC-MS-MS and LC-NMR for the optimization/selection of culture media for high-throughput fermentation of novel strains. Targeted HTS methods are important for the speed

and accuracy of identification of novel antimicrobials. From these evaluation models, many crude extracts or purified compounds were obtained as positive hits. In addition to evaluate the microorganisms, it is worthy to note that these screening assays also provide mode of action hypothesis from the crude extracts.

2.4 Natural product derived drug molecules

Drugs of natural origin have been classified as (i) original natural products, (ii) products derived or chemically synthesized from natural products or (iii) synthetic products based on natural product structures. Evidence of the importance of natural products in the discovery of leads for the development of drugs for the treatment of human diseases and aquaculture are provided by the fact that close to half of the best-selling pharmaceuticals and antibiotics in 1990-2000 were either natural products or their derivatives (Cragg et al. 1997). In this regard, of the 25 top-selling drugs reported in 1997, 42% were natural products or their derivatives and of these, 67% were antibiotics. Today, the structures of around 140 000 secondary metabolites have been elucidated. Applications of chemically synthesized natural metabolites include the use of a natural product derived from plant salicylic acid derivatives present in wintergreen and meadowsweet to relieve pain and suffering. Synthetic salicylates were produced initially by Bayer in 1874, and later in 1897, by Arthur Eichengrün. The plant-based systems continue to play an essential role in health care, and it has been estimated by the World Health Organization (WHO) that approximately 80% of the world's inhabitants rely mainly on traditional medicines for their primary health care (Farnsworth et al. 1985). The alkaloid quinine, the active constituent of *Cinchona succirubra*, has been known for centuries by South American Indians to control malaria. During the twentieth century, massive programs to synthesize quinoline derivatives, based on the quinine prototype, were carried out. The first of the new quinolones to be used clinically as an antibacterial agent was nalidixic acid (Topliss et al. 2002). The compound 7-chloro-1, 4-dihydro-1-ethyl-4-oxoquinolone-3-carboxylic acid was obtained as a side product during purification of chloroquine and found to have antibacterial activity against Gram-negative bacteria and was shown to be an inhibitor of DNA gyrase. Its discovery led to a whole series of synthetic quinolone

and fluoroquinolone antibiotics (pefloxacin, norfloxacin, ciprofloxacin, levofloxacin, ofloxacin, lomefloxacin, sparfloxacin, etc.), which have been very successful in medicine and have achieved major commercial success. Secondary metabolites have exerted a major impact on the control of infectious diseases and other medical conditions, and the development of pharmaceutical industry. Their use has contributed to an increase in the average life expectancy in the world. In 2000, the market for major antiinfectives from bacteria and other natural sources was US\$55 billion and in 2007 it was US\$66 billion.

Table 2.1
Various classes of antibiotics/drugs from microbial flora(upto 2000)
 (Barber 2001)

Sl. No.	Antibiotics/drugs	Market share (US billion \$)
1	Antiviral compounds	10.2
2	Penicillins	8.2
3	Cephalosporins	9.9
4	Beta lactam antibiotics	1.5
5	Quinolines	6.4
6	Other antibacterials	6.0
7	Tetracyclines	1.5

Two antivirals (acyclovir and cytarabine) that are chemically synthesized today were originally isolated from the marine organisms. Acyclovir was found to be active against the herpes virus and cytarabine was reported to be active against non-Hodgkin's lymphoma. These compounds are nucleoside analog drugs, originally isolated from sponges (Rayl 1999). Other antiviral applications of natural compounds are related to human immunodeficiency virus (HIV) treatment. Furthermore, reports have been published on natural product inhibitors of HIV integrase obtained from among the marine ascidian alkaloids; that is, the lamellarins (produced by the mollusk *Lamellaria* sp.), and from terrestrial plants (*Baccharis genistelloides* and *Achyrocline satureioides*). The most consistent anti-HIV activity was observed with extracts prepared from several *Baccharis* sp (Robinson et al. 1996).

2.5 Bioactivities of molecules from microbial flora

The pharmaceutical and aquaculture industry has extended to explore new molecules as potential antibacterial, antifungal, antiviral, in their programs to combat several deleterious diseases (Sum 2006). Marine microorganisms are fascinating resources due to their production of novel natural products with several bioactivities. Increases in both the number of new chemical entities found and the substantiation of indigenous marine actinobacteria present a fundamental difficulty in the future discovery of novel bioactive molecules, namely, dereplication of those compounds already discovered. The immunosuppressants have revolutionized medicine by facilitating organ transplantation. Other applications include antitumor drugs, enzyme inhibitors, gastrointestinal motor stimulator agents, hypocholesterolemic drugs, pesticides and other pharmacological activities. Further applications are possible in various areas of pharmacology, aquaculture, and bioremediation. The details of the activities of these potential molecules from microbes towards different bioactivities are illustrated under the following subheads.

2.5.1 Immunosuppressant molecules from marine microbial flora

A number of antimicrobial compounds capable of suppressing the immune response have been discovered from marine microbial flora. Cyclosporin A, a family of neutral, cyclic undecapeptides containing some unusual amino acids, produced by marine fungus *Tolypocladium nivenum* by aerobic fermentation (Borel 2002). Cyclosporins were reported to inhibit lymphokine production and interleukin release, and therefore lead to a reduced function of effector T cells. Other important transplant agents include sirolimus (rapamycin macrolide) and tacrolimus (FK506), which were produced by the marine bacterial flora *S. hygroscopicus*, and had potent immunosuppressive and antiproliferative properties (Aggarwala et al. 2006). Rapamycin analogs, everolimus, and tensirolimus have been developed with improved pharmaceutical properties. Everolimus were isolated from bacteria is currently used as an immunosuppressant to prevent the rejection of organ transplants (Eisen et al. 2003). AP23573 is a novel non-prodrug

rapamycin analog that has demonstrated antiproliferative activity against several human tumor cell lines *in vitro* and against experimental tumors *in vivo* (Dancey 2006). This agent is currently under evaluation in phase I–II trials, including patients with different tumors.

2.5.2 Antitumor drugs from microbial sources

Microbial metabolites are among the most important of the cancer chemotherapeutic agents. They started to appear around 1940 with the discovery of actinomycin isolated from *Streptomyces antibioticus*, and since then many compounds with anticancer properties have been isolated from natural sources (Waksman and Woodruff 1941). More than 60% of the current compounds with antineoplastic activity were originally isolated as natural products or are their derivatives. Streptozotocin, a glucosamine-nitroso-urea compound is a marine microbial metabolite with antitumor properties, produced by marine *Streptomyces achromogenes*. Pentostatin (deoxycoformycin) is an anticancer chemotherapeutic drug produced by *S. antibioticus*. It is classified as a purine analog, which mimic the nucleoside adenosine and thus tightly binds and inhibit adenosine deaminase (Showalter et al. 1992). Among other approved products deserving special attention are actinomycin D, anthracyclines, bleomycin, mitosanes, anthracenones, enediynes, taxol and epothilones to treat a wide range of cancers. Valrubicin is a semisynthetic analog of doxorubicin approved as a chemotherapeutic drug in 1999, and used to treat bladder cancer.

2.5.3 Microbial products in agriculture

Insecticides are used in agriculture, medicine, industry and households. Microbially produced insecticides are especially valuable because their toxicity to non-target animals and humans is extremely low. Spinosyns (A83543 group) are a group of natural products produced by marine *Saccharopolyspora spinosa*. They are active on a wide variety of insect pests, especially lepidopterans and dipterans (Kirst et al. 2002). The spinosyns are a family of macrolides with 21 carbon atoms, containing four connected rings of carbon atoms at their core to which two

deoxysugars (forosamine and 2,3,4, tri-o-methylrhamnose, which are required for bioactivity) are attached. A mixture of spinosyn A (85%) and D (15%) (spinosad) is being produced through fermentation, and was introduced to the market in 1997 for the control of chewing insects on a variety of crops. Recently, a new naturally occurring series of insect-active compounds was discovered from a marine microbial isolate, *Saccharopolyspora pogona* NRRL30141 (Hahn et al. 2006).

2.5.4 Aquaculture grade chemicals from marine microbes

Disease caused by the bacterial pathogens has been widely recognized as a major cause of economic loss in many commercially cultured fish and shellfish species in India, with mortality of larval stages in hatcheries and the growing stages in different mariculture systems. Pathogenic vibrios are involved in significant mortalities in the larviculture and growout phases of famed finfish and shellfishes. In an attempt to control the proliferation of pathogenic vibrios, the prophylactic and therapeutic use of antibiotics have been practiced in commercial hatcheries, creating more serious problem of antibiotic resistance among the microflora in the environment. With safety concerns about synthetic antibiotics, considerable interest has arisen in finding alternative natural sources (Gomez-Gil et al. 2000). Screening and development of aquaculture-grade chemicals from bacterial flora could be a highly promising approach to produce these bioactive molecules. Members of the genus *Pseudomonas* and *Bacillus* either free living or associated with marine flora are common beneficial bacterial candidates, and were known to produce a wide range of secondary metabolites (Raaijmakers et al. 1997) inhibiting a wide range of pathogenic bacteria (Rengpipat et al. 1998). The metabolites 6-oxo-de-o-methylsiodiplodin, (E)-9-etheno-lasiodiplodin, lasiodiplodin, de-o-methylsiodiplodin, and 5-hydroxy-de-o-methylsiodiplodin, were isolated from the mycelium extracts of a microbe obtained from South China Sea (Yang et al. 2006). Studies conducted at CIBA, Chennai isolated two bacteria, *Pseudomonas* sp. PM 11 as potential candidate probionts from a pool of bacteria isolated from gut of farm reared sub-adult shrimp (Alavandi et al. 2004). Marine bacterial strain, *Pseudomonas* I-2, producing inhibitory compounds against shrimp pathogenic vibrios including *Vibrio harveyi*, *V. fluvialis*, *V. parahaemolyticus*, *V.*

damsela and *V. vulnificus* was reported by Chaitanya et al. (2002). Bioactive compounds were isolated from a marine bacterium *Bacillus circulans* (Chakraborty et al., 2010). Labda-14-ene-3a,8a-diol and labda-14-ene-8a-hydroxy-3-one were found to be inhibitory to the growth of *Vibrio parahaemolyticus* with minimum inhibitory concentrations of 30-40 µg/mL (Chakraborty et al. 2010), and their structures have been elucidated by ¹H NMR and ¹³C NMR spectra, including 2D NMR. Several bacterial flora were isolated from marine ecosystem (*Bacillus subtilis*, *Bacillus amyloliquifaciens*, *Pseudomonas putida*, and *Pseudomonas aeruginosa*) with potential activities of greater than 20 mm inhibition zone against pathogenic Vibrios (Chakraborty et al. 2010). The antibacterial component in the chloroform fraction of *P. aeruginosa* was found to be N-substituted methyl octahydro-1-phenazinecarboxylate. The other important antibacterial molecules were found to be propyl 2-oxoacetate and phenethyl 2-oxoacetate.

2.6 New molecules from marine bacteria as a solution towards multiresistant antibiotic and drug molecules

In recent times, several scientific groups are making concerted efforts to find novel antimicrobial agents as a solution towards multiresistant antibiotic and drug molecules. Novel glycylicyclines (modified tetracyclines) developed to treat tetracycline-resistant bacteria. These show potent activity against a broad spectrum of Gram-positive and Gram-negative bacteria, including strains that carry the two major tetracycline-resistance determinants, involving efflux and ribosomal protection. Two of the glycylicycline derivatives, DMG-MINO and DMG-DMDOT, have been tested against a large number of clinical pathogens isolated from various sources. The spectrum of activity of these compounds includes organisms with resistance to antibiotics other than tetracyclines; for example, methicillin-resistant staphylococci, penicillin-resistant *S. pneumoniae* and vancomycin-resistant enterococci (Sum 2006). Tigecycline was approved by the FDA in 2005 as an injectable antibiotic (Bacque et al. 2005). A new glycopeptide antibiotic, teicoplanin, was developed against infections with resistant Gram-positive bacteria, especially bacteria resistant to the glycopeptide vancomycin. In another instance, the approach involved the redesign of a mixture of two compounds,

called streptogramin, into a new mixture, called pristinamycin, to allow administration of the drug parenterally and in higher doses than the earlier oral preparation (Bacque et al. 2005). The two components of streptogramin, quinupristin and dalfopristin, were chemically modified to allow intravenous administration. The new combination, pristinamycin, was approved by the FDA for use against infections caused by vancomycin-resistant *Enterococcus faecium*. Among the novel class of antimicrobial agents used in treating resistance to Gram-positive infections, we can also mention the cyclic lipopeptide antibiotic daptomycin produced by *Streptomyces roseosporus*. This compound was approved in 2003 by the FDA for skin infections resulting from complications following surgery, diabetic foot ulcers and burns (Laplante et al. 2004). Telithromycin, a macrolide antibiotic, is the first orally active compound of a new family of antibacterials named the ketolides. It shows potent activity against pathogens implicated in community acquired respiratory tract infections, irrespective of their β -lactam, macrolide or fluoroquinolone susceptibility (Leclercq 2001).

2.7 Symbiotic role of marine microbes and bioactive compound production

In recent years, the investigation of marine natural products has moved to the microscopic level, due to numerous findings of similar structures between marine microorganisms and macroorganisms, such as, marine sponges and ascidians, indicating that microorganisms would seem to be a better biological source to tackle the supply problem of marine invertebrates (Peng et al. 2009), and might be the actual source of such compounds (Kubaneck 2003). The embryos of the shrimp *Palaemon macrodactylus* were found to be resistant to infection by the fungus *Lagenidium callinectes*, a recognized pathogen of many crustaceans. A bacterial strain *Alteromonas* sp isolated from the surface of the embryos was reported to produce 2, 3-indolinedione (isatin), a compound that inhibits the pathogenic fungus.

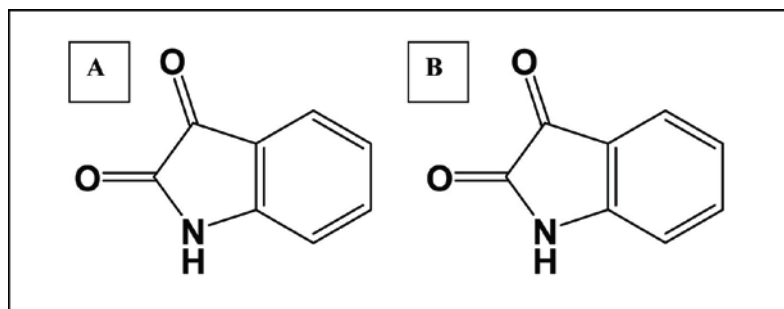


Figure 2.7

The antifungal compounds (A) isatin and (B) 2, 3-indolinedione produced by symbiotic *Alteromonas* sp.

If exposed to the fungus, bacteria-free embryos were found to quickly die, whereas similar embryos reinoculated with the bacteria or treated only with 2, 3-indolinedione lived well. The commensal *Alteromonas* sp bacteria was demonstrated to protect shrimp embryos from the fungal infection by producing and liberating the antifungal metabolite 2, 3-indolinedione (Giltunes 1989).

Every surface immersed in the sea rapidly becomes covered with a biofilm. On inanimate surfaces, this is often followed by colonisation by larger organisms, and general macrofouling. On the other hand, the majority of marine organisms remain relatively free from macrofouling, although some may be covered in a thin film of epibiotic bacteria. The role of these bacteria in maintaining the health of the host has received little attention (Amstrong et al. 2001).

The alkaloid harman, previously reported from some marine invertebrates, was identified as the antibiotic substance of the tunicate-associated bacterium *Enterococcus faecium*. Harman was initially isolated from a number of terrestrial plants, marine organisms as a minor component from the marine dinoflagellate *Noctiluca miliaris* and from the bryozoans. This study suggested that symbiotic microorganisms may be responsible for its occurrence previously reported in marine invertebrates, pointing to an ecologic role of harman for these marine invertebrates. Studies on microorganisms associated with invertebrates will provide a better understanding of marine microbial ecology, which is essential to

maximize the efficiency of research in the discovery of novel secondary metabolites (Aassila et al. 2003).

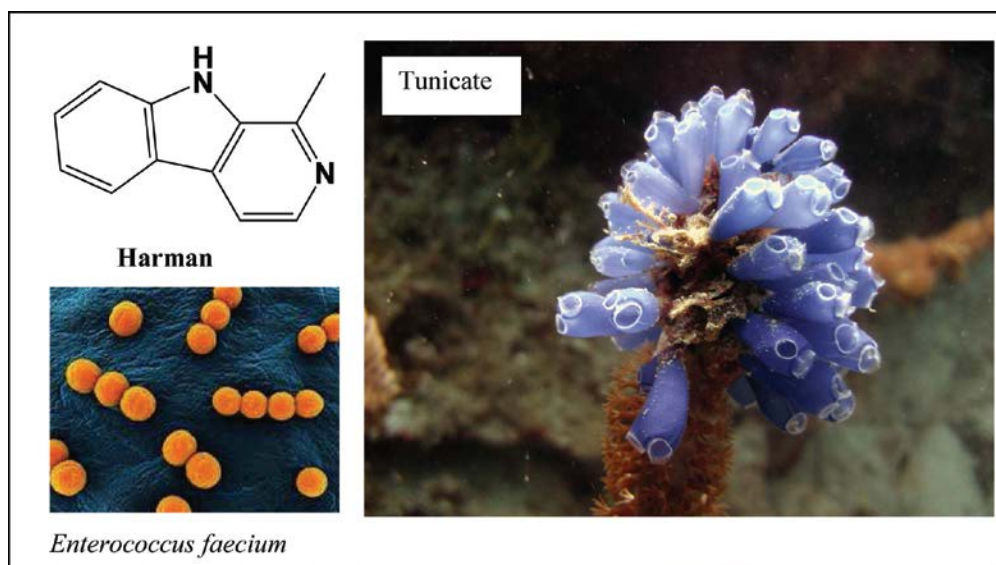


Figure 2.8

The antibiotic harman isolated from the tunicate-associated bacterium *Enterococcus faecium*

2.8 Why seaweed associated bacteria?

Marine seaweeds have been challenged throughout their evolution by microorganisms, and have developed in a world of microbes. Therefore, it is not surprising that a complex array of interactions has evolved between seaweeds and bacteria, which basically depend on chemical interactions of various kinds (Goecke et al. 2010). The increasing number of duplications and the demand for new leading structures in pharmacology has enforced the search for metabolites in novel and promising habitats (Laatsch 2006). The intertidal zone is an important coastal habitat in terms of biological productivity and economic value. Biofilms form protective micro-environments in the changing environments of intertidal regions, where surface dwelling microbes to develop adaptive response and antagonistic strategies to prevent potential competitors occupying their habitat (Mitra et al. 2014). Competition amongst microbes for space and nutrients in the marine environment is a powerful selective force which has led to the evolution of

a variety of effective strategies for colonizing and growing on surfaces (Burgess et al. 1999). Seaweeds and associated bacteria were reported to use targeted antimicrobial chemical defense strategies to deter microbial infection (Kubaneck et al. 2003, Kozubek 2001). Weinberger and Friedlander (2000) found that rhodophytan seaweed *Gracilaria conferta* exhibits an antagonistic response to the deleterious bacterial populations. Antibacterial labdane diterpenoids of *Ulva fasciata* Delile from the southwestern coast of Indian Peninsula were reported (Chakraborty et al. 2009).

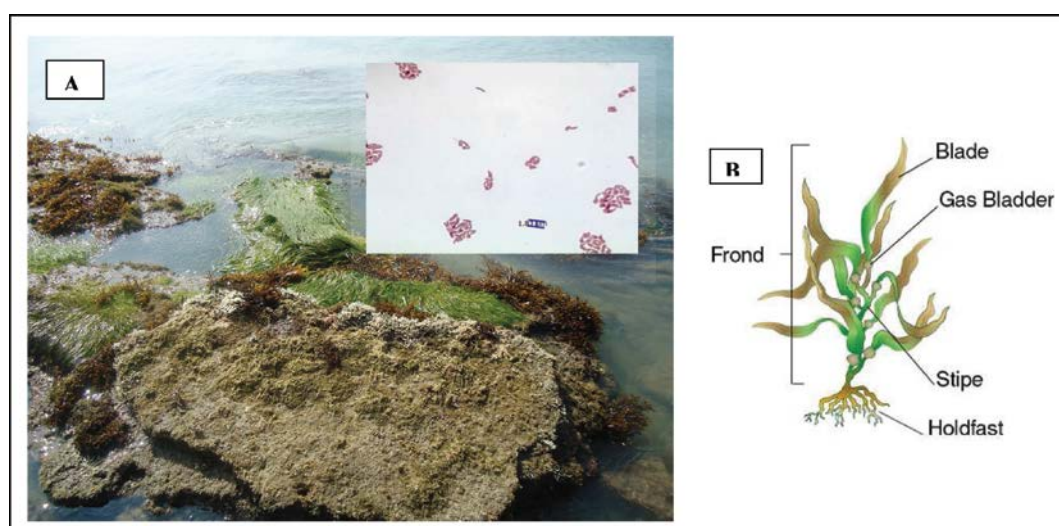


Figure 2.9

- (A) The seaweeds and the bacterial flora associated with them;**
(B) Different parts of seaweed

2.8.1 Seaweed associated bioactive bacterial isolates

Seaweeds and microbial populations associated with seaweeds constitute the major biologically active flora of marine food pyramid due to their enormous biodiversity. As a pioneer study survey of antibiotic-producing bacteria from the microbial flora attached to seaweeds and the study of their antibiotic capacities were carried out. From five species of green and brown seaweeds, a total of 224 bacterial strains were isolated and tested for antibiotic production. A total of 38 strains displayed antibiotic activity, and it was a higher proportion than some other marine environments (Lemose et al. 1985). Further the proportion of active

bacteria associated with marine invertebrates (20%) and seaweeds (11%) was found to be higher than that isolated from seawater (7%) and sediment (5%) in a study to explore marine organisms with medical potential using marine bacteria isolated from seawater, sediment, marine invertebrates and seaweeds collected from different coastal areas of China sea. (Zeng et al. 2005). One hundred and sixteen epibiotic bacteria were isolated from the surface of nine species of brown algae at Awaji Island, Japan. Among the bacteria isolated 20% exhibited antibacterial activity (Kanagasabhapathy et al. 2006). From the surfaces of marine algae *Delisea pulchra* and *Ulva australis* also 12% of the isolated strains showed to have antimicrobial activity (Penesyant et al. 2009). Heterotrophic aerobic bacteria species associated with coralline red alga *Jania rubens* (Northern coast of Tunisia, southern Mediterranean Sea) were isolated. 36% of the isolates were antibiotic-like producers with in vitro inhibition against Gram positive and Gram negative bacteria and the yeast *Candida albicans* (Ali et al. 2012). A *Pseudomonas* sp. was cultured which was associated with the Japanese seaweed *Digenea* sp. Crude extracts prepared from this bacterial culture were found to inhibit the growth of other marine bacterial strains. From this bacterial culture, two new peptides cyclo-[phenylalanyl-prolyl-leucylprolyl] and cyclo-[isoleucyl-prolyl-leucyl-alanyl] have been isolated together with two known peptides. None of the individual peptides isolated in this study showed antibiotic activity (Rungprom et al. 2008). Evaluation the antibacterial and anticancer activities of extracts from the seaweeds *Egregia menziesii*, *Codium fragile*, *Sargassum muticum*, *Endarachne binghamiae*, *Centroceras clavulatum* and *Laurencia pacifica* collected from Todos Santos Bay, México. Organic extracts were obtained from bacteria-free algae and from surface-associated bacteria. The strains Cc51 isolated from *Centroceras clavulatum*, Sm36 isolated from *Sargassum muticum*, and Eb46 isolated from *Endarachne binghamiae* showed anticancer activity. Likewise, the extracts from the seaweed and its associated bacteria inhibited the growth of the Gram negative bacterium *Proteus mirabilis* (Gomez et al. 2010).

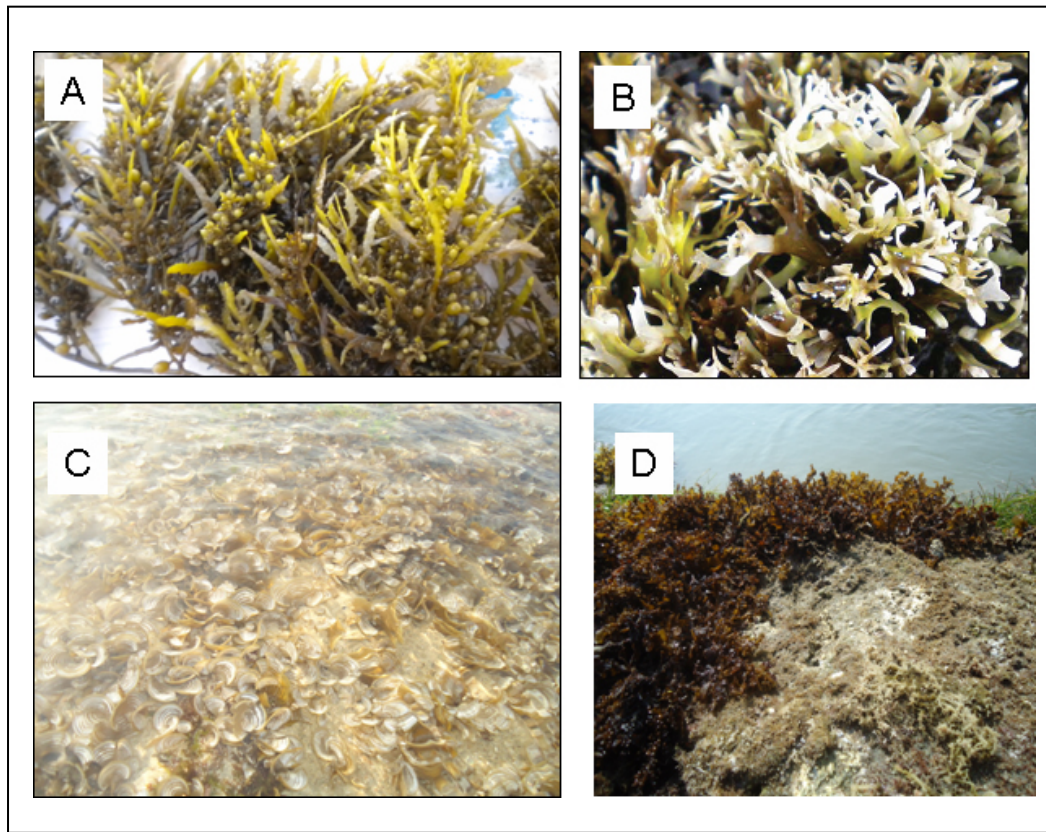


Figure 2.10

Different seaweed species (A) *Sargassum* sp; (B) *Gracillaria* sp,(C) *Padina* sp., (D) A seaweed collection site

2.8.2 Protective role of seaweed associated bacteria against fouling

Antifouling chemical defenses have long been acknowledged as a protection mechanism for marine organism (Pereira et al. 2011). The protective role of bacteria associated with seaweed surfaces was also proposed in the study. These strains were isolated from macroalgae using a variety of substrates including low-nutrient agars and were found to inhibit the pathogenic strains (Boyd et al. 1998). Associated bacteria isolated from *Ulva lactuca* samples collected from the intertidal zones of Laucala Bay, Suva, Fiji were tested for their antibacterial and anti-diatom properties that may regulate surface colonization on the algae. Sixty percent of the epiphytic isolates expressed antibacterial properties against other resident bacteria and 80% had anti-diatom activity against the pennate diatom, *Cylindrotheca fusiformis* (Kumar et al. 2011).

2.8.3 Seaweed associated bacteria against fish pathogens

The activity of seaweed-associated antibiotic-producing marine bacteria was assayed against bacterial fish pathogens belonging to the genera *Vibrio*, *Aeromonas*, *Pasteurella*, *Edwardsiella*, *Yersinia* and *Pseudomonas* and proposed the possible use of these marine strains for controlling epizootics in aquaculture. Inhibition tests on solid medium showed that, in general, the majority of fish bacteria were strongly sensitive to the marine bacteria and the production of antibiotics give these marine strains ;in antagonistic capacity against most of the fish pathogenic bacteria. (Dopazo et al. 1989). This might explain why the seaweeds are rarely been infected. Further the production of inhibitory substances could play a significant role in competition phenomena in some concrete microhabitats, such as those that can be formed on algal surfaces, where these producer strains are relatively common was proposed (Lemose et al. 1985).

2.9 Seaweed associated bacterial as a source of antimicrobial compounds

Due to a competitive role for space and nutrient, the marine bacteria associated with marine macroorganisms, invertebrates and seaweeds could produce more antibiotic substances. These marine bacteria were expected to be potential resources of natural antibiotic products (Zeng 2005).

Seaweed associated bacteria are able to produce antimicrobial compounds and this response represents a chemically induced defense response when the antibiotic producer strain is faced with a potential competing organism in the marine environment. Over 400 strains of surface-associated bacteria from various species of seaweed and invertebrate from Scottish coastal waters were isolated and 35% of them shown to produce antimicrobial compounds. This is a much higher proportion than free living marine isolates or soil bacteria (Burgess et al. 1999).

Haliangicin, is a the novel antifungal polyunsaturated antibiotic with a β methoxyacrylate moiety produced by a marine myxobacterial strain AJ-13395 was isolated from a seaweed sample collected at a sandy beach in the Miura Peninsula,

Kanagawa, Japan. The strain was tentatively named as *Haliangium luteum* (Fudou et al. 2001)

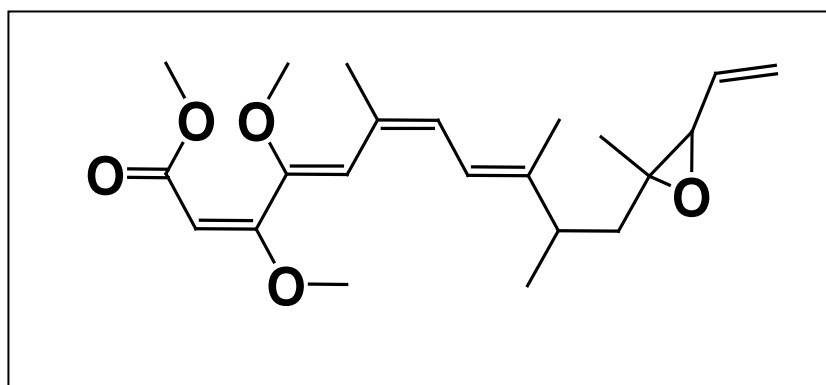


Figure 2.11
Chemical structure of haliangicin

Recent research progresses reported that many bioactive natural products from seaweeds have striking similarities to metabolites of microorganisms (Kubaneck 2003; Goecke et al. 2010). Using bioassay guided fractionation, a 22-membered cyclic lactone, lobophorolide, of presumed polyketide origin, with activity against pathogenic and saprophytic marine fungi was isolated and characterized. Lobophorolide is structurally unprecedented, yet parts of the molecule are related to tolytoxin, the scytophycins, and the swinholides, macrolides previously isolated from terrestrial cyanobacteria and from marine sponges and gastropods. Because of the low yield of the compound, its structural similarity to microbial metabolites, and the fact that polyketides of this type are unprecedented from seaweeds, a microbial origin warrants further exploration. This suggests seaweeds use targeted antimicrobial chemical defense strategies and that secondary metabolites important in the ecological interactions between marine macroorganisms and microorganisms could be a promising source of novel bioactive compounds.

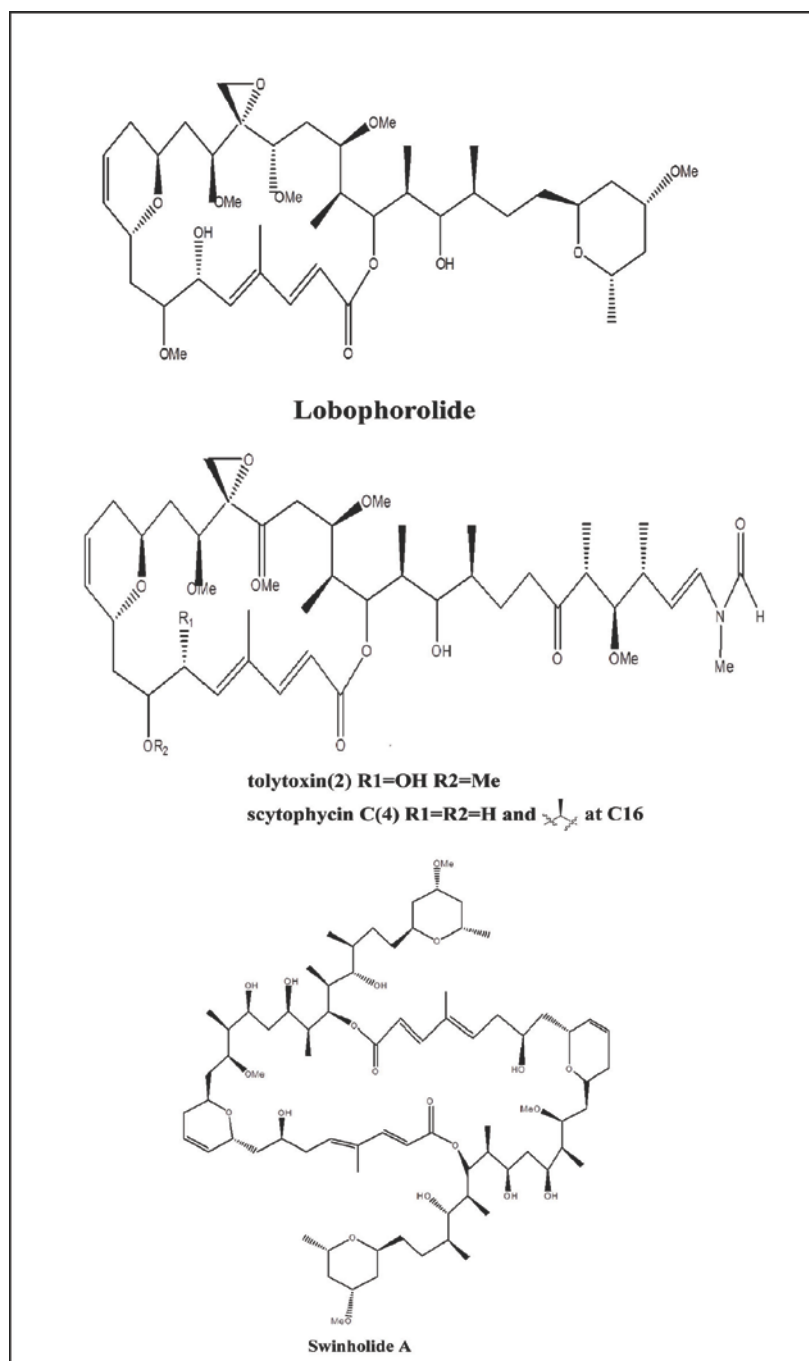


Figure 2.12

Chemical structure of lobophorolide and related macrolides

Many seaweed associated bacteria have been reported as a source of antibacterial compounds. A few interesting studies have been presented on associates of seaweeds, but a detailed knowledge of the interaction of seaweeds with their associated microbes and among microbes on algal surfaces and tissues is

still lacking (Goecke et al. 2010). Although examples are rare (Giltunes 1989; Kubaneck 2003; Aassila et al. 2003), the symbionts may be an important source of antimicrobial chemical defenses for plants and animals. Thus it is important to highlight the possible role of seaweed associated bacteria in the production of bioactive compounds of the seaweeds.

2.10 Diversity of seaweed associated antibiotic producers

From the surfaces of seaweeds *Delisea pulchra* and *Ulva australis*, the majority of the isolates with antimicrobial activity were found belonged to be α and γ -proteobacteria. Other antimicrobial isolates obtained in this study belonged to the phyla Actinobacteria, Firmicutes and Bacteroidetes (Penesyan et al. 2009). The seaweeds from the coastal area of the Autonomous University of Baja California (UABC) Ensenada, BC, México was found to harbor bioactive isolates that could be classified within three main phyla *Actinobacteria*, *Proteobacteria* and *Firmicutes* (Gomez et al. 2010). From *Ulva lactuca* surface associated bacteria with antibacterial and antidiatom activity showed that the strains were belonged to readily culturable genera, including *Pseudoalteromonas*, *Vibrio*, *Shewanella* and *Bacillus* (Kumar et al. 2011). The surface-associated community of the *Jania rubens* with antibacterial activity were α and γ -proteobacteria, Bacteroidetes and Firmicutes. Results demonstrated that Proteobacteria (about 73%) constitute the majority of bacterial cells, bacteroidetes representing 21% and only one strain was found assigned to the Firmicutes and was identified as closely related to *Bacillus* (Benali et al. 2012). Marine bacteria in particular, antibiotic production has been reported in *Actinomyces*, *Aeromonas*, *Alcaligenes*, 'Alginovibrio', *Alteromonas*, *Bacillus*, *Chromobacterium*, *Flavobacterium*, *Micrococcus*, *Serratia*, *Streptomyces* and *Vibrio* (Austin 1989). In a study of antibacterial activities of marine epibiotic bacteria isolated from brown algae of Japan, all the strains with antibacterial activity isolated were found to be from *Bacillus* (Bacillaceae family) (Kanagasabavathy et al. 2006). Burgess et al. (2003) isolated bacteria with antifouling activity belonged to the genus *Bacillus*, such as *B. pumilus*, *B. licheniformis*, and *B. subtilis*.



Figure 2.13
Collection site of seaweeds at Gulf of Mannar region
of South East coast of India

2.11 Antibiotic Compounds from *Bacillus*: Why are they so amazing?

The recent advances in genome sequencing highlighted the genus *Bacillus* as an unexpected source of antibiotic-like compounds. *Bacillus* sp is known to produce bacteriocin, polyketides and non-ribosomal peptides. *Bacillus* sp were also found able to synthesize others unusual antibiotic peptides, such as, rhizotocins (Fickers 2012). Gramicidin and tyrocidine hydrochloride have been prepared in crystalline form from cultures of an aerobic sporulating *Bacillus brevis* (Hotchkiss and Renti 1941). The production of bacillibactin-related siderophores seems a common characteristic for this family, since the *dhb* cluster is present in nine published genomes (Donadio et al. 2007). To date, it is estimated that only a small fraction of the antimicrobial molecules potentially produced by Gram-positive bacteria has been identified. Research to discover these compounds are sure to be ongoing for many more years (Fickers 2012). All the complete genome sequences of members of this genus contain TMS genes, with the exception of *B. halodurans* C-125 (Donadio et al. 2007). Several strains belonging to the genus *Bacillus* and particularly to the *B. subtilis* and *B. amyloliquefaciens* species were reported to be effective for the biocontrol of multiple plant diseases (Arias et al. 2009). A new 24-membered ring lactone named macrolactin S, along with the known compound

macrolactin B, has been isolated from the mycelium of liquid fermentation cultures of *Bacillus* sp. AT28. The structure of macrolactin S was determined on the basis of MS and NMR data. Macrolactin S showed a dose dependent inhibition of *Staphylococcus aureus* FabG. Also macrolactin S was reported to inhibit the growth of *S. aureus*, *Bacillus subtilis*, and *Escherichia coli* (Sohn et al. 2008)

The *Bacillus subtilis* is considered as the model system for Gram-positive organisms, was demonstrated to produce more than two dozen antibiotics with an amazing variety of structures. The produced anti-microbial bioactive compounds included peptides in predominance that are either ribosomally synthesized and post-translationally modified (lantibiotics and lantibiotic-like peptides) or non-ribosomally generated, as well as a couple of non-peptidic compounds such as polyketides, an aminosugar, and a phospholipid (Stein 2005). Difficidin and oxydifficidin were reported to be two novel macrocyclic polyene lactone phosphate esters that were discovered in the fermentation broths of each of two strains of *Bacillus subtilis* ATCC 39320 and *B. subtilis* ATCC 39374. Difficidin and oxydifficidin showed a broad spectrum of activity against aerobic and anaerobic bacteria (Zimmerman et al. 1986).

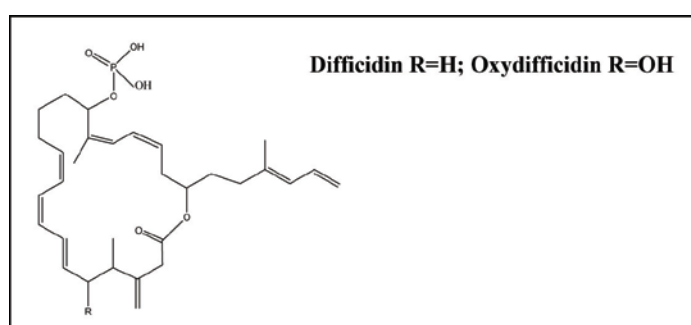


Figure 2.14
Difficidin and oxydifficidin (macrocyclic polyene lactone phosphate esters) from *Bacillus subtilis* ATCC 39320 and *B. subtilis* ATCC 39374, respectively.

Bacillaene, a novel polyene antibiotic, was discovered and isolated from the fermentation broths of *Bacillus subtilis*. The novel antibiotic has a nominal molecular weight of 580 and an empirical formula of $C_{35}H_{48}O_7$. Bacillaene is active against a broad spectrum of bacteria in agar-plate diffusion assays. In vitro studies indicate that the antibiotic inhibited prokaryotic protein synthesis but not

eukaryotic protein synthesis. Cell survival studies performed with strains of *Escherichia coli* indicated that the antibiotic is a bacteriostatic agent (Pattel et al. 1995).

B. subtilis strain 168 has long been a model system for prokaryote differentiation and was the first sequenced Gram positive. The sequenced *B. subtilis* strain was reported to an inactive allele of the PPTase gene *sfp* (Donadio et al. 2007). This strain is therefore unable to convert TMS enzymes into the active holoforms and unable to produce polyketides. In addition to the bacillibactin 4 cluster, this strain contains three TMS clusters, some of which direct the synthesis of compounds known in other *B. subtilis* strains: the *pps* operon encodes five NRPSs, and is responsible for the synthesis of the lipodecapeptide, plipastatin, the *srf* cluster consists of three NRPS genes and directs formation of the lipopeptide surfactin; the *pks* cluster consists of nine *pks* genes, and probably directs the synthesis of bacillaene or difficidin, produced by the related strain (Donadio et al. 2007).

The genome of plant-associated *Bacillus amyloliquefaciens* FZB42 harbors an array of giant gene clusters involved in synthesis of lipopeptides and polyketides with antifungal, antibacterial and nematocidal activity. The gene clusters were shown to direct synthesis of the cyclic lipopeptides surfactin, bacillomycin, fengycin, an unknown peptide, and the iron-siderophore bacillibactin. In addition, one gene cluster encoding enzymes involved in synthesis and export of the antibacterial dipeptide bacilysin is also functional in FZB42. Three gene clusters were shown to direct synthesis of the antibacterial acting polyketides macrolactin, bacillaene, and difficidin. In total, FZB 42 dedicates 8.5% of its total genetic capacity, to synthesis of secondary metabolites. On the contrary, genes involved in ribosome-dependent synthesis of lantibiotics and other peptides are scarce (Chen et al. 2009).

B. amyloliquefaciens strain GA1 (formerly *B. subtilis* GA1, Table 2.2) was demonstrated to display high *in vitro* inhibitory activity towards growth of multiple fungal and oomycete plant pathogens (Arguelles-Arias et al. 2009).

Table 2.2

Metabolite production of *B. amyloliquefaciens* GA1 detected by HPLC-ESI mass spectrometry (Arguelles-Arias et al. 2009)

Metabolite	Observed mass peak	Assignment	Reference
Surfactin	1030.8, 1046.8 [M+Na, K] ⁺	C13-surfactin	[Ongena 2008]
	1044.8, 1060.8 [M+Na, K] ⁺	C14-surfactin	[Ongena 2008]
	1058.8, 1074.8 [M+Na, K] ⁺	C15-surfactin	[Ongena 2008]
Fengycin	1471.9, 1487.9 [M+Na, K] ⁺	Ala-6 C15-fengycin	[Ongena 2008]
	1485.9, 1501.9 [M+Na, K] ⁺	Ala-6 C16-fengycin	[Ongena 2008]
	1499.9, 1515.9 [M+Na, K] ⁺	Ala-6 C17-fengycin	[Ongena 2008]
	1513.9, 1529.9 [M+Na, K] ⁺	Val-6 C16-fengycin	[Ongena 2008]
	1527.8, 1543.8 [M+Na, K] ⁺	Val-6 C17-fengycin	[Ongena 2008]
Iturin A	1066.1 [M+Na] ⁺	C14-iturin A	[Ongena 2008]
	1079.7 [M+Na] ⁺	C15-iturin A	[Ongena 2008]
Macrolactin	425.4 [M+Na] ⁺	Macrolactin A	[Schneider K 2007]
	511.4 [M+Na] ⁺	7-o-malonyl macrolactin A	[Schneider K 2007]
	525.4 [M+Na] ⁺	7-o-succinyl macrolactin A	[Schneider K 2007]
	629.3 [M+H-H ₂ O] ⁺	Macrolactin D	[Schneider K 2007]
Difficidin	559.2 [M-H] ⁻	Oxydifficidin	[Chen X 2006]
Bacillaene	583.5 [M+H] ⁺	Bacillaene A	[Chen X 2006]
	605.5 [M+Na] ⁺	Bacillaene B	[Chen X 2006]
Chlorotetaine	289.2 [M+H] ⁺	Chlorotetaine (³⁵ Cl)	[Rapp C, 1988]
	291.1 [M+H] ⁺	Chlorotetaine (³⁷ Cl)	[Rapp C 1988]

2.12 Functional genes related to the antimicrobial activity of the seaweed associated bacteria

Microorganisms usually carry all the relevant genes in a contiguous DNA segment known as a gene cluster. With the help of chemistry-driven studies, the genes participated in the synthesis of known natural products were characterized. The data obtained have confirmed that the biosynthesis of a large number of natural products requires the participation of sophisticated molecular machines

known as polyketide synthases (PKS) and nonribosomal peptide synthetases (NRPS) (Donadio et al, 2007). Moreover, the structural characteristics of marine natural products have revealed that they mainly belong to two important chemical families, namely, polyketides and cyclopeptides, and are synthesized by multifunctional enzymes called polyketide synthases (PKSs) and nonribosomal peptide synthases (NRPSs) (Peng et al. 2009). PKSs and NRPSs are key players in the synthesis of natural products, since they carry out the oligomerization of small building blocks into often complex structures. Both systems are molecular assembly lines that direct product formation on a protein template by maintaining reaction intermediates covalently bound as thioesters on the same phosphopantetheine prosthetic group. Usually, a 4 phosphopantetheinyltransferase (PPTase) specific for modular enzymes modifies an active site serine residue in the thiolation (T) and acyl carrier protein (ACP) domains of NRPSs and PKSs, respectively, to generate the corresponding holoenzymes. Each monomer is handled by a separate set of enzymatic domains known as a module, and usually there are as many modules as monomers incorporated in the final product. For these reasons, PKSs and NRPSs are thio-template modular systems (TMS) or TMS genes (Donadio et al. 2007).

NRPSs use amino or hydroxy acids as building blocks, catalyzing the formation of amide or ester bonds, respectively. Each *nrps* module consists of three core domains: an adenylation (A) domain, which select the cognate amino acid, activates it as an amino acyl adenylate and transfers it to the T domain (also known as peptidyl carrier protein, or PCP) where a thioester bond is formed, a condensation (C) domain, responsible for peptide bond formation between the amino acid present on the T domain of the same module and the peptidyl intermediate bound to the T domain of the preceding module, and the T domain itself. Usually, all elongation modules present these core domains. A dedicated loading module (carrying just A and T domains) and a termination module, containing a thioesterase (TE) domain, usually complete the *nrps* assembly line. Additional reactions may be carried out by specialized domains within a module, such as amino acid epimerization (E), methylation (M) and reduction (R) activities. Additional variations include the presence of a heterocyclization domain (Cy) in

place of a C domain, or the occurrence of C domains capable of epimerization (Donadio et al. 2007).

Polyketides constitute one of the major classes of natural products. Many of these compounds or derivatives thereof have become important therapeutics for clinical use; in contrast, various polyketides are infamous food-spoiling toxins or virulence factors, comprising of polyethers, polyenes, polyphenols, macrolides, and enediynes. They are mainly derived from one of the simplest building blocks available in nature: acetic acid (Hertweck 2009). Bacterial type I polyketide synthases (PKSs) produce a wide range of biomedically important secondary metabolites. These enzymes possess a modular structure that can be genetically re-engineered to yield novel drug candidates not found in nature (Piel et al. 2003).

On the basis of the architecture and mode of action of the enzymatic assembly lines, PKSs are classified into various types (Table 2.3). As in FAS nomenclature, type I refers to linearly arranged and covalently fused catalytic domains within large multifunctional enzymes, whereas the term type II indicates a dissociable complex of discrete and usually monofunctional enzymes. Furthermore, a third group of multifunctional enzymes of the chalcone synthase type is denoted as type III PKSs. Apart from the structures of the enzymes or enzyme complexes, the PKSs are also categorized as iterative or noniterative, that is, whether or not each KS domain catalyzes more than one round of elongation acid (Hertweck 2009).

Table 2.3

Survey of the types of PKSs.

PKS type	Building blocks	Organisms
Modular type I (non-iterative); subtypes: cis-AT, trans-AT	ACP, various extender units; (in situ methylation possible)	Bacteria, Protist

Iterative type I subtypes: NR-, PR-, HR-PKS	ACP, only malonyl-CoA extenders (in situ methylation possible)	Mainly fungi, some bacteria
(Iterative) type II	ACP, only malonyl-CoA extenders	Exclusively bacteria
(Iterative) type III	Acyl-CoA, only malonyl-CoA extenders	Mainly plants, some bacteria and fungi
PKS-NRPS hybrid	ACP, malonyl-CoA, amino acids	Bacteria (modular) fungi (iterative)

The type I polyketide synthases are a diverse group of multifunctional enzymes. They contain the activities required to complete a cycle of β -keto acyl chain elongations. Within the type I classification, there are two subgroups dividing the synthases by enzymatic activity and the type of host organism i.e. modular polyketides and iterative synthases. The most common types of enzyme domains used in the type I synthases are ketoacyl synthase (KS), acyl transferase (AT), ketoreductase (KR), dehydratase (DH), enoyl reductase (ER), and thioesterases (TE). Minimal modules contain the KS, AT, and the acyl carrier protein (ACP). This group is responsible for lengthening of the polyketide through the addition of acyl groups. The chains are then reduced using KR, DH, and ER. The polyketide is released from the PKS by a thioesterase, by hydrolysis or macrolactonization (Castoe 2007).

2.13 Conclusions

The ability of marine microorganisms to produce novel antimicrobial compounds has been well demonstrated, and apparently they have a future role in the fight against antibiotic-resistant pathogens. Ongoing research efforts to isolate and screen new marine microorganism species should be accompanied by efforts to understand their ecology. Extensive culture-dependent and culture -independent surveys of marine microorganisms are a prioritized research area to determine the

extent to which marine diversity differs. The isolation of seawater-obligate and symbiotic microorganisms has proved that marine adaptation has occurred in this lineage, but so far this property has only been identified at the genus and species level, an indication that marine adaptation is a comparatively recent evolutionary event. If such adaptation is rare within the microorganisms, it is reasonable to expect that seawater-obligate strains will represent species that have no terrestrial counterparts, and thus they are unlikely to have been previously screened for antimicrobial compounds. This raises the intriguing possibility that there are antimicrobial compounds unique to marine species. Genomic analysis of the marine microbial flora indicates the differences in secondary metabolite biosynthetic genes may be a driver of speciation, supporting the hypothesis that the marine microbial species will produce new compounds. Finally, if antimicrobial compounds are to make it from the ocean to the clinic, big pharma must re-engage in drug discovery from microbes. Currently, small pharmaceutical and biotechnology companies have been, or are currently engaged in antimicrobial lead molecule discovery from marine microorganisms.

CHAPTER 3

ISOLATION OF ANTAGONISTIC BACTERIAL FLORA ASSOCIATED WITH SEAWEEDS

3.1 Background

Bacteria with inhibitory characteristics exist symbiotically on the seaweed surface, providing it with a microbial-mediated defense community. Macroalgae (seaweeds) and their associated bacteria have been studied over a hundred years. It has been shown that these chemically mediated interactions are based on the exchange of nutrients, minerals, and secondary metabolites, the diversity and specificity of macroalgal–bacterial relationships have not been thoroughly investigated (Hollants et al. 2012). Seaweeds are potential sources of high biotechnological interest due to the production of a great diversity of compounds exhibiting a broad spectrum of biological activities. More than 2500 secondary metabolites have been isolated from seaweeds (Chakraborty et al. 2008). But still it's a puzzle whether the bacteria or the seaweed is the actual producer (Kubaneck et al. 2003)? Although examples are rare (Kubaneck et al. 2003), it is believed that marine eukaryotes may use their surface-associated bacteria as a source of antimicrobial chemical defenses in competition and in protection of the host (Penesyan et al. 2009). Investigations of seaweed–bacterial associations lag behind these of other marine eukaryotes (Goecke et al. 2010; Hollants et al. 2012). Seaweed–bacterial associations are appealing from evolutionary, ecological, and applied perspectives and there is a strong need to integrate the aspects of different biological disciplines, such as, microbiology, phycology, ecology, and chemistry in future macroalgal–bacterial studies (Hollants et al. 2012). Hence the objective of the present study was to assess the diversity of cultivable antagonistic heterotrophic bacterial communities associated with seven species of intertidal seaweeds present at the Gulf of

Mannar region in the south-east coast of India and to explore them as a source for potentially useful antimicrobial substances. The present chapter describes the isolation of the antagonistic isolates, their preservation and identification as a primary step to precede the further work.

3.2 Materials and Methods

3.2.1 Seaweed sample collection

Intertidal seaweeds belonging to *Phaeophyceae* and *Rhodophyceae* were collected by scuba diving from the intertidal zone of Mandapam situated at 9° 17' 0" North, 79° 7' 0" East, Gulf of Mannar region in South-East coast of India. The brown seaweeds collected were *Anthophycus longifolius*, *Sargassum myriocystum*, *Padina gymnospora*, *Turbinaria ornata* and *Dictyota dichotoma*, whereas red seaweeds were *Hypnea valentiae* and *Laurencia papillosa* (Figure 3.1). Seaweed samples were placed in a sterile polythene bag filled with seawater. Samples were kept in the dark at 4°C until subsequent processing in the laboratory.



Figure 3.1

Indicative pictures showing (A) sample collection site (B) *Padina gymnospora* (C) *Sargassum myriocystum* (D) *Sargassum wightii*

3.2.2 Isolation of seaweed-associated bacteria

Specimens of seaweed samples were thoroughly washed with the sterile seawater for three times to remove loosely attached bacteria from the surface. Seaweed samples were processed and the associated bacterial strains were isolated by a modified protocols as reported in earlier studies (Wiese et al. 2009; Wilson et al. 2010; Kanagasabhapathy et al. 2006; Lemose et al.1985; Ali et al. 2012, Penesyany et al. 2009). Briefly for isolation of seaweed-associated bacteria the specimen samples (10 g) were suspended in sterile seawater (10 mL) and homogenized using a pestle and mortar in a laminar airflow hood aseptically. The suspension was serially diluted in sterile seawater (9 mL), and different dilutions were plated on isolation media organized. Isolation media used involved Nutrient agar supplemented with sodium chloride (NA, NaCl, and 1% w/v), Zobell marine agar (ZMA), Seawater agar (SWA) and Nutrient agar (half strength). Incubation was performed in the dark at 30°C for 7 days. Pure cultures were obtained by several subsequent isolation and purification steps on Nutrient agar medium supplemented with sodium chloride (NA, NaCl, 1% w/v)

3.2.3 Purification of seaweed-associated bacterial isolates

3.2.3.1 The streak-plate method for isolation of pure cultures

In microbiology, a prerequisite to the characterization of a microbial species is that it be available for study as a pure culture. The term pure culture denotes that all the cells in the culture had a common origin and are simply descendants of the same cell. In the current study, streak plate method has been used to isolate an axenic culture. Samples can then be taken from the resulting colonies and a microbiological culture can be grown on a new plate so that the organism can be identified, studied, or tested (Pelczar and Chan 1977).

Quadrant Streak Method The solidified agar plates were marked into four quadrants. Inoculation loop was sterilized on a flame and cooled, then remove one colony from the mixed culture by the loop and streak the first quadrant. The loop was

flame sterilized and cooled to repeat the procedure. The culture was dragged from the second quadrant back into the first quadrant three times and streaked the second quadrant. The loop was sterilized again as stated earlier, and cooled before being streak the third quadrant. The loop was again sterilized and dragged from the fourth quadrant into the third quadrant one time and then streaked the fourth quadrant with one wavy line. The agar plate was labeled and incubated. (dedicated website: <http://www.drcarman.info/bio2511b/09lab251.pdf> ; Pelczar and Chan 1977).

3.2.4 Pathogenic test organisms used for the study

Pathogenic organisms other than the isolates procured from culture collections were maintained, and their pathogenicities were assessed (Figure 3.2) at the Mariculture Facility of Central Marine Fisheries Research Institute. All the strains were maintained in Brain heart infusion broth supplemented seawater/NaCl as per the requirement.

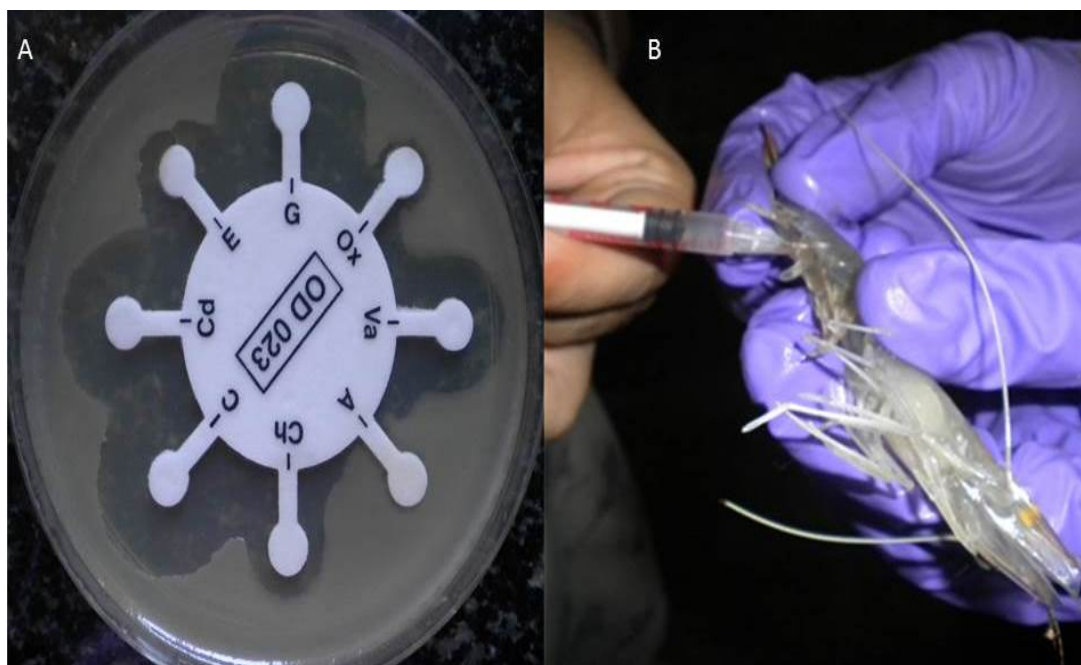


Figure 3.2

Indicative pictures showing (A) Antibiotic susceptibility testing for *A. hydrophilla* used for the study (B) Pathogen challenging via injection of the pathogenic bacteria in shrimp.

3.2.4.1 *Vibrio parahaemolyticus*

Vibrio parahaemolyticus is a Gram-negative, halophilic, non-spore forming, curved rod-shaped bacterium. Infections usually present in one of three major clinical syndromes: 60-80% of infections cause gastroenteritis, 34% wound infections, and 5% septicemia. Fatal cases of septicemia may occur in immunocompromised patients or those with a pre-existing medical condition (such as liver disease, cancer, heart disease, recent gastric surgery, antacid use, or diabetes) (Public Health Agency of Canada dedicated website: www.publichealth.gc.ca).

3.2.4.1.1 *Vibrio parahaemolyticus* (ATCC® 17802™)

Vibrio parahaemolyticus is a halophilic bacterium that occurs naturally in estuarine environments worldwide. This organism is the leading cause of seafood-associated bacterial gastroenteritis in the United States, and it is one of most important food-borne pathogens in Asia, causing approximately half of the food poisoning outbreaks in Taiwan, Japan, and South-East Asian countries. The reference strain ATCC® 17802™, was reported to be isolated from a patient with food poisoning in Japan (Fujino et al. 1965).

3.2.4.1.2 *Vibrio parahaemolyticus* MTCC451

A type strain of *Vibrio parahaemolyticus* (MTCC 451) was procured from the Microbial Type Culture Collections of the Institute of Microbial Technology (IMTECH), Chandigarh. The shrimp pathogenesis of *Vibrio parahaemolyticus* MTCC 451 is characterized, and their LD50 values have been evaluated (Ramalingam et al. 2006). Penaeid shrimp production is a worldwide economic activity, primarily important for inter-tropical developing countries. The bacterial strains responsible for vibriosis in the successive stages are usually considered to be different, and their virulence specificity has been reported both at the species level and at the stage levels.

3.2.4.2 *Vibrio vulnificus* MTCC1145

Vibrio vulnificus strain used in the current study is a fish pathogen (Kiran et al, 2010) procured from Microbial Type Culture Collection, Chandigarh (India). *Vibrio vulnificus* is infrequent cause of disease in New Zealand, but has a high associated case fatality rate. It is a marine organism (grows in 6% NaCl) that can grow both in the presence and absence of air. It causes wound infections, gastroenteritis and primary septicaemia. It is the leading cause of foodborne illnesses that result in death in Florida (www.foodsafety.govt.nz/.../Vibrio_Vulnificus-Science_Research.pdf)

3.2.4.3 *Vibrio harveyi*

Vibrio harveyi strain used in the current study is an aquaculture pathogen that has been obtained from National Institute of Fish Health, Cochin University of Science and Technology. *Vibrio harveyi* is a Gram-negative, bioluminescent, marine bacterium in the genus *Vibrio*. *V. harveyi* is rod-shaped, motile (via polar flagella), facultatively anaerobic, halophilic, and competent for both fermentative and respiratory metabolism. It does not grow below 4°C or above 35°C. *V. harveyi* can be found free-swimming in tropical marine waters, commensally in the gut microflora of marine animals, and as both a primary and opportunistic pathogen of marine animals, including Gorgonian corals, oysters, prawns, lobsters, the commonsnook, barramundi, turbot, milk fish, and seahorses. It is responsible for luminous vibriosis, a disease that affects commercially farmed penaeid prawns (dedicated website http://en.wikipedia.org/wiki/Vibrio_harveyi).

3.2.4.4 *Aeromonas hydrophilla*

Aeromonas hydrophilla strain used in the current study is an aquaculture pathogen that has been obtained from National Institute of Fish Health, Cochin University of Science and Technology. *Aeromonas hydrophilla* is a species of bacterium that is present in all freshwater environments and in brackish water. Some strains of *A. hydrophilla* are capable of causing illness in fish and amphibians as well as in humans

who may acquire infections through open wounds or by ingestion of a sufficient number of the organisms in food or water. *A. hydrophila* may cause gastroenteritis in healthy individuals or septicemia in individuals with impaired immune systems or various malignancies (dedicated website: <http://www.fda.gov/food/foodborneillnesscontaminants/causesofillnessbadbugbook/ucm070523.htm>).

3.2.4.5 *Vibrio alginolyticus*

Vibrio alginolyticus strain used in the current study is an aquaculture pathogen that was obtained from Central Marine Fisheries Research Institute, Karwar. *Vibrio alginolyticus* is a Gram-negative marine bacterium. It is medically important since it causes otitis and wound infection. It is also present in the bodies of animals such as pufferfish, where it is responsible for the production of the potent neurotoxin, tetrodotoxin (dedicated website: http://en.wikipedia.org/wiki/Vibrio_alginolyticus).

3.2.4.6 *Vibrio anguillarum*

Vibrio anguillarum strain used in the current study is an aquaculture pathogen that was obtained from Central Institute of Brackish Aquaculture, Chennai. *Vibrio anguillarum*, also known as *Listonella anguillarum*, is the causative agent of vibriosis, a deadly haemorrhagic septicaemic disease affecting various marine and fresh/brackish water fish, bivalves and crustaceans. In both aquaculture and larviculture, this disease is responsible for severe economic losses worldwide (Frans et al. 2011).

3.2.5 Screening of isolated strains for their antibacterial activity against the pathogens

For preliminary characterization of antagonistic bacteria an inhibition test on solid media was carried out by a spot over lawn assay (Figure 3.3). Briefly pathogenic bacteria were grown in their respective Nutrient broth (NB) and incubated for 18 h (10^8 CFU/ml). The OD is adjusted according to McFarland turbidity standard. About 0.1mL from the above described inoculated broth was spread over the Muller Hinton agar (MHA) plates to form a lawn of test pathogenic bacteria. To perform bioassay, the seaweed-associated isolates were simultaneously cultured on NA plates at 20°C until it

acquires a visible growth. Purified isolates (as explained under section 3.2.2 and 3.2.3) were then picked and spotted (6mm diameter) onto the agar cast with pathogens under sterile conditions. The plates were incubated at 30°C for 24–72 h. The clearing zones in the turbid growth of pathogen were scored as antibacterial activity. Measure of antagonistic activity was recorded as the diameter of inhibition zones determined as a distance of ≥ 1 mm between the circular area (=lawn of the isolate) and the end of the clear zone bounded by the lawn of the test strain (Gram et al. 2010; Lemose et al. 1985). The live cells were stained with 3-(4, 5-dimethylthiazol-2-yl)-2, 5-diphenyltetrazolium bromide (MTT) to visualize the growth inhibition around the spotted isolates.

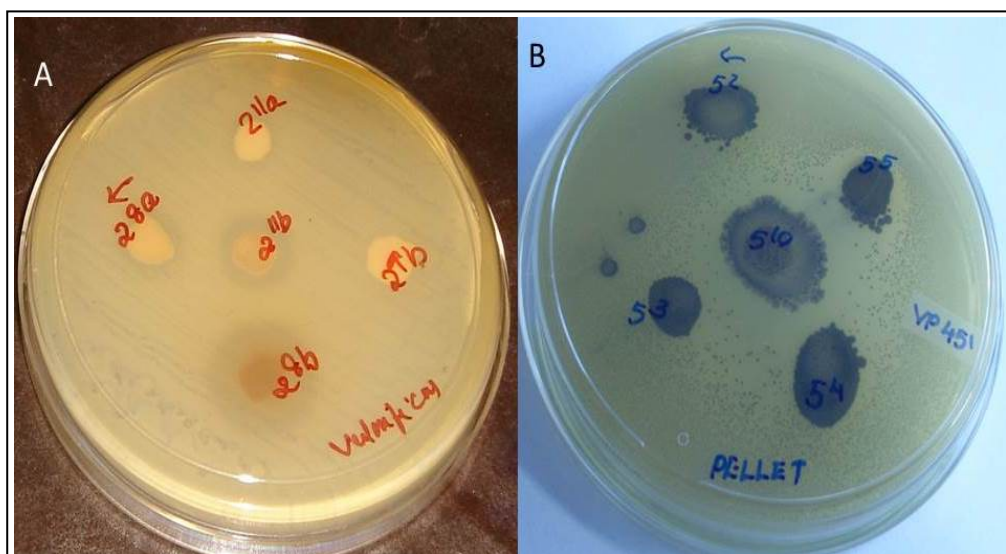


Figure 3.3

Indicative pictures showing preliminary screening (spot over lawn assay) of seaweed associated bacterial isolates (A) Bacterial isolates of brown seaweed *Dictyota dichotoma* are spotted against *V. vulnificus* (B) Bacterial isolates of brown seaweed *Anthophycus longifolium* against *V. parahaemolyticus* MTCC451. Live cells are stained in blue with MTT solution and the bactericidal zones are visualized as yellowish clear zone around the spotted seaweed associated bacterial isolates.

3.2.6 Preservation of isolated strains with antibacterial activity against the tested pathogens

Laboratory test procedures requiring the used microorganisms must be preserved in a manner that will allow for their genetic stability and long term survival. The chief methods of preservation utilized during the study were serial sub culture on agar slants, oil sealing and freeze-drying (Goldman and Green 2009; Pelczar et al. 1957).

3.2.6.1 Serial sub culture on agar slants

This is a simple method in which cultures are periodically passed in agar media in sealed tubes. It is not a satisfactory method for long term preservation due problems with contamination, culture death and unintended selection of mutants. In the current study this method was employed for routine laboratory works (Goldman and Green, 2009; Pelczar et al. 1957).

3.2.6.2 Oil sealing

Cultures can be preserved for periods greatly exceeding the viability of ordinary agar cultures by sealing them with sterile paraffin oil (Figure 3.4.A). The process prevents the moisture loss from the medium and suppresses the growth by excluding oxygen. Screw capped tubes were autoclaved with agar media, and allowed to solidify. The cultures were inoculated and incubated until the growth was visible. The oil is poured aseptically over the culture until the entire agar is covered. The oiled cultures were kept at 20°C (Goldman and Green, 2009; Pelczar et al. 1957).

3.2.6.3 Storage at low temperature

Cultures in agar plates/slants were preserved at 4 to 8°C. Agar slants/broths of the viable cultures were overlaid with 10% glycerol and stored at -80 °C (Goldman and Green, 2009; Pelczar et al. 1957).

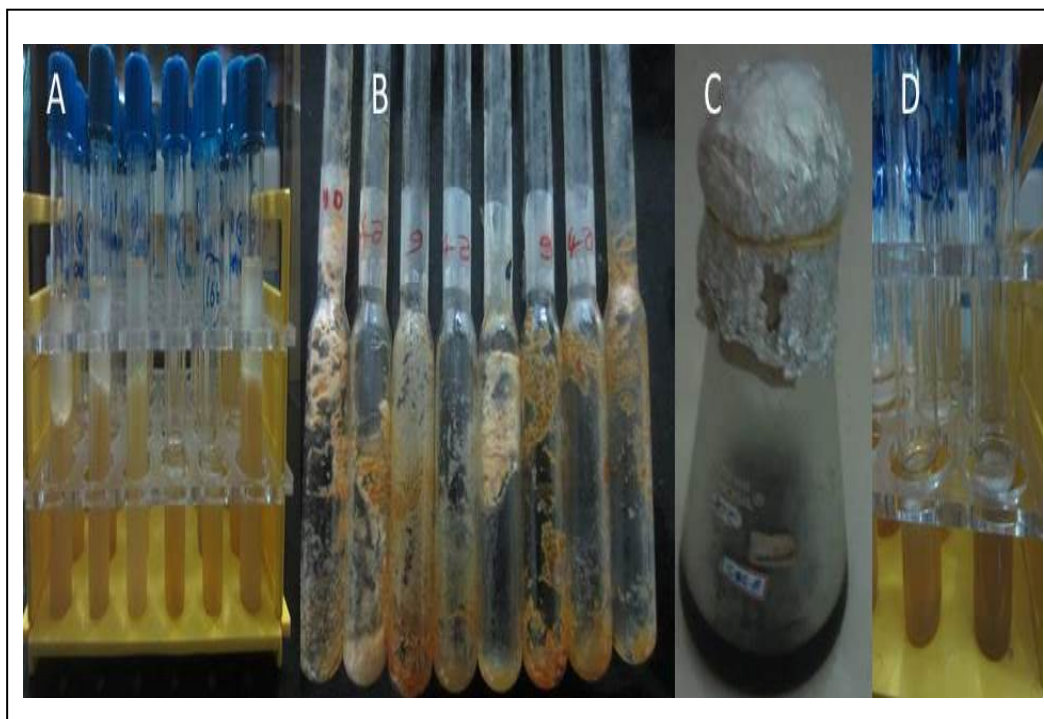


Figure 3.4

Preservation techniques used (A) Cultures preserved with oil sealing (B) Cultures preserved with Lyophilization (C) Seaweed Extract used for preservation media enrichment (D) Cultures preserved with oil sealing in Seaweed extract agar.

3.2.6.4 Preservation by lyophilization

Microorganism to be preserved was streaked on nutrient agar plate and incubated overnight to form a lawn of growth. Sterile crimp-cap vials were autoclaved ahead of time, with the caps placed loosely on top. Lyophilization buffer (4mL) was added to the plate and the cells were suspended using a sterile glass rod. The culture suspension (approximately 1.5 mL) was transferred to the sterilized vials before being sealed with the rubber cap. The culture suspension inside the vials was frozen by placing the vials in a -20 °C freezer. The freeze drier was prepared by turning it on and allowing time for the appropriate temperature and vacuum conditions to stabilize according to the manufacturer's instructions. The vial caps were placed loosely on top of the vials in an aseptic condition to escape during the freeze drying process before

being placed into the freeze drier chamber. Vacuum was applied for a time period to completely lyophilize (dry out). The samples from the freeze drier chamber were removed according to the manufacturer's instructions, was stored before being sealed. The lyophilized culture collection was stored at room temperature (Figure 3.4B) and the tubes were assessed for viability in a random manner (Desmons et al. 1998; Milanovic et al. 2001). The lyophilization buffer used was a mixture of 10% skimmed milk in 5% glycerol and 0.1% CaCO₃, which was prepared aseptically.

3.2.6.5 Preservation using Seaweed Extract Agar

Seaweed Extract agar was prepared by agitating seaweed in autoclaved water for 12 hours before being centrifuged to obtain the aqueous extract (Figure 3.4.C). The extract was lyophilized and the lyophilized powder was used to supplement the media to afford a final concentration of 10g/L (Boyd et al. 1999). Each culture isolate was sub cultured on their respective seaweed extract media, and overlaid with paraffin oil as described under the section 3.2.6.2 (Figure 3.4.D).

3.2.7 Identification of isolated strains with antibacterial activity

3.2.7.1 Biochemical identification

Colony morphology was analyzed on agar plates and Gram staining was performed. Strains were identified by carrying out biochemical and physiological tests as described in the Bergey's Manual of Determinative Bacteriology. Conventional tests, such as motility, gas from glucose, starch hydrolysis, indole, nitrate reduction, Vogues-prosker, Citrate, gelatin hydrolysis, esculin hydrolysis, growth at various temperature and NaCl Concentration etc. were used

3.2.7.2 Molecular identification based on 16S rRNA genes

3.2.7.2.1 DNA isolation

The selected pure bacterial colonies were inoculated in Luria Bertani broth (LB) supplemented with NaCl and grown for 6-8 h in a shaking incubator. Culture pellet was collected by centrifugation (at 8000 rpm, 4°C, 10 min, Thermo Centrifuge, USA) and

DNA extraction was carried out using phenol-chloroform extraction method. The culture (1mL) was centrifuged at 10,000 rpm for 5 min. The pellet was resuspended in 180µL of glucose Tris-EDTA buffer. Lysozyme was added to a final concentration of 5mg/mL and the solution was vortexed (Spinnot, India) and incubated in ice for 10min. In to the tube, 20 µL of 10%SDS was added and incubated at room temperature (30°C). An equal volume of neutral phenol was added to the tube before being mixed by inversion. The contents of the tube were kept at room temperature for 10min before being centrifuged (10,000rpm for 10min at 4°C). The aqueous layer was collected and extracted with chloroform:isoamyl alcohol (24:1). To the mixture 1/10th volume of 3Msodium acetate was added, before being precipitated with ethanol. The DNA pellet was suspended in Tris-EDTA buffer (pH 8.0) and stored at -20°C.

3.2.7.2.2 PCR

Genomic DNA was quantified and diluted to 50-75 ng for PCR amplification using 16s rRNA primers. The primer sequences used were forward primer “AGAGTTTGATCCTGGCTCAG” and reverse primer “ACGGCTACCTTGTTACGACTT” (Weisburg et al. 1991). PCR was performed in a total volume of 25 µL containing 1x reaction buffer with MgCl₂ (Sigma), 0.25 mM of each dNTP (Fermentas), 0.5mM of each primers (Sigma), 1 ng DNA and 0.3 U Taq DNA polymerase (Sigma). The following cycling conditions were used: initial denaturation at 94°C for 5 min, followed by 30 cycles of 95°C for 1 min, 58°C for 1 min and 72°C for 2 min, with a final extension 72°C for 5 min. The molecular sizes of the amplified fragments were estimated by comparing with a 1 Kb ladder on a 1.5% (w/v) agarose gel using 1X TAE buffer at 80V. Fragments with the expected size were gel-purified using GelElute™ gel extraction kit (Sigma) following the manufacturer’s protocol and sequenced.

3.2.7.2.3 BLAST

Sequence data were deposited in GenBank and compared with existing sequences using blastn (<http://blast.ncbi.nlm.nih.gov/Blast.cgi?>) search program.

3.2.7.2.4 Phylogenetic tree construction

Sequences were aligned against reference sequences with CLUSTALW software of Bioedit program, and the aligned dataset was used as input for phylogenetic analysis program. The evolutionary history was inferred by using the Maximum Likelihood method based on the Kimura 2-parameter model (Kimura 1980), and the bootstrap analysis with 1000 replications. Evolutionary analyses were conducted in MEGA5 (Tamura et al. 2011).

3.2.7.2.5 Nucleotide Accession numbers

Partial 16S rRNA gene sequences were deposited under the Accession numbers, KC559432-KC559434; KC510279-KC510286; JX203227-JX203230

3.2.7.3 Chemotaxonomy based on analysis of fattyacid profiles

3.2.7.3.1 Analysis of cellular fatty acids

The bacterial cells were cultured on the Trypticase soy broth agar plates, and were removed from the plate by scraping the surface of the culture medium with a sterile 4 mm inoculating loop. The loop containing the live bacterial wet cells has been inserted with the cells into a clean, dry screw cap culture tube. The bacterial cells were saponified, methylated, and extracted to afford bacterial fatty acid methyl esters (BAMEs) as described previously (Zhu et al. 2005). Fatty acid methyl esters were analyzed using the standard procedure of the Microbial Identification System and compared to the fatty-acid database (Ali et al. 2009). Briefly, a saponification reagent was prepared by combining the NaOH pellets (45 grams) to the solution of deionized distilled water and methanol (HPLC grade) (150 ml each). The bacterial pellets (50 mg) were saponified with the saponification reagent (1 mL), which was taken into each of the culture tubes in the batch, and was tightly sealed. The tubes were vortexed and the sample tubes were placed into a circulating water bath at 100°C for 30 min before being cooled under the tap water. Methylation converts the fatty acids (as sodium salts) to fatty acid methyl esters, which increase the volatility of the fatty acids for the GC analysis. The tubes were uncapped in the batch, and then added with the methylation

reagent (6N HCl, 325 ml and methanol, 275 mL) (2 mL) before being heated at 80°C for 10 min, followed by cooling to room temperature. Fatty acid methyl esters (FAMES) thus prepared were removed from the acidic aqueous phase and transferred to an organic phase with a liquid-liquid extraction procedure. The tubes were uncapped and were added with 1.25 mL of the extraction solvent (*n*-hexane 200 mL and methyl tert-butyl ether 200 mL). The tubes were tightly sealed and the batches of the tubes were gently mixed for 10 min. The aqueous (lower) phase was discarded. The extract was washed and neutralized with a dilute base solution, which was added to the sample tubes to remove free fatty acids and residual reagents from the organic extract. In brief sodium hydroxide (10.8 g) was added with the deionized distilled water (900 mL) to prepare the base wash reagent solution. This reagent (3 mL) was added to each tube, tightly capped, and gently rotated end-over-end for 5 min. About two-third of the organic (upper) phase from the tube was taken by using a sterile Pasteur pipette, and was transferred to the GC sample vial for analysis (Zhu et al. 2005).

3.2.7.3.2 Gas liquid chromatography

Fatty acid profiles were evaluated on a Perkin-Elmer (USA) AutoSystem XL gas chromatograph (HP 5890 Series II) equipped with an Elite-5 (crossbond 5% diphenyl 95% dimethyl polysiloxane) capillary column (30m X 0.53mm i.d., Supelco, Bellfonte, PA) with split/splitless injector, using a flame ionization detector as described previously (Wilkinson et al. 2005). Fatty acid methyl ester mixtures were analyzed with the Microbial Identification System software (MIS) and a fatty acid identification program (MIDI; Sherlock 4.5 Microbial Identification System) (MIDI Inc., Newark, Delaware, USA) (Stead et al. 1992).

3.2.7.3.3 Reproducibility of FAME analysis

The reproducibility of FAME profiles for all the samples was determined by analyzing each isolate three times under standard conditions. For each peak in the chromatogram the coefficient of variation (standard deviation/ mean) x 100 was calculated (Mukwaya and Welch 1989). Peak area values for each fatty acid were calculated as percentages of the total peak area to eliminate the effect of inoculum size

variation. A standard procedure for the adequate structural identification of bacterial fatty acids by mass spectrometry has been followed.

3.3 Results and discussion

3.3.1 Algal samples

Algal samples collected were identified as *Sargassum myriocystum*, *Dictyota dichotoma*, *Anthophycus longifolium*, *Padina gymnospora*, *Chondrococcus hornemanii*, *Acanthophora spicifera*, *Hypnea valentiae*, *Halymenia floresia*, *Hydroclathrus clatratus*, *Jania rubens*, *Laurencia papillosa*, *Turbinaria ornatae*, *Gelidium* sp .

3.3.2 Isolation and antimicrobial screening

Seaweeds are proposed to have chemical defense strategies against targeted microorganisms (Kubaneck et al. 2003), and the significant proportion of antagonistic isolates from seaweeds further confirmed this hypothesis (Lemose et al. 1985; Burgess et al. 1999; Wiese et al. 2009). Among the total number of 234 isolates screened during isolation, 53, i.e. about 22% were found to be active against at least one test pathogen used in the preliminary screening (Figure 3.5; Table 3.1). Details of the active isolates from each algae were depicted in Table 3.1. About 9 percent of the isolates showed consistent results on further screening, and these results were found to be similar to those observed by other researchers (Burgess et al. 1999; Lemose et al. 1985). From these isolates only 23 were succeeded in overcoming further laboratory sub culturing strategies, and could withstand the activity. The antimicrobial patterns of these isolates against the pathogens used in the study have been summarized in the Table 3.2 . Reports have shown that the proportion of bacteria with inhibitory activity associated with seaweeds and invertebrates was higher than that of seawater and sediments (Zeng et al. 2005). Bacteria associated with live or inert surfaces were more likely to display antibacterial activity (Gram et al. 2010). There are several reports that compounds of the associated bacterium which assist the host in certain ways, or the bioactive compounds isolated from the host have some structural similarities to the

compounds of the microbial origin (Kubanek et al. 2003; Zhang et al. 2009). The bacterial isolates with antibiotic activities in the present study were pigmented, which further corroborate the observation of the earlier study that antibiotic producing bacteria were pigmented (Lemose et al. 1985).



Figure 3.5

Indicative pictures of the algal samples screened for antagonistic activity and their isolates. (A) Seaweed sample *Bacterial isolates of brown seaweed *Anthophycus longifolium* (5) and inset shows antibacterial activity assay of its isolates against *V.parahaemolyticus* MTCC451(5⁵ and 5¹⁰ are with inhibitory zones) (B) Seaweed sample *Halimeda sp.* and its isolates Isolate 3³ inhibiting *V.parahaemolyticus* ATCC17802*

Table 3.1
Active isolates used for preliminary screening

Seaweed host	C.F.U*	Number of Active isolates obtained in preliminary screening
<i>Sargassum myriocystum</i>	39x10 ⁴	6
<i>Dictyota dichotoma</i>	32x10 ⁴	6
<i>Anthophycus longifolium</i>	46x10 ⁴	5
<i>Padina gymnospora</i>	44x10 ⁴	3
<i>Chondrococcus hornemanii</i>	42x10 ⁴	6
<i>Acanthophora spicifera</i>	40x10 ⁴	4
<i>Hypnea valentiae</i>	71x10 ⁴	4
<i>Halymenia floresia</i>	32x10 ⁵	2
<i>Hydroclathrus clatratus</i>	31x10 ⁴	5
<i>Jania rubens</i>	76x10 ⁴	3
<i>Laurencia papillosa</i>	47x10 ⁵	6
<i>Turbinaria ornatae</i>	18x10 ⁵	3

* Colony forming units

Table 3.2
Antimicrobial spectrum of candidate strains

Strains	Seaweed host	Seaweed-associated strains	Antimicrobial activity (mm) against test pathogens						
			<i>V. parahaemolyticus</i> ATCC® 17802™	<i>V. parahaemolyticus</i> MTCC 451	<i>V. vulnificus</i> MTCC 1145	<i>A. hydrophila</i>	<i>V. harveyi</i>	<i>V. anguillarum</i>	<i>V. alginolyticus</i>
SW1 1	<i>Anthophycus longifolium</i>	<i>B. cereus</i> MTCC 10404	17±1.00	17±1.00	12±2.50	12±1.00	8±1.15	ND	ND
SW1 2	<i>Anthophycus longifolium</i>	<i>B. subtilis</i> MTCC 10403	20±2.00	22±2.50	17±0.20	13±1.00	14±1.53	12±2.00	14±1.50
SW1 3	<i>Padina gymnospora</i>	<i>B. subtilis</i> MTCC 10403 ^B	15±1.15	17±1.50	22±1.50	12±2.00	15±1.00	11.3±1.20	15±1.00
SW1 4A	<i>Laurencia papillosa</i>	<i>B. subtilis</i> MTCC 10402	13±1.15	15±1.20	18±1.50	14±1.00	13±1.15	11.3±1.20	13±1.20
SW1 4B	<i>Laurencia papillosa</i>	<i>B. amyloliquefaciens</i> MTCC 10456 ^C	16±1.53	14±1.50	18±1.00	15±3.00	ND	ND	ND
SW1 5	<i>Turbinaria ornata</i>	<i>B. amyloliquefaciens</i> MTCC 10456	18±1.15	14±0.60	16±1.00	14±2.00	14±0.58	12.3±0.60	13±1.20
SW1 6	<i>Hypnea valentiae</i>	<i>B. amyloliquefaciens</i> MTCC 10456 ^D	14±0.58	15±1.00	18±0.60	14±0.00	13±0.58	11.3±1.20	14±0.60
SW1 7	<i>Padina gymnospora</i>	<i>B. amyloliquefaciens</i> MTCC 10456 ^B	19±1.53	16±0.60	17±1.00	12±1.00	12±2.00	11.3±1.20	9.7±0.60
SW1 8	<i>Laurencia papillosa</i>	<i>B. subtilis</i> MTCC 10407 ^B	5±2.08	12±0.60	16±1.00	2±2.00	ND	ND	ND
SW1 9	<i>Hypnea valentiae</i>	<i>S. algae</i> MTCC 10455 ^B	17±5.03	16±0.60	22±3.00	ND	18±0.58	ND	ND
SW1 10	<i>Laurencia papillosa</i>	<i>S. algae</i> MTCC 10609	14±3.21	14±1.00	24±3.20	ND	ND	ND	ND
SW1 11	<i>Padina gymnospora</i>	<i>S. algae</i> MTCC 10608	19±2.65	5±0.60	21±2.10	ND	15±0.58	ND	ND
SW1 12	<i>Hypnea valentiae</i>	<i>S. algae</i> MTCC 10455	19±2.00	ND	17±1.50	ND	ND	ND	ND
SW1 12B	<i>Hypnea valentiae</i>	<i>V. alginolyticus</i> [*]	ND	ND	12±2.00	ND	3±0.58	4.67±0.60	ND
SW1 13	<i>Padina gymnospora</i>	<i>S. algae</i> MTCC 10609 ^B	17±1.15	ND	ND	ND	20±1.53	ND	ND
SW1 14	<i>Anthophycus longifolium</i>	<i>S. algae</i> MTCC 10608 ^B	17±0.58	5±0.60	11±1.20	ND	21±1.15	ND	ND
SW1 16A	<i>Anthophycus longifolium</i>	<i>B. subtilis</i> MTCC 10407	17±1.15	14±1.50	ND	12±2.00	ND	ND	ND
SW1 16B	<i>Anthophycus longifolium</i>	<i>B. subtilis</i> MTCC 10402 ^B	15±1.53	13±1.20	16±1.20	12±2.00	14±0.58	11.3±1.20	12±2.10
SW1 17	<i>Dictyota dichotoma</i>	<i>S. algae</i> MTCC 10609 ^C	19±2.08	ND	17±1.00	ND	10±0.58	8.67±0.60	ND
SW1 18	<i>Dictyota dichotoma</i>	<i>S. algae</i> MTCC 10608 ^C	14±2.00	ND	13±1.20	ND	5±0.58	ND	2.3±0.60
SW1 19	<i>Sargassum myriocystum</i>	<i>B. subtilis</i> MTCC 10407 ^C	17±0.58	11±0.60	17±1.00	11±1.00	16±0.58	11±1	11±1.20
SW1 20	<i>Laurencia papillosa</i>	<i>Vibrio</i> sp [*]	ND	ND	13±1.00	ND	ND	ND	ND
SW1 21	<i>Laurencia papillosa</i>	<i>P. putida</i> MTCC 10458	ND	ND	12±2.00	ND	4±0.58	2.67±0.60	ND

3.3.3 Preservation of candidate strains

It is known that several epiphytic bacteria lose their ability to produce antimicrobial compounds after many subcultures on artificial growth media (Ali et al, 2012). In the present study we also faced the problem on repeated sub culturing on agar slants (3.2.6.1) and low temperature freezing (3.2.6.3). However the cultures preserved on seaweed extract agar could retain the activity for a longer time (more than 3 years) and we could preserve it for a longer period by overlaying with mineral oil at 20° C in an incubator giving the identical inhibitory pattern against the growth of pathogens. This might be because of the fact that marine surface associated microorganisms might require conditions that resemble their native environment in order to produce the maximum amount of bioactives, as mentioned by Penesyana et al. (2010). Ali et al. (2012) reported that the decrease of activity for bacterial culture J9, isolated from *Jania rubens* when grown after several transfers on marine agar. They further reports this species might require different growth conditions for optimal production of desired metabolites. Further Boyd et al. (1999) tried different culture media for better bacterial growth that reflect the types and quantities of nutrients present in the environments sampled. They have reported maximum strains on maine agar with 22% having antibiotic activity that showed the utility of specific growth media for culturing of heterotrophic bacteria. The seaweed extract based media was reported to give a lesser number of viable strains with 24% with antibiotic activity, which apparently suggested it as a better media to study bioactive isolates.

3.3.4 Identification

3.3.4.1 Biochemical Identification

Gram staining (Figure 3.6) and KOH screening showed that among the isolated strains, 12 falls under Gram positive and 11 to Gram negative. The Table 3.3 describes the detailed morphological, physiological and biochemical characteristics exhibited by isolated strains of the study. Biochemical analysis had clustered the promising bacterial isolates in to four species i.e, *Bacillus*, *Shewanella*, *Vibrio*^{*} and *Pseudomonas*.(*Biochemical analysis reports of SWI 20 and SWI 12B not included in Table 3.3)

Table 3.3. A
Morphological tests of the test bacteria

Tests	SWI9	SWI2	SWI 4B	SWI 5	SWI 21	SWI 6
Colony morphology						
Configuration	Circular	Circular	Wrinkled	Wrinkled	Circular	Wrinkled
Margin	Entire	Entire	Rhizoidal	Rhizoidal	Entire	Rhizoidal
Elevation	Convex	Convex	Flat	Flat	Convex	Flat
Surface	Smooth	Smooth	Rough	Rough	Smooth	Rough
Pigment	Yellow	Yellow	Off white	Off white	Cream	Off white
Opacity	Translucent	Translucent	Opaque	Opaque	Opaque	Opaque
Gram's reaction	-	-	+	+	-	+
Cell shape	Short	Short	Rods	Rods	IrregularRo	Rods
Size (μm)	1-2 μm	1-2 μm	3-5 μm	3-5 μm	1-2 μm	2-4 μm
Arrangement	Scattered	Scattered	Chains	Chains	Scattered	Chains
Spore(s)	-	-	+	+	-	+
Postion	-	-	Sub	Sub	-	Sub
Shape	-	-	Ellipsoidal	Ellipsoidal	-	Ellipsoidal
Sporangia bulging	-	-	Non bulged	Non bulged	-	Non bulged
Motility	+	+	+	+	+	+

Table 3.3. A (Continued...)
Morphological tests of the test bacteria

Tests	SWI 10	SWI 11	SWI 13	SWI 17	SWI	SWI 18
Colony morphology						
Configuration	Circular	Circular	Circular	Circular	Circular	Circular
Margin	Entire	Entire	Entire	Entire	Entire	Entire
Elevation	Convex	Convex	Convex	Convex	Convex	Convex
Surface	Smooth	Smooth	Smooth	Smooth	Smooth	Smooth
Pigment	Yellow	Yellow	Yellow	Yellow	Yellow	Yellow
Opacity	Translucent	Translucent	Translucent	Translucent	Translucent	Translucent
Gram's reaction	-	-	-	-	-	-
Cell shape	Rods	Rods	Rods	Rods	Rods	Rods
Size (μm)	1-2 μm	1-2 μm	1-2 μm	1-2 μm	1-2 μm	1-2 μm
Arrangement	Scattered	Scattered	Chains	Chains	Scattered	Chains
Spore(s)	-	-	-	-	-	-
Postion						
Shape						
Sporangia bulging						
Motility	+	+	+	+	+	+

Table 3.3. A (Continued...)
Morphological tests of the test bacteria

Tests	SWI4a	SWI 2	SW 1	SWI 16A	SWI 8	SWI 19
Colony morphology						
Configuration	Wrinkled	Wrinkled	Wrinkled	Wrinkled	Wrinkled	Wrinkled
Margin	Rhizoidal	Rhizoidal	Rhizoidal	Rhizoidal	Rhizoidal	Rhizoidal
Elevation	Flat	Flat	Flat	Flat	Flat	Flat
Surface	Rough	Rough	Rough	Rough	Rough	Rough
Pigment	Off white	Off white	Off white	Off white	Off white	Off white
Opacity	Opaque	Opaque	Opaque	Opaque	Opaque	Opaque
Gram's	+	+	+	+	+	+
Cell shape	Rods	Rods	Rods	Rods	Rods	Rods
Size (μm)	2-3.5 μm	2-4 μm	3-5 μm	2-3 μm	2-3 μm	2-3 μm
Arrangement	Chains	Scattered	Regular Chains	Chains	Chains	Chains
Spore(s)	+	+	+	+	+	+
Postion	Sub	Sub	Sub	Central	Central	Central
Shape	Ellipsoidal	Ellipsoidal	Ellipsoidal	Ellipsoidal	Ellipsoidal	Ellipsoidal
Sporangia bulging	Non bulged	Non bulged	Bulged	Non bulged	Non bulged	Non bulged
Motility	+	+	+	+	+	+

Table 3.3. A (Continued...)
Morphological tests of the test bacteria

Tests	SWI 16B	SWI 3	SWI 6	SWI 7
Colony morphology				
Configuration	Wrinkled	Wrinkled	Wrinkled	Wrinkled
Margin	Rhizoidal	Rhizoidal	Rhizoidal	Rhizoidal
Elevation	Flat	Flat	Flat	Flat
Surface	Rough	Rough	Rough	Rough
Pigment	Off white	Off white	Off white	Off white
Opacity	Opaque	Opaque	Opaque	Opaque
Gram's reaction	+	+	+	+
Cell shape	Rods	Rods	Rods	Rods
Size (μm)	2-3.5 μm	2-4 μm	3-5 μm	3-5 μm
Arrangement	Chains	Scattered	Chains	Chains
Spore(s)	+	+	+	+
Postion	Sub terminal	Sub terminal	Sub terminal	Sub terminal
Shape	Ellipsoidal	Ellipsoidal	Ellipsoidal	Ellipsoidal
Sporangia bulging	Non bulged	Non bulged	Non bulged	Non bulged
Motility	+	+	+	+

Table 3.3. B

Physiological tests of the test bacteria

Tests	SWI9	SWI I2	SWI 4B	SWI 5	SWI2I	PW-15
Growth at temperatures						
4°C	-	-	-	-	-	-
10°C	-	-	-	-	+	-
20°C	+	+	+	+	+	+
30°C	+	+	+	+	+	+
37°C	+	+	+	+	+	+
42°C	+	+	+	+	+	+
55°C	-	-	+	+	-	-
Growth at pH						
pH 4.0	-	-	-	-	(+)	-
pH 5.0	-	-	-	-	+	(+)
pH 6.0	+	+	+	+	+	+
pH 7.0	+	+	+	+	+	+
pH 8.0	+	+	+	+	+	+
pH 9.0	+	+	+	+	+	+
pH 10.0	+	+	+	+	+	+
pH 11.5	+	+	+	+	+	+
Growth on NaCl (%)						
2.0	+	+	+	+	+	+
4.0	+	+	+	+	+	+
6.0	+	+	+	+	+	+
8.0	+	+	+	+	+	+
10.0	-	-	+	+	-	+
Growth under anaerobic condition	-	-	-	-	-	-

Table 3.3. B (Continued...)
Physiological tests of the test bacteria

Tests	SWI 10	SWI 11	SWI 13	SWI 17	SWI 14	SWI 18
Growth at temperatures						
4°C	-	-	-	-	-	-
10°C	-	-	-	-	-	-
20°C	+	+	+	+	+	+
30°C	+	+	+	+	+	+
37°C	+	+	+	+	+	+
42°C	+	+	+	(+)	+	(+)

55°C	-	-	-	-	-	-
Growth at pH						
pH 4.0	(+)	-	+	+	-	-
pH 5.0	+	+	+	+	+	+
pH 6.0	+	+	+	+	+	+
pH 7.0	+	+	+	+	+	+
pH 8.0	+	+	+	+	+	+
pH 9.0	+	+	+	+	+	+
pH 10.0	+	+	+	+	+	+
pH 11.5	+	+	+	+	+	+
Growth on NaCl (%)						
2.0	+	+	+	+	+	+
4.0	+	+	+	+	+	+
6.0	+	+	+	+	+	+
8.0	+	+	+	+	+	+
10.0	-	-	-	-	-	-
Growth under anaerobic condition	-	-	-	-	-	-

Table 3.3. B (Continued...)
Physiological tests of the test bacteria

Tests	SWI4a	SWI 2	SWI 1	SWI 16A	SWI 8	SWI 19
Growth at temperatures						
4°C	-	-	-	-	-	-
10°C	-	-	(+)	-	-	-
20°C	+	+	+	+	+	+
30°C	+	+	+	+	+	+
37°C	+	+	+	+	+	+
42°C	+	+	+	+	+	+
55°C	+	+	+	+	+	+

Growth at pH						
pH 4.0	-	-	-	-	-	-
pH 5.0	-	-	-	-	-	-
pH 6.0	+	+	+	+	+	+
pH 7.0	+	+	+	+	+	+
pH 8.0	+	+	+	+	+	+
pH 9.0	+	+	+	+	+	+
pH 10.0	+	+	+	+	+	+
pH 11.5	+	+	+	+	+	+
Growth on NaCl (%)						
2.0	+	+	+	+	+	+
4.0	+	+	+	+	+	+
6.0	+	+	+	+	+	+
8.0	+	+	+	+	+	+
10.0	+	+	+	+	+	+
Growth under anaerobic condition	-	-	+	+	+	+

Table 3.3. B (Continued...)
Physiological tests of the test bacteria

Tests	SWI 16B	SWI 3	SWI 6	SWI 7
Growth at temperatures				
4°C	-	-	-	-
10°C	-	-	-	-
20°C	+	+	+	+
30°C	+	+	+	+
37°C	+	+	+	+
42°C	+	+	+	+
55°C	+	+	+	+
Growth at pH				
pH 4.0	-	-	-	-

pH 5.0	-	-	-	-
pH 6.0	+	+	+	+
pH 7.0	+	+	+	+
pH 8.0	+	+	+	+
pH 9.0	+	+	+	+
pH 10.0	+	+	+	+
pH 11.5	+	+	+	+
Growth on NaCl (%)				
2.0	+	+	+	+
4.0	+	+	+	+
6.0	+	+	+	+
8.0	+	+	+	+
10.0	+	+	+	+
Growth under anaerobic condition	-	-	-	-

Table 3.3. C
Biochemical tests of the test bacteria:

Tests	<i>SWI9</i>	<i>SWI2</i>	<i>SWI 4B</i>	<i>SWI 5</i>	<i>SWI21</i>	<i>SWI 6</i>
Growth on MacConkey	+(NLF)	+(NLF)	-	-	+(LF)	-
Indole test	-	-	-	-	-	-
Methyl red test	-	-	-	-	-	-
Voges Proskauer test	+	(+)	(+)	+	-	+
Citrate utilization	-	-	-	-	+	-
H ₂ S production	+	+	-	-	-	-
Gas production from glucose	-	-	-	-	-	-
Casein hydrolysis	+	+	+	+	-	+
Esculin hydrolysis	-	-	+	+	(+)	+
Gelatin hydrolysis	+	+	+	+	-	+
Starch hydrolysis	-	-	+	+	-	+
Urea hydrolysis	+	+	(+)	(+)	-	+
Nitrate reduction	+	+	+	+	+	+
Ornithine decarboxylase	-	-	(+)	(+)	-	+
Lysine decarboxylase	-	-	-	-	-	-

Arginine Dihydrolase	+	+	+	+	ND	ND
Catalase test	+	+	+	+	+	+
Oxidase test	+	+	-	-	+	+
Tween 20 hydrolysis	+	+	-	-	-	+
Tween 40 hydrolysis	+	+	-	-	-	(+)
Tween 60 hydrolysis	+	+	-	-	-	-
Tween 80 hydrolysis	-	-	-	-	-	-
Acid Production from						
Dextrose	-	-	+	+	+	+
Lactose	-	-	(+)	(+)	+	(+)
Maltose	-	-	+	+	-	+
Sucrose	-	-	+	+	-	+
Xylose	-	-	(+)	(+)	+	(+)

Table 3.3. C (Continued...)
Biochemical tests of the test bacteria:

Tests	SWI 10	SWI 11	SWI 13	SWI 17	SWI 14	SW-18
Growth on MacConkey	+	+	+	+	+	+
	(NLF)	(NLF)	(NLF)	(NLF)	(NLF)	(NLF)
Indole test	-	-	-	-	-	-
Methyl red test	-	-	-	-	-	-
Voges Proskauer test	+	+	+	+	+	+
Citrate utilization	-	-	-	-	-	-
H ₂ S production	+	+	+	+	+	+
Gas production from glucose	-	-	-	-	-	-
Casein hydrolysis	+	+	+	+	+	+
Esculin hydrolysis	-	-	-	-	-	-
Gelatin hydrolysis	+	+	+	+	+	+
Starch hydrolysis	-	-	-	-	-	-
Urea hydrolysis	+	+	+	+	+	+
Nitrate reduction	+	+	+	+	+	+
Catalase test	+	+	+	+	+	+
Oxidase test	+	+	+	+	+	+

Tween 20 hydrolysis	+	+	+	+	+	+
Tween 40 hydrolysis	+	+	+	+	+	+
Tween 60 hydrolysis	+	+	+	+	+	+
Tween 80 hydrolysis	-	-	-	-	-	-
Acid Production from						
Dextrose	-	-	-	-	-	-
Lactose	-	-	-	-	-	-
Maltose	-	-	+	-	-	-
Sucrose	-	+	-	-	-	-

Table 3.3. C (Continued...)
Biochemical tests of the test bacteria:

Tests	SWI4a	SWI 2	SWI 1	SWI 16A	SWI 8	SWI 19
Growth on MacConkey	-	-	-	-	-	-
Indole test	-	-	-	-	-	-
Methyl red test	-	-	+	-	-	-
Voges Proskauer test	+	(+)	(+)	+	+	+
Citrate utilization	-	-	+	+	+	+
H ₂ S production	-	-	-	-	-	-
Gas production from glucose	-	-	-	-	-	-
Casein hydrolysis	+	+	+	-	-	-
Esculin hydrolysis	+	+	+	+	+	+
Gelatin hydrolysis	+	+	+	+	+	+
Starch hydrolysis	+	+	+	+	+	+
Urea hydrolysis	+	+	+	+	+	+
Nitrate reduction	+	+	+	+	+	+
Ornithine decarboxylase	+	+	+	+	+	+
Lysine decarboxylase	-	-	+	(+)	(+)	(+)
Catalase test	+	+	+	+	+	+
Oxidase test	+	-	+	-	-	-
Tween 20 hydrolysis	-	-	-	+	+	+
Tween 40 hydrolysis	-	-	(+)	+	+	+
Tween 60 hydrolysis	-	-	(+)	+	+	+
Tween 80 hydrolysis	-	-	-	-	-	-
Acid Production from						
Dextrose	+	+	+	+	+	+
Lactose	+	+	+	+	+	+
Sucrose	+	+	+	+	+	+

Table 3.3. C (Continued...)
Biochemical tests of the test bacteria:

Tests	SWI 16B	SWI 3	SWI 6	SWI 7
Growth on MacConkey	-	-	-	-
Indole test	-	-	-	-
Methyl red test	-	-	-	-
Voges Proskauer test	+	(+)	(+)	+
Citrate utilization	-	-	-	-
H ₂ S production	-	-	-	-
Gas production from glucose	-	-	-	-
Casein hydrolysis	+	+	+	+
Esculin hydrolysis	+	+	+	+
Gelatin hydrolysis	+	+	+	+
Starch hydrolysis	+	+	+	+
Urea hydrolysis	+	+	(+)	(+)
Nitrate reduction	+	+	+	+
Ornithine decarboxylase	+	+	(+)	(+)
Lysine decarboxylase	-	-	-	-
Catalase test	+	+	+	+
Oxidase test	+	-	-	-
Tween 20 hydrolysis	-	-	-	-
Tween 40 hydrolysis	-	-	-	-

Tween 60 hydrolysis	-	-	-	-
Tween 80 hydrolysis	-	-	-	-
Acid Production from				
Dextrose	+	+	+	+
Lactose	+	+	(+)	(+)
Sucrose	+	+	+	+

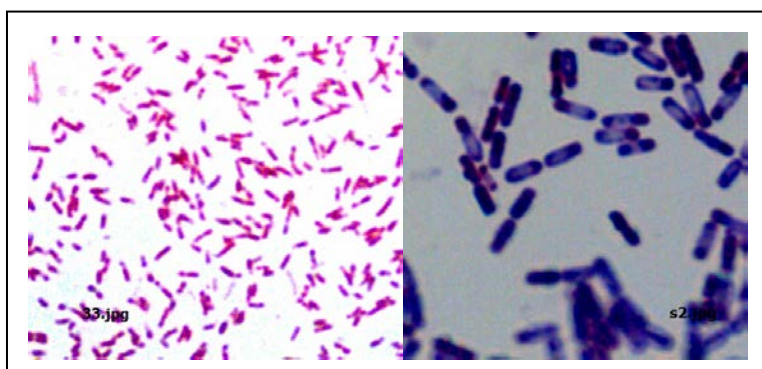


Figure 3.6

Indicative pictures showing the Gram staining of the isolates
 (a) Gram negative strains (*S. algae*) (b) Gram positive strains (*B. subtilis*)

3.3.5 16S rRNA based phylogeny

The 16S rRNA of the isolated strains was compared with the closest relatives in the GeneBank and a phylogenetic tree was constructed by comparing the sequences of the 23 isolates with their closest relatives (Figure 3.7). The isolates were identified as *Bacillus subtilis*, *Bacillus amyloliquefaciens*, *Vibrio alginolyticus*, *Shewanellae algae* and *Pseudomonas putida*. Biochemical identification results were further confirmed by 16S rRNA gene phylogeny. The 16S rRNA gene sequence based homology searches shown that most of the isolates of the present study were closely related to each other (>99 percent similarity). However, each isolates were included in the study as individual isolates as they were found to be different in their inhibition and growth patterns. In the present survey of antagonistic bacteria associated with seaweeds, the representatives from two bacterial phyla, *Firmicutes* and *Proteobacteria*

were found. These results found harmony with earlier research findings (Ali et al. 2012; Kennedy et al. 2009; Wiese et al. 2009). Ali et al. (2012) have shown that Proteobacteria constitute the predominant of bacterial cells on the surface of *J. rubens* (about 73%), whilst *Bacteroidetes* made the second and *Firmicutes* followed. Bacteria isolated from *L. saccharina* were found to be affiliated to bacterial domain, the Gram-positive *Actinobacteria* and *Firmicutes*, the Gram-negative *Proteobacteria* and *Bacteroidetes*. The representatives of the *Proteobacteria* were most abundant, the majority of which were affiliated with the γ -subgroup (Wiese et al. 2009). The γ -*proteobacterial* phylum has proven to be the most dominant cultivable group in a recent study of sponge-associated bacteria from *Haliclona simulans* collected from Irish waters (Kennedy et al. 2009). The predominant bacterial group found in the *H. simulans* total 16S rRNA gene library was the γ -*Proteobacteria*, which constituted 77 percent of clones obtained during the study (Kennedy et al. 2008). The γ -*proteobacterial* *Shewanellae algae*, however, would be less likely to be enriched by the selection process and are probably dominant group of cultivable bacteria from the seaweeds. The entire set of isolates of *Firmicutes* belonged to the genus *Bacillus*. The greater number of *Bacillus* isolates found in this study might be due to the selectivity of the media used in the present study, as also supported by published literature (Zhang et al. 2009). Within the *Firmicutes*, especially strains of the genus *Bacillus* are common producers of antimicrobial compounds. Approximately 800 bacterial metabolites with antibiotic activity have been isolated from *Bacillus* spp (Wiese et al. 2009). The *Bacillus* clade in the present study had the representatives of the species *B. cereus*, *B. subtilis* and *B. amyloliquefaciens*. The DNA similarity searches of the partial 16s rRNA gene sequences of the isolated strains in the study with the Gene Bank databases had shown *B. amyloliquefaciens* and *B. subtilis* are clustered as one, and difficult to distinguish. *B. amyloliquefaciens* and *B. subtilis* were reported to harbor several rRNA gene clusters in which 16S rDNA sequence variation exists (Hu et al. 2010). However we could not differentiate them with the sequence results of the present study, possibly due to the fact that the regions amplified with the primers used in the present study did not belong to those clusters with sequence variation.

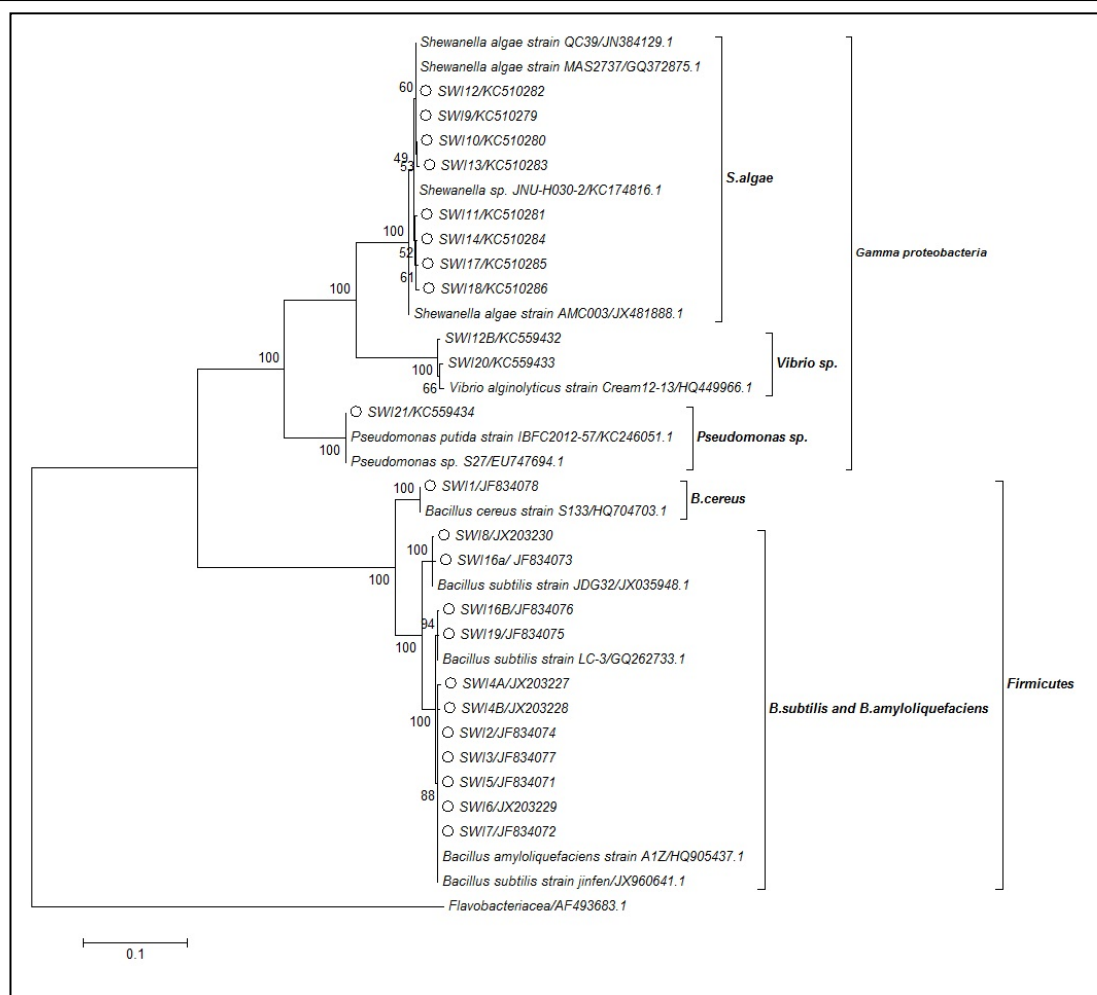


Figure 3.7

Phylogenetic tree derived from nearly complete 16S rRNA gene sequences, showing relationships between the antagonistic bacterial isolates associated with seaweeds and their phylogenetic neighbors. The evolutionary history was inferred by using the Maximum Likelihood method based on the Kimura 2-parameter model. Evolutionary analyses were conducted in MEGA5.

3.3.6 Identification by Fatty acid profiles

The cellular fatty acid profiles of the strains were further confirmed the results obtained from the biochemical and molecular taxonomic studies that the strains were belonged to the *Firmicutes* and *Gamma Proteobacteria*. The results of the FAME analysis (Table 3.4 and 3.5) confirmed the results, and further demonstrated that there were differences between *Bacillus* sp. A detailed analysis report were depicted in table 3.4 and 3.5. The *vibrio* and *Pseudomonas* isolates were not included in fatty acid analysis as they were not taken in to consideration for the further studies.

Table 3.4

Comparison of fatty acids present in *Bacillus* sp (greater than or equal to 3 % of the total percentage FAME area).

Fatty acids	Shorthand designation	SWI 19	SWI 3	SWI 2	SWI4a	SWI 4B	SWI 5	SWI 6	SWI 7	SWI 1
Fatty acids (% w/w of total fatty acids) ^a										
11-Methyldodecanoic acid	C13:0 iso	ND	ND	ND	ND	ND	ND	ND	ND	3.91
12-Methyltridecanoic acid	C14:0 iso	ND	2.02	ND	ND	1.09	1.08	ND	ND	2.96
Tetradecanoate	C14:0	ND	1.83	ND	ND	1.35	1.61	1.95	2.76	3.21
13-Methyltetradecanoate	C15:0 iso	21.10	20.11	31.48	21.42	30.93	24.53	23.03	21.83	29.43
12-Methyltetradecanoate	C15:0 anteiso	34.13	34.31	38.65	32.96	35.86	35.22	33.84	44.62	4.76
3-Hydroxytetradecanoic acid	C14:0 3OH	ND	ND	ND	ND	ND	ND	ND	ND	2.83
14-Methylpentadecanoic acid	C16:0 iso	ND	4.51	ND	ND	1.89	2.00	1.78	ND	7.88
cis-Hexadec-5-enoic acid	C16:1 ω11c	ND	2.77	ND	4.15	2.77	3.23	3.38	ND	ND
2-Hydroxy-13-methyltetradecanoic acid	C15:0 iso 2OH	ND	ND	ND	ND	ND	ND	ND	ND	9.69
Hexadecanoate	C16:0	9.58	12.13	17.23	18.00	9.03	12.64	13.91	15.11	10.00
cis-16-Methylheptadec-7-enoic acid	C17:1 iso-ω10c	ND	ND	ND	ND	1.54	1.39	1.95	ND	3.28
cis-16-Methylheptadec-12-enoic acid	C17:1 iso-ω5c	ND	ND	ND	ND	ND	ND	ND	ND	4.76
cis-14-Methylhexadec-3-enoic acid	C17:1 anteiso	ND	ND	ND	ND	ND	0.60	ND	2.18	ND
15-Methylhexadecanoate	C17:0 iso	11.37	7.74	12.63	9.08	8.97	9.27	10.06	7.08	10.73
14-Methylhexadecanoate	C17:0 anteiso	13.30	7.22	ND	7.16	6.57	7.63	7.46	6.43	2.48
Octadecanoate	C18:0	10.51	4.39	ND	7.23	ND	0.80	2.65	ND	4.08
Icosanoic acid	C20:0	ND	2.97	ND	ND	ND	ND	ND	ND	ND
ΣIso-fatty acids		32.47	34.38	44.11	30.5	42.88	36.88	34.87	28.91	54.91
ΣAnteiso fatty acids		47.43	41.53	38.65	40.12	42.43	42.85	41.3	51.05	7.24
ΣIso + anteiso fatty acids		79.9	75.91	82.76	70.62	85.31	79.73	76.17	79.96	62.15
ΣAnteiso / ΣIso fatty acids		1.46	1.21	0.88	1.32	0.99	1.16	1.18	1.77	0.13
C15 anteiso / C15 iso fatty acids		1.62	1.71	1.23	1.54	1.16	1.44	1.47	2.04	0.16
C15 anteiso / C17 anteiso fatty acids		2.57	4.75	ND	4.60	5.46	4.62	4.54	6.94	1.92
Monoenoic fatty acids		ND	2.77	ND	4.15	4.31	5.22	5.33	2.18	8.04
Hydroxy fatty acids		ND	ND	ND	ND	ND	ND	ND	ND	12.52
Straight chain saturated fatty acids		20.09	21.32	17.23	25.23	10.38	15.05	18.51	17.87	17.29

Some minor fatty acid components are not shown in this table. Individual fatty acids comprising less than 1% of the FA content were ignored. . ND: Not detected in the GC trace. The typical bacterial fatty acids such as 3-hydroxydecanoic acid (C10:0 3OH), undecanoate (C11:0), dodecanoate (C12:0), 3-hydroxyundecanoate (C11:0 3OH), 2-hydroxydodecanoic acid (C12:0 2OH), 3-hydroxydodecanoic acid (C12:0 3OH), tridecanoate (C13:0), 3-hydroxydodecanoate (C12:0 3OH), 3-hydroxy-11-methyldodecanoic acid (C13:0 iso 3OH), 3-hydroxytridecanoic acid (C13:0 3OH), cis-pentadec-7-enoic acid (C15:1 ω8c), cis-pentadec-9-enoic acid (C15:1 ω6c), pentadecanoate (C15:0), cis-Hexadec-7-enoate (C16:1 ω9c), 3-hydroxy-13-methyltetradecanoic acid (C15:0 iso 3OH), methylenehexadecanoate (C17:0 cyclo), heptadec-9-enoate (C17:1 ω8c), cis-heptadec-11-enoate (C17:1 ω6c), cis-heptadecanoate (C17:0), cis-octadec-9-enoate (C18:1 ω9c), and cis-octadec-11-enoate (C18:1 ω7c) were not detected in GC trace, and were therefore, not reported in the table.

Table 3.5

Comparison of fatty acids present in *Shewanella algae* isolated from the seaweeds (greater than or equal to 1 % of the total percentage FAME area).

Fatty acids	Nomenclature	SWI9	SWI2	SWI 10	SWI 11	SWI 13	SWI 17	SWI 14	SWI 18
Fatty acids (% total fatty acids)									
Undecanoate	C11:0	0.38	0.32	0.43	0.00	0.00	0.00	0.00	0.51
Dodecanoate	C12:0	2.13	1.65	3.65	3.52	3.13	2.13	3.73	2.72
3-Hydroxyundecanoate	C11:0 3OH	0.92	0.73	0.78	0.73	0.00	0.75	0.00	0.91
3-Hydroxydodecanoic acid	C12:0 3OH	0.00	1.88	0.00	0.00	0.00	0.00	0.00	0.00
11-Methyl dodecanoic acid	C13:0 iso	7.86	7.03	6.81	8.02	6.00	6.72	6.37	5.97
Tridecanoate	C13:0	1.68	1.27	1.74	1.54	1.87	1.74	2.27	1.85
3-Hydroxydodecanoate	C12:0 3OH	2.29	1.88	3.00	2.96	2.37	1.19	2.38	2.18
12-Methyltridecanoic acid	C14:0 iso	0.59	0.53	0.79	0.00	0.00	0.00	0.00	0.61
Tetradecanoate	C14:0	0.55	0.39	0.98	0.00	0.00	0.00	0.00	0.76
3-Hydroxy-11-methyl dodecanoic acid	C13:0 iso 3OH	7.15	6.99	4.11	5.93	4.08	4.37	3.70	4.02
3-Hydroxytridecanoic acid	C13:0 3OH	3.71	3.23	3.17	3.22	3.04	3.34	4.04	3.60
13-Methyltetradecanoate	C15:0 iso	27.16	29.95	29.32	27.75	27.79	37.44	24.69	25.61
12-Methyltetradecanoate	C15:0 ante-iso	0.00	0.37	0.00	0.00	0.00	0.00	0.00	0.00
cis-Pentadec-7-enoic acid	C15:1 ω8c	0.55	0.44	0.00	0.00	0.00	0.00	0.00	0.00
cis-Pentadec-9-enoic acid	C15:1 ω6c	0.67	0.65	0.00	0.00	0.00	0.00	0.00	0.00
3-Hydroxytetradecanoic acid	C14:0 3OH	1.63	1.26	1.63	1.90	1.59	1.17	0.00	1.29
14-Methylpentadecanoic acid	C16:0 iso	0.00	0.46	0.00	0.00	0.00	0.00	0.00	0.00
cis-Hexadec-7-enoate	C16:1 ω9c	0.78	0.00	1.55	0.95	0.00	0.00	0.00	1.02
2-Hydroxy-13-methyltetradecanoic acid	C15:0 iso 2OH	6.74	0.00	11.32	9.30	9.01	6.94	12.05	8.66
Hexadecanoate	C16:0	5.99	5.44	7.64	7.14	10.31	5.73	9.07	9.03
3-Hydroxy-13-methyltetradecanoic acid	C15:0 iso 3OH	1.68	1.56	0.78	1.33	0.00	1.21	0.00	0.00
cis-14-Methylhexadec-3-enoic acid	C17:1 ante-iso 13	0.00	0.00	0.00	0.00	0.00	0.00	0.00	0.00
15-Methylhexadecanoate	C17:0 iso	2.35	3.12	1.45	2.35	2.28	2.04	0.00	1.68
Heptadec-9-enoate	C17:1 ω8c	16.98	16.25	14.39	14.07	17.41	17.94	21.73	19.05
cis-Heptadec-11-enoate	C17:1 ω6c	1.08	1.36	0.00	0.89	0.00	1.13	0.00	1.34
14-Methylhexadecanoate	C17:0 ante-iso	0.00	0.00	0.00	0.00	0.00	0.00	0.00	0.00
cis-Heptadecanoate	C17:0	3.39	3.47	2.60	3.31	4.64	4.49	4.51	4.14
cis-Octadec-9-enoate	C18:1 ω9c	1.89	2.05	2.09	2.81	3.55	1.69	2.50	2.80
cis-Octadec-11-enoate	C18:1 ω7c	1.86	2.14	1.79	2.26	2.92	0.00	2.97	2.24
ΣIso-fatty acids		53.53	49.64	54.58	54.68	49.16	58.72	46.81	46.55
Odd carbon iso fatty acids		52.94	48.65	53.79	54.68	49.16	58.72	46.81	45.94
Even carbon iso fatty acids		0.59	0.99	0.79	0	0	0	0	0.61
ΣAnte-iso fatty acids		0	0.37	0	0	0	0	0	0
Monoenoic fatty acids		23.81	22.89	19.82	20.98	23.88	20.76	27.2	26.45
Hydroxy fatty acids		24.12	17.53	24.79	25.37	20.09	18.97	22.17	20.66

^a Some minor fatty acid components are not shown in this table. Individual fatty acids comprising less than 1% of the FA content were ignored.

MTCC Accession Numbers: MTCC 10608-MTCC10609; MTCC10455-MTCC10456; MTCC10458; MTCC10402-MTCC10407. Details are available with Table 3.2

3.4 Conclusions

Seaweeds possess much potential as valuable source for screening bioactive bacterial isolates with bioactive potential, which facilitates novel natural product discovery from marine environment. These seaweed-associated epibionts might be beneficial to the seaweeds by limiting or preventing the development of competing, pathogenic and fouling bacteria. Seaweeds are potential sources of bioactive compound producing bacterial isolates when compared to other marine sources such as seawater, sediments etc. A greater percentage of a isolates with antibacterial activity against pathogenic microorganisms as demonstrated (22%) in this study found good agreement with the literature. These candidate isolates were found to have a broad spectrum activity against different pathogens. The taxonomic classifications showed that a greater proportion of the marine isolates belonged to the *Firmicutes* genera belonging to *Bacillus* sp. The remaining isolates in our study were belonging to γ -Proteobacteria. The cultures preserved on a medium supplemented with seaweed extract were found to retain the bioactivity for a prolonged time period. This might due to the fact that marine surface associated microorganisms required conditions that resemble their native environment on seaweed host in order to produce greater quantities of antibacterial lead molecules.

CHAPTER 4

CHARACTERIZATION OF ANTAGONISTIC POTENTIAL OF SEAWEED ASSOCIATED BACTERIAL ISOLATES

4.1 Background

Seaweeds use targeted antimicrobial chemical defense strategies and that secondary metabolites important in the ecological interactions between marine macroorganisms and microorganisms could be a promising source of novel bioactive compounds (Lemose et al. 1985). There are scanty information regarding the interaction of seaweeds with their associated microbial flora (Goeke et al. 2010). Despite the seaweed associated microbial flora have been reported as a source of natural compounds very little is known about the chemical nature of such compounds and their role on antimicrobial activity. Polyketide synthetases (PKS) and non-ribosomal peptide synthetases (NRPS) are multifunctional enzymes catalyzing the biosynthesis of structurally diverse bioactive natural products (Hutchinson 2003), and therefore, been commonly employed for designing molecular tools to assess metabolically active bacterial groups (Ayuso-Sacido and Genilloud 2005; Zhang et al. 2009; Kennedy et al. 2009). Despite being very important marker gene systems, little is known about the presence of *nrps* and *pks-I* in the diverse seaweed-associated microbiota.

4.2 Materials and Methods

4.2.1 Release of antibiotic substances to the culture medium

Nutrient broth was prepared and inoculated with 5% inoculum of producer strains and kept on an orbital shaker for 7 days. The fermentation broth was collected by centrifugation (10,000 rpm for 15 min). The process was repeated for every 24 hours and the cells were washed three times with TS buffer (Tris 50 mM,

NaCl 0.1 M, pH 8) on a vortex mixer. The *in vitro* antibacterial activity of the medium, cell-free wash supernatants and pellets was measured against *Vibrio parahaemolyticus* ATCC 17802 by the disc-diffusion method (for supernatant) and spot over lawn assay (for pellet) (Boyd et al. 1998, Lemose et al. 1985) on Muller Hinton Agar.

4.2.2 Antagonism assays among the isolated marine bacteria and their auto inhibition

To determine the possible role of antibacterial substances produced by the epiphytic bacteria in the amensalist competition, assays were conducted with the producer strains to test the mutual antagonism, and also against other epiphytic bacteria. The antagonism between the isolated bacterial strains was studied on a solid media. Marine bacteria were grown in broth for a period of 8 hours, and a swab of organism has been employed as test cultures. Marine bacterial cells were scraped off from a pre-inoculated plate, and kept over the plates with test organisms. The plates were incubated overnight to analyze inhibitory zone. The antagonistic effect was indicated by an inhibition zone in the confluence area (Lemose et al. 1985).

4.2.3 Plasmid profiling

The plasmid of the strain was extracted by alkaline method, and identified by agarose gel electrophoresis. Briefly, the cells were grown overnight in Luria Bertane broth containing sodium chloride (LBS, NaCl, 2% w/v), and incubated at 37°C in a shaker incubator (120 rpm) for 16-18 h. The culture (1.5 mL) was used for plasmid preparation following the method of alkaline lysis (Sambrook et al. 1989). The nucleic acid was re-dissolved in Tris-EDTA buffer (50µL, 10 mM Tris-HCl, 1mM Na₂EDTA, pH 8.0) containing DNAase free RNAase (20mg/mL), vortexed briefly and stored at -20°C. Electrophoresis was performed using 0.8% agarose gel system in Tris borate buffer. Gels were stained with ethidium bromide (0.5µg/mL). The resolved bands were visualized on a UV transilluminator at a wavelength of 360 nm, and photographed using an UV gel documentation system (Biorad, USA) (Devi et al. 2009).

4.2.4 Plasmid curing

Plasmid curing was carried out to determine whether the antibacterial substance was plasmid-encoded. For curing experiment, a chemical agent sodium dodecyl sulphate (SDS) was used. Each bacterial isolate was inoculated into the LBS broth and incubated at 37°C under shaking in an incubator at 150rpm. Thereafter, 50µL (10%) of the cultured strain was added in to 5mL of fresh LB medium containing 0.005% SDS with three consecutive transfers every 24h. Every day a portion of each culture was withdrawn and checked for the presence of plasmid in the agarose gel (0.8% w/v) electrophoresis. The antimicrobial activity of the colonies identified after plasmid curing by the method used to identify antagonistic bacteria, i.e., spot over lawn assay against test pathogens (Devi et al. 2009; Hu et al. 2010).

4.2.5 Identification and analysis of PKS and NRPS gene fragments

The highly conserved sequences of β -ketoacyl synthase (KS) domains are shared among all PKSs, and therefore, the KS domains are useful in the screening for PKS genes in bacteria. Similarly, the most conserved adenylation (A) domain can be used for PCR primer design to survey NRPSs gene diversity. Different sets of degenerate primers targeting genes encoding *pks-I* and *nrps* were used to screen the biosynthetic potential of the bacterial isolates to elicit bioactive polyketide compounds characterized by the repetitive occurrence of ketide (-CH₂-CO-) moieties and non-ribosomal peptides. The primers have been listed under Table 1. PCR was performed in a total volume of 25 µL containing 1X reaction buffer with MgCl₂ (Sigma), 0.25 mM of each dNTP (Fermentas), 0.5 mM of each primers (Sigma), 1 ng DNA and 0.3 U Taq DNA polymerase (Sigma). The PCR process was set as initial denaturation 5 min at 94°C followed by 35 cycles of 1 min at 95°C, 1 min at 45°C, 1 min at 72°C, and a final extension of 5 min at 72°C. All of the amplification products were examined by 1.5% agarose gel electrophoresis, and bands of 700 to 800 bp and 1000 to 1,400 bp were classified as products of *pks-I* and *nrps* genes, respectively. Polymerase chain reaction amplicons were separated by agarose gel electrophoresis and the bands of expected size were gel-

purified using electrophoresis and bands of 700-800 bp (*pks-I*) and 1000-1400 bp (*nrps*) were gel-purified using Gel Elute™ Gel Extraction Kit (Sigma) and cloned into the pGET-Blunt M13 vector (Fermentas) following the manufacturer's instructions and transformed into chemocompetent *E. coli* cells. The positive recombinants were screened by ampicillin resistant recombinant selection method assisted with colony PCR with M13 specific primers. The positive clones were used for plasmid isolation using GenJET™ Plasmid isolation kit (fermentas) and sequenced using M13 F and m13 R primers.

4.2.6 Sequence analysis

Forward and reverse sequences of the PKS gene amplified product were assembled using Dna Baser v2.exe and the vector sequences were removed using Vescreen (NCBI). The sequence data were subjected to GeneBank searches with blastx algorithm. Nucleotide sequences were translated in to peptide sequences EMBOSS Transeq (EMBL-EBI) and blastp searches of deduced amino acid sequences were also performed. Multiple alignments of amino acid sequences with reference sequences of the GeneBank was carried out with CLUSTALW software of Bioedit program and then the aligned dataset was used as input for phylogenetic analysis program (Zhu et al. 2009). The evolutionary history was inferred by using the Maximum Likelihood method based on the Whelan And Goldman model (Whelan and Goldman, 2001) and the bootstrap analysis with 1000 replications in MEGA5 (Tamura et al. 2011). Multiple alignment of active sites of type I KS domains with reference sequences were also performed to verify the conserved sequence motifs.

4.3 Results and Discussion

4.3.1 Release of antibiotic substances to the culture medium

Assays were conducted to determine the degree of excretion of the antibiotic substances. This assay showed that the bacteria released compounds into the bacterial supernatant that had antimicrobial activity. For the cultures analyzed in our study we could found that the active compounds were released in the

medium. But the pellets were still active after several wash. The inhibitory zones exhibited by the supernatant were not as prominent as pellet. This justified the earlier finding that the antibiotic activity remained associated with cells in algal epiphytes. This is in agreement with the report of Lemose et al. (1985). In the present study, the amount of antibacterial substances released in the medium was found to be low. For the *Bacillus* sp inhibition zones were evident in 24 hours, whereas *Shewanellae* exhibited zone on the third day of inoculation. However, both cases the inhibition zone clearance exhibited by the centrifuged supernatant was lesser than that observed on the agar plates, i.e the solid media. This demonstrated that the bacteria are likely to release bioactive compounds into the surrounding slowly. In general, the antibiotic substances produced by the epiphytic bacteria used in the study remained strongly bound to the cells. Particularly *Shewanellae* sp showed very less activity in the spent broth, whereas cells were active on solid agar. The specific role of the cell wall in the secretion processes is still unknown, although there are evidences indicating the limited release of exocellular proteins by Gram-negative bacteria. In this process the protein remain bound to the cell in the periplasmic space after excretion. A rapid release of antibiotic substances by producer epiphytic bacteria probably would not provide them with any competitive advantage because inhibitors would be immediately washed away by seawater. However, if antibiotics remained linked to cells, they could be excreted slowly and continually to the environment, preventing colonization by competitors of the adjacent space on the seaweed surface. The cultures showed a greater activity when they are grown as surface culture, and the activity were found to be lower in shake flasks. The present study supported the earlier finding that bacteria grown on surfaces released bioactive compounds that had greater activity against target strains compared with those from the same strain grown in shake flask cultures (Amstrong et al. 2001). This increase in production might be due to the expression of different genes in a similar manner to those known to be involved in extracellular polysaccharide production once bacteria have settled on a surface (Amstrong et al. 2001).

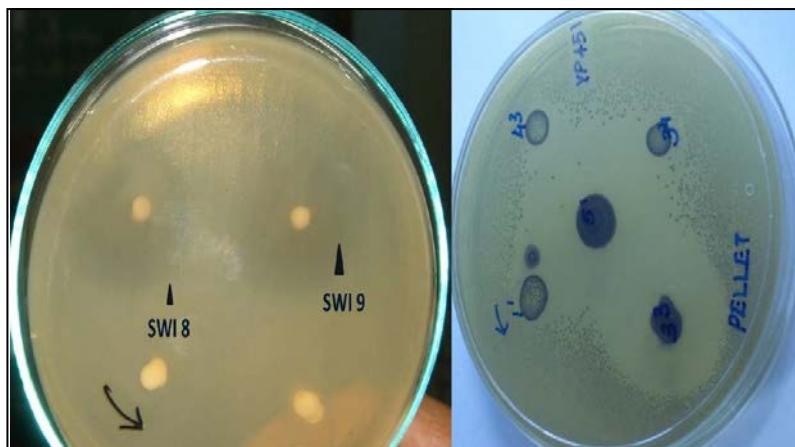


Figure 4.1

Indicative pictures showing the release of antibacterial compound (A) Disc diffusion assay of the broth and (B) Spot over lawn assay of the culture pellet against *V.parahaemolyticus* MTCC 451

4.3.2 Antagonism assays among the isolated marine bacteria and their autoinhibition

The absence of inhibitory activity of producer strains against other epiphytic producers indicated that the production of inhibitors could be of great importance in microhabitats such as an algal surface, where competition for an attachment site is surely a frequent event. In general, a few producer strain inhibited the growth of the other producers, while the activity among majority of the strains were non inhibitory. Only one strain SWI 1 was inhibited by all the producers tested. Interestingly, this particular strain showed a clear autoinhibitory activity. On the other hand, a greater number of antagonistic relationships between producer strains isolated from the seaweeds was not observed which contradicts the Lemose's (1985) observation. Most of the cells under the study were not inhibitory to each other except SWI1.A detailed autoinhibition and mutual inhibition pattern is shown in Table 4.1. These results suggested that these beneficial populations coexists in the seaweed biofilm, and may be protecting seaweeds from deleterious population or other colonizers.

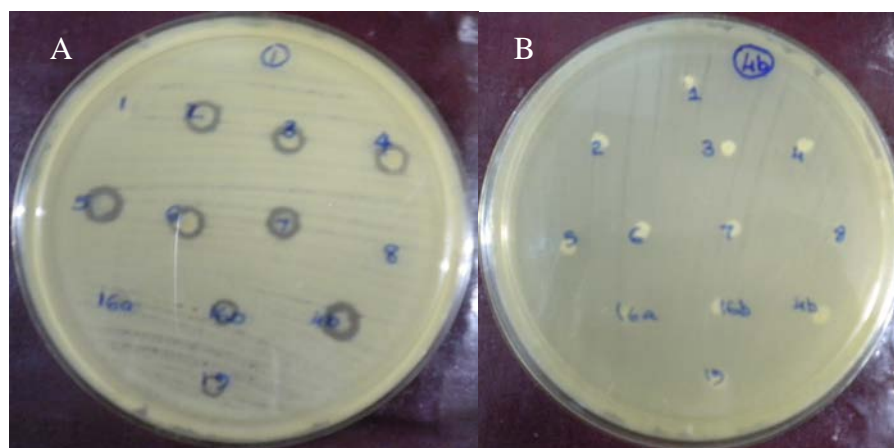


Figure 4.2

Indicative pictures for autoinhibition and mutual inhibition of seaweed associated isolates (A) SWI 1 MTCC10404 (B) SWI 4b MTCC 10456

Table 4.1
Autoinhibition and mutual inhibition pattern (expressed in mm) of antagonistic isolates associated with seaweed

	SWI1	SWI2	SWI3	SWI4A	SWI4B	SWI5	SWI6	SWI7	SWI8
SWI1	NI	10.3±1.5	10.3±1.53	12.7±0.58	0	9±1	9.33±1.15	10±1	NI
SWI2	3.0±2.0	NI	NI	NI	NI	NI	NI	NI	NI
SWI3	3.7±1.5	NI	NI	NI	NI	NI	NI	NI	NI
SWI4A	2.3±0.6	NI	NI	NI	NI	NI	NI	NI	NI
SWI4B	NI	NI	NI	NI	NI	NI	NI	NI	NI
SWI5	1.7±0.6	NI	NI	NI	NI	NI	NI	NI	NI
SWI6	2.7±0.6	NI	NI	NI	NI	NI	NI	NI	NI
SWI7	2±0	NI	NI	NI	NI	NI	NI	NI	3.33±0.58
SWI8	0.7±0.6	2.67±0.51	10.7±1.15	9.67±0.58	11.3±1.15	10.3±0.58	10.7±1.15	2.7±0.6	NI
SWI9	NI	NI	NI	NI	NI	NI	NI	NI	NI
SWI10	NI	NI	NI	NI	NI	NI	NI	NI	NI
SWI11	NI	NI	NI	NI	NI	NI	NI	NI	NI
SWI12	NI	NI	NI	NI	NI	NI	NI	NI	NI
SWI12B	NI	NI	NI	NI	NI	NI	NI	9.3±1.2	NI
SWI13	1±1.7	NI	9.33±0.58	11.3±1.15	14±1	11±1	NI	2±0	NI
SWI14	0.7±1.2	2.33±0.19	1.33±0.58	1.67±0.58	NI	NI	NI	9.7±0.6	NI
SWI16A	0.7±1.2	9.33±0.19	11.7±1.53	11±1	13±1	11.7±0.58	9±1	12±0.6	2.67±0.58
SWI16B	NI	NI	NI	NI	NI	NI	NI	NI	NI
SWI17	NI	NI	NI	NI	NI	NI	NI	9.7±0.6	NI
SWI18	10±1.5	12±1	14.3±0.58	12±1	11.7±1.53	17.7±0.58	15±1	11±1.2	NI
SWI19	NI	NI	NI	NI	NI	NI	NI	NI	NI
SWI20	NI	NI	1.67±0.58	2.33±0.58	1.33±0.58	NI	NI	NI	NI
SWI21	NI	NI	NI	NI	NI	NI	NI	NI	NI

	SWI9	SW I10	SW I11	SWI12	SW I13	SW I14	SWI 16A	SWI1 6B	SW I17	SW I18	SWI19	SW I20	SW I21
SWI1	NI	NI	NI	NI	NI	NI	NI	NI	NI	NI	2.67±0.58	NI	NI
SWI2	NI	NI	NI	NI	NI	NI	NI	NI	NI	NI	NI	NI	NI
SWI3	NI	NI	NI	NI	NI	NI	NI	NI	NI	NI	NI	NI	NI
SWI4A	NI	NI	NI	NI	NI	NI	NI	NI	NI	NI	NI	NI	NI
SWI4B	NI	NI	NI	NI	NI	NI	NI	NI	NI	NI	NI	NI	NI
SWI5	NI	NI	NI	NI	NI	NI	NI	NI	NI	NI	NI	NI	NI
SWI6	NI	NI	NI	NI	NI	NI	NI	NI	NI	NI	NI	NI	NI
SWI7	NI	NI	NI	NI	NI	NI	NI	NI	NI	NI	NI	NI	NI
SWI8	NI	NI	NI	NI	NI	NI	NI	NI	NI	NI	NI	NI	NI
SWI9	NI	NI	NI	NI	NI	NI	NI	NI	NI	NI	NI	NI	NI
SWI10	NI	NI	NI	NI	NI	NI	NI	NI	NI	NI	NI	NI	NI
SWI11	NI	NI	NI	NI	NI	NI	NI	NI	NI	NI	NI	NI	NI
SWI12	NI	NI	NI	NI	NI	NI	NI	NI	NI	NI	NI	NI	NI
SWI13	NI	NI	NI	NI	NI	NI	NI	NI	NI	NI	NI	NI	NI
SWI14	NI	NI	NI	11.3±1.15	NI	NI	NI	NI	NI	NI	NI	15.7±0.58	NI
SWI16A	NI	NI	NI	NI	NI	NI	NI	1±1.7321	NI	NI	2±1	0	NI
SWI16B	NI	NI	NI	NI	NI	NI	NI	NI	NI	NI	NI	NI	NI
SWI17	NI	NI	NI	NI	NI	NI	NI	NI	NI	NI	NI	NI	NI
SWI18	NI	NI	NI	NI	NI	NI	NI	NI	NI	NI	14.7±0.58	NI	NI
SWI19	NI	NI	NI	NI	NI	NI	NI	NI	NI	NI	NI	NI	NI
SWI20	NI	NI	NI	NI	NI	NI	NI	NI	NI	NI	NI	NI	NI
SWI21	NI	NI	NI	NI	NI	NI	NI	NI	NI	NI	NI	NI	NI

4.3.3 Plasmid profiling, curing and antibacterial activity

The *Shewanellae* sp demonstrated to possess a plasmid longer than 10kb whilst *Bacillus* sp SWI1 (~>10kb) shown the presence of a single plasmid. The bacterial strain SWI8 showed a plasmid above 10kb and two plasmids of <10kb. No bands appeared after plasmid curing. The cultures retained their antagonistic activity even after plasmid curing, suggesting that the antagonistic activity of the bacterial isolates used in the present study was not encoded by plasmid, and the genes encoding the antagonistic product might be present within the genome. The antibiotic whose biosynthesis was determined by the SCPI plasmid of *Streptomyces coelicolor* ~3(2) had been characterized as methylenomycin A (2-methylene-cyclopentan-3-one-4,5-epoxy-4,5-dimethyl-carboxylic acid) (Wright 1975). Plasmid linkage of bacteriocin activity was reported (Schillinger, 1989). In contrast, chromosomally encoded a class II bacteriocin LCI protein of *Bacillus amyloliquefaciens* Bg-C31 was also reported (Hu et al. 2010).

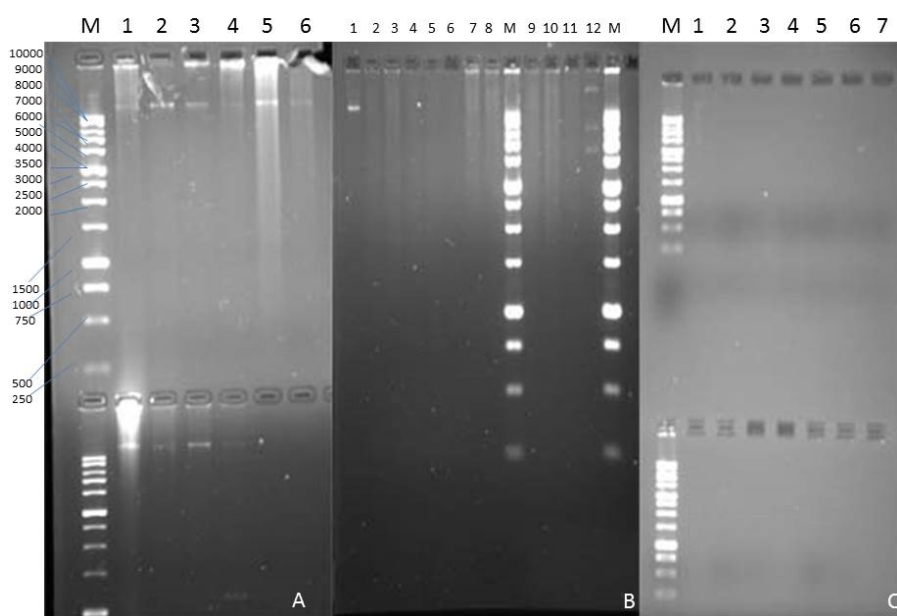


Figure 4.3

Plasmid profiles of the antagonistic isolates before and after curing. (A) Gram negative plasmid profile 4th lane (down) *V. alginolyticus*, M(Molecular marker) (B) Plasmid profiles of *Bacillus* strain Lane 1 (SWI1), 12th Lane (SWI8), M(Molecular marker) (C) Plasmid profiles of the strains after curing, M(Molecular marker). Molecular marker used is Gene Ruler™ 1kb DNA Ladder (Thermo scientific, 250bp-10,000bp).

4.3.4 Identification and analysis of PKS and NRPS gene fragments

The PKS specific primers were successful in obtaining the PCR amplicons that showed any significant homology to the sequences deposited in Gene bank. No correct products were detected when the NRPS primers were used for PCR. The negative results from the initial NRPS and PKS PCRs were also confirmed through subsequent annealing-temperature gradient NRPS and PKS PCRs. The primers used in the study are shown in the Table 1. Among the 23 candidate antagonistic isolates 8 were found to be PKS positive with an amplicon of PKS gene (~0.7kb). All the positives were found to be the genus *Bacillus*. The PKS primers couldn't amplify the *Shewanella* isolates. To verify the amplified product, the sequenced results obtained through cloning were subjected to blastx analysis in GeneBank. Further the DNA sequences were translated and the deduced amino acid sequences were also analyzed through blastp program of NCBI. From the

blast analysis report it has found that 4 of the *pks-I* positive isolates were having sequence similarity with *Bacillus subtilis* (99%) PKS and remaining 4 sequences were similar to the gene sequences reported from *Bacillus amyloliquefaciens* (99%). All of the 8 bacterial isolates with an amplified *pks-I* gene product exhibited antibacterial activities against multiple aquaculture pathogens reporting broad spectrum antagonistic potential (Table 2). PCR detection of type I polyketide synthase genes in myxobacteria has shown that most of the sequences detected in *Sorangium cellulosum* EW-4 were similar to those in *S. cellulosum* YA-2. Often, but not always, PKS in one strain of *Cystobacterineae* was similar to that in another strain of *Cystobacterineae*; however, most other sequences were nonredundant, indicating that different strains have different PKS genes. (Komaki et al. 2008). We chose to limit our analysis to PKSs and NRPSs, since these two classes participate in the synthesis of many diverse secondary metabolites. In addition, they usually encode easily recognizable large multimodular polypeptides that often comprise a large fraction of gene clusters (Donadio et al. 2007).

Polyketides and nonribosomal peptides have been immensely concerned over the past few decades, and numbers of various novel polyketide and non-ribosomal peptide compounds have been found from marine-derived microbes, most of which showed different biological activities and ecological functions (Zhou et al. 2011). Polyketides, nonribosomal peptides, and PKS/NRPS hybrid compounds are important classes of natural products and include many important drugs. Phycochemical studies showed the ability of seaweeds to produce and store polyketide as polycyclic ether macrolides and open chain polyketides. Although macrolides produced by terrestrial microorganisms have been used for long in human therapeutics, microlides from marine algae is a recent citation (Cardozo et al. 2007). Compounds of polyketide origin, with bioactivity have been isolated from seaweed and have reported to have structural similarity to the known compounds of terrestrial cyanobacteria. It is apparent that seaweeds use targeted antimicrobial chemical defense strategies and that secondary metabolites important in the ecological interactions between marine macroorganisms and microorganisms could be a promising source of novel bioactive compounds, but this hypothesis has rarely been tested (Kubanek et al. 2003). In support, it was found that the deduced

amino acid sequence of type III PKS (SbPKS) from a brown seaweed, *Sargassum binderi*, sharing a higher sequence similarity with bacterial PKSs (38% identity) than plant PKSs (Baharum et al. 2011). This further strengthened the hypothesis of ecological interactions between the seaweed host and their associated bacterial flora.

In the present report 23 antagonistic isolates with broad spectrum activities against aquaculture pathogens were further screened for the secondary metabolite genes. Among these only 8 were able to amplify the desired genes. The possible absence of the screened amplicons might be because the primers used were not suitable for the strains (Schirmer et al. 2005) or the coding genes for the antimicrobial products of the screened strains might be different from that of *pks* or *nrps* genes. Our results validated the statement that there are examples of strains possessing the functional genes with no inhibitory activity and vice versa (Zhao et al. 2011). Further the existence of cultured isolates with potential to synthesize bioactive compound and without a metabolite gene amplified product showed that culturing remains a powerful resource for exploring bioactive metabolites of bacterial origin (Penesyanyan et al. 2009). Even though the cultivation based studies possess some limitations, it remains essential as it provides opportunities to study and understand microbial ecology, physiology, and to design antibiotic screening assays (Ali et al. 2012). Further the absence of screened metabolite gene products in the tested active strain indicated the possibility of other biosynthetic genes in those strains. It is therefore that the biosynthetic gene guided screening of bioactive bacterial population needs to consider the conserved gene sequences of other biosynthetic pathways (Zhu et al. 2009).

On the basis of the architecture and mode of action of the enzymatic assembly lines, PKSs are classified into type I, type II and type III. Type I PKSs refers to linearly arranged and covalently fused catalytic domains within large multifunctional enzymes, whereas the term type II indicates a dissociable complex of discrete and usually monofunctional enzymes. Furthermore, a third group of multifunctional enzymes of the chalcone synthase type is denoted as type III PKSs (Hertweck 2009). A phylogeny based on the KS domain sequences from other well

described organisms can be employed to determine the structural similarity of the obtained KS domain sequences (Zhu et al. 2009). The phylogeny of the sequence KS domains characterized the deduced amino acid sequences as of type I bacterial PKSs (Figure 3). The deduced amino acid sequences obtained in the study were aligned with the relative sequences of the GeneBank (Figure 3). The phylogenetic study showed that amplified gene products of the present study were of bacterial type I PKSs. Earlier studies in sponge associated bacteria too found that the bacterial strains to harbor type I bacterial PKSs (Zhu et al. 2009; Zhang et al. 2009). The KS domain sequence based phylogeny further clustered four sequences under the present study with *B. subtilis*, and the remaining four with *B. amyloliquefaciens*. Hence the KS domain sequences enabled us to clearly differentiate *B. subtilis* from the *B. amyloliquefaciens* strains, which could be done through 16S rRNA gene based phylogenetic approach. *B. cereus* strain isolated in the present study was unable to amplify the metabolite gene product. Multiple sequence alignment of the sequenced data with the known sequences from the GeneBank further enabled to identify the conserved sequence motif TACSSSLVA. KS domain conserved residues from the sponge, *Hymeniacidon perleve* associated bacteria has been reported as VDTACSSSLVA (Zhu et al. 2009). In our study this sequence motif amino acids have shown some variations at certain specific sites. In *B. subtilis* the acidic amino acid, aspartate, located at the third position from the cysteine active site in the N terminal is replaced by glutamate. Likewise in *B. amyloliquefaciens* the amino acid, valine, was located at the fourth position from the cysteine active site in the N terminal is replaced by isoleucine. However, due to the structural similarities of acidic amino acids aspartate (2-aminosuccinic acid) with glutamate (2-aminopentanedioic acid) and isoleucine (2-amino-3-methylpentanoic acid) with valine (2-amino-3-methylbutanoic acid), it is apparent that the KS domains of the bioactive *Bacillus* strains in the present study shared a common catalytic mode of action. Due to their versatile assemblage mechanism, polyketides exhibited remarkable diversity both in terms of structure and biological activities. To date, only a small fraction of the antimicrobial molecules potentially produced by Gram-positive bacteria has been characterized for their structures. The

recent advances in genome sequencing highlighted the genus *Bacillus* as a potentially important source to produce antibiotic-like compounds (Fickers 2010).

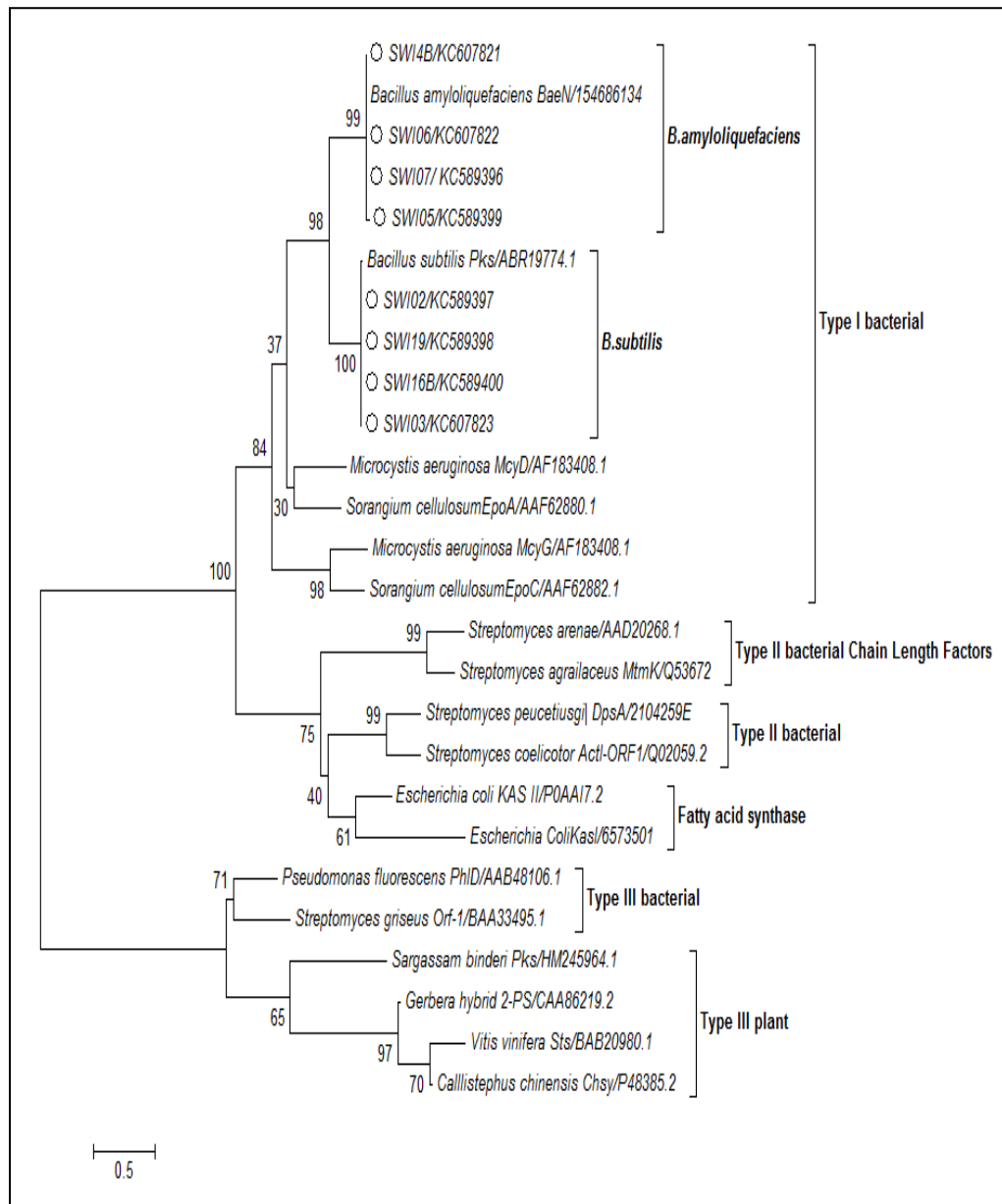


Figure 4.4

Molecular phylogeny analysis of ketosynthase regions with respect to diverse range of ketosynthase domains including Type I, II and III. The evolutionary history was inferred by using the Maximum Likelihood method based on the Whelan and Goldman model. A discrete gamma distribution was used to model evolutionary rate differences among sites. The tree with the highest log likelihood is shown. The sequences in the experiment are preceded by circles

			*	
SWI02	MIPSVGNRM	SYFLNIHGPS	EEVETACSSS	LVAIHRAVTA
SWI19	MIPSVGNRM	SYFLNIHGPS	EEVETACSSS	LVAIHRAVTA
SWI16B	MIPSVGNRM	SYFLNIHGPS	EEVETACSSS	LVAIHRAVTA
SWI03	MIPSVGNRM	SYFLNIHGPS	EEVETACSSS	LVAIHRAVTA
Pks	IIPSVGNRM	SYFLNIHGPS	EEVETACSSS	LVAIHRAVTA
NidKS2	SAGSVASGRV	AYTLGLQGPA	LTVDTACSSS	LVALHLAVQS
EryA	NSASVLSGRI	AYTFGWEGPA	LTVDTACSSS	LVGIHLAMQA
PimS0	TAGSAVSGRI	AYTYGLEGPA	LTVDTACSSS	LVALHLACRS
EpoA	TMPSVGAGRI	SYVLGLRGPC	VAVDTAYSSS	LVAVHLACQS
McyD	TSVSMAAGRL	SYVLGLQGPA	MTIDTACSSS	LVAIHLAYNA
NJ6-3-2	VMMTMLSRI	SHTFDNFGPS	MSIDTACSSS	IVALDMACKS
SWI05	TSPSVGNRV	SYTLNLHGPS	EEIDTACSSS	LVAIHHA VSS
SWI07	TSPSVGNRV	SYTLNLHGPS	EEIDTACSSS	LVAIHHA VSS
SWI06	TSPSVGNRV	SYTLNLHGPS	EEIDTACSSS	LVAIHHA VSS
SWI4B	TSPSVGNRV	SYTLNLHGPS	EEIDTACSSS	LVAIHHA VSS
BaeN	TSPSVGNRV	SYTLNLHGPS	EEIDTACSSS	LVAIHHA VSS

Figure 4.5

Amino acid sequence alignments of active sites of Type I KS domains. The characteristic conserved motifs of Type I KS domains were predicted from the multiple alignments of active sites. The cysteine active site and the conserved amino acid sequence motif are marked by asterisk and frame, respectively. The sequences in this study are from seaweed associated bacteria and are SWI02, SWI19, SWI03, SWI16B, SWI05, SWI07, SWI4B and SWI06. Other reference sequences aligned sequences in the GeneBank were derived from *pks* (*B. subtilis*, ABR19774.1), *NidKS2* (*Streptomyces aelestis*, AF016585), *EryA* (*Saccharopolyspora erythraea*, CAA44448), *PimS0* (*Streptomyces natalensis*, AJ278573), *EpoA* (*Sorangium cellulosum* AF217189), *McyD* (*Microcystis aeruginosa*, AF183408.1), *NJ6-3-2* (*Pseudoalteromonas sp.*, DQ666948), and *BaeN* (*B. amyloliquefaciens* 154686134)

4.4 Conclusions

The results demonstrated that antimicrobial activity cannot be solely assessed by metagenomic studies as some strains may escape the amplification of the desired genes. In that case antimicrobial potential may only be assessed by screening of the inhibition potential with the desired indicator organisms. Further metabolite gene based screening of bioactive organisms that exploit the gene clusters of biosynthetic pathways other than *pkss* and *nrpss* is recommended. It can be concluded that the polyketides are the widespread metabolites of seaweed-associated bacterial population particularly belonging to *Bacillus* species. The present work may have an impact on the exploitation of seaweed associated bacterial polyketides for pharmaceutical and biotechnological applications.

CHAPTER 5

BIOPROSPECTING OF ANTIBACTERIAL METABOLITES IN SEAWEED ASSOCIATED BACTERIAL FLORA

5.1 Background of the study

Novel secondary metabolites from marine epibiotic bacteria are attracting attention because of the growing demand for new compounds of natural origin, having potential applications in pharmaceutical or industrial fields (Kanagasabavathy et al. 2006). Marine algae and bacteria are an inexhaustible source of chemical compounds that produce a wide variety of biologically active secondary metabolites (Gomez et al. 2010). The recovery of strains with antimicrobial activity suggests that seaweed represent an ecological niche which harbors a specific microbial diversity worthy of further secondary metabolites investigation. Despite the seaweed associated microbial flora have been reported as a source of natural compounds with inhibitory activity very little is known about the chemical nature of such compounds. Seaweed–bacterial associations are appealing from evolutionary, ecological, and applied perspectives and there is a strong need to integrate aspects of ecology, cell biology, and in order to understand the production and the distribution of the bioactive molecules *in situ* as well as their ecological impact on the macroalgal–bacterial interactions (Hollants et al. 2012; Goecke et al. 2010). Hence the current chapter is directed towards chemical nature and the mode of action of the extracellular antibacterial compounds produced by seaweed-associated bacterial isolates with antibacterial activity through bioassay guided purification .

5.2 General materials and methods

5.2.1 Microbial strains used in the study

Pathogenic microbes used for the study have been described under the section 3.2.4. of chapter 3 The seaweed associated bacterial isolates were isolated (chapter 3 section 3.2.2) and assayed for their ability to inhibit selected pathogenic microbes (chapter 3 section 3.2.5). The isolates for metabolite purification with antibacterial activity used in the study were selected based on their inhibition spectrum (Chapter 3, Table 3.2) and the positive hit for metabolite gene (Chapter 4. 2.5 and 4.3.4).

The selected strains are

- 1) *B. subtilis* MTCC 10403 associated with *Anthophycus longifolium*(SWI2)
- 2) *B. subtilis* MTCC 10407 associated with *Sargassum myriocystum*(SWI 19)
- 3) *B. amyloliquefacens* MTCC 10456 associated with *Laurentia papillosa*(SWI4B)
- 4) *B. amyloliquefacens* MTCC 10456^B associated with *Padina gymnospora* (SWI 7)

#B (Biochemically identical to MTCC 10456)

5.2.2 Antibiotic resistance and abiotic stress tolerance

The candidate strains were assayed for their antibiotic resistance patterns by using the commercially available antibiotic discs (Himedia, India) following the disc diffusion method (Bauer et al. 1966). The selected isolates were screened for their ability to survive under differing environmental conditions like temperature, pH and salinity on Nutrient agar plates.

5.2.3 Optimization of growth conditions for optimized compound production

Production of antibacterial substance(s) by bacterium was evaluated in nutrient broth. The effect of temperature and initial pH on growth and antibacterial

production were monitored by using a modifying method of Hasegawa et al. (2005). The optimum time for maximized production was also noted.

5.2.3.1 Optimization of time

The microorganism under the study was inoculated in nutrient broth and incubated at 30°C for 5 days. Every 24 hours, 5 mL broth was withdrawn, centrifuged (10000 rpm for 5 min). The culture free supernatant was assayed for antibacterial activity by disc diffusion over Muller Hinton Agar plates. The plates were incubated overnight at 30°C and the inhibitory activity was recorded.

5.2.3.2 Optimization of temperature

The microorganism under the study was inoculated in nutrient broth and allowed to grow for 4 days at different temperatures (4°C, 10°C, 20°C, 30°C, 37°C, 50°C, and 60°C). After the fifth day the broth was withdrawn and centrifuged (10000 rpm for 5 min). The supernatant was assayed for activity to inhibit selected pathogenic microorganisms using disc diffusion method over Muller Hinton Agar plates. The plates were incubated overnight at 30°C, and the inhibitory activity was recorded.

5.2.3.3 Optimization of pH

Nutrient broth was prepared at varying pH (5, 7, 8, 9, 10, 11 and 12). The microorganisms under the study was inoculated in nutrient broth and allowed to grow for 4 days at different pH. The broth was harvested after the fifth day and clarified by centrifugation. The supernatant was assayed for activity to inhibit selected pathogenic microorganisms using disc diffusion method over Muller Hinton Agar plates. The plates were incubated overnight at 30°C and the inhibitory activity was recorded.

5.2.4 Chemicals and reagents

All chemicals were of analytical, spectroscopic or chromatographic reagent grade, and were obtained from E-Merck (Darmstadt, Germany). All reagents and chemical solvents used for products isolation were of analytical grade or higher.

5.2.5 Preparation of crude extracts from cultures

The preparation and recovery of secondary metabolites were carried out by a surface culturing method over solid nutrient agar plates. Briefly 4 liters of Nutrient agar media was prepared and plated to furnish 200 Nutrient agar plates. The plates were allowed to solidify and were inoculated with the microbial culture in a zigzag manner by utilizing the entire plate surface. The cultures were incubated for 5 days to allow the maximum secretion of secondary metabolites. The microbial cultures were then scraped off aseptically and the spent agar was collected in a sterile beaker. The adsorbed products were subsequently extracted with solvent by homogenization (Arrow Engineering CO; INC, Pennsylvania Ave, U.S.A) followed by refluxing. The extract filtered through the filter paper (Whatman No.1) assisted with a drying agent (sodium sulphate), and the pooled filtrate was concentrated (50°C) in a rotary vacuum evaporator (Heidolf, Germany). Evaporation of the solvent under reduced pressure yielded the crude extract from the total culture volume of 4 liters.

5.2.6 Determination of antibacterial activities by agar diffusion method

Sterile disks (HiMedia, India) containing 10 µl of crude extract or 10 µl of purified compound in solvent (the solvent traces were removed by drying in nitrogen and the final compound concentration on the disk was 100 µg) were placed on fresh plates of Mueller-Hinton agar (Difco) seeded with suspensions (10^5 CFU/ml) of overnight cultures of the test microorganisms. The diameters of the zones of inhibition of growth around the disks were measured after incubation periods of 18 h at 37°C. Antibiotic disc for gram negatives namely Octodiscs[®] G-I minus (OD005) (HiMedia, India) was used to compare the results. The antibiotics used were ampicillin (A, 10 µg/disk), ciprofloxacin (Cf, 10 µg/disk), colistin (Cl, 10 µg/disk), co-trimoxazole (Co, 25 µg/disk), gentamicin (G, 10 µg/disk), nitrofurantoin (Nf, 300 µg/disk), streptomycin (S, 10 µg/disk), and tetracycline (T, 30 µg/disk).

5.2.7 Analysis

5.2.7.1 Chromatographic analyses

5.2.7.1A Preparative thin layer chromatography (*prep-TLC*)

Prep-TLC was performed on pre-coated TLC plates with silica gel 60 F₂₅₄ (layer thickness 0.2 mm; 20 x 20 cm; Merck KGaA, Darmstadt, Germany) using different solvent systems as needed. The band separation on TLC was detected under UV lamp at 254 and 366 nm.

5.2.7.1B Flash column chromatography (*FCC*)

Flash column chromatography was performed on Biotage SP, SP1-B1A, and Biotage AB, Sweden using pre-packed flash chromatography cartridges (Biotage No. 25 + M 0489-1). The flash cartridges were packed with Biotage® HP-Sphere™ spherical silica; these cartridges have the highest loading capacity, lowest backpressure and can withstand greater flow rates. The solvent systems were decided based on the TLC data. Samples were dissolved in a small volume of the same solvent used and the resulting mixture was packed onto the column using a special syringe. The cartridges were dried by purging nitrogen and assembled to the instrument. The collection wavelength was set prior to loading by scanning the compound in a UV spectrophotometer. Using step gradient elution with non-polar solvent (here, *n*-hexane or DCM) and increasing amounts of polar solvents (e.g. EtOAc or MeOH) successive fractions were collected. The samples are collected in 12mL test tubes and pooled based on the chromatogram pattern.

5.2.7.1C Vacuum column chromatography (*CC*)

Normally, the columns were dry silica gel GF₂₅₄ pre-packed, of 18 cm height and inner diameter of 12 cm, vertically clamped. The column was filled and saturated with the desired non-polar solvent in the mobile phase (eg: *n*-hexane) prior to sample loading. The samples were dissolved in a small volume of the same solvent used and the resulting mixture was then packed onto the top of the column using special syringe. Using step gradient elution with non-polar solvent (here, *n*-hexane or DCM) and increasing amounts of polar solvents (e.g. EtOAc or MeOH)

successive fractions were collected. The mobile phase (gradient elution) was pumped through the column with the help of peristaltic pump resulting in sample separation.

5.2.7.1D High Performance Liquid Chromatography (HPLC)

HPLC was used for the evaluation of the efficiency of separation, and to understand the product purity. HPLC was performed on Prominence UFLC (Shimadzu, Japan) equipped with a SPD-M20A High Performance Liquid Chromatography PDA

5.2.7.2 Spectroscopic analyses

5.2.7.2A Fourier Transform Infra Red spectrometry (FTIR) and UV-visible spectroscopy

Fourier Transform Infra Red spectrometer (FTIR) spectra of the compounds under KBr pellets were recorded in a Thermo Nicolet, Avatar 370. The scanning was conducted in to mid IR range, i.e., between 4000-400 cm^{-1} . UV spectra were obtained on a Varian Cary 50 UV-VIS spectrophotometer (Varian Cary, USA).

5.2.7.2B Mass spectrometry (MS) and elemental analysis

The Gas Chromatography-Mass Spectrometry (GC-MS) analyses were performed in electronic impact (EI) ionization mode in a Varian GC (CP-3800) interfaced with a Varian 1200L single quadrupole Mass Spectrometer. ESI-MS spectra were acquired in the positive and negative modes with a turboionspray voltage, curtain gas, turbo temperature, and nebulizer gas of -4500 V, 30 psi, 500 °C, and 50 psi (positive mode) at a flow rate of 1.5 ml/min. Elemental analysis of the compounds was carried out using a Euro Vector elemental analyzer (model no. EA3011). Liquid chromatography-mass spectrometry experiments were performed on an Applied Biosystems QTrap 2000 (Applied Biosystems, Darmstadt, Germany) coupled to an Agilent 1100 HPLC system (Agilent, Waldbronn, Germany) using a Luna 5 μ C₁₈ column (100 Å, 100 × 4.6 mm, Phenomenex,

Aschaffenburg, Germany) or a Luna 3 μ C₁₈ column (100 Å, 50 × 1.0 mm, Phenomenex, Aschaffenburg, Germany) and a gradient of solvents A (0.1% HCOOH) and B (CH₃CN + 0.1% HCOOH; gradient 0% B to 100% B in 10 min) with a flow rate of 1.5 ml/min or 60 μ l/min, respectively. ESI-MS spectra were acquired in the positive and negative modes with a turboion spray voltage, curtain gas, turbo temperature, and nebulizer gas of -4500 V, 30 psi, 500 °C, and 50 psi (positive mode, flow rate at 1.5 ml/min. The exact molecular ion weights of the pure compounds have been acquired by direct injection in a high resolution mass spectrometer, and were compared with the MarinLit database (Royal Society of Chemistry, London, Burlington House, London W1J 0BA) dedicated to marine natural products.

5.2.7.2C Nuclear Magnetic Resonance Spectroscopy (NMR)

The ¹H and ¹³C-NMR spectra were recorded on a Bruker AVANCE III 500 MHz (AV 500) DRX 500 NMR spectrometer (Bruker, Karlsruhe, Germany) in CDCl₃ as aprotic solvent at ambient temperature with TMS as the internal standard (δ 0 ppm) equipped with 5 mm probes. The number of attached protons for the ¹³C-NMR signals was determined from DEPT experiments. Standard pulse sequences were used for Distortionless Enhancement by Polarization Transfer (DEPT), ¹H-¹H Correlation spectroscopy (¹H-¹H COSY for determining basic connectivity via J couplings through-bond), Nuclear Overhauser Effect Spectroscopy (NOESY for see through-space and conformation and for determining proximity of adjacent spin systems), Heteronuclear Single Quantum Correlation (HSQC for determining the narrower resonances for ¹H - ¹³C correlations), and Heteronuclear Multiple Bond Correlation (HMBC to correlate X-nucleus shifts that are typically 2-4 bonds away from a proton) experiments.

5.3 Isolation and purification of secondary metabolites

Description of isolation and purification of the secondary metabolites from seaweed associated bacterial isolates were divided into three different sections under chapter 5 based on the culture strains used as starting material..

CHAPTER 5A

BIOPROSPECTING OF *Bacillus subtilis* MTCC 10403 ASSOCIATED WITH *Anthophycus longifolium* (SWI 2) FOR ANTIBACTERIAL METABOLITES

5A.1 Materials and Methods

5A.1.1 Microbial strain used under the study

The microbial strain used for bioprospecting of antimicrobial compounds in the present study is MTCC 10403 associated with the brown seaweed *Anthophycus longifolium*. The seaweed associated bacterial isolates were isolated (chapter 3, section 3.2.2) and assayed for their ability to inhibit selected pathogenic microorganisms (chapter 3, section 3.2.5). The isolates for metabolite purification with antibacterial activity used in the study were selected based on their inhibition spectrum (chapter 3, Table 3.2; Figure 5A.1), and the positive hit for metabolite gene (chapter 4.2.5 and 4.3.4).

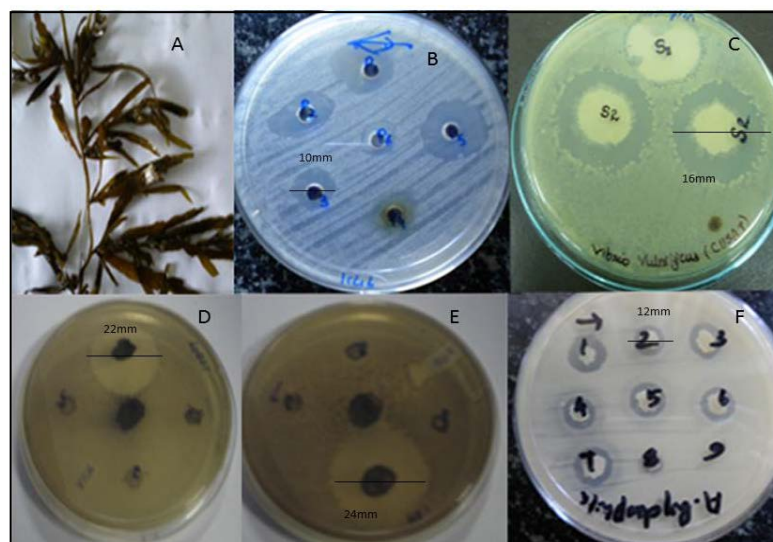


Figure 5A.1

Antagonistic spectrum of seaweed isolates SWI2: (A) Seaweed sample used for isolation of bacteria; (B) Well diffusion of culture SWI2 supernatant against *V. vulnificus* 1145; Spot over lawn assay of culture SWI2 against (C) *V. vulnificus* 1145; (D) *V. parahaemolyticus* 17802 (E) *V. parahaemolyticus* 451, and (F) *A. hydrophilla*

5A.1.2 Antibiotic resistance, abiotic stress tolerance

Antibiotic resistance and abiotic stress tolerance and enzyme production profile of the strain MTCC 10403 were analyzed using the methodology explained in 5.2.2.

5A.1.3 Optimization of time

The microorganism under the study was inoculated in nutrient broth and the optimum time for the antibiotic production with maximum inhibitory activity was analyzed as explained in 5.2.3.

5A.1.4 Optimization of temperature

The optimum temperature for the production of antibacterial compound for the strain MTCC 10403 was analyzed using the methodology explained under the section 5.2.4.

5A.1.5 Optimization of pH

The pH for the production of the active metabolite was standardized as described under the section 5.2.5.

5A.1.6 Preparation of crude extract for purification of secondary metabolites

The antibiotic-producing bacterium, *Bacillus subtilis* MTCC 10403 (SWI 2) was isolated from *Anthophycus longifolius*. The preparation and recovery of the secondary metabolites were carried out by a surface culturing method over solid nutrient agar plates (section 5.2.7). The adsorbed products were subsequently extracted with ethyl acetate at 70°C on a water bath under reflux. Evaporation of the solvent under reduced pressure yielded the ethyl acetate (EtOAc) extract. Subsequently the residual agar was extracted with CH₂Cl₂ (DCM) and CHCl₃ to furnish dichloromethane extract and chloroform extracts, respectively. These solvent extracts were evaluated for antibacterial activities (section 5.2.8); against the pathogens (listed in chapter 3 section 3.2.4) and the fractions, which showed significantly broad spectrum antibacterial activities and higher yields, were further purified by chromatographic techniques.

5A.1.7 Purification of secondary metabolites

The EtOAc fraction (2.3 g) of the *Bacillus subtilis* MTCC 10403 was subjected to flash column chromatographic purification (Biotage SP, SP1-B1A, Biotage AB, Sweden) (Fig.5.1) over silica gel (180-230 mesh, Biotage No. 25+M 0489-1), with a stepwise gradient of CH₂Cl₂/MeOH (0-100% MeOH). A collection wavelength of 236 nm was programmed in the flash chromatograph to provide a total of forty-three fractions (12 ml, F1–F23). These column fractions were evaluated for antibacterial activities (section 5.2.4), against the pathogens (listed in chapter 3, section 3.2.4) and the fractions, which showed significantly broad spectrum antibacterial activities and higher yield were further subjected to column chromatographic or preparative TLC (P-TLC)-guided purification using different solvent systems (EtOAc:*n*-hexane, MeOH:CHCl₃ or MeOH:EtOAc as mobile phases), whichever required. The schematic diagram showing the purification of *B. subtilis* MTCC 10403 associated with *Anthophycus longifolium* (SWI2) ethyl acetate extract was shown in Figure 5A.2.

5A.1.8 Analysis of pure fractions

The active fractions were subjected to chromatographic and spectroscopic analysis as explained earlier (section 5.2.9).

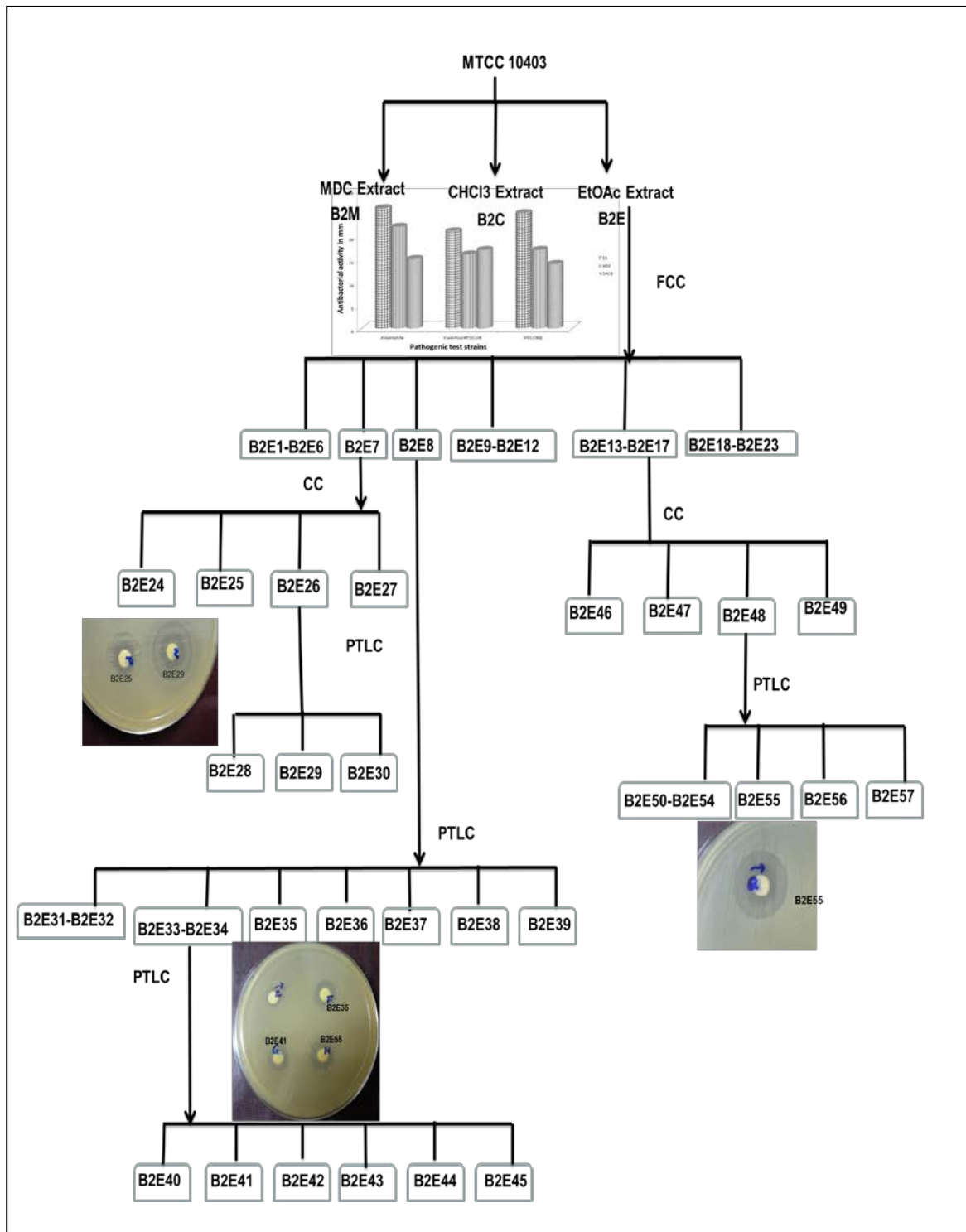


Figure 5A.2

Schematic representation of bioprospecting of *Bacillus subtilis* MTCC 10403

5A.2 Results and discussion

5A.2.1 Antibiotic resistance and abiotic stress tolerance

The bacterial strain was susceptible to all the antibiotics tested (Figure 5A.3) and was proved to be safe for laboratory work. The strain was able to grow from 25°C up to 55°C, and could withstand a pH range of 6 to 11.5 (Figure 5A.4). The bacterial strain could able to grow at a NaCl concentration from 2 to 10%. The ability of the seaweed associated bacterial isolate to grow under a wide range of environmental conditions might be a functional adaptation for their protective function in varying aquatic environment.

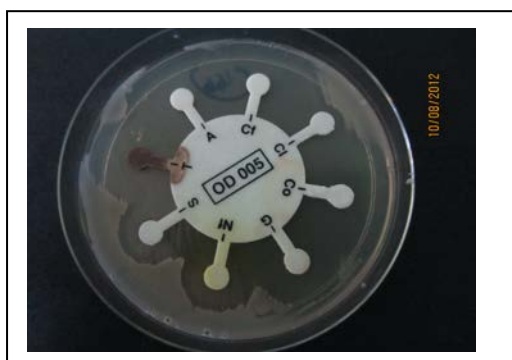


Figure 5A.3

Antibiotic sensitivity profile of MTCC10403

5A.2.2 Optimization of time, temperature and pH

Optimum production time is found to be after 72 hours and it declined after 96 hours. Optimum temperature for greater production of the antibacterial compound was found to be 20°C, whilst the optimum pH was 8.

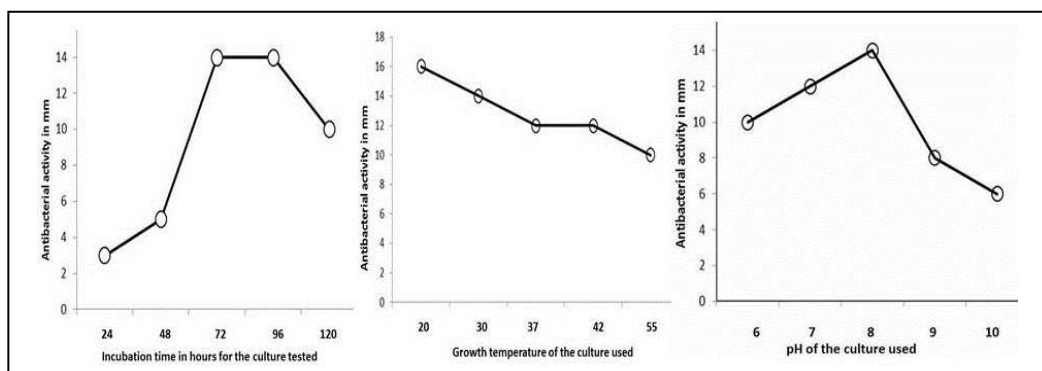


Figure 5A.4

Graphical representation of antibacterial compound production at different incubation time, temperature and pH

5A.2.3 Yield

The yield (g/L of the spent broth) of the EtOAc extracts of *B. subtilis* MTCC 10403 (0.570 g/L of the spent broth) was recorded maximum yield as compared with DCM (0.375 g/L of the spent broth) extract and CHCl_3 (0.207 g/L of the spent broth).

5A.2.4 Antibacterial activities of the crude extracts by agar diffusion method.

Antibacterial activity of *B. subtilis* MTCC 10403 solvent extracts to different pathogens *Aeromonas hydrophilla*, *V. vulnificus* MTCC 1145 and *V. parahaemolyticus* ATCC17802 were shown in the Figure 5A.5. It was apparent that the EA fractions were more active than other fractions of the *B. subtilis* MTCC 10403.

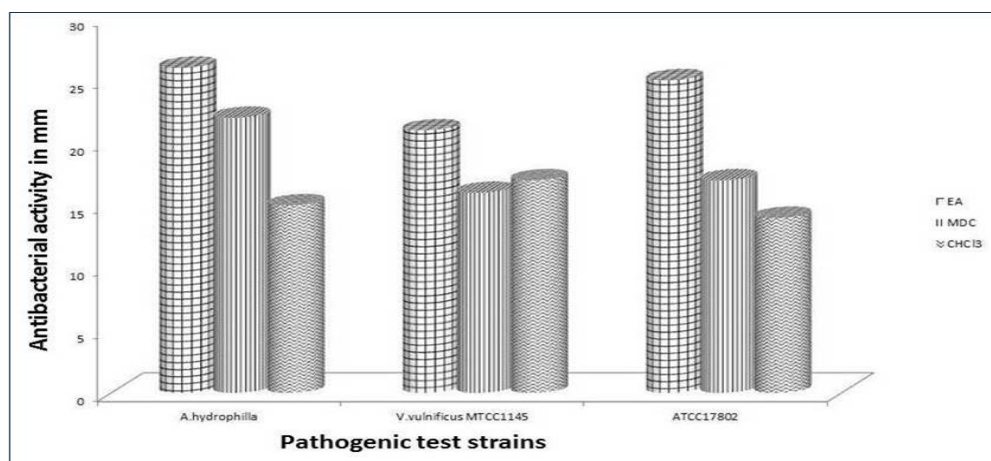


Figure 5A.5
Graphical presentation showing antibacterial activities of solvent extracts of *B. subtilis* MTCC10403 against the pathogenic strains

5A.2.5 Secondary metabolites from *B. subtilis* MTCC 10403 associated with *Anthophycus longifolium* (SWI2)

The yield, antibacterial activities of each column/P-TLC fractions were given in Table 5(1). The R_f values of all the P-TLC fractions were shown in Table 5A.1. Among the column fractions obtained from the EtOAc fraction of the MTCC 10403 extract, the fractions B2E13-B2E17 exhibited significantly greater antibacterial activity and similar TLC pattern.

Fraction B2E13-B2E17 as eluted by CH₂Cl₂/MeOH (3:2 to 1:1, v/v) was pooled together (81.8 mg) , and further applied to a silica gel column (80-120 mesh) to yield four sub-fractions (B2E46 to B2E49). Among these fractions, B2E48 (58mg) showed significantly higher antibacterial activity followed by B2E49 (6.2mg; 14mm). The sub-fraction B2E48 was purified by preparatory TLC (CH₂Cl₂/MeOH, 4:1, v/v) to afford B2E55 (**compound 1**) (99% purity, 10.2 mg; 16mm) and B2E57 (**compound 2**) (99% purity, 8 mg; 13 mm).

The column fraction B2E7 obtained from the EtOAc fraction of the MTCC 10403 extract, was a mixture with an inhibitory zone diameter of 12mm (123.6 mg). The fraction B2E7 was further charged on a silica gel column (80-120 mesh) to yield four sub-fractions (B2E24 through B2E27). The sub-fraction B2E25 seems to be pure to afford **compound 3** (99% purity, 9.6 mg). The sub-fraction B2E26 was purified by preparatory TLC (CH₂Cl₂/MeOH, 4:1, v/v) to afford B2E29 (**compound 4**) (99% purity, 8.3 mg).

Fraction B2E8 (92.3 mg) was purified by preparatory TLC (CH₂Cl₂/MeOH, 4:1, v/v) to afford nine sub-fractions (B2E31 to B2E39). Evaporation of solvents from the fractions followed by TLC over precoated silica gel GF₂₅₄ (particle size 15 mm, E-Merck, Germany) using CH₂Cl₂/MeOH (99:1, v/v) supported the purity of B2E35, **compound 5** (7.9 mg). The sub-fractions B2E33 and B2E34 were pooled together (24.3mg) and was purified by preparatory TLC (CH₂Cl₂/MeOH, 4:1, v/v) to yield B2E41 as **compound 6** (7.2 mg) (99% purity). Evaporation of the solvents from the fractions followed by TLC over precoated silica gel GF₂₅₄ (particle size 15 mm, E-Merck, Germany) using CH₂Cl₂/MeOH (99:1, v/v) supported the purity. The remaining fractions were not considered for purification due to either of lower yield or lesser activity.

Table 5A.1

Yield, activity and R_f values of the fractions at different purification stages

	Yield	R _t	R _f	Antibacterial activity
B2 EtOAc fraction (CC M/D)				
B2E-1 (100% D)	129g	-	0.9	NA
B2E -2 (0-5% M/D)	735mg	-	-	NA
B2E -3 (0-5% M/D)	178mg	-	-	NA
B2E -4 (0-5% M/D)	31mg	-	-	NA
B2E -5 (0-5% M/D)	104mg	-	-	10mm
B2E -6 (0-5% M/D)	87mg	-	-	13mm
B2E -7 (5-10% M/D)	123.6mg	-	-	12mm
B2E -8 (5-10% M/D)	92.3mg	-	-	15mm
B2E -9 (5-10% M/D)	28mg	-	-	10mm
B2E -10 (5-10% M/D)	86mg	-	-	2mm
B2E -11 (10-50% M/D)	26mg	-	-	15mm
B2E -12 (10-50% M/D)	3mg	-	-	3mm
B2E -13 (10-50% M/D)	16.3mg	-	-	20mm
B2E -14 (10-50% M/D)	18.5mg	-	-	24mm
B2E -15 (10-50% M/D)	12mg	-	-	25mm
B2E -16 (10-50% M/D)	21mg	-	-	18mm
B2E -17 (10-50% M/D)	14mg	-	-	21mm
B2E -18 (10-50% M/D)	15mg	-	-	11mm
B2E -19 (10-50% M/D)	13mg	-	-	3mm
B2E -20 (10-50% M/D)	88mg	-	-	1mm
B2E -21 (50-100% E)	36mg	-	-	13mm
B2E -22 (50-100% E)	9mg	-	-	1mm
B2E -23 (50-100% E)	3mg	-	-	2mm
B2E -7(CC)				
B2E -24(100%D)	42mg		-	NA
B2E -25(5%D)	9.6mg	41.793	0.6	13mm

B2E -26(2(10%D))	3.2mg	-	0.8	5mm
B2E -27(100%M)	1.6mg	-	0.96	NA
B2E 26(4:1MDC/M)PTLC				
B2E 28	6.9mg	-	0.2	NA
B2E 29	8.3mg	34.358	0.5	10mm
B2E 30	7mg	-	0.7	NA
B2E -8 (PTLC 100% DCM)				
B2E 31	2.3mg	-	0.15	NA
B2E 32	1.2mg	-	0.18	NA
B2E 33	5.7mg	-	0.22	NA
B2E 34	1.3mg	-	0.34	5mm
B2E 35	7.9mg	21.595	0.4	14mm
B2E 36	27.5mg	-	0.5	NA
B2E 37	13.6mg	-	0.6	NA
B2E 38	21.2mg	-	0.82	NA
B2E39	3.5mg	-	0.9	NA
B2E 33- B2E 34(PTLC)				
B2E 40	9.2mg	-	0.15	NA
B2E 41	7.2mg	29.395	0.2	12mm
B2E 42	10.9mg	-	0.3	NA
B2E 43	4.6mg	-	0.45	NA
B2E 44	2.3mg	-	0.6	NA
B2E 45	6.9mg		0.9	NA
B2E 13- B2E 17 (CC M/D)	81.8mg			
B2E 46	9.1mg	-	-	NA
B2E 47	5.6mg	-	-	
B2E 48	58mg	-	-	17mm
B2E 49	7.8mg	-	-	14mm
B2E 48 (PTLC)	58mg			

B2E 50	6.2mg	-	0.12	NA
B2E 51	4.3mg	-	0.25	NA
B2E 52	8.2mg	-	0.32	NA
B2E 53	1.8mg	-	0.4	5mm
B2E 54	12.6mg	-	0.5	6mm
B2E 55	10.2mg	6.220	0.7	16mm
B2E 56	8mg	9.171	0.9	12mm
B2E 57	2.6mg	-	0.96	NA

It is significant to note that the antibacterial activities of the crude extract against the test pathogens were greater than those exhibited by the purified bioactive compounds (Table 5A.1 and Figure 5A.5). It is apparent that many bioactive compounds may act synergistically to impart greater antibacterial activities against the test pathogenic bacteria used in this study.

5A.2.6 Structural characterization of secondary metabolites with antibacterial activity

5A.2.6.1 Structural characterization of Compound I (B2E55)

7-O-methyl-5'-hydroxy-3'-heptenoate-macrolactin: Amorphous solid; UV (MeOH) λ_{\max} (log ϵ): 226nm (3.72) and 248 nm (3.21); TLC (Si gel GF₂₅₄ 15 mm; CH₂Cl₂/MeOH 1:99, v/ v) R_f: 0.70; Rt: 6.22 min, IR ν_{\max} (KBr) cm⁻¹ : 970 (trans C=C oop bending), 1073.71 (unsaturated sec. alcohol C-O str.), 1121.80 (C-O-C symmetrical str.), 1282.20 (CH-OH in plane bending), 1376.96 (O=C-CH₂, C-H bending), 1461.43 (C-H asym-bending), 1640.23 (C=C str.), 1753.96 (α,β -unsaturated C=O str.), 2854.74 (-O-CH₂ sym C-H str.), 2923.22 (alkane C-H str.), 3014 (asym.alkene C-H str.), 3437.24cm⁻¹ (O-H str.); ¹H (CDCl₃, 500 MHz, δ ppm) and ¹³C NMR (CDCl₃, δ ppm) data, see Table 5A.2; HRMS (ESI) *m/z*: calcd. for C₃₁H₄₅O₇ 529.6422; found 529.6894 [M+H]⁺.

7-O-methyl-5'-hydroxy-3'-heptenoate-macrolactin, a new derivative of the macrolactin was isolated as amorphous solid upon chromatography over silica columns. The IR absorption band (in MeOH) at 3014cm^{-1} was due to $-\text{CH}$ stretching vibrations. The $-\text{OH}$ group in the skeleton exhibited free $-\text{OH}$ stretching vibrations near 3437cm^{-1} . The bending vibration bands near 1753cm^{-1} denoted the ester carbonyl absorption. The olefinic ($\text{C}=\text{C}$), and ether ($\text{C}-\text{O}-\text{C}$) groups have been symbolized by the absorption bands at 1640 and 1073cm^{-1} . The IR spectrum revealed a broad absorption band at ν_{max} 3500 to 3000cm^{-1} , attributed to hydroxyl functionality, and to olefinic system ($1200, 1121\text{cm}^{-1}$). The ultraviolet absorbance at λ_{max} ($\log \epsilon$) 226 (3.72) and 248 (3.21) nm were assigned to a chromophore with extended conjugation. Its mass spectrum exhibited a molecular ion peak at m/z 528 (HRESIMS m/z 529.689 $[\text{M}+\text{H}]^+$; D 0.0 amu), which in combination with its ^1H and ^{13}C NMR data (Table 5A.2, Figure 5A.6) indicated the elemental composition of $\text{C}_{31}\text{H}_{44}\text{O}_7$ as 7-O-methyl-5'-hydroxy-3'-heptenoate-macrolactin with ten degrees of unsaturation (Figure 5A.7). Seven degrees of unsaturation from double bonds of macrolactin ring, two degrees of unsaturation from double bonds of the substitution as (S, E) -methyl 5-hydroxyhept-3-enoate ($\text{C}_8\text{H}_{14}\text{O}_3$), and one degree from the ring of macrolactin were demonstrated. The molecular ion peak at m/z 528 appeared to undergo elimination of (5-hydroxyhept-3-enoic acid ($\text{C}_7\text{H}_{12}\text{O}_3$, m/z 144.1708) to yield 7-hydroxy substituted macrolactin at m/z 402.2450 ($\text{C}_{24}\text{H}_{34}\text{O}_5$), which underwent dehydration ($-\text{H}_2\text{O}$) to afford a fragment with m/z 386.2580 ($\text{C}_{24}\text{H}_{34}\text{O}_4$). The appearance of the fragment at m/z 126.1507 indicated the presence of 6-ethyl-3H-pyran-2 (6H) -one moiety ($\text{C}_7\text{H}_{10}\text{O}_2$), resulted from the intramolecular rearrangement and dehydration of 5-hydroxyhept-3-enoic acid via the intermediate 6-ethyl-3H-pyran-2, 2 (6H) -dial (Figure 5A.8)

The ^1H NMR in conjugation with ^{13}C -NMR recorded the presence of two methyl signals at δ 0.81 and δ 1.30 ppm. The former was assigned to be due to the terminal methyl group at the side chain 5-hydroxyhept-3-enoate moiety, whereas the methyl group at δ 1.30 shifted downfield due to the acrylate moiety ($-\text{OC}(=\text{O})-\text{C}=\text{C}-$) at the β -position with respect to the deshielded methyl group. The methylene group protons at δ 2.60 and δ 2.04 ppm were assigned to be at 6 carbon position of the macrolactin ring structure, and the downfield shift (about δ 0.5 ppm) was due to

the presence of the conjugated butadiene moiety at one side and the side chain acetate group (-OC(=O)-C) attached to the macrolactin ring at its 7 carbon position. Three methylene groups have been assigned to occupy at the C20-22 positions of the macrolactin ring structure as heptenyl formate moiety. The protons of the -CH₂- group at δ 1.45, 1.43 ppm were at C22, and were deshielded due to the presence of the acrylate moiety (-OC(=O)-C=C-) at the β -position with respect to the deshielded methyl group. The methyl group protons at δ 2.07, 1.96 ppm (C-20) too appeared to be deshielded due to the conjugated double bond structure (butadiene) spanning from C16-C19 position of the macrolactin ring. The methylene protons at C21 position appeared at δ 1.81 and 1.60 ppm. The -CH₂- protons appeared in δ 1.94 and 1.78 ppm were due to the presence of the propanediol group, and have been assigned to be present at the C14 position in the macrolactin ring structure. The protons at δ 2.68 and 2.33 ppm shifted downfield due to the presence of -C=C- group at its α -position and a β -OH group. The methylene protons at δ 2.35, 2.26 ppm have been assigned to be present at the side chain 5-hydroxyhept-3-enoate moiety, and their downfield shift was due to the ester functionality at the α -position of the methylene protons and -C=C- at its β -position. The other -CH₂- group at δ 1.21 was a part of the terminal ethyl group of 5-hydroxyhept-3-enoate. The methine protons at δ 3.42 and 4.84 ppm were assigned to be present at the C13 and C15 positions in the macrolactin ring structure. The downfield shift appeared to be due to the propane-1, 3-diol moiety at C13 to C15. The methine proton at δ 4.84 appeared to be deshielded due to the presence of β -olefinic group extended by further conjugated structure. The carboxyl ester group at the C1 position of the macrolactin ring resulted in strong deshielding of the -CH- proton at δ 4.99 ppm, and therefore, has been assigned to be present at the C23 position of the macrolactin ring structure. The methine proton (given triplet of the doublet) at δ 5.05 ppm is characteristic of the junction point of the macrolactin ring (C-7) to that of the side chain 5-hydroxyhept-3-enoate moiety. The ¹H-NMR spectrum showed three exchangeable hydroxyl proton at δ 4.23 (1H, bs in CDCl₃), δ 3.79 (1H, bs in CDCl₃), and δ 3.16 ppm (1H, bs in CDCl₃), which disappeared upon addition of D₂O. The ¹³C NMR spectrum of the purified compound in combination with DEPT experiments indicated the occurrence of 31 carbon atoms in the molecule, including two ester carbonyl carbon at δ 165.16 and δ 168.2, fourteen methine carbons between δ 116.1 and 146 assigned to seven double

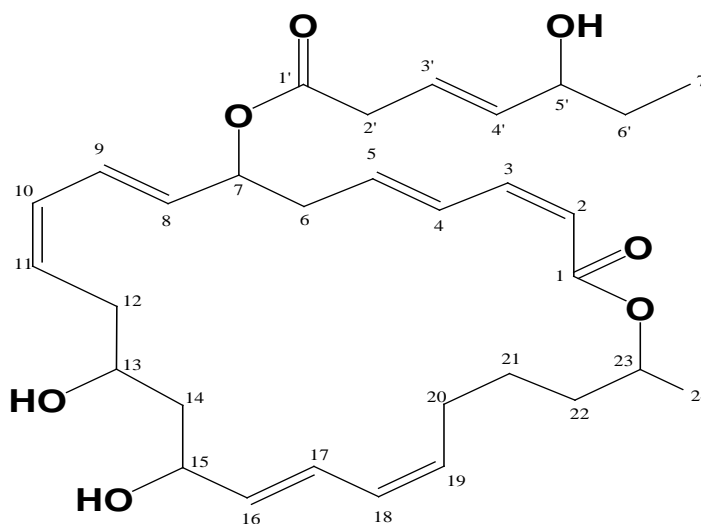
bonds, five oxygenated methine carbons between δ 67.5 and 75.4; and ten aliphatic carbons between δ 20.10 and 50.8 ppm. The ^{13}C NMR spectrum displayed two quaternary carbon (δ 165.16, 169.54 ppm) atoms bearing the carbonyl groups. The low field quaternary signals (^{13}C NMR) were in agreement with that to a quaternary carbon signal carrying the carbonyl groups at C-1 of the macrolactin ring structure and C-1' of the side chain (5-hydroxyhept-3-enoate) attached to the macrolactin framework at the 7-C position of the ring. This was supported by the relatively downfield shift of the H₂, 23 signals (δ 5.60, t and δ 4.99 ddq, respectively) and methylene signals at C-2' (δ 2.26, 2.35), which referred to a possible oxygenation in its vicinity. The side chain is substituted at C-7 with either a α - or β -oriented hydroxyl group at the 5' position. The position of the hydroxyl group at C-5' was further confirmed from the ^1H - ^1H COSY, HSQC, NOESY, and HMBC spectra. In the ^1H - ^1H COSY spectrum, the couplings were apparent between H-7/H-6, 8; H-13/H-12, 14; H-15/H-14, 16, and H-20/H-21/H-22/H-23, which support the presence of macrolactin skeleton. The point of cyclization of the ester in macrolactone ring was indicated by the low-field shift of H-23 at δ 4.99, which has been coupled with the H-24 methyl group at δ 1.30 (d, J = 6.1 Hz), which also gives clear ^1H - ^1H COSY correlation. Also, the ^1H - ^1H COSY correlations between H'-5/H-6/H-7 supported the presence of the terminal propanol moiety at the 5-hydroxyhept-3-enoate side chain. The proton and carbon connectivity deduced from HSQC and HMBC experiments confirmed the macrolactin framework attached to the side chain 5-hydroxyhept-3-enoate moiety at the 7th position of the macrolactin. The H-H and C-H connectivity apparent in the ^1H - ^1H COSY and HMBC spectra, respectively indicate that one of the three unsaturations was due to the macrolactin ring framework (Table 5A.2). In the HMBC spectrum, it was observed that H-12/C-10, 14; H-15/C-13, 16; H-20/C-19, 22; and H-21/C-1, 23, 24 were correlated with each other. In addition, a methine proton (H-7) was coupled to the olefinic tertiary carbon (C-9) and methine H-15 with C-16, 17. This indicated that these protons (H-7 and H-15) were connected to the olefinic tertiary carbon atoms. The proton at C-21 appeared to demonstrate long range HMBC correlation with ester carbonyl carbon at δ 165.16 (C-1). The proton at C-7 realized HMBC correlation at δ 169.54, which belong to the second ester carbon. The HMBC analysis revealed that the carbon at δ

75.4 (C-5'), bearing the hydroxyl group, correlated with a primary methyl proton δ 0.81 (H'-7).

The HMQC spectrum of the purified compound also revealed connections of the protons (H-2') to the methylene carbon at δ 50.8 ppm. Placement of the 5-hydroxyhept-3-enoic acid group at the C-7 was confirmed by the downfield shift of H-7 (δ 5.05) in the compound as compared to the baseline value (δ 4.34), and also by the long-range correlation of H-7 to the carbonyl carbon at δ 169.54 (C-1') in the HMBC spectrum (Jaruchoktawechai et al. 2000). The HMBC spectrum demonstrated long-range correlations of the methine proton (H-5') to the vinylic carbon at δ 139.0 (C-3') and methyl carbon at δ 14.1 (C-7'). These observed spectral data were indicative of the presence of the hydroxyheptenoic acid half-ester moiety, which was supported by the IR spectral data exhibiting intensely broad hydroxyl absorption from 3500 to 3000 cm^{-1} and ester carbonyl absorption at 1710 cm^{-1} . The geometric isomerisms of the olefinic protons have been established by the ^1H coupling constants suitable for the geometries (Z and E form). The relative stereochemistry of the chiral centers, particularly that of C-13 and 15 carrying the hydroxyl group of the macrolactin framework and that of C'-5, was deduced from the NOESY spectrum of the compound and the J-values. NOE couplings were observed between H α -13/H α -7 thus indicating that these groups must be equatorial and on the α -side of the molecule. NOE correlations between H β -23/H β -15/H β -20 and those among H-5'/H-15/H-23, indicated the close proximity of these groups and their β -disposition. Therefore, the C-1 carboxyl group is equatorial and α -oriented. The methine proton at C'-5 group did not exhibit NOE interactions with H-7 and H-13, and the methylene proton at C-14 (δ 1.78, m), which is in the α -face of the molecule, thereby indicating that H-7 is at the equatorial disposition. An interaction through the space of the hydroxyl protons at C-5' (δ 3.16, 1H, bs) and C-15 (δ 3.79, 1H, bs) with H-7 (δ 5.05, td) and H α -14 (δ 1.94, m in CDCl_3) is only possible for the α -orientation of the tertiary hydroxyl group on C-5' and C-15. The stereochemistry at the tertiary alcohol at C-15 position was established by the fact that H-15 has mutual NOE correlations with H-23, which had shown to be in the β -face of the molecule (axial configuration) under observation, and the secondary alcohol group that appeared as a broad singlet (at δ 4.23 ppm) has NOE interactions with H-13 and

H-7 in the molecule. This is only possible if the C-15 hydroxyl group lies on the α -side of the molecule.

Table 5A.2
NMR spectroscopic data of 7-O-methyl-5'-hydroxy-3'-heptenoate-macrolactin in CDCl₃.^a



Carbon no.	¹³ C NMR (DEPT)	H	$\delta^1\text{H}$ NMR (int., mult., J in Hz) ^b	¹ H- ¹ H COSY	HMBC (¹ H- ¹³ C)
1	165.16(C)	-	-	-	-
2	116.11 (CH)	2H	5.60(d, J=11.2)	-	-
3	143 (CH)	3H	6.74(t, J=11.1)	H-2, H-4	C-4
4	127 (CH)	4H	7.25(dd, 15.2, 11.1)	-	-
5	142.7 (CH)	5H	6.19(dt , J=15.3, 7.1)	-	-
6	42.69 (CH ₂)	6H ^a 6H ^b	6H ^a at 2.60(m); 6H ^b at 2.04(m)	H-7	-
7	73.2(CH)	7H	5.05 (td)	H-8, H-6	C-1 ¹ , C-8
8	139 (CH)	8H	5.71(dd, J=15.2, 6.1)	H-9	-
9	125.02(CH)	9H	6.40dd, 15.1, 11.3)	-	-
10	130.3.08(CH)	10H	6.17(m)	H-11	-
11	127 (CH)	11H	5.71(dt, J=10.6, 8.4)	H-12, H-10	-
12	38.08(CH ₂)	12 H ^a	12 H ^a at 2.68(m), 12H ^b	H-13	C-14

		12H ^b	at 2.33(m)		
13	67.5(CH)	13H	3.42(dd) (4.02,OH)	H-14	-
14	45.41(CH ₂)	14H ^a 14H ^b	14H ^a at 1.94(m); 14H ^b at 1.78(m)	-	-
15	67.5 (CH)	15H	4.84(dt,J=6.1,6.1) (3.79,OH)	-	C-13,C-16
16	135.20 (CH)	16H	5.80 (dd, J=15.4,6.2)	H-17	-
17	127 (CH)	17H	6.29(dd, J=15.1,10.6)	-	-
18	130.3 (CH)	18H	6.19(t,10.6)	H-19	-
19	135 (CH)	19H	5.72(ddd,J=14.2,7.0,6.7)	-	-
20	31.9 (CH ₂)	20H ^a 20H ^b	20H ^a at 2.07(m); 20H ^b at 1.96	-	-
21	24.30 (CH ₂)	21H ^a 21H ^b	21H ^a at 1.60(m); 21H ^b at 1.81(dt,11.2,5.2)	H-22	C-1,C-24,C-23
22	35.93(CH ₂)	22H ^a 22H ^b	22H ^a at 1.54(m); 22H ^b at 1.43(m)	-	-
23	71.72(CH)	23H	4.99(ddq,J=4.5,7.1,5.1)	H-24	-
24	20.10(CH ₃)	-	1.30(d, J=6.1)	-	-
1 ¹	169.54(C)	-		-	-
2 ¹	50.8 (CH ₂)	H ^a , H ^b	H ^a at 2.26; H ^b at 2.35	H-3 ¹	-
3 ¹	139 (CH)	-	4.06(dt, J=15.6,7.4)	H-4 ¹ , H-2 ¹	-
4 ¹	147 (CH)	-	6.18(dd,J=17.4,7.2)	H-3 ¹	-
5 ¹	75.4 (CH)	-	4.94(m) (3.16,OH)	H-4 ¹	-
6 ¹	31.94 (CH ₂)	-	1.21(m)	H-7 ¹	C-4 ¹ , C-7 ¹
7 ¹	14.1 (CH ₃)	-	0.81(t)	-	C-6 ¹

^a NMR spectra were recorded using the Bruker DPX 300 and AVANCE 300 MHz spectrometers.

^b Values in ppm, multiplicity and coupling constants (J/Hz) are indicated in parentheses. Assignments were made with the aid of the ¹H-¹H COSY, HMQC, and HMBC experiments.

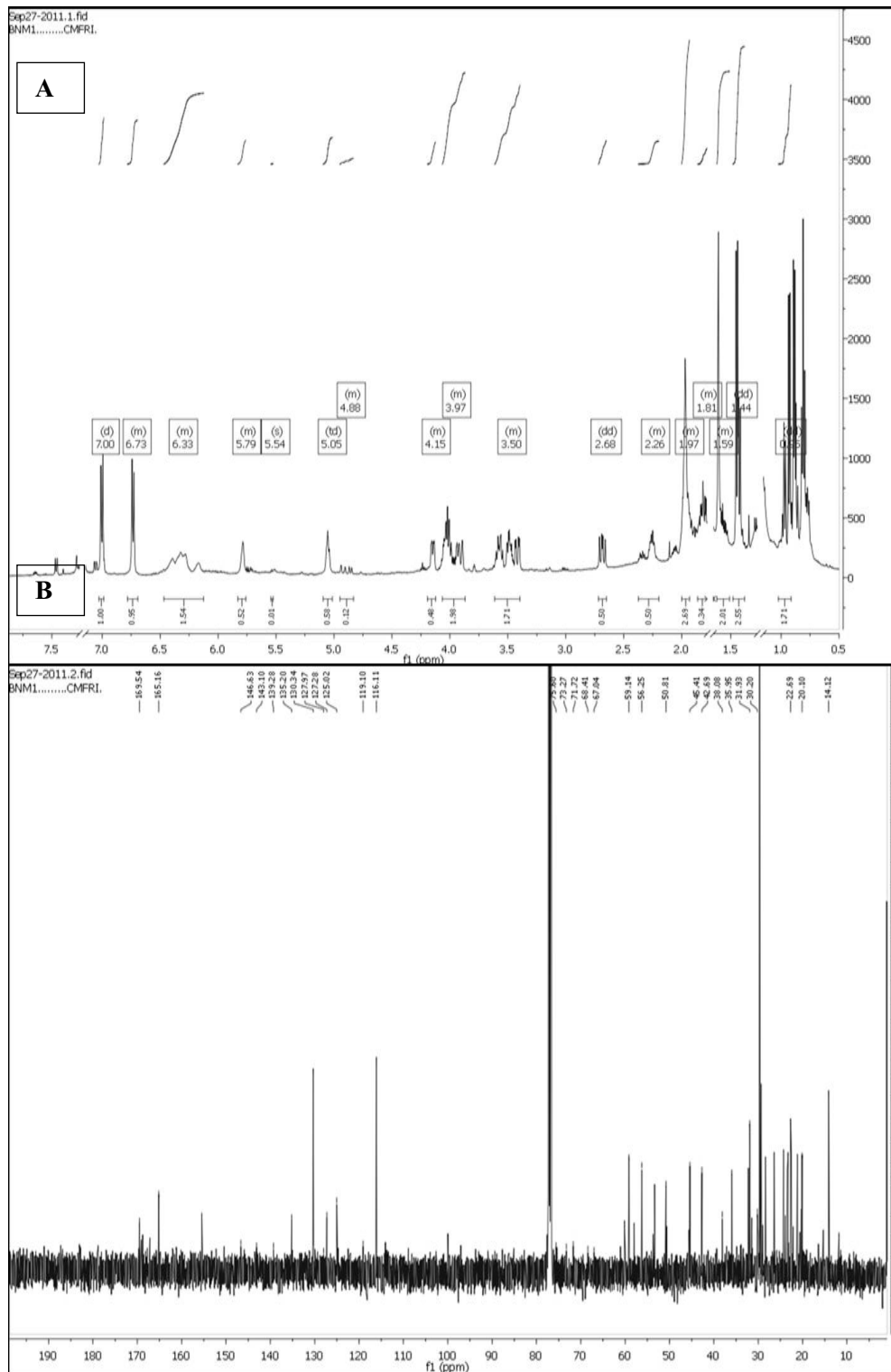


Figure 5A.6
(A) ¹H, (B) ¹³C NMR spectrum of compound 1

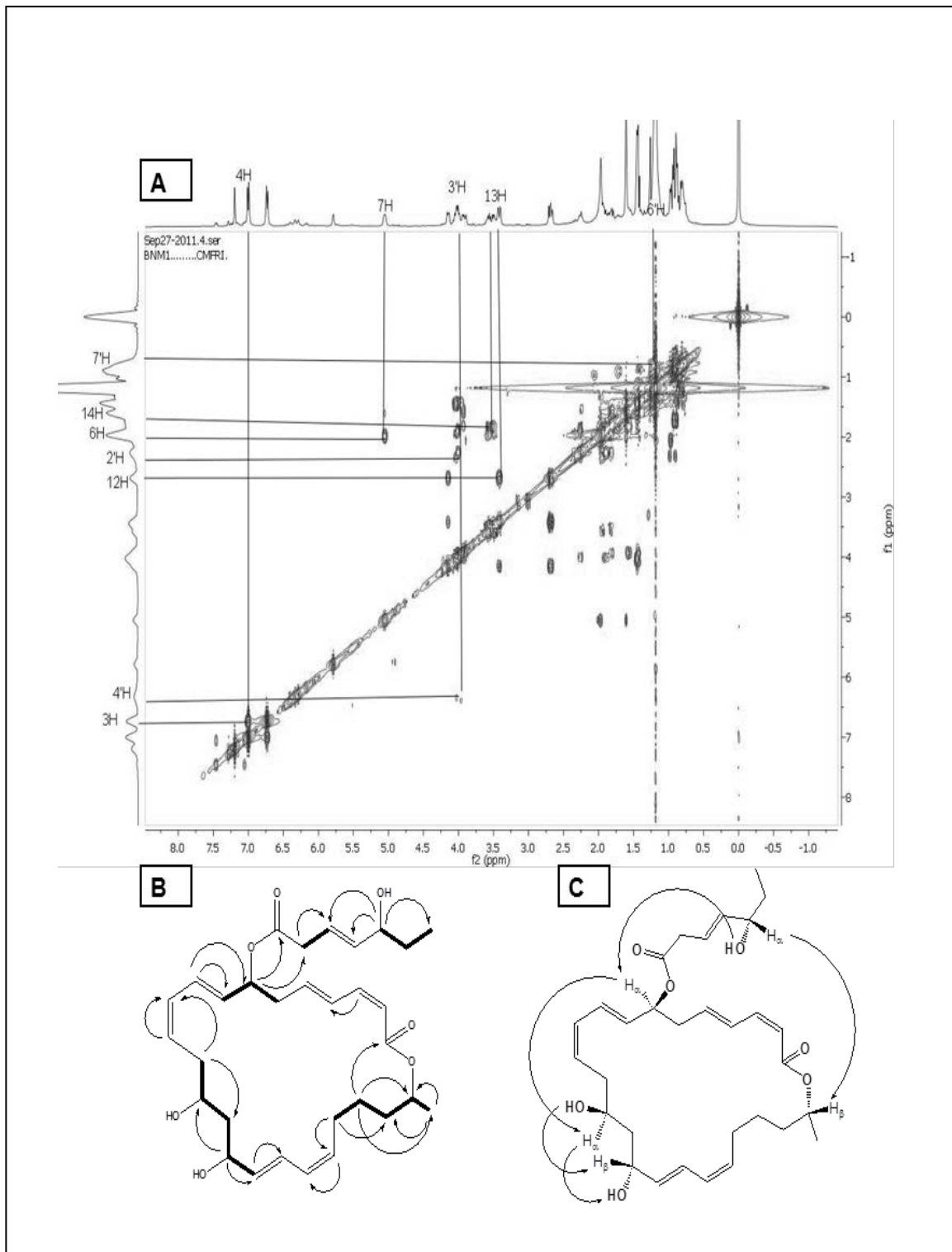


Figure 5A.7

2D NMR correlations as observed in 7-O-methyl-5-hydroxy-3-heptenoate-macrolactin. (A) The key ^1H - ^1H COSY couplings; (B) The ^1H - ^1H COSY couplings have been represented by the bold face bonds; The HMBC couplings are indicated as a double barbed arrow; (C) Key NOESY correlations.

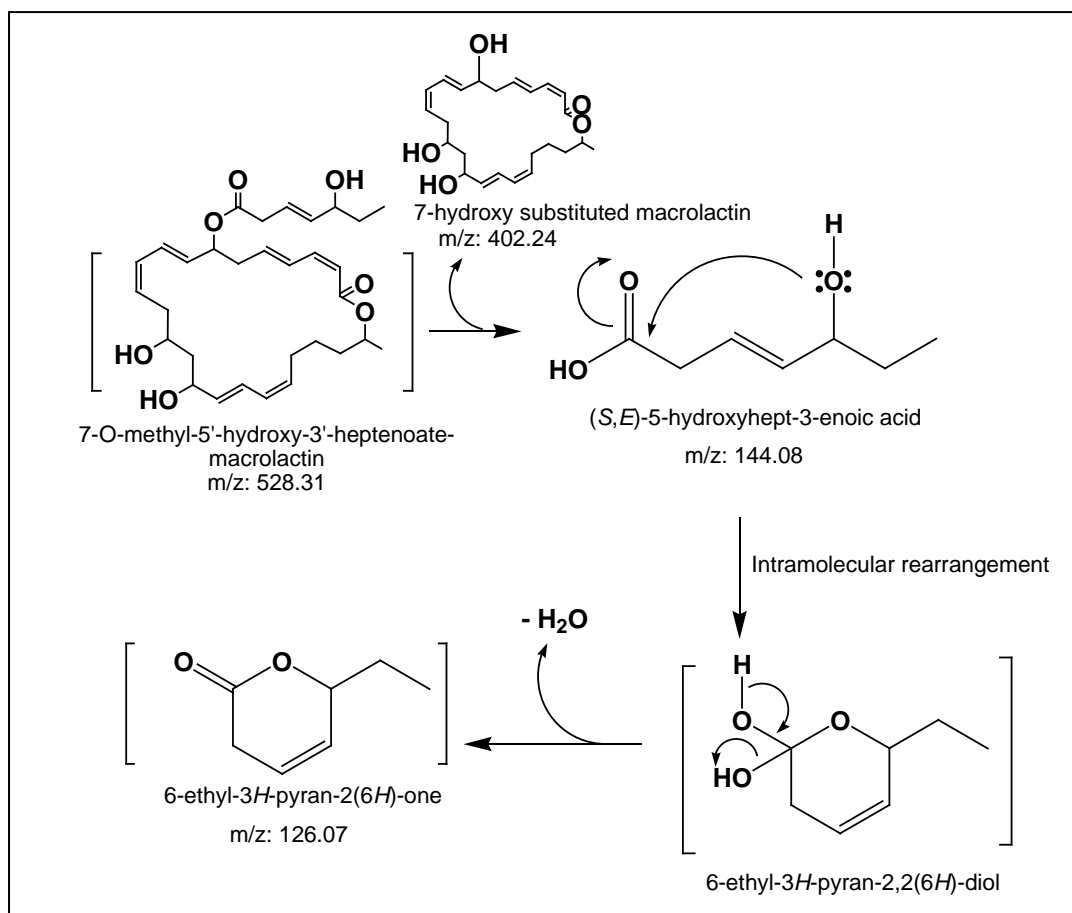


Figure 5A.8

Mass fragmentation pattern of 7-O-methyl-5'-hydroxy-3'-heptenoate-macrolactin.

The macrolactins possess twenty-four membered lactone ring with three isolated diene elements, and have been originally isolated from deep sea bacterium and *Actinomadura* sp (Gustafson et al. 1989; Nagao et al. 2001). A total of sixteen macrolactins have been chemically characterized (Gustafson et al. 1989; Marino et al. 2002). Macrolactin A was found to be most active compound in this series with potent antiviral properties, and was reported to possess antibacterial and anticancerous activities (Jaruchoktawechai et al. 2000; Gustafson et al. 1989). 7-O-succinyl macrolactin F and 7-O-succinyl macrolactin A were isolated from the ethylacetate extract of the marine *Bacillus* sp SC026, and were reported as antiviral (Jaruchoktawechai et al. 2000). The antibacterial activities of the macrolactins have

been compared by Nagao et al. (2001) who reported that the C₁₅-OH group is responsible for the target bioactivity of this group of compounds. However, there were no studies regarding the effects of the side chain attached at the C₇-OH position of the macrolactin ring system.

The physicochemical parameters of bioactive molecules such as polarizability, steric, and hydrophobic descriptors (lipophilicity, partition coefficients) have a major role to influence with biological activities (Chakraborty and Paulraj 2008; Clinq-Mars et al. 2008). The ability of any molecule to penetrate biological membranes is a primary factor in controlling the interaction of compounds with biological systems, and is dependent on lipophilicity factors as determined by the partition coefficient between 1-octanol and water (log P). It is of note that the terminal functional group as the 5-hydroxyhept-3-enoate moiety at the side chain C-7 position of the macrolactin ring system increase lipophilicity. The increased lipophilicity (log P 4.43) of 7-O-methyl-5'-hydroxy-3'-heptenoate-macrolactin as compared to the parent compound (log P 3.28) affords better penetration of the former through the lipoidal membrane barrier to arrive at the receptor site, thereby resulting in greater antibacterial activity of 7-O-methyl-5'-hydroxy-3'-heptenoate-macrolactin than the parent compound. The lipophilicity factors of the related compounds have been compared to demonstrate the lesser log P value of 7-O-methyl-5'-hydroxy-3'-heptenoate-macrolactin than 7-O-succinyl macrolactin (log P 3.24) with succinate side chain (-C(=O)CH₂CH₂COOH) and 7-O-malonyl macrolactin (log P 3.18) with malonyl side chain (-C(=O)CH₂COOH) are lesser than 7-O-methyl-5'-hydroxy-3'-heptenoate-macrolactin (log P 4.43) with 5-hydroxyhept-3-enoate side chain. 7-O-Methyl-5'-hydroxy-3'-heptenoate-macrolactin exhibited significant greater activity against test pathogens (at a concentration of 20µg per disc) than the parent macrolactin apparently due to the presence of more polarisable (polarisability 59.91 X 10⁻²⁴ cm³) C-7,5-hydroxyhept-3-enoate group as compared to the less polarisable succinate or malonate groups (52-24 X 10⁻²⁴ cm³). It can be inferred that 5-hydroxyhept-3-enoate moiety with highly electronegative acetyl and olefinic groups withdraw the electron cloud by a combination of inductive (-I effect) and mesomeric effect (+M-effect) from the substituted macrolactin ring of 7-O-methyl-5'-hydroxy-3'-heptenoate-macrolactin, thus acting as

the nucleophilic centre of the molecule resulting in a high level of activity (Figure 5A.9). This lead demonstrated in the present study will be significant in explaining the pharmacophore-fit in the macromolecular receptor site and exploring the primary site and mode of action of this class of the substituted macrolactone analogues.

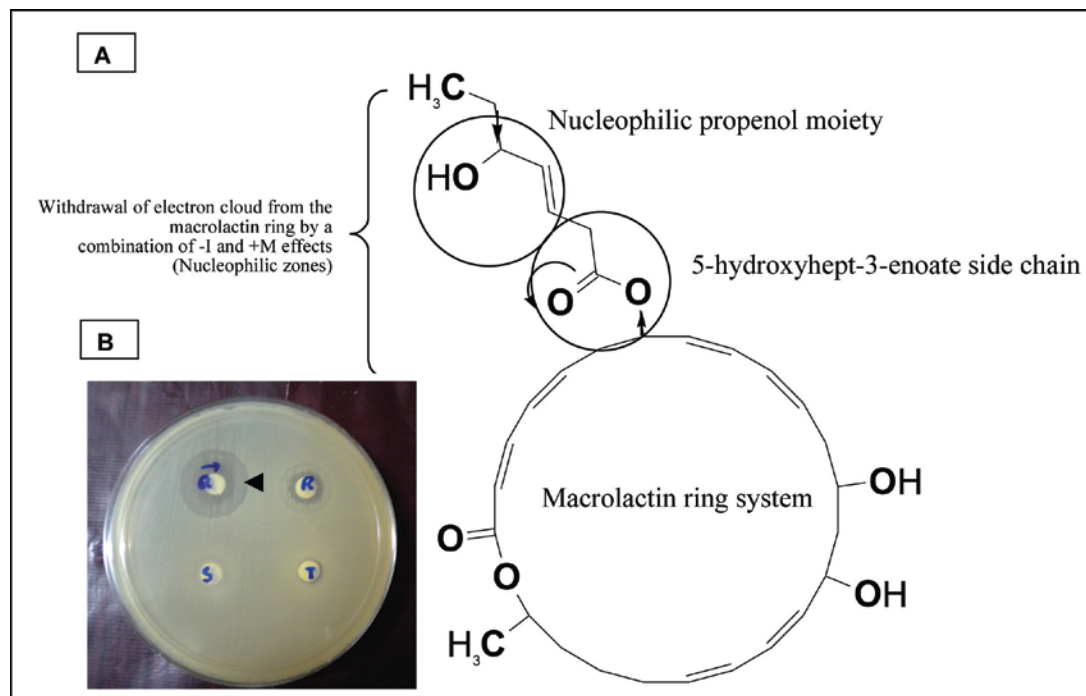


Figure 5A.9

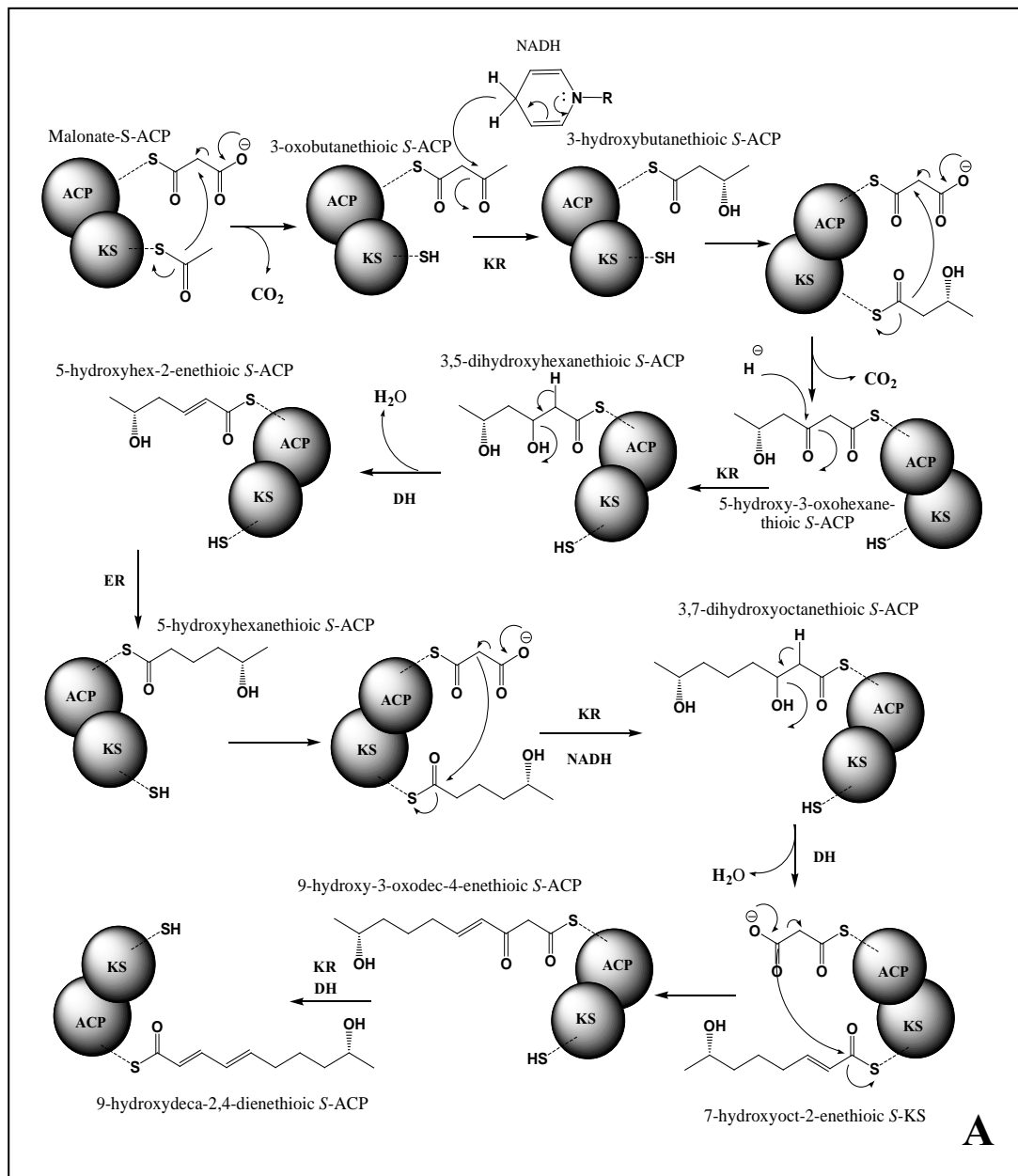
(A) Sketch model of 7-O-methyl-5'-hydroxy-3'-heptenoate-macrolactin. Induction of bioactivity is directly proportional to the inductive (field/polar effect) and resonance effects of the 5-hydroxyhept-3-enoate side chain attached to the macrolactin ring system at C-7. The 5-hydroxyhept-3-enoate moiety with a highly electronegative acetyl group withdraw the electron cloud by a combination of inductive (-I effect) and mesomeric effect (+M-effect) from the substituted macrolactin ring, thus acting as the nucleophilic center of the molecule resulting in a high level of activity; (B) Antibacterial activity of 7-O-methyl-5'-hydroxy-3'-heptenoate-macrolactin against *V. parahemolyticus* ATCC17802. The inhibition zone is indicated by an arrow.

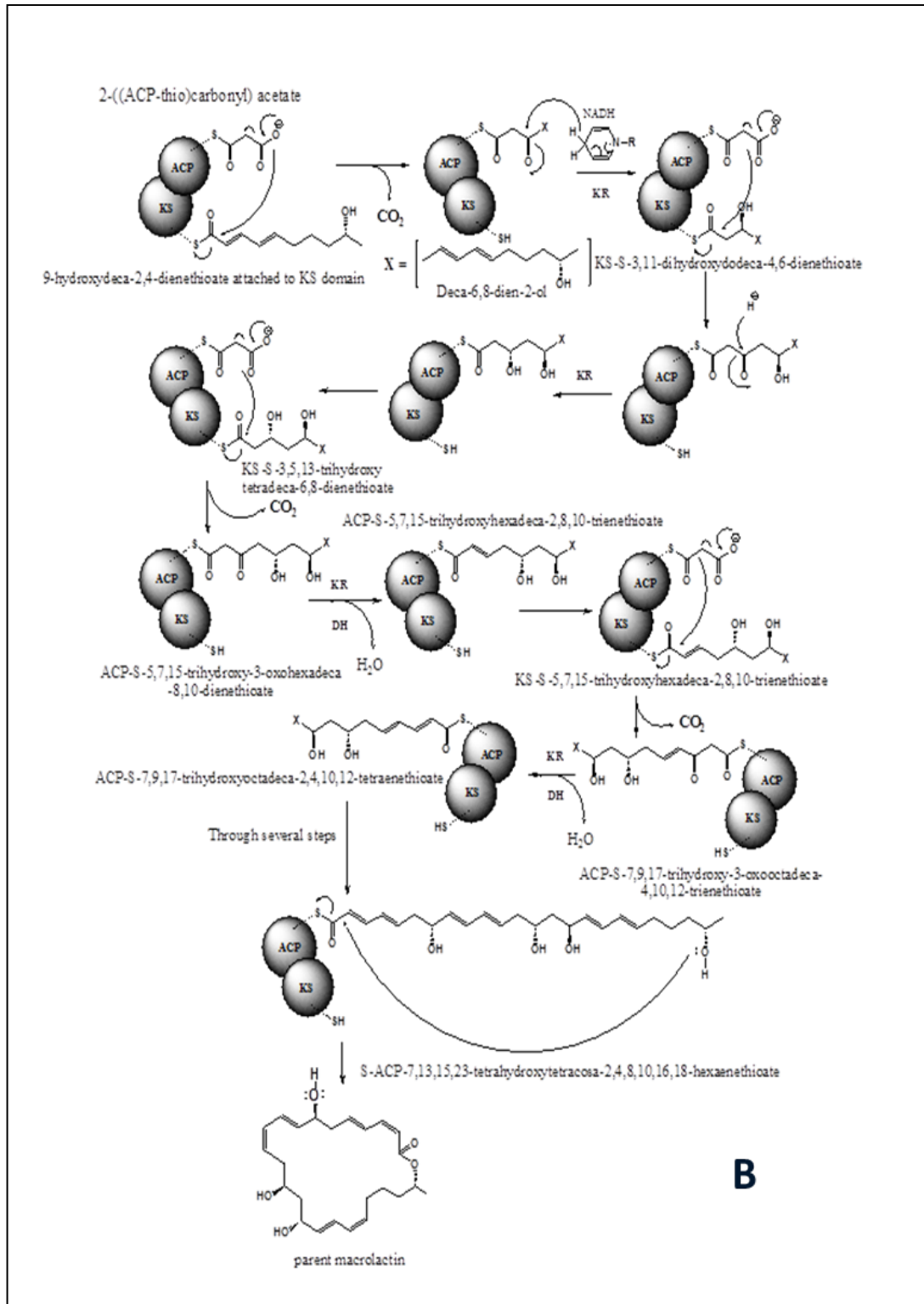
The elongation module of type-I PKS harbors the acyl carrier protein (ACP), acyltransferase, (AT) and ketosynthase (KS) domains that synergistically catalyze a series of decarboxylative Claisen condensation involving malonyl units to result in the elongation of the polyketide chain affording the formation of the intermediate biosynthetic product as β -ketoacyl-S-ACP. A series of condensation, dehydration, reduction, and hydrolysis of the intermediate polyketides result in the biosynthesis of 7-O-methyl-5'-hydroxy-3'-heptenoate-macrolactin (Figure 5A.10.A). It is, however, of note that the ketoreductase (KR), dehydratase (DH) and enoyl reductase (ER) are

active in a few steps to reduce the carbonyl group to -OH, olefinic double bond or a fully reduced end product.

The correlations of metabolite genes such as *pks* with secondary metabolites belonging to polyketides and their putative biosynthesis pathway in related bacteria were reported in earlier studies (Moldenhauer et al. 2007, Scotti et al. 1993). The *pks* gene has been assigned to the biosynthesis of bacillane, a polyketide product in *Bacillus amyloliquefaciens* FZB 42 genome. The *pks* gene cluster was identified from *B. amyloliquefaciens* CH12, a genetically engineered strain, and the putative biosynthetic pathway of bacillane was demonstrated. A bacillaene multienzyme complex of *trans*-AT PKSs with *pks*-like chemistry was characterized in an earlier study, where introduction of the β -branch and subsequent incorporation of olefinic bonds into the noncanonical bimodules have been comprehended (Moldenhauer et al. 2007). The *pksX* polyketide synthase (PKS) genes were also reported in *Bacillus subtilis* (Scotti et al. 1993). A stepwise aldol addition of acetyl-ACP and Grob fragmentation on the enzymatically loaded acyl carrier proteins were demonstrated to result *pks*-derived antibacterial metabolites bacillane and curacin (Calderone et al. 2006; Gu et al. 2006). Mupirocin H, a novel metabolite resulting from mutation of the HMG-CoA synthase analogue, *mupH* in *Pseudomonas fluorescens*, has been reported (Wu et al. 2007). Previous work demonstrated that unlike fatty acid biosynthesis, the biosynthesis of polyketide products don't follow a rigid sequence (Weissman and Leadlay, 2005). Instead, some or none of these steps and reduction reactions occurs in different biosynthetic steps to result in various combinations of structural diversity of the PKS products. It is of note that some of the domains remain inactive at one or more steps of macrolactin biosynthesis thereby leading to the formation of conjugation at three positions (C2-5, C8-11, and C16-19 of the macrolactin ring system) and three hydroxyl groups of the intermediate polyketide product (S-ACP-7,13,15,23-tetrahydroxytetracos-2,4,8,10,16,18-hexaenethioate). The later undergoes intramolecular cyclization by the nucleophilic attack of the terminal hydroxy group on the thioester-activated carbonyl to result the formation of -C(=O)-O- linkage in the 24-membered macrolactin ring location system with the elimination of ACP-SH.

The post-biosynthetic modifications of the macrolactin ring at the C7 position of macrolactin have been reported in earlier literature (Jaruchoktawechai et al. 2000). In general, type I PKSs use malonyl/methylmalonyl/ethylmalonyl derivatives of CoA and hydroxymalonyl/aminomalonyl/methoxymalonyl ACP extender units to biosynthesize diverse natural products bearing the polyketide backbone (Jaruchoktawechai et al. 2000). It is of note that in the biosynthetic route leading to the formation of the side chain 5-hydroxyhept-3-enoate moiety is also a polyketide biosynthetic product. A model for biosynthesis of 5-hydroxyhept-3-enoate can be proposed (Figure 5A.10.B), which accounts for the fact that propanethioate/malonate as the starting building blocks instead of acetate/malonate in the biosynthesis of this polyketide backbone. Accordingly, the biosynthetic route starts from propanethioate (KS-S-C(=O)C₂H₅) attached with the KS domain, and is accomplished by two alternate steps of decarboxylative Claisen condensations and ketoreduction. Finally, DH catalyzes the elimination of the water molecule in the intermediate KR product S-ACP-3, 5-dihydroxyheptanethioate to afford the S-ACP-5-hydroxyhept-3-enethioate. The nucleophilic attack of the terminal hydroxyl group (as butanol moiety) on the thioester-activated carbonyl carbon atom of S-ACP-5-hydroxyhept-3-enethioate results in the formation of a cyclic polyketide product as 6-ethyl-3, 6-dihydro-2-(ACP-thio) -2H-pyran-2-one in the 6-membered pyran ring location system. A subsequent elimination of ACP-SH afforded 6-ethyl-3, 6-dihydro-2H-pyran-2-one. The carbonyl carbon atom of the latter undergoes a nucleophilic attack by the 7-OH group in the macrolactin ring system followed by ring opening yielding the final PKS product as 7-O-methyl -5'-hydroxy-3'-heptenoate-macrolactin (Figure 5A.10.C). It is apparent from this study that various combinations of the starter and elongation units used for polyketide biosynthesis lead to the formation of multiple stereocenters and structurally diverse polyketide backbone.





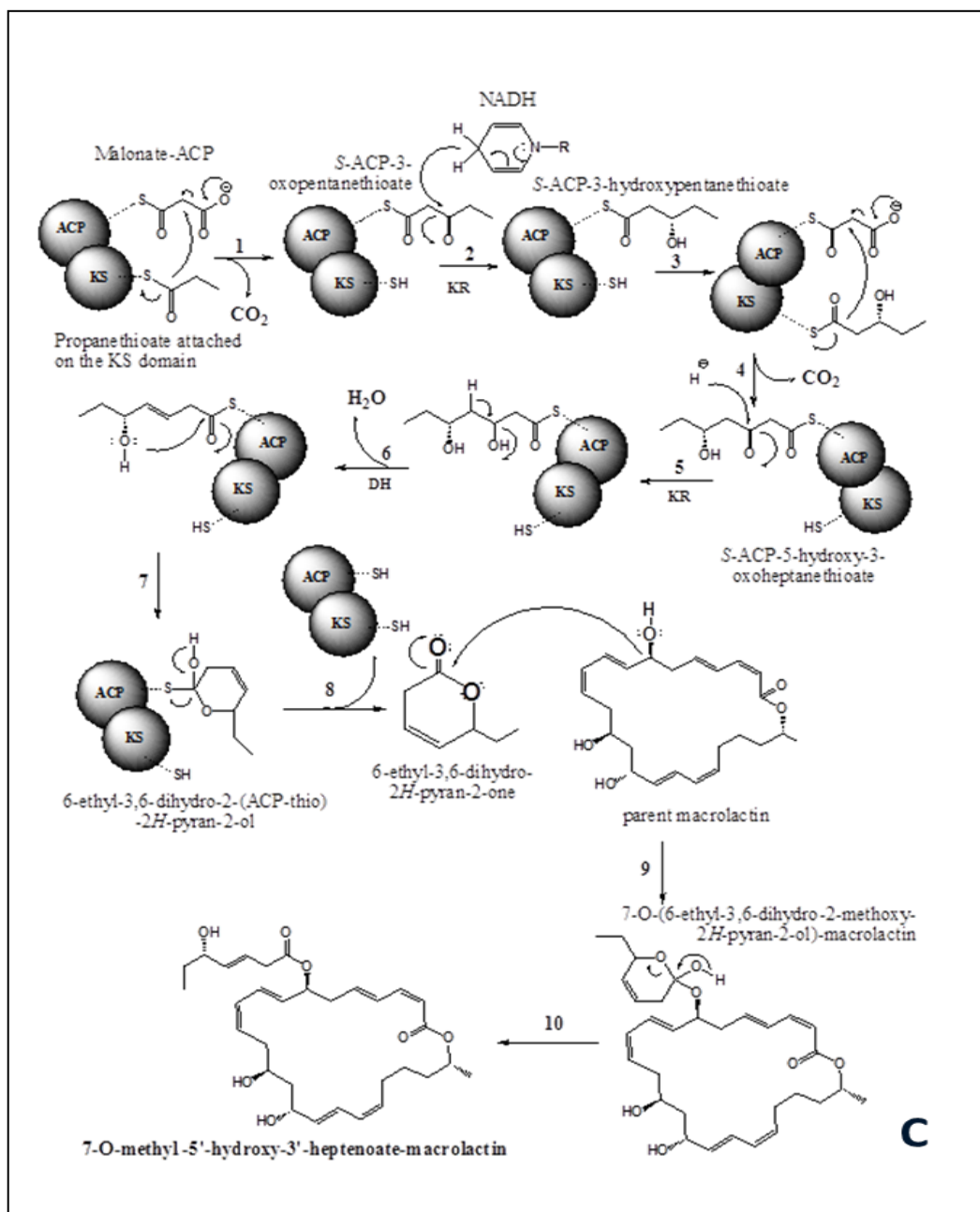


Figure 5A.10

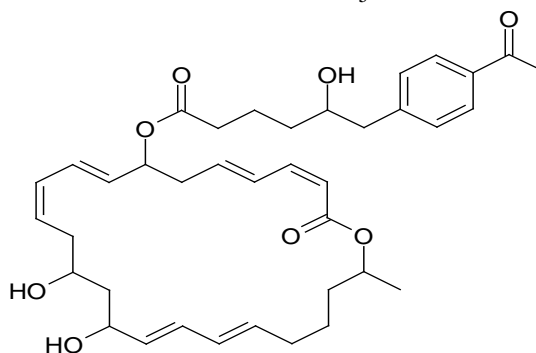
Hypothetical pathways for biosynthesis of the bacterial metabolite 7-O-methyl-5'-hydroxy-3'-heptenoate-macrolactin, showing the loading, decarboxylation and elongation steps catalyzed by the PKS-1. Both enzymes build their products from an acetate starter unit and malonate extender units. The intermediates shown bound to the PKSs are hypothetical, but consistent with experimental results(B,C). Sequence of events in the biosynthesis of side chain 5-hydroxyhept-3-enoate moiety attached to the macrolactin ring system at C-7, and the final PKS product as 7-O-methyl-5'-hydroxy-3'-heptenoate-macrolactin.

5A.2.6.2 Structural Characterization of Compound 2 (B2E56)

6-(4-Acetylphenyl)-5-hydroxyhexanoic macrolactin : Amorphous solid; UV (MeOH) λ_{\max} (log ϵ): 268nm (3.85); TLC (Si gel GF₂₅₄ 15 mm; CH₂Cl₂/MeOH 40:60, v/ v) R_f: 0.90; R_t: 9.171 min(HPLC)(Figure 5A.11), IR ν_{\max} (KBr) cm⁻¹ : 976 (trans C=C bending), 1072.32(unsaturated sec. alcohol C-O str.), 1122.45(C-O-C symmetrical str.), 1284.22(CH-OH in plane bending), 1378.54(O=C-CH₂,C-H bending), 1466.42(C-H asym-bending), 1642.78(C=C str.), 1680.12 (aromatic C=C),1754.13(α,β -unsaturated C=O str.), 2848.26(-O-CH₂ sym C-H str.), 2934.44(alkane C-H str.), 3022 (asym.alkene C-H str.), 3446.26cm⁻¹(O-H str.); ¹H(CDCl₃, 500 MHz, δ ppm) and ¹³C NMR (CDCl₃, δ ppm) data, see Table 5A.3; HRMS (ESI) *m/z*: calcd. for C₃₈H₅₀O₈ 634.3506; found 634.3582 [M]⁺.

Table 5A.3

NMR spectroscopic data of **6-(4-acetylphenyl)-5-hydroxyhexanoic macrolactin** in CDCl₃,^a



Carbon no.	¹³ C NMR (DEPT)	H	δ^1 H NMR (int., mult., J in Hz) ^b	¹ H- ¹ H COSY	HMBC (¹ H- ¹³ C)
1	165.30(C)	-	-	-	-
2	116.12 (CH)	2-H	5.40(d, J=11.2)	-	-
3	143.95 (CH)	3-H	6.68(t, J=11.1)	2-H, 4-H	C-4
4	127.53 (CH)	4-H	7.06(dd,15.2,11.1)	-	-
5	141.11(CH)	5-H	6.34(dt , J=15.3,7.1)	-	-
6	42.43 (CH ₂)	6-H ^a 6-H ^b	6H ^a at 2.75(m); 6H ^b at 2.41(m)	7-H	-
7	73.2(CH)	7-H	5.01 (dt)	8-H, H-6	C-1 ¹ ,C-8
8	139.28 (CH)	8-H	5.79(dd , J=15.2,6.1)	9-H	-
9	123.73(CH)	9-H	6.50dd,15.1,11.3)	-	-

10	130.33(CH)	10-H	5.96(m)	11-H	-
11	128.81(CH)	11-H	5.40(dt, J=10.6,8.4)	12-H, 10-H	-
12	37.27(CH ₂)	12-H ^a 12-H ^b	12 H ^a at 2.51(m), 12H ^b at 2.32(m)	13-H	C-14
13	66.55(CH)	13-H	3.42(dd) (4.02,OH)	14-H	-
14	45.62(CH ₂)	14-H ^a 14-H ^b	14H ^a at 1.81(m); 14H ^b at 1.68(m)	-	-
15	67.00 (CH)	15-H	4.13(dt,J=6.1,6.1)(3.79,OH)	-	C-13,C-16
16	135.19 (CH)	16-H	5.80 (dd, J=15.4,6.2)	17-H	-
17	127 (CH)	17-H	6.36(dd, J=15.1,10.6)	-	-
18	130.3 (CH)	18-H	6.23(t,10.6)	19-H	-
19	135.21 (CH)	19-H	5.72(ddd,J=14.2,7.0,6.7)	-	-
20	31.92 (CH ₂)	20-H ^a 20-H ^b	20H ^a at 2.05(m); 20H ^b at 1.93	-	-
21	23.99 (CH ₂)	21-H ^a 21-H ^b	21H ^a at 1.62(m); 21H ^b at 1.82(dt,11.2,5.2)	22-H	C-1,C-24,C-23
22	35.96(CH ₂)	22-H ^a 22-H ^b	22H ^a at 1.48(m); 22H ^b at 1.42(m)	-	-
23	72.18(CH)	23-H	4.04(ddq,J=4.5,7.1,5.1)	24-H	-
24	21.66(CH ₃)	-	1.20(d, J=6.1)	-	-
25	169.55				
26	33.13	26-H	2.23(t,2H)	27-H	C-25
27	57.74	27-H	2.93(m,2H)		
28	29.69	28-H	1.82(dd,2H)	29-H	C-27,29
29	59.03	29-H	4.22(m,1H)	30-H	
30	40.53	30-H	3.13/3.07(dt,2H)		
31	144.63				
32	128.77	32-H	7.30(d,1H)	33-H	C-33
33	129.91	33-H	7.20(d,1H)		
34	133.08	34-H			
35	129.32	35-H	7.22(d,1H)	36-H	C-34,36
36	127.77	36-H	7.29(d,1H)		
37	207				
38	30.92	38-H	2.17(s,3H)		C-37

^a NMR spectra were recorded using the Bruker DPX 300 and AVANCE 300 MHz spectrometers.

^b Values in ppm, multiplicity and coupling constants (J/4 Hz) are indicated in parentheses. Assignments were made with the aid of the ¹H-¹H COSY, HMQC, and HMBC experiments.

The methylene group protons at δ 2.75 and δ 2.45 were assigned to be at 6 carbon position of the macrolactin ring structure, and the more downfield shift

(about δ 0.15) was due to the presence of the conjugated butadiene moiety at one side and the side chain (4-acetylphenyl)-5-hydroxyhexanoate attached to the macrolactin ring at its 7 carbon position (**Figure 5A.12**). Three methylene groups have been assigned to occupy at the C20-22 positions of the macrolactin ring structure as heptenyl formate moiety. The protons of the $-\text{CH}_2-$ group at δ 1.48, 1.42 are at C-22, and are deshielded due to the presence of the acrylate moiety ($-\text{OC}(=\text{O})-\text{C}=\text{C}-$) at the β -position with respect to the deshielded methyl group. Most of the proton signal shown similarity with earlier reported macrolactin. Mainly aromatic signals appeared in $^1\text{H-NMR}$ around 7.20-7.30 strongly supports the presence of disubstituted aromatic ring. H-7(5.01) shown HMBC with C-25(169.55) indicates the attachment of side chain at C-7. Strong H-H COSY correlation between 26-H(2.23)/27-H(2.93)/28-H(1.82)/29-H(4.22)/30-H^a(3.13) and 30-H^b(3.07) indicated the presence of 5-hydroxyhexanoate. Acetyl group attached to aromatic ring in para substitution confirmed by HMBC spectra and mass fragment shown 249 ($\text{C}_{14}\text{H}_{17}\text{O}_4$)⁺ indicated the presence of (4-acetylphenyl)-5-hydroxyhexanoate moiety.

The methyl group protons at δ 2.05, 1.93 (C-20) appeared to be deshielded due to the conjugated double bond structure (butadiene) spanning from C16-C19 position of the macrolactin ring. The methylene protons at C-21 position appeared at δ 1.81 and 1.60 ppm. The $-\text{CH}_2-$ protons appeared in δ 1.94 and 1.78 ppm were due to the presence of the propanediol group, and have been assigned to be present at the C-14 position in the macrolactin ring structure. The protons at δ 2.68 and 2.33 ppm shifted downfield due to the presence of $-\text{C}=\text{C}-$ group at its α -position and a β -OH group. The methine protons at δ 3.42 and 4.84 ppm were assigned to be present at the C13 and C15 positions in the macrolactin ring structure. The downfield shift appeared to be due to the propane-1, 3-diol moiety at C13 to C15. The methine proton at δ 4.84 appeared to be deshielded due to the presence of β -olefinic group extended by further conjugated structure. The carboxyl ester group at the C1 position of the macrolactin ring resulted in strong deshielding of the $-\text{CH}-$ proton at δ 4.99 ppm, and therefore, was assigned to be present at the C23 position of the macrolactin ring structure. The methine proton (gives triplet of the doublet) at δ 5.05 ppm is characteristic of the junction point of the macrolactin ring (C-7) to that of the

side chain (4-acetylphenyl)-5-hydroxyhexanoate. The $^1\text{H-NMR}$ spectrum showed three exchangeable hydroxyl proton at δ 4.23 (1H, bs in CDCl_3), δ 3.79 (1H, bs in CDCl_3), and δ 3.16 ppm (1H, bs in CDCl_3), which disappeared upon addition of D_2O . The ^{13}C NMR spectrum of the purified compound displayed two quaternary carbon (δ 165.30, 169.55) atoms bearing the carbonyl groups. The low field quaternary signals (^{13}C NMR) are in agreement with that to a quaternary carbon signal carrying the carbonyl groups at C-1 of the macrolactin ring structure and C-25 of the side chain (4-acetylphenyl)-5-hydroxyhexanoate attached to the macrolactin framework at the 7C position of the ring. The position of the hydroxyl group at C-29 was further confirmed from the $^1\text{H-}^1\text{H}$ COSY, HSQC, NOESY, and HMBC spectra. In the $^1\text{H-}^1\text{H}$ COSY spectrum, the couplings were apparent between H-7/H-6, 8; H-13/H-12, 14; H-15/H-14, 16, and H-20/H-21/H-22/H-23 support the presence of macrolactin skeleton. The point of cyclization of the ester in macrolactone ring was indicated by the low-field shift of H-23 at δ 4.99, which has been coupled with the H-24 methyl group at δ 1.30 (d, $J = 6.1$ Hz), which also gives clear $^1\text{H-}^1\text{H}$ COSY correlation. Also, the $^1\text{H-}^1\text{H}$ COSY correlations between 26-H/27-H/28-H /29-H supports the presence of the terminal (4-acetylphenyl)-5-hydroxyhexanoate chain. The proton and carbon connectivity deduced from HSQC and HMBC experiments confirmed the marolactin framework attached to the side chain (4-acetylphenyl)-5-hydroxyhexanoate moiety at the 7th position of the macrolactin. The H-H and C-H connectivities apparent in the $^1\text{H-}^1\text{H}$ COSY and HMBC spectra, respectively indicate that one of the three unsaturations was due to the macrolactin ring framework. In the HMBC spectrum, it was observed that H-12/C-10, 14; H15/C-13, 16; H-20/C-19, 22; and H-21/C-1, 23, 24 were correlated with each other. In addition, a methine proton (H-7) was coupled to the olefinic tertiary carbon (C-9) and methine H-15 with C-16, 17. This indicated that these protons (H-7 and H-15) were connected to the olefinic tertiary carbon atoms. The proton at C-21 appeared to demonstrate long range HMBC correlation with ester carbonyl carbon at δ 165.16 (C-1). The proton at C-7 realized HMBC correlation at δ 169.55, which belong to the second ester carbon. The HMQC spectrum of the purified compound also revealed connections of the protons (H-26) to the methylene carbon at δ 50.8. Placement of the(4-acetylphenyl)-5-hydroxyhexanoate group at the C-7 was confirmed by the downfield shift of H-7 (δ 5.05) in the compound as compared to

the baseline value (δ 4.34) [Jaruchoktawechai *et al.* 2000] and also by the long-range correlation of H-7 to the carbonyl carbon at δ 169.55 (C-25) in the HMBC spectrum. The geometric isomerisms of the olefinic protons have been established by the ^1H coupling constants suitable for the geometries (Z and E form). The relative stereochemistry of the chiral centres, particularly that of C-13 and 15 carrying the hydroxyl group of the macrolactin framework and that of C-29, was deduced from the NOESY spectrum of the compound and the J-values. NOE couplings were observed between $\text{H}\alpha$ -13/ $\text{H}\alpha$ -7 thus indicating that these groups must be equatorial and on the α -side of the molecule. NOE correlations between $\text{H}\beta$ -23/ $\text{H}\beta$ -15/ $\text{H}\beta$ -20 and those among H-29/H-15/H-23 indicated the close proximity of these groups and their β -disposition. Therefore, the C-1 carboxyl group is equatorial and α -oriented. An interaction through the space of the hydroxyl protons at C-29 (δ 4.22, 1H, bs) and C-15 (δ 3.79, 1H, bs) with H-7 (δ 5.05, td) and $\text{H}\alpha$ -14 (δ 1.94, m in CDCl_3) is only possible for the α -orientation of the tertiary hydroxyl group on C-29 and C-15. The stereochemistry at the tertiary alcohol at C-15 position was established by the fact that H-15 has mutual NOE correlations with H-23, which had shown to be in the β -face of the molecule (axial configuration) under observation, and the secondary alcohol group that appeared as a broad singlet (at δ 4.23 ppm) has NOE interactions with H-13 and H-7 in the molecule. This is only possible if the C-15 hydroxyl group lies on the α -side of the molecule.

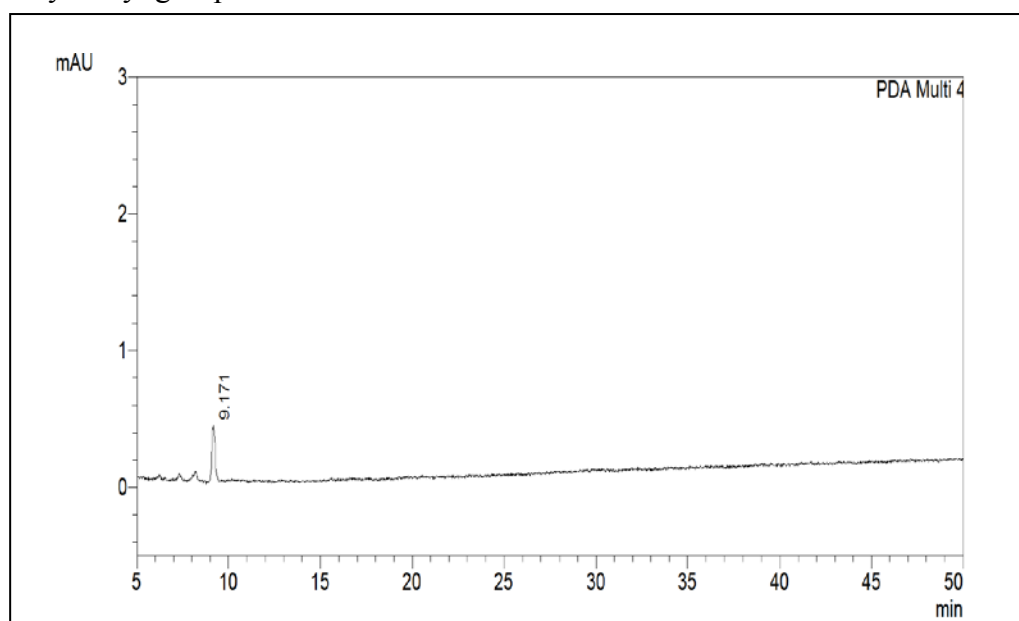


Figure 5A.11
HPLC Chromatogram of Compound 2

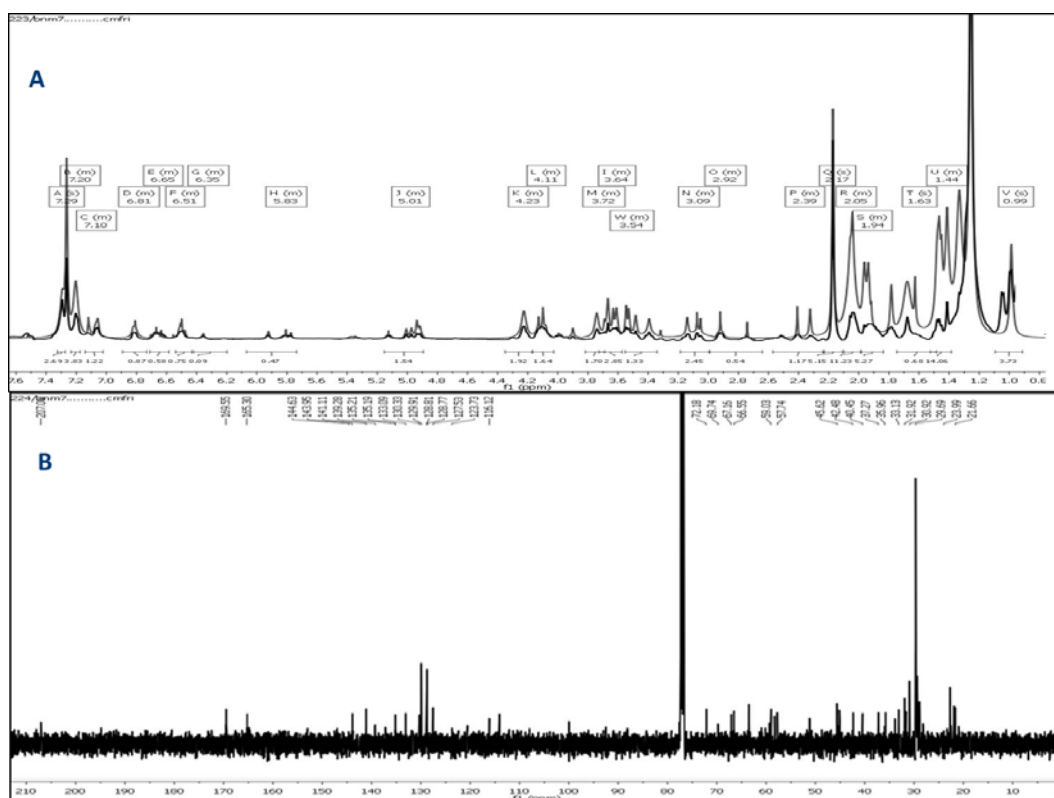


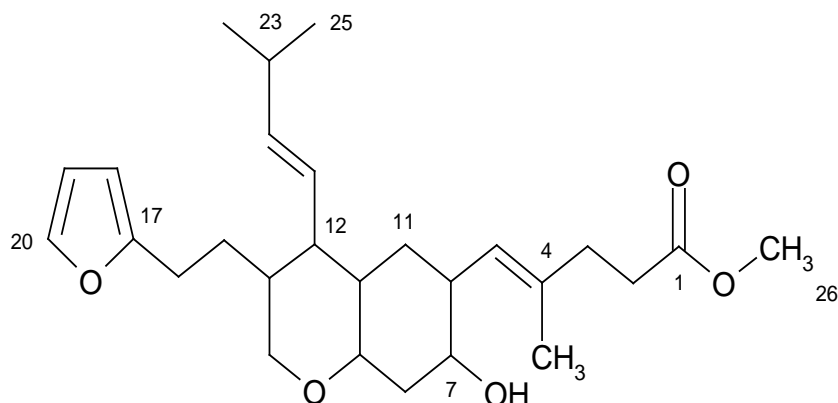
Figure 5A.12
(A) ¹H, (B) ¹³C NMR spectrum of Compound 2

5A.2.6.3 Structural Characterization of Compound 3(B2E25)

(4E)-methyl 5-(3-(2-(furan-2-yl)ethyl)-octahydro-7-hydroxy-4-((E)-3-methyl but-1-enyl)-2H-chromen-6-yl)-4-methylpent-4-enoate: yellow oil; UV(MeOH) λ_{\max} (log ϵ): 315 (4.12) nm TLC (Si gel GF₂₅₄ 15 mm; 1% MeOH/CHCl₃, v/v) R_f: 0.60; R_t: 41.793 min (HPLC)(Figure 5A.13); IR (KBr, cm⁻¹) ν_{\max} 722.2 (C-H ρ), 1052.32(C-O v), 1372.22 (CH δ), 1560.22 (C=C v), 1732.02(-COO v), 2854.74 (C-H ν_{as}), 3325(O-H v); ¹H NMR (500 MHz, Chloroform-d) δ 7.47 (d, 1H), 7.20 (dd, 1H), 7.06 (d, J=8.4Hz 1H), 5.83 – 5.59 (m, 1H), 5.37 – 5.17 (m, 1H), 4.92 (m, 1H), 4.21 (m, 1H), 4.05 (m, 1H), 3.85 (s, 2H), 3.58 (s, 3H), 3.46 (s, 2H), 3.34 – 3.09 (m, 2H), 2.90 (s, 3H), 2.53 -2.22 (m, 7H), 1.96 (d, 4H), 1.72-1.53 (m, 5H), 1.30 (d, 2H), 1.02 – 0.71 (m, 6H). ¹H-¹H COSY and HMBC data (details under the Table 5A.4); HRMS (ESI) m/e : 445.6854 calcd. for C₂₇H₄₁O₅:445.4528 [M+H]⁺. Molecular formula C₂₇H₄₀O₅

Table 5A.4

NMR spectroscopic data of 6-(4-acetylphenyl)-5-hydroxyhexanoic macrolactin in CDCl₃,^a



Position	¹³ C ppm	H	¹ H NMR	¹ H- ¹ H COSY	HMBC → ¹ H ¹³ C
1	174.33				
2	34.13	2-H	2.25(t,2H)		C-3,C-1
3	24.84	3-H	1.52(t,2H)	2-H	
4	130				
5	129.75	5-H	5.28(d,1H)	6-H	
6	28.17	6-H	1.93(m,1H)	7-H	C-11
7	58.07	7-H	4.06(m,1H)	8-H	C-5,C-6
8	29.36	8-H	2.32(m,2H)		C-9
9	70.14	9-H	4.22(m,1H)	10-H	C-10,C-14
10	29.69	10-H	1.65(m,1H)	11-H	
11	31.92	11-H	1.72(m,2H)		C-7
12	30.2	12-H	2.04(m,1H)	21-H	C-13,C-21
13	53.6	13-H	1.94(m,1H)	14-H	
14	60.2		3.49(m,2H)		C-12
15	38.46	15-H	2.53(m,2H)		C-16
16	50.61	16-H	3.20(m,2H)	15-H	C-17
17	138.74				
18	126.91	18-H	7.29(s,1H)	19-H	C-20
19	128.98	19-H	7.09(d,1H)	20-H	C-17,C-18
20	129.17	20-H	7.48(d,1H)		

21	134.14	21-H	5.70 (dd,1H)		
22	114.05	22-H	4.98(m,1H)	23-H	C-23
23	29.33	23-H	1.98(m,1H)	24-H	C-22,C-24
24	22.69	24-H	1.21(d,3H)		C-23
25	14.11	25-H	1.26(d,3H)	23-H	
26	51.44	26-H	3.60(s,3H)		C-1
27	40.67	27-H	2.90(s,3H)		C-4

- ^a NMR spectra were recorded using the Bruker DPX 300 and AVANCE 300 MHz spectrometers.
- ^b Values in ppm, multiplicity and coupling constants ($J/4$ Hz) are indicated in parentheses. Assignments were made with the aid of the ^1H - ^1H COSY, HMQC, and HMBC experiments.

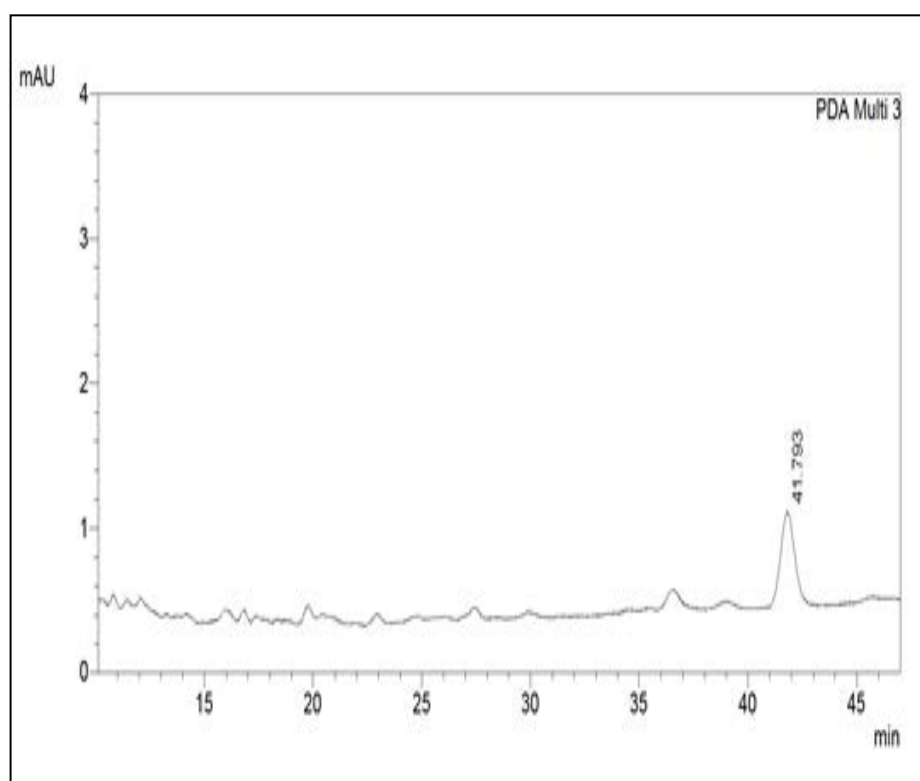


Figure 5A.13
HPLC Chromatogram of Compound 3

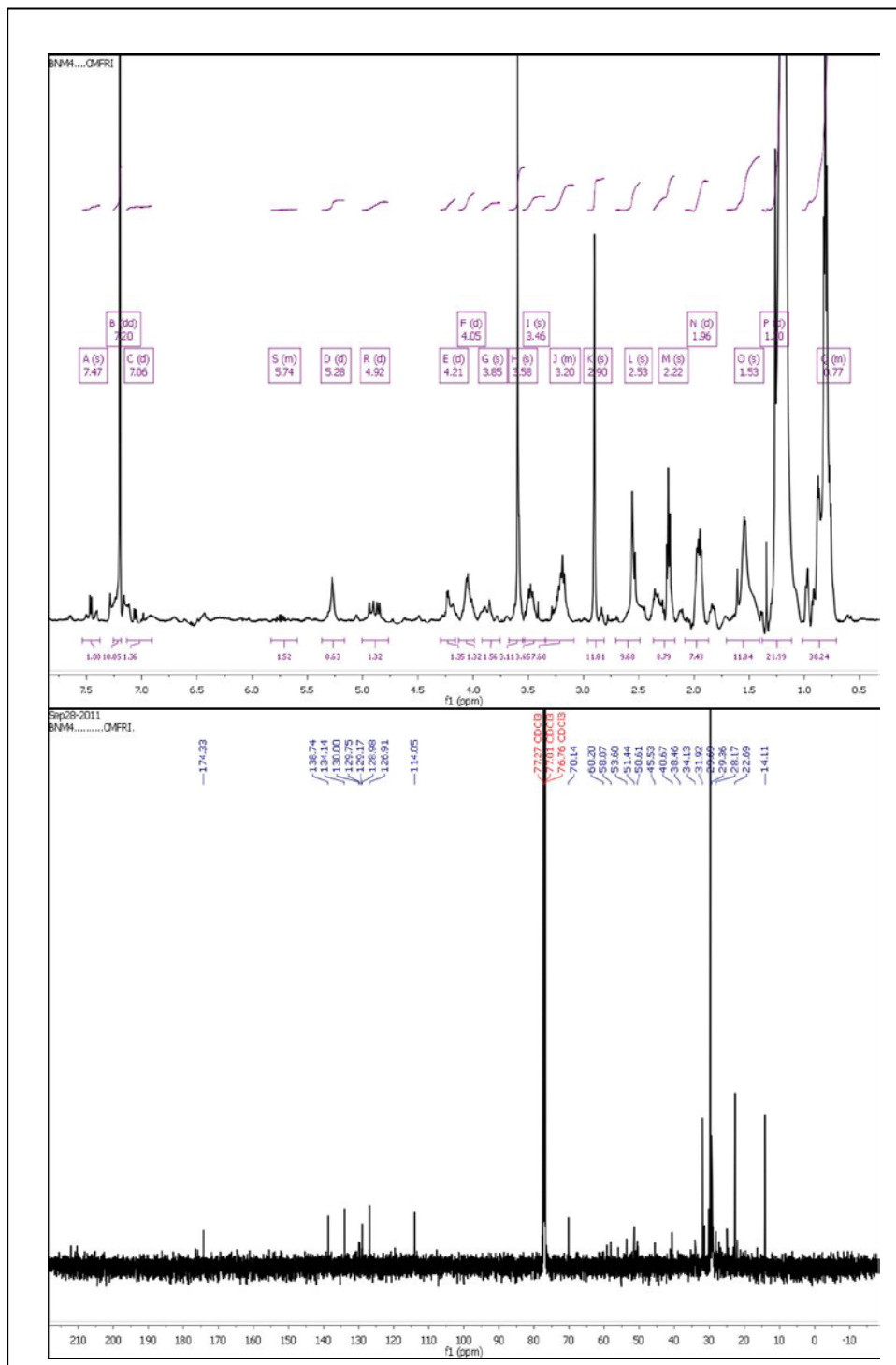


Figure 5A.14
(A) ^1H , (B) ^{13}C NMR spectrum of Compound 3

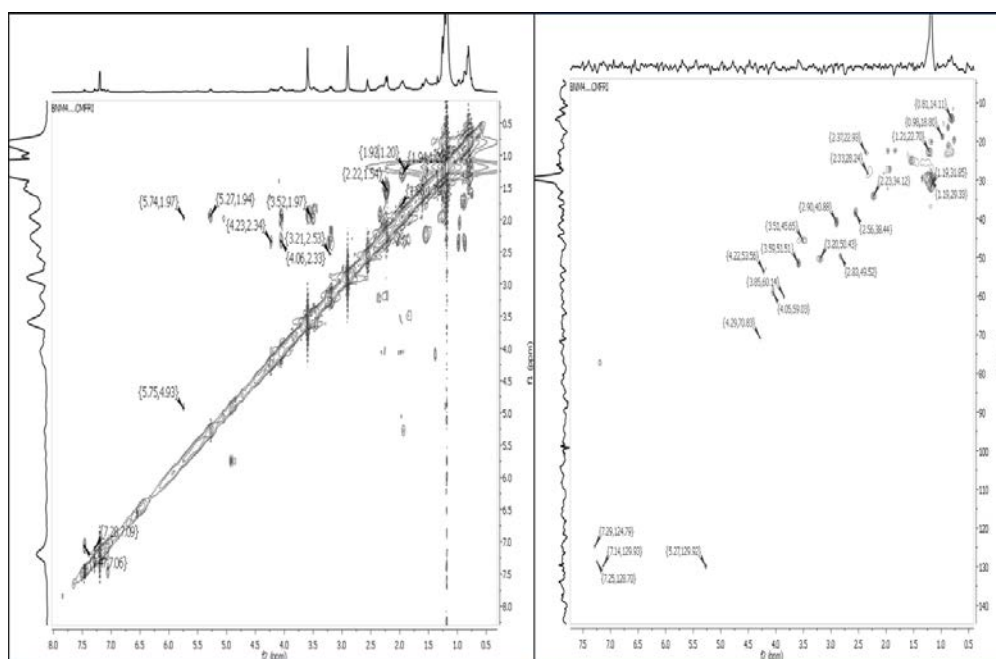


Figure 5A.15
(A) HMBC correlation spectrum of compound 3 (B) Prominent HSQC correlation spectrum of compound 3

2-(7-(2-Ethylbutyl)-2,3,4,4a,6,7-hexahydro-2-oxopyrano [3,2-b] pyran-3-yl) ethyl benzoate. The IR bending vibration bands near of compound compound 3 at 1732.02 cm^{-1} attributed to the ester carbonyl absorption and that near 1560.22 cm^{-1} was due to the presence of C=C-stretching vibrations. The ultraviolet absorbance at $\lambda_{\text{max}} (\log \epsilon) 248\text{ nm} (3.12)$ was assigned to a chromophore with extended conjugation. Its mass spectrum exhibited a molecular ion $[M-H]^-$ peak at $m/e 443$, which in combination with its ^1H and ^{13}C NMR data (Table 5A.4) indicated the elemental composition of $\text{C}_{27}\text{H}_{40}\text{O}_5$. The ^1H NMR in conjugation with ^{13}C -NMR and DEPT spectra recorded the presence of seven methylene, thirteen methine, four methyl, and three quaternary carbon atoms. Its mass spectrum exhibited a molecular ion peak at $m/z 445$ (HRESIMS $m/e 445.6854 [M+H]^+$; D 0.0 amu), which in combination with its ^1H and ^{13}C NMR data (Table 5A.4) indicated the elemental composition of $\text{C}_{27}\text{H}_{40}\text{O}_5$ as with eight degrees of unsaturation (Figure 5A.14). four degree of unstruration from double bonds and three degrees of unstruration from the ring systems, one from the carbonyl moieties. Couplings were apparent between the

protons at δ 1.21 (H-24)/ δ 1.98 (H-23)/ δ 1.26 (H-25) with δ 4.98 (H-22)/ δ 5.70 (H-21) in the ^1H - ^1H COSY spectrum, which supported the presence of 2-methyl pentene moiety.

The methylene signal at δ 4.06 appeared downfield due to the presence of multiple electronegative systems at close proximity. Two methylene groups have been assigned to occupy at the C2-3 positions, and the one with δ 2.25 shifted downfield due to the presence of a carbonyl group. The HMBC correlation of the proton at δ 2.25 and δ 3.60 with the carbon atom at δ 174.33 apparently indicated the presence of -C=O(O) group. The HSQC and HMBC experiments revealed that the ester group linked to the methane group at δ 3.60 was attached to the oxygen of carboxylic group. The aromatic protons showed their characteristic signals at δ 7.40-7.07. Extensive HMBC (Figure 5A.15.A) and HSQC(Figure 5A.15.B) experiments revealed the presence of substituted furan moiety in the compound.

^1H - ^1H COSY experiments revealed that the protons at δ 5.28 (d) correlate with the methine proton at δ 1.93 (assigned to be as H-6) and that at δ 4.06 (H-7), the later is assigned to be attached to a strongly electronegative group. HMBC correlations were apparent between H-6 (δ 1.93) with that of a olefinic carbon at δ 129.75. The -CH- proton appeared downfield at δ 4.24 apparently due to the presence of the electronegative oxygen group and was assigned to be present at the C-9 position of compound 3. The carboxyl group at the C-1 position of the compound resulted in strong deshielding of the -CH- proton at δ 2.25, and therefore, has been assigned to be present at the C-2 position of the structure.

The chemical shift of the protons at δ 4.24, 1.65, 2.04, 1.97, and 3.49 along with detailed 2D NMR experiments established the presence of *O*-heterocyclic pyran ring system. The -CH- proton (q) at δ 4.24 is characteristic of the junction point of the bicyclic system. The ^{13}C NMR spectrum of the purified compound in combination with DEPT experiments indicated the occurrence of 27 carbon atoms in the molecule including one carbonyl carbon at δ 174.33 and olefinic carbons at δ 134.14 and 114 (Table 5A.4). The low field quaternary signals (^{13}C NMR) was in agreement with that to a quaternary carbon signal carrying the carbonyl groups at C-1 of the compound 3, and this was supported by the relatively downfield shift of the

H-7 signal (δ 4.06), which referred to a possible oxygenation in its vicinity. The position of the hydroxyl group at C-7 was further confirmed from the HSQC, NOESY, and HMBC spectra. The H–H and C–H connectivities apparent in the ^1H – ^1H COSY and HMBC spectra respectively indicate that one of the eight unsaturations was due to the three ring and five double bonds.

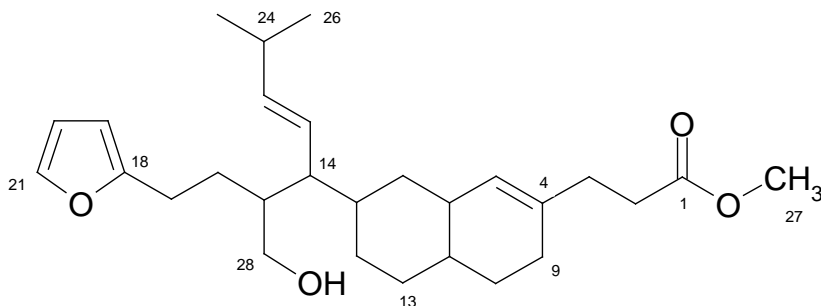
The relative stereochemistry of the chiral centre particularly that of C-7 cyclic framework was deduced from the NOESY experiment and the *J*-values. NOE couplings were observed between H α -5/H α -7 thus indicating that these groups must be equatorial and on the α -side of the molecule. Therefore, the H-6 axial and β -oriented. The methine proton at C-13 group did not exhibit NOE interactions with H-12 and H-9, which are at the β -face of the molecule, thereby indicating that H-10 is at the equatorial disposition.

5A.2.6.4 Structural characterization of Compound 4 (B2E29)

Methyl3-(2-((E)-2-(2-(furan-2-yl)ethyl)-1-hydroxy-6-methylhept-4-en-3-yl)-1,2,3,4,4a,5,6,8a-octahydronaphthalen-7-yl) propanoate: yellowish oil (8.3mg; 10mm) ; UV(MeOH) λ_{max} (log ϵ): 254 (2.83) nm TLC (Si gel GF₂₅₄ 15 mm; 1% MeOH/CHCl₃, v/v) R_f: 0.50; R_t:34.358 min (HPLC)(Figure 5A.16).; IR (KBr, cm⁻¹) ν_{max} 734.22 (C-H ρ), 1050.36(C-O ν), 1370.26 (CH δ), 1640.25 (C=C ν), 1736(-COO ν), 2854.74 (C-H ν_{as}), 3402(O-H ν); ^1H NMR (500 MHz, Chloroform-d) δ 7.46 (d, 1H), 7.14 (dd, 1H), 7.09(d,1H), 5.83 – 5.27 (m, 2H), 5.02 – 4.74 (m, 1H), 4.31 – 4.15 (m, 2H), 3.65 – 3.49 (m, 4H), 2.36 – 2.18 (m, 4H), 2.10 – 1.83(m,6 H), 1.80 – 1.66 (m, 6H), 1.63 – 1.48 (m, 3H), 1.45 – 1.29 (m, 4H), 1.29 – 0.98 (m, 6H); ^1H - ^1H COSY and HMBC data (details under the Table 5A.5); HRMS (ESI) *m/e* : 441.9864 calcd. for C₂₈H₄₁O₄:441.4528 [M-H]⁻. Molecular formula: C₂₈H₄₂O₄

Table 5A.5

NMR spectroscopic data of Methyl3-(2-((E)-2-(2-(furan-2-yl) ethyl)-1-hydroxy-6-methylhept-4-en-3-yl)-1,2,3,4,4a,5,6,8a-octahydronaphthalen-7-yl) propanoate in CDCl₃.^a



Position	¹³ C ppm	H-TYPE	¹ H NMR	¹ H- ¹ H COSY	HMBC ¹ H → ¹³ C
1	175.46				
2	34.13	2-H	2.30(t,2H)	3-H	C-1,C-3
3	24.84	3-H	1.57(t,2H)	2-H	C-4
4	134.14				
5	129.75	5-H	5.30(d,1h)	6-H	C-6,C-7
6	28.17	6-H	1.93(m,1H)	7-H	C-4
7	26.75	7-H	1.33(m,1H)	8-H	C-5
8	29.29	8-H	1.62(m,2H)		C-9
9	30.19	9-H	2.04(m,1H)	8-H	C-4
10	27.22	10-H	1.72(m,1H)		
11	31.92	11-H	2.97(m,1H)	12-H	C-12
12	30.2	12-H	2.11(m,2H)	13-H	C-13,C-10
13	29.89	13-H	1.54(m,2H)		
14	45.53	14-H	2.53(m,2H)	22-H	C-22,C-11
15	53.60	15-H	3.49(m,2H)	14-H	C-14
16	38.94	16-H	1.83(m,2H)		
17	41.12	17-H	3.20(m,2H)	16-H	C-16
18	139.79				
19	123.00	19-H	7.29(s,1H)	²⁰ -H	C-18
20	127.15	20-H	7.09(d,1H)	21-H	C-19,C-21
21	129.17	21-H	7.48(d,1H)		
22	131.76	22-H	5.70 (dd,1H)	23-H	

23	115.89	23-H	4.98(m,1H)	24-H	C-22
24	29.33	24-H	1.98(m,1H)		C-26,C-25
25	19.19	25-H	1.21(d,3H)	26-H	C-24
26	14.11	26-H	1.26(d,3H)		C-25
27	51.49	27-H	3.60(s,3H)		C-1
28	69.09	28-H	4.30(d,2H)	15-H	C-15,C-14

Compound 4 was isolated as yellowish oil upon chromatography over silica columns. The IR absorption band (in MeOH) exhibited close resemblance with that of compound 3, which apparently indicated that these compounds shared close structural similarities. The ultraviolet absorbance at λ max (log e) 254 nm (2.83) was assigned to a chromophore with extended conjugation. Its mass spectrum exhibited a molecular ion peak at m/e 441 (HRESIMS m/e 441.9864 [M-H]⁻; D 0.0 amu), which in combination with its ¹H and ¹³C NMR data (Table 5A.5, Figure 5A.17) indicated the elemental composition of compound 4 as C₂₈H₄₂O₄ with eight degrees of unsaturation. One degree of unsaturation from the carbonyl group, four degrees of unsaturation from the double bonds and three degrees of unsaturation from the rings were demonstrated. The ¹H-NMR in conjugation with ¹³C-NMR recorded the signals at δ 5.80, 4.99, 1.97, 1.21 and 1.31, and the ¹H-¹H COSY(Figure 5A.17.C) couplings were apparent between these protons assigned to be at H-23/H-24/H-25 and H-26; which support the presence of 2-methyl pentene system in compound 4. The relatively downfield shift of the methylene protons at δ 4.32 and the C-28 carbon at δ 65.60 referred to a possible hydroxyl group. The aromatic protons were assigned to be present at δ 7.42-7.09 and the proton integral of the protons revealed the presence of furan ring. The methylene group protons at δ 2.30 and δ 1.57 were assigned to be at C-2 and 3 positions respectively, and the downfield shift was apparently due to the presence of carbonyl and olefinic moiety in its vicinity. Strong HMBC correlations were found between H-27 (δ 3.67) and H-2 (δ 2.30) with C-1(δ 175) (Table 5A.5), which apparently indicated the presence of the carbonyl carbon near the methylene group. The presence of two quaternary carbons at δ 130.75 and δ 138.74 were due to the presence of substituted furan moiety. The ¹H-¹H COSY correlations between H-21 (δ 7.45)/H-20 (δ 7.06)/H-19 (δ 7.20) along with the proton and carbon connectivities deduced from HSQC (Figure 5A.17.D) and HMBC

(Figure 5A.17.E) experiments (Table 5A.5) confirmed the presence of the furan framework. No peaks observed in the ^1H NMR at 2.90 (s, 3H), 4.04, 4.24 indicates absence of oxygen in their vicinity. Also additional olefinic signals were apparent at δ 129.75, 131.34, and 115.89. The ^1H - ^1H COSY correlation between H-6/H-7/H-13/H-12/H-11/H-10 indicate the hexane ring. These results were supported by detailed HMBC experiment (Table 5A.5).

The presence of $-\text{CH}_2\text{OH}$ group at the C-15 position of compound 4 was confirmed by ^1H - ^1H COSY and HMBC experiments (Table 5A.5). The methine proton at δ 2.97 was characteristic of the junction point of the bicyclic ring with that of the side chain ethyl furan moiety as established by ^1H - ^1H COSY correlations and detailed HMBC experiments (Table 5A.5). The ^{13}C NMR spectrum of the purified compound in combination with DEPT experiments indicated the occurrence of 28 carbon atoms in compound 4 including one ester carbonyl carbon at δ 174 (Table 5A.5). The $-\text{CH}-$ proton at δ 34.23 exhibited HMBC correlation with the carbonyl carbon atom assigned to be as C-1 (δ 174.33). The low field quaternary signal (^{13}C NMR) at C-18 was in agreement with that of a quaternary carbon signal carrying furan ring C-18 of the structure (δ 138.74). The point of cyclization of H-5(5.30)/H-6(1.92)/H-7(1.33)/H-8(1.62)/H-9(2.04) forms six member ring similarly strong cosy relation between H-13(1.54) /H-12(2.11)/H-11(2.97)/H-10(1.72) support the presence of second ring. The proton and carbon connectivity deduced from HSQC and HMBC experiments confirmed the bicyclic framework attached to the aromatic side chain at the C-12 position of the compound. The $-\text{CH}_2$ proton at C-2 (δ 2.30) appeared to demonstrate long range HMBC correlation (Figure 5A.17.E)) with ester carbonyl carbon at δ 174 (C-1). The relative stereochemistry of the chiral centres particularly that of C-6, 11 and 14 of the bicyclic framework was deduced from the NOESY spectrum (Figure 5A.17.F) of the compound and the J -values. NOE couplings were observed between $\text{H}\alpha$ -5 (δ 5.30)/ $\text{H}\alpha$ -7 (δ 1.33) thus indicating that these groups must be equatorial and on the α -side of the molecule. The methine proton at C-14 group did not exhibit NOE interactions with H-11 and H-15, which is at the α -face of the molecule, thereby indicating that H-14 is at the axial disposition.

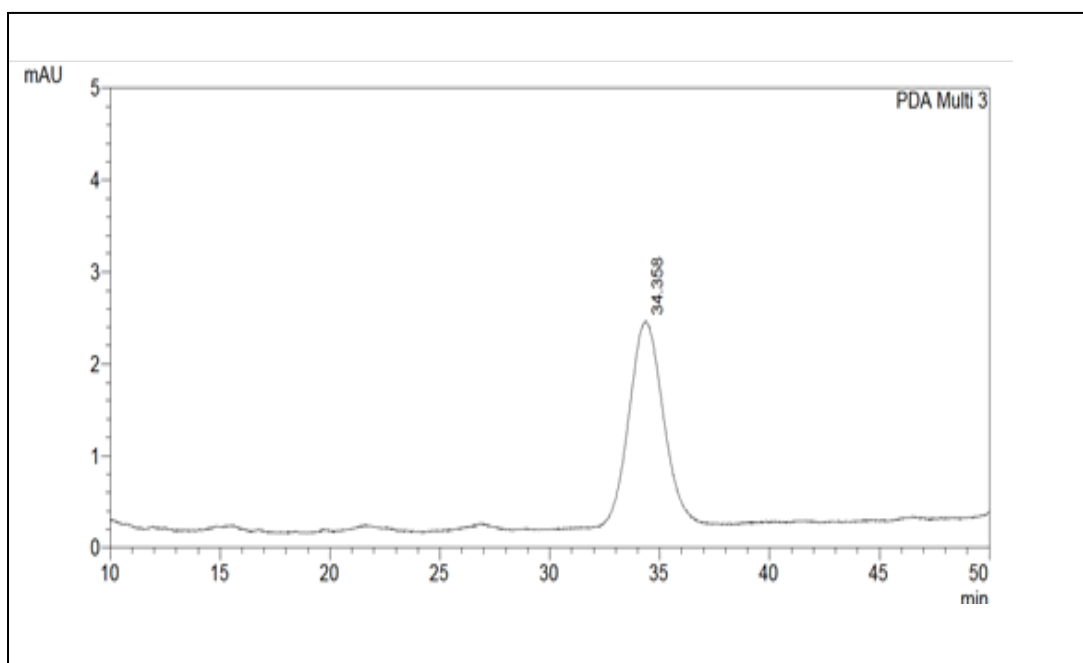


Figure 5A.16
HPLC chromatogram of Compound 4

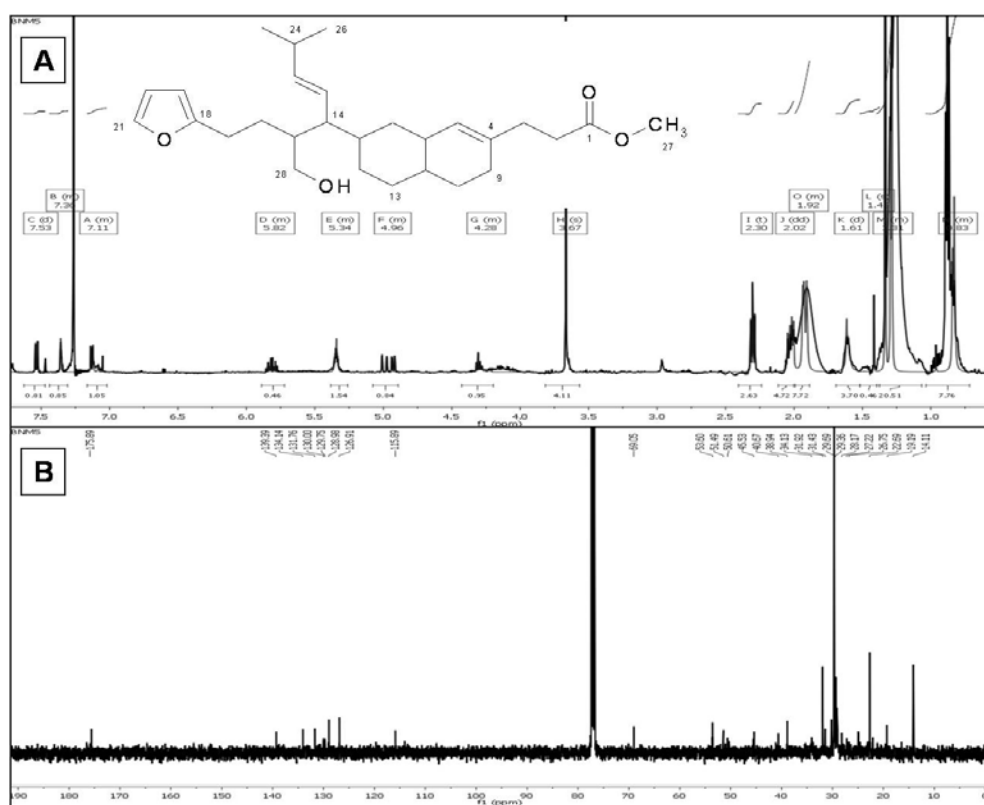


Figure 5A.17
(A) ¹H, (B) ¹³C NMR spectrum of compound 4

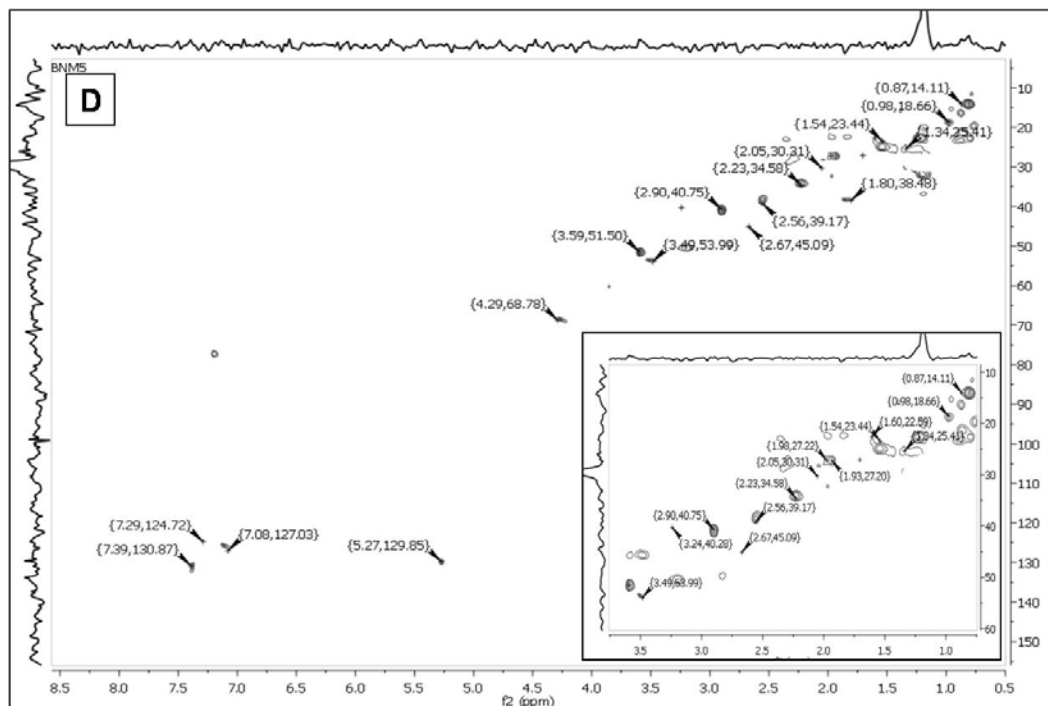
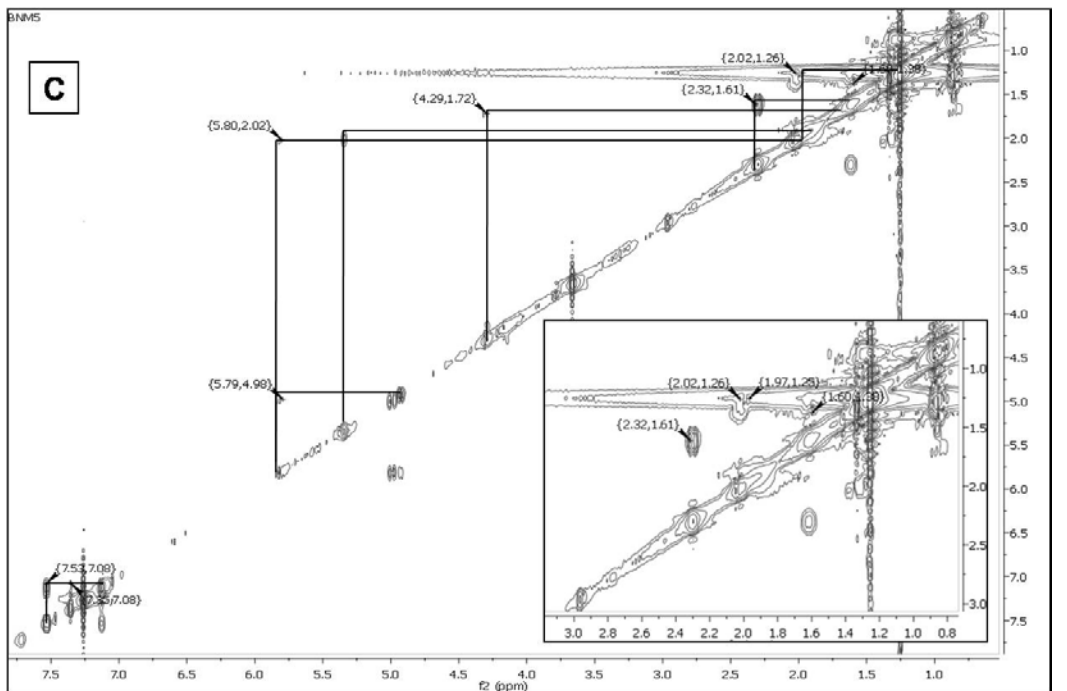


Figure 5A.17

(C) ^1H - ^1H COSY - NMR spectrum of compound 4 (D) Prominent HSQC correlation spectrum of compound 4

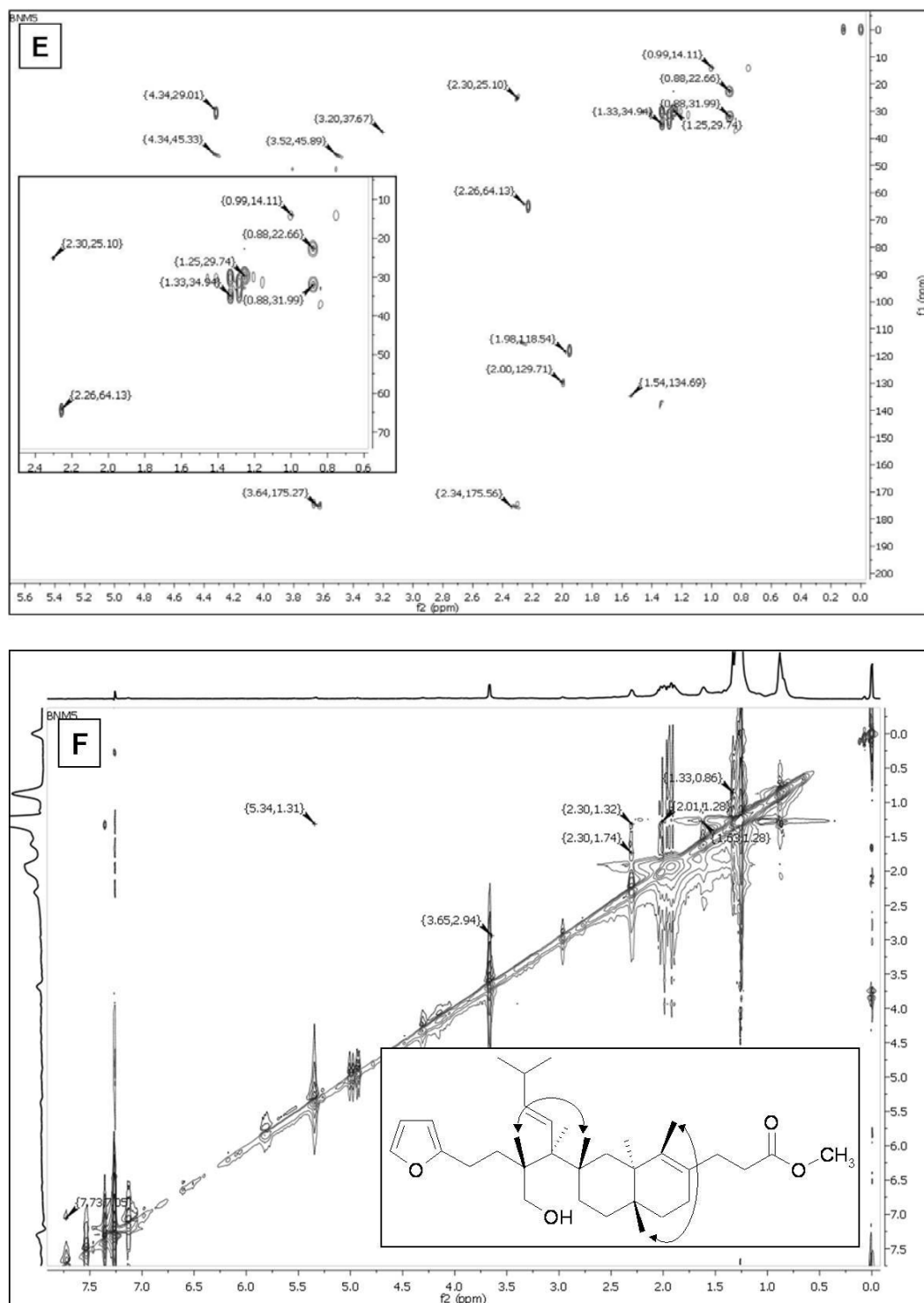


Figure 5A.17

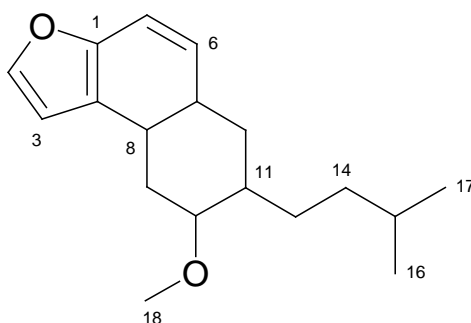
(E) HMBC and **(F)** NOESY spectra of compound 4. The key HMBC couplings have been indicated as double barbed arrow. The NOESY spectrums have been indicated as two sided arrows.

5A.2.6.5 Structural characterization of Compound 5(B2E35)

5a,6,7,8,9,9a-Hexahydro-7-isopentyl-8-methoxynaphtho[2,1-b]furan: Yellowish oil UV (MeOH) λ_{\max} (log ϵ): 238 nm (3.12); TLC (Si gel GF₂₅₄ 15 mm; EtOAc/*n*-hexane (3:17, v/v) R_f: 0.40; R_t: 21.595 min(Figure 5A.18); IR (KBr, cm⁻¹) ν_{\max} 818.24 (aromatic C-H_δ), 1309.16 (C-O_v), 1372.34 (C-H_ρ), 1618.46 (C=C_v), 2935.35 (alkane C-H_v), 3011.22 cm⁻¹ (aromatic C-H_v); ¹H NMR (500 MHz, Chloroform-d) δ 7.61 – 7.50 (m, 1H), 7.13 (d, 2H), 5.93 – 5.71 (m, 1H), 5.08 – 4.83 (m, 1H), 4.30 (d, 1H), 3.67 (s, 3H), 2.43 – 2.20 (m, 1H), 2.15 – 1.93 (m, 3H), 1.65–1.31 (m, 6H), 1.27–1.20(m,3H), 0.90(d,3H), 0.88 (d, 3H). ¹³C NMR (125 MHz, CDCl₃ δ in ppm), ¹H-¹H-COSY, and HMBC data, see Table 5A.6; HRMS (ESI) *m/e*: 275.6846(M+H)⁺ calcd. for C₁₈H₂₇O₂ 275.4072; found 275.6846(M+H)⁺.

Table 5A.6

NMR spectroscopic data of 5a,6,7,8,9,9a-hexahydro-7-isopentyl-8-methoxynaphtho[2,1-b]furan in CDCl₃.^a



Position	¹³ C ppm	H-type	¹ H NMR	¹ H- ¹ H COSY	HMBC ¹ H → ¹³ C
1	148.59				
2	124.45				
3	115.57	3-H	7.06(d,1H)	4-H	C-1
4	144.96	4-H	7.38(d,1H)		
5	117.06	5-H	4.98(d,1H)	6- H	C-1,6
6	133.18	6-H	5.82(m,1H)	7-H	
7	41.17	7-H	2.03(m,1H)	12-H	C-6
8	48.46	8-H	2.29(t, 1H)	7- H	C-7

9	31.93	9-H	1.55 (m, 2H),		C-10
10	62.09	10-H	4.26(m, 1H),		C-9,11
11	34.87	11-H	1.98(m,1H)	12-H	C-12
12	31.44	12-H	1.36(m,2H)		
13	30.20	13-H	1.65 (m, 2H)	11-H	C-14,11
14	29.36	14-H	1.27(m,2H)		C-15
15	22.69	15-H	1.21(m,1H)	14-H	
16	14.11	16-H	0.91(d,3H)	15-H	C-17
17	13.91	17-H	0.88(d,3H)		
18	53.22	18-H	3.67(s,3H)		C-10

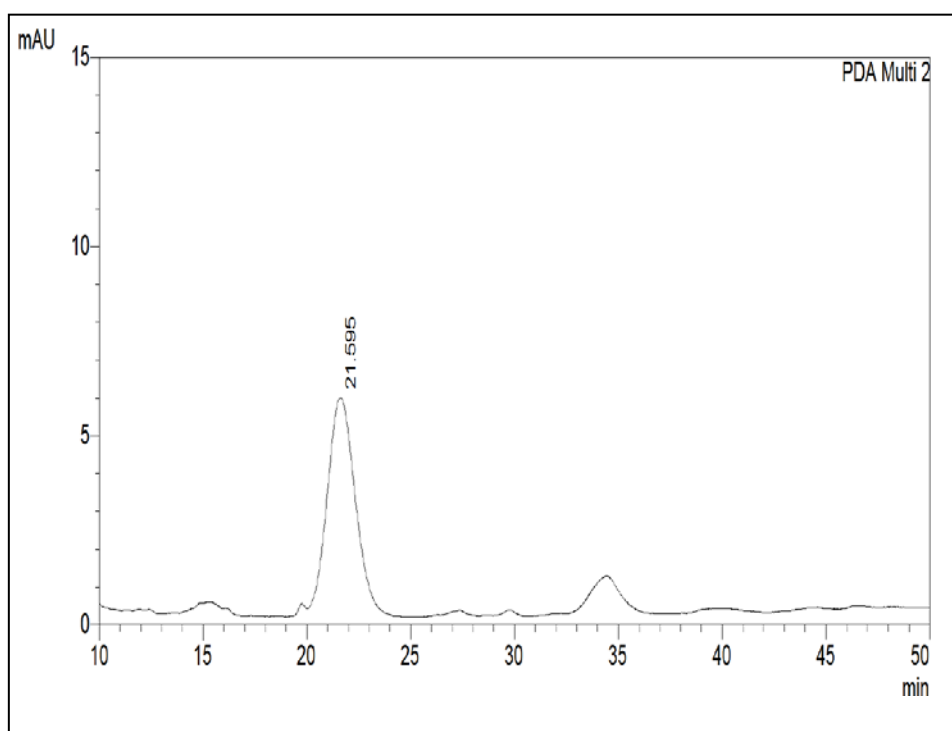


Figure 5A.18
HPLC chromatogram of compound 5

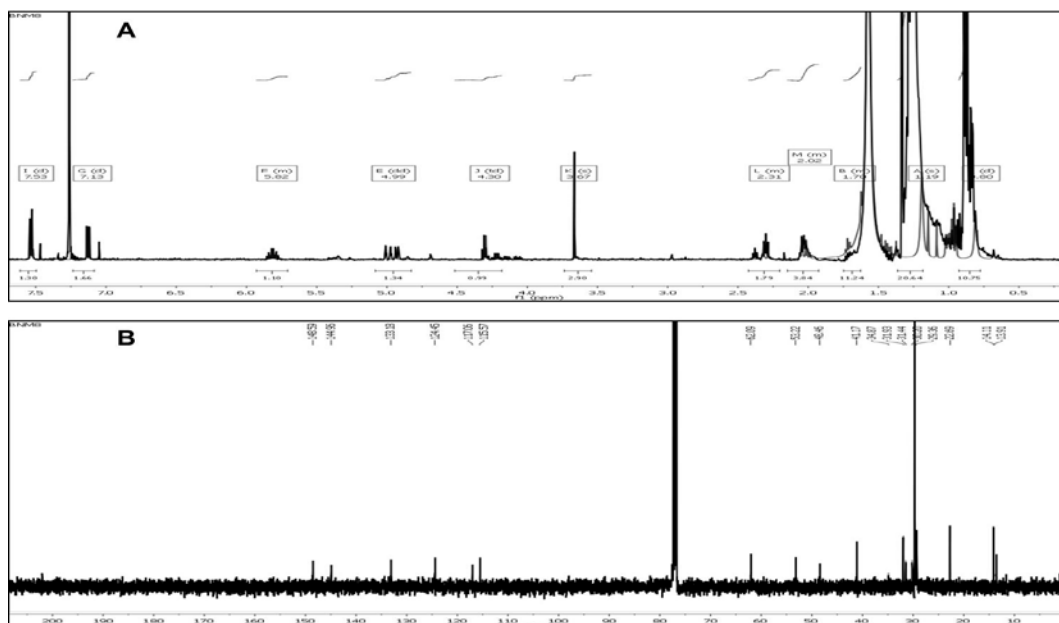


Figure 5A.19
(A) ^1H , (B) ^{13}C NMR spectrum of Compound 5

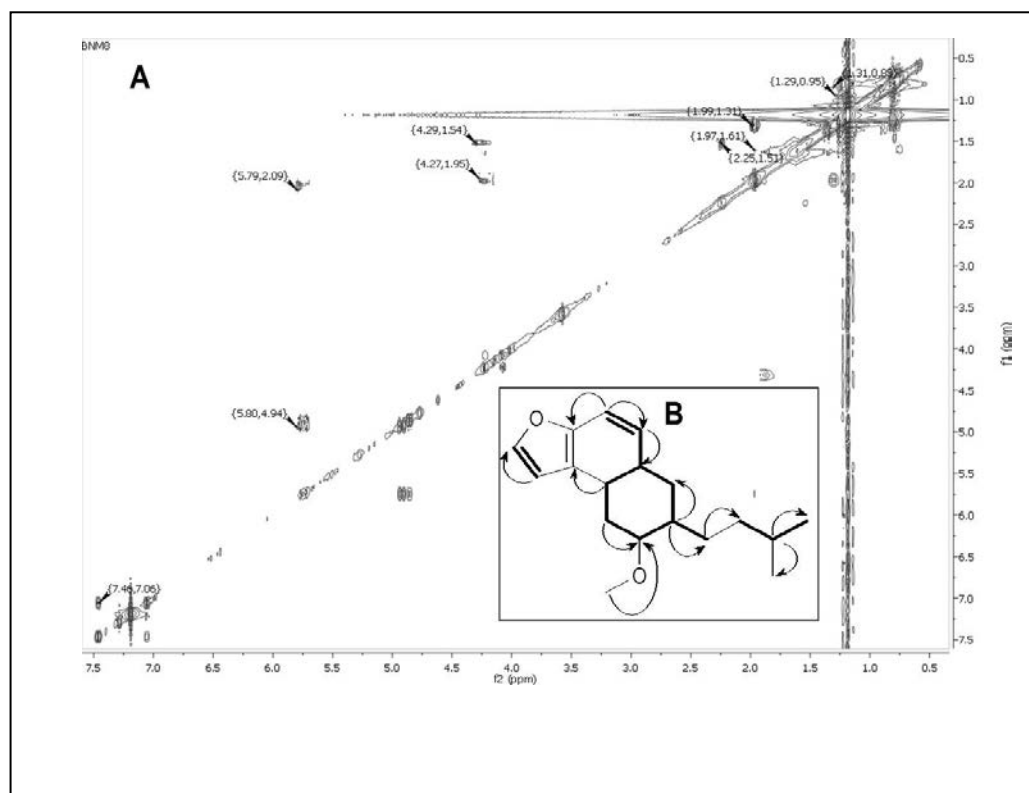


Figure 5A.20
2D NMR correlations as observed in compound5 (A) The key ^1H - ^1H COSY couplings; (B) The ^1H - ^1H COSY couplings have been represented by the bold face bonds; The HMBC couplings are indicated as a double barbed arrow

Compound 5 was isolated as yellowish oil upon chromatography over silica columns. The ultraviolet absorbance at λ max (log e) 238 nm (3.12) was assigned to a chromophore with extended conjugation. Its mass spectrum exhibited a molecular ion peak at m/e 275 (HRESIMS m/e 275.6846 $[M+H]^+$; D 0.0 amu), which in combination with its ^1H and ^{13}C NMR data (Table 5A.6; Figure 5A.19) indicated the elemental composition of compound 5 as $\text{C}_{18}\text{H}_{26}\text{O}_2$ with six degrees of unsaturation. Three degrees of unsaturation from the double bonds and three degrees of unsaturation from the rings were demonstrated. The ^1H -NMR in conjugation with ^{13}C -NMR recorded the signals at δ 1.98, 1.65, 1.27, 1.21, 0.88 and 0.91 showed ^1H - ^1H COSY couplings were apparent between these protons assigned to be at H-11/H-13/H-14/H-15/H-16 and H-17; which support the presence of 2-methyl pentane system in compound 5. The relatively downfield shift of the methylene protons at δ 4.26 and the C-10 carbon at δ 62.09 referred to a possible oxygen group. The aromatic protons were assigned to be present at δ 7.48-7.06 and the proton integral of the protons revealed the presence of furan ring. Signal at 148.59 (C-1) downfield shifts was apparently due to the furan ring and olefinic moiety in its vicinity. Strong HMBC correlations were found between H-5 (δ 4.98) and H-6 (δ 5.82) with C-1 (δ 148.59) (Table 5A.6), which apparently indicated the presence of the olefinic carbons near the furan group. The presence of two quaternary carbons at δ 148.59 and δ 124.45 were due to the presence of substituted furan moiety. The ^1H - ^1H COSY correlations between H-3 (δ 7.11)/H-4 (δ 7.38) along with the proton and carbon connectivities deduced from HSQC and HMBC experiments (Table) confirmed the presence of the furan framework. Also additional olefinic signals were apparent at δ 133.18 and 117.06. The ^1H - ^1H COSY correlation with H-5 (δ 4.98 dd, 1H)/H-6 (δ 5.82, m, 1H)/H-7 (δ 2.03, m, 1H) and H-8 (δ 2.29, t, 1H) which support the presence of the cyclic hexane moiety (Figure 5A.20.A). These results were supported by detailed HMBC experiment (Figure 5A.20.B). The presence of $-\text{CH}_2\text{OCH}_3$ group at the C-10 position of compound 5 was confirmed by ^1H NMR and HMBC experiments (Table 5A.6). The methine proton at δ 2.29 was characteristic of the junction point of the bicyclic ring with that of the side furan moiety as established by ^1H - ^1H COSY correlations and detailed HMBC experiments (Table 5A.6). The ^{13}C NMR spectrum of the purified compound in combination with DEPT experiments indicated the occurrence of 18 carbon atoms in compound 5.

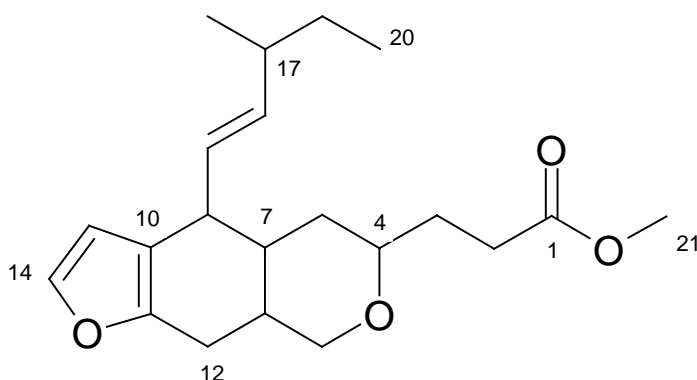
(Table 5A.6). The –CH– proton at δ 53.22 exhibited HMBC correlation with the carbon atom assigned to be as C-10 (δ 62.09). The low field quaternary signal (^{13}C NMR) at C-1 was in agreement with that of a quaternary carbon signal carrying furan ring C-18 of the structure (δ 148.59). The aromatic furan attached to the bicyclic group was substituted side by side. The point of cyclization of H-8(2.29)/H-9(1.55)/H-10(62.09)/H-11(1.98)/H-12(1.36) forms six member ring support the presence of second cyclohexane ring. The proton and carbon connectivity deduced from HSQC and HMBC experiments confirmed the bicyclic framework attached to the aromatic furan ring. The HMBC spectrum of the purified compound also revealed connections of the protons at C-18 (δ 3.67) to the methylene carbon at δ 62.09. The relative stereochemistry of the chiral centers particularly that of C-8, 10, 11 and 7 of the bicyclic framework was deduced from the NOESY spectrum of the compound and the *J*-values. NOE couplings were observed between H α -8 (δ 2.29)/H α -11 (δ 1.98) thus indicating that these groups must be equatorial and on the α -side of the molecule. The methine proton at C-10 group did not exhibit NOE interactions with H-11 and H-8, which is at the α -face of the molecule, thereby indicating that H-10 is at the axial disposition.

5A.2.6.6 Structural characterization of Compound 6(B2E41)

Methyl 3-(4a,5,6,8,8a,9-hexahydro-4-((E)-3-methylpent-1-enyl)-4H-furo [3,2-g]isochromen-6-yl)propanoate: Yellowish oil UV (MeOH) λ_{max} (log ϵ): 259 nm (2.86); TLC (Si gel GF₂₅₄ 15 mm; EtOAc/*n*-hexane (3:17, v/v) R_f: 0.20; R_t: 29.395 min(HPLC) (**Figure 5A.21**) ; IR (KBr, cm⁻¹) ν_{max} 812.06 (aromatic C-H δ), 1310.16 (C-O ν), 1378.22 (C-H ρ), 1612.94 (C=C ν), 1690.28 cm⁻¹ (C-C-O ν), 1738.96 (C=O ν), 2923.22 (alkane C-H ν), 3010.12 cm⁻¹ (aromatic C-H ν); ^1H NMR (500 MHz, Chloroform-d) δ 7.40 (d, 1H), 7.14 – 6.89 (m, 1H), 5.83 – 5.67 (m, 2H), 5.02 – 4.74 (m, 2H), 4.31 – 4.15 (m, 1H), 4.15 – 3.98 (m, 1H), 3.65 – 3.49 (m, 1H), 2.36 – 2.18 (m, 2H), 2.10 – 1.87 (m, 10H), 1.80 – 1.66 (m, 13H), 1.63 – 1.48 (m, 6H), 1.45 – 1.29 (m, 5H), 1.29 – 1.16 (m, 5H), 1.00 – 0.85 (m, 3H). ^{13}C NMR (125 MHz, CDCl₃ δ in ppm), ^1H - ^1H -COSY, and HMBC data, see Table 5A.7 ; HRMS (ESI) *m/e*: 369.3892(M+Na)⁺ calcd. for C₂₁H₃₀O₄ Na 369.4008; found 369.3892 [M+Na]⁺.

Table 5A.7

NMR spectroscopic data of methyl 3-(4a,5,6,8,8a,9-hexahydro-4-((E)-3-methylpent-1-enyl)-4H-furo[3,2-g]isochromen-6-yl)propanoate in CDCl_3 .^a



Position	^{13}C ppm	H	^1H NMR	^1H - ^1H COSY	HMBC $^1\text{H} \rightarrow$ ^{13}C
1	173.59				
2	33.82	2-H	2.25 (m, 1H)	3-H	C-3,1
3	25.24	3-H	1.55 (m, 1H)	4-H	C-4
4	60.69	4-H	4.06(m, 1H)	8-H	C-5
5	65.46	5-H	4.26(m, 1H)	6- H	
6	29.7	6-H	1.65 (m, 1H)	12-H	C-12
7	22.69	7-H	1.36(m,1H)		C-9
8	31.93	8-H	1.94 (t, $J = 6.7$ Hz, 2H)		C-4
9	29.42	9-H	1.97(m,1H)	15-H	C-10
10	146.26				
11	127.34				
12	29.36	12-H	1.72(d,1H)	6- H	
13	124.03	13-H	7.06(d,1H)	14-H	C-14,10

14	133.76	14-H	7.38(d,1H)		
15	139.28	15-H	5.70(dt,1H)	16-H	C-16
16	114.06	16-H	4.98(dd,1H)		C-17
17	27.09	17-H	1.80 (m, 1H)	18-H	
18	24.98	18-H	1.23(d,1H)		C-17
19	22.63	19-H	1.21(m,2H)	17-H	C-12
20	14.12	20-H	0.88(d,3H)	19- H	C-19,17
21	58.69	21-H	3.59(s,3H)		C-1

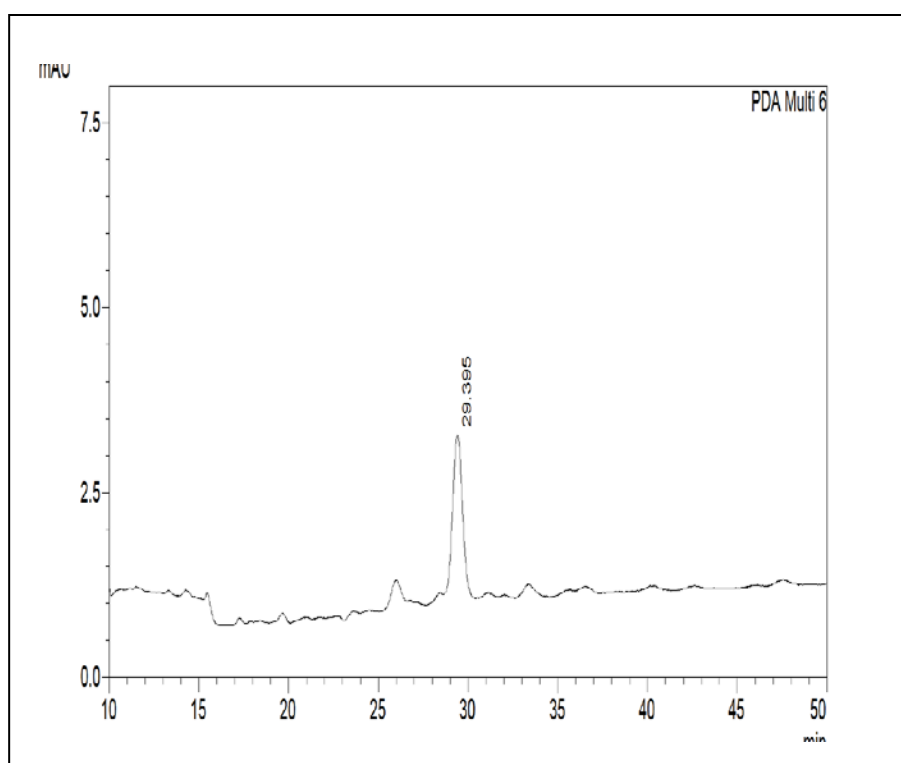


Figure 5A.21
HPLC chromatogram of Compound 6(B2E41)

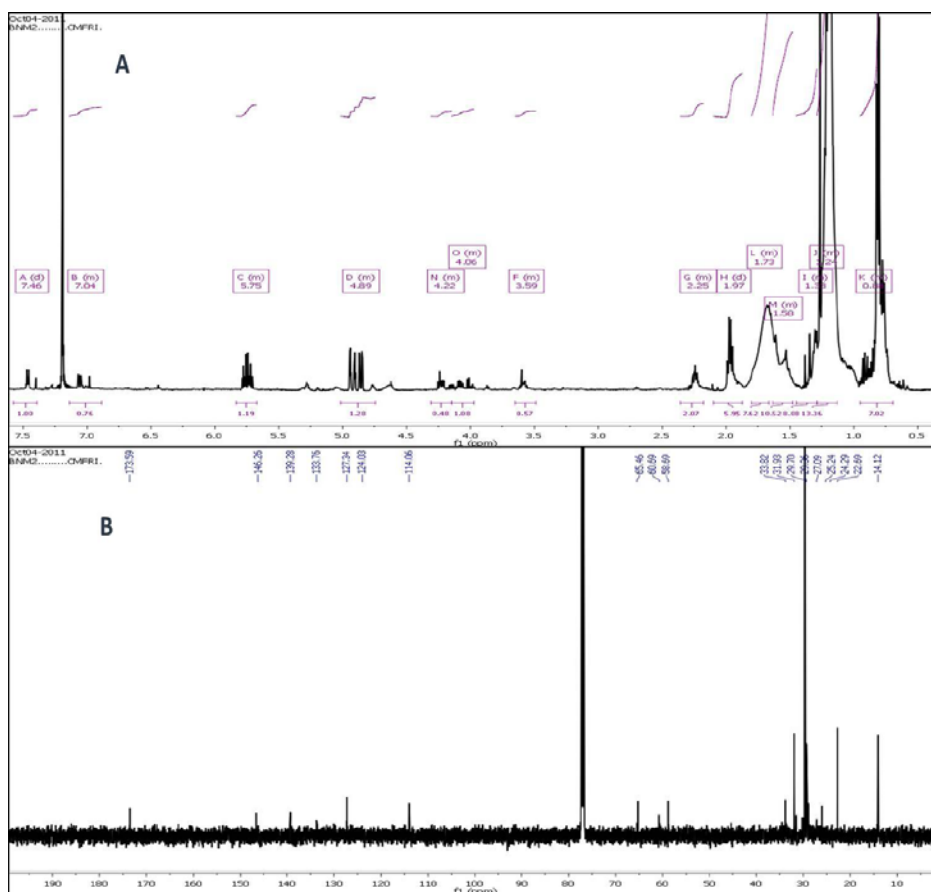


Figure 5A.22
(A) ^1H , (B) ^{13}C NMR spectrum of compound 6

The IR bending vibration bands of compound 6 at 1738.96 cm^{-1} attributed to the ester carbonyl absorption. The IR spectrum revealed broad absorption band at $\nu_{\text{max}} 1612.94\text{ cm}^{-1}$, symbolizing the olefinic system. The bending vibration bands near 812.06 cm^{-1} and stretching vibration at 3010.12 cm^{-1} denoted the aromatic C-H vibrations. The ultraviolet absorbance at $\lambda_{\text{max}} (\log \epsilon) 259\text{ nm} (2.86)$ was assigned to a chromophore with extended conjugation. Its mass spectrum exhibited a molecular ion peak at $m/e 369$, which in combination with its ^1H and ^{13}C NMR data (Table 5A.7) indicated the elemental composition of $\text{C}_{21}\text{H}_{30}\text{O}_4\text{Na}$. The ^1H -NMR in conjunction with ^{13}C -NMR and DEPT spectra recorded the presence of six methylene, nine methine, three methyl, and three quaternary carbon atoms. Its mass spectrum exhibited a molecular ion peak at $m/z 346$ (HRESIMS $m/e 369.3892$ $[\text{M}+\text{Na}]^+$; D 0.0 amu), which in combination with its ^1H and ^{13}C NMR data (Table 5A.7; Figure 5A.22) indicated the elemental composition of compound 6 as

$C_{21}H_{30}O_4Na$ with seven degrees of unsaturation (Figure 5A.22). Three degree of unstaruration from double bonds, three degrees of unstaruration from the aryl and pyran ring systems, one from the carbonyl moieties. Couplings were apparent between the protons at δ 5.80 (H-15)/ δ 4.98 (H-16)/ δ 1.97 (H-17)/ δ 1.23 (H-18) and 1.21(H-19)/ δ 0.88 (H-20) in the 1H - 1H COSY spectrum, which supported the presence of 3-methyl pentene moiety. The methine signal H-4 at δ 4.06 appeared downfield due to the presence of electronegative systems at close proximity. One methylene groups have been assigned to occupy at the C-5 position, shifted downfield due to the presence of oxygen moiety. The HMBC correlation of the proton at δ 4.26 with the carbon atom at δ 60.69 apparently indicated the presence of pyranose moiety. The HSQC and HMBC experiments revealed that the ester group linked to the methoxy group at δ 3.59. The aromatic protons showed their characteristic signals at δ 7.38-7.04. Extensive HMBC and HSQC experiments revealed the presence of substituted furan moiety in compound 6. The 1H - 1H COSY experiments revealed that the protons at δ 2.25(t) correlate with the methylene protons at δ 1.53 (assigned to be as H-3) and, the later is assigned to be attached to a carbonyl electronegative group.

The $-CH_2-$ proton appeared downfield at δ 4.26 apparently due to the presence of the electronegative oxygen group and was assigned to be present at the C-5 position of compound 6. The carboxyl group at the C-1 position of compound 6 resulted in strong deshielding of the $-CH-$ proton at δ 2.25, and therefore, has been assigned to be present at the C-2 position of the structure. The chemical shift of the protons at δ 1.94, 1.36, 1.65, and 4.26 along with detailed 2D NMR experiments established the presence of *O*-heterocyclic pyran ring system. The $-CH-$ proton at δ 4.06 is characteristic of the junction point of the cyclic system with carboxylic side chain. The ^{13}C NMR spectrum of the purified compound in combination with DEPT experiments indicated the occurrence of 21 carbon atoms in the molecule including furan carbons at δ 146-114, and olefinic carbons at δ 139.77 and 124 (Table 5A.7). The low field quaternary signals (^{13}C -NMR) were in agreement with that to a quaternary carbon signal carrying the furan ring. The H-H and C-H connectivities apparent in the 1H - 1H COSY and HMBC spectra respectively indicate that one of the seven unsaturations was due to the three ring and four double bonds. The relative stereochemistry of the chiral centre particularly that of C-6 cyclic

framework was deduced from the NOESY experiment and the *J*-values. NOE couplings were observed between H α -4/H α -6 thus indicating that these groups must be equatorial and on the α -side of the molecule. Therefore, the C-7 proton is axial and β -oriented.

5A.3 Conclusions

Bacillus subtilis MTCC 10403 (SWI2) associated with *Anthophycus longifolium* demonstrated it as a promising bacterial candidate to isolate the potential antibacterial metabolites. A total of six antibacterial metabolites were purified from the crude solvent extract of the bacterium, namely, 7-O-methyl-5'-hydroxy-3'-heptenoate-macrolactin, 6-(4-acetylphenyl)-5-hydroxyhexanoic macrolactin, 2-(7-(2-ethylbutyl)-2,3,4,4a,6,7-hexahydro-2-oxopyrano [3,2-b] pyran-3-yl) ethyl benzoate, methyl 3-(2-((E)-2-(2-(furan-2-yl)ethyl)-1-hydroxy-6-methylhept-4-en-3-yl)-1,2,3,4,4a,5,6,8a-octahydronaphthalen-7-yl)propanoate, 5a,6,7,8,9,9a-hexahydro-7-isopentyl-8-methoxynaphtho[2,1-b]furan and methyl 3-(4a,5,6,8,8a,9-hexahydro-4-((E)-3-methylpent-1-enyl)-4H-furo[3,2-g]isochromen-6-yl)propanoate.

The potential of polyketide derived antibacterial candidate to develop a new generation of drug candidates for use against the multiresistant microbial pathogens. The newly evolving antibacterials bearing the polyketide backbone will be increasingly important keeping in mind the development of multi-drug resistant bacteria and pathogenic microorganisms against the existing antibiotics and related molecules. In this study, a new variant of macrolactin, 7-O-methyl -5'-hydroxy-3'-heptenoate-macrolactin has been described. This novel polyketide product holds promise to develop a new generation of drug candidate for use against the multiresistant microbial pathogens. Evidence for a biosynthetic route of this compound was provided in this study, which may lead to the identification of a new target for antimicrobial lead molecule discovery programs. The results demonstrated that these polyene antibiotics are widespread metabolites of seaweed-associated bacterial populace particularly belonging to *Bacillus* species. The present work may have an impact on the exploitation of macrolactins for food, pharmaceutical and biotechnological applications.

CHAPTER 5B

BIOPROSPECTING OF ANTAGONISTIC BACTERIA

Bacillus amyloliquefacens MTCC 10456 ASSOCIATED WITH SEAWEED *Laurenciae papillosa* (SWI4B) FOR ANTIBACTERIAL METABOLITES

5B.1 Materials and Methods

5B.1.1 Microbial strain under the study

The microbial strain used for bioprospecting of antimicrobial compound in the current study is MTCC 10456 associated with *Laurenciae papillosa*. The seaweed associated bacterial isolates were isolated (chapter 3 section 3.2.2) and assayed for their ability to inhibit selected pathogenic microorganisms (chapter 3 section 3.2.5). The isolates used in the study for purification of secondary metabolites with antibacterial activities were selected based on their inhibition spectrum (Figure 5B.1) (chapter 3 Table 3.2) and the positive hit for metabolite gene (Chapter 4. 2.5 and 4.3.4).

5B.1.2 Antibiotic resistance and abiotic stress tolerance

Antibiotic resistance, abiotic stress tolerance and enzyme production profile of the strain MTCC 10456 was analyzed using the methodology explained in 5.2.2.

5B.1.3 Optimization of time

The microorganism under the study was inoculated in nutrient broth and the optimum time for the antibiotic production with maximum inhibitory activity was analyzed as explained in 5.2.3.

5B.1.4 Optimization of temperature

The optimum temperature for the production of antibacterial compound for the strain MTCC 10456 was analyzed using the methodology explained under the section 5.2.4.

5B.1.5 Optimization of pH

P^H for the production of the active metabolite was standardized as described under the section 5.2.5.

5B.1.6 Preparation of crude extract for purification of secondary metabolites

The antibiotic-producing bacterium, *B. amyloliquefacens* MTCC 10456 associated with *Laurentia papillosa* (SWI4B). The preparation and recovery of secondary metabolites were carried out by a surface culturing method over solid nutrient agar plates (5.2.3). The adsorbed products were subsequently extracted with ethyl acetate by homogenization (Arrow Engineering Inc., Pennsylvania Ave, USA) followed by refluxing. Evaporation of the solvent under reduced pressure (Heidolph Instruments GmbH & Co., Schwabach, Germany) yielded the ethyl acetate extract (6.3g) from the total culture volume of 4 L. Subsequently the residual agar was extracted with CH₂Cl₂ to furnish dichlorometane extract. These solvent extracts were evaluated for antibacterial activities (5.2.4), against the pathogens (listed in chapter 3 section 3.2.4) and the fractions which showed significantly broad spectrum antibacterial activities and higher yield were further purified by chromatographic techniques.

5B.1.7 Purification of secondary metabolites

The pooled ethyl acetate extract (6.3 g) was subjected to vacuum liquid chromatography on silica gel (180-230 mesh), with a stepwise gradient of *n*-hexane/EtOAc (0-100%). The column was initially eluted with *n*-hexane and the eluent polarity was gradually increased by addition of EtOAc (*n*-hexane: EtOAc 19:1 to 1:4, v/v) to furnish fourteen fractions of 50 ml each (B₄E₁-B₄E₁₄). These column

fractions were evaluated for antibacterial activities(5.2.4), against the pathogens (listed in chapter 3 section 3.2.4) and the fractions which showed significantly broad spectrum antibacterial activities and higher yield were further purified by column chromatography or preparative TLC (P-TLC) using EtOAc:*n*-hexane or MeOH:CHCl₃ or MeOH:EtOAc as mobile phase when required. The schematic diagram showing the purification of *B. amyloliquefaciens* MTCC 10456 associated with *Laurentia papillosa* (SWI4B) was shown in Figure 5B.2

5B.1.8 Analysis of pure fractions

Active fractions were subjected to chromatographic and spectroscopic analysis as explained earlier (5.2.9).

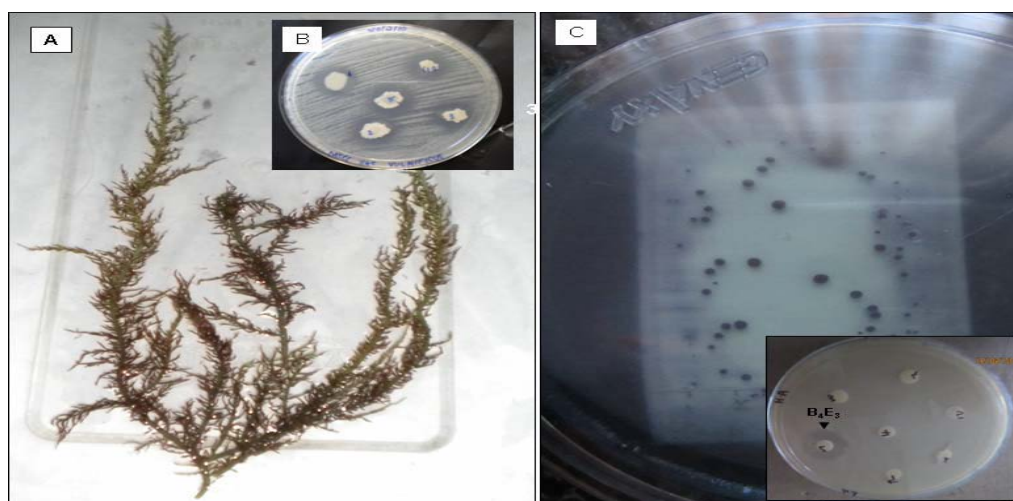


Figure 5B.1

(A) *Laurenciae papillosa* at harvest location (9° 17' 0" North, 79° 7' 0" East). (B) Spot over lawn assay of *B. amyloliquefaciens* MTCC 10456 culture against pathogenic *Vibrio vulnificus* MTCC 1145. The clearance zones realized by the isolates signify the antibacterial activity. (C) Bioautographic plate showing inhibitory activity of the column fraction B₄E₃ from crude culture extract (shown as hallow). The antagonistic activity of B₄E₃ was indicated as an arrow on the plate (inset). Antagonistic activity was recorded as the diameter of inhibition zones determined as a distance of ≥ 1 mm between the circular area (= lawn of the isolate) and the end of the clear zone bounded by the lawn.

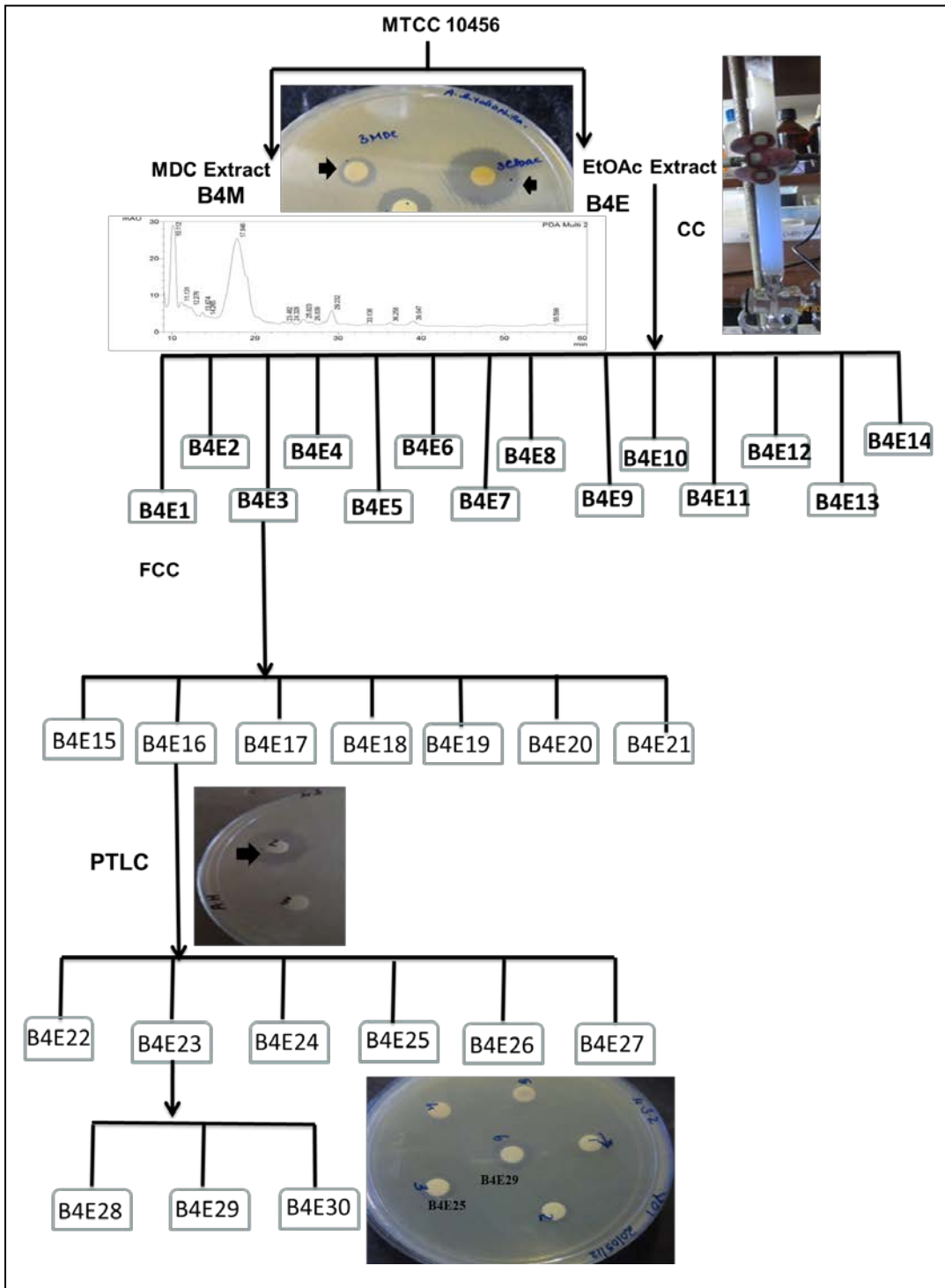


Figure 5B.2

Schematic representaion of bioprospecting of *B. amyloliquefacens* MTCC 10456

5B.2 Results and discussion

5B.2.1 Antibiotic resistance and abiotic stress tolerance

The strain was susceptible to all the antibiotics tested and was proved to be safe for laboratory work. The strain was able to grow above 20°C up to 55°C and could with stand a pH range of 6 to 11.5. Strain could grow an NaCl concentration from 2% to 10%. The ability of the seaweed associated bacterial isolate to grow under a wide range of environmental conditions may be a functional adaptation for their protective function in varying aquatic environment.

5B.2.2 Optimization of time, temperature and pH

Optimum time of production for the culture is found to be within 72 to 96 hours. The pH was found to be 8 and the culture grown at 20°C is shown a maximum activity (Figure 5B.3).

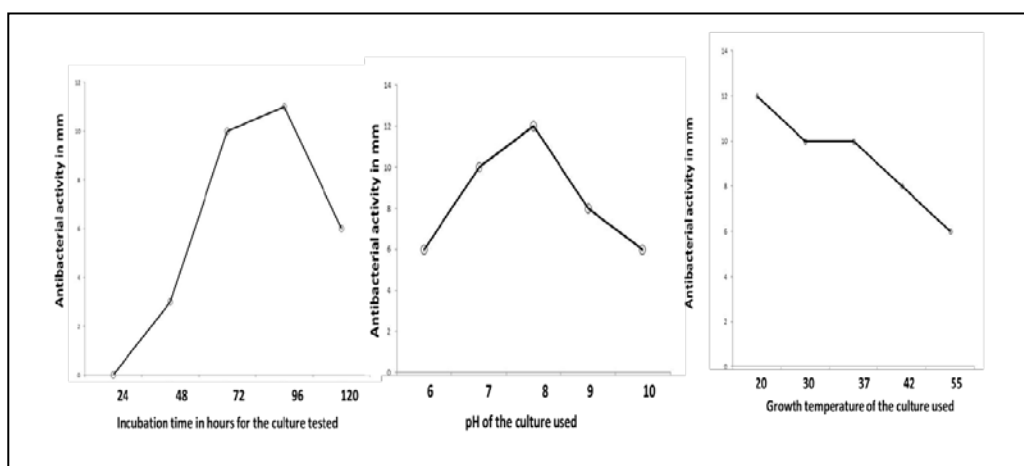


Figure 5B.3
Graphical representation of antibacterial activity of cultures
incubated at different pH, temperature and time

5B.2.3 Yield

The yield (g/L of the spent broth) of the EtOAc extracts of SWI 4 was recorded as 1.575g/L of the spent broth is higher than DCM (0.4365 g/L of the spent broth) extract.

5B.2.4 Antibacterial activities of the crude extracts by agar diffusion method.

Antibacterial activity of *B. amyloliquefacens* MTCC 10456 extracts to different pathogens *Aeromonas hydrophilla* V. *vulnificus* MTCC 1145 and *V. parahaemoliticus* ATCC17802 are shown in Fig. 5B.4. The figure indicated that the EA fractions are more active than other fractions of the *B. amyloliquefacens* MTCC 10456 associated with *Laurentia papillosa* (SWI4B). The ethyl acetate extract (100 mcg on disk) of *Bacillus amyloliquefaciens* MTCC10456 exhibited an inhibitory zone diameter of about 21-26 mm against the experimental pathogens (Figure 5B.1 and Figure 5B.2)

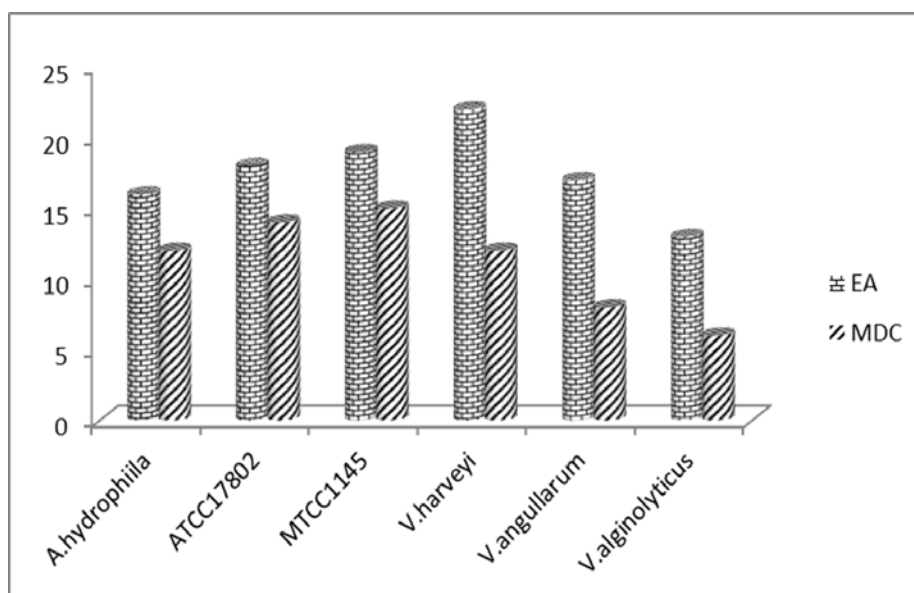


Figure 5B.4
Graphical representation of antibacterial activity of different crude solvent extracts to the tested pathogens

5B.2.5 Secondary Metabolites from *B. amyloliquefacens* MTCC 10456 associated with *Laurentia papillosa*(SWI4B)

The fraction B₄E₃ (773 mg) was found to be a mixture with an antibacterial activity of 24 mm, which was flash chromatographed (Biotage AB SP1-B1A, 230–400 mesh, 12 g; Biotage AB, Uppsala, Sweden) on a silica gel column (Biotage, 230–400 mesh, 12 g; Sweden, Biotage No. 25+M 0489-1) at a collection UV wavelength at 242 nm using a step gradient of CH₂Cl₂/ MeOH (0-100% MeOH) to afford 125 fractions (9 ml each). The fractions with similar patterns were pooled together to afford seven pooled fractions (B₄E₁₅– B₄E₂₁) after TLC analysis (*n*-hexane: EtOAc, 9:1, v/v). The sub-fraction B₄E₁₆ (159 mg) as eluted with CH₂Cl₂/ MeOH (19:1, v/v) was further separated by chromatography on silica gel GF₂₅₄ (particle size 15 µm) coated on a preparatory thin layer plate using a stepwise gradient system from 0.5% MeOH/CH₂Cl₂ yielding B₄E₂₅, 3- (octahydro-9-isopropyl-2H- benzo [h] chromen-4-yl) - 2- methylpropyl benzoate (**compound 7**, inhibition zone diameter of 12 mm, 25 mcg per disk). The active fraction B₄E₂₃ (72 mg) eluted at 0.3% MeOH/CH₂Cl₂ was further chromatographed over preparatory TLC on silica gel GF₂₅₄ (particle size 15 mm, E-Merck, Germany) using MeOH/CH₂Cl₂ (0.5:95.5, v/v) to afford B₄E₂₉ methyl 8- (2- (benzoyloxy) ethyl) – hexahydro -4- ((E) – pent - 2- enyl) - 2H-chromene-6-carboxylate (**compound 8**, ~99% purity, 6.2 mg, inhibition zone diameter of 14 mm, 25 mcg per disk). Evaporation of solvents from B₄E₂₉ followed by TLC over precoated silica gel GF₂₅₄ (particle size 15 mm, E-Merck, Germany) using EtOAc/ *n*-hexane (1:4, v/v) supported the purity. The remaining fractions were not considered for purification either of low yield or less activity.

The compound **7** and **8** isolated from *Bacillus amyloliquefaciens* MTCC10456 demonstrated significant antibacterial activity (inhibitory zone diameter of greater than 18 mm against *A. hydrophilla*, 25 mcg on disk) against these pathogenic bacteria (Fig. 5B(2), Table 5B(1). The antibacterial activities of **7** and **8** against *Vibrio vulnificus* (14-16 mm, 25 mcg on disk) and *V. parahemolyticus* ATCC® 17802™ (inhibitory zone diameter of 12-14 mm, 25 mcg on disk) were

found to be lesser than *A. hydrophilla*. It is of note that the compound **8** exhibited greater antibacterial activities against the experimental pathogens than **7** (Table5B.1).

Table 5 B.1

Yield, activity and R_f values of the fractions at different purification stages

	Yield (mg)	R _t	R _f	Antibacterial activity
B4 EtOAc fraction (CC E/H)				
B4E-1(100% H)	49.2	-	NP	NA
B4E-2(0-5% E/H)	3.7	-	NP	NA
B4E-3(5-7% E/H)	773	-	NP	24mm
B4E-4(7-10% E/H)	2.59	-	NP	NA
B4E-5(10-15% E/H)	470	-	NP	NA
B4E-6(15-17% E/H)	624	-	NP	NA
B4E-7(17-20% E/H)	720	-	NP	NA
B4E-8(20-25% E/H)	56.3	-	NP	NA
B4E-9(25-30% E/H)	104.5	-	NP	NA
B4E-10(25-30% E/H)	398.6	-	NP	16mm
B4E-11(30-40% E/H)	1176.33	-	NP	NA
B4E-12(40-50% E/H)	417.46	-	NP	NA
B4E-13(50-100% E/H)	9.685	-	NP	NA
B4E-14(100% E)	1.655	-	NP	NA
B4E-3 ((FCC M/D)				
B4E-15(100%D)	6.5	-	NP	NA
B4E-16(0-5% M/D)	159	-	NP	18mm
B4E-17(0-10% M/D)	3.7	-	NP	NA
B4E-18(10-20% M/D)	2.1	-	NP	NA
B4E-19(25-50% M/D)	1	-	NP	NA
B4E-20(50-100%M)	4.6	-	NP	NA
B4E-21(50-100% M)	12.6	-	NP	NA

B4E-16 (PTLC 0.5% M/D)				
B4E-22	8.8	-	0.18	NA
B4E-23	20.6	-	0.25	18mm
B4E-24	1.9	-	0.48	NA
B4E-25	12.6	31.963	0.55	14mm
B4E-26	12.8	-	0.72	NA
B4E-27	19.6	-	0.90	NA
B4E-23(PTLC 0.3%M/D)				
B4E-28	3.2		0.30	NA
B4E-29	9.8	37.684	0.48	12
B4E-30	4.8		0.98	NA

NP-Not pure NA-Not active.

5B.2.6 Structural characterization of antibacterial metabolites from *Bacillus amyloliquefaciens* MTCC 10456

5B.2.6.1 Structural characterization of compound 7

3- (Octahydro-9-isopropyl-2H- benzo [h] chromen-4-yl) - 2-methylpropyl benzoate. Yellowish oil; UV (MeOH) λ_{\max} (log ϵ): 254 nm (3.11); TLC (Si gel GF₂₅₄ 15 mm; CHCl₃/MeOH 1:9, v/ v) R_f: 0.6; R_t: 31.963 min (HPLC RP C18) (**Figure 5B.5**); IR ν_{\max} (KBr) cm⁻¹ (δ_{OOP} = out of plane bending, ν = stretching, δ = bending, ρ = rocking vibrations): 726.24 (C-H ρ), 1000.14 (aromatic C-H δ), 1352.24 (C-H ρ), 1526.21(C=C aromatic ν), 1654.40 (C=C ν), 1692.21 (C-CO-O ν), 1722.86 (C=O ν), 2923.22 (C-H ν), 2955.04 cm⁻¹ (C-H ν), 3067.12 (C-H aromatic ν); ¹H NMR (500 MHz, CDCl₃ δ in ppm), ¹³C NMR (125 MHz, CDCl₃ δ in ppm), ¹H-¹H-COSY, and HMBC data, see Table 5B.2; HRMS (ESI) m/z : calcd. for C₂₇H₃₇O₃ 409.2984; found 409.6062 [M+H]⁺.

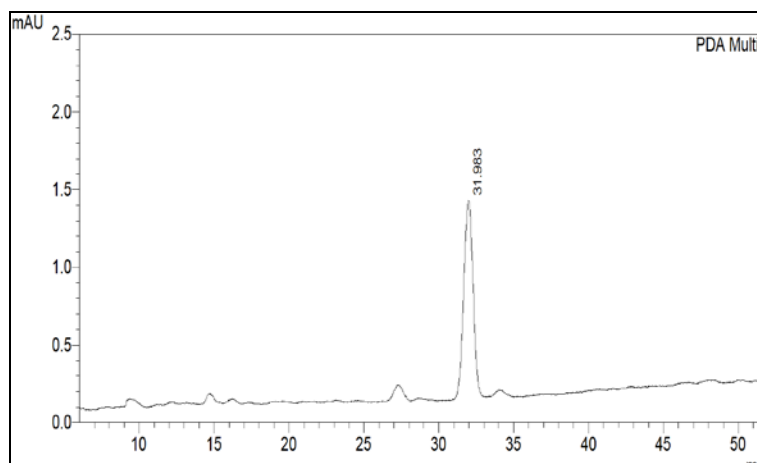
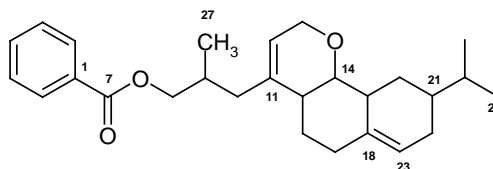


Figure 5B.5
HPLC Chromatogram of compound 7

Table 5B.2
NMR spectroscopic data of 7 in CDCl₃^a



C. No.	$\delta^{13}\text{CNMR}$	H	$\delta^1\text{H NMR}$ (int., mult., J in Hz) ^b	¹ H- ¹ H COSY	HMBC ¹ H → ¹³ C
1	132.31	-	-	-	-
2	130.9	2-H	7.77-7.65 (qd, 1H)	3-H	C-3,4
3	129.79	3-H	7.51 – 7.37 (m, 1H)	-	-
4	128.84	4-H	7.51 – 7.37 (m, 1H)	-	-
5	128.84	5-H	7.51 – 7.37 (m,1H)	6- H	-
6	130.90	6-H	7.77-7.65 (qd, 1H).	-	-
7	167.71	-	-	-	-
8	65.57	8-H	4.31 (d, J = 6.7 Hz,	9- H	C-9,7
9	30.58	9-H	1.71 (m,1H)	27-H	C-8
10	34.12	10-H	1.62 (m,2H)	-	C-11
11	148.59	-	-	-	-
12	135.04	12-H	5.26 (m,1H)	13- H	-
13	72.4	13-H	4.14 (H ^α)4.29(H ^β)(d)	12-H	C-12
14	82.92	14-H	4.22 (dd,1H)	15-H	-
15	44.98	15-H	2.29 (td,1H)	16-H	C-17
16	28.24	16-H	1.60 (m,2H)	17-H	-
17	24.33	17-H	1.53 (m,2H)	-	C-13

18	132.5	-	-	-	-
19	41.02	19-H	2.30 (td,1H)	20-H	C-20
20	27.40	20-H	1.62 (dd,2H)	21-H	-
21	19.75	21-H	1.31 (m,1H)	22-H	-
22	22.35	22-H	2.04 (m,2H)	23-H	-
23	128.71	23-H	5.34 (d,1H)	22-H	C-17
24	18.68	24-H	1.44 (m,1H)	21-	C-25
25	13.96	25-H	0.89 (d,3H)	24-H	-
26	13.74	26-H	0.94 (d,3H)	-	-
27	19.76	27-H	1.21 (d,3H)	-	C-9

^a NMR spectra recorded using Bruker AVANCE III 500 MHz (AV 500) spectrometers. ^bValues in ppm, multiplicity and coupling constants ($J = \text{Hz}$) are indicated in parentheses. Assignments were made with the aid of the ¹H-¹H COSY, HSQC, HMBC and NOESY experiments.

5B.2.6.2 Structural characterization of compound 8

Methyl 8- (2- (benzoyloxy) ethyl) – hexahydro -4- ((E) – pent - 2- enyl) - 2H-chromene-6-carboxylate. Colorless oil; UV (MeOH) λ_{max} (log ϵ): 362 nm (3.62); TLC (Si gel GF₂₅₄ 15 mm; CHCl₃/MeOH 1:9, v/ v) R_f: 0.5; R_t: 32.684 min (HPLC RP C18) (Figure 5B.6); IR ν_{max} (KBr) cm⁻¹ (δ_{OOP} = out of plane bending, ν = stretching, δ = bending, ρ = rocking vibrations): 838.17 (C-H ρ), 968.1 (HC=CH δ), 1454.38 (C-C ν), 1578.21(C-C aromatic ν), 1642 (C=C ν), 1742 (C=O ν), 2923.22 (C-H ν), 3010.04 (C-H ν); ¹H NMR (500 MHz, CDCl₃ δ in ppm), ¹³C NMR (125 MHz, CDCl₃ δ in ppm), ¹H-¹H-COSY, and HMBC data, see Table Table 5B.2; HRMS (ESI) m/z : calcd. for C₂₅H₃₃O₅ 413.5239; found 413.6684 [M+H]⁺.

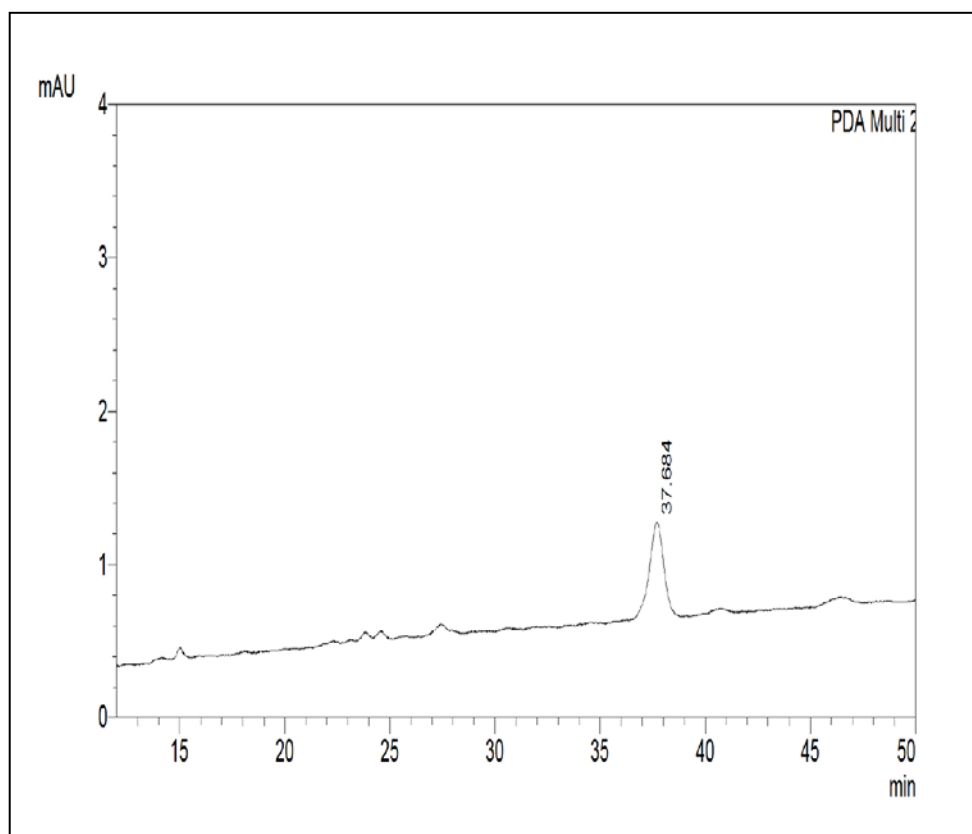
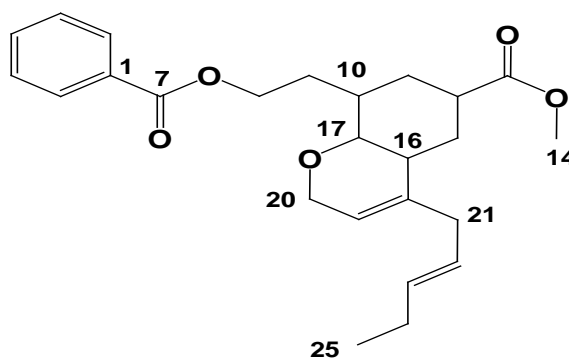


Figure 5B.6
HPLC Chromatogram of compound 8

Table 5B.3
NMR spectroscopic data of 8 in CDCl₃^a



C. No.	$\delta^{13}\text{C}$ NMR	H	$\delta^1\text{H}$ NMR (int., mult., J in Hz) ^b	¹ H- ¹ H COSY	HMBC $\xrightarrow{\text{H}} \text{C}^{13}$
1	132.0	-	-	-	-
2	130.84	2-H	7.78-7.65 (qd, 1H)	3-H	C-3,4
3	129.79	3-H	7.51 – 7.37 (m, 1H)	-	-
4	128.84	4-H	7.51 – 7.37 (m, 1H)	-	-
5	128.84	5-H	7.51 – 7.37 (m,1H)	6- H	-
6	130.90	6-H	7.78-7.65 (qd, 1H)	-	-
7	167.69	-	-	-	-
8	65.55	8-H	4.23 (t, J = 6.7 Hz, 2H)	9- H	C-9,7
9	32.05	9-H	1.68 (m,2H)	-	C-7
10	22.60	10-H	1.42 (m,1H)	17- H	C-11
11	29.66	11-H	1.58 (m,2H)	12-H	-
12	34.06	12-H	2.23(m,1H)	15- H	-
13	173.28	-	-	-	C-11
14	56.67	14-H	3.59(s,3H)	-	-
15	22.69	15-H	1.29(m,2H)	16-H	C-17
16	33.80	16-H	1.96 (m,1H)	-	-
17	68.88	17-H	3.98 (dt, 1H)	10- H	C-13
18	139.28	-	-	-	-
19	128.33	19-H	5.19 (dt,1H)	-	C-20
20	62.13	20-H	4.10 (dd,2H)	19- H	-
21	27.40	21-H	1.94(m,1H/1.96(m,1H)	22-H	-
22	122.98	22-H	5.86(m,1H)	23-H	-
23	114.05	23-H	4.88(m,1H)	-	C-16
24	19.18	24-H	1.30(m,2H)	25- H	C-23
25	14.11	25-H	0.89(t,3H)	24-H	-
-	-	-	-	-	-
-	-	-	-	-	-

^a NMR spectra recorded using Bruker AVANCE III 500 MHz (AV 500) spectrometers.
^bValues in ppm, multiplicity and coupling constants ($J = \text{Hz}$) are indicated in parentheses. Assignments were made with the aid of the ¹H-¹H COSY, HSQC, HMBC and NOESY experiments.

Two novel substituted carboxylate analogues, **7** and **8** (as stated in the materials section) were isolated upon repeated bioassay guided chromatography over silica columns (Table 5B.2).

3- (Octahydro-9-isopropyl-2H- benzo [h] chromen-4-yl) - 2- methylpropyl benzoate(, a new derivative of the substituted carboxylate was isolated as

yellowish oil upon chromatography over silica columns. The $^1\text{H-NMR}$ in conjugation with $^{13}\text{C-NMR}$ (**Figure 5B.7**) recorded the signals at δ 5.26, 4.27, 4.22 and 2.29. The $^1\text{H-}^1\text{H}$ COSY (5B.8.A) couplings were apparent between these protons assigned to be as H-12/H-13/H-14/H-15; which support the presence of six membered lactone ring system. The relatively downfield shift of the methylene proton at δ 4.31 and the C-8 carbon at δ 65.57 referred to a possible carboxyl group with extended conjugated aromatic moiety in its vicinity. The aromatic protons were assigned to be present at δ 7.42-7.77 and the proton integral of the protons revealed the presence of aryl ring. The methylene group protons at δ 4.31 and 1.71 were assigned to be at C-8 and 9 positions respectively, and the downfield shift (about δ 0.75) was apparently due to the presence of the possible extended conjugated moiety in its vicinity. A strong HMBC correlation was found between H-8 (δ 4.31)/ C-7 (δ 167.71) (Table 5B.2), which apparently indicate the presence of the carbonyl carbon near the methylene group.

The presence of two quaternary carbons at δ 132.31 and δ 167.71 were due to the presence of substituted benzyl moiety. The protons of the $-\text{CH}-$ groups at δ 4.27, 4.22, and 4.31 were deshielded due to the possible oxygenation at its vicinity. Also, the $^1\text{H-}^1\text{H}$ COSY (Fig. 5B.8.A) correlations between H-12 (δ 5.26)/ H α -13(δ 4.27), H β -13(δ 4.14) and H-14 (δ 4.22)/ H-15 (δ 2.29), along with the proton and carbon connectivities deduced from HSQC (Fig. 5B.8.B) and HMBC (Fig. 5B.9.A) experiments (Table 5B.2) confirmed the pyran framework. The aromatic ring and carboxyl ester group at the C-7 position of the structure resulted in strong deshielding of proton at δ 4.31, the quaternary $-\text{C}-$ at δ 132.51, and therefore, has been assigned to be present at the junction point between the aromatic ring and carboxyl ester group.

The methine proton at δ 2.29 was characteristic of the junction point of the pyran ring with that of the side six membered ring moiety as established by $^1\text{H-}^1\text{H}$ COSY correlations and detailed HMBC experiments (Table 5B.2)). The ^{13}C NMR spectrum of the purified compound in combination with DEPT experiments indicated the occurrence of 27 carbon atoms in the molecule including one ester carbonyl carbon at δ 167.71 and two methylene carbons between δ 65.57, 72.4

and methine carbon at δ 82.92 (Table 5B.2)). The latter was found to be significantly deshielded due to the presence of oxygen in its vicinity. The $-\text{CH}$ -proton at δ 34.12 exhibited HMBC correlation with the olefinic quaternary carbon atom assigned to be as C-11 (δ 148.59). The low field quaternary signals (^{13}C NMR) is in good agreement with that to a quaternary carbon signal carrying the carbonyl groups at C-7 of the structure (δ 167.71) and C-1 of the aromatic carbon (δ 132.31) attached with the ethyl benzoate side chain.

The aromatic side chain attached to the pyran ring was substituted at C-11. The point of cyclization of the pyran ring was indicated by the low-field shift of $\text{H}\alpha$ -13 at δ 4.27 and $\text{H}\beta$ -13 at δ 4.14, which has been coupled with the H-12 methine proton at δ 5.26. The latter demonstrated clear $^1\text{H}-^1\text{H}$ COSY correlation with $\text{H}\alpha$ / $\text{H}\beta$ -13/ H-12, and between H-14 at δ 4.22 with H-15 at δ 2.29, which support the presence of the pyran moiety in the compound. The proton and carbon connectivity deduced from HSQC and HMBC experiments confirmed the pyran framework attached to the aromatic side chain at the C-11 position of the compound. In the HMBC spectrum, it was observed that H-14 (δ 4.22)/C-15 (δ 44.98), H-15(2.29)/C-16, C-17(δ 24.16); H-17 (δ 1.53)/C-19(δ 41.02) were correlated with each other (Table 1), which support the presence of the bicyclic framework. The $-\text{CH}$ proton at C-14 (δ 4.22) appeared to demonstrate long range HMBC correlation (Fig. 5B.9.A) with the quaternary carbon at δ 132.5 (C-18).

The HMBC spectrum of the purified compound also revealed connectivity between the protons at C-8 (δ 4.31) to the methylene carbon at δ 65.57. The relative stereochemistry of the chiral centers particularly that of C-14 and 15 of the bicyclic octahydronaphthalene framework was deduced from the NOESY spectrum (Fig. 5B.9.B) and the J -values. NOE couplings were apparent between H-12 (δ 5.26)/ H-14 (δ 4.22) thus indicating that these groups must be equatorial and on the α -side of the molecule. The methine proton at C-15 group did not exhibit NOE interactions with H-12 and H-14, which is at the α -face of the molecule, thereby indicating that H-15 is at the axial disposition.

The IR absorption band (in MeOH) exhibited bending vibration bands near 1722.86 cm^{-1} , which denote the ester carbonyl absorption. The olefinic (C=C), and ether (C-O-C) groups have been symbolized by the absorption bands at 1654.40 and 1692.21 cm^{-1} . The ultraviolet absorbance at λ_{max} (log e) 259nm (3.11) was assigned to a chromophore with extended conjugation. Its mass spectrum exhibited a molecular ion peak at m/z 409 (HRESIMS m/z 409.6062 $[\text{M}+\text{H}]^+$; D 0.0 amu), which in combination with its ^1H and ^{13}C NMR data (Table 5B.2) indicated the elemental composition of $\text{C}_{27}\text{H}_{37}\text{O}_3$ as 3- (octahydro-9-isopropyl-2H- benzo [h] chromen-4-yl) - 2- methylpropyl benzoate with ten degrees of unsaturation. One degree of unsaturation from the carbonyl group, four degrees of unsaturation from the double bonds of the aromatic ring system, two double bonds, and three degrees of unsaturation from the ring system were demonstrated.

The molecular ion peak at m/z 409 appeared to undergo elimination of benzoic acid (m/z 122) to yield octahydro-4-isobutyl-9-isopropyl-2H-benzo [h] chromene at m/z 288. The appearance of the fragment at m/z 190 indicated the presence of octahydro-2H-benzo [h] chromene moiety, resulted from the side chain elimination (Fig. 5B.10). Intramolecular rearrangement of the latter resulted in the formation of tetrahydro-2H-pyran (m/z 86), octahydronaphthalene (m/z 136), and cyclohexane (m/z 84) via the intermediate decahydronaphthalene (m/z 138). The presence of tropylium ion (m/z 91) supports the presence of aryl ring system in 7.

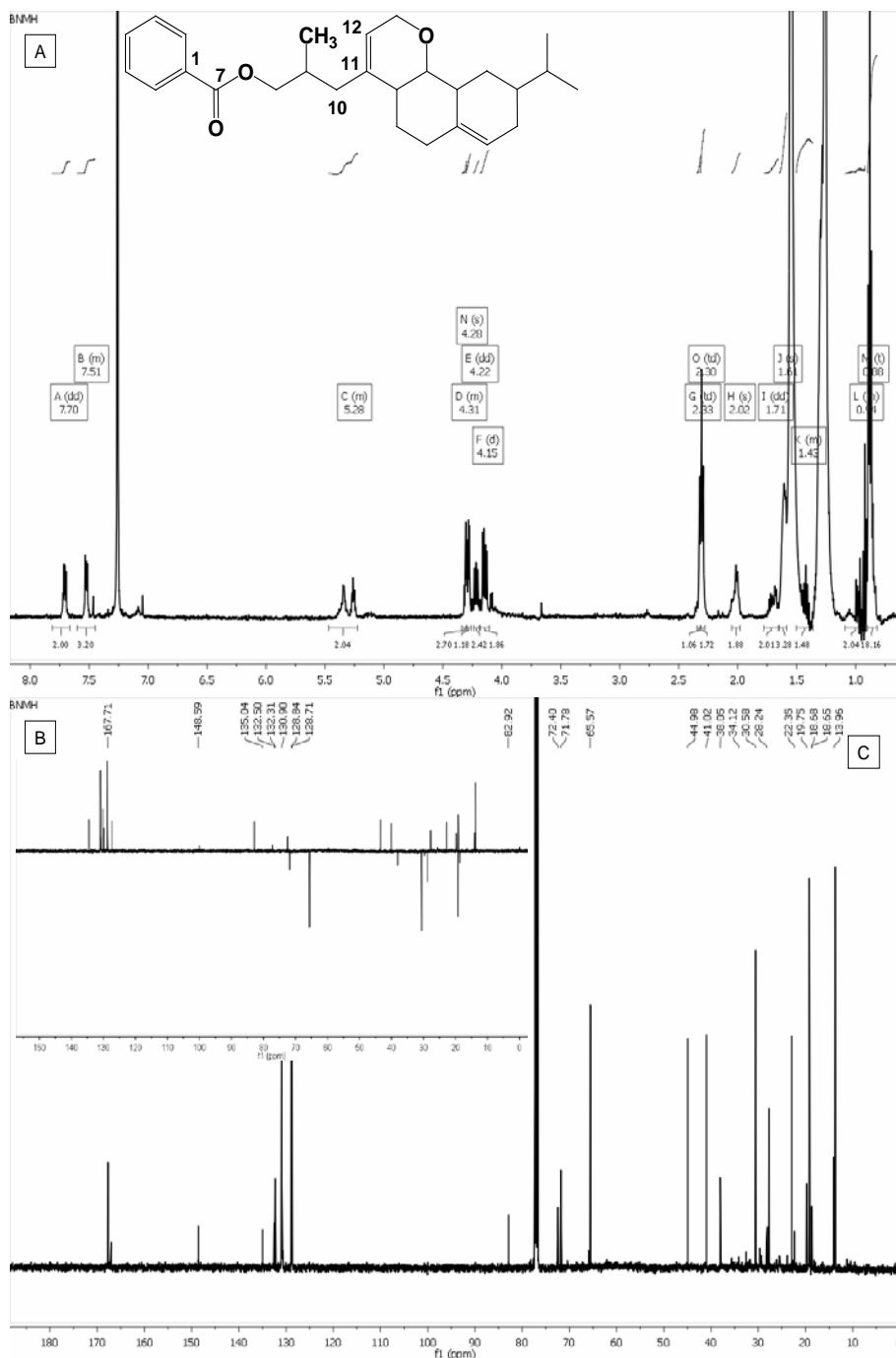


Fig. 3

Figure 5B.7
 (A) ¹H, (B) DEPT₁₃₅ and (C) ¹³C NMR spectrum of compound 7.

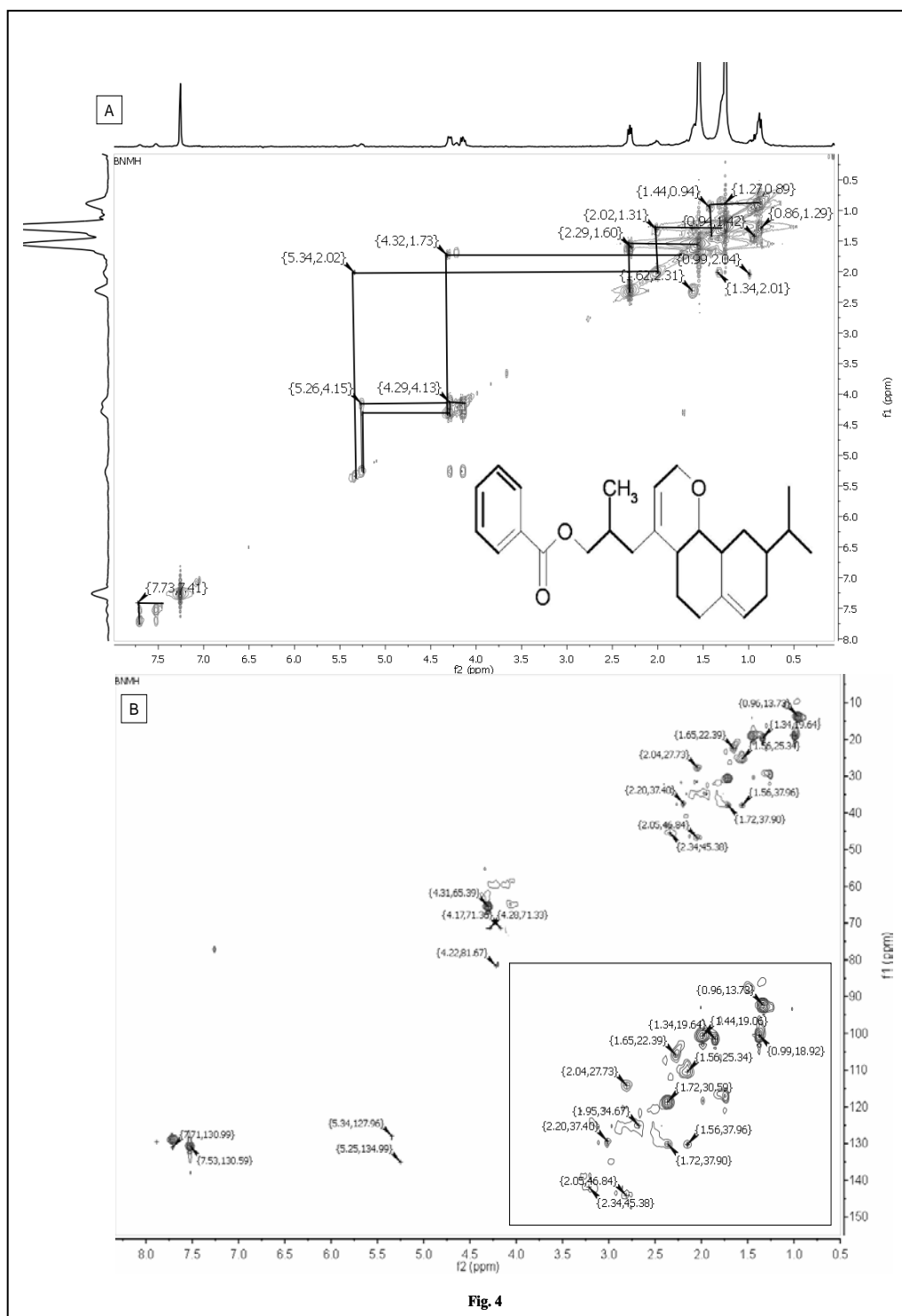


Figure 5B.8

(A) ^1H - ^1H COSY - NMR spectrum of 7. The key ^1H - ^1H COSY couplings have been represented by the bold face bonds. (B) Prominent HSQC correlation spectrum of 7.

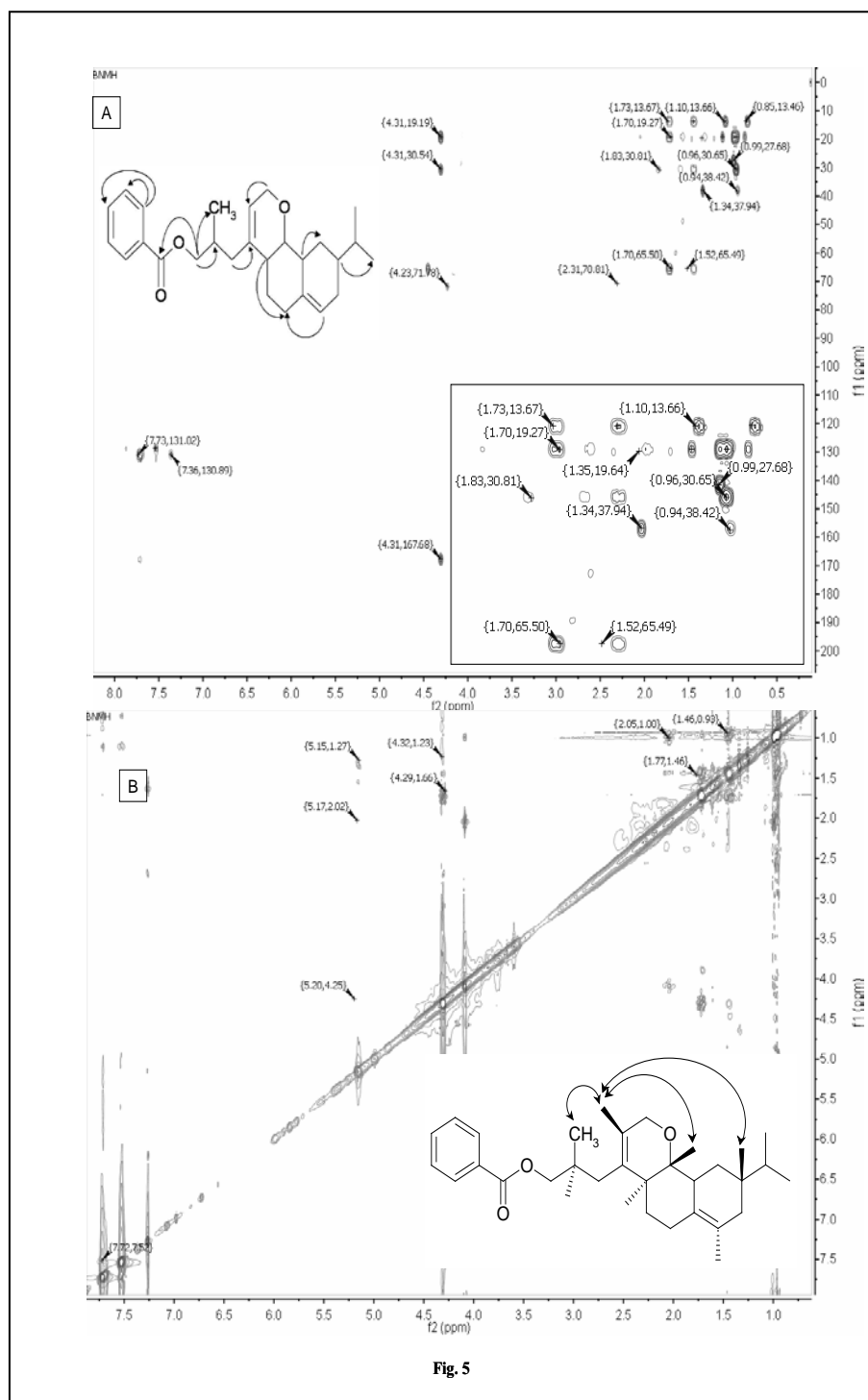


Fig. 5

Figure 5B.9

(A)HMBC and (B) NOESY spectra of 7. The key HMBC couplings have been indicated as double barbed arrow. The NOESY spectrum have been indicated as two sided arrows.

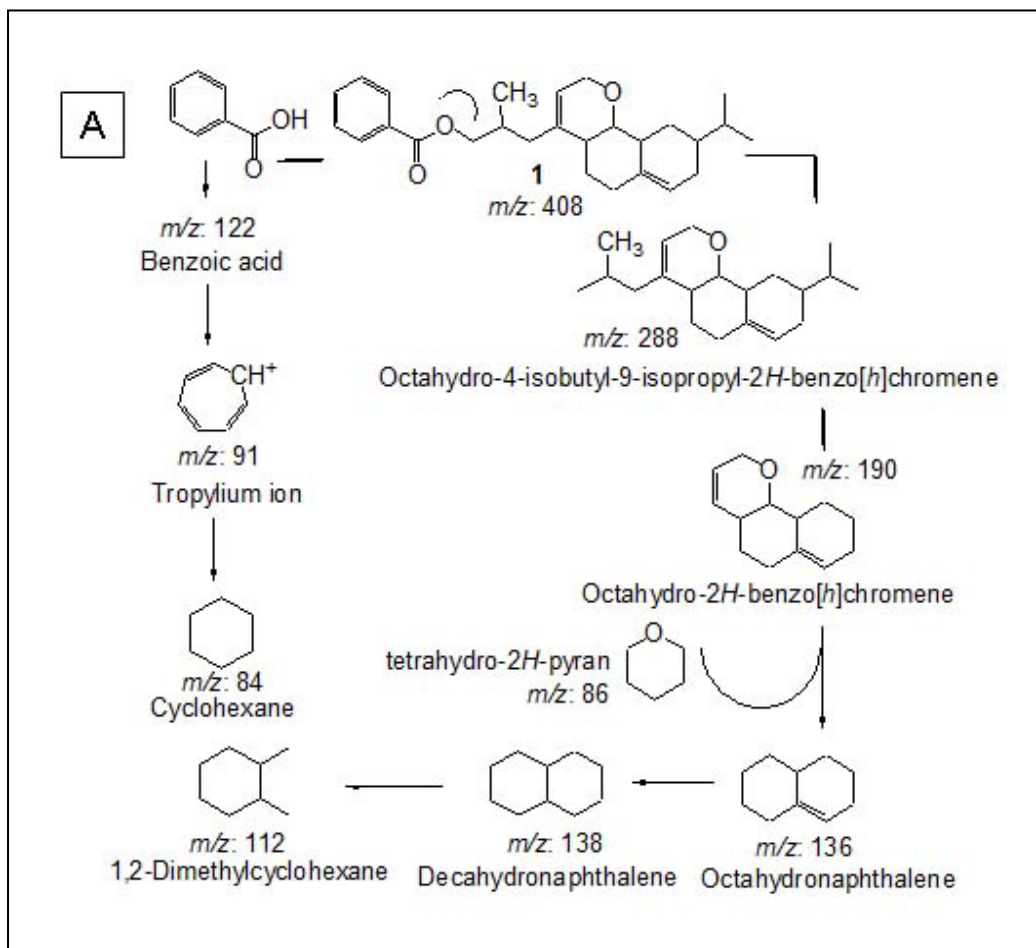


Figure 5B.10
Mass fragmentation pattern of 3-(Octahydro-9-isopropyl-2H-benzo [h] chromen-4-yl) - 2- methylpropyl benzoate

Methyl 8-(2-(benzyloxy) ethyl) – hexahydro -4- ((E) – pent - 2- enyl) - 2H-chromene-6-carboxylate (Fig. 5B.11.A-C), a new derivative of the substituted carboxylate was isolated as colorless oil upon chromatography over silica columns. Its mass spectrum exhibited a molecular ion peak at m/z 412 $[M]^+$ (HRESIMS m/z 413.6684 $[M+H]^+$; D 0.0 amu), which in combination with its 1H and ^{13}C NMR data (Table 5B.2) indicated the elemental composition of **8** as $C_{25}H_{32}O_5$ with ten degrees of unsaturation. Two degree of unsaturation from the carbonyl groups, three degrees of unsaturation from the double bonds of the aromatic ring system and two double bonds, and three degrees of unsaturation from the rings were

demonstrated. The $^1\text{H-NMR}$ in conjugation with $^{13}\text{C-NMR}$ recorded the signals at δ 1.42, 1.58, 2.23, 1.29, 1.98 and 3.98. The $^1\text{H-}^1\text{H}$ COSY couplings (Figure 5B.12.A) were apparent between these protons assigned to be at H-10/H-11/H-12;H-14/H-15/H-16, which supported the presence of six member ring system of **8**. The relatively downfield shift of the methylene protons at δ 4.23 and the C-8 carbon at δ 65.55 referred to a possible carboxyl group with extended conjugated aromatic moiety in its close vicinity. The aromatic protons were assigned to be present at δ 7.37-7.78. The methylene group protons at δ 4.23 and δ 1.68 were assigned to be at C-8 and 9 positions respectively, and the downfield shift (about δ 0.75) was apparently due to the presence of the possible extended conjugated moiety in its vicinity. A strong HMBC correlation was found between H-8 (δ 4.23)/ C-7(δ 167.69) (Table 5B(2)), which apparently indicate the presence of the carbonyl carbon near the methylene group. The presence of two quaternary carbons at δ 132.0 and δ 167.69 were due to the presence of substituted benzyl moiety. The protons of the $-\text{CH}-$ groups at δ 4.10, 3.98, and 3.59 were deshielded due to the possible oxygenation at its vicinity. The $^1\text{H-}^1\text{H}$ COSY correlations between H-17 (δ 3.98)/H-16 (δ 1.96), H-20 (δ 4.10), and H-19 (δ 5.19), along with the proton and carbon connectivity deduced from HSQC (Figure 5B.12.B) and HMBC experiments (Figure 5B.13.A) confirmed the presence of the pyran framework. Unlike the compound 7, additional olefinic $-\text{CH}-$ DEPT signals were apparent at δ 122.98 and 114.05, which demonstrated the presence of an extra *trans* oriented double bond as also confirmed based on the *J* values. The $^1\text{H-}^1\text{H}$ COSY correlation with H-21 (δ 1.94, m, 2H)/ H-22 (δ 5.86, m, 1H)/ H-23 (δ 4.88, m, 1H)/ H-24 (δ 1.30, m, 2H)/ H-25 (δ 0.89, t, 3H) support the presence of the pentene moiety. These results were supported by detailed HMBC experiment (Table 5B.2). The $-\text{CH}-$ proton at δ 34.06 exhibited HMBC correlation with the carbonyl carbon atom assigned to be as C-13 (δ 173.28) (Table 5B.2). The aromatic ring and carboxyl ester group at the C-7 position of **8** resulted in strong deshielding of proton at δ 4.31 along with the quaternary carbon atom at δ 132.0, and therefore, has been assigned to be present at the junction point between the aromatic ring and carboxyl ester group. The methoxy protons at δ 3.59 were attached to carbonyl carbon at C-13 was confirmed by the HMBC correlation at H-14 (δ 3.59)/ C-13. The ^{13}C NMR

spectrum in combination with DEPT experiments indicated the occurrence of 25 carbon atoms in **8** including two ester carbonyl carbon at δ 167.69 and 173.28, two methylene carbons between δ 32.0 and 65.55 (Table 5B(2)). The latter was found to be significantly deshielded due to the presence of possible conjugation in the form of the aromatic ring system. The point of cyclization of the substituted ring was indicated by clear ^1H - ^1H COSY correlation with H-10/H-11/H-12/H-15/H-16/H-17, which supports the presence of the six member ring moiety in **8** (Fig. 5B(11)A). The proton and carbon connectivity deduced from HSQC (Fig. 5B.12.B) and HMBC experiments (Fig. 5B.13.A) confirmed the presence of hexahydro-2H-chromene framework attached to the aromatic side chain at the C-10 position of the compound. HMBC correlations between H-17 (δ 3.98)/C-18 (δ 138.28), H-16(1.96)/C-17; H (δ 4.10)/C-23(δ 114.05) (Table 5B.2) also supported the presence of the hexahydro-2H-chromene ring system. The $-\text{CH}_2$ proton at C-8 (δ 4.23) appeared to demonstrate long range HMBC correlation with ester carbonyl carbon at δ 167.69 (C-7). The relative stereochemistry of the chiral centres particularly that of C-10, 17 and 12 of the methyl hexahydro-2H-chromene-6-carboxylate framework was deduced from the NOESY spectrum (Fig. 5B.13.B) of the compound and the J -values. NOE couplings were demonstrated between $\text{H}\alpha$ -17 (δ 3.98)/ $\text{H}\alpha$ -12 (δ 2.23) thus indicating that these groups might be equatorial and on the α -side of the molecule. The methine proton at C-16 group did not exhibit NOE interactions with H-17 and H-12, which is at the α -face of the molecule, thereby indicating that H-16 is at the axial disposition. The IR absorption band (in MeOH) exhibited close resemblance with that of **7**, except the presence of greater trans olefinic bending signals near 968.1 cm^{-1} , which apparently indicated that **7** and **8** shared close structural similarities. The ultraviolet absorbance at λ max (log e) 254 nm (3.62) was assigned to a chromophore with extended conjugation. Similar mass fragments were detected in **8** (m/z 122, 91, and 84) (Fig. 5B.14) as in **7** (Fig. 5B.10), which supported the structural similarities between these compounds. However, two intense peaks at m/z 288 and 190 as described in **7** were absent in **8**. It is of note that two mass fragment peaks appeared at m/z 224 and 140 were due to the presence of methyl hexahydro-4, 8-dimethyl-2H-chromene-6-carboxylate and octahydro-2H-chromene, respectively.

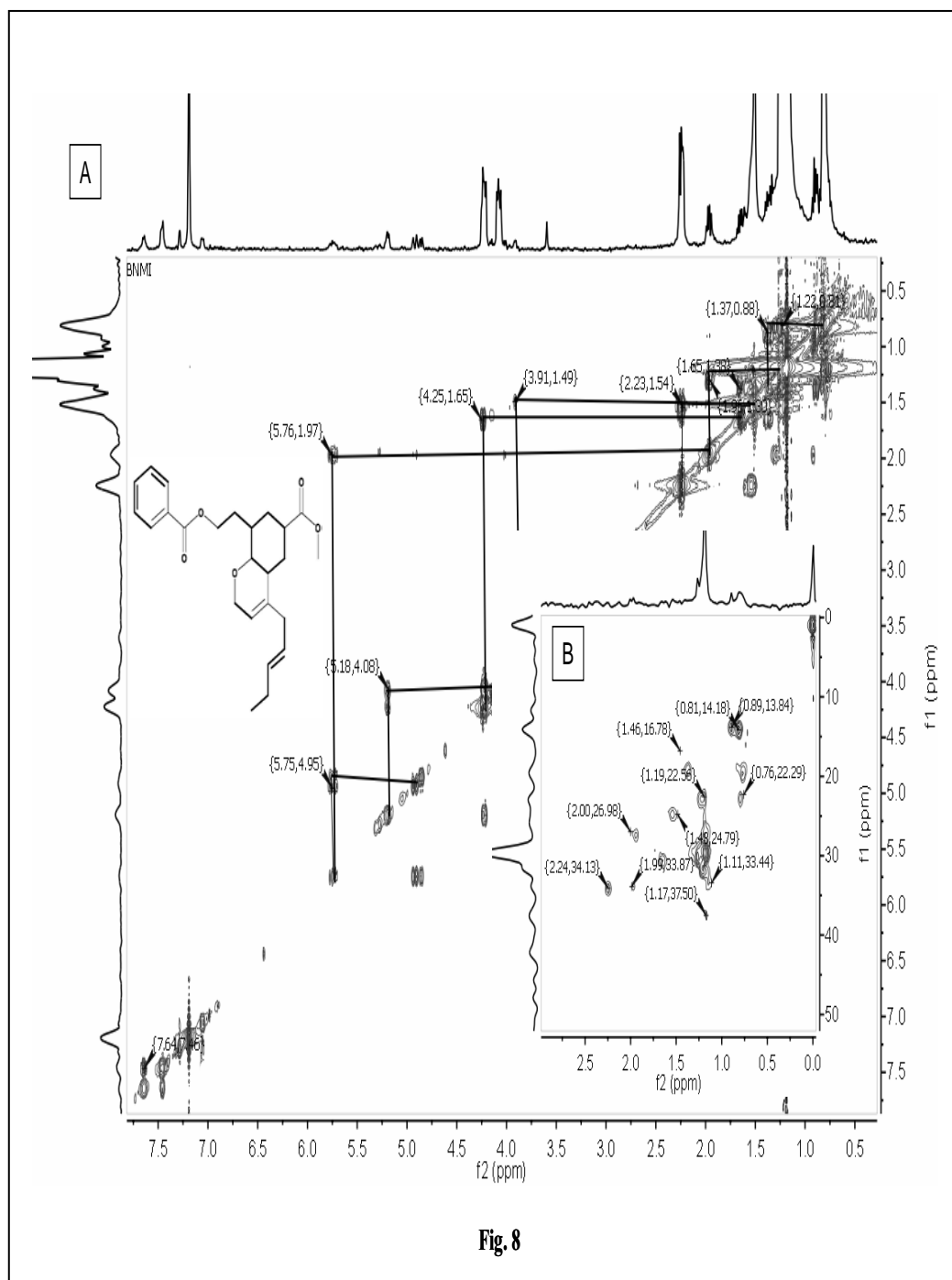


Figure 5B.12

(A) ^1H - ^1H COSY - NMR spectrum of 8. The key ^1H - ^1H COSY couplings have been represented by the bold face bonds. (B) Prominent HSQC correlation spectrum of 8.

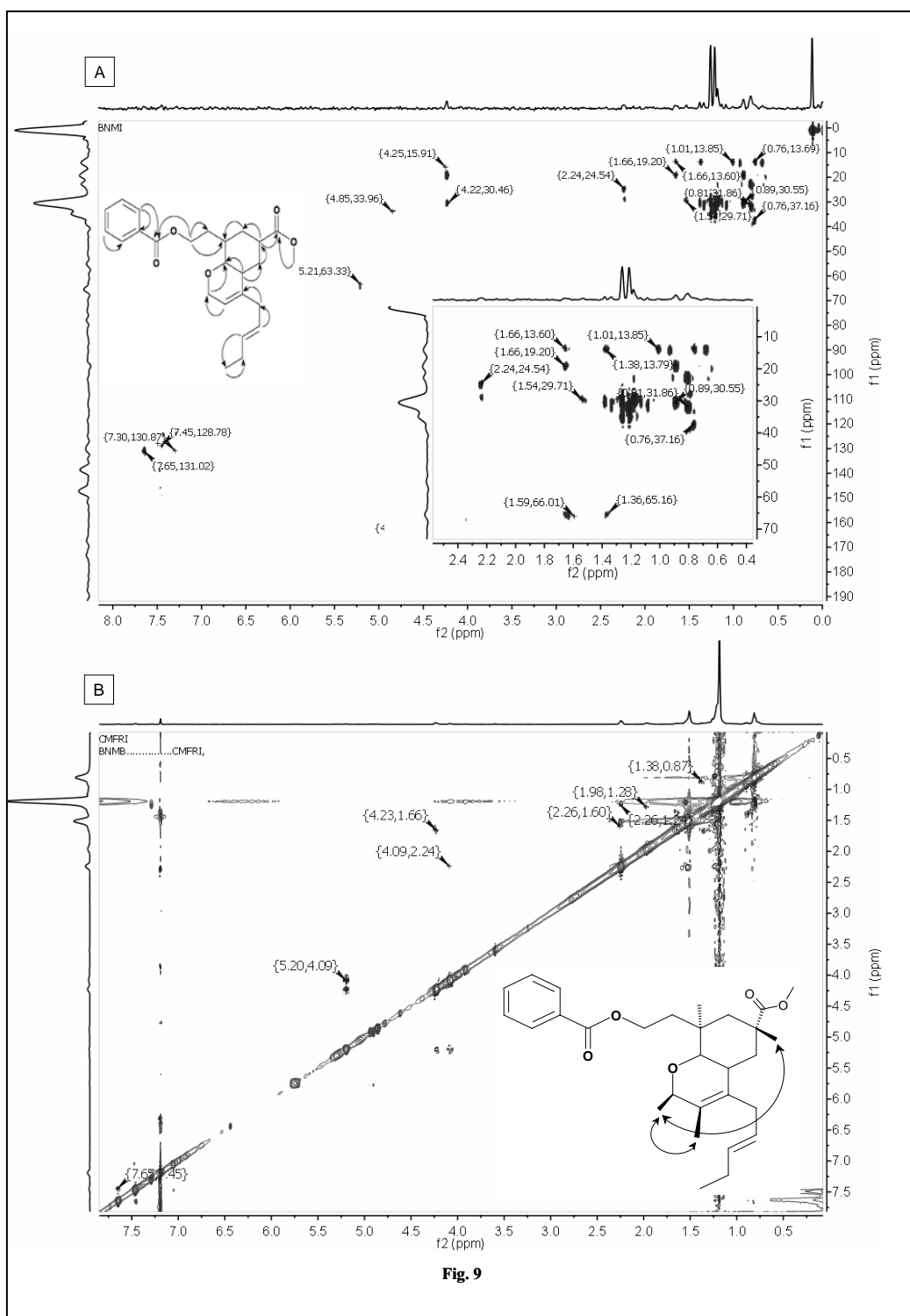


Figure 5B.13
(A) HMBC and (B) NOESY spectra of 8. The key HMBC couplings have been indicated as double barbed arrow. The NOESY spectrum have been indicated as two sided arrows.

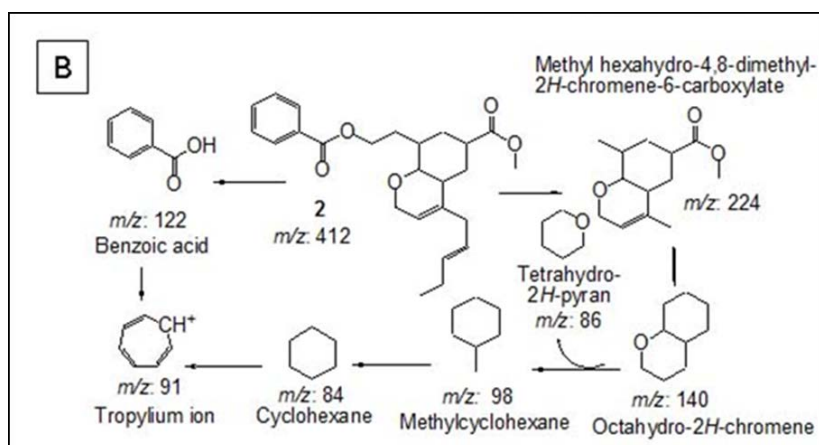


Figure 5B.14

Mass fragmentation pattern of Methyl 8- (2- (benzoyloxy) ethyl) – hexahydro -4- ((E) – pent - 2- enyl) - 2H-chromene-6-carboxylate.

Utilizing bioassay-guided fractionation, two antibacterial compounds **7** (3-(octahydro-9-isopropyl-2H- benzo [h] chromen-4-yl) - 2- methylpropyl benzoate) and **8** (methyl 8- (2- (benzoyloxy) ethyl) – hexahydro -4- ((E) – pent - 2- enyl) - 2H-chromene-6-carboxylate) that represent the scaffold of *pks-1* gene encoded products, with activity against pathogenic bacteria, have been isolated from the ethyl acetate extract of from *Bacillus amyloliquefaciens* MTCC10456. In each stage TLC bioautography overlay assay ensured the bioassay guided purification. The live microbes converted MTT to formazan dye to give a blue color, whereas the inhibition zones were clear in purple background. The active fractions demonstrated a qualitative inhibition zone in the TLC plate which was further affirmed through Disc diffusion assay. Polyketides have discovered an application as bioactive leads in drug based products for utilization against pathogenic microorganisms and diverse immunocompromising afflictions. The common examples of polyketides are rapamycin, epothilone B, and erythromycin with antibacterial, anticarcinogenic and immunosuppressant properties.

Among different bacterial genera, *Bacillus* spp have been perceived to contain different *pks* gene groups and bioactive molecules bearing the polyketide backbone. The highly conserved sequences of β -ketoacyl synthase (KS) domains

are imparted among all *pks*, and along these lines, the KS domains are valuable in the screening for PKS genes in bacteria. Thus, the positive results in a PCR-based screening for *pks* gene doesn't simply give affirmation of the generation of relating metabolites furthermore may show the vicinity of further metabolic pathways. In the present study the secondary metabolites of *Bacillus amyloliquefaciens* MTCC10456 with potent antibacterial activities against bacterial pathogens was perceived to represent the platform of *pks*-1 gene encoded products. The multifactorial polyketide structures are endowed with supplementary *O*-heterocyclic moieties as in **7** and **8** contributing meticulousness to the polyketide functionality. The crude extract from *Bacillus amyloliquefaciens* MTCC10456, the purified compounds (**7** and **8**) and, commercial antibiotics (as control) were analyzed against human opportunistic pathogens *V. parahaemolyticus*, *V. vulnificus* and *A. hydrophilla*. 3- (Octahydro-9-isopropyl-2H- benzo [h] chromen-4-yl) - 2-methylpropyl benzoate (**7**) demonstrated a great subjective inhibitory spectrum to the tested isolates. It is significant to note that the antibacterial activities of the crude extract against the test pathogens were greater than those exhibited by the pure compounds **7** and **8** with substituted *O*-heterocyclic moiety. It is evident that there might be other bioactive compounds alongside the purified *O*-heterocycles, which acted synergistically to confer more noteworthy antibacterial activities against the test food pathogenic organisms utilized as a part of this study.

The physicochemical parameters such as polarizability, steric, and hydrophobic descriptors (lipophilicity, partition coefficients) have a major role to influence with biological activities (cinq-Mars et al. 2008). The electronic descriptors namely polarizability (PI); hydrophobic parameter log P_{ow} to calculate *n*-octanol/water partition coefficient; steric (or bulk descriptor), molar volume (MV), molar refractivity (MR), and parachor (P) as calculated by ChemDraw 12.0 were taken into consideration It is of note that the ability of any molecule to penetrate biological membranes is a primary factor in controlling the interaction of compounds with biological systems, and is dependent on lipophilicity factors as determined by the partition coefficient between 1-octanol and water (log P). The increased lipophilicity (log P 5.77) of **7** due to the terminal functional group as the 4-isobutyl-9-isopropyl-octahydro-2H-benzo[h]chromene as compared to that in **8**

(log P 4.46) affords better penetration of the former through the lipoidal membrane barrier to arrive at the receptor site, thereby resulting in greater antibacterial activity of **7** than **8**. The compound **7** exhibited significant greater activity against test pathogens (at a concentration of 20 µg per disc) than **8** apparently due to the presence of more polarizable (polarizability $48.99 \times 10^{-24} \text{ cm}^3$) 4-isobutyl-9-isopropyl-octahydro-2H-benzo[h]chromene group as compared to the less polarisable methyl 8-ethyl-4-[(E)-2-pentenyl]-hexahydro-2H-6-chromene carboxylate group ($45.85 \times 10^{-24} \text{ cm}^3$). This lead demonstrated in the present study will be significant in explaining the pharmacophore-fit in the macromolecular receptor site and exploring the primary site and mode of action of this class of the substituted O-heterocyclic analogues. It is therefore imperative that the presence of octahydro-2H-benzo[h]chromene system is essentially required to impart the greater activity (IZD 20 mm, 25 mcg on disk against *A. hydrophila*). It is significant to note that the compound **7** has greater values of steric descriptors (P 977.7 cm^3 , MR $123.58 \text{ cm}^3/\text{mol}$, MV 385.4 cm^3) than **8** (P 940.6 cm^3 , MR $115.66 \text{ cm}^3/\text{mol}$, MV 378.9 cm^3) purified from *Bacillus amyloliquefaciens* MTCC10456. The antibacterial compounds **7** and **8** isolated from the ethyl acetate extract of from *Bacillus amyloliquefaciens* MTCC10456 shared similar structures, and therefore, might be the result of the identical metabolic pool. In particular the presence of isobutyl benzoate moiety in **7** and propyl benzoate moiety in **8** strongly suggested the metabolic relationship between these compounds. It is of note that the hydrophobic (log P_{ow}) and electronic descriptor (PI) had a major role to describe the bioactivity of compound **7** isolated from *Bacillus amyloliquefaciens* MTCC10456. Although there is no significant differences in the polarizability depicting the electronic descriptor ($46-49 \times 10^{-24} \text{ cm}^3$) in **7** and **8**, the activity of the latter was lesser (IZD 18 mm; 25 mcg on disk) than of the former (IZD >20 mm; 25 mcg on disk), apparently due to the greater hydrophobic values of **7** (log P 5.57) than that recorded in **8** (log P 4.46). The direct involvement of log P with the target bioactivity in **7** implied that hydrophobic rather than the electronic and steric effect appears to be the key factor influencing the induction of antibacterial activity. This leads demonstrated in the present study will be significant in explaining the pharmacophore-fit in the macromolecular receptor site and

exploring the primary site and mode of action of this class of the substituted *O*-heterocyclic compounds.

The correlations of metabolite genes, for example, *pks* with auxiliary metabolites having a place with polyketides, and their putative biosynthesis pathway in related microorganisms were accounted for in prior studies (Moldenhauer et al. 2007; Scotti et al. 1993). *B. amyloliquefaciens* FZB42 distinguished gene clusters responsible for synthesis of several antibacterial polyketide compounds, for example, difficidin and bacillaene (Chen et al. 2009). The *pks* gene has been doled out to the biosynthesis of bacillaene, a polyketide product in the *Bacillus amyloliquefaciens* FZB42 genome. The *pks* gene cluster was identified from *B. amyloliquefaciens* CH12, a genetically engineered strain, and the putative biosynthetic pathway of bacillane was elucidated. Cao et al. (2011) reported the isolation of *Bacillus amyloliquefaciens* G1 with potential antimicrobial activities from the brackishwater sediment against pathogenic *A. hydrophila*. Polyketide compounds of various types were isolated from a marine *Bacillus amyloliquefaciens* associated with the gorgonian, *Junceella juncea* (Gao et al. 2010). A bacillaene multienzyme complex of *trans*AT PKSs with *pks*-like chemistry was described in a prior study, where introduction of the β -branch and subsequent incorporation of olefinic bonds into the noncanonical bimodules has been comprehended (Moldenhauer et al. 2007). The *pksX* polyketide synthase (PKS) genes were likewise reported in *Bacillus subtilis* (Scotti et al. 1993). A step-wise aldol addition of acetyl-ACP and Grob fragmentation on the enzymatically loaded acyl carrier proteins was exhibited to result *pks*-derived antibacterial metabolites bacillaene and curacin (Calderone et al. 2006; Gu et al. 2006)). Mupirocin H, a novel metabolite resulting from mutation of the HMG-CoA synthase analogue, *mupH* in *Pseudomonas fluorescens* has been accounted for (Wu et al. 2007). A previous work demonstrated that unlike fatty acid biosynthesis, the biosynthesis of polyketide products don't follow a rigid sequence (Weissman and Leadlay 2005). A model for biosynthesis of polyketide product 7-O-methyl-5'-hydroxy-3'-heptenoate-macrolactin was proposed in our prior chapter (chapter 5A), which represents the way that propanethioate/malonate as the initial building blocks.

5B.3 Conclusions

The bacterial strain under the study is *Bacillus amyloliquefaciens* MTCC10456 with a 16S rRNA gene bank accession number JX203228. The bacterium demonstrated a promising antibacterial spectrum and therefore was utilized to isolate potential antibacterial metabolites. Macroalgal-associated bacterial communities seem to contain a consistent functional profile with features identified with an algal host-associated lifestyle (Hollants et al. 2012). The strain under study demonstrated a positive hit for polyketide synthase gene (with an accession number of KC607821). This showed the conceivable vicinity of polyketide metabolite pathway. The recognition of antimicrobial metabolite from marine macroalga associated marine bacterium, further reinforced the theory that microbial metabolites of the symbiotic microorganisms helps in chemical defenses of the marine macroalgae against pathogenic and fouling microorganisms, indicating an ecological role of microbial metabolites in host bacterial interaction for these marine organisms. The recently advancing antibacterials bearing the polyketide backbone will be progressively vital remembering the development of multi-drug resistant bacteria and pathogenic microorganisms against the existing antibiotics and related molecules. With the expanding requirement for novel medication revelation, marine macroalgae-associated marine epibiotic bacteria with potential antimicrobial activity proposes the marine macroalgal species as an ideal ecological niche harboring specific bacterial diversity representing a largely underexplored source of novel antimicrobial secondary metabolites.

CHAPTER 5C

BIOPROSPECTING OF ANTAGONISTIC BACTERIA *B.subtilis* MTCC 10407 ASSOCIATED WITH SEAWEED *Sargassum myriocystum* (SWI 19) FOR ANTIBACTERIAL METABOLITES

5C.1 Materials and methods

5C.1.1 Microbial strain under the study

The microbial strain used for bioprospecting of antimicrobial compound in the current study is *B. subtilis* MTCC 10407, which was found to be associated with brown seaweed *Sargassum myriocystum*. The seaweed associated bacteria were isolated (chapter 3 section 3.2.2) and assayed for their ability to inhibit selected pathogenic microorganisms (chapter 3 section 3.2.5). The isolates for metabolite purification with antibacterial activity used in the study were selected based on their inhibition spectrum (chapter 3 Table 3.2) and the positive hit for metabolite gene (chapter 4.2.5 and 4.3.4).

5C.1.2 Antibiotic resistance and abiotic stress tolerance

Antibiotic resistance, abiotic stress tolerance and enzyme production profile of the strain *B. subtilis* MTCC 10407 was analyzed using the methodology explained in 5.2.2.

5C.1.3 Optimization of time

The microorganism under the study was inoculated in nutrient broth and the optimum time for the antibiotic production with maximum inhibitory activity was analyzed as explained in 5.2.3.

5C.1.4 Optimization of temperature

The optimum temperature for the production of antibacterial compound for the strain MTCC 10407 was analyzed using the methodology explained under the section 5.2.4.

5C.1.5 Optimization of pH

P^H for the production of the active metabolite was standardized as described under the section 5.2.5.

5C.1.6 Preparation of crude extract for purification of secondary metabolites

The antibiotic-producing bacterium, *B. subtilis* MTCC 10407 (SWI 19) was isolated from the brown seaweed *Sargassum myriocystum*. The preparation and recovery of secondary metabolites were carried out by a surface culturing method over solid nutrient agar plates (5.2.7). The adsorbed products were subsequently extracted with ethyl acetate by homogenization (Arrow Engineering Inc., Pennsylvania Ave, USA) followed by refluxing. Evaporation of the solvent under reduced pressure (Heidolph Instruments GmbH & Co., Schwabach, Germany) yielded the ethyl acetate extract (5.56 g) from the total culture volume of 4 L. Subsequently the residual agar was extracted with CH₂Cl₂ to furnish dichlorometane extract. These solvent extracts were evaluated for antibacterial activities (5.2.8), against the pathogens (listed in chapter 3 section 3.2.4), and the fractions which showed significantly broad spectrum antibacterial activities and higher yield were further purified by chromatographic techniques.

5C.1.7 Bioassay guided purification of antibacterial compound from *B. subtilis* MTCC 10407 associated with seaweed *Sargassum myriocystum*

The pooled ethyl acetate extract (5 g) was fractionated by chromatography over silica gel (180–230 mesh) on a flash column chromatograph (Biotage SP, SP1-B1A, Biotage AB, Sweden), with a stepwise gradient of CH₂Cl₂/MeOH (0–100% MeOH) using the flash silica gel cartridge (Biotage no. 25+M 0489-1) at a collection UV wavelength at 256 nm to provide 112 fractions (12 mL). Based on analytical TLC, the fractions with similar patterns were pooled together to afford seventeen pooled fractions (B3E1–B3E17). These column fractions were evaluated for antibacterial activities (5.2.8), against the pathogens (listed in chapter 3 section 3.2.4) and the fractions which showed significantly broad spectrum antibacterial activities and higher yield were further purified by column chromatography or preparative TLC (P-TLC) using EtOAc:*n*-hexane, MeOH:CHCl₃, or MeOH:EtOAc as mobile phase, whichever required. The schematic diagram showing the

purification of *B. subtilis* MTCC 10407 associated with *Sargassum myriocystum* (SWI19) ethyl acetate extract is shown in Figure 5C.1.

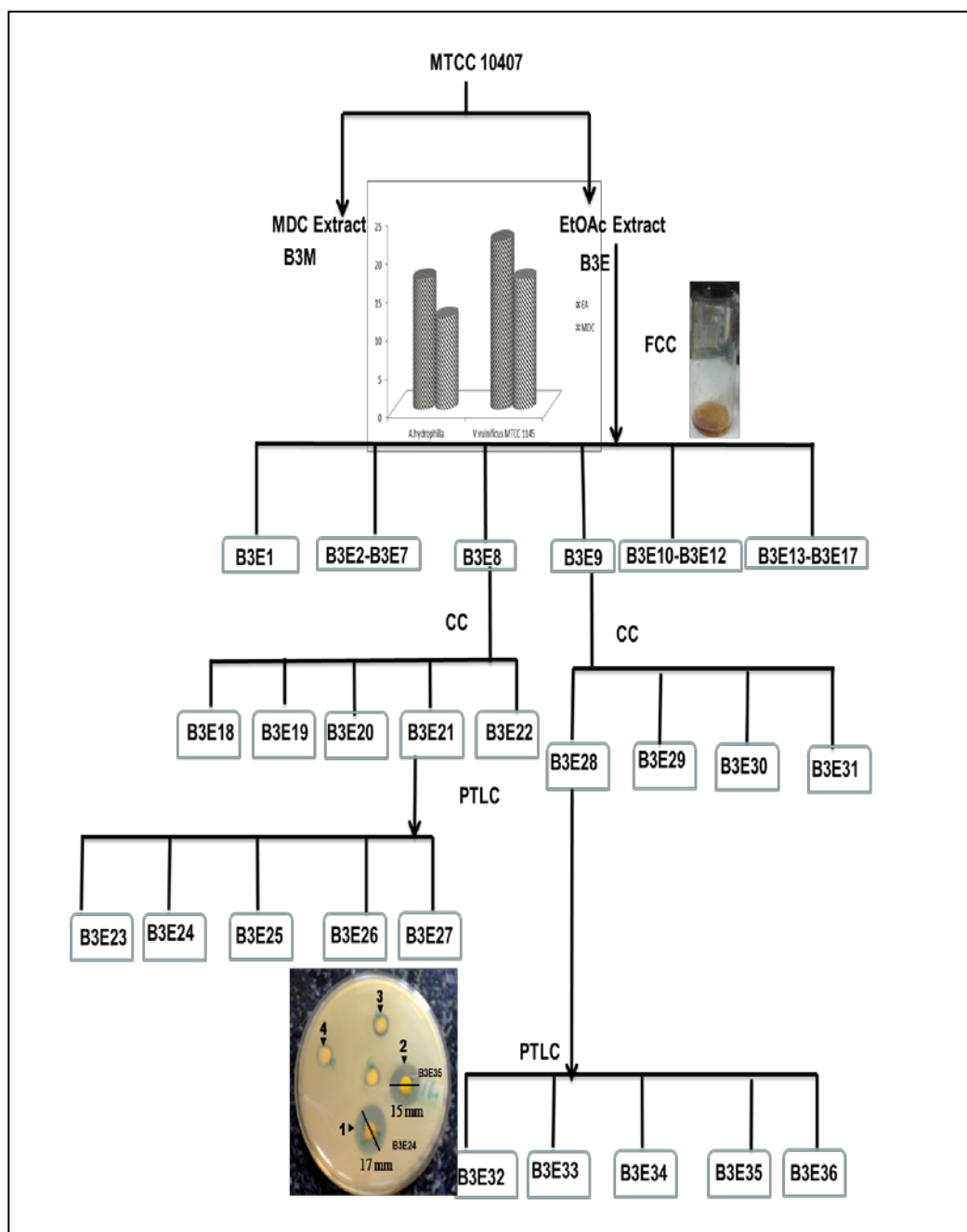


Figure 5C.1
Purification scheme for bioactive secondary metabolites from MTCC 10407.

5C.2 Results and discussion

5C.2.1 Antibiotic resistance and abiotic stress tolerance

The strain was susceptible to all the antibiotics tested and was proved to be safe for laboratory work. The strain was able to grow from 25°C up to 55°C and could with stand a pH range of 6 to 11.5. Strain could grow an NaCl concentration from 2% to 10%. The ability of the seaweed associated bacterial isolate to grow under a wide range of environmental conditions may be a functional adaptation for their protective function in varying aquatic environment.

5C.2.2 Optimization of time, temperature and pH

Optimum production time is found to be after 72 hours and it declined after 96 hours. Optimum temperature for production of the compound is found to be 20°C, whilst the optimum pH for the production is 8 (Figure 5C.2).

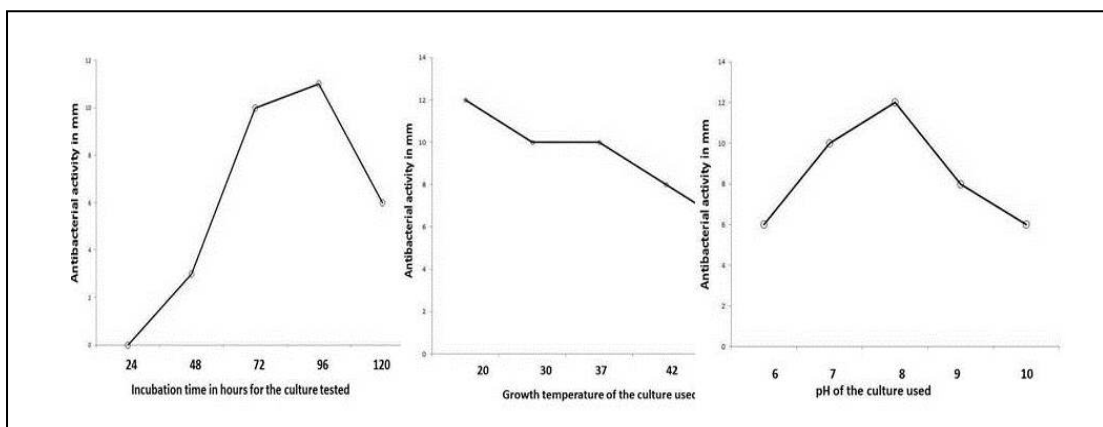


Figure 5C.2
Graphical representation of antibacterial compound production at different incubation time, temperature and pH

5C.2.3 Yield

The yield (g/L of the spent broth) of the EtOAc extracts of MTCC10407 SWI 19 (1.3g/L of the spent broth) was recorded maximum yield as compared with DCM (0.3465 g/L of the spent broth) extract.

5C.2.4 Antibacterial activities of the crude extracts by agar diffusion method.

Antibacterial activity of culture 3 extracts to different pathogens *Aeromonas hydrophilla* and *V. vulnificus* MTCC 1145 is shown in Figure 5C.3. The Figure 5C.3 indicates that the EA fractions are more active than DCM fractions of the culture 3.

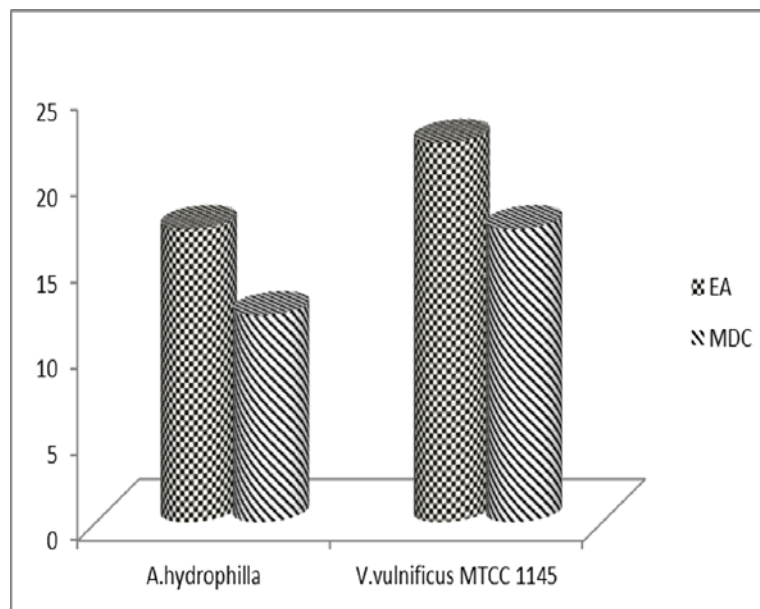


Figure 5C.3
Graphical representation of antibacterial activity of different solvent extracts to test pathogens

5C.2.5 Secondary Metabolites from *B. subtilis* MTCC 10407 associated with *Sargassum myriocystum* (SWI19)

The yield, antibacterial activities of each column/P-TLC fractions are given in Table 5C.1 The R_f of all the P-TLC fractions are also shown in Table 5C.1 Among the column fractions obtained from the EtOAc fraction of the MTCC 10407 extract, the fractions B3E8 and B3E9 exhibited significantly higher antibacterial activity. The fraction B3E8 (106 mg) was found to be a mixture, and was subjected to vacuum liquid chromatography on silica gel (180-230 mesh). The column was initially eluted with *n*-hexane and the eluent polarity was gradually increased by addition of EtOAc (*n*-hexane: EtOAc 19:1 to 1:3, v/v) to furnish twenty fractions of 15 ml each, which were reduced to five groups (B3E18 –

B3E22) after TLC analysis (*n*-hexane: EtOAc, 9.5:0.5, v/v). The fraction B3E21(52 mg) was further separated by chromatography on silica coated on a preparatory thin layer plate using a stepwise gradient system from 0.5% MeOH/CH₂Cl₂ to afford B3E24 2-(7-(2-ethylbutyl)-2,3,4,4a,6,7-hexahydro-2-oxopyrano[3,2-*b*]pyran-3-yl)ethyl benzoate (**9**, ~98% purity, 6.3 mg). Evaporation of solvents from the fractions followed by TLC over precoated silica gel GF₂₅₄ (particle size 15 mm, E-Merck, Germany) using EtOAc/*n*-hexane (3:17, v/v) supported the purity. The active fraction B3E9 (542.3 mg) eluted at 4% MeOH/CH₂Cl₂ was fractionated by chromatography over silica gel (180-230 mesh), with a stepwise gradient of CH₂Cl₂/MeOH (0-100%) to provide four sub-fractions (45 mL, B3E28 through B3E31). The active fraction B3E28 (23 mg) was found to be a mixture, which was further chromatographed over preparatory TLC on silica gel GF₂₅₄ using MeOH/CH₂Cl₂ (0.5:95.5, v/v) to afford **B3E35**, 2-((4*Z*)-2-ethyl-octahydro-6-oxo-3-((*E*)-pent-3-enylidene) pyrano[3,2-*b*]pyran-7-yl)ethyl benzoate (**10**, ~99% purity, 5.9 mg). Evaporation of solvents from **10** followed by TLC over precoated silica gel GF₂₅₄ (particle size 15 mm, E-Merck, Germany) using CHCl₃/MeOH (9:1, v/v) supported the purity.

Table 5C.1

Yield, activity Rt and R_f values of the fractions at different purification stages

	Yield (mg)	R _t	R _f	Antibacterial activity
EtOAc fraction (FCC M/D)				22.66±0.577
B3E-1(100%D/M)	127.8	-	-	NA
B3E-2(100%D/M)	20.3	-	-	NA
B3E-3(100%D/M)	8.3	-	-	NA
B3E-4(3%D/M)	6.4	-	-	NA
B3E-5(3%D/M)	10.5	-	-	NA
B3E-6(5%D/M)	5.6	-	-	10mm
B3E-7(7%D/M)	12.9	-	-	12mm
B3E-8(9%D/M)	106	-	-	20
B3E-9(10%D/M)	542.3	-	-	16
B3E-10(10%D/M)	214.4	-	-	6mm

Chapter - 5 C Bioprospecting of antagonistic bacteria *B.subtilis* MTCC 10407 associated with seaweed *Sargassum myriocystum* (SWI 19) for antibacterial metabolites

B3E-11(10%D/M)	132.9	-	-	5mm
B3E-12(20%D/M)	195.0	-	-	4mm
B3E-13(20%D/M)	216.4	-	-	7mm
B3E-14(30%D/M)	48.3	-	-	NA
B3E-15(50%D/M)	211.6	-	-	NA
B3E-16(100%M)	167.3	-	-	NA
B3E-17(100%M)	220.2	-	-	NA
B3E -8 (CC H/E)	106	-	-	20
B3E-18(100% H)	14mg	-	-	NA
B3E-19(10-25% E/H)	22mg	-	-	NA
B3E-20(25-50% E/H)	12mg	-	-	6
B3E-21(50-100% E/H)	52mg	-	-	15
B3E-22(100% E)	16mg	-	-	7
B3E -21 (4:1M/D)	52mg	-	NP	15
B3E-23	9.8	-	0.12	12
B3E-24	6.3mg	47.377	0.65	17
B3E-25	6.2	-	0.74	5
B3E-26	5.2	-	0.82	NA
B3E-27	4.3		0.98	2
B3E 9(CC M/D)	542.3	-	-	16
B3E-28(0-5% M/D)	23	-	-	14
B3E-29(10-25% M/D)	40.4	-	-	NA
B3E-30(25-50% M/D)	9.4	-	-	5
B3E-31(100%M)	11.3	-	-	7
B2E -28 (PTLC 100% DCM)	23	-	NP	14
B3E-32	2.3	-	0.15	7
B3E-33	5.77	-	0.23	NA
B3E-34	1.36	-	0.36	7
B3E-35	5.9	32.101	0.57	15
B3E-36	7.2	-	0.8	4

#NP-Not pure NA-Not active

5C.2.6 Structural characterization of antibacterial O-heterocycle pyran derivatives from *B. subtilis* MTCC 10407.

5C.2.6 .1 Structural characterization of Compound 9

2-(7-(2-Ethylbutyl)-2,3,4,4a,6,7-hexahydro-2-oxopyrano [3,2-b] pyran-3-yl) ethyl benzoate (9). Yellowish oil UV (MeOH) λ_{\max} (log ϵ): 315 nm (3.14); TLC (Si gel GF₂₅₄ 15 mm; EtOAc/*n*-hexane (3:17, v/v) R_f: 0.16; HPLC(Figure 5C.4) R_t: 47.377 min.; IR (KBr, cm⁻¹) ν_{\max} 814.06 cm⁻¹ (aromatic C-H_δ), 1312.76 (C-O_v), 1378.29 cm⁻¹ (C-H_p), 1648.94 cm⁻¹ (C=C_v), 1690.28 cm⁻¹ (C-CO_v), 1738.96 (C=O_v), 2923.22 cm⁻¹ (alkane C-H_v), 3010.12 cm⁻¹ (aromatic C-H_v); ¹H NMR (500 MHz, CDCl₃ δ in ppm), ¹³C NMR (125 MHz, CDCl₃ δ in ppm), ¹H-¹H-COSY, and HMBC data, see Table 5C.2; HRMS (ESI) *m/e*: 386.4489 calcd. for C₂₃H₃₀O₅ 386.4268; found 387.8689 [M+H]⁺.

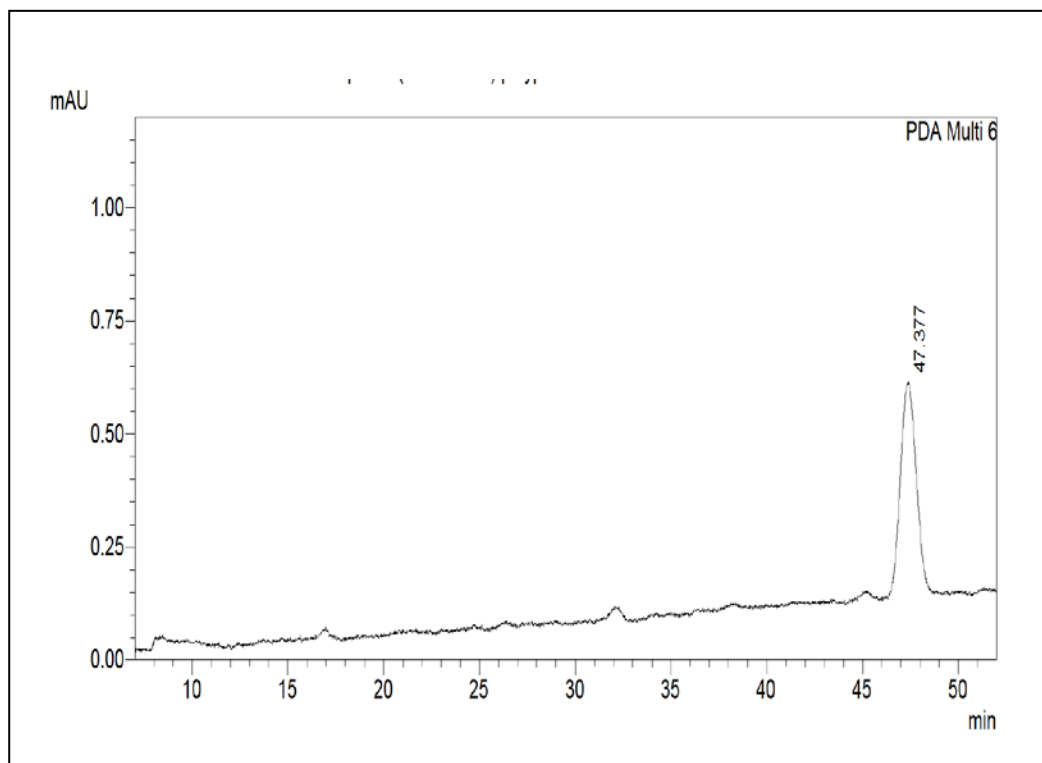
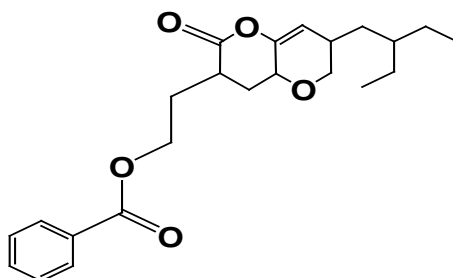


Figure 5C.4
HPLC Chromatogram of compound 9

Table 5C.2
¹H and ¹³C-NMR spectroscopic data of compound 9



C. No.	$\delta^{13}\text{CNMR}$	H	$\delta^1\text{H NMR}$ (int., mult., J in Hz) ^b	¹ H- ¹ H COSY	HMBC (¹ H- ¹³ C)
1	132.51				
2	131.32	2-H	7.78 – 7.65(m, 1H)	3-H	C-7,3
3	128.84	3-H	7.57 – 7.43 (m, 1H)		
4	128.11	4-H	7.57 – 7.43 (m, 1H)		
5	128.71	5-H	7.57 – 7.43 (m, 1H)	4-H	C-6
6	130.75	6-H	7.78 – 7.65 (m, 1H)	5-H	
7	167.72				
8	65.57	8-H	4.31 (t,J=7.2Hz, 2H)	9-H	C-7,9
9	30.58	9-H	1.72 (m, 2H)		C-10
10	43.76	10-H	2.38 (m, 1H)	13-H	C-11
11	179.99				
12	--		--		
13	27.73	13-H	1.68(t,2H)	14-H	C-14
14	72.41	14-H ^a	4.23(dq, J=6.7 Hz,1H)		C-15,18
15	138.77				
16	123.12	16-H	5.34 (d, 1H)	17-H	C-17
17	38.05	17-H	2.04(m,1H)	18-H	C-18
18	71.79	18-H	4.09 (d,J=6.67Hz, 2H)		C-20
19	27.73	19-H	1.53(m, 2H)		
20	22.7	20-H	1.46 (m, 2H).	19-H	C-25
21	19.16	21-H	1.01 (m, 2H)	22-H	C-22
22	14.12	22-H	0.88(m, 3H)		
23	--		--		
24	19.76	24-H	1.26(m,2H)	25-H	
25	13.12	25-H	0.92(t,3H)		

IR bending vibration bands of compound 1 at 1738 cm^{-1} attributed to the ester carbonyl absorption. The IR spectrum revealed a broad absorption band at $\nu_{\text{max}}1648 \text{ cm}^{-1}$, symbolized the olefinic system. Its mass spectrum exhibited a molecular ion peak at m/e 386 (HRESIMS m/e 387.8689 $[\text{M}+\text{H}]^+$), which in

combination with its ^1H and ^{13}C NMR data (Table 5C.2; Figure 5C.5.A-B) indicated the elemental composition of $\text{C}_{23}\text{H}_{30}\text{O}_5$ with nine degrees of unsaturation. The ^{13}C NMR spectrum in combination with DEPT experiments indicated the occurrence of 23 carbon atoms in the molecule, including two carbonyl carbon at δ 179.99 and δ 167.72, and olefinic carbons at δ 138.77 and 123.12 (Table 5C.2)). ^1H - ^1H COSY couplings (Figure 5C.5C) were apparent between the protons at δ 0.92 (H25) / δ 1.26 (H24) / δ 1.44 (H20) / δ 1.01 (H21) / δ 0.88 (H22) in the spectrum, which supported the presence of 3-ethyl butane moiety. Two methylene groups have been assigned to occupy at the C8-9 positions, and the one with δ 4.31 shifted downfield due to the presence of an extended conjugation probably linked to an aromatic moiety. The aromatic protons showed their characteristic signals at δ 7.78-7.58. ^1H - ^1H COSY experiments revealed that the protons at δ 4.31 (t) correlate with the methylene protons at δ 1.72 (assigned to be as H-9) and that at δ 2.38, the latter is assigned to be attached to a strongly electronegative group. HMBC correlations were apparent between H-9 (δ 1.72) with that of a carboxyl carbon at δ 179.99. The $>\text{C}=\text{O}$ group at the C-11 position of **9** resulted in strong deshielding of the $-\text{CH}-$ proton at δ 2.38, and therefore, has been assigned to be present at the C-10 position of the structure. The chemical shift of the protons at δ 1.53, 2.04, 5.37, and 4.09 along with detailed 2D NMR experiments established the presence of *O*-heterocyclic pyran network. The $-\text{CH}-$ proton (t) at δ 4.23 is characteristic of the junction point of the bicyclic system. The low field quaternary signal (^{13}C NMR) was in agreement with that to a quaternary carbon signal carrying the carbonyl groups at C-7 of **9**, and this was supported by the relatively downfield shift of the H-8 signal (δ 4.31), which referred to a possible oxygenation in its vicinity. The H-H and C-H connectivities apparent in the ^1H - ^1H COSY and HMBC spectra, respectively indicate that one of the nine unsaturations was due to the three rings and six double bonds. The relative stereochemistry of the chiral center particularly that of the C-10 cyclic framework was deduced from the NOESY experiment and the *J*-values. NOE couplings were observed between $\text{H}\alpha$ -14/ $\text{H}\alpha$ -10 thus indicating that these groups must be equatorial and on the α -side of the molecule. Therefore, the C-11 carboxyl group is axial and β -oriented. The methine proton at C-16 group did not exhibit NOE interactions with H-14 and H-

18, which are in the α -face of the molecule, thereby indicating that H-16 is at the axial disposition. The molecular ion peak at m/e 386 appeared to undergo elimination of benzoic acid (m/e 122) to yield 3-ethyl-7-(2-ethylbutyl)-tetrahydropyrano[3,2-b]pyran-2(3H)-one at m/e 266. The appearance of the fragment at m/e 154 indicated the presence of tetrahydropyrano [3, 2-b] pyran-2 (3H) -one moiety, resulted from the side chain elimination in 3-ethylpentane (Fig. 5C(2)A). Intramolecular rearrangement of tetrahydropyrano [3, 2-b] pyran-2 (3H) -one resulted in the formation of heptenoic acid (m/e 128) via the intermediate (E) -6-ethylidene-tetrahydropyran-2-one (m/e 126). The presence of tropylium ion (m/e 91) supports the presence of aryl ring system in 9 (Figure 5C.6).

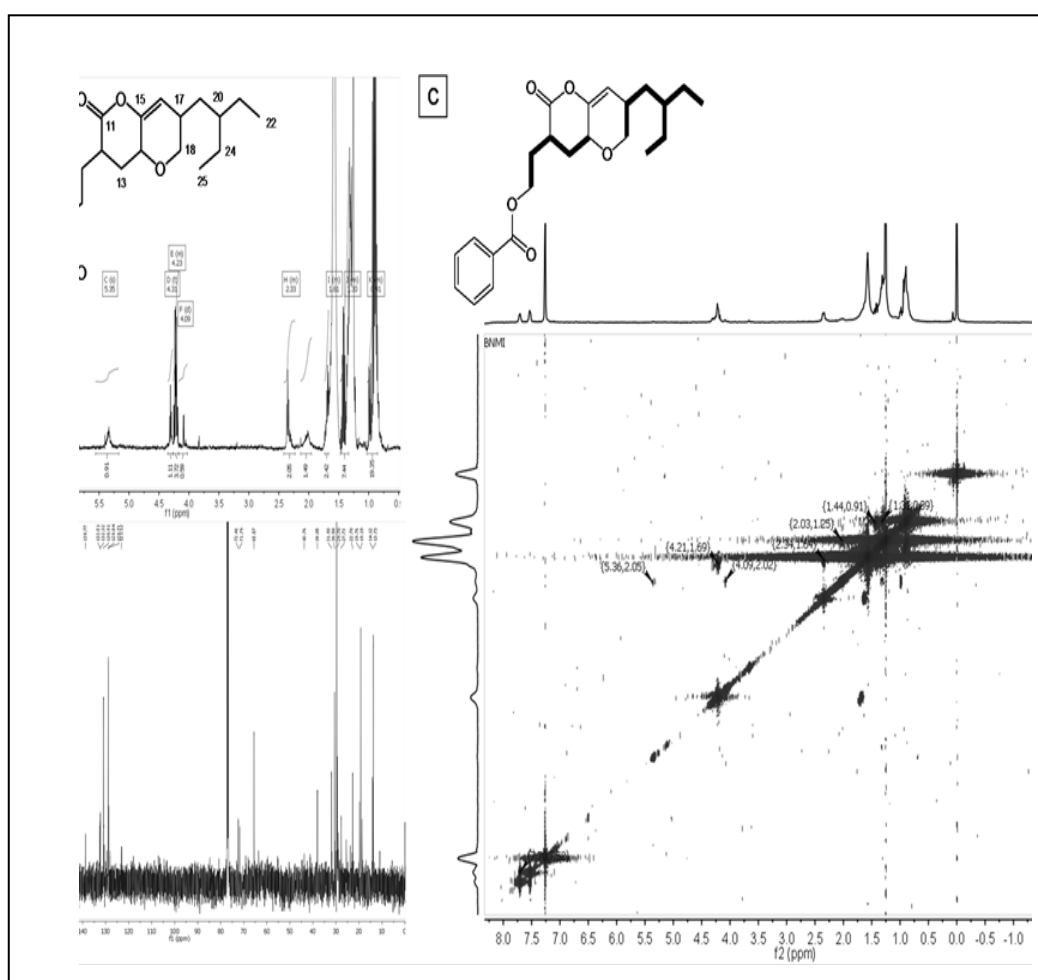


Figure 5C.5
(A) ^1H , (B) ^{13}C and (C) ^1H - ^1H COSY - NMR spectrum of 9. The key ^1H - ^1H COSY couplings have been represented by the bold face bonds.

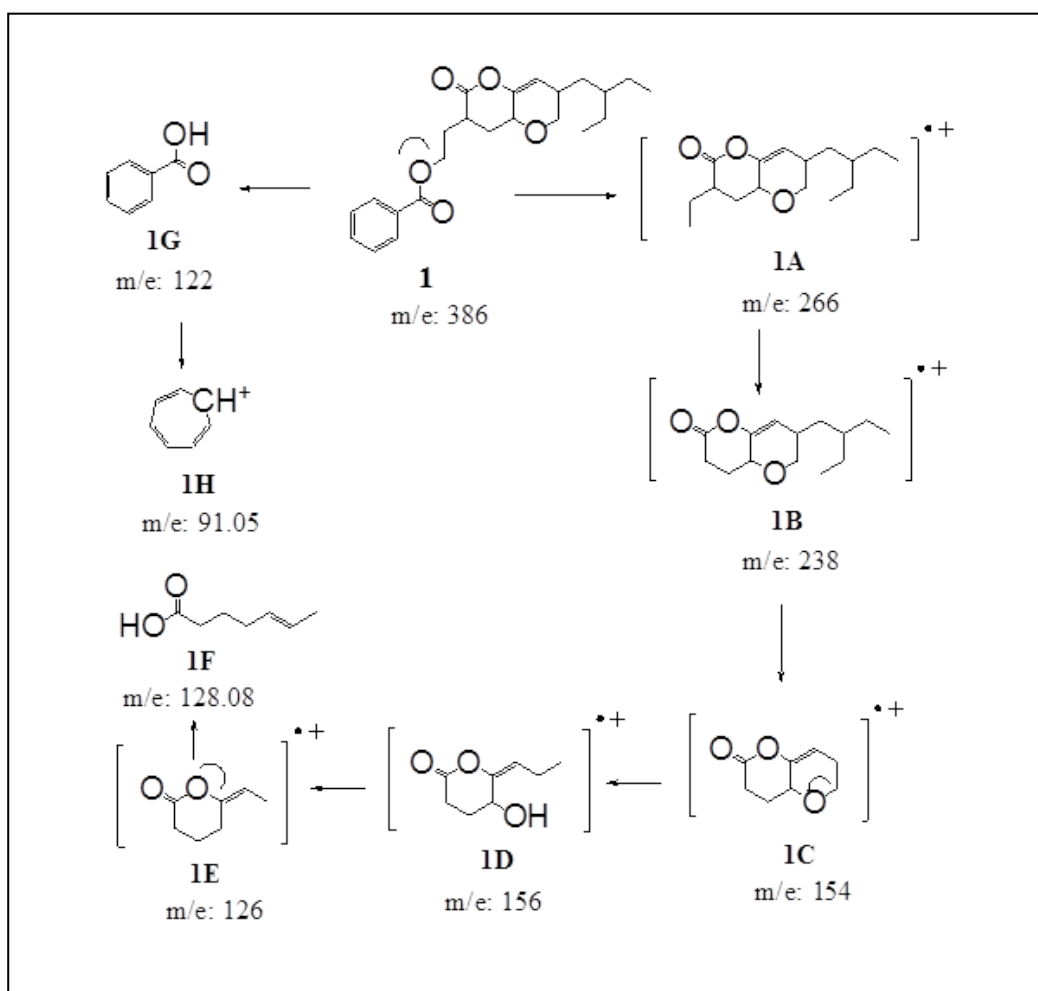


Figure 5C.6

Mass fragmentation pattern of *O*-heterocycle pyran derivative compound **9** from *B. subtilis* MTCC 10407. The compound **9** undergoes mass fragmentation to yield (**1A**) 3-ethyl-7-(2-ethylbutyl)-4,4a,6,7-tetrahydropyrano[3,2-b]pyran-2(3H)-one, (**1B**) 7-(2-ethylbutyl)-4,4a,6,7-tetrahydropyrano[3,2-b]pyran-2(3H)-one, (**1C**) 4,4a,6,7-tetrahydropyrano[3,2-b]pyran-2(3H)-one, (**1D**) (E)-tetrahydro-5-hydroxy-6-propylidenepyran-2-one, (**1E**) (E)-6-ethylidene-tetrahydropyran-2-one, (**1F**) heptenoic acid, (**1G**) benzoic acid, and (**1H**) tropylium ion as major peaks.

5C.2.6 .2Structural characterization of Compound 10

2-((4Z)-2-Ethyl-octahydro-6-oxo-3-((E)-pent-3-enylidene) pyrano [3, 2-b]pyran-7-yl) ethyl benzoate (**10**). Yellowish oil; UV (MeOH) λ_{\max} (log ϵ): 410 nm (2.83); TLC (Si gel GF₂₅₄ 15 mm; CHCl₃/MeOH 9:1, v/v) R_f: 0.50; R_t: 32.101 min(Figure 5C.7); IR (KBr, cm⁻¹) ν_{\max} 727.22 cm⁻¹ (C-H_p), 814.16 cm⁻¹ (aromatic C-H_δ), 1371.26 cm⁻¹ (C-H_p), 1526.21(aromatic C=C_v), 1652.42 cm⁻¹ (C=C_v), 1690.21 cm⁻¹ (C-CO-O_v), 1726.86 cm⁻¹ (C=O_v), 2923.22 cm⁻¹ (alkane C-H_v), 3346 cm⁻¹

(broad O-H_v); ¹H NMR (500 MHz, CDCl₃ δ in ppm), ¹³C NMR (126 MHz, CDCl₃ δ in ppm), ¹H-¹H-COSY, and HMBC data, see Table 5C.3; HRMS (ESI) *m/e*: 399.6984 calcd. for C₂₄H₃₁O₅ 399.1268; found 399.6984 [M+H]⁺.

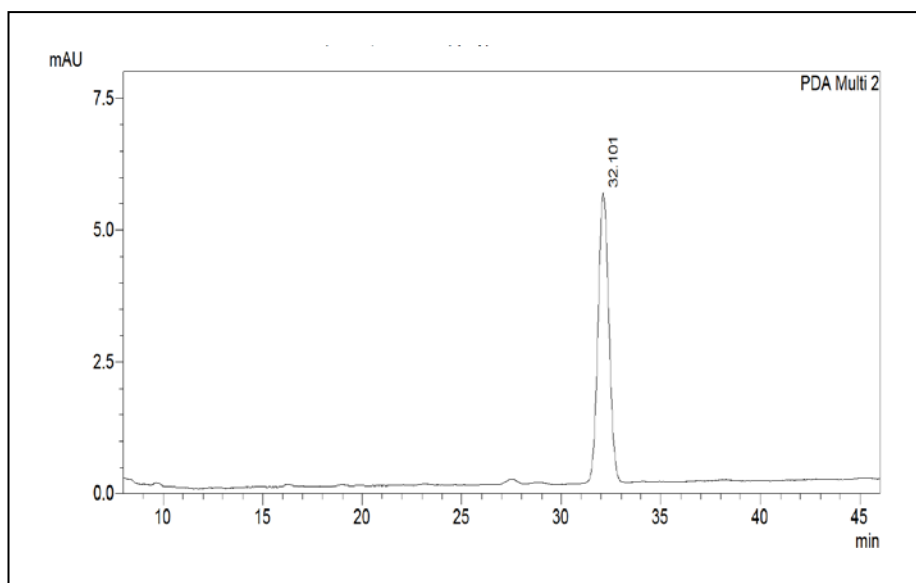


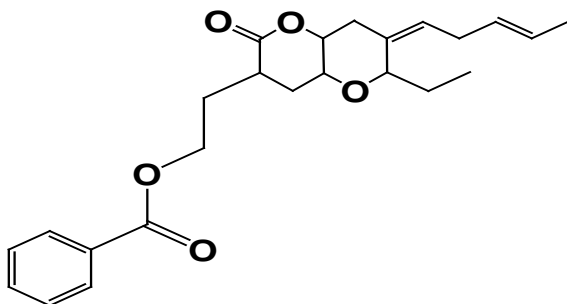
Figure 5C.7
HPLC chromatogram of compound 10

The IR absorption band of **10** exhibited close resemblance with that of **9**, except the presence of greater olefinic signals near 1653 cm⁻¹, which apparently indicated that **9** and **10** shared close structural similarities. Its mass spectrum exhibited a molecular ion peak at *m/e* 399 (HRESIMS *m/e* 399.6984 [M+H]⁺), which in combination with its ¹H and ¹³C NMR data (Table 5C.3) indicated the elemental composition of **10** as C₂₄H₃₀O₅ with ten degrees of unsaturation. A significant similarity in the NMR spectral data between **10** and **9** was apparent (Figure 5C.8.A-B), which indicated their structural similarity. However, unlike the compound **9**, no DEPT signal was apparent for the C-16 for **10**, which indicated the carbon as quaternary (δ 142.78) (Figure 5C.8.C). Additional olefinic signals were apparent at δ 130.14, 123.78, and 114.63. The ¹H-¹H COSY correlation with H-18 (δ 5.27 dd, 1H)/H-19 (δ 1.94-1.97, m, 2H)/H-20 (δ 5.80, m, 1H)/H-21 (δ 4.97, dd, 1H)/H-22 (δ 0.87, d, 3H) support the presence of the six member hexadiene moiety (Figure 5C.9.A). These results were supported by detailed HSQC and HMBC experiments (Fig. 5C.9.B and Fig. 5C.10.A). The ¹H-NMR in conjugation

with ^{13}C -NMR recorded the signals at δ 2.38, 1.62, 3.91, and 3.51, and the ^1H - ^1H COSY couplings were apparent between these protons assigned to be as H-10/H-14/H-13/H-12; which supported the presence of six member tetrahydropyranone ring system. The aromatic ring and carboxyl ester group at the C-7 position resulted in strong deshielding of proton at δ 4.32 along with the quaternary carbon atom at δ 132.96, and therefore, has been assigned to be present at the junction point between the aromatic ring and carboxyl ester group. The methine proton at δ 2.38 was characteristic of the junction point of the tetrahydropyranone ring with that of the side chain ethyl benzoate moiety as established by ^1H - ^1H COSY correlations and detailed HMBC experiments. The point of cyclization of the substituted lactone ring was indicated by the low-field shift of H-10 at δ 2.38, which has been coupled with the H-14 methylene group at δ 1.62, which also gives clear ^1H - ^1H COSY correlation with H-10/H-14/H-13, thus supporting the presence of the six member lactone moiety. The relative stereochemistry of the chiral centres, particularly that of C-10, 12 and 17 of the hexahydropyrano [3, 2-b] pyranone framework was deduced from the NOESY spectrum of the compound and the J -values. NOE couplings were observed between H α -13 (δ 3.91)/H α -10 (δ 2.38) thus indicating that these groups must be equatorial and on the α -side of the molecule (Figure 5C.10.B). The methine proton at C-12 group did not exhibit NOE interactions with H-13 and H-10, which is in the α -face of the molecule, thereby indicating that H-12 is at the axial disposition. The compound **10** undergoes mass fragmentation to afford similar mass fragments as in **9** (m/e 154, 156, 128, 126, 122, and 91), which supported the structural similarities between these compounds (Figure 5C.6 and Figure 5C.11). Two intense peaks at m/e 266 and 238 as described in **9** were absent in **10**, which apparent signified the modifications in the side chain attached at C-17 position of the hexahydropyrano [3,2-b] pyran-2(3H)-one ring system of the latter. Two mass fragment peaks appeared at m/e 278 and 250 apparently due to the presence of diethyl-hexahydro-7-(pentenylidene) pyrano [3,2-b] pyranone and ethyl-hexahydro-7-(pentenylidene) pyrano [3,2-b] pyranone, respectively.

Table 5C.3

^1H and ^{13}C -NMR spectroscopic data of compound 10



C. No.	δ ^{13}C NMR	H	$\delta^1\text{H}$ NMR (int., mult., J in Hz) ^b	^1H - ^1H COSY	HMBC (^1H - ^{13}C)
1	132.3				
2	130.87	2-H	7.50 – 7.42 (m, 1H)	3-H	C-3,4
3	129.95	3-H	7.69 – 7.61 (m, 1H)		
4	128.84	4-H	7.69 – 7.61 (m, 1H)		
5	128.84	5-H	7.69 – 7.61 (m, 1H)	6- H	
6	130.90	6-H	7.50 – 7.42 (m, 1H)		
7	167.73	-			
8	65.57	8-H	4.23 (t, J = 6.7 Hz, 2H)	9- H	C-9,10
9	30.58	9-H	1.67(m,1H)		C-10
10	34.84	10-H	2.34(m,1H)	14- H	C-11
11	173.52				
12	53.61	12-H	3.59(m,1H)	15- H	
13	69.06	13-H	3.91(m,1H)		C-11
14	30.12	14-H	1.62(t,2H)		C-10
15	29.38	15-H	1.45(d,2H)		C-17
16	142.78				
17	62.16	17-H	4.08(dt, 1H)	23- H	C-13
18	130.14	18-H	5.27(dd,1H)	19- H	C-12
19	27.40	19-H ^a /19-H ^b	1.94/1.97(m,2H)		C-20
20	123.78	20-H	5.80(m,1H)	21- H	
21	114.63	21-H	4.97(dd,1H)		
22	14.14	22-H	0.87(d,3H)		
23	19.80	23-H	1.48(m,2H)		C-16
24	13.81	24-H	0.81(t,3H)	23- H	C-23
25	--	--	--		

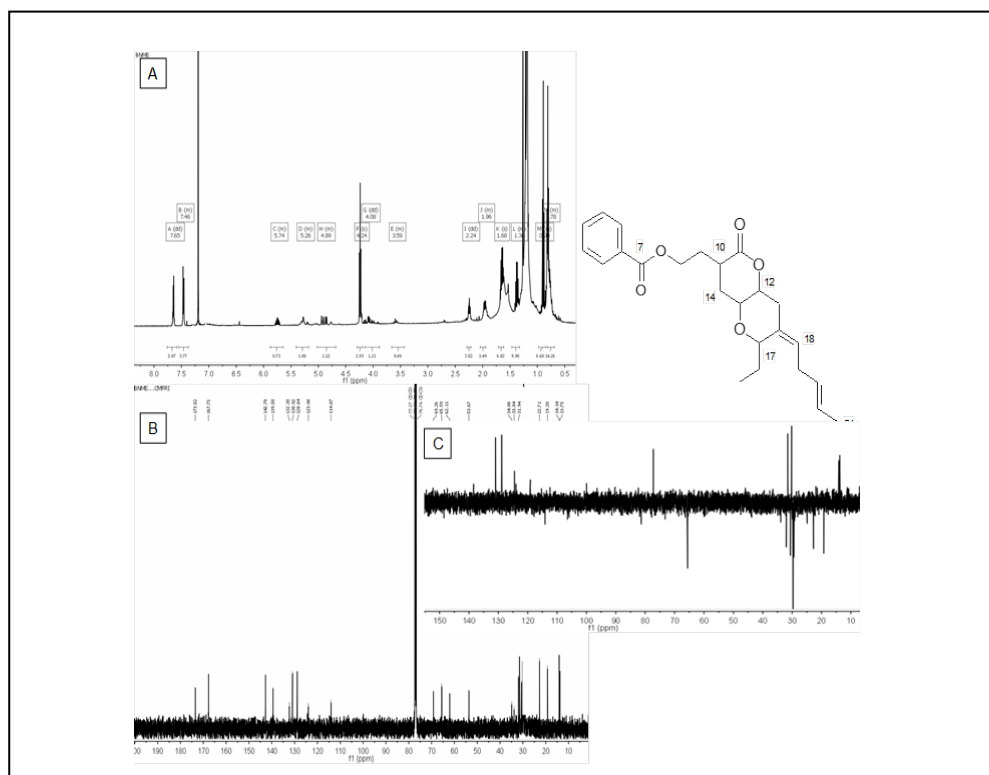


Figure 5C.8
(A) ^1H , (B) ^{13}C and (C) DEPT_{135} - NMR spectrum of 10.

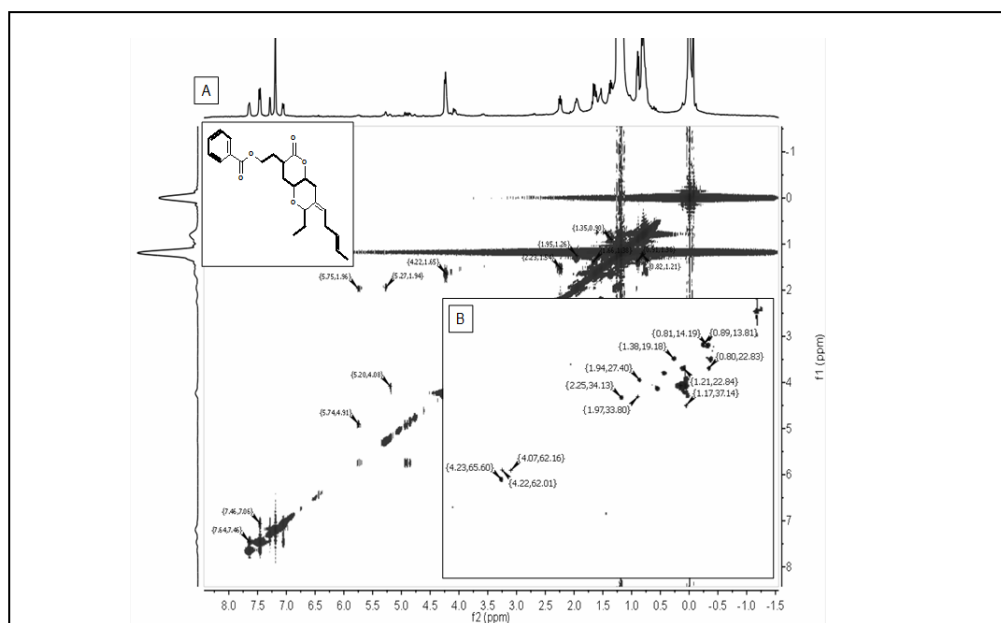


Figure 5C.9
(A) ^1H - ^1H COSY and (B) prominent HSQC correlation spectra of 10. The key ^1H - ^1H COSY couplings have been represented by the bold face bonds.

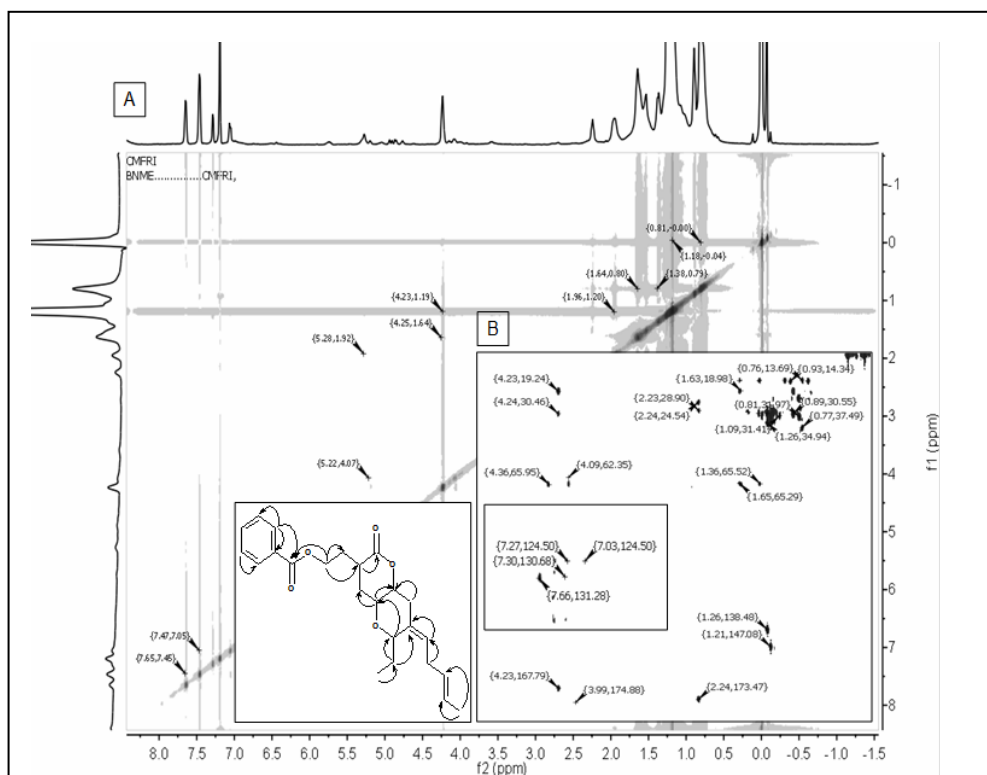


Figure 5C.10
(A) HMBC and (B) NOESY spectra of 10. The key HMBC couplings have been indicated as double barbed arrow.

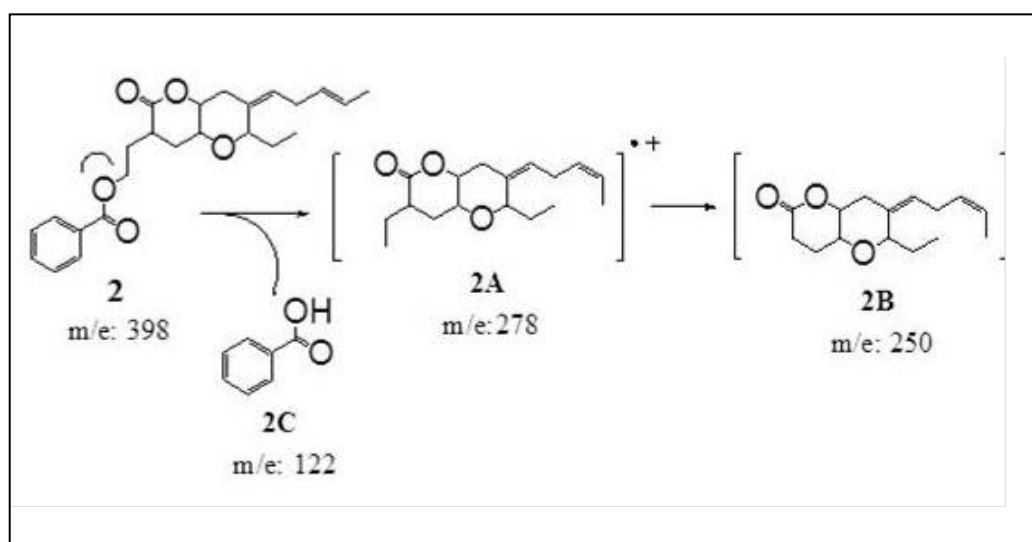


Figure 5C.11 Mass fragmentation pattern of *O*-heterocycle pyran derivative compound 10 from *B. subtilis* MTCC 10407.

5C.3 Conclusions

Two novel *O*-heterocycle pyrans, 2-(7-(2-ethylbutyl)-2,3,4,4a,6,7-hexahydro-2-oxopyrano[3,2-*b*]pyran-3-yl)ethyl benzoate (**9**) and 2-((4*Z*)-2-ethyl-octahydro-6-oxo-3-((*E*)-pent-3-enylidene)pyrano[3,2-*b*]pyran-7-yl)ethyl benzoate (**10**) were isolated from the ethylacetate extract of the *B. subtilis* MTCC 10407, which was found to be associated with brown seaweed *Sargassum myriocystum* upon repeated chromatography over silica columns.

CHAPTER 5D

BIOPROSPECTING OF ANTAGONISTIC BACTERIA *B. amyloliquefaciens* ASSOCIATED WITH SEAWEED *Padina gymnospora*(SWI7)FOR ANTIBACTERIAL METABOLITES

5D.1 Materials and methods

5D.1.1 Microbial strain under the study

The microbial strain used for bioprospecting of antimicrobial compound in the current study is *Bacillus amyloliquefaciens* associated with *Padina gymnospora*. The seaweed associated bacterial isolates were isolated (chapter3 section 3.2.2) and assayed for their ability to inhibit selected pathogenic microorganisms (chapter3 section 3.2.5). Isolates for metabolite purification with antibacterial activity used in the study were selected based on their inhibition spectrum (Chapter3 Table 3.2) and the positive hit for metabolite gene (Chapter4. 2.5 and 4.3.4).

5D.1.2 Antibiotic resistance and abiotic stress tolerance

Antibiotic resistance, Abiotic stress tolerance and Enzyme production profile of the strain was analyzed using the methodology explained in 5.2.2.

5D.1.3 Optimization of time

The microorganism under the study was inoculated in nutrient broth and the optimum time for the antibiotic production with maximum inhibitory activity was analysed as explained in 5.2.3.

5D.1.4 Optimization of temperature

The optimum temperature for the production of antibacterial compound for the strain was analyzed using the methodology explained under the section 5.2.4.

5D.1.5 Optimization of pH

The optimum P^H for the production of the active metabolite was standardized as described under the section 5.2.5.

5D.1.6 Preparation of crude extract for purification of secondary metabolites

The antibiotic-producing bacterium, *B. amyloliquefacens* associated with *Padina gymnospora* (SWI 7). The preparation and recovery of secondary metabolites were carried out by a surface culturing method over solid nutrient agar plates (5.2.3). The adsorbed products were subsequently extracted with ethyl acetate by homogenization (Arrow Engineering Inc., Pennsylvania Ave, USA) followed by refluxing. Evaporation of the solvent under reduced pressure (Heidolph Instruments GmbH & Co., Schwabach, Germany) yielded the ethyl acetate extract (2.87 g) from the total culture volume of 4 L. Subsequently the residual agar was extracted with CH₂Cl₂ to furnish dichloromethane extract. These solvent extracts were evaluated for antibacterial activities (5.2.4), against the pathogens (listed in Chapter 3 section 3.2.4) and the fractions which showed significantly broad spectrum antibacterial activities and higher yield were further purified by chromatographic techniques.

5D.1.7 Purification of secondary metabolites

The pooled ethyl acetate extract (2.87 g) was subjected to vacuum liquid chromatography on silica gel (180-230 mesh). The column was initially eluted with *n*-hexane and the eluent polarity was gradually increased by addition of EtOAc (*n*-hexane: EtOAc 19:1 to 1:3, v/v) to furnish nine fractions of 50 ml each (B7E1-B7E9). These column fractions were evaluated for antibacterial activities (5.2.4), against the pathogens (listed in Chapter 3 section 3.2.4) and the fractions which showed significantly broad spectrum antibacterial activities and higher yield were further purified by column chromatography or preparative TLC (P-TLC) using EtOAc:*n*-hexane or MeOH:CHCl₃ or MeOH:EtOAc as mobile phase when required. The schematic diagram showing the purification of *B. amyloliquefacens*

associated with *Padina gymnospora* (SWI7) ethyl acetate extract is shown in Figure 5D.1.

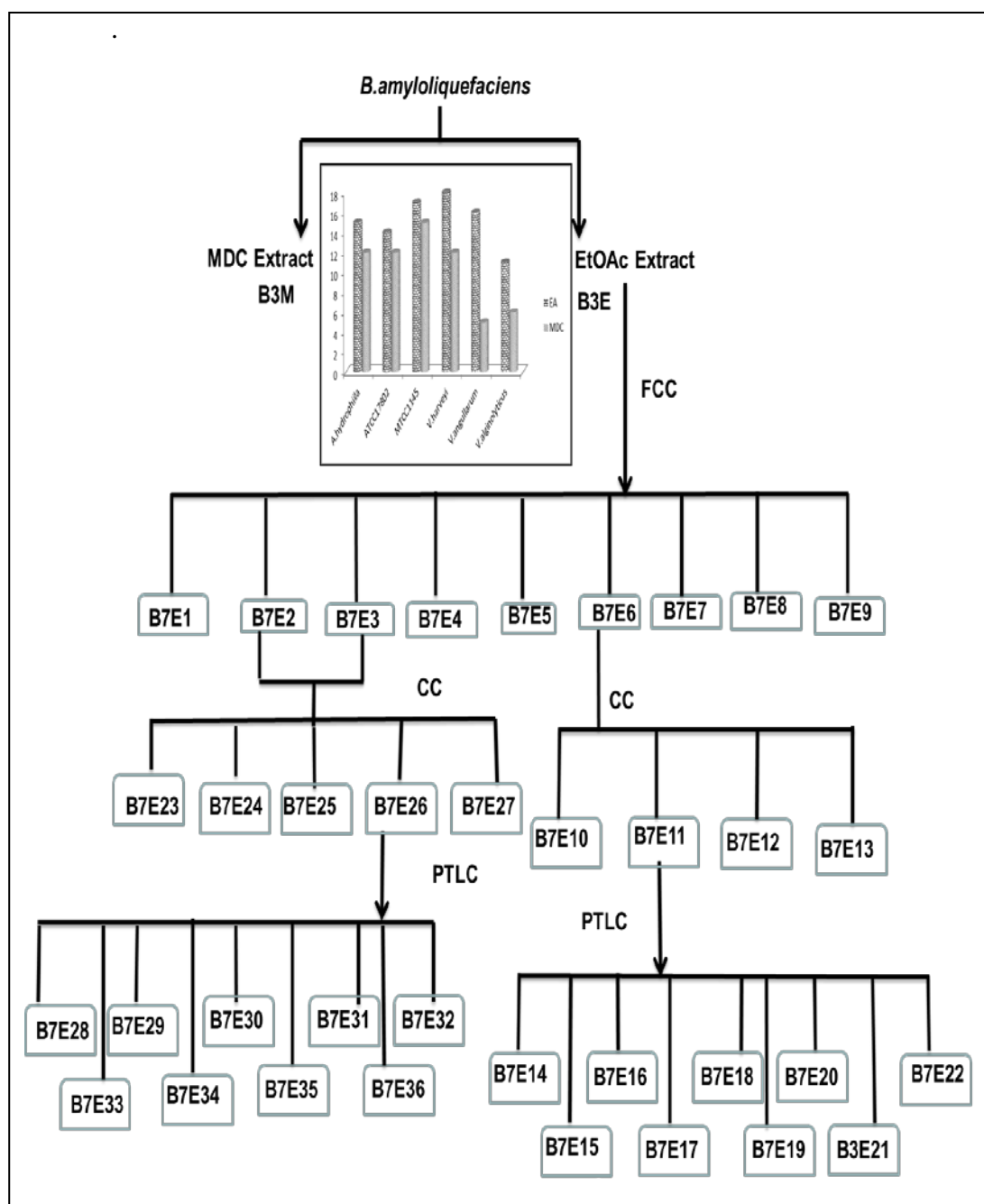


Figure 5D.1

Schematic representation showing the purification scheme for bioprospecting of antibacterial metabolites in *B. amyloliquefaciens* associated with *Padina gymnospora*

5D.2 Results and Discussion

5D.2.1 Antibiotic resistance, abiotic stress tolerance and optimization of growth conditions

The bacterial isolate under the study was sensitive to the tested antibiotics and had similar abiotic stress tolerance as exhibited by SWI 4B (Chapter 5B).The growth conditions were also similar to the above described culture.

5D.2.2 Yield

The yield (g/L of the spent broth) of the EtOAc extracts of SWI 4 is recorded as 0.7175g/L of the spent broth is higher than DCM (0.2675 g/L of the spent broth) extract.

5D.2.3 Antibacterial activities of the crude extracts by Agar Diffusion Method.

Antibacterial activity of *B. amyloliquefacens* MTCC 10456^B extracts to different pathogens *Aeromonas hydrophilla* V. *vulnificus* MTCC 1145 and *V. parahaemoliticus* ATCC17802 were shown in Figure 5D.2. The Figure 5D.2 indicates that the EA fractions are more active than other fractions of the *B. amyloliquefacens* MTCC 10456^B associated with *Padina gymnospora* (SWI7).

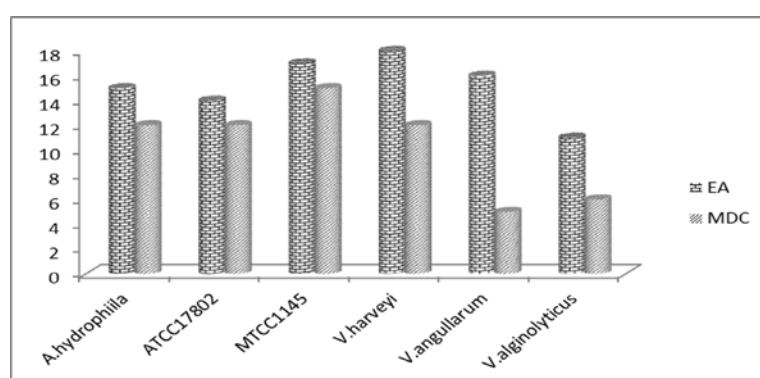


Figure 5D.2

Graphical representation of antibacterial activity of solvent extracts of bacterial metabolites against test pathogens.

5D.2.4 Secondary metabolites from *B. amyloliquefacens* MTCC 10456^B associated with *Padina gymnospora* (SWI7)

The fraction B7E6 (780mg) was subjected to vacuum liquid chromatography on silica gel (180-230 mesh). The column was initially eluted with *n*-hexane and the eluent polarity was gradually increased by addition of EtOAc (*n*-hexane: EtOAc 1:9 to 1:2, v/v) to furnish twenty three fractions of 15 ml each, which were reduced to four groups (B7E10 – B7E13). The fraction B7E11(159 mg) was further separated by chromatography on silica coated on a preparatory thin layer plate using a stepwise gradient system from 0.5% MeOH/CH₂Cl₂ to afford B7E18 and B7E21. Evaporation of solvents from the fractions followed by TLC over precoated silica gel GF₂₅₄ (particle size 15 mm, E-Merck, Germany) using EtOAc/*n*-hexane (3:17, v/v) supported the purity.

The fraction B7E2 and B7E3 were pooled after TLC analysis (*n*-hexane: EtOAc, 9.5:0.5, v/v) was found to be a mixture with an antibacterial activity of 25mm (300mg), and was subjected to vacuum liquid chromatography on silica gel (180-230 mesh). The column was initially eluted with *n*-hexane and the eluent polarity was gradually increased by addition of EtOAc (*n*-hexane: EtOAc 19:1 to 1:3, v/v) to furnish twenty fractions of 15 ml each, which were reduced to five groups (B7E23– B7E27) after TLC analysis (*n*-hexane: EtOAc, 9.5:0.5, v/v). The fraction B7E26 (109 mg) was further separated by chromatography on silica coated on a preparatory thin layer plate using a stepwise gradient system from 0.8% MeOH/CH₂Cl₂ to afford B4E29 and B7E 36(Table 5D.1).Evaporation of solvents from the fractions followed by TLC over precoated silica gel GF₂₅₄ (particle size 15 mm, E-Merck, Germany) using EtOAc/*n*-hexane (3:17, v/v) supported the purity.

Table 5D.1
Yield, activity ,R_t and R_f values of the fractions
at different purification stages

	Yield	R _t	R _f	Antibacterial
B7EtOAc fraction (FCC)E/H)				
B7E1(100% H)	49.2 g	-	-	-
B7E2(5-10% E/H)	3.7 mg	-	-	22mm
B7E3(10-20% E/H)	773 mg	-	-	24mm
B7E4(20-25% E/H)	2.59 mg	-	-	-
B7E5(25-30% E/H)	470 mg	-	-	-
B7E6(30-35% E/H)	624 mg	-	-	-
B7E7(30-40% E/H)	720 mg	-	-	18mm
B7E8(50% E/H)	56.3 mg	-	-	-
B7E9(100% E)	104.5 mg	-	-	-
B7E6(CC E/H)	-	-	NP	18mm
B7E10(0-25% E/H)	6.5 mg	-	-	6mm
B7E11(25-50% E/H)	159 mg	-	-	14mm
B7E12(50-100% E/H)	3.7 mg	-	-	5mm
B7E13(100% E)	2.1 mg	-	-	NA
B7E11 (PTLC			NP	14mm
B7E14	1.0 mg	-	0.1	NA
B7E15	8.8 mg	-	0.2	NA
B7E16	4.6 mg	-	0.3	8mm
B7E17	1.9 mg	-	0.4	6mm
B7E18	8.2 mg	25.1	0.4	14mm
B7E19	6 mg	-	0.5	NA
B7E20	5 mg	-	0.7	NA
B7E21	9.2mg	15.9	0.8	12mm
B7E22	-	-	0.9	5mm
B7E-(2-3) (CC E/H)	-	-	NP	24mm

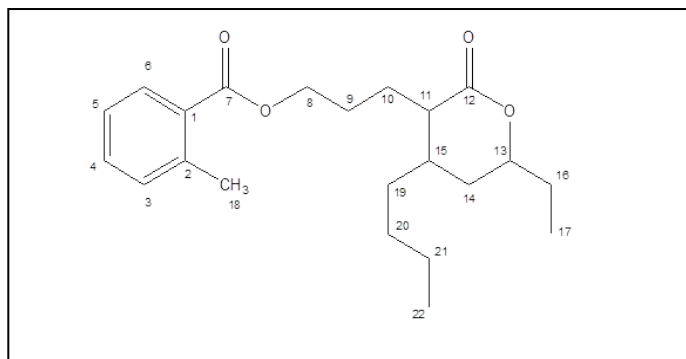
B7E23(0-10% E/H)	12mg	-	-	NA
B7E24(10-25%E/H)	8.9mg	-	-	NA
B7E25(25-50% E/H)	2.6mg	-	-	NA
B7E26(50-100% E/H)	25mg	-	-	17mm
B7E27(100% E)	12.8mg	-	-	9mm
B7E26 (PTLC 0.8%	25mg	-	NP	17mm
B7E28	6.2mg	-	0.1	NA
B7E29	9.2mg	37.0	0.2	15mm
B7E30	2.1mg	-	0.3	6mm
B7E31	1.2mg	-	0.4	NA
B7E32	1.6mg	-	0.4	NA
B7E33	3.2mg	-	0.5	NA
B7E34	1.5mg	-	0.6	NA
B7E35	1.8mg	-	0.7	5mm
B7E36	7.9mg	32.1	0.9	13mm

5D.2.4.1 Structural characterization of the compound 11

10-(15-butyl-13-ethyl-2-oxotetrahydro-2H-pyranyl)propyl-2 methylbenzionate (**11**) Yellowish oil; UV (MeOH) λ_{\max} (log ϵ): 242 nm (3.42); TLC (Si gel GF254 15 mm; EtOAc/*n*-hexane (3:17, v/v) R_f : 0.48; R_t : 25.176 min(; IR (KBr, cm^{-1}) ν_{\max} 818.24 (aromatic C-H δ), 1310.16 (C-O ν), 1372.12 (C-H ρ), 1619.48 (C=C ν), 2935.34 (alkane C-H ν), 3012.24 (aromatic C-H ν); $^1\text{H-NMR}$ (500 MHz, Chloroform- d) δ 7.72 (d,1H),7.53 (d,1H), 7.08 (d,1H), 7.06 (m,1H) , 4.22 (t, 1H), 4.08 (m, 2H), 2.31 (s,3H), 2.29 (m,1H), 2.03 (m,1H), 1.97 (d,2H), 1.72 (m, 2H), 1.61 (m,1H), 1.36 (m,2H), 1.26(m,2H), 1.28(m,2H), 1.12(m,2H), 1.01 (d,3H), 0.88(t,3H), $^{13}\text{C-NMR}$ (125 MHz, CDCl_3 δ in ppm), $^1\text{H-}^1\text{H}$ COSY and HMBC data, see Table 5D.2; HRMS (ESI) m/e : 361.4871(M+H) $^+$ calcd. for $\text{C}_{22}\text{H}_{32}\text{O}_4$ 360.2301; found 361.4871(M+H) $^+$.

Table 5D.2

NMR spectroscopic data of compound 11 in CDCl₃.^a



Position	¹³ C	H-type	¹ H NMR	¹ H- ¹ H COSY	HMBC → ¹ H ¹³ C
1	139.77				
2	148.45				
3	129.66	3-H	7.72 (d,1H)	4-H	C-2
4	128.84	4-H	7.53 (d,1H)		
5	130.84	5-H	7.08 (d,1H)	6- H	C-1,6
6	129.66	6-H	7.06 (m,1H)		
7	171.15				
8	63.27	8-H	4.22 (t, 1H)	9- H	C-7
9	31.92	9-H	1.72 (m, 2H),		C-10
10	24.99	10-H	1.61 (m, 1H),	11-H	C-11
11	38.26	11-H	2.29 (m,1H)	15-H	C-12
12	172.34				
13	68.09	13-H	4.08 (m, 2H)	16-H	C-14
14	29.69	14-H	1.36 (m,2H)		
15	21.02	15-H	2.03 (m,1H)	14-H	
16	29.35	16-H	1.97 (d,2H)	17-H	C-17
17	22.81	17-H	1.01 (d,3H)		
18	38.44	18-H	2.31 (s,3H)		C-3

19	29.65	19-H	1.26(m,2H)	20-H	C-20
20	22.76	20-H	1.28(m,2H)		
21	19.74	21-H	1.12(m,2H)	22-H	C-22
22	14.11	22-H	0.88(t,3H)		

The compound 10-(15-butyl-13-ethyl-2-oxotetrahydro-2H-pyranyl)propyl-2-methylbenzoate (**11**) was isolated as yellowish oil upon chromatography over silica columns. The IR absorption band (in MeOH) exhibited close resemblance with that of **compound 11**. The ultraviolet absorbance at λ max (log e) 242 nm (3.42) was assigned to a chromophore with extended conjugation. Its mass spectrum exhibited a molecular ion peak at m/e 360 (HRESIMS m/e 361.4871 [M+H]⁺; D 0.0 amu), which in combination with its ¹H and ¹³C NMR data (Table 5D.2) indicated the elemental composition of compound as C₂₂H₃₂O₄ with seven degrees of unsaturation. Three degrees of unsaturation from the double bonds and two degrees of unsaturation from the rings were demonstrated. Remaining two were from the carbonyl groups.

The ¹H-NMR in conjugation with ¹³C-NMR recorded the signals at δ 2.31, 1.26, 1.28, 1.12 and 0.88 shows ¹H–¹H COSY couplings(Figure 5D.4.A) were apparent between these protons assigned to be at H-18/H-19/H-20/H-21 and H-22; which support the presence of pentane system in compound 11. The relatively downfield shift of the methylene protons at δ 4.22 and the C-8 carbon at δ 63.27 referred to a possible aromatic conjugated carbonyl group. The aromatic protons were assigned to be present at δ 7.72-7.06 and the proton integral of the protons revealed the presence of aromatic ring. Signal at 148.45(C-2) downfield shift was apparently due to the ring contain methyl substitution. Strong HMBC correlations were found between H-8 (δ 4.22) and H-9 (δ 1.72) with C-7(δ 171.15) (Table 5D.2), which apparently indicated the presence of the propyl benzoate group. The presence of two quaternary carbons at δ 148.45 and δ 139.77 were due to the presence of substituted aromatic moiety. The ¹H–¹H COSY correlations between H-11 (δ 2.29)/H-15(δ 2.03)/H-14(δ 1.36) and H-13(δ 4.08) along with the proton and carbon connectivities deduced from HSQC (Figure 5D.4.B) and HMBC

experiments (Table 5D.2) confirmed the presence of the pyranone framework. Also additional ethyl signals were apparent at δ 29.35 and 22.81 attached to C-13 position. These results were supported by detailed HMBC experiment (FIGURE 5D.4.C). The presence of $-\text{CH}_3$ group at the C-18 position of the compound was confirmed by ^1H NMR and HMBC experiments (Table 5D.2).

The methine proton at δ 2.29 was characteristic of the junction point of the pyranone ring with that of the side propyl methyl benzoate moiety as established by ^1H - ^1H COSY correlations and detailed HMBC experiments (Table 5D.2). The ^{13}C NMR spectrum of the purified compound in combination with DEPT experiments indicated the occurrence of 22 carbon atoms in the compound. (Table 5D.2). The low field quaternary signal (^{13}C NMR) at C-7 was in agreement with that of a quaternary carbon signal carrying aromatic ring C-1 of the structure (δ 139.77). The point of cyclization of H-11(2.29)/H-15(2.02)/H-14(1.36)/H-13(4.08) forms six member ring support the presence of pyranone ring.

The proton and carbon connectivity deduced from HSQC and HMBC experiments confirmed the pyranone framework attached to the aromatic ring. The relative stereochemistry of the chiral centers particularly that of C-11, 13 and 15 of the pyranone framework was deduced from the NOESY spectrum(FIGURE 5D.4.D) of the compound and the J -values. NOE couplings were observed between $\text{H}\alpha$ -11 (δ 2.29) and $\text{H}\alpha$ -13 (δ 4.08) thus indicating that these groups must be equatorial and on the α -side of the molecule. The methine proton at C-15 group did not exhibit NOE interactions with H-11 and H-13, which is at the α -face of the molecule, thereby indicating that H-15 is at the axial disposition.

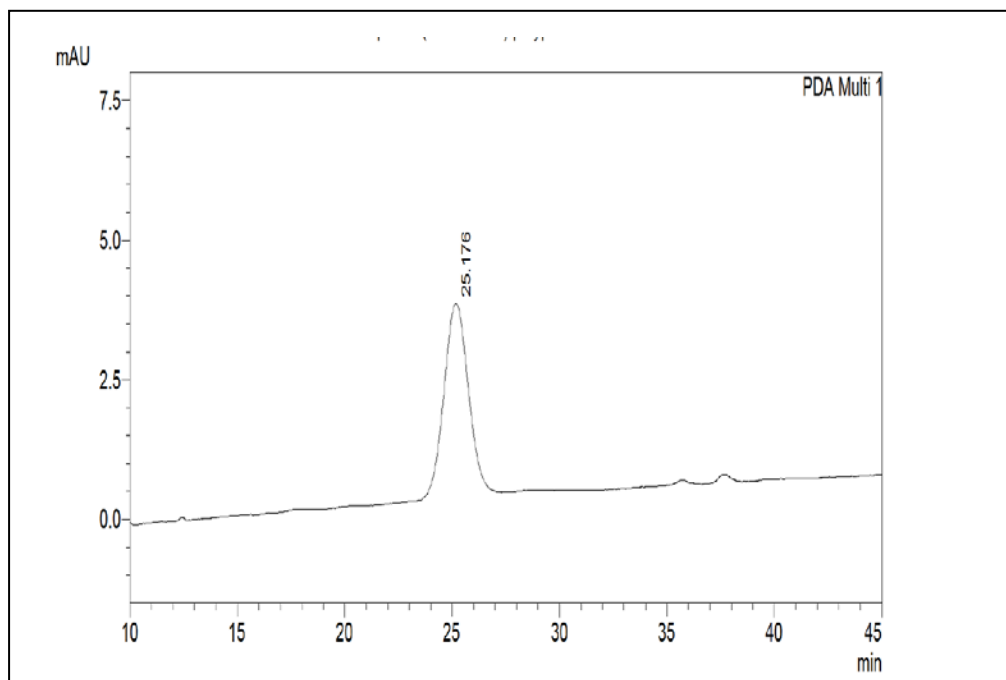


Figure 5D.3
HPLC Chromatogram of compound11

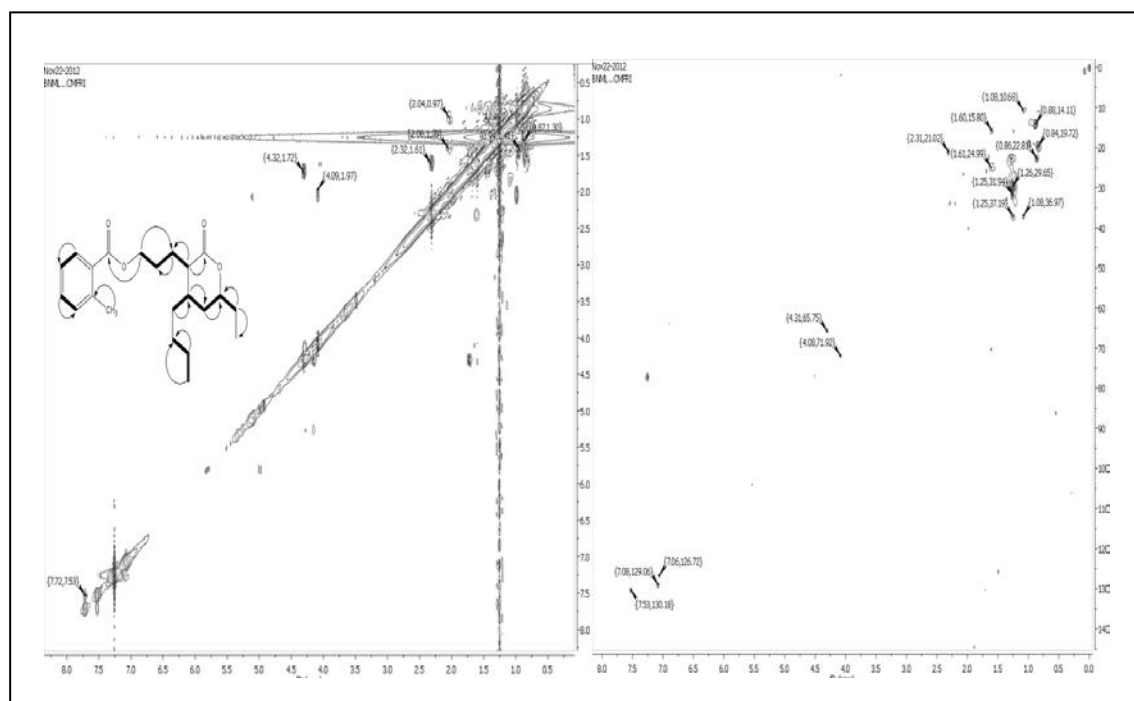


Figure 5D.4
(A) ^1H - ^1H COSY - NMR spectrum of compound11 (B) Prominent HSQC correlation spectrum of compound11

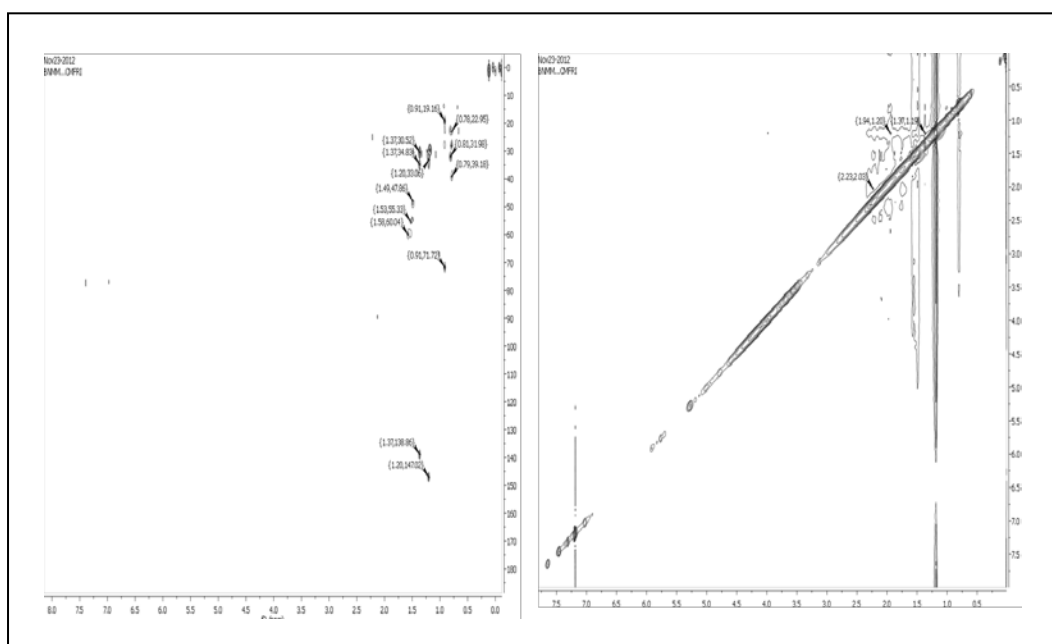


Figure 5D.4

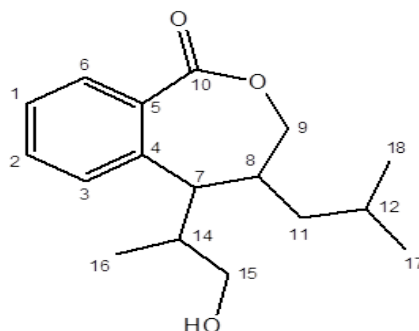
(C) HMBC and (D) NOESY spectra of compound 11

5D.2.4.2 Structural characterization of the compound 12(B7E21)

7,8-Dihydro -7- (15-hydroxypropan-14-yl) -8- isobutylbenzo [c] oxepin-1(9H)-one (12): Brown oily ; UV (MeOH) λ_{\max} (log ϵ): 296 (3.82) nm TLC (Si gel GF₂₅₄ 15 mm; 2% MeOH/CHCl₃, v/v) R_f:0.82; HPLC(Figure 5D.5) R_t:15.951 min.; IR (KBr, cm⁻¹) ν_{\max} 732.25 (C-H ρ), 1372.28 (C-H ρ), 1652 (C=C ν), 1690.21 (C-CO-C ν), 2854.74 (C-H ν); ¹H-NMR (500 MHz, Chloroform-d) δ 7.75(dd,1H), 7.70 (dd, 1H), 7.53 (dd, 1H), 7.50 (dd, 1H), 4.32(dt,2H), 4.09 (d,2H), 2.36(d,1H), 2.09(m,1H), 1.75(m,1H), 1.42(m,1H), 1.28(t,2H), 0.99(dd,3H), 0.96(dd,3H), 0.94(dd,3H). ¹³C-NMR (125 MHz, CDCl₃); ¹H-¹H COSY and HMBC data (details under the Table 5D.3; Figure 5D.6); (HRESIMS m/e 321.1424 [M+Na]⁺; D 0.0 amu, cald for C₁₇H₂₄O₃Na, 321.3362).

Table 5D.3

NMR spectroscopic data of compound 11 in CDCl₃.^a



Carbon no.	¹³ C NMR (DEPT)	H-type	δ ¹ H NMR (int., mult., J in Hz) ^b	¹ H- ¹ H COSY	HMBC (¹ H- ¹³ C)
1	128.83	1-H	7.75(dd,1H)	2-H	
2	128.7	2-H	7.70 (dd, 1H)	3-H	C-3
3	130.72	3-H	7.53 (dd, 1H)		C-2,4
4	132.34				
5	132.53				
6	130.87	6-H	7.50 (dd, 1H)	7-H	
7	38.06	7-H	2.36(d,1H)	6-H	C-13,8
8	30.58	8-H	1.75(m,1H)	9-H	
9	65.55	9-H	4.32(dt,2H)		
10	167.68				
11	22.67	11-H	1.28(t,2H)	12-H	C-12
12	19.18	12-H	1.42(m,1H)		
13	29.69	13-H	2.09(m,1H)	14-H	C-12,11
14	71.77	14-H	4.09 (d,2H)		C-15
15	19.73	15-H	1.09(dd,3H)	13-H	
16	14.08	16-H	0.94(dd,3H)	12-H	C-17
17	13.7	17-H	0.96(dd,3H)		

The ^{13}C NMR spectrum of the purified compound in combination with DEPT experiments indicated the occurrence of 17 carbon atoms in the molecule including three quaternary carbons, eight $-\text{CH}$, three $-\text{CH}_2$, and three $-\text{CH}_3$ carbons. The ^{13}C NMR spectrum of the purified compound displayed one quaternary carbon (δ 167.46) atoms bearing the carbonyl group and 132.53 and 132.34 were two quaternary carbons are located in substituted aromatic ring. The side chain isopropyl is substituted at C-8 (δ 30.60) based on HMBC and COSY relations. The cyclic ring was confirmed by the strong $^1\text{H}-^1\text{H}$ COSY signals of $-\text{CH}_2$ and $-\text{CH}$ protons supported HSQC and HMBC signals as detailed under Table 5D.3. The proton at 7-H (δ 2.36) exhibited strong $^1\text{H}-^1\text{H}$ COSY correlation (Figure 5D.7.A) with the proton at δ 2.09 (assigned to be 13-H), which in turn exhibited $^1\text{H}-^1\text{H}$ COSY correlations between 13-H/14-H and 15-H (Table 5D.3). These correlations assigned the 15-hydroxypropan-14-yl system. In the $^1\text{H}-^1\text{H}$ COSY spectrum, couplings were apparent between H-7/H-8/H-9 which supports the presence of oxepin-1(9H)-one skeleton. The $^1\text{H}-^1\text{H}$ COSY correlations between H-9 (δ 1.73)/H-11(1.28)/H-11(δ 1.42) and H-16(0.96)/H-12(1.42)/H-17(0.94) supports the presence of the 8-isobutyl moiety. The proton and carbon connectivity deduced from HSQC (Figure 5D.7.B) and HMBC experiments (Figure 5D.8.A) confirmed the (15-hydroxypropan-14-yl)-8-isobutylbenzo[c]oxepin-1(9H)-one framework. Placement of the 15-hydroxypropan-14-yl group at C-7 of the benzoxepinone was confirmed by the upfield shift about δ 0.65 of $-\text{CH}$ (δ 2.95) group attached to aromatic ring in the compound. NOE couplings were observed between $\text{H}\alpha$ -13 (δ 2.09)/ $\text{H}\alpha$ -8 (δ 1.75) indicating that these groups must be equatorial and on the α -side of the molecule (Figure 5D.8.B). The methine proton at C-7 group (δ 2.36) did not exhibit NOE interactions with H-13 (δ 2.09), which is at the β -face of the molecule, thereby indicating that H-7 is at the equatorial disposition.

The olefinic ($\text{C}=\text{C}$) groups have been symbolized by the absorption bands at 1652 and 1056 cm^{-1} . The ultraviolet absorbances at λ_{max} ($\log e$) 296 (3.82) nm indicating the presence of more than one conjugated system in the compound. Its

mass spectrum exhibited a molecular ion peak at m/e 276 (HRESIMS m/e 321.1424 $[M+Na]^+$; D 0.0 amu, cald for $C_{17}H_{24}O_3Na$, 321.3362), which in combination with its 1H and ^{13}C NMR data (Table 5D.3) indicated the elemental composition of $C_{17}H_{24}O_3$ as 7,8-dihydro-7-(15-hydroxypropan-14-yl)-8-isobutylbenzo[c]oxepin-1(9H)-one with six degrees of unsaturation. Four degree of unsaturation from aromatic ring and one due to carbonyl group. The additional degree of unsaturation was due to the cyclic ring.

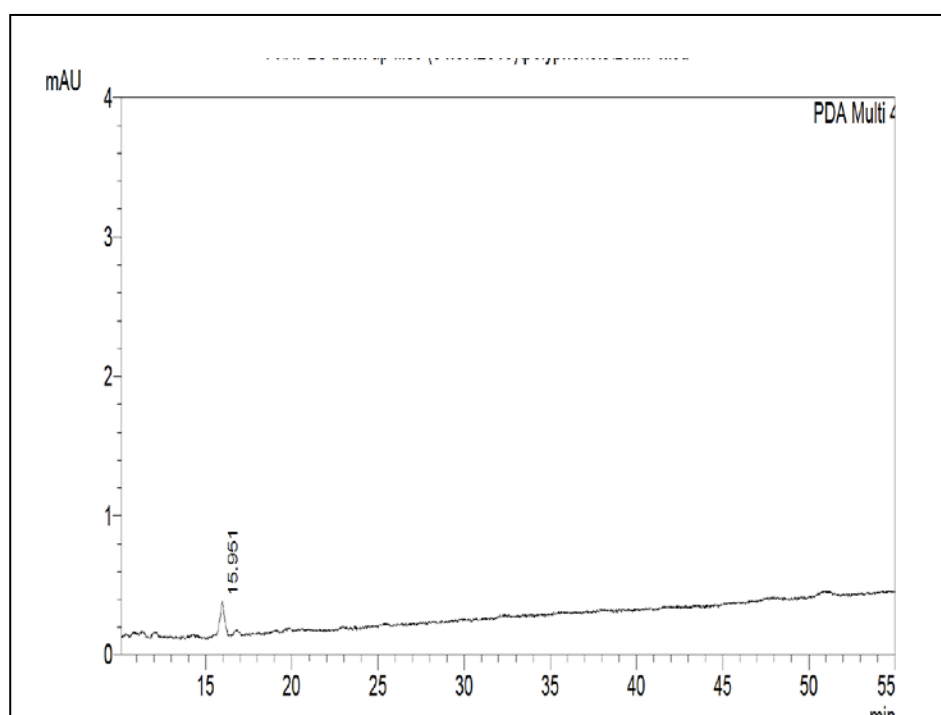


Figure 5D.5
HPLC Chromatogram of compound 12

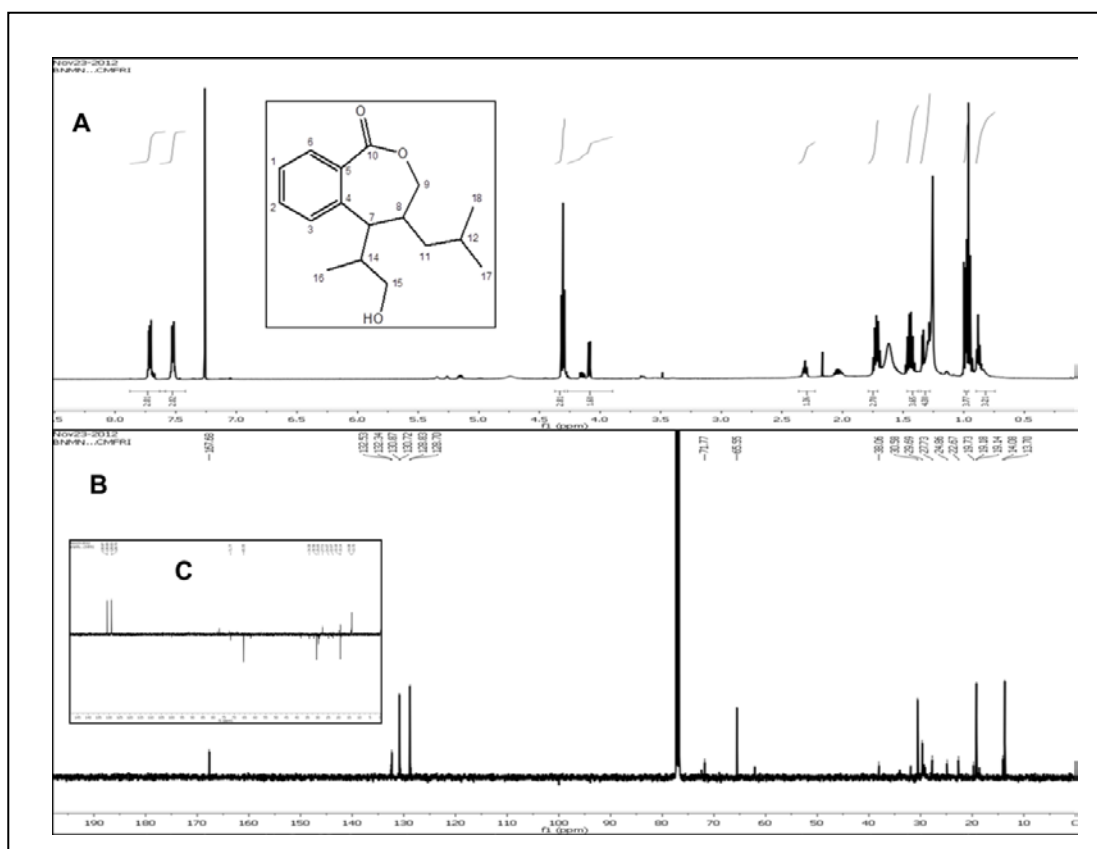


Figure 5D.6
(A) ^1H , (B) ^{13}C NMR spectrum of compound 12

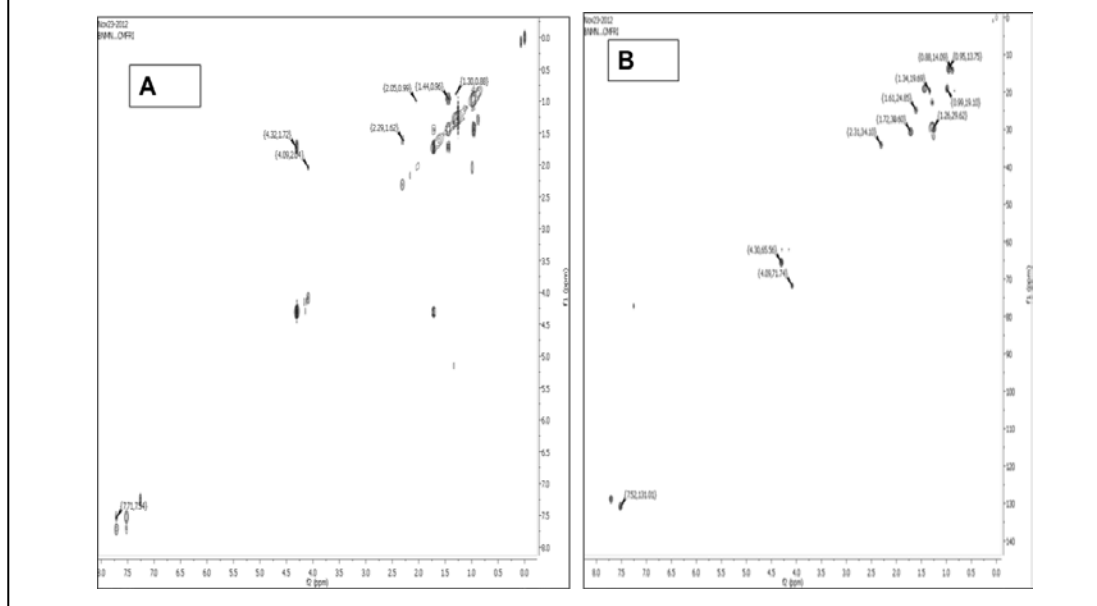


Figure 5D.7
(A) ^1H - ^1H COSY - NMR spectrum of compound 12 (B) Prominent HSQC correlation spectrum of compound 12

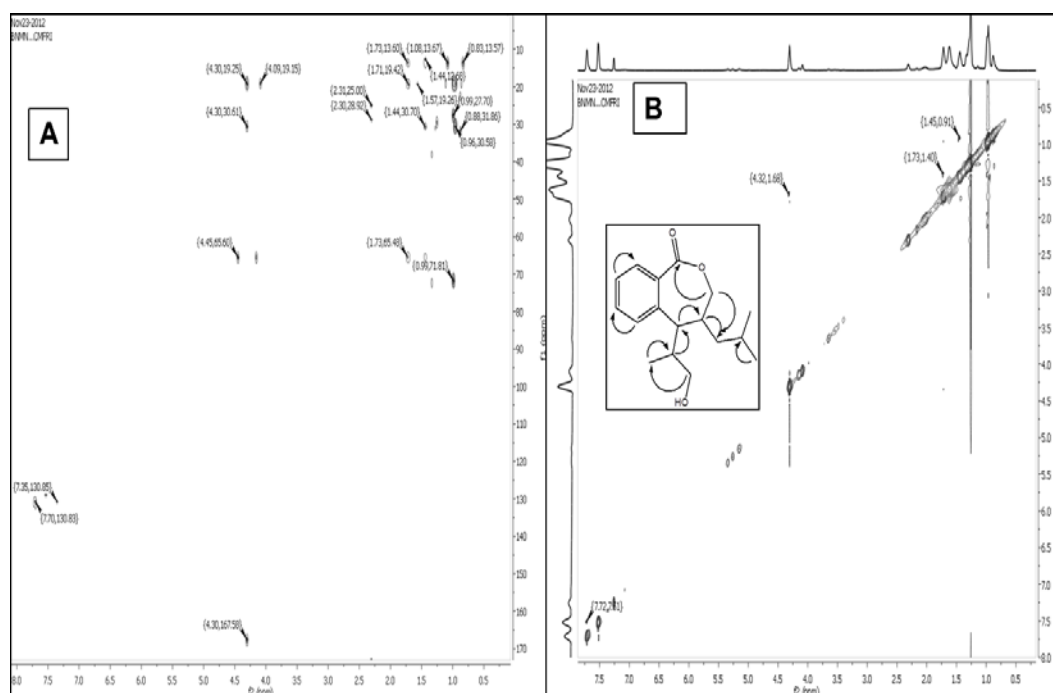


Figure 5D.8

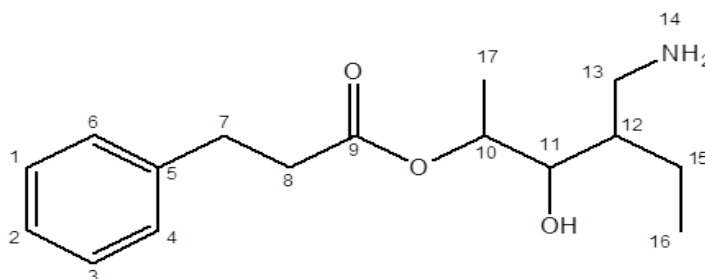
(A) HMBC and (B) NOESY spectra of **compound 12**. The key HMBC couplings have been indicated as double barbed arrow. The NOESY spectrum have been indicated as two sided arrows.

5D.2.4.3 Structural characterization of the compound 13(B7E29)

13-(Amino methyl)-11-hydroxyoctanyl 10-phenylpropanoate (**13**) : yellow oil: UV (MeOH) λ_{\max} (log ϵ): 268 nm (3.15); TLC (Si gel GF₂₅₄ 15 mm; CC 30% EtOAc:n-hexane, v/v); R_t: 37.079 min(Figure 5D.9) ; R_f 0.24; IR (KBr, cm⁻¹) ν_{\max} 718.29 (C-H ρ), 812.47 (aromatic C-H δ), 1372.96 (C-H ρ), 1458.33 (C-H δ), 1467.92 (C-H δ), 1560.32(C=C ν), 1693.18 (C-CO-C ν), 1720.81 (C=O ν), 2946.85 (C-H ν), 3340 (br O-H ν); ¹H-NMR (500 MHz, Chloroform-d) δ 7.34 -7.25(m, 3H), 7.22-7.20(m,2H) , 4.24(m,1H), 3.68(t,1H), 2.96(t,2H), 2.69(t,2H), 2.36(dt,1H), 2.16(s,2H), 1.72(d,3H), 1.62(m,1H), 1.28(m,2H), 0.89(t,3H); ¹³C-NMR, ¹H-¹H-COSY and HMBC data (details under the Table 5D.4); HRMS (ESI) m/e: 279.6824 calcd. for C₁₆H₂₅O₃ 279.2825; found 279.6824 [M⁺].

Table 5D.4

NMR spectroscopic data of compound 13 in CDCl₃.^a



Carbon no.	¹³ C NMR (DEPT)	H-type	δ ¹ H NMR (int., mult., J in Hz) ^b	¹ H- ¹ H COSY	HMBC (¹ H- ¹³ C)
1	128.53	1-H	7.29(m,1H)	2-H	
2	129.35	2-H	7.34 (m, 1H)	3-H	C-3
3	127.28	3-H	7.26 (m, 1H)	4-H	C-4,5
4	126.34	4-H	7.20 (t, 2H)		
5	140.22				
6	128.24	6-H	7.21 (m,1H)	1-H	
7	31.91	7-H	2.96(t,2H)	8-H	C-8
8	37.57	8-H	2.69(t,2H)		
9	176.93				
10	67.29	10-H	4.24(m,1H)	11-H	C-11
11	40.33	11-H	3.68(t,1H)		C-12
12	24.79	12-H	1.62(m,1H)		
13	34.5	13-H	2.36(dt,1H)	12-H	C-12,11
14	N	14-H	2.16 (s,2H)		
15	22.67	15-H	1.28(m,2H)	16-H	C-16
16	14.09	16-H	0.89(t,3H)		
17	29.69	17-H	1.72(d,3H)	10-H	

The phenylpropanoate derivative 13-(amino methyl)-11-hydroxyoctanyl 10-phenylpropanoate (**13**) was isolated as semisolid upon repeated column

chromatography using silica gel as adsorbent. The ^1H , ^{13}C , DEPT, ^1H - ^1H COSY, HSQC and HMBC NMR spectra of 13-(amino methyl)-11-hydroxyoctanyl 10-phenylpropanoate is shown in Figure 5D.10, Figure 5D.11 and Figure 5D.12 respectively. The IR absorption band (in MeOH) exhibited free -OH stretching vibrations near 3340 cm^{-1} . The bending vibration bands near 1720.81 cm^{-1} denotes the ester carbonyl absorption. The IR spectrum revealed broad absorption band at $\nu_{\text{max}} 3400\text{ to }3100\text{ cm}^{-1}$, attributed to hydroxyl functionality. The ultraviolet absorbance at $\lambda_{\text{max}} (\log e) 268\text{ nm} (3.15)$; was assigned to a chromophore with extended conjugation. Its mass spectrum exhibited a molecular ion peak at $m/e 279$ (HRESIMS $m/e 279.6824 [M]^+$; D 0.0 amu), which in combination with its ^1H and ^{13}C NMR data (Table 5D.4) indicated the elemental composition of $\text{C}_{16}\text{H}_{25}\text{O}_3$ as 13-(amino methyl)-11-hydroxyoctanyl 10-phenylpropanoate with five degrees of unsaturation.

The ^1H NMR in conjugation with ^{13}C -NMR (Figure 5D.10 A-B) recorded the presence of methane signals at $\delta 0.89$ and 1.72 and the ^1H - ^1H COSY couplings (Figure 5D.11.A) were apparent between these protons assigned to be at H-16 and H-17 which support the presence of two methyl groups. The relatively downfield shift of the methylene proton at $\delta 2.96$ at H-7 and the $\delta 2.69$ at H-8 indicates the methylene protons were attached to aromatic ring. The aromatic protons were assigned to be present at $\delta 7.19\text{-}7.24$, $\delta 7.27\text{-}7.34$ and the proton integral of the protons revealed the presence of five aromatic protons. The broad IR absorption band (in MeOH) at $3100\text{-}3350\text{ cm}^{-1}$ was due to the -OH groups in the skeleton exhibit free -OH stretching vibrations, which has been supported by the ^1H -NMR signals at about $\delta 6.50$. The exchangeable hydroxyl protons at $\delta 6.50$ (1H, bs in CDCl_3) disappeared upon addition of D_2O . The methine group protons at $\delta 4.24$ (H-10) and $\delta 3.68$ (H-11) are assigned to be at C-10 and 11 positions, respectively, and the downfield shift (about $\delta 1.25$) is apparently due to the presence of the carbonyl groups. A strong HMBC correlation was found between H-10 ($\delta 4.22$)/ C-9 ($\delta 174$) (Table 5D.4), which apparently indicated the presence of the carbonyl carbon near the methine group. The presence of two quaternary carbons at $\delta 140.22$ and $\delta 174$ are due to the presence of substituted benzyl moiety. The ^1H - ^1H COSY correlations between H-7 ($\delta 2.96$) and H-8 ($\delta 1.2.69$) along with

the proton and carbon connectivities deduced from HSQC (Figure 5D.11.B) and HMBC(Figure 5D.12.A) experiments (Table 5D.4) confirmed the phenyl propanoate framework. The –CH proton at δ 1.62(assigned to be at C-12) exhibited strong ^1H – ^1H COSY correlations with the methylene protons at δ 1.28(H-15)/0.89(H-16)/2 and 2.36(H-8) which established the presence of 13-(amino methyl)-11-hydroxyoctanyl chain of the compound. The methylene group at the C-7 position of the structure resulted in strong deshielding of the aromatic quaternary –C- at δ 140.22 and therefore, has been assigned to be present at the junction point attached with aromatic ring. The methine proton at δ 4.22 is characteristic of the junction point of the phenylpropanoate ring with that of the side chain amino methyl-11-hydroxyoctanyl moiety was established by ^1H – ^1H COSY correlations and detailed HMBC experiments (Table 5D.4). The ^{13}C NMR spectrum in combination with DEPT experiments indicated the occurrence of 16 carbon atoms in the molecule including one ester carbonyl carbon at δ 174 (Table 5D.4). The proton and carbon connectivity deduced from HSQC and HMBC experiments confirmed the 13-(amino methyl)-11-hydroxyoctanyl framework attached at C-10 position.

The –CH protons at C-11 (δ 3.68) appeared to demonstrate the presence of hydroxyl group. Long range HMBC correlation δ 2.96(H-7) and δ 2.69(H-8) with aromatic carbon at δ 140(C-5) and 128.15(C-6) indicates these methylene groups attached to aromatic ring. This along with extensive 2D NMR analyses assigned the presence of phenyl propanoate, amino methyl and one hydroxyl moieties. The relative stereochemistry of the chiral centres particularly that of C-10, 11 and 12 of the compound was deduced from the NOESY spectrum (Figure 5D.12.B) of the compound and the J-values. The methine proton at C-11 group did not exhibit NOE interactions with H-10 and H-12, which is at the α -face of the molecule, thereby indicating that H-11 is at the axial disposition.

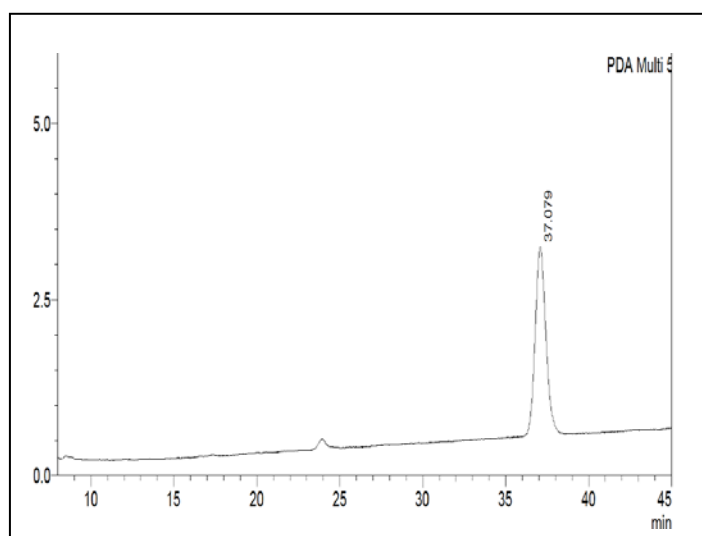


Figure 5D.9

HPLC Chromatogram of compound 13

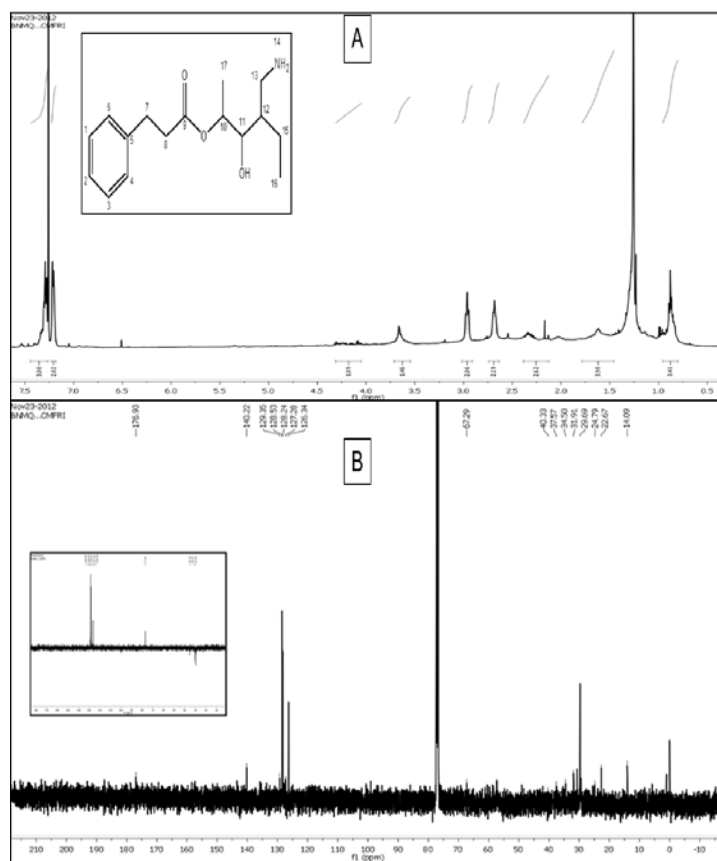


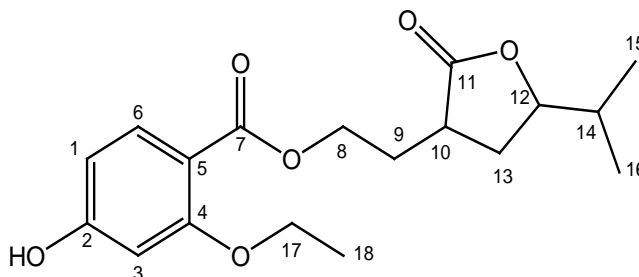
Figure 5D.10

(A) ¹H, (B) ¹³C NMR (Inset DEPT)spectrum of compound13

5D.2.4.4 Structural characterization of the compound 14(B7E29)

9-(tetrahydro-12-isopropyl-11-oxofuran-10-yl) ethyl 4-ethoxy-2-hydroxybenzoate (14): Yellowish oil UV (MeOH) λ_{\max} (log ϵ): 253 nm (2.63); TLC (Si gel GF₂₅₄ 15 mm; EtOAc/*n*-hexane (3:17, v/v) R_f: 0.98; R_t: 32.175 min.(Figure 5D.13); IR (KBr, cm⁻¹) ν_{\max} 814.02 (aromatic C-H δ), 1310.16 (C-O ν), 1377.22 (C-H ρ), 1614.92 (C=C ν), 1691.24 (C-C-O ν), 1736.92 (C=O ν), 2924.21 (alkane C-H ν), 3010.11 (aromatic C-H ν); ¹H NMR (500 MHz, Chloroform-d) δ 7.65(dd, 1H), 7.45 (dd,1H), 6.51 (s, 1H), 4.22(dt,2H), 4.02 (dt,2H), 3.56 (dd,2H), 2.29(m,1H), 1.98(m,1H), 1.65(m,2H), 1.59(m,2H), 0.93(dd,3H), 0.81(dd,3H), 1.08(t,3H) ¹³C NMR (125 MHz, CDCl₃ δ in ppm), ¹H-¹H-COSY, and HMBC data, see Table 5D.5; HRMS (ESI) *m/e*: 336.1573(M)⁺ calcd. for C₁₈H₂₄O₆ 336.4008; found 336.4008 [M]⁺.

Table 5D.5
NMR spectroscopic data of compound 14 in CDCl₃.^a



Carbon no.	¹³ C NMR (DEPT)	H-type	$\delta^1\text{H}$ NMR (int., mult., J in Hz) ^b	¹ H- ¹ H COSY	HMBC (¹ H- ¹³ C)
1	131.14	1-H	7.45 (dd,1H)	6-H	C-2
2	157.62				
3	101.6	3-H	6.51 (s, 1H)		
4	158.02				

5	148.45				
6	128.79	6-H	7.65 (dd, 1H)	7-H	C-5,1
7	173.42				
8	66.33	8-H	4.22(dt,2H)	9-H	C-7,9
9	30.24	9-H	1.65(m,2H)	10-H	C-8,10
10	33.51	10-H	2.29(m,1H)	13-H	C-11
11	177.26				
12	71.76	12-H	4.02 (dt,2H)	14-H	
13	24.81	13-H	1.59(m,2H)		C-12,11
14	29.5	14-H	1.98(m,1H)	12-H	C-15
15	19.16	15-H	0.93(dd,3H)	13-H	
16	14.11	16-H	0.81(dd,3H)	12-H	C-17
17	72.25	17-H	3.56 (dd,2H)	18-H	
18	22.6	18-H	1.08(t,3H)		

The IR bending vibration bands near of compound **14** at 1736.92 cm^{-1} attributed to the ester carbonyl absorption. The IR spectrum revealed broad absorption band at $\nu_{\text{max}} 1614.92\text{ cm}^{-1}$, symbolized the olefinic system. The bending vibration bands near 814.02 cm^{-1} and stretching vibration at 3010.11 cm^{-1} denoted the aromatic C-H vibrations. The ultraviolet absorbance at $\lambda_{\text{max}} (\log \epsilon) 253\text{ nm}$ (2.63) was assigned to a chromophore. Its mass spectrum exhibited a molecular ion peak at m/e 336, which in combination with its ^1H and ^{13}C NMR data (Table 5D.5) indicated the elemental composition of $\text{C}_{18}\text{H}_{24}\text{O}_6$. The ^1H NMR in conjugation with ^{13}C -NMR and DEPT spectra recorded the presence of four methylene, six methine, three methyl, and five quaternary carbon atoms. Its mass spectrum exhibited a molecular ion peak at m/z 336 (HRESIMS m/e 336.1573 $[\text{M}]^+$; D 0.0 amu), which in combination with its ^1H and ^{13}C NMR data (Table 5D.5) indicated the elemental composition of $\text{C}_{18}\text{H}_{24}\text{O}_6$ as compound 14 with

seven degrees of unsaturation (Figure 5D.14). Three degree of unstruration from double bonds, two degrees of unstruration from the aryl and furan ring systems, two from the carbonyl moieties. Couplings were apparent between the protons at δ 4.22 (H-8)/ δ 1.65 (H-9)/ δ 2.30 (H-10)/ δ 1.59 (H-13) and 4.02(H-12) in the ^1H - ^1H COSY spectrum (Figure 5D.15.A), which supported the presence of 10-ethyl furan moiety.

The methine signal H-12 at δ 4.02 appeared downfield due to the presence of electronegative systems at close proximity. One methylene groups have been assigned to occupy at the C-17 position, shifted downfield due to the presence of oxygen moiety. The HSQC (Figure 5D.15.B) and HMBC experiments (Figure 5D.16.A) revealed that the ester group linked to the isopropyl at δ 4.02. The aromatic protons showed their characteristic signals at δ 7.65 -7.45and 6.51. Extensive HMBC and HSQC experiments revealed the presence of substituted furan moiety in the compound. ^1H - ^1H COSY experiments(Figure 5D.15.A) revealed that the protons at δ 2.29(m) correlate with the methylene protons at δ 1.65 (assigned to be as H-9) and, the later is assigned to be attached to a carbonyl electronegative group.

The $-\text{CH}_2-$ proton appeared downfield at δ 4.22 apparently due to the presence of the electronegative oxygen group and was assigned to be present at the C-8 position of the above stated compound. The carboxyl group at the C-11 position of the compound resulted in strong deshielding of the $-\text{CH}-$ proton at δ 2.29, and therefore, has been assigned to be present at the C-10 position of the structure. The chemical shift of the protons at δ 1.98, 0.89 and 0.84 along with detailed 2D NMR experiments established the presence of *O*-heterocyclic furan ring system. The $-\text{CH}-$ proton at δ 4.02 is characteristic of the junction point of the cyclic system with carboxylic side chain. The ^{13}C NMR spectrum of the purified compound in combination with DEPT experiments indicated the occurrence of 18 carbon atoms in the molecule including furan carbons at δ 158-101. (Table 5D.5). The low field quaternary signals (^{13}C NMR) were in agreement with that to a quaternary carbon signal carrying the furan ring. The H-H and C-H connectivities apparent in the ^1H - ^1H COSY and HMBC spectra respectively indicate that one of

the seven unsaturations was due to the two ring and five double bonds. The relative stereochemistry of the chiral centre particularly that of C-12 cyclic framework was deduced from the NOESY experiment (Figure 5D.15.B) and the *J*-values. NOE couplings were observed between H α -10/H α -14 thus indicating that these groups must be equatorial and on the α -side of the molecule. Therefore, the C-12 proton is axial and β -oriented.

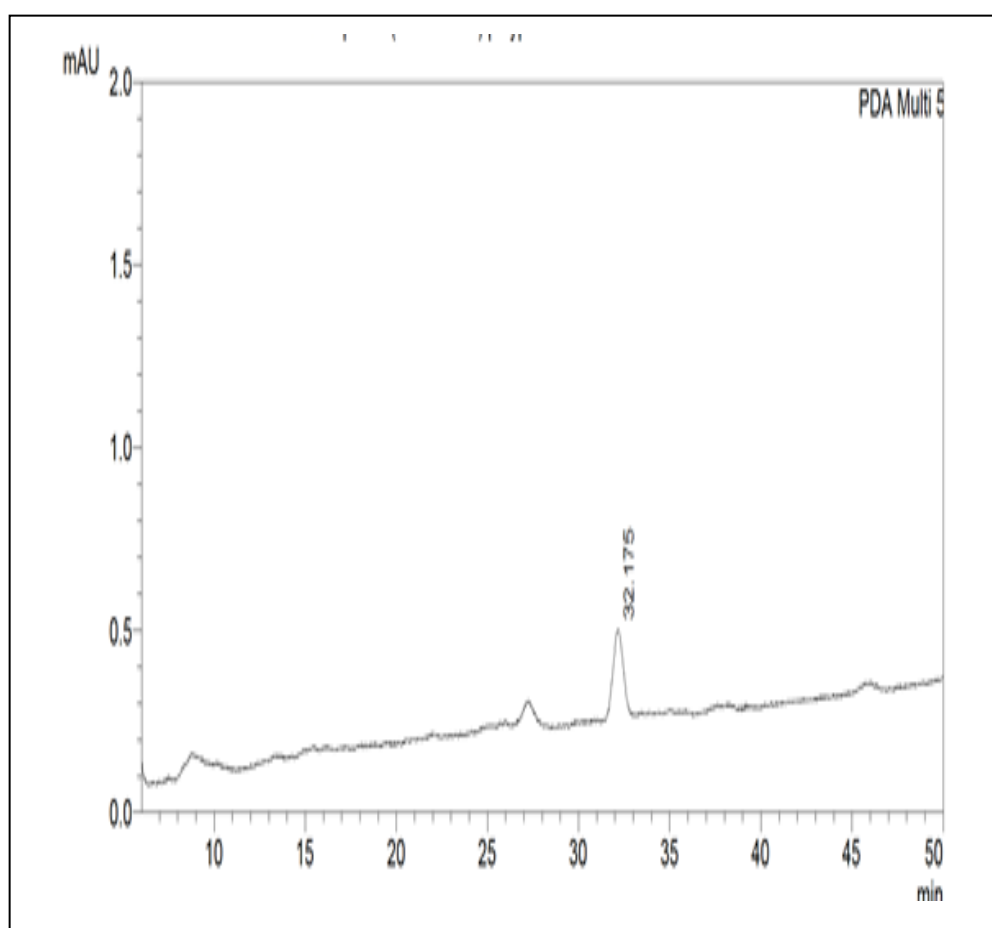


Figure 5D.13
HPLC Chromatogram of compound 14

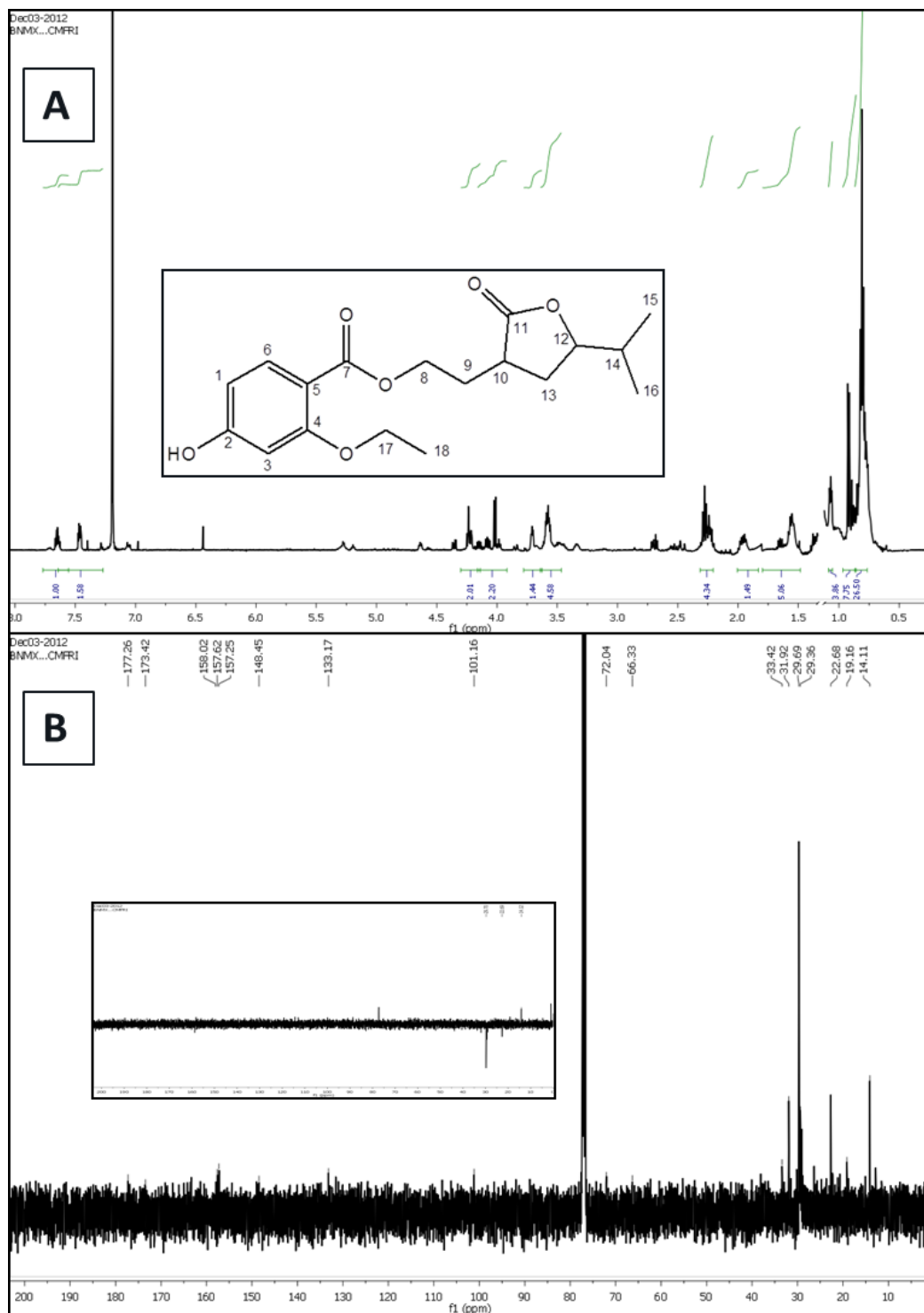


Figure 5D.14

(A) ^1H , (B) ^{13}C NMR (Inset DEPT) spectrum of compound 14

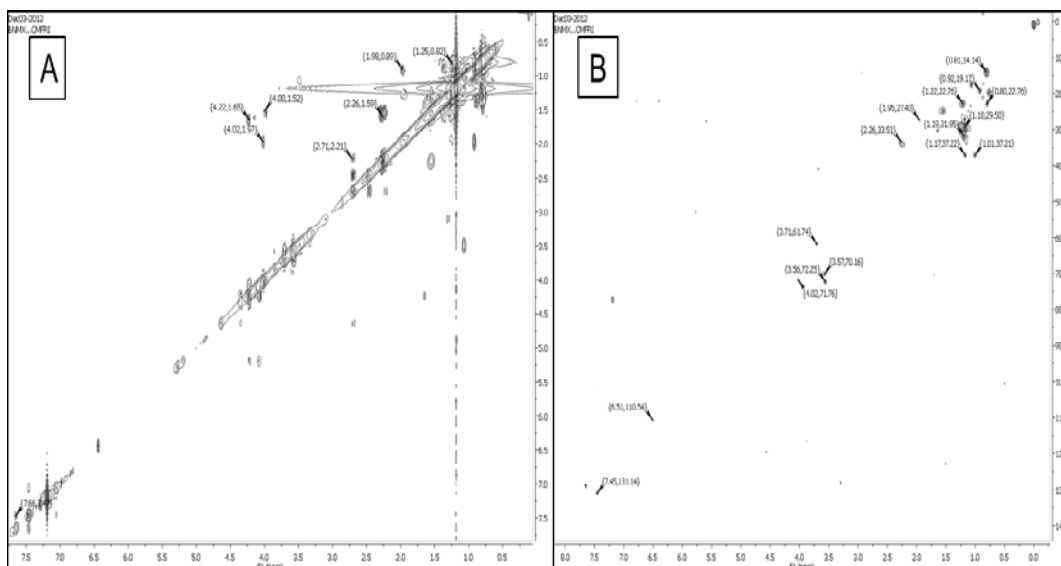


Figure 5D.15
A) ¹H-¹H COSY - NMR spectrum of compound14 (B) Prominent HSQC correlation spectrum of compound14

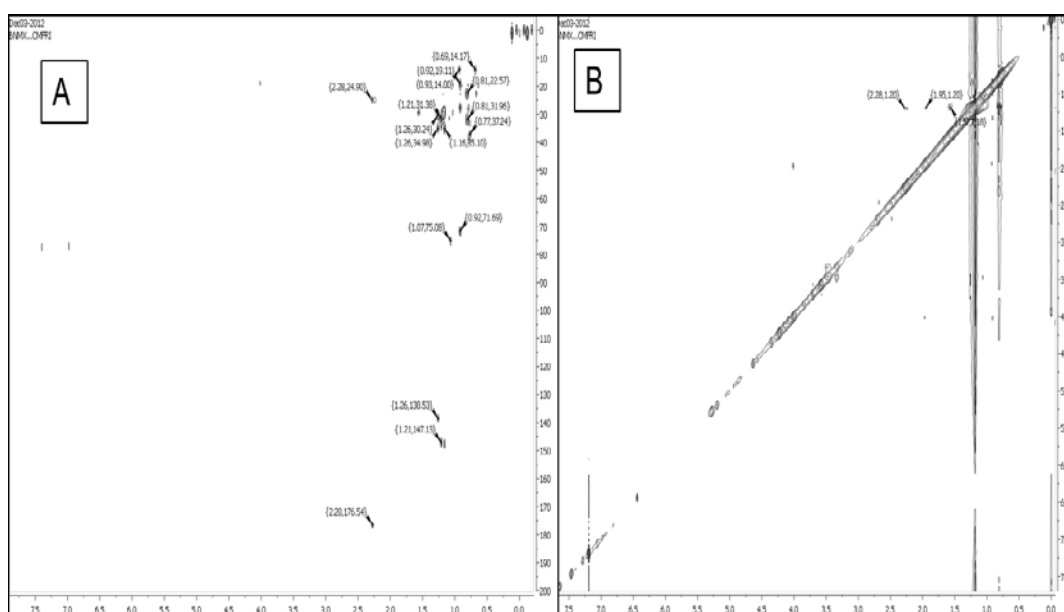


Figure 5D.16
A) HMBC and (B) NOESY spectra of compound14. The key HMBC couplings have been indicated as double barbed arrow. The NOESY spectrum have been indicated as two sided arrows.

5D.3 Conclusion

Bioprospecting of antibacterial metabolites in antagonistic bacteria *B. amyloliquefacens* associated with seaweed *padina gymnospora* (SWI7) revealed a multi component mode of antagonism. The crude ethyl acetate extract of the bacterial metabolites yielded four antibacterial compounds **11** through **14**. The compounds were 10-(15-butyl-13-ethyl-2-oxotetrahydro-2H-pyranyl)propyl-2-methylbenzoate (**11**), 7,8-dihydro-7-(15-hydroxypropan-14-yl)-8-isobutylbenzo [c] oxepin-1 (9H)-one (**12**), 13-(amino methyl)-11-hydroxyoctanyl 10-phenylpropanoate (**13**) and 9-(tetrahydro-12-isopropyl-11-oxofuran-10-yl) ethyl 4-ethoxy-2-hydroxybenzoate(**14**).

CHAPTER 6

Secondary metabolites and seaweed-bacterial interactions

6.1 Background of the study

Seaweeds are highly productive components of the coastal ecosystem releasing dissolved organic carbon into surrounding waters, thus harboring suitable living substrata for microbial colonization (Ali et al. 2012). It has been shown that these chemically mediated interactions between the seaweeds and their associated bacteria are based on the exchange of nutrients, minerals, and secondary metabolites. However, the interactions of seaweeds with their associated microbes have not been thoroughly investigated (Hollants et al. 2012). Emergence of antibiotic resistant bacteria and the need for novel, antimicrobial compounds lead to the exploration of new habitats to screen the production of bioactive substances. These seaweed species was reported to suffer remarkably low levels of microbial infection, despite lacking cell-based immune systems (Kubanek et al. 2003). In recent years, it has been suggested that certain seaweed species may utilize surface associated bacteria that produce inhibitory compounds to prevent surface fouling (Kumar et al. 2011).

Although the ecological relevance of most bacterial associates on or within seaweeds remains unclear, nutrient-rich seaweed surfaces attract many opportunistic micro and macroorganisms, thereby creating a greatly competitive environment in which the production of defensive compounds can serve as powerful tools for bacteria to out compete other surface colonizers. Seaweed–bacterial associations are appealing from evolutionary, ecological, and applied

perspectives, and there is a strong need to integrate the aspects of different biological disciplines such as microbiology, phycology, ecology, and chemistry in seaweed–bacterial interactions (Hollants et al. 2012).

Keeping these reports in background in the current chapter we are making an attempt to illustrate the ecological interaction between seaweed host and its associated active bacterial flora. Seaweed–bacterial interactions were studied by comparing the antibacterial metabolites of colonizing bacteria with its host derived seaweed secondary metabolites in Chapter 6A. We have extended the analysis to understand the effect of seaweed extract and the metabolic precursors of the seaweed extract on the growth and fatty acid profile of the bacterial species to understand the interactions between the host seaweed and their associated bacterial flora in chapter 6B.

Chapter 6A

ANTIBACTERIAL SECONDARY METABOLITES AND SEAWEED BACTERIAL INTERACTIONS

6A.1 Background of the study

Seaweeds along with their associated bacterial communities are potential sources of biotechnological interest due to the production of a great diversity of compounds exhibiting broad spectrum biological activities. Marine microbial symbionts are possibly the true producers or take part in the biosynthesis of some bioactive marine natural products isolated from the eukaryotic hosts as reported in similar studies (Kubaneck et al. 2003; Zhao et al. 2011). Pluralities of culture dependent and independent studies on sponges and their associated microbiota validated this hypothesis (Zhang et al. 2009; Li 2009). Investigations of seaweed–bacterial associations lag behind those of other marine eukaryotes (Hollants et al 2012; Goecke et al. 2010). Although examples are rare (Kubaneck et al. 2003), it is believed that marine eukaryotes may use their surface-associated bacteria as a source of antimicrobial chemical defenses in competition and in the protection of the host (Penesyanyan et al. 2010). Similarly, studies in sponges have shown co-detection of the chemical fingerprints of the bacterial metabolites in the host extracts and some bacterial compounds, which were shown to have a role as chemical mediators of interactions within the sponge-associated bacterial compartment (Quevrain et al. 2014).

In this study, we have adopted a culture dependent method to isolate heterotrophic *B. subtilis* MTCC 10407 (chapter 3 section 3.2.2) associated with brown seaweed *Sargassum myriocystum* at the Gulf of Mannar in the southeast coast of India to explore them as a source to isolate *O*-heterocycle pyran

derivatives of presumed polyketide origin, with activity against human opportunistic food pathogenic bacteria. The potential of the seaweed-associated *B. subtilis* MTCC 10407 to produce antimicrobial secondary metabolites was analyzed by polymerase chain reaction employing amplifying genes encoding for polyketide synthetase (*pks*). Seaweed–bacterial interactions were studied by comparing the antibacterial metabolites of colonizing bacteria with its host derived seaweed secondary metabolites. The PKS-assisted biosynthetic pathway of the *O*-heterocycle pyrans was proposed and the ecological interactions of seaweed and its associated bacterial metabolites have been demonstrated based on co-detection of the chemical fingerprint of the bacterial metabolites in the host extracts.

6A.2 Materials and methods

6A.2.1 General

Reagents and analysis as explained in chapter 5 (5.2.4 and 5.2.7). Bacterial pathogens as in chapter 3 (3.2.4)

6A.2.2 Seaweed samples and associated antibacterial isolates

The brown seaweed *Sargassum myriocystum* was collected by scuba diving from the intertidal zone of the Gulf of Mannar region in South-East coast of India situated at 9° 17' 0" North, 79° 7' 0" East. The seaweed samples were processed and the associated bacterial strains were isolated as described earlier (chapter 3.2.2). The isolated strains were assayed for antagonistic activity against test pathogens (chapter 3.2.4). The inhibitory activity was assayed by a spot over lawn assay as described earlier (chapter 3.2.5). Bacteria with antagonistic properties were identified using classical biochemical methods followed by 16S rRNA gene sequencing using the primers AGAGTTTGATCCTGGCTCAG (forward) and ACGGCTACCTTGTTACGACTT (reverse) (Weisburg et al. 1991) as described in chapter 3 (3.2.7.2). The isolate under the present study was *B. subtilis* MTCC 10407 isolated from *Sargassum myriocystum* (chapter 3 section 3.2.2). The candidate strain was subjected to metabolite gene (*pks*) screening using the primer RTRGAYCCNCAGCAICG (forward) and VGTNCCNGTGCCRTG (reverse) as reported earlier (chapter 4 section 4.2.5).

6A.2.3 Bioassay guided purification of antibacterial compound from *B. subtilis* MTCC 10407 associated with seaweed *Sargassum myriocystum*

B. subtilis MTCC 10407 was cultured over solid nutrient agar plates. The preparation and recovery of secondary metabolites from antibiotic-producing bacterium *B. subtilis* MTCC 10407 was carried out as described in chapter 5C(section 5C.1.4) and structural characterization as explained in Chapter 5C(section 5C.2.6). Purified bacterial secondary metabolites compound 9 and compound 10 are used for present study.

6A.2.4 Bioassay guided chromatographic purification of the ethyl acetate extract of *Sargassum myriocystum*

The ground shade-dried seaweed samples (400 g) were extracted with MeOH (2000 ml x 3) at an elevated temperature (40-45°C) for 3 h. The samples were filtered through filter paper (Whatman No. 1) and the pooled filtrate was concentrated (50 °C) *in vacuo* to one-third volume, before being partitioned with *n*-hexane (150 ml x3), CH₂Cl₂ (150 ml x3) and EtOAc (150 ml x3) in succession. Evaporation of the solvents from these fractions under reduced pressure furnished *n*-hexane (3.6g), CH₂Cl₂ (4.24g), and EtOAc (7.5g) fractions. The aliquot of the EtOAc extract (7.5 g) of *S. myriocystum* was slurried in silica gel (3 g, 60–120 mesh), and loaded into a glass column (90 cm X 4 cm) packed with silica gel (60–120 mesh, 50 g) as adsorbent before being subjected to vacuum liquid chromatography. The column was initially eluted with *n*-hexane, to remove the waxy material. The eluent polarity was gradually increased by addition of EtOAc (*n*-hexane: EtOAc 199:1 to 1:19, v/v) to furnish twenty-five fractions of 30 ml each, which were reduced to 9 groups (SM₁₋₉) after TLC analysis (*n*-hexane: EtOAc, 9:1, v/v). The fraction 4 (SM₄) obtained by eluting with *n*-hexane: EtOAc (5:1, v/v) was found to be a mixture, which was flash chromatographed (Biotage AB SP1-B1A, 230–400 mesh, 12 g; Biotage AB, Uppsala, Sweden) on a silica gel column (Biotage, 230–400 mesh, 12 g; Sweden, Biotage No. 25+M 0489-1) at a collection UV wavelength at 242 nm using a step gradient of ethyl acetate/*n*-

hexane (0-20% EtOAc) to afford 95 fractions (9 ml each). The fractions with similar patterns were pooled together to afford four pooled fractions (SM₄₋₁ - SM₄₋₄). The sub-fraction SM₄₋₃ as eluted with EtOAc/*n*-hexane (3:17, v/v) was further separated by chromatography on silica gel GF₂₅₄ (particle size 15 µm) coated on a preparatory thin layer plate using a stepwise gradient system from 0.5% MeOH/CH₂Cl₂ yielded compound **15**, *i.e.*, 2-(8-butyl-3-ethyl-3,4,4a,5,6,8a-hexahydro-2H-chromen-6-yl)ethyl benzoate (6.2 mg). The fractions SM₇ and SM₈ as eluted with *n*-hexane: EtOAc (3:7 and 1:4 v/v, respectively) were pooled together before being chromatographed on a silica gel column (180-230 mesh, 3.5x15cm) using a step gradient of CHCl₃: MeOH (100:0 to 9:1, v/v) to afford fifty-three fractions (10 ml each). Based on analytical TLC (*n*-hexane: EtOAc, 9:1, v/v), the fractions with similar patterns were pooled together to afford five pooled fractions (SM₇₋₁ through SM₇₋₅). The sub fraction SM₇₋₄ eluted with CHCl₃: MeOH (23:2, v/v) was fractionated over preparatory TLC on silica gel GF₂₅₄ using a stepwise gradient system from 3% CH₂Cl₂: MeOH to obtain four sub-fractions (SM₇₋₄₋₁ - SM₇₋₄₋₄). Repeated chromatographic separation of PG₇₋₄₋₄ on silica gel GF₂₅₄ using CH₂Cl₂: MeOH (97:3, v/v) afforded 3-(methoxycarbonyl)-4-(5-(2-ethylbutyl)-5, 6-dihydro-3-methyl-2H-pyran-2-yl) butyl benzoate (**16**, 6.15 mg) as major component. Evaporation of solvents from **16** followed by TLC over silica gel GF₂₅₄ (particle size 15 mm) using CHCl₃: MeOH (99:1, v/v) supported the purity.

6A.2.5 Antimicrobial assay

Antibacterial activities of the compounds were analyzed using a disc diffusion method with compound impregnated discs as explained in chapter 5(5.2.6).

6A.3 Results

6A.3.1 Isolation and antibacterial activities of *Bacillus subtilis* MTCC 10407 associated with intertidal seaweed *Sargassum myriocystum*

The bacterial isolate with antibacterial activity was identified as a *Bacillus subtilis* strain and has been submitted at Microbial Type Culture Collection and

Gene Bank (MTCC) of Institute of Microbial Technology (Chandigarh, India). The strain under the present study has been designated as MTCC10407 (Figure 6A.1). It was identified through biochemical, fatty acid methyl ester analysis and 16S rRNA gene sequencing, and the sequence was deposited under the accession number JF834077 (Chapter 3 section 3.2.7). The strain was found to be positive for the polyketide synthase gene (*pks*), and the KS domain sequences obtained during the study have been deposited under the accession number KC607823 (Chapter 4 section 4.2.5). Although it is difficult to predict the products of *pks* based upon the derived sequences due to the presence of smaller gene fragments, an attempt was made to correlate the structural properties of produced secondary metabolites with the presence of *pks* gene. The strain possessed a broad spectrum antibacterial activity against human opportunistic food pathogenic bacteria *V. parahaemolyticus* ATCC®17802™ (15 mm), *V. parahemolyticus* MTCC 451 (17 mm), *V. vulnificus* MTCC 1145 (22 mm), *A. hydrophilla* (12 mm), *V. harveyi* (15 mm), *V. anguillarum* (11.3 mm), and *V. alginolyticus* (15 mm).

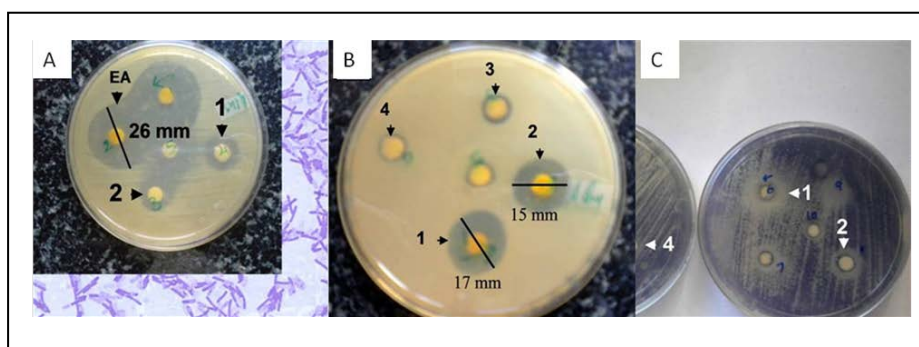


Figure 6A.1

(A) The Gram stained *B. subtilis* MTCC 10407. The antibacterial activities of ethyl acetate extract of *B. subtilis* MTCC 10407 and the compounds purified (compound 9(1) compound 10(2) against *Aeromonas hydrophilla* on Mueller Hinton agar plates were shown as inset. 'EA' designates the ethyl acetate extract of *B. subtilis* MTCC 10407. The bactericidal inhibition zones are visualized as clearance around the disc impregnated with the test materials. (B) Antibacterial activities of the purified compounds (1-4) against *Aeromonas hydrophilla* on Mueller Hinton agar plates. (C) Inhibitory activities of the purified compounds (1-4) against *Vibrio alginolyticus* MTCC 4439 as visualized on MTT sprayed Mueller Hinton agar plates. The live cells were changed to blue color. The bactericidal zones of the active compounds were visualized as yellow color. [#compound 15(3) and compound 16(4)]

6A.3.2 Antibacterial activities of chromatographic fractions of *Sargassum myriocystum* and its associated *B. subtilis* MTCC 10407 by agar diffusion method

The ethyl acetate extract (10mcg on disk) of *B. subtilis* MTCC 10407 exhibited an inhibitory zone diameter of greater than 20 mm against the experimental pathogens (Figure 6A.1.B, Table 6A.1). The compound 9(1) and 10(2) isolated from *B. subtilis* MTCC 10407 demonstrated significant antibacterial activity (inhibitory zone diameter of greater than 15 mm against *A. hydrophilla*, 10 mcg on disk) against these pathogenic bacteria (Figure 6A.1.B, Table 6A.1). The seaweed derived compounds (3 and 4) showed a negligible inhibition zone (<10mm) (Figure 6A.1.B, Table 6A.1). These results were further validated by spraying the plates with 3-(4, 5-dimethylthiazol-2-yl)-2, 5-diphenyltetrazolium bromide (MTT) sprayed on the Mueller Hinton agar plates (Figure 6A.1.C).

Table 6A.1
Antibacterial activity of the crude ethyl acetate extract and the *O*-heterocyclic pyrans (1, 2) from *B. subtilis* MTCC 10407 and the homologous compounds (3, 4) from the brown seaweed *Sargassum myriocystum*

		<i>Antimicrobial activity (mm) against test pathogens</i>			
	Crude extract [#]	1 ^a (9)	2 ^a (10)	3 ^b (15)	4 ^b (16)
<i>V. parahemolyticus</i> *	24.33±0.577	11.0±1.00	11.0±1.00	7.00±1.0	3.33±0.58
<i>Vibrio vulnificus</i>	22.66±0.577	12.66±0.577	14.0±1.00	7.33±0.58	4.60±0.58
<i>Aeromonas hydrophilla</i>	26.0±1.00	17.66±0.577	15.0±1.00	8.33±0.58	7.00 ±1.00

[#] Ethyl acetate extract of *B. subtilis* MTCC 10407 associated with brown seaweed *Sargassum myriocystum*

^a Compounds from *B. subtilis* MTCC 10407(9 and 10)

^b Compounds from *Sargassum myriocystum*(15 and 16)

* *V. parahemolyticus* ATCC® 17802™

6A.3.3 Structural characterization of antibacterial O-heterocycle pyrans from *B. subtilis* MTCC 10407

Two novel O-heterocycle pyrans, **9** and **10** (as stated in the materials section) were isolated upon repeated chromatography over silica columns (as explained earlier chapter 5C section 5C.2.7).

6A.3.4 Structural characterization of secondary metabolites from *Sargassum myriocystum*

Two compounds **15** and **16** (as stated in the materials section 6A.2.4) were isolated upon repeated chromatography over silica columns. The structural details of the compounds were as follows.

6A.3.4.1 Structural characterization of compound **15**

2-(8-Butyl-3-ethyl-3, 4, 4a, 5, 6, 8a-hexahydro-2H-chromen-6-yl) ethyl benzoate (**15**). White semisolid; UV (MeOH) λ_{\max} (log ϵ): 235 nm (3.84); TLC (Si gel GF₂₅₄ 15 mm; CHCl₃/MeOH 99:1, v/v) R_f: 0.45; GC R_t: 8.6 min; IR (KBr, cm⁻¹) ν_{\max} 729.29 (C-H_p), 1376.26 (C-H_p), 1454.38 (C-H_δ), 1466.91 (C-H_δ), 1506 (aromatic C-H_v), 1642 (C=C_v), 1736.96 (C=O_v), 2854.7 (C-H_v); ¹H NMR (500 MHz, CDCl₃ δ in ppm), ¹³C NMR (126 MHz, CDCl₃ δ in ppm), ¹H-¹H-COSY, and HMBC data, see Table 6A.2; HRMS (ESI) *m/e*: 416.5668 calcd. for C₂₅H₃₇O₅ 416.4814; found 416.5668 [M+H]⁺.

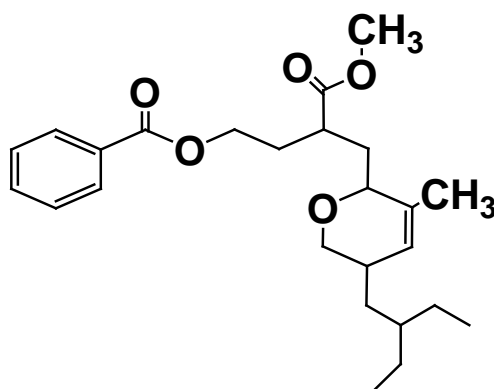
The IR bending vibration bands of compound **9** at 1736.96 cm⁻¹ attributed to the ester carbonyl absorption. Its mass spectrum exhibited a molecular ion peak at *m/e* 416, which in combination with its ¹H (Figure 6A.2.A) and ¹³C NMR data (Table 6A.2) indicated the elemental composition of C₂₅H₃₆O₅ with eight degrees of unsaturation. The ¹³C NMR spectrum in combination with DEPT experiments (Figure 6A.2.B) indicated the occurrence of 25 carbon atoms, including two carbonyl carbons at δ 173.30 and δ 167.70 and olefinic carbons at δ 132.46 and 114.05 (Figure 6A.3.B). The -CH₂- protons appeared at δ 4.11 was due to the presence of the dihydropyran ring system and has been assigned to be present at the C-18 position of the ring structure. ¹H-¹H COSY experiments revealed that the protons at δ 4.33 (d) correlated with the methylene protons at δ 1.72 (assigned to

Bioprospecting of antibacterial metabolites in seaweed associated bacterial flora along the southeast coast of India

be as H-9) and the –CH proton at δ 2.34, the latter was assigned to be attached to a strongly electronegative group (Figure 6A.4.A). A typical signal characteristic of –OCH₃ group was apparent at δ 3.69, which enabled to deduce the presence of methyl 4-methoxybutanoate moiety in the compound. The methine proton (*t*) at δ 4.24 is characteristic of the junction point of the 3, 6-dihydro-2H-pyran moiety with that of the side chain. The proton and carbon connectivity deduced from ¹H–¹H COSY, HSQC(Figure 6A.4.B) and HMBC experiments(Figure 6A.5.A) confirmed the C4 framework attached to the dihydro-2H-pyran moiety at the C-17 position of the ring structure . Strong ¹H–¹H COSY correlations were apparent between the protons at δ 2.02 (-CH, assigned to be as C-17)/ δ 1.52 (-CH₂, C-19)/ δ 1.44 (-CH₂, C-20)/ δ 1.02 (-CH₂, C-21)/ δ 0.88 (-CH₃, C-22), which along with the results detailed above support the presence of 3-butyl-3,6-dihydro-5-methyl-2H-pyran moiety. The detailed spectral analyses demonstrating the presence of the relative stereochemistry of the chiral centers, particularly that of C-10 (with the proton chemical shift at δ 2.34 as deduced from HSQC experiments) carrying the –COOMe group of the framework, and that of C-14 (bearing the –CH group proton at δ 4.24) and C-17 (bearing the –CH group proton at δ 2.02), was deduced from the NOESY spectrum (Figure 6A.5.B) and the *J*-values. NOE couplings were observed between H α -10 (δ 2.34)/ H α -17 (δ 2.02) thus indicating that these groups must be equatorial and on the α -side of the molecule (Fig. 6A.5.B).

Table 6A.2

NMR spectroscopic data of 15 in CDCl₃^a



C. No.	$\delta^{13}\text{C}$ NMR	H	$\delta^1\text{H}$ NMR (int., mult., J in Hz) ^b	^1H - ^1H COSY	HMBC (^1H - ^{13}C)
1	132.45				
2	130.87	2-H	7.77 – 7.69 (m, 1H)	3-H	C-1
3	129.95	3-H	7.55 (dq, J = 6.8Hz, 1H)	4-H	
4	128.80	4-H	7.55 (dq, J = 6.8Hz, 1H)		
5	128.84	5-H	7.55 (dq, J = 6.8Hz, 1H)	6-H	
6	130.90	6-H	7.77 – 7.69 (m, 1H)		C-5,7
7	167.70				
8	65.57	8-H	4.33 (t, J = 6.7 Hz, 2H)	9-H	C-7,9
9	30.37	9-H	1.72(m,2H)	10-H	
10	34.13	10-H	2.34(m,1H)	13-H	C-8,11
11	173.30				
12	51.43	12-H	3.69(s,3H)		C-11
13	29.70	13-H	1.61(m,2H)	14-H	C-14
14	68.16	14-H	4.24 (t, J = 5.9 Hz, 1H)		
15	114.05				
16	129.93	16-H	5.38 (d, J = 9.3Hz, 2H)	17-H	
17	38.74	17-H	2.02(m,1H)	18-H,19-H	C-18,20
18	71.79	18-H	4.11 (d, J = 6.7 Hz, 1H)		C-16
19	22.69	19-H	1.52(m,2H)		
20	22.63	20-H	1.44(m,2H)	21-H	C-25
21	19.05	21-H	1.03(m,2H)	22-H	C-22
22	14.96	22-H	0.88(m,2H)		
23	24.89	23-H	2.16(s,3H)		
24	22.99	24-H	1.26(m,2H)		
25	13.96	25-H	0.92(m,3H)		

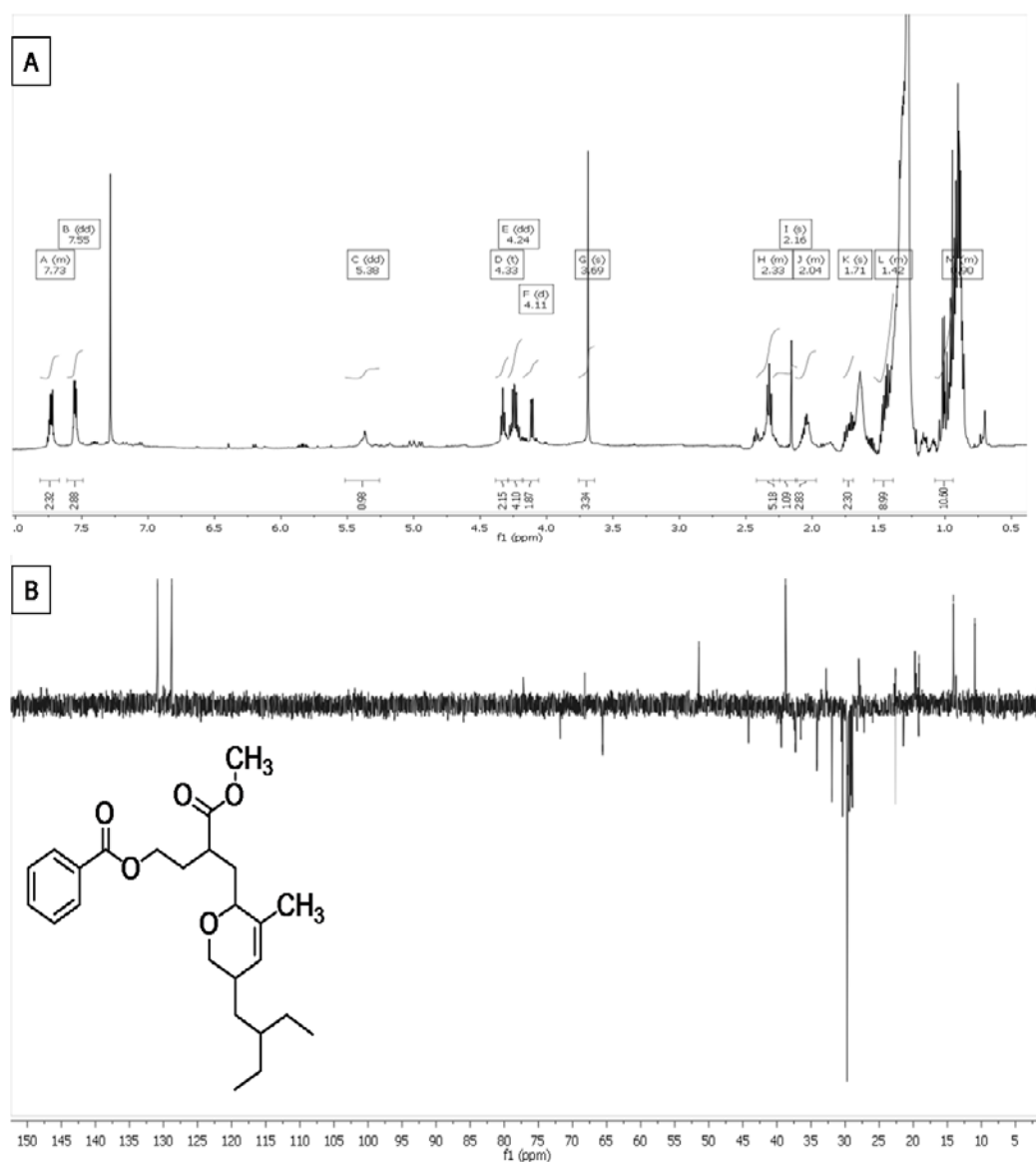


Figure 6A.2
(A) ^1H and (B) DEPT₁₃₅ - NMR spectrum of 15

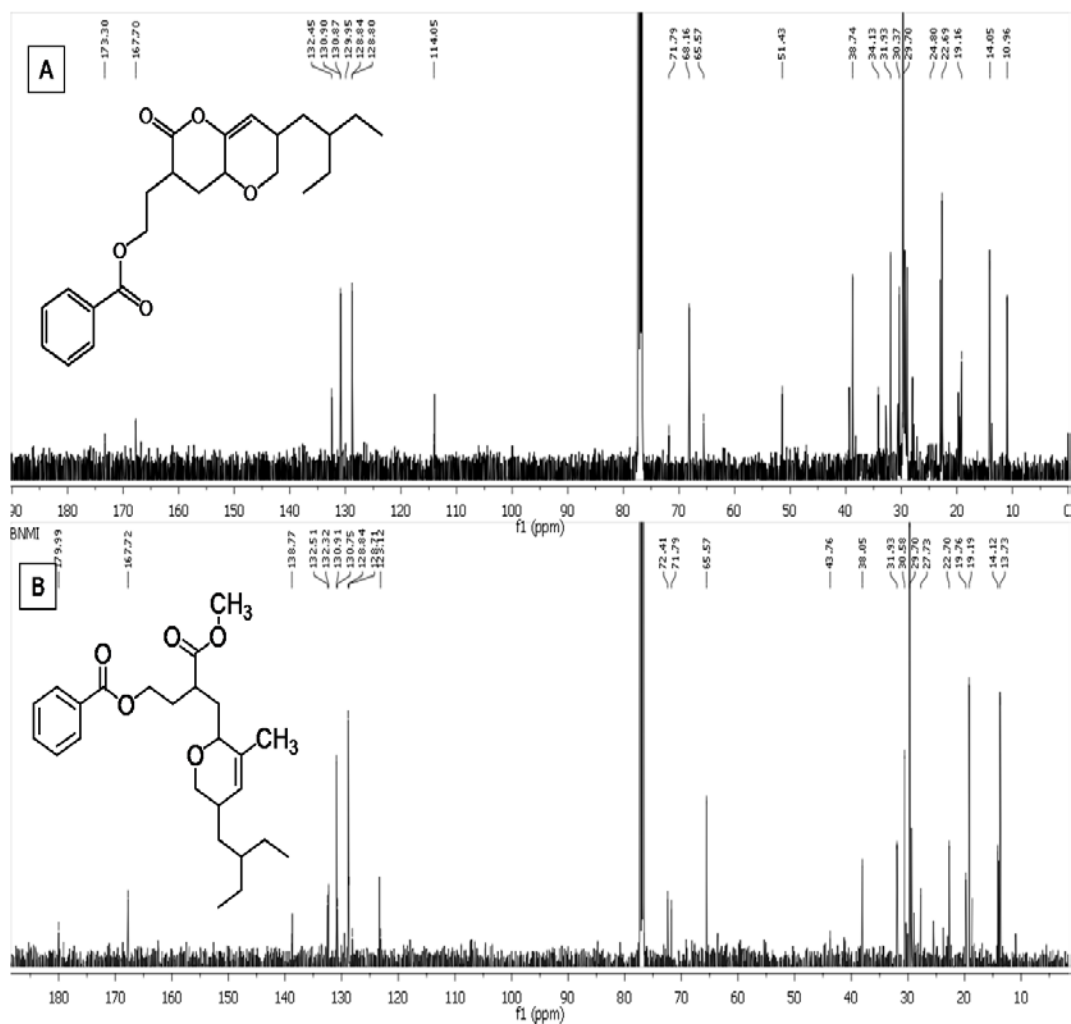


Figure 6A.3

Comparison of ^{13}C -NMR between the compounds (A) 9 isolated from *B. subtilis* MTCC 10407 and (B) 15 from seaweed *Sargassum myriocystum*

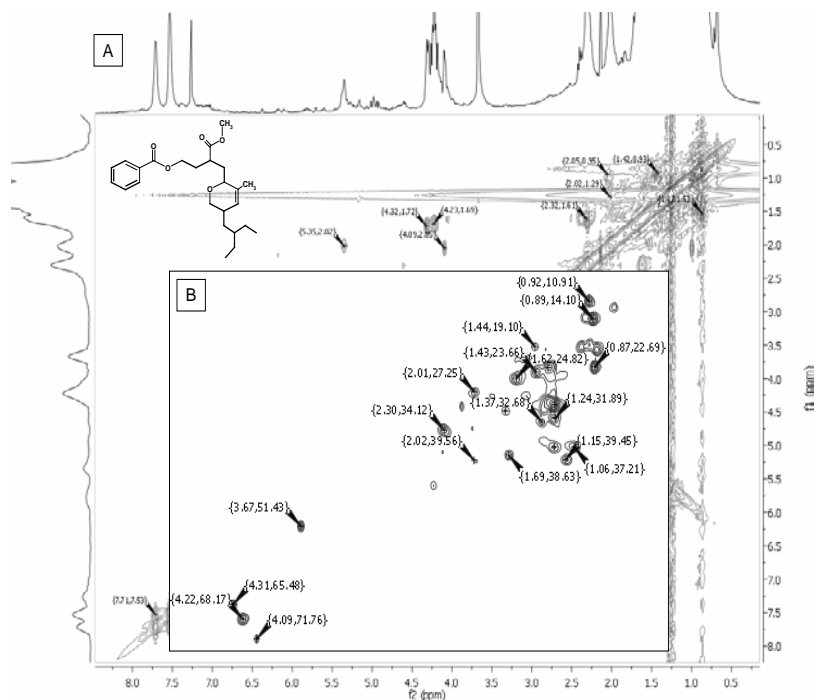


Figure 6A.4
(A) ^1H - ^1H COSY and (B) prominent HSQC correlation spectra of 15. The key ^1H - ^1H COSY couplings have been represented by the bold face bonds.

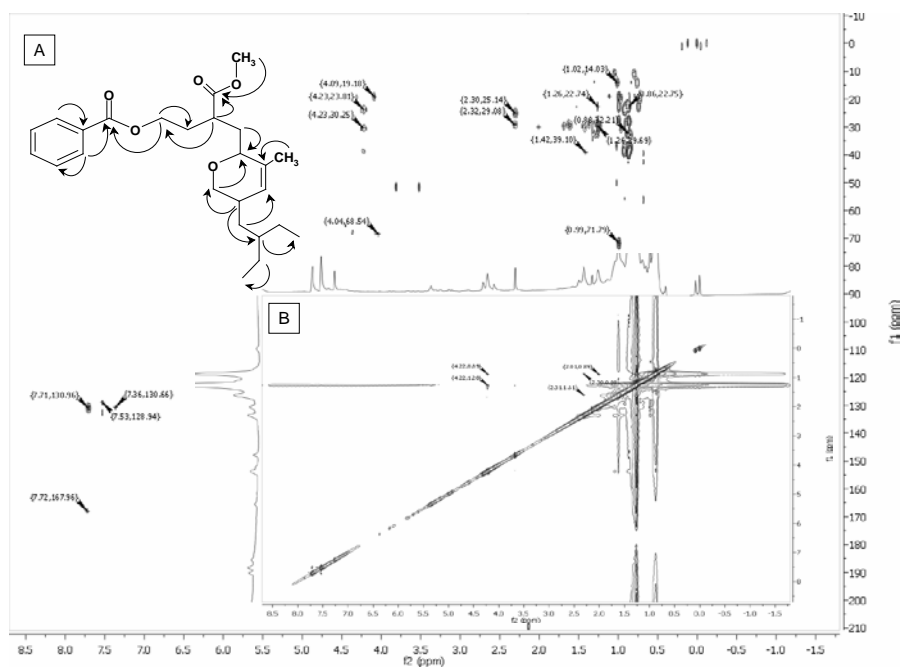


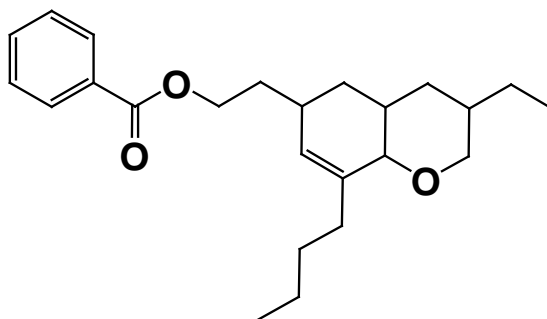
Figure 6A.5
(A) HMBC and (B) NOESY spectra of 15. The key HMBC couplings are indicated as double barbed arrow.

6A.3.4.2 Structural characterization of compound 16

3 - (Methoxycarbonyl) -4- (5-(2-ethylbutyl) - 5, 6-dihydro - 3 - methyl - 2H - pyran-2-yl) butyl benzoate (**16**). Pale yellow powder; UV (MeOH) λ_{\max} (log ϵ): 229 nm (3.40); TLC (Si gel GF₂₅₄ 15 mm; CHCl₃: MeOH 99:1, v/v) R_f: 0.86; GC R_t:17.22 min; IR (KBr, cm⁻¹) ν_{\max} 731.29 (C-H_p), 812.06 (aromatic C-H₆), 1376.26 (C-H_p), 1466.91 (C-H₆), 1650.12 (C=C_v) 1690.21 (C-CO-C_v), 1742.02 (C=O_v), 2856.74 (C-H_v), 2921.22 (C-H_v), 3010.12 (aromatic C-H_v); ¹H NMR (500 MHz, CDCl₃ δ in ppm), ¹³C NMR (126 MHz, CDCl₃ δ in ppm), ¹H-¹H-COSY, and HMBC data, see Table 6A.3; HRMS (ESI) *m/e*: calcd. for C₂₄H₃₅O₃ 371.2462; found 371.7478 [M+H]⁺.

Table 6A.3

NMR spectroscopic data of 16 in CDCl₃^a



C. No.	δ ¹³ CNMR	H	δ ¹ H NMR (int., mult., J in Hz) ^b	¹ H- ¹ H COSY	HMBC (¹ H- ¹³ C)
1	132.50				
2	130.91	2-H	7.55 (dq, J = 6.8Hz, 1H)	3-H	C-7,3,4
3	128.86	3-H	7.77 – 7.69 (m, 1H)		C-4,6
4	128.71	4-H			
5	128.84	5-H	7.55 (dq, J = 6.8Hz, 1H)	6-H	
6	132.31	6-H	7.77 – 7.69 (m, 1H)		
7	167.72				
8	65.58	8-H	4.22 (t, J = 6.8Hz, 2H)	9-H,21-H	C-7,9,10
9	38.05	9-H	1.72(m,2H)	10-H	C-10
10	30.57	10-H	1.36(m,1H)	11-H	C-11,9
11	126	11-H	5.15(m,1H)		
12	130.76				
13	72.41	13-H	3.78(m,1H)	14-H	C-14,9
14	40.97	14-H	2.30(m,1H)	15-H	C-13,18,17
15	37.88	15-H	1.63(m,2H)		
16	45.02	16-H	2.18(m,2H)	14-H	

17	34.62	17-H	2.02(m,1H)	18-H	C-16
18	71.79	18-H	4.08(d,2H)		C-20,14
19	19.76	19-H	0.98(m,2H)	17-H	C-18,17
20	13.74	20-H	0.81(t,3H)	19-H	C-19
21	29.9	21-H	1.44(t,2H)	9-H	C-9
22	18.65	22-H	1.26(m,2H)	21-H	C-21
23	27.73	23-H	0.91(t,3H)		
24	--		--		
25	--		--		

The IR bending vibration bands of compound **16** at 1742 cm^{-1} attributed to the ester carbonyl absorption. Its mass spectrum exhibited a molecular ion peak at m/e 370 [HRESIMS m/e 371.7478 ($M+H$)⁺] (Figure 6A.6), which in combination with its ^1H and ^{13}C NMR data (Table 6A.3) indicated the elemental composition of $\text{C}_{24}\text{H}_{34}\text{O}_3$ with eight degrees of unsaturation. Two methylene groups have been assigned to occupy at the C8-9 positions, and the one with δ 4.22 shifted downfield due to the presence of an extended conjugation probably linked to an aromatic moiety (Fig. 6A.8.A). The ^{13}C NMR spectrum in combination with DEPT experiments (Figure 6A.8.B-C) indicated the occurrence of 24 carbon atoms in **16** including one carbonyl carbon at δ 167.70 and olefinic carbons at δ 130 and 125.98 (Table 6A.3). The HMBC correlation of the proton at δ 4.22 with the carbon atom at δ 167.72 apparently indicated the presence of $-\text{C}=\text{O}(\text{O})$ moiety. $^1\text{H}-^1\text{H}$ COSY experiments revealed that the protons at δ 4.22(*t*) correlate with the methylene protons at δ 1.72 (assigned to be as H-9) and HMBC correlations were apparent between H-9 (δ 1.72) with that of a carboxyl carbon at δ 167.72, which apparently indicated the presence of ethyl benzoate moiety. The C-18 position of the compound resulted in strong deshielding of the $-\text{CH}_2-$ proton at δ 4.08 ppm probably linked to oxygen. The chemical shift of the protons at δ 4.08, 2.02, 1.57, 2.18 and 3.78 ppm along with detailed 2D NMR experiments established the presence of pyranose moiety. The proton and carbon connectivity deduced from $^1\text{H}-^1\text{H}$ COSY (Figure 6A.8.A), HSQC (Figure 6A.8.B) and HMBC experiments (Figure 6A.9.A) confirmed the C4 framework attached to the C-10 position of the hexahydro-2H-chromene framework. The H-H and C-H connectivities apparent in the $^1\text{H}-^1\text{H}$ COSY and HMBC spectra respectively indicate that bicyclic framework. The relative stereochemistry of the chiral centers,

Bioprospecting of antibacterial metabolites in seaweed associated bacterial flora along the southeast coast of India

particularly that of C-10 (with the proton chemical shift at δ 1.36 as deduced from HSQC experiments) carrying the $-C=C-$ group and that of C-7 (bearing the $-CH_2$ group proton at δ 4.29) and C-18 (bearing the $-CH_2$ group proton at δ 4.08), was deduced from the NOESY spectrum (Figure 6A.9.B) of the compound and the J -values. NOE couplings were observed between H_{α} -10 (δ 1.36)/ H_{α} -18 (δ 4.08) thus indicating that these groups must be equatorial and on the α -side of the molecule. NOESY correlation between 10-H (δ 1.36) and 11-H (δ 5.17) indicated that they were on the same side of **16**.

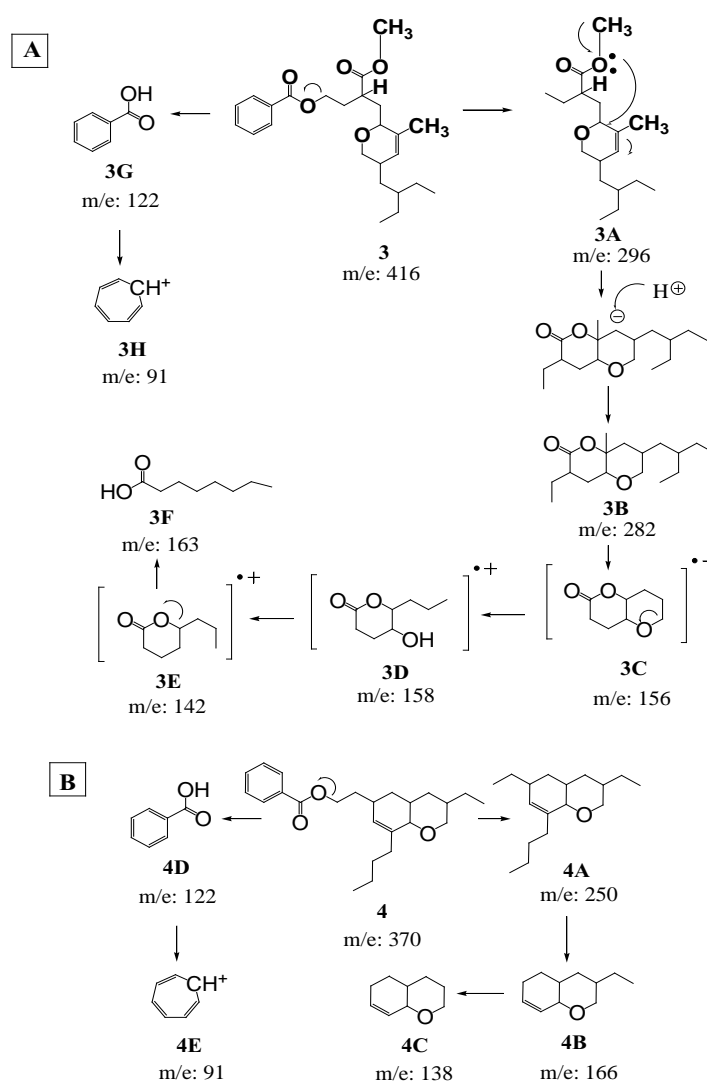


Figure 6A.6

(A) Mass fragmentation pattern of **15** from seaweed *Sargassum myriocystum*; The compound **15** undergoes mass fragmentation to yield (**3A**) methyl 2-((5-(2-ethylbutyl)-5,6-dihydro-3-methyl-2H-pyran-2-yl)methyl)butanoate, (**3B**) 3-ethyl-7-(2-ethylbutyl)-hexahydro-8a-

methylpyrano[3,2-b]pyran-2(3H)-one, (3C) hexahydropyrano[3,2-b]pyran-2(3H)-one, (3D) tetrahydro-5-hydroxy-6-propylpyran-2-one, (3E) tetrahydro-6-propylpyran-2-one, (3F) octanoic acid, (3G) benzoic acid, and (3H) tropylium ion as major peaks. The molecular ion peak at m/e 416 appeared to undergo elimination of benzoic acid (m/e 122) to yield methyl 2-((5-(2-ethylbutyl)-5,6-dihydro-3-methyl-2H-pyran-2-yl)methyl)butanoate at m/e 296, which underwent intramolecular rearrangement to afford a fragment with m/e 282 (3-ethyl-7-(2-ethylbutyl)-hexahydro-8a-methylpyrano[3,2-b]pyran-2(3H)-one). The appearance of the fragment at m/e 156 indicated the presence of hexahydropyrano[3,2-b]pyran-2(3H)-one, (3D) tetrahydro-5-hydroxy-6-propylpyran-2-one moiety, resulted from the side chain elimination of 3-ethylpentane (Figure 2B). Intramolecular rearrangement of tetrahydro-propylpyranone resulted in the formation of octanoic acid (m/e 163). The presence of tropylium ion (m/e 91) supports the presence of aryl ring system in 1. (B) Mass fragmentation pattern of 16 from seaweed *Sargassum myriocystum* (A) The compound 16 undergoes mass fragmentation to yield (4A) 8-butyl-3,6-diethyl-3,4,4a,5,6,8a-hexahydro-2H-chromene, (4B) 3-ethyl-7-(2-ethylbutyl)-hexahydro-8a-methylpyrano[3,2-b]pyran-2(3H)-one from the 1-butyl-3-ethylcyclohex-1-ene moiety upon the elimination of alkyl side chains from the C-1 and C-3 positions, (4C) 3,4,4a,5,6,8a-hexahydro-2H-chromene derived from the elimination of ethyl side chain from the C-3 carbon atom of the 3-ethyl-tetrahydro-2H-pyran moiety, (4D) benzoic acid, and (4E) tropylium ion as major peaks. The molecular ion peak at m/e 370 appeared to undergo elimination of benzoic acid (m/e 122) to yield 8-butyl-3,6-diethyl-3,4,4a,5,6,8a-hexahydro-2H-chromene at m/e 250, which underwent elimination of alkyl side chains from the C-1 and C-3 positions from the 1-butyl-3-ethylcyclohex-1-ene moiety to afford a fragment with m/e 166 (3-ethyl-7-(2-ethylbutyl)-hexahydro-8a-methylpyrano[3,2-b]pyran-2(3H)-one). The latter underwent elimination of ethyl side chain from the C-3 carbon atom of the 3-ethyl-tetrahydro-2H-pyran moiety to afford 3, 4, 4a, 5, 6, 8a-hexahydro-2H-chromene at m/e 138.

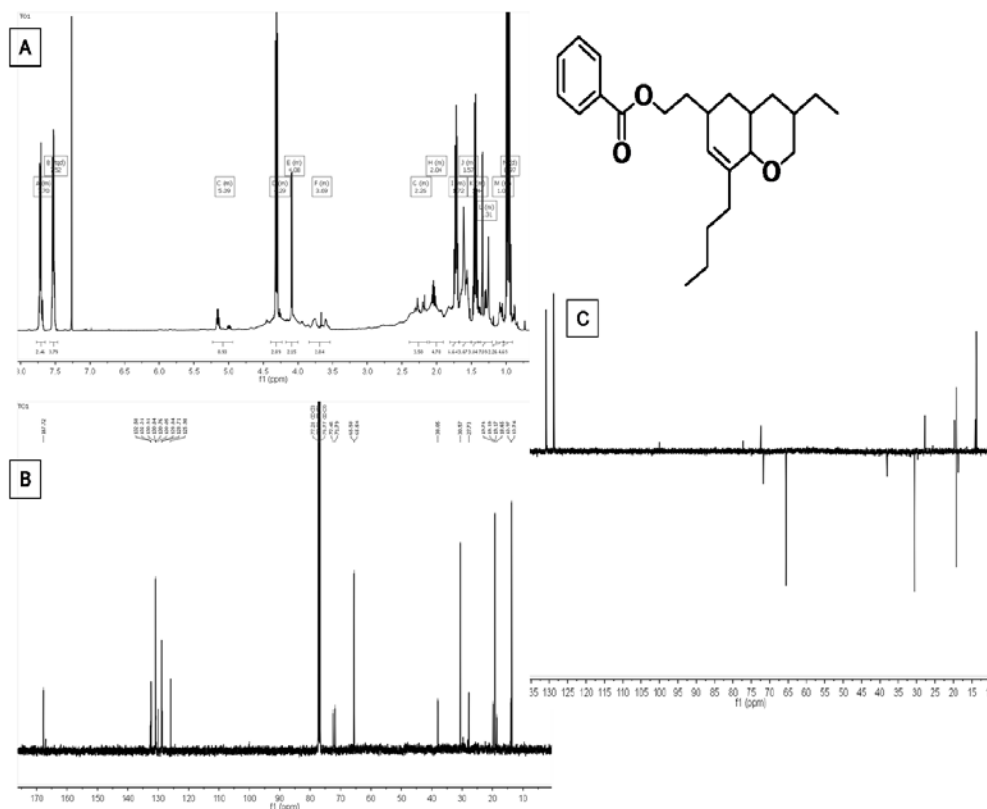


Figure 6A.7
(A) ^1H , (B) ^{13}C and (C) DEPT₁₃₅ - NMR spectra of 16.

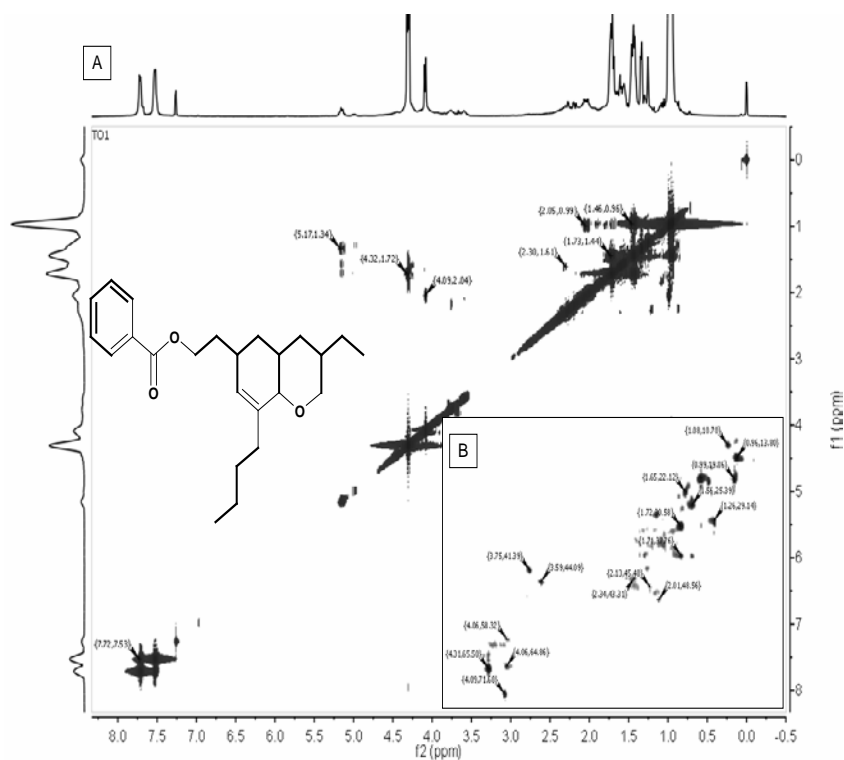


Figure 6A.8

(A) ^1H - ^1H COSY and (B) prominent HSQC correlation spectra of 16. The key ^1H - ^1H COSY couplings have been represented by the bold face bonds.

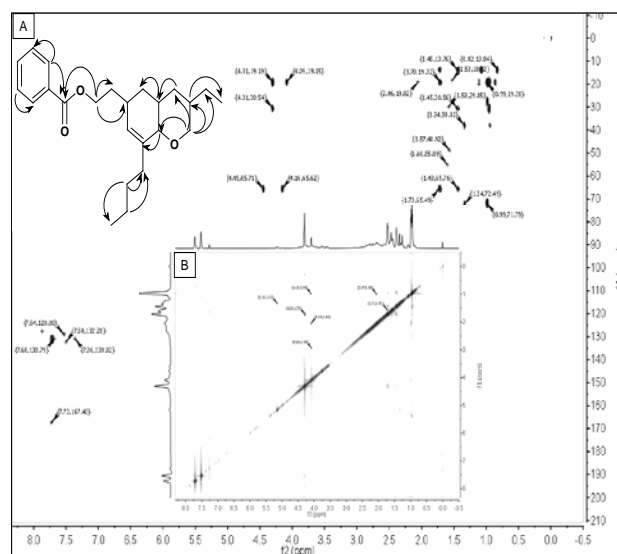


Figure 6A.9

(A) Prominent HMBC and (B) NOESY spectra of 16. The key HMBC couplings are indicated as double barbed arrow.

6A.4 Discussion

The surface of marine organisms such as seaweeds is more nutritious than inanimate material and seawater (Penesyany et al. 2009), and have long been known to support abundant populations of bacteria (Kubaneck et al. 2003). The seaweed associated bacterial flora was reported to be predominant as symbiotic organisms on seaweeds, and are potential sources of antibacterial metabolites. *Aeromonas hydrophila*, *Vibrio vulnificus* and *Vibrio parahaemolyticus*, which were reported to be as human pathogens, and cause gastroenteritis and lethal instances of septicemia in immunocompromised individuals, were used to understand the antagonistic properties of the seaweed-associated bacteria.

The study of the chemical ecology of living surfaces of marine organisms and the symbiotic relationships between seaweeds and their microbial flora can provide important biotechnological information with significance for the production of bioactive secondary metabolites. Marine *Bacillus* species was reported to produce versatile secondary metabolites including lipopeptides, polypeptides, macrolactones, fatty acids, polyketides, and isocoumarins (Amstrong et al. 2001). Kanagasabhapathy et al. (2008) investigated the antimicrobial activity of epiphytic bacteria from several red seaweeds, and found that the highest activity was produced by certain *Bacillus* species especially *B. cereus* and *B. pumilus*. Our results are in agreement with these studies since the major populations of our isolates were *Bacillus* comprising of *B. subtilis*, *B. amyloliquefaciens* and *B. cereus*.

In our survey the antagonistic bacteria associated with seaweed *Sargassum myriocystum* predominantly represented by the phylum *Firmicutes* (*Bacillus* spp) that was reported to dominate among the strains with polyketide synthase (*pks*) genes (Chapter 4). The bacterial strain used in the present study MTCC10407 (NCBI accession number-JF834077) showed identity to *Bacillus subtilis* strain *jinfen 1* (JX960641). Although the ecological relevance of most bacterial associates on or within the seaweeds remained unclear, *Bacillus* species are

efficient producers of compounds with antimicrobial and antifouling characteristics, making them greatly successful colonizers of seaweed surfaces (Goecke et al.2010) .

Bacteria with inhibitory characteristics exist symbiotically on the seaweed surface, providing it with a microbe-mediated defense community. Although examples are rare, studies in seaweeds (Kubaneck et al. 2003) and sponges (Quevrain et al. 2014) have shown the chemical fingerprint of the bacterial metabolites in the host extracts and host derived compounds. It is hypothesized that marine eukaryotes may use their surface-associated bacteria as a source of antimicrobial chemical defences in competition and in the protection of the host (Penesyan et al. 2009). The biosynthesis of a large number of natural products require the participation of sophisticated molecular machines known as *pks* (Donadio et al. 2007). *B. subtilis* MTCC 10407 under the present study is found to be positive for *pks* gene with an NCBI accession number KC607823. The phylogenetic study shown that the amplified gene products of the present study were of bacterial type I *pks* (results not shown). Earlier studies in sponge associated bacteria too found that the bacterial strains to harbor type I bacterial *pks* (Zhang et al. 2009). Bacterial type I *pks* was reported to produce a wide range of biomedical important secondary metabolites (Piel et al. 2004). During our study of biologically active natural products from seaweeds and its associated bacteria(Chakraborty et al.2010) we could notice that the antibacterial activities of seaweed derived compounds were lesser than those of the associated bacterial communities. This led us to investigate whether bacteria or the seaweed is the original source of antibacterial compounds. In the present study, we have taken a *Bacillus subtilis* strain MTCC10407 associated with the seaweed host *Sargassum myriocystum* with a broad spectrum activity with important tested pathogens as a model organism to explain the chemical interactions of seaweed and its associated bacteria.

The guiding principles to determine the bioactivity of the secondary metabolites from bacteria *vis-à-vis* seaweed was designed by utilizing different descriptor variables *viz.*, electronic, hydrophobic, and steric parameters (Chakraborty et al.2010). The electronic descriptors *viz.*, molecular polar surface

area based on fragment contributions (tPSA), polarisability (PI); hydrophobic parameter $\log P_{ow}$ to calculate *n*-octanol/water partition coefficient; steric (or bulk descriptor), molar volume (MV), molar refractivity (MR), and parachor (P) as calculated by ChemDraw 12.0 were taken into consideration (Table 6A.4).

Using bioassay-guided fractionation, two antibacterial compounds **9** (2-(7-(2-ethylbutyl)-2,3,4,4a,6,7-hexahydro-2-oxopyrano[3,2-b]pyran-3-yl)ethyl benzoate) and **10** [2-((3Z)-2-ethyl-octahydro-6-oxo-3-((E)-pent-3-enylidene)pyrano[3,2-b]pyran-7-yl)ethyl benzoate] of presumed polyketide origin, with activity against pathogenic bacteria, have been isolated from the ethyl acetate extract of from *B. subtilis* MTCC 10407(Chapter 5C). The multifactorial polyketide structures are endowed with supplementary *O*-heterocyclic moieties that contribute rigor to polyketide structure. Two homologous compounds **15** (3-(methoxycarbonyl)-4-(5-(2-ethylbutyl)-5, 6-dihydro-3-

methyl-2H-pyran-2-yl)butyl benzoate) and **16** [2-(8-butyl-3-ethyl-3,4,4a,5,6,8a-hexahydro-2H-chromen-6-yl)ethyl benzoate] also have been isolated from the ethyl acetate extract of host seaweed *Sargassum myriocystum*. It is interesting to note that the tetrahydropyran-2-one moiety of the tetrahydropyrano[3,2-b]pyran-2(3H)-one system of **9** might be cleaved by the metabolic pool of seaweeds to afford methyl 3-(dihydro-3-methyl-2H-pyranyl) propanoate moiety of **15**, which was found to have no significant antibacterial activity (Figure 6A.10, Table 6A.1). It is therefore imperative that the presence of dihydro-methyl-2H-pyran-2-yl propanoate system is essentially required to impart the greater activity (IZD 17 mm, 10 mcg on disk). It is significant to note that seaweed might metabolically engineer the parent compound **9** of bacterial origin in its metabolic pool for some other reasons probably related to the structural integrity and rigidity of the seaweed cell wall. This hypothesis can further be supported by the fact that transformed product **15** has greater values of steric descriptors (P 982.5 cm³, MR 118.59 cm³/mol, MV 402.4 cm³) than the parent compound **9** (P 872.9 cm³, MR 107.71 cm³/mol, MV 338.0 cm³) purified from *B. subtilis* MTCC 10407. The biotransformation of the bacterial metabolite to **15** in seaweed might thus contribute to the adaptive mechanism of the seaweed to form a

tougher cell wall to resist the pathogenic bacterial flora in the oceanic ecosystem. Thus, there exists an interesting chemical ecological interaction between the secondary metabolites produced by the seaweed bacteria and the seaweed host organism.

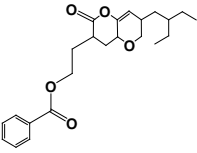
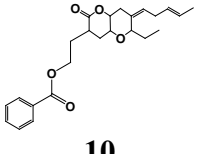
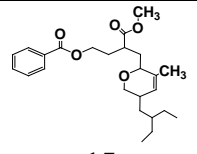
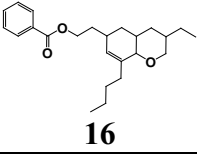
The antibacterial compound **10** isolated from the ethyl acetate extract of from *B. subtilis* MTCC 10407 and **16** from seaweed *Sargassum myriocystum* shared similar structures, and therefore, might be the result of the identical metabolic pool of seaweed and bacteria. In particular the presence of ethyl benzoate moiety in **10** and **16** from seaweed-associated bacteria and seaweed strongly suggested the ecological and metabolic relationship between these compounds. The seaweed derived metabolite **16** did not show an appealing antibacterial property, and therefore, it can be concluded that the compound has a different role, probably related to structural functionality of seaweed. It is interesting to note the greater hydrophobic coefficient of **16** (log P 5.68) than that recorded in **10** (log P 4.28), which apparently support its role in cell wall structure and its integrity.

Polyketides have discovered an application as bioactive leads in drug based products for utilization against disease causing microorganisms and different immunocompromising ailments. Among different bacterial genera, *Bacillus* spp have been perceived to contain different *pks* gene groups and bioactive atoms bearing the polyketide backbone. The much rationed successions of β -ketoacyl synthase (KS) areas are imparted among all *pks*, and hence, the KS spaces are valuable in the screening for *pks* genes in microbes. Consequently, the positive results in a PCR-based screening for *pks* gene doesn't just give confirmation of the generation of relating metabolites additionally may demonstrate the presence of further metabolic pathways of auxiliary metabolite union. In the present study the secondary metabolites of *B. subtilis* MTCC 10407 with potent antibacterial action against bacterial pathogens was recognized to represent the platform of *pks*-1 gene encoded products.

It is of note that the hydrophobic ($\log P_{ow}$) and steric descriptors (P, MR and MV) had a major role to describe the bioactivity of compound **9** isolated from *B. subtilis* MTCC 10407 and compound **15** from the host seaweed. Although the tPSA depicting the electronic descriptor is identical (61.83) in **9** and **15**, the activity of the latter was lesser (IZD 8mm; 10 mcg on disk) than of the former (IZD 17mm; 10mcg on disk), apparently due to the greater steric values (P= 982.5 cm^3) of **3** than that recorded in **1** (P= 872.9 cm^3) (Table 6A.4).

Table 6A.4

Physicochemical descriptor variables of **9** and **15** derived from *B. subtilis* MTCC 10407 vis-à-vis **10** and **16** isolated from brown seaweed *Sargassum myriocystum*

Compounds	Physicochemical descriptor variables					
	Electronic		Hydrophobic	Steric		
	tPSA	PI ($\times 10^{-24} \text{cm}^3$)	Log P	MR (cm^3/mol)	P (cm^3)	MV (cm^3)
 9	61.83	42.19	3.97	107.71	872.9	338.0
 10	61.83	44.84	4.28	113.11	900.6	354.7
 15	61.83	46.66	5.21	118.59	982.5	402.4
 16	35.53	43.35	5.68	110.11	887.4	368.7

PI: Polarisability (cm^3/mol), P: Parachor (cm^3); tPSA: Calculation of polar surface area based on fragment contributions; CLogP to calculate *n*-octanol/water partition coefficient ($\log P_{ow}$); MR: molar refractivity (cm^3/mol); CMR to calculate molar refractivity; MV: molar volume (cm^3).

The compound **10** isolated from *B. subtilis* MTCC 10407 also demonstrated to possess greater antibacterial activities against pathogenic organisms than **16** purified from *Sargassum myriocystum*. It is of note that unlike compound **9**, the compound **10** with 6-oxo-3-(pentenylidene) pyrano[3,2-b]pyran-2-yl moiety showed greater polarisability ($44.8 \times 10^{-24} \text{ cm}^3$), and therefore, the electronic descriptors might play a predominant role in determining the antibacterial activity. The electronic factor such as tPSA was found to significantly contribute towards the greater antibacterial activity of **10**. In particular, the tPSA of **10** was recorded to be significantly greater (61.8) than the related seaweed metabolite **16**, which recorded a lesser tPSA value (35.5). This might be due to the absence of the -O-C=O group from **16**, possibly due to the biochemical transformation of **10** in the seaweed metabolic pool.

The direct involvement of polarisability (PI) with the target bioactivity in **10** implied that inductive (field/polar) rather than the steric effect (parachor) appears to be the key factor influencing the induction of antibacterial activity. This leads demonstrated in the present study will be significant in explaining the pharmacophore-fit in the macromolecular receptor site and exploring the primary site and mode of action of this class of the substituted *O*-heterocyclic compounds belonging to pyran-2-yl ethyl benzoate analogues.

Polyketides emblemize a highly diverse group of natural products having structurally intriguing carbon skeletons. The extraordinary divergence of polyketide structures results from the type of biosynthetic starter and extender units (Khosla et al. 1999). The chain extension module of type-I *pks* harbors the acyl carrier protein (ACP) and ketosynthase (KS) domains that synergistically catalyze a series of decarboxylative Claisen condensation involving different starter and extender units on ACP and KS subunits of *pks* to result in the elongation of the polyketide chain affording the formation of the intermediate biosynthetic product as ACP-S-7-(2-ethylbutyl)-2,3,4,4a,6,7-hexahydro-3-(2-hydroxyethyl)-2-mercaptopyrano[3,2-b]pyran-2-ol (Figure 6A.11.A). A series of

condensation, dehydration, and ketoreduction of the intermediate polyketides result in the biosynthesis of 2-(7-(2-ethylbutyl)-2,3,4,4a,6,7-hexahydro-2-oxopyrano[3,2-b]pyran-3-yl)ethyl benzoate. It is of note that in the biosynthetic route leading to the formation of 2-((7Z)-octahydro-2-oxo-7-((E)-pent-3-enylidene) pyrano [3, 2-b]pyran-3-yl) ethyl benzoate is also a *pks* biosynthetic product (Figure 6A.11.B). A model for biosynthesis of the *pks* gene product can be proposed (Figure 6A.11.C), which account for the fact that S-3-(1-hydroxypropyl)-4, 7-dioxooctanethioate as the starting building blocks instead of acetate/malonate in the biosynthesis of this polyketide backbone.

Earlier reports indicated the concerted zipper-type cyclization reaction of polyepoxides by *pks-1* system(Bhatt et al. 2005; Gallimore et al 2006)through a semiacetal hydroxy group. Similar biosynthetic routes have been postulated in the formation of the polyether ladders of marine toxins maitotoxin (Gallimore et al 2006) and pyran rings of tetronomycin and ambruticin. The connections of *pks* metabolite gene with auxiliary metabolites fitting in with polyketides, and their putative biosynthesis pathway in related microbes was accounted for in prior studies (Moldenhauer et al.2007).

All in all, *pks* uses malonyl/methylmalonyl/ethylmalonyl subsidiaries of CoA and hydroxymalonyl/aminomalonyl/methoxymalonyl ACP extender units to biosynthesize a widely diverse natural products bearing the polyketide backbone. It is of note that during the course of *pks*-catalyzed biosynthesis of 2-(7-(2-ethylbutyl)-2,3,4,4a,6,7-hexahydro-2-oxopyrano[3,2-b]pyran-3-yl)ethyl benzoate, the ACP and KS subunits of the enzyme build their products from an 2-(7-(2-ethylbutyl)-hexahydro-2-oxopyrano[3,2-b]pyran-3-yl)ethyl benzoate starter unit and malonate extender units.

The biosynthetic route of 2-(7-(2-ethylbutyl)-hexahydro-2-oxopyrano[3,2-b]pyran-3-yl)ethyl benzoate starts from thioacetate unit attached to the ACP domain, and is accomplished by a stepwise process of decarboxylative Claisen condensations and ketoreduction. In particular, the biosynthetic route of the pyran

ring system features the extraordinary blueprint of nature to yield complex molecules from simpler units by *pks* enzymatic cascade.

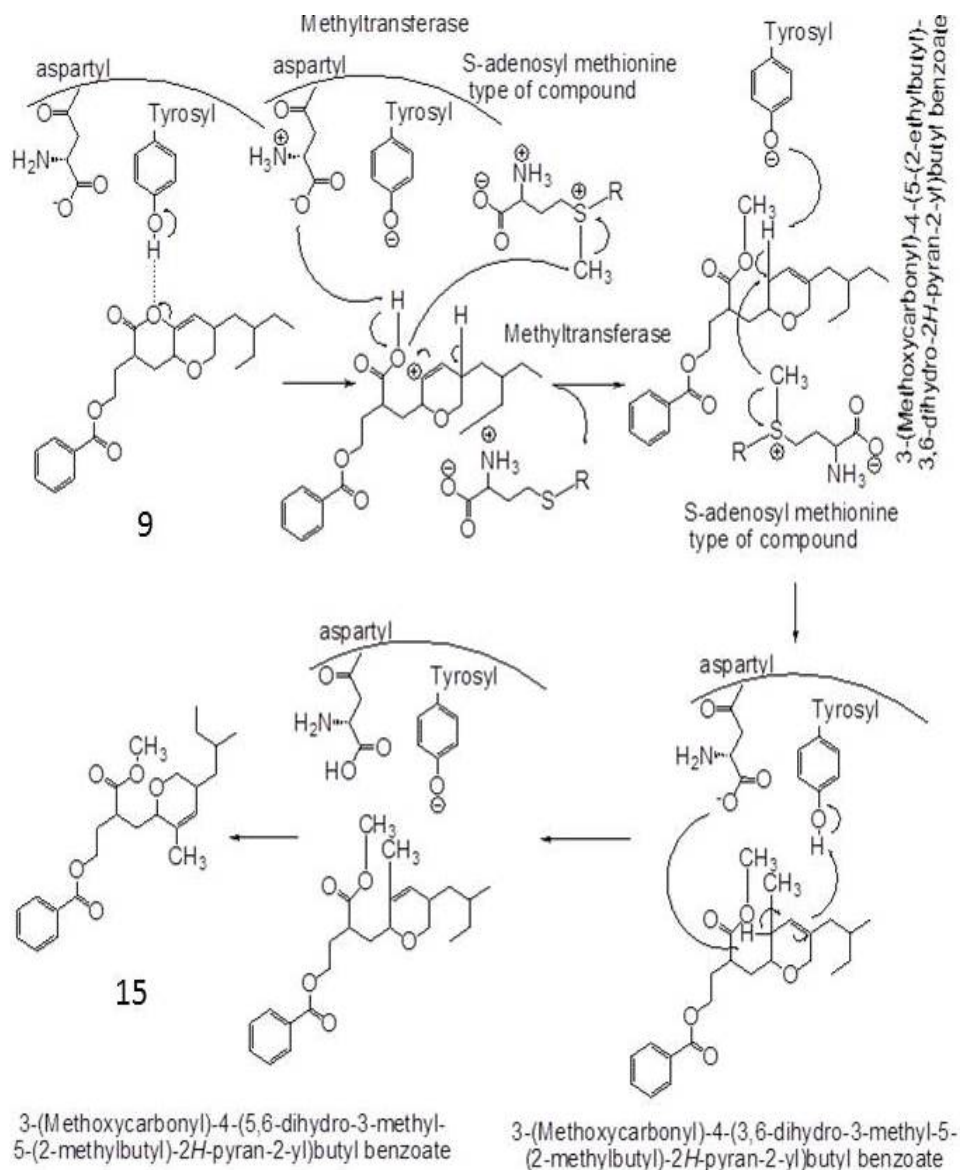
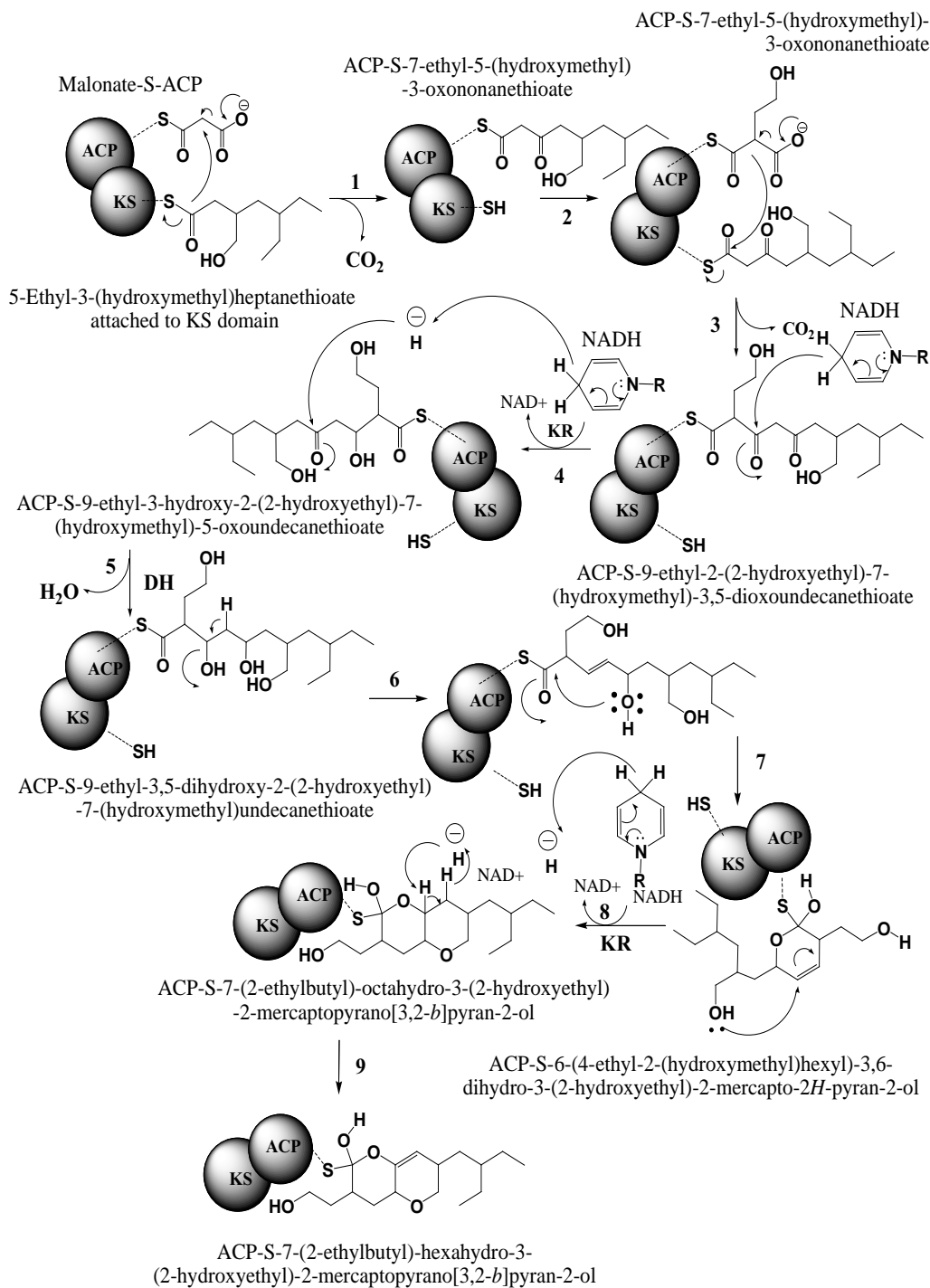


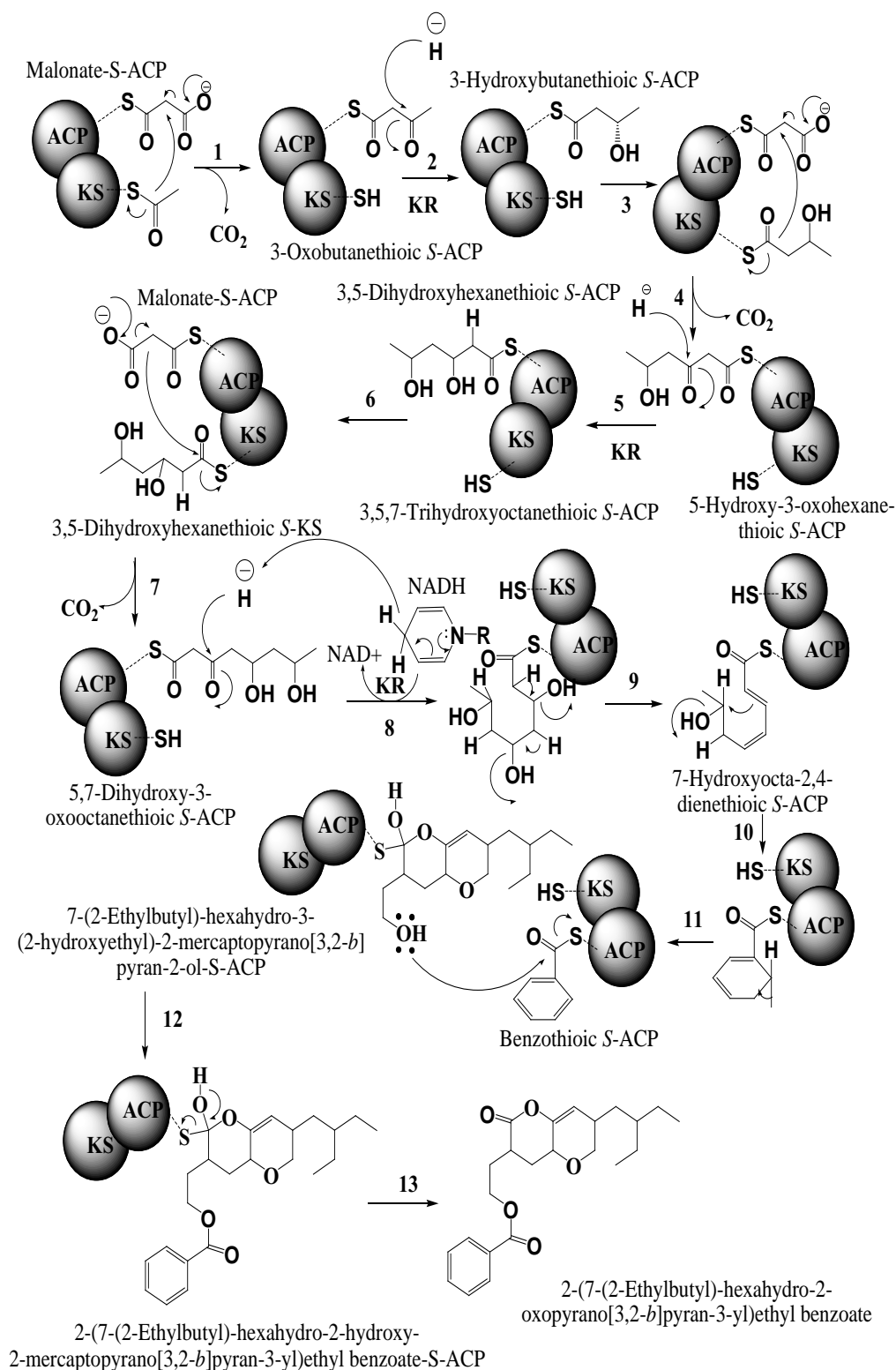
Fig. 6A.10

Hypothetical biosynthetic transformation of 9 in the seaweed metabolic pool by methyltransferase reactions that utilized S-adenosyl methionine type of compound. The oxygen atom of 9 engages in S_N2 nucleophilic attack on the electrophilic methyl carbon of S-adenosyl methionine to afford 3-(methoxycarbonyl)-4-(5-(2-ethylbutyl)-3,6-dihydro-2H-pyran-2-yl) butyl benzoate. This followed the electrophilic addition reactions to asymmetrical alkenes, where the nucleophile is a π -bond on 4-

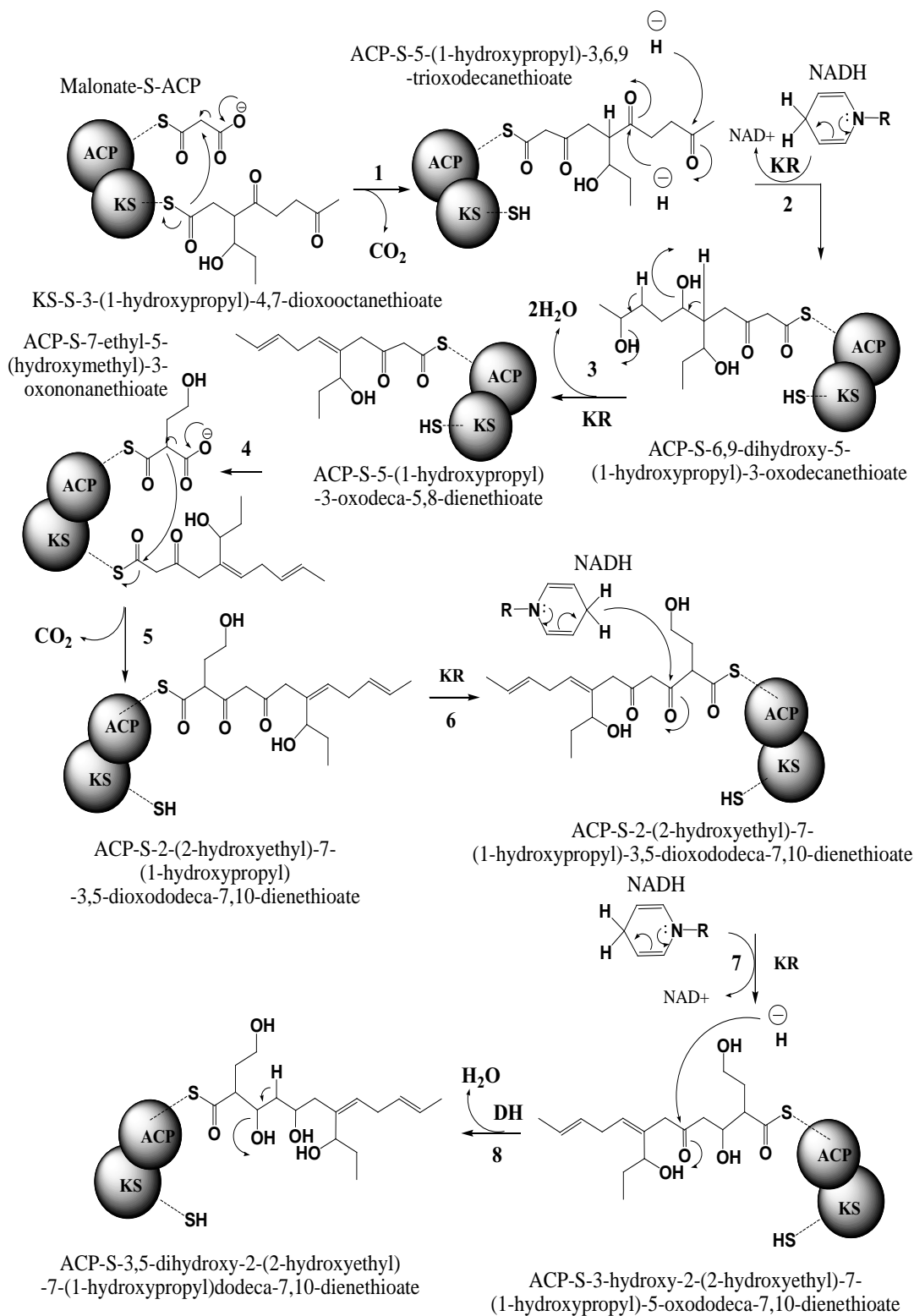
(benzoyloxy)-2-((5-(2-ethylbutyl)-5, 6-dihydro-2H-pyran-2-yl)methyl) butanoic acid, proceed through the stabilization of the carbocation intermediate to yield 3-(methoxycarbonyl)-4-(3,6-dihydro-3-methyl-5-(2-methylbutyl)-2H-pyran-2-yl)butyl benzoate. This was followed by the double bond shifting in the pyran ring system of 3,6-dihydro-3-methyl-5-(2-methylbutyl)-2H-pyran-2-yl to 5,6-dihydro-3-methyl-5-(2-methylbutyl)-2H-pyran-2-yl.



6A.11.A



6A.11.B



6A.11.C

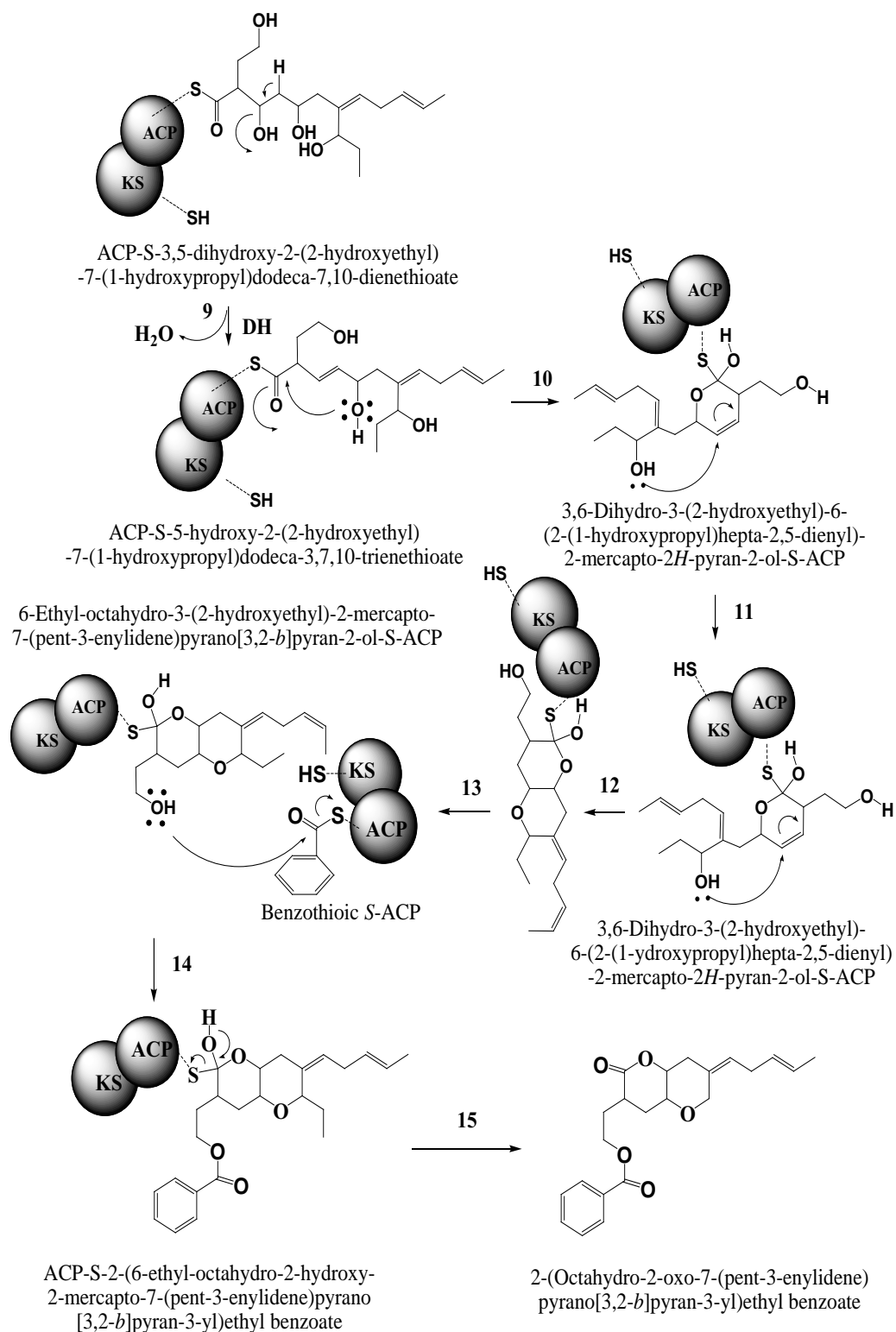


Fig. 6A.11.C

Fig. 6A.11

(A) Hypothetical biosynthetic pathways of **1**, showing the loading, decarboxylation and elongation steps catalyzed by the *pks-1*. Both enzymes build their products from 5-ethyl-3-(hydroxymethyl) heptanethioate starter unit and malonate extender units. The intermediates shown bound to the *pks* are hypothetical, but consistent with experimental results. Chain extension is initiated by decarboxylation of malonyl-ACP to ACP-S-7-ethyl-5-(hydroxymethyl)-3-oxononanethioate by the KS domain. The 7-ethyl-5-(hydroxymethyl)-3-oxononanethioate group is then passed from the ACP to the active site cysteine of the KS. The ACP is loaded with 7-ethyl-5-(hydroxymethyl)-3-oxononanethioate and then KS-catalysed decarboxylative Claisen condensation takes place resulting in ACP-S-9-ethyl-2-(2-hydroxyethyl)-7-(hydroxymethyl)-3,5-dioxoundecanethioate. The latter undergoes ketoreduction followed by dehydration to afford ACP-S-9-ethyl-3,5-dihydroxy-2-(2-hydroxyethyl)-7-(hydroxymethyl) undecanethioate. The mercaptyl sulfur atom of the latter undergoes nucleophilic attack by the 5-OH group in the substituted undecanethioate system yielding ACP-S-6-(4-ethyl-2-(hydroxymethyl)hexyl)-3,6-dihydro-3-(2-hydroxyethyl)-2-mercapto-2H-pyran-2-ol. C₅ olefinic carbon atom of the 2H-pyran ring system undergoes intramolecular nucleophilic attack by the 2'-OH group of 4-ethyl-2-(hydroxymethyl) hexyl moiety to afford ACP-S-7-(2-ethylbutyl)-octahydro-3-(2-hydroxyethyl)-2-mercapto-3,2-b]pyran-2-ol, which undergoes dehydrogenation yielding ACP-S-7-(2-ethylbutyl)-hexahydro-3-(2-hydroxyethyl)-2-mercapto-3,2-b]pyran-2-ol. (B) The biosynthetic route of **1** starts from thioacetate unit attached on the ACP domain, and is accomplished by stepwise process of decarboxylative Claisen condensations and ketoreduction. DH catalyzes the elimination of the water molecule in the intermediate KR product 5, 7-dihydroxy-3-oxooctanethioic S-ACP to afford benzothioic S-ACP. The nucleophilic attack of the terminal 2-hydroxy group (as 2-hydroxyethyl moiety) of 7-(2-ethylbutyl)-hexahydro-3-(2-hydroxyethyl)-2-mercapto-3,2-b]pyran-2-ol-S-ACP on the thioester-activated carbonyl carbon atom of benzothioic S-ACP result in the formation of 2-(7-(2-ethylbutyl)-hexahydro-2-hydroxy-2-mercapto-3,2-b]pyran-3-yl)ethyl benzoate-S-ACP. A subsequent elimination of ACP-SH afforded 2-(7-(2-ethylbutyl)-hexahydro-2-oxopyrano[3,2-b]pyran-3-yl)ethyl benzoate. (C) Sequence of events in the hypothetical biosynthetic pathway of *pks* product as compound **2**, showing the loading, decarboxylation and elongation steps catalyzed by the *pks-1*. Both enzymes build their products from an S-3-(1-hydroxypropyl)-4, 7-dioxooctanethioate starter unit and malonate extender units. Chain extension is initiated by decarboxylation of malonyl-ACP to ACP-S-5-(1-hydroxypropyl)-3,6,9-trioxododecanethioate by the KS domain. The latter undergoes ketoreduction and dehydration to afford ACP-S-5-(1-hydroxypropyl)-3-oxodeca-5,8-dienethioate. The ACP-S-5-(1-hydroxypropyl)-3-oxodeca-5,8-dienethioate group is then passed from the ACP to the active site cysteine of the KS. The ACP is loaded with one unit of ACP-S-7-ethyl-5-(hydroxymethyl)-3-oxononanethioate and then KS-catalysed decarboxylative Claisen condensation takes place resulting in ACP-S-2-(2-hydroxyethyl)-7-(1-hydroxypropyl)-3,5-dioxododeca-7, 10-dienethioate. Two alternate steps of ketoreduction of the latter yielded ACP-S-3-hydroxy-2-(2-hydroxyethyl)-7-(1-hydroxypropyl)-5-oxododeca-7, 10-dienethioate. DH catalyzes the elimination of the water molecule in the intermediate KR product to afford ACP-S-5-hydroxy-2-(2-hydroxyethyl)-7-(1-hydroxypropyl) dodeca-3,7,10-trienethioate. The nucleophilic attack of the 5-OH group (as 5-hydroxy-2-(2-hydroxyethyl)) on the thioester-activated carbonyl carbon atom of ACP-S-5-hydroxy-2-(2-hydroxyethyl)-7-(1-hydroxypropyl)dodeca-3,7,10-trienethioate result in the formation of a cyclic 2H-pyran product as 3,6-dihydro-3-(2-hydroxyethyl)-6-(2-(1-hydroxypropyl)hepta-2,5-dienyl)-2-mercapto-2H-pyran-2-ol in the 6-membered pyran ring lactone system. A subsequent intramolecular nucleophilic attack by the 1-hydroxypropyl-OH group in the 2-(1-hydroxypropyl)hepta-2,5-dien-1-yl)- system on the C-3 of the 2H-pyran ring system yielded 6-ethyl-3-(2-hydroxyethyl)-2-mercapto-7-(pent-3-en-1-ylidene) octahydro-3,2-b]pyran-2-ol-S-ACP. The carbonyl carbon atom of benzothioic S-ACP undergoes nucleophilic attack by the 3-OH group in the 3-(2-hydroxyethyl)-system of 6-ethyl-3-(2-hydroxyethyl)-2-mercapto-7-(pent-3-en-1-ylidene)octahydro-3,2-b]pyran-2-ol-S-ACP yielding pyrano [3,2-b]pyran-3-yl) ring system of ACP-S-2-(6-ethyl-octahydro-2-hydroxy-2-mercapto-7-(pent-3-enylidene)pyrano[3,2-b]pyran-3-yl)ethyl benzoate. A subsequent elimination of ACP-SH afforded the final PKS product as 2-(octahydro-2-oxo-7-(pent-3-enylidene) pyrano [3, 2-b]pyran-3-yl) ethyl benzoate.

6A.5 Conclusions

The previous decade saw the disclosure of different bacterial polyketide leads with colossal significance as novel alternatives to the existing antibiotics for use against multi-drug resistant human opportunistic food pathogens. In this study, we depicted two new variants of antibacterial *O*-heterocyclic pyran derivatives of polyketide origin. These novel polyketide products may be promising to develop a new generation of drug candidate for utilization against the multiresistant microbial pathogens. The fact that polyketides of this type are unprecedented from seaweed and the structural similarity of the seaweed derived homologous compounds to the microbial metabolites suggests that these could be the products of symbiont, and it is biotransformed by the seaweed metabolic pool. We have likewise given confirmation to a biosynthetic course of these compounds, and this may prompt to identify novel drug target. The present work may have a footprint on the use of *O*-heterocyclic polyketide products for biotechnological, food and pharmaceutical applications.

Chapter 6B
CHEMICAL ECOLOGY OF SEAWEED-ASSOCIATED ANTAGONISTIC
***BACILLUS sp* BASED ON DIFFERENTIAL MEMBRANE FATTY ACID**
COMPOSITION

6B.1 Background of the study

Seaweeds or marine macroalgae have been challenged throughout their evolution by microorganisms, and have developed in a world of microbes. Therefore, it is not surprising that a complex array of interactions has evolved between seaweeds and bacteria, which depend on chemical interactions of various kinds (Goecke et al. 2010). Seaweeds harbor a rich diversity of associated microorganisms with functions related to host health and defense. In particular, epiphytic bacterial communities have been reported as essential for normal morphological development of the seaweed host, and bacteria with antifouling properties are thought to protect chemically undefended seaweeds from detrimental, secondary colonization by other microscopic and macroscopic epibiota. This tight ecological relationship suggests that seaweeds and epiphytic bacteria interact as a unified functional entity or holobiont (Egan et al. 2013). Bacterial communities belonging to the phyla *Proteobacteria* and *Firmicutes* are generally the most abundant on seaweed surfaces (Singh and Reddy 2014; Chakraborty et al. 2014). Although surface-associated marine bacteria may be potential sources of novel secondary metabolites of various bioactivities, the literature contains a few reports relating to the chemical ecology of these organisms (Boyd et al. 1999).

The bioactivity of bacterial species grown under symbiotic condition depends on several abiotic and biotic factors, among which the growth environment plays a major role. The extreme forms of salinity and oxidative stress in oceanic

ecosystems made the bacterial species to modulate their biochemical profile to adapt and survive in the stressed conditions (Hazel 1995). This adaptation is largely accomplished by changing membrane fatty acid chain length, unsaturation degree, and branching pattern (Hazel 1995). Since the symbiotic bacteria could be able to grow on the host organism, i.e., the seaweed, it is imperative that the seaweed metabolites may play an important role in determining the growth, bioactivity, and viability of the resident bacterial flora. It was also reported that the addition of seaweed extract to the culture medium caused the increased formation of *anteiso* fatty acids (*anteiso*_{C17:0}) related to these fatty acid substrates, and the tolerance of marine bacteria grown at laboratory culture conditions depends to a significant extent on a greater proportion of the above-described fatty acids in the membrane. There is, therefore, a need to investigate the bacterial communities living on different coexisting seaweeds using new technologies, and to investigate the production, localization and secretion of the biologically active metabolites involved in those possible ecological interactions (Goecke et al. 2010).

Seaweed associated bacteria were found to be rich in bacterial strains with polyketide synthase (*pks*) gene (Chakraborty et al. 2014). Polyketides constitute one of the major classes of natural products many of these compounds or derivatives thereof have become important therapeutics for clinical use (Hertweck et al. 2009). Bacterial *pks* genes are structurally type I, but act in an iterative manner to produce aromatic polyketides (Zhang et al. 2013). Polyketide biosynthesis has much in common with fatty acid biosynthesis. Not only are they alike in the chemical mechanisms involved in chain extension but also in the common pool of simple precursors employed, such as acetylcoenzyme A (CoA) and malonyl-CoA (MCoA) units. In general, both polyketides and fatty acids are constructed by repetitive decarboxylative Claisen thioester condensations of an activated acyl starter unit with malonyl-CoA derived extender units (Hertweck et al. 2009). The type I iterative *pks* genes can be further divided to non-reducing *pks*, the products of which are true polyketides; partially reducing *pks* and fully reducing *pks*, the products of which are fatty acid derivatives (Hertweck et al. 2009).

The fatty acid profile of *Bacillus subtilis*, the gram-positive bacteria, is dominated by the *iso*- and *anteiso*-branched fatty acids. Branched chain amino acids are used as the precursors for their synthesis of isoleucine for *anteiso*; and valine and leucine for *iso*-branched fatty acids. *Bacillus subtilis* cells use two distinct mechanisms of adaptation to stress conditions such as those cultured in laboratory using artificial growth medium. This may explain the role of these branched fatty acids in surviving in the stressed oceanic environments. The long-term membrane adaptation employs an increase in low melting *anteiso*-branched fatty acids (mostly *anteiso*_{C15:0} and *anteiso*_{C17:0}) that effectively fluidize the membrane (Suutari and Laakso 1992) thereby preventing the stress related conditions. Modulation of fatty acid composition to ensure survival at the stressed conditions is an important bacterial strategy for growth (Suutari and Laakso 1994).

It was reported that 2-methylbutyric acid, a precursor of *anteiso* fatty acids, restored the *anteiso*_{C15:0} content, membrane fluidity, and growth of the mutants, whereas isobutyrate and isovalerate, precursors of *iso* fatty acids, did not (Zhu et al. 2005). Hence, as far as stress factor adaptation of the bacterial species is concerned, the central strategy is to increase the proportion of *anteiso*_{C15:0} and the compounds related to 2-methyl butyric acid. The vast majority of previous studies of the fatty acid composition of bacteria have employed complex media for growth. Tsai and Hodgson described a minimal medium that does not require BCFA supplements. Such capacities have been suggested to be related to its atypically high *iso* and *anteiso*, odd-numbered BCFA content (Annous et al. 1997).

The fatty acid profiles of the seaweed associated antagonistic bacilli are found to have an increased amount of *iso* and *anteiso* fatty acids. The *pks* gene is the functional gene determining the bacterial active metabolite, and also there were reports that the seaweed derived polyketide metabolites are related to bacterial metabolites (Kubaneck et al. 2003; Chakraborty et al. 2014). Polyketide biosynthesis has much in common with fatty acid biosynthesis, and was reported to have multiple role determining the bioactivity and growth in artificial culture media. Not only are they alike in the chemical mechanisms involved in chain extension but also in the common pool of simple precursors employed, such as

acetylcoenzyme A (CoA) and malonyl-CoA (MCoA) units (Hertweck et al. 2009). Based on these facts we hypothesized that there might be a relation in the presence of fatty acids, antibacterial activity, and the presence of functional *pks* genes responsible for the antibacterial activity. We have adopted a culture dependent method to assess the bioactivity of the cultivable antagonistic heterotrophic bacterial communities associated with the intertidal seaweeds at the Gulf of Mannar in the Southeast coast of India bordering the Bay of Bengal. We extended the analysis to understand the effect of seaweed extract and the metabolic precursors of the seaweed extract on the growth and fatty acid profile of the bacterial species to understand the chemical ecological relationship between the host seaweed and their associated bacterial flora. The possible biosynthetic route of the 2-methyl butyric acid from the seaweed metabolite has been proposed, which also corroborates the role of isoleucine and 2-methyl butyric acid for greater growth, bioactivity and viability of the seaweed associated bacterial flora in a culture dependent method. The ecological interaction between seaweed host and its associated active bacterial flora and their importance in the growth and antibacterial activities have been illustrated.

6B.2 Materials and methods

6B.2.1 Isolation and molecular identification of the seaweed associated antagonistic bacteria

Intertidal seaweeds belonging to *Phaeophyceae* and *Rhodophyceae* were collected by scuba diving from the intertidal zone of Mandapam situated at 9° 17' 0" North, 79° 7' 0" East, Gulf of Mannar region in southeast coast of India. The brown seaweeds were *Anthophyscus longifolius*, *Sargassum myriocystum*, *Padina gymnospora*, *Turbinaria ornata* and *Dictyota dichomata*, whereas red seaweeds were *Hypnea valentiae* and *Laurentiae pappilosa*. The seaweed samples were processed and the associated bacterial strains were isolated as reported earlier (chapter 3). The bacterial strains were assayed for antagonistic activity against pathogens (chapter 3). Measure of antagonistic activity was recorded as the diameter of inhibition zones and bacteria with antagonistic properties were

identified using classical biochemical methods followed by 16S rRNA gene sequencing (chapter 3). The bacteria were screened for the presence of metabolite genes encoding polyketide synthetase (*pks-I*) involved in natural product biosynthetic pathway. Different sets of degenerate primers targeting *pks-I* were used to screen the biosynthetic potential of the bacterial isolates to elicit bioactive polyketides (chapter 4).

6B.2.2 Preservation of bacterial strains on seaweed extract agar

The seaweed species used to isolate the associated *Bacillus* sp were used to prepare the seaweed extract agar. For each bacterial strain the respective host derived dried powder of seaweed aqueous extract was used (chapter 3)

6B.2.3 Chemistry

Chemical reagents and analytical methods used were explained in chapter 5

6B.2.4 Fatty acid analyses and gas chromatography

The bacterial cells were saponified, methylated, and extracted to afford bacterial fatty acid methyl esters (FAMES) as described previously (chapter 3). Fatty acid profiles were evaluated on a Perkin-Elmer (USA) AutoSystem XL gas chromatograph (HP 5890 Series II) equipped with an Elite-5 (crossbond 5% diphenyl 95% dimethyl polysiloxane) capillary column (30m X 0.53mm i.d., Supelco, Bellfonte, PA) with split/splitless injector, using a flame ionization detector as described previously (chapter 3).

6B.2.5 Seaweed material and preparation of crude extracts

The brown seaweed *Anthophycus longifolium* was used to isolate the associated antagonistic bacteria *Bacillus subtilis* SWI 2. This seaweed species was used as a model to understand the chemical ecology of seaweed derived secondary metabolites and their relationship with the fatty acid biosynthesis, growth and antagonistic properties of the associated bacterial species (*Bacillus subtilis* SWI 2). The seaweed was freshly collected from the Gulf of Mannar in Mandapam region located between 8°48' N, 78°9' E and 9°14' N, 79°14'E on the southeast coast of

India. The samples collected were washed in running water for 10 min, transported to the laboratory and shade dried (35 ± 3 °C) for 36 h. The shade dried seaweeds were powdered and used for further experiments. The powdered seaweed samples (100 g) were extracted three times with ethylacetate-methanol (1:1 v/v, 50–60 °C, 3 h), filtered through Whatman No. 1 filter paper and the pooled filtrate was concentrated (50 °C) *in vacuo* (Heidolph Instruments GmbH & Co., Schwabach, Germany) to furnish the seaweed crude methanol-ethyl acetate (MeOH-EtOAc) extract.

6B.2.6 Chromatographic purification of substituted vinylphenanthrenyl-2-methylbutanoate from *Anthophycus longifolium*

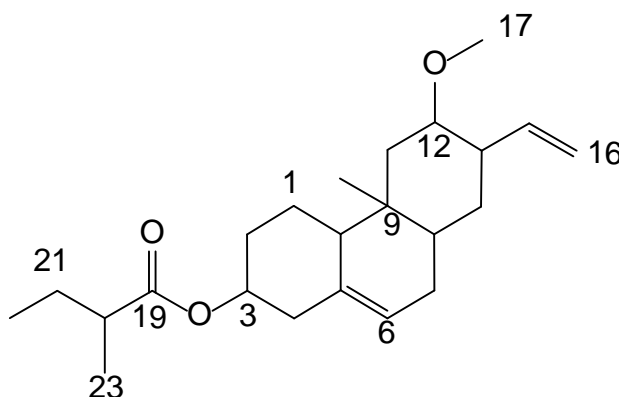
An aliquot of the crude MeOH-EtOAc extract (10 g) of *Anthophycus longifolium* was slurried in silica gel (4 g, 80–120 mesh), and loaded into a glass column (120 cm X 4 cm) packed with silica gel (80–120 mesh, 50 g) as adsorbent before being subjected to vacuum liquid chromatography. The column was initially eluted with *n*-hexane, followed by addition of EtOAc (*n*-hexane: EtOAc 99:1 to 0:100, v/v) to furnish 18 fractions of 50 ml each, which were reduced to 5 groups (F₁-F₅) after TLC analysis (*n*-hexane: EtOAc, 4:1, v/v). Fraction 3 (F₃) obtained by eluting with *n*-hexane: EtOAc (1:1, v/v) was found to be a mixture, which was flash chromatographed (Biotage AB SP1-B1A, 230–400 mesh, 12 g; Biotage AB, Uppsala, Sweden) on a silica gel column (Biotage, 230–400 mesh, 12 g; Sweden, Biotage No. 25+M 0489-1) at a collection UV wavelength at 256 nm using a step gradient of CH₂Cl₂:MeOH (CH₂Cl₂:MeOH 99.5:0.5 to 19:1, v/v) to afford 160 fractions (8 ml each), which were reduced to three pooled fractions (F₃₋₁-F₃₋₃) after TLC analysis (*n*-hexane: EtOAc, 5:1, v/v). The fraction F₃₋₂ eluted with CH₂Cl₂:MeOH (49:1, v/v) on subsequent preparatory thin layer chromatographic purification using *n*-hexane: EtOAc (4:1, v/v) afforded dodecahydro-3-methoxy-4a-methyl-2-vinylphenanthren-7-yl-2-methyl butanoate (**17**, 6.5 mg). Evaporation of solvents followed by TLC over precoated silica gel GF₂₅₄ (particle size 15 mm, E-Merck, Germany) using using 5% ethylacetate /*n*-hexane supported the purity.

6B.2.7 Structural characterization of compound 13

Physicochemical data of 1, 2, 3, 4, 4a, 4b, 5, 6, 7, 8, 10, 10a-dodecahydro-3-methoxy-4a-methyl-2-vinylphenanthren-7-yl-2-methyl butanoate (**1**): colorless liquid; UV (MeOH) $\lambda_{\max}(\log \epsilon)$: 243nm (2.89) and 265nm (2.35) ; TLC (Si gel GF₂₅₄ 15 mm; *n*-hexane/EtOAc 95:5, v/v) R_f: 0.45; R_t: 4.6min.; IR ν_{\max} (KBr) cm⁻¹ (δ_{OOP} = out of plane bending, ν = stretching, δ = bending vibrations): 481.08 δ_{OOP} (C-CO), 1056.71 ν (C-O), 1121.80 ν_s (C-O-C), 1282.20 $\delta_{in-plane}$ (CH-OH), 1376.96 δ (C-H) of(O=C-CH₂), 1461.43 δ_{as} (C-H), 1728.15 δ (C=O), 1656.80 ν (C=C), 2854.74 ν_s (C-H) of (-O-CH₂), 2923.22 (alkane ν (C-H), 2957.04 alkanes ν_{as} (C-H), 3437.24 ν (O-H); ¹H-NMR(CDCl₃, 500MHz, δ ppm) δ 5.82 (ddt, J =16.9,10.2,6.7Hz, 1H), 5.53–5.15 (m,1H), 5.09–4.81 (m,2H), 4.30 (p,1H), 4.19–4.06 (m,1H), 1.53–1.31 (m,2H), 1.28 (t, J=14.7Hz,1H), 0.94 (d, J=20.5Hz,3H), 0.88 (t, J=6.9Hz,3H), 0.85–0.81 (s,3H), 2.38 (d, J=4.09Hz,2H), 2.31 (td, J=7.5, 4.1Hz, 1H), 2.10–1.96 (m,4H), 1.78–1.52 (m,6H), 1.45–1.34 (m,2H); ¹³C-NMR (CDCl₃,125MHz, δ ppm) δ 167.70, 139.27, 130.89, 128.84, 114.05, 74.29, 65.56, 56.14, 38.70, 35.07, 34.06, 33.82,31.93, 31.44, 30.58, 30.20, 29.70, 29.66, 29.51, 28.96, 22.69, 19.19, 14.11, 13.72; 2D-NMR data, see Table 6B.1(Figure 6B.3.A-B); HRMS (ESI) *m/z*: calcd. for C₂₃H₃₇O₃ 361.5422; found 361.5842 [M+H]⁺.

Table 6B.1

NMR spectroscopic data of 1,2,3,4,4a,4b,5,6,7,8,10,10a-dodecahydro-3-methoxy-4a-methyl-2-vinylphenanthren-7-yl 2-methylbutanoate in CDCl₃.^a



Carbon no.	¹³ C NMR (DEPT)	H	$\delta^1\text{H}$ NMR (int., mult., J in Hz) ^b	¹ H- ¹ H COSY	HMBC (¹ H- ¹³ C)
1	30.20	1-H	1.38 (m, 2H)	2-H	C-2,10
2	28.96	2-H	1.72 (m, 2H)	3-H	
3	74.29	3-H	4.30 (p, 1H)		C-19,4,2,1
4	34.06	4-H	2.38 (d, J= 4.09Hz, 1H)	3-H	C-6,5,7
5	130.89	-	-	-	-
6	128.84	6-H	5.33 (m, 1H)	-	C-7
7	29.70	7-H ^a 7-H ^b	1.98 (m, 1H), 2.00 (m,1H)	6-H	C-6,8,9
8	31.44	8-H	1.52 (m, 2H)	7-H ^a	C-14,18,9
9	35.07	-	-	-	-
10	31.93	10-H	1.28 (t, J=7.5Hz,1H),	1-H	C-1,18
11	29.66	11-H	1.58 (m, 2H)	12-H	C-12
12	65.56	12-H	4.13 (m, 1H)	13-H	C-13,17
13	38.70	13-H	2.03 (m,1H)	15-H	C-15,16
14	30.58	14-H	1.60 (t, 2H)	8-H	C-13
15	139.27	15-H	5.82 (ddt, J=16.9Hz,1H)	-	-
16	114.05	16-H ^a 16-H ^b	4.97 (dd,1H) 5.09 (dd,1H)	15-H	C-13,14
17	56.14	17-H	3.66 (s,3H)	-	C-12
18	19.19	18-H	1.33(s,3H)	-	C-11
19	167.70			-	-
20	33.82	20-H	2.31 (m,1H)	23-H, 21-H	-
21	22.69	21-H	1.68 (p,2H)	-	-
22	13.72	22-H	0.87 (d,3H)	21-H	C-21
23	14.11	23-H	0.98 (t,3H)	-	C-20,21

^aNMR spectra recorded using Bruker DPX 300 and AVANCE 300 MHz spectrometers.

^bValues in ppm, multiplicity and coupling constants (J/4 Hz) are indicated in parentheses.

Assignments were made with the aid of the 1H–1H COSY, HMQC, and HMBC experiments.

6B.3 Results

6B.3.1 Isolation, Molecular Identification and Preservation of the Seaweed Associated Antagonistic Bacteria

About 22% of the seaweed associated bacterial isolates shown inhibition against at least one pathogen used in the study, with 9% of this showing broad spectrum activity against the pathogen screened. Among these potential bacterial species, twelve belonged to *Bacillus* sp,(Chapter3;) which were considered in the present study. The preserved cultures were found be to be viable and active for more than three years during random testing. The antimicrobial patterns of these isolates against the pathogens used in the study have been summarized in the Table 3.2(Chapter3). The identifications of the bacterial isolates were confirmed through 16S rRNA gene based molecular evolutionary analysis using the neighbor-joining method as described earlier (Chapter 3). The PKS positive gene sequences were deposited under NCBI accession numbers KC589396- KC589400; KC607821- KC607823 as reported earlier (Chapter 4).

6B.3.2 Analysis of Cellular Fatty Acid of *Bacillus* sp isolated from seaweeds

Bacillus subtilis (SWI 19, SWI 3, SWI 2, and SWI 4a) had considerable amounts of *anteiso* fatty acids (38.65% in SWI 2 to as high as 47.43% in SWI 19 than their *iso* counterpart fatty acids (0.88-1.46%) (Table 3.4, Figure 6B.1.A-B). No unsaturated fatty acids were detected in *Bacillus subtilis* SWI 19 and SWI 2, whereas *B. subtilis* SWI 3 and SWI 4a produced monounsaturated fatty acid to the tune of 2.77 and 4.15%, respectively. The *anteiso* fatty acids content is found to be 41-51% of the total fatty acids when *Bacillus amyloliquefaciens* (SWI 5, SWI 7, SWI 6, and SWI 4B) (Table 3.4). The representative FAME profiles for *Bacillus subtilis* (SWI 19, SWI 3, SWI 2, and SWI 4a) and *Bacillus amyloliquefaciens* (SWI 5, SWI 7, SWI 6, and SWI 4B) along with one strain of *Bacillus cereus* SWI 1 were shown in Fig. 6B.2.A-D. In *Bacillus subtilis* maximum of 5-6 peaks were recognized as typical of this isolate, of which 4 peaks belonging to *iso* and *anteiso* series of C₁₅ and C₁₇ fatty acids had areas equal to or greater than 70 percent of the total percentage FAME area (Fig. 6B.1.B), and these peaks were identified using

the MIDI system. In *Bacillus amyloliquefaciens* SWI 5, a total of ten peaks were recognized as typical of FAME profiles. A total of fourteen peaks were recognized as typical of *Bacillus cereus* SWI 1 on the basis of their presence in repeated samples of the two isolates used in this study. Fatty acids present in *Bacillus subtilis* (SWI 19, SWI 3, SWI 2, and SWI 4A), *Bacillus amyloliquefaciens* (SWI 5, SWI 7, SWI 6, and SWI 4B), and *Bacillus cereus* SWI 1 were shown in Table 3.4

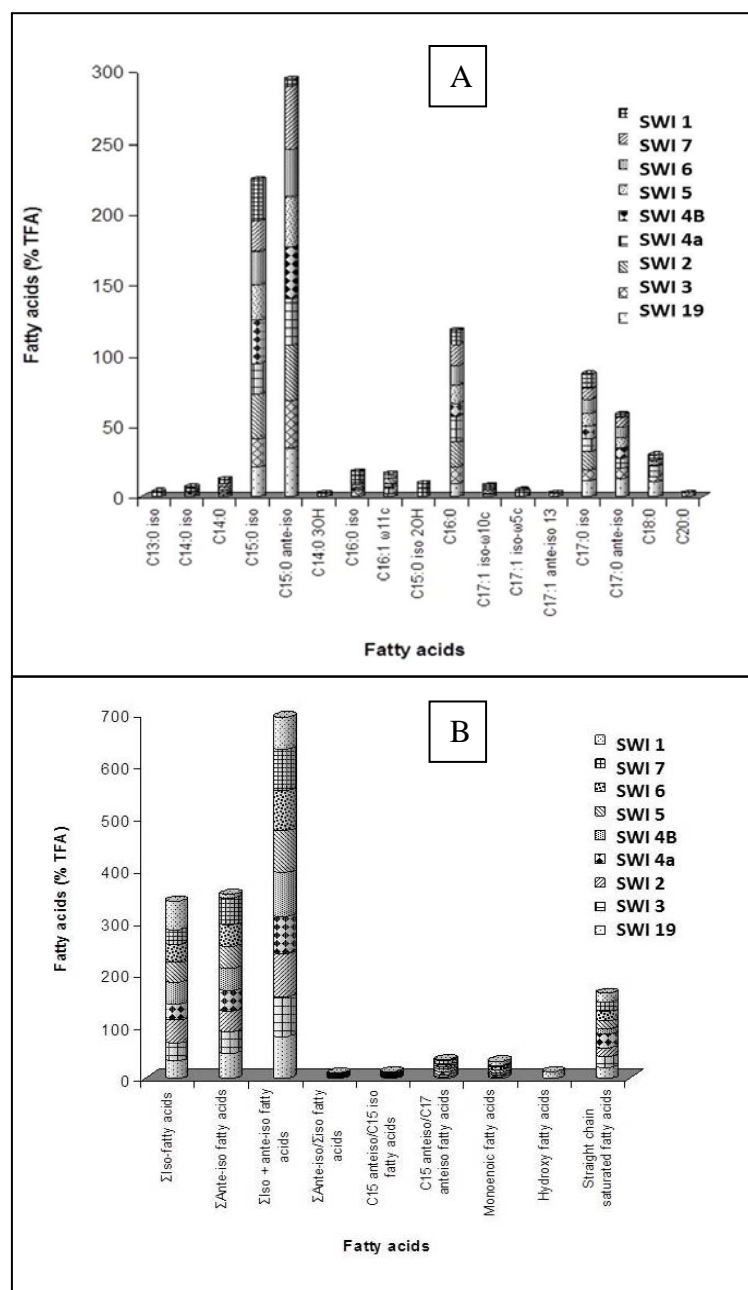


Fig. 6B.1
(A) FAME profile of *Bacillus* sp. (B) Comparison of specific group of fatty acids in different bacterial isolates and the ratio of different FAMES.

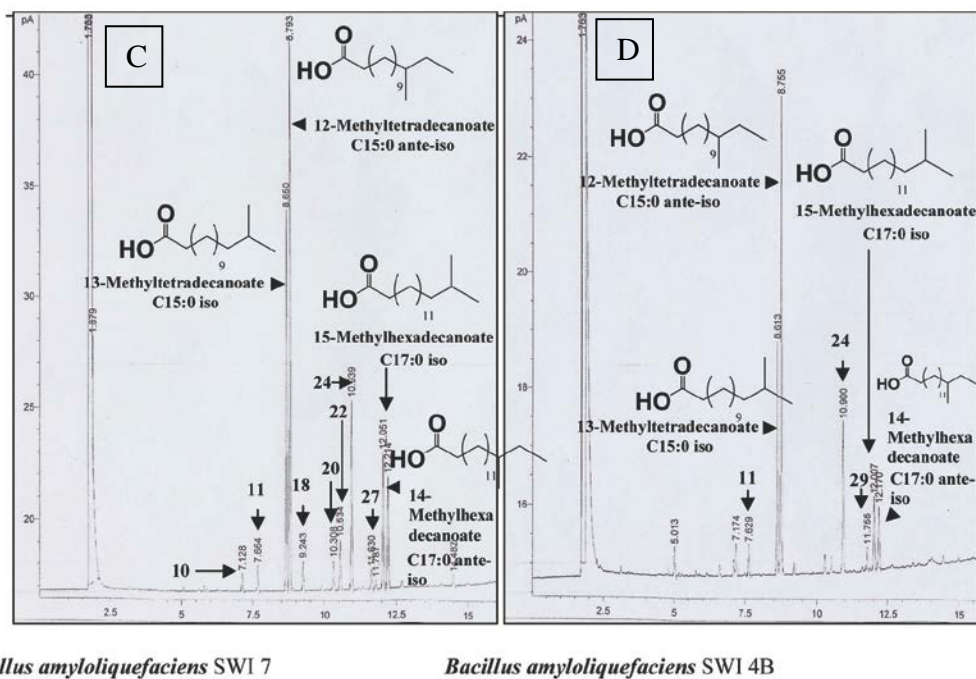
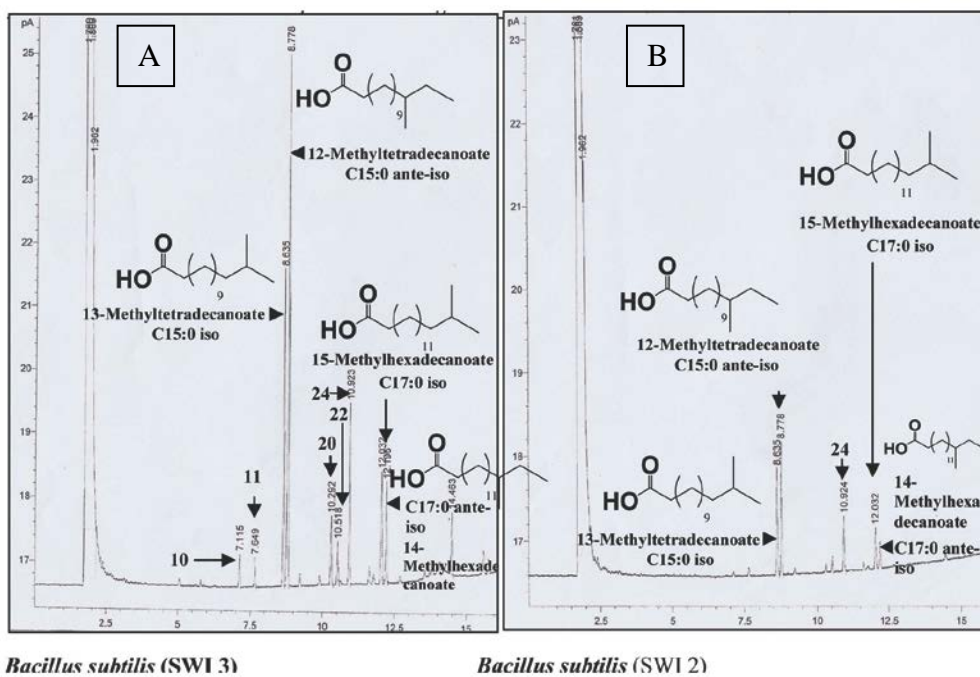


Fig. 6B.2

Representative FAME profile of (A) *Bacillus subtilis* SWI 3, (B) *Bacillus subtilis* SWI 2, (C) *Bacillus amyloliquefaciens* SWI 7, and (D) *Bacillus amyloliquefaciens* SWI 4B. Peaks labeled 1-20 correspond to the fatty acids in Table 3.4.

6B.3.3 Structural Characterization of Vinylphenanthrenyl-2-Methylbutanoate from *Anthophycus longifolium*

The brown seaweed *Anthophycus longifolium* was used to isolate the associated antagonistic bacteria *Bacillus subtilis* SWI 2. The compound dodecahydro-3-methoxy-4a-methyl-2-vinylphenanthren-7-yl 2-methylbutanoate was obtained from the EtOAc-MeOH extract of the seaweed *Anthophycus longifolium* as a colorless liquid, and was isolated upon chromatography over silica columns. The compound has the molecular formula of $C_{23}H_{36}O_3$ on the basis of HRMS showing a molecular ion peak at m/z 361.5842 $[M+H]^+$ (calcd for $C_{23}H_{37}O_3$, 361.5422). The IR spectrum revealed broad absorption band at ν_{max} 1728 cm^{-1} attributed to be due to the presence of carbonyl carbon, to the olefinic system (1656 cm^{-1}), and carbons attached to oxygen C-O stretching (1056 cm^{-1}). The IR absorption band (in MeOH) at 3437.24 cm^{-1} is due to -O-H stretching vibrations. The ^{13}C NMR signals afforded characteristic methylene signals (-CH₂) at δ 114.05 (Figure 6B.3A), which showed strong 1H - 1H -COSY correlation with the protons at δ 5.82 belonging to the carbon atom at δ 139.27. This indicated that the olefinic bond situated to external to ring system by continuous 1H - 1H -COSY correlation to 13-H (δ 2.03) of C-13. The carbon atom at C-5 (δ 130.89) was evident in the ^{13}C -NMR spectrum, although no signal of the same was apparent in the DEPT spectrum. The HSQC correlation between the carbon atom at C-6 (δ 128.84) and the proton at δ 5.33 (ddt) indicates the signature peak of exocyclic bond of A ring in the bicyclic ring system. Based upon the spectral information from the DEPT and ^{13}C -NMR signals, it can be concluded that there are three quaternary carbons, eight -CH, eight -CH₂, and four -CH₃ carbons. The four ^{13}C -NMR signals at C-5, C-6 and C-15, C-16 indicated the presence of two olefinic bonds. A total of six degrees of unsaturation with three double bonds and three ring system has been established by detailed spectroscopic analysis. The cyclic rings confirmed by the strong 1H - 1H -COSY (Figure 6B.4.A-B) correlation signals also support the HSQC (Figure 6B.4.C) and HMBC (Figure 6B.5.A-B) signals. The ^{13}C NMR spectrum of the purified compound displayed a quaternary carbon (δ 167.7) atom bearing the carbonyl group. The low field quaternary signals (^{13}C NMR) is in agreement with

that to a quaternary carbon signal carrying the carbonyl groups at C-19 of the phenanthrene ring structure and C-3 of the side chain (2-methyl butanoate) attached with the phenanthrene framework at the 3C position of the ring. This was supported by the relatively downfield shift of the methylene H_{3, 4} signals (δ 4.30 and δ 2.38, respectively), which referred to a possible oxygenation in its vicinity. The carboxyl carbon attached to ring A at position 3 confirmed by the HMBC experiment (Table 6B.1). The mass fragment at m/z 101 (C₅H₉O₂) formed due to 2-methyl butyric carboxy radical. The proton at 20-H (δ 2.31) exhibited downfield shift and was attributed to be attached to the carbonyl carbon, and exhibited ¹H-¹H-COSY correlation with the protons at 23-H and 21-H. The ring systems A, B, and C has been affirmed to be connected, and this has been confirmed by the strong ¹H-¹H-COSY correlations between 1-H/2-H, 2-H/3-H/4-H, 6-H/7-H^b/8-H/14-H/13-H, 13-H/15-H/16-H, 12-H/11-H (Figure 6B.4A-B). The methoxy carbon at C-17 (δ 56.14) gives HSQC at 17-H (δ 3.66) singlet (Figure 6B.4C) situated on C-12 by HMBC and hydrogen 12-H attached to C-12 gives peaks at down field δ 4.13 (m) due to it attached to oxygen (Figure 6B.5A-B). The NOESY (Figure 6B.5.C) signal showed that the protons at 3-H and 6-H are aligned to one side, which indicate that the C-O bond at C-3 remains above the plane. In the ¹H-¹H COSY spectrum, couplings were apparent between 1-H (δ 1.38)/2-H (δ 1.72)/3-H (δ 4.30)/4-H (δ 2.38), 6-H (δ 5.33)/7-H (δ 2.00)/8-H (δ 1.52)/11-H (δ 4.13)/12-H (δ 4.13)/13-H (δ 2.03), which support the presence of substituted phenanthrene skeleton with olefinic bonds and oxygenation in the side chain. The proton and carbon connectivity deduced from HSQC and HMBC experiments confirmed the phenanthrene framework attached to the side chain 2-methylbutanoate moiety at the 3rd position of the former (Fig. 6B.4 and 6B.5). The H-H and C-H connectivities apparent in the ¹H-¹H COSY and HMBC spectra respectively indicate that three of the six unsaturations were due to the ring framework. The relative stereochemistry of the chiral centres, particularly that of C-3 and 12 carrying the side chains of the framework and that of C-8, 10, and 20 were deduced from the NOESY spectrum of the compound and the *J*-values. NOE couplings were observed between 3-H α (δ 4.30)/13-H α (δ 2.03) thus indicating that these groups must be equatorial and on the α -side of the molecule (Fig. 6B.5C-D). NOE

correlations between 12-H β (δ 4.13)/10-H β (δ 1.28)/8-H β (δ 1.52) indicated the close proximity of these groups and their β -disposition. Therefore, the C-3 2-methyl butanoate group is axial and β -oriented.

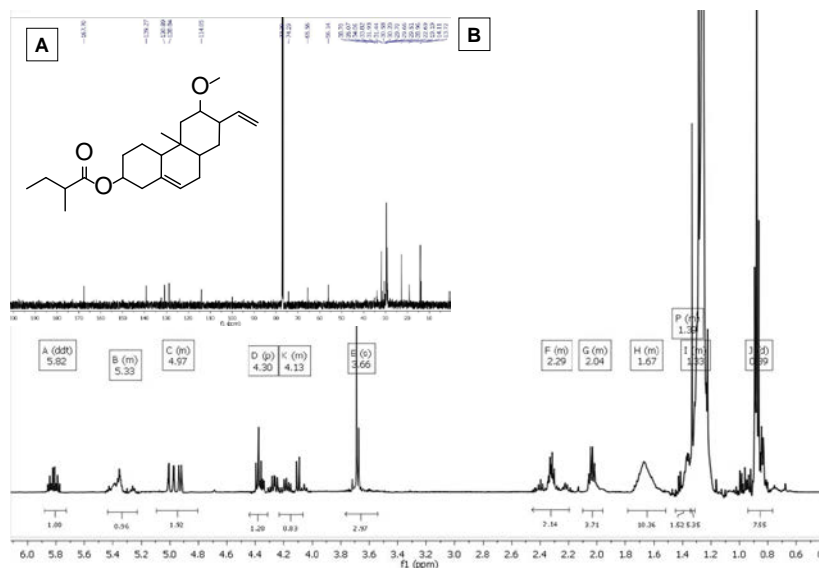


Figure 6B.3
(A) ^{13}C -NMR and (B) ^1H -NMR spectra of 1,2,3,4,4a,4b,5,6,7,8,10,10a-dodecahydro-3-methoxy-4a-methyl-2-vinylphenanthren-7-yl -2-methylbutanoate.

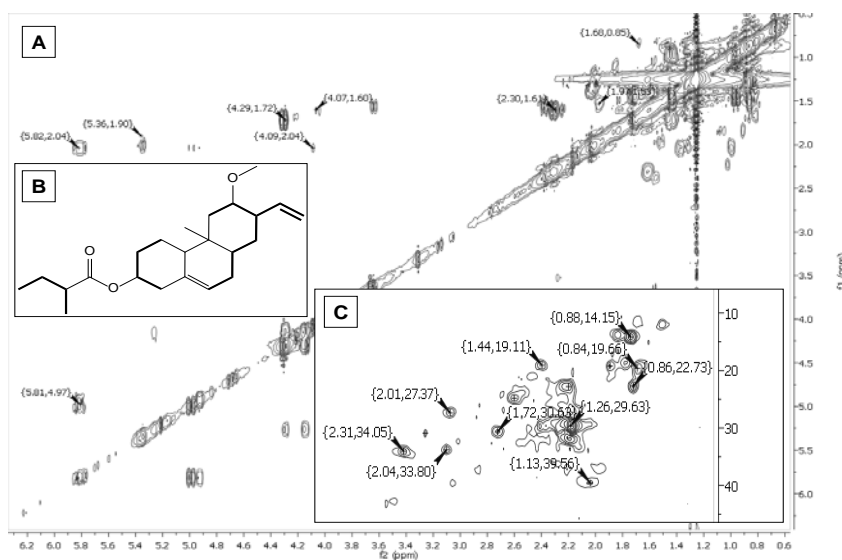


Figure 6B.4
2D NMR correlations in 1,2,3,4,4a,4b,5,6,7,8,10,10a-dodecahydro-3-methoxy-4a-methyl-2-vinylphenanthren-7-yl -2-methylbutanoate. (A) Key ^1H - ^1H COSY couplings; (B) the key ^1H - ^1H COSY couplings have been represented by the bold face bonds; (C) key HSQC correlations.

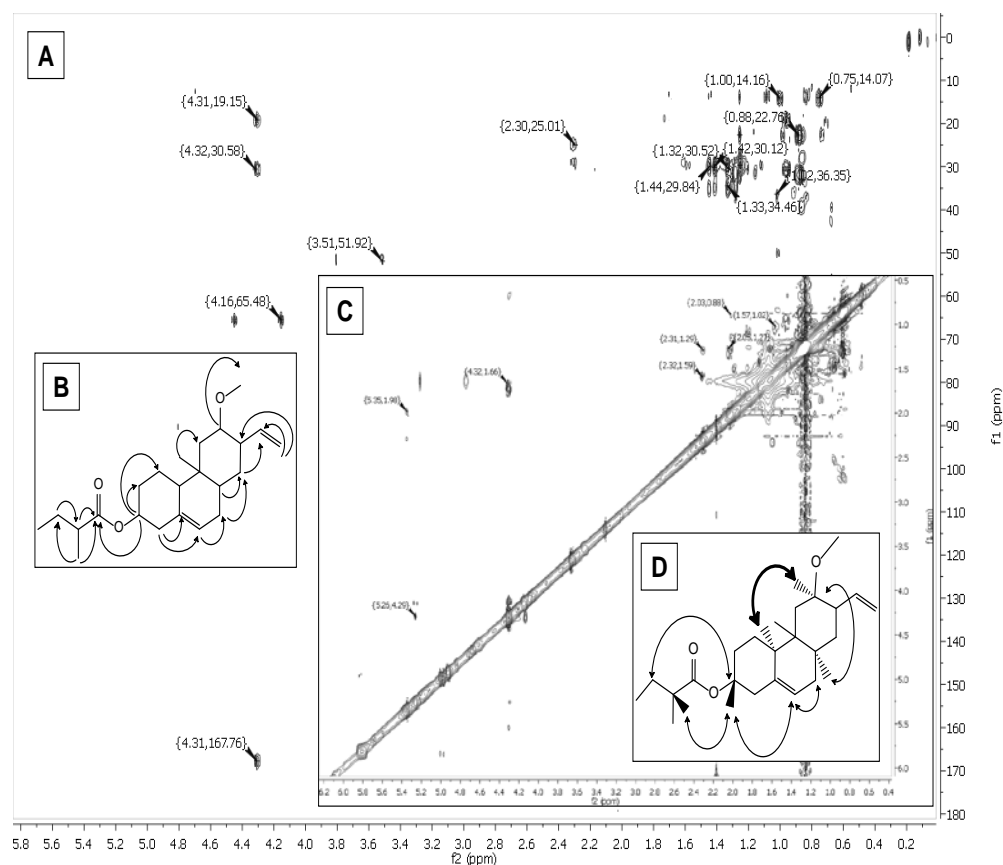


Figure 6B.5

2D NMR correlations in 1,2,3,4,4a,4b,5,6,7,8,10,10a-dodecahydro-3-methoxy-4a-methyl-2-vinylphenanthren-7-yl -2-methylbutanoate. (A) Key HMBC couplings; (B) the key HMBC couplings are indicated as double barbed arrow; (C) key NOESY correlations; (D) The NOE couplings are indicated as double barbed arrow.

6B.3.4 Correlations between Fatty Acids and antibacterial Activity

While analyzing the fatty acid composition of the seaweed associated bacterial flora with antibacterial activity, it was interesting to note that the *Bacillus* strains were found to be rich in *iso* and *anteiso* fatty acid content. A significant correlation between branched chain fatty acids and antibacterial activity of seaweed associated *Bacillus* sp was realized by Pearson correlation analysis (Fig. 6B.6). Antibacterial activity *vis-à-vis iso* and *anteiso* fatty acids were found to be positively correlated, thereby realizing the role branched chain fatty acids in antibacterial properties of seaweed associated *Bacillus* sp.

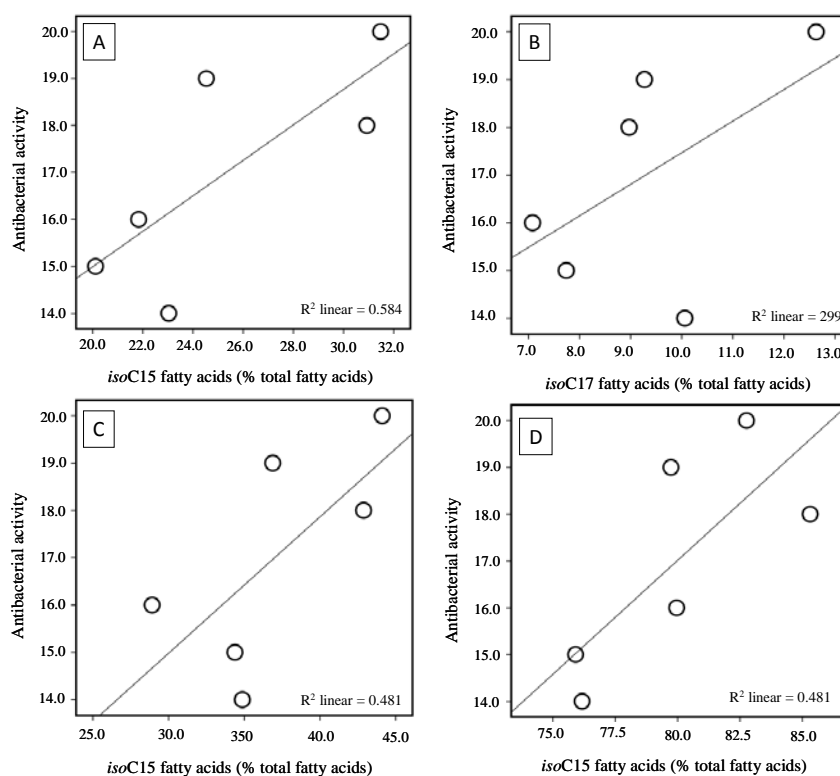


Fig. 6B.6

Correlation between antibacterial activities activity to fatty acid content of the seaweed associated *Bacillus* spp by scatterplot analyses. Scatterplot diagrams showing the correlation of antibacterial activity were shown as A-D.

6B.4 Discussion

The surface of marine organisms such as seaweeds are more nutritious than inanimate material and seawater (Zeng et al. 2005), and have long been known to support abundant populations of bacteria (Ali et al. 2012). Studies of the surface associated microbial communities of seaweeds have provided a considerable deal of knowledge regarding chemical interactions with their host and between members of the microbial community (Penesyan et al. 2009). The study of the chemical ecology of living surfaces of marine organisms and the symbiotic relationships between them and their microbial flora can also provide important biotechnological information with significance for the production of bioactive secondary metabolites. Marine *Bacillus* species was reported to produce versatile

secondary metabolites including lipopeptides, polypeptides, macrolactones, fatty acids, polyketides, and isocoumarins (Amstrong et al. 2001). These structurally diverse compounds exhibit a wide range of biological activities, such as antimicrobial, anticancer, and antialgal activities (Mondol et al. 2013). Kanagasabhpathy et al. (2008) investigated antimicrobial activity of epiphytic bacteria from several red algae and found that the highest activity was produced by certain *Bacillus* species especially *B. cereus* and *B. pumilus*. Our results are in agreement with these studies since the major populations of our isolates were *Bacillus* comprising of *B. subtilis*, *B. amyloliquefaciens* and *B. cereus*.

Marine surface associated microorganisms may require conditions that resemble their native environment in order to produce the maximum amount of bioactives (Penesyany et al. 2009; Ben Ali et al. 2012). It has been known that several epiphytic bacteria lose their ability to produce antimicrobial compounds after many subcultures on artificial growth media (Ben Ali et al. 2012). In the present report the seaweed-associated bacterial strains were maintained on agar slants with a modified seaweed extract agar that mimic the native environment. The active isolates preserved their abilities to produce inhibitory substances against the sensitive pathogens after successive sub-culturing on marine agar giving the persistent inhibition of growth of pathogens over the years, whereas they exhibited reduction in inhibitory zone diameter when they were subjected to routine subculture on marine agar with seaweed supplements. A similar result was reported by Ben Ali et al. (2012) that the antibacterial activity of *Bacillus* sp J9 isolated from seaweed *Jania rubens* showed a decrease of activity when grown after several transfers on marine agar.

A fatty acid profile is a stable phenotypic expression of a bacterial genotype when the bacteria under the study were grown in controlled culture conditions (Welch 1991). Fatty acid metabolism is constitutive and directed by the chromosome, and is not known to be under plasmid control. The presence of certain fatty acids in bacteria has been shown to correlate with taxonomic conventions (Drucker 1976). Hence the patterns of fatty acids, once identified, have resulted in the production of 'fingerprints' of bacteria. This has led to the use

of fatty acid profiles as a key for chemotaxonomic classification. The fatty acid patterns of the various species of *Bacillus* can be divided into two groups, either the *anteiso*_{C15:0} or the *iso*_{C15:0} that are most abundant among the fatty acids (Kaneda 1966). The group, in which the *anteiso*_{C15:0} is most abundant, includes most *Bacillus* species (*B. subtilis* group), whereas the other group, in which *iso* fatty acids are predominantly present (~55%), among which *iso*_{C15} is most abundant (29.4%), includes only the *B. cereus*. The *B. cereus* group had two other features distinguishing it from the remaining species: (i) the range of chain length of the fatty acids is wider, containing C₁₃-*iso* fatty acids (~4%) and small but significant amounts of monounsaturated fatty acids (8.04% of the total) were present (Table 3.4).

The hydroxyl fatty acids such as 3-hydroxytetradecanoic acid (C14:0 3OH) and 2-hydroxy-13-methyltetradecanoic acid (C15:0 *iso* 2OH) were not present in *Bacillus subtilis* (SWI 19, SWI 3, SWI 2, and SWI 4a) and *Bacillus amyloliquefaciens* (SWI 5, SWI 7, SWI 6, and SWI 4B). The only exception being *Bacillus cereus* SWI 1, for which it has been recorded to the tune of 2.83 and 9.69 percent, respectively (Table 3.4, Figure 6B.1A). Hydroxyl fatty acids play a major role in antibacterial activity of *Bacillus cereus*. The hydroxyl group of this group of fatty acids gives them special properties, such as higher viscosity and reactivity when compared with other fatty acids (Hou and Forman 2000). It is significant that these bacteria belonging to *Bacillus subtilis* and *Bacillus amyloliquefaciens* don't contain hydroxyl fatty acids, which have been implicated in the pathogenesis of several diseases such as 3-hydroxymyristic acid (3OH C14:0) that are also associated with lipopolysaccharide compounds (Galanos et al. 1977). Hydroxy fatty acids also reported to exhibit a wide range of antimicrobial activities (Sjogren et al. 2003). Sjogren et al. (2003) proposed that hydroxyl fatty acids readily partition into the lipid bilayers of fungal membrane and increase membrane permeability and the release of intracellular electrolytes and proteins.

Bacillus subtilis and *Bacillus amyloliquefaciens* as in the present study were found to contain many of the cellular fatty acids known to be present in the related species (Kondo and Ueta 1972). The fatty acid compositions of bacteria,

including *Bacillus*, are significantly different from those of higher organisms in having no polyunsaturated fatty acids (fatty acids with more than one unsaturation). The predominance of terminally methyl branched *iso* and *anteiso* fatty acids having 12 to 17 carbons is a characteristic observed in all species of *Bacillus* studied (Weerkamp and Heinen 1972). The normal fatty acids such as myristic and palmitic, the most common fatty acids in the majority of organisms, are generally minor constituents in the genus *Bacillus*. The total content of monoenoic fatty acids was found to be 8.04 percent in *B. cereus* SWI 1 as compared to 2-4 percent in *B. amyloliquefaciens* and 0-4 percent in *B. subtilis* (Figure 6B.1B).

Most common monounsaturated fatty acids in nature are ω -9-isomers (Dart and Kaneda 1970). However, in the present study, *Bacillus subtilis* (SWI 19, SWI 3, and SWI 4a) predominantly were found to contain *cis*-hexadec-5-enoic acid (C16:1 ω 11c) as the sole monoenoic fatty acid (2.77 and 4.15 percent, respectively) (Figure 6B.2). No monoenoic fatty acid was apparent in *Bacillus subtilis* SWI 19 and SWI 2. Interestingly, *cis*-16-methylheptadec-7-enoic acid (C17:1 *iso*- ω 10c) was found to be present in *Bacillus amyloliquefaciens* (SWI 5, SWI7, SWI6, and SWI4B) (<2 percent) other than C16:1 ω 11c (2.8-3.4 percent). In *Leptospira*, up to 50 percent of the cellular fatty acids were reported to be as methyl hexadecanoate (C16:0), the remainder being unsaturated, whilst *T. pallidurn* was found to possess predominantly methyl hexadecanoate, methyl octadecenoate (C18:1) and methyl octadecanoate (C18:0) (Welch 1991). However, the major straight chain fatty acid components of *Bacillus subtilis* (SWI 19, SWI 3, SWI 2, and SWI 4a), as demonstrated in this study were hexadecanoate (C16:0, 10-18 percent in different *Bacillus subtilis* species) and octadecanoate (C18:0, 7-10 percent). The fatty acid C17:0 was found to be absent in *Bacillus subtilis* SWI 2. These fatty acids (saturated straight chain) represent about 10-18 percent in the different species of *Bacillus amyloliquefaciens* (SWI5, SWI 7, SWI 6, and SWI 4B) used in the present study. In addition, minor variations in the fatty acid composition of the different *Bacillus* species studied were recorded. These 'fingerprints' of the *Bacillus* species may therefore have an application for determining their genetic and taxonomic relationships.

The two branched series (*iso* and *anteiso*) of the fatty acids account for 70 to 82 percent of the total acids in *Bacillus subtilis*, and 76 to 85 percent of the total acids in *Bacillus amyloliquefaciens* (Figure 6B.1B). The unsaturated fatty acids are generally absent or present only in very small amounts in the *Bacillus* species as also supported by earlier studies (Kaneda 1969). Earlier it has been reported that bacterial cells can maintain membrane fluidities at stress environmental conditions (Hazel 1995). This adaptation is largely accomplished by changing membrane fatty acid chain length, unsaturation degree, and branching pattern. Proper membrane fluidity of the bacterial cells grown at extreme conditions can be achieved by increasing unsaturated fatty acid, branched chain fatty acids, and shorter-chain fatty acids (Suutari, and Laakso 1994).

The tolerance of marine bacteria grown at laboratory culture conditions depends to a significant extent on a greater proportion of the above-described fatty acids in the membrane. Earlier reports indicated that *L. monocytogenes* increased its *anteiso*_{C15:0} content to more than 70 percent when grown at low temperatures because lipids containing *anteiso*_{C15:0} have significantly lower phase transition temperatures than those containing *iso* fatty acids and/or *anteiso*_{C17:0} (Kaneda 1991). The higher contents of *anteiso*_{C15:0}, with its effects on membrane fluidity (Jones et al. 2002), enables this organism to grow at artificial growth media. We wanted to demonstrate how *Bacillus subtilis* and *Bacillus amyloliquefaciens* produce their characteristically high content of *anteiso*_{C15:0}. Fatty acid chain shortening was a critical response to further increase the *anteiso*_{C15:0} level when the total *anteiso* content was already high (Kaneda 1991). Therefore, a greater proportion of *anteiso*_{C17:0} probably could not support growth at culture conditions as also evident from the higher proportion of *anteiso* fatty acids (*anteiso*_{C15} and *anteiso*_{C17}) in the *Bacillus* species (higher than 4% in SWI 3 and SWI 4a). It is noteworthy that *B. subtilis* could increase its *anteiso*:*iso* fatty acid ratio (>1.0), but could not efficiently shorten fatty acid chain length under their symbiotic growth condition. As a result, *anteiso*_{C15:0} content in *B. subtilis* was significantly higher (~40%) in *Bacillus subtilis*.

The fatty acid pattern of a given species of *Bacillus* can act as a "fingerprint" if the organism is grown under culture conditions where the exogenous supply of the precursors of chain initiators including the "naturals" supplied through the host extract is significant. It was reported that 2-methylbutyric acid, a precursor of *anteiso* fatty acids, restored the *anteiso*_{C15:0} content, membrane fluidity, and growth of the mutants at low temperatures, whereas isobutyrate and isovalerate, precursors of *iso* fatty acids, did not (Zhu et al. 2005). Hence, as far as adaptation of the bacterial species in the artificial culture conditions is concerned, the central strategy is to increase the proportion of *anteiso*_{C15:0} and the compounds related to 2-methyl butyric acid (Zhu et al. 2005).

The complex seaweed extract medium might provide considerable amounts of dodecahydro-3-methoxy-4a-methyl-2-vinylphenanthren-7-yl 2-methylbutanoate to the culture medium that biosynthetically converted to the precursor molecules (isoleucine and 2-methylbutyric acid) of the branched-chain α -keto acids and branched chain amino acids (Figure 6B.7), thereby causing the increased formation of *anteiso* C₁₅ and C₁₇ fatty acids. It is significant to note that the fatty acids present in *Bacillus subtilis* (SWI 2) grown on a medium containing Zobell Marine agar supplemented with seaweed extract with substituted vinylphenanthrenyl methylbutanoate resulted in the optimum growth of the bacterial species. In support of this, recent reports have shown that two species of thermophilic *Bacillus* (Weerkamp and Heinen 1972) and some species of *Propionibacterium* (Moss et al. 1969) synthesize *iso*_{C15:0} acid most abundantly, but neither shorter-chain fatty acids (C12 and C13) nor unsaturated fatty acids are synthesized in any significant amounts. Although the number of species examined in the present study in a given genus is rather limited, the pattern seems to be uniform within these genera.

The preferential incorporation of α -(2)-methyl butyrate into *anteiso*_{C15} indicates that the terminal isobutyryl group (C-15 and C-17) must be derived from isobutyrate. Furthermore, the greatly increased formation of *anteiso*_{C15:0} in the presence of precursor compounds present in the seaweed extract might provide the

substrate for biosynthesis of branched chain fatty acids in the culture medium. This also indicated that the formation of the terminal isobutyryl group is a rate-limiting factor for the synthesis of *anteiso*_{C15:0} in *B. subtilis* (Brock et al. 1967). In the present study, the secondary metabolite dodecahydro-3-methoxy-4a-methyl-2-vinylphenanthren-7-yl 2-methylbutanoate isolated from the CH₂Cl₂/MeOH extract of seaweed *Anthophycus longifolium* might be the precursor, which possibly undergoes the elimination of dodecahydro-6-methoxy-4b-methyl-7-vinylphenanthren-2-ol to afford 2-methylbutyric acid. The latter is a known precursor compound of isoleucine, which subsequently afford the branched chain amino acids belonging to *anteiso*_{C15:0} and *anteiso*_{C17:0} series. As shown under the Figure 6B.7, 2-amino-3-methylpentanoic acid (isoleucine), which might be synthesized from 2-methylbutyric acid undergo deamination by branched-chain amino acid transaminase yielding 2-keto-3-methyl valerate. The later undergo dehydrogenation by branched-chain 2-keto acid dehydrogenase to afford enzyme bound 2-methyl-butyryl-S-CoA.

The enzyme fatty acyl synthase builds the fatty acid products from a 2-methyl butyrate starter unit and malonate extender units. The chain extension might be initiated by decarboxylation of malonyl-S-ACP to 4-methyl-3-oxo-hexanoyl S-ACP by the KS domain. A series of condensation and chain extension reactions involving the enzyme cascades β -hydroxyacyl-ACP-dehydrase (DH), enoyl reductase (ER), and ketoreduactase (KR) afforded ante-iso C_{15:0} S-ACP via the reaction intermediates such as 6-methyl-3-hydroxy-octanoyl S-ACP, 6-methyl-oct-2-enoyl S-ACP, and 4-methyl-octanoyl S-ACP. Thiolase catalyzed elimination of the water molecule from *anteiso*_{C15:0} S-ACP afforded *anteiso*_{C15:0} followed by another extension cycle of fatty acid synthase that resulted in *anteiso*_{C17:0}. The fact that the seaweed extract led to the formation of appreciable quantities of *anteiso*_{C15:0} and *anteiso*_{C17:0} supported the hypothesis that the compound present in the seaweed might provided the substrate for biosynthesis.

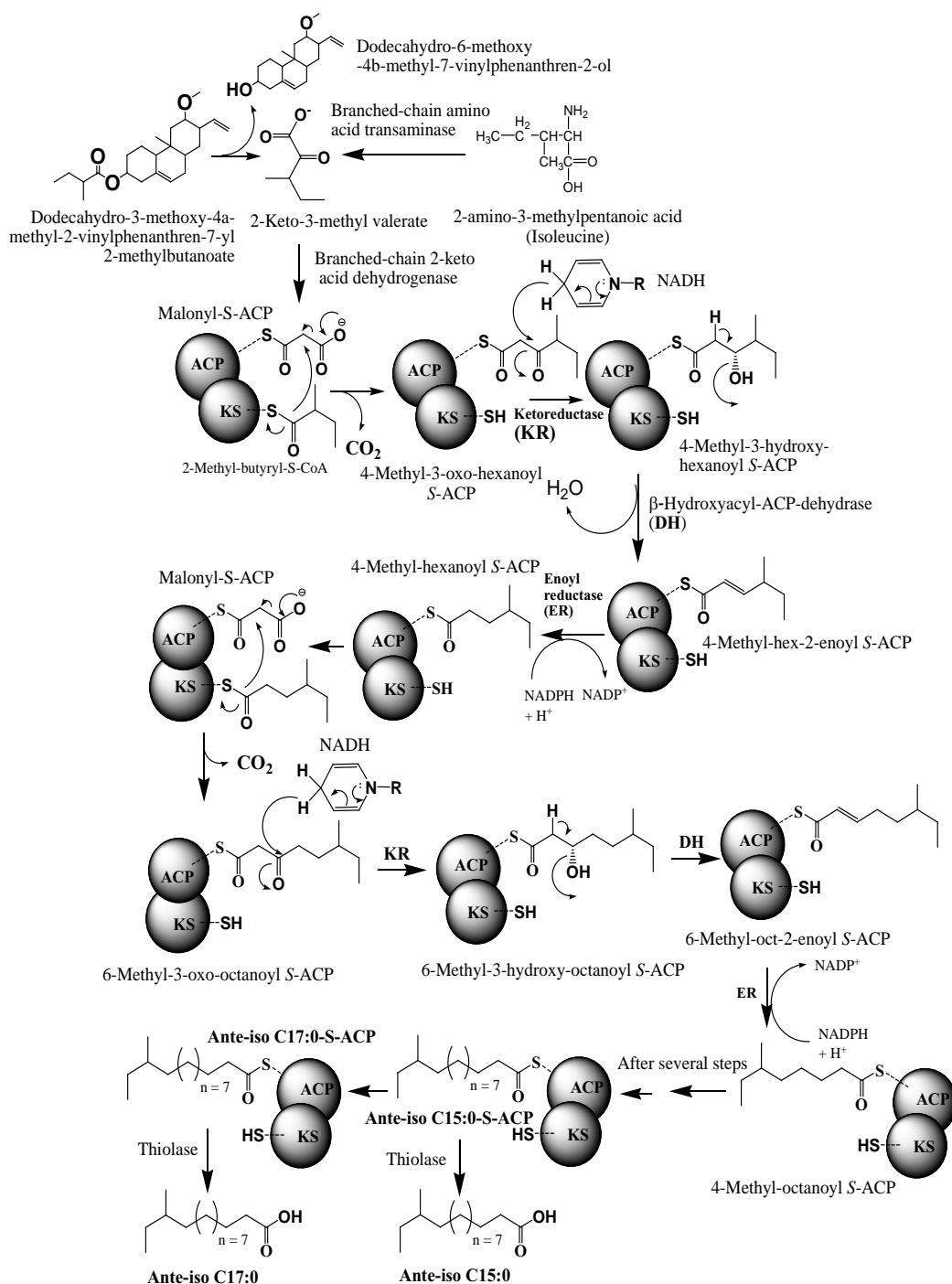


Fig. 6B.7

Hypothetical sequence of events for biosynthesis of the bacterial fatty acids *anteiso*_{C15:0} and *anteiso*_{C17:0} fatty acids from the precursor 2-keto-3-methyl valerate, showing the loading, decarboxylation and elongation steps catalysed by the fatty acid synthase.

Dodecahydro-3-methoxy-4a-methyl-2-vinylphenanthrenyl-2-methylbutanoate isolated from the MeOH-EtOAc extract of seaweed *Anthophycus longifolium* transformed to dodecahydro-6-methoxy-4b-methyl-7-vinylphenanthren-

2-ol and 2-methylbutyric acid (2-keto-3-methyl valerate), the biosynthetic precursor of branched chain *anteiso* fatty acids. The enzyme builds the fatty acid products from a 2-methyl butyrate starter unit and malonate extender units. The intermediates shown bound to the PKSs are hypothetical, but consistent with experimental results. (1) Chain extension is initiated by decarboxylation of malonyl-S-ACP to 4-methyl-3-oxo-hexanoyl S-ACP by the KS domain, (2) 4-methyl-3-hydroxy-hexanoyl S-ACP converted to 4-methyl-hex-2-enoyl S-ACP by the enzymatic action of β -Hydroxyacyl-ACP-dehydrase (DH); (3) enoyl reductase (ER) converts 4-methyl-hex-2-enoyl S-ACP to 4-methyl-hexanoyl S-ACP; (4) the 4-methyl-hexanoate group is then passed from the ACP to the active site cysteine of the KS and the ACP is loaded with another unit of malonate and then KS-catalysed condensation takes place resulting in 6-methyl-3-oxo-octanoyl S-ACP; (5) Another cycle of chain extension starts to yield *ante-iso* C_{15:0} S-ACP via the reaction intermediates such as 6-methyl-3-hydroxy-octanoyl S-ACP, 6-methyl-oct-2-enoyl S-ACP, and 4-methyl-octanoyl S-ACP; (6) thiolase catalyzes the elimination of the water molecule in the intermediate product to afford *anteiso* C_{15:0}; (6) Another extension cycle of fatty acid synthase results in *anteiso* C_{17:0} S-ACP and resultant thiolase catalyzed *anteiso* C_{17:0}.

In this study, we have attempted to make a correlation of the fatty acid contents of the seaweed-associated bacteria with their antibacterial activity. Antibacterial activity and *iso/anteiso* fatty acids were found to be positively correlated (Figure 6B.6). The Pearson correlation analysis of the fatty acid contents of the seaweed associated bacterial isolates *vis-à-vis* the antibacterial activities of these isolates to the pathogen tested.

A positive correlation between the total branched chain *iso* and *anteiso* fatty acids *vis-à-vis* the antibacterial activities ($r^2=0.570$) against pathogenic bacteria demonstrated the ecological relationship between the *pks* genes regulating branched chain fatty acid biosynthesis and antibacterial activity of the seaweed-associated *Bacillus* sp. It is of note that during the correlation analysis *pks* negative strains were omitted as they were found to deviate from this correlation. This apparently demonstrated the role of PKS enzymes in the production of antibacterial compounds as also demonstrated in our earlier study (chapter 5A). The strains with *pks* genes were found to possess greater antibacterial activity whereas *pks* negatives had lesser activity even though they had a greater content of branched chain *iso* and *anteiso* fatty acids.

6B.5 Conclusions

Fatty acid methyl ester derivatives were examined as a means of characterizing seaweed-associated bacterial isolates *Bacillus subtilis* (SWI 19, SWI 3, SWI 2, and SWI 4a), *Bacillus amyloliquefaciens* (SWI 5, SWI 7, SWI 6, and SWI 4B), and *Bacillus cereus* SWI 1, and studying the differential composition of branched chain *iso* and *anteiso* fatty acids to understand their effects on the bioactivity and viability. The group, in which the *anteiso*_{C15:0} was most abundant, includes most *Bacillus* species (*B. subtilis* group), whereas the other group, in which *iso* fatty acids were predominantly present (~55 percent), among which iso-C₁₅ was most abundant (29.4 percent), includes only the *B. cereus*. This also accounts for the dominance of *Bacillus* sp in seaweed associated culturable isolates. Fatty acids present in grown on a medium containing Marine agar supplemented with seaweed extract resulted in optimum growth of the bacterial species. The addition of seaweed extract containing dodecahydro-3-methoxy-4a-methyl-2-vinylphenanthren-7-yl 2-methylbutanoate, to the culture medium caused the increased formation of *anteiso* fatty acids (*anteiso*_{C15:0}) related to these fatty acid substrates. The present study demonstrated how the seaweed associated epiphytic bacterial flora utilize the precursors from the host seaweeds to biosynthesize greater contents of the branched chain fatty acids, which provide greater stability and antibacterial activity of the bacterial flora under laboratory culture conditions.

CHAPTER 7

SUMMARY AND CONCLUSION

Disease caused by bacterial pathogens has been widely recognized as a major cause of economic loss in many commercially cultured fish and shellfish species the world over, with mortality of larval stages in hatcheries and the growout stages in different mariculture systems. Pathogenic vibrios are involved in significant mortalities in the larviculture and grow out phases of famed fishes. In an attempt to control the proliferation of pathogenic vibrios, the prophylactic and therapeutic use of antibiotics has been practiced in commercial hatcheries, creating more serious problem of antibiotic resistance among the microflora in the environment. The problem of antibiotic resistance and its epidemiological consequences led to the exploration of several alternate approaches for disease management in mariculture systems. Amongst them the most popular and practical approach is the use of aquaculture-grade chemicals from beneficial bacterial sources as prophylactics.

Control of the unwanted microorganisms is essential in all aspects of life, and microbial diseases must be treated in humans, animals, and plants. Emergence of antibiotic resistant bacteria and the need for novel, antimicrobial compounds led to the exploration of new habitats to screen the production of bioactive substances. Seaweeds and microbial populations associated with seaweeds constitute the major biologically active flora of marine food pyramid due to their enormous biodiversity. Due to a competitive role for space and nutrient, the marine bacteria associated with marine macroorganisms, invertebrates and seaweeds could produce more antibiotic substances. These marine microbial symbionts are possibly the true producers or take part in the biosynthesis of potential antimicrobial substances. These seaweed associated bacteria are able to produce antimicrobial compounds

and this response represents a chemically induced defense response when the host seaweed is faced with a potential competing organism in the marine environment. Kubaneck et al. (2003) have found antifungal compounds from seaweeds, which were structurally related to microbial compounds. The antimicrobial compounds could be the byproduct of symbiosis between the seaweed and an as-yet unidentified microbe. This hypothesis could explain why the seaweeds are rarely infected, despite constant exposure to potentially deleterious microorganisms. Quevarin et al. (2014) have carried out similar studies in sponges, and have proven to have homologous compounds in both host and their associated microbes. Based on this background it is necessary to have insight into the ecological interactions between different seaweed species and related marine ecosystem. Therefore the potential of exploring the antimicrobial lead molecules of seaweed-associated microbial flora is highly promising one, and offer a multitude of potential applications in various fields of biotechnology.

Seaweed-associated heterotrophic bacterial communities were screened to isolate potentially useful antimicrobial strains. In this study, 234 bacterial strains were isolated from 7 seaweed species in Gulf of Mannar of the South-East coast of India. The strains having consistent antagonistic activity were chosen for further studies, and this constituted about 9.8% of the active strains isolated. The bioactive strains were shortlisted and phylogenetically analyzed. Phylogenetic analysis using 16S rDNA sequencing, assisted with classical biochemical identification indicated the existence of two major phyla, *Firmicutes* and *Proteobacteria*. The antagonistic bacterial isolates have been submitted to the Microbial Type Culture Collection and Gene Bank (MTCC) of Institute of Microbial Technology (Chandigarh, India), an International Depository Authority under the Budapest Treaty. The possibility to encode the active metabolite gene by plasmids were further analysed and they were subsequently screened for the presence of metabolite genes involved in important natural product biosynthetic pathway.

Antimicrobial activity analysis combined with the results of amplifying genes encoding for polyketide synthetase (PKS-I) and nonribosomal peptide synthetase (NRPS) shown that seaweed-associated bacteria had broad-spectrum

antimicrobial activity and potential natural product diversity, which further proved that these microbes are valuable reservoirs of novel bioactive metabolites. These epibionts might be beneficial to the seaweeds by limiting or preventing the development of competing or fouling bacteria. Phylogenetic analysis of ketosynthase regions with respect to the diverse range of ketosynthase (KS) domains showed that the KS domains from the candidate isolates were of type I. Seaweed-associated bacteria with potential antimicrobial activity suggests the seaweed species as an ideal ecological niche harboring specific bacterial diversity representing a largely underexplored source of novel antimicrobial secondary metabolites.

Further studies with these isolates were focussed to identify the potential lead antimicrobial compounds from the seaweed-associated bacterial flora, and to unravel their biotechnological potential. Bioprospecting of antibacterial metabolites in *Bacillus subtilis* MTCC 10403 (SWI2) associated with brown seaweed *Anthophycus longifolium* revealed the bacterium is a promising bacterial candidate for bioprospecting. A total of six antibacterial metabolites, namely, 7-O-methyl-5'-hydroxy-3'-heptenoate-macrolactin (**1**), 6-(4-acetylphenyl)-5-hydroxyhexanoic macrolactin (**2**), 2-(7-(2-ethylbutyl)-2,3,4,4a,6,7-hexahydro-2-oxopyrano [3,2-b] pyran-3-yl) ethyl benzoate (**3**), methyl-3-(2-((E)-2-(2-(furan-2-yl)ethyl)-1-hydroxy-6-methylhept-4-en-3-yl)-1,2,3,4,4a,5,6,8a-octahydronaphthalen-7-yl) propanoate (**4**), 5a,6,7,8,9,9a-hexahydro-7-isopentyl-8-methoxynaphtho[2,1-b]furan (**5**) and methyl 3-(4a,5,6,8,8a,9-hexahydro-4-((E)-3-methylpent-1-enyl)-4H-furo[3,2-g]isochromen-6-yl) propanoate (**6**) were purified from the crude ethyl acetate-methanol extract (1:1, v/v) of the bacterial isolate. All the isolated compounds exhibited broad spectrum antagonistic activities to the tested pathogens.

The past decade witnessed the discovery of various polyketide leads from bacterial sources with tremendous importance in food control and human health perspective. The newly evolving antibacterials bearing the polyketide backbone will be increasingly important keeping in mind the development of multi-drug resistant bacteria and pathogenic microorganisms against the existing antibiotics

and related molecules. In this study, two new variants of macrolactin, 7-O-methyl - 5'-hydroxy-3'-heptenoate-macrolactin and 6-(4-acetylphenyl)-5-hydroxyhexanoic macrolactin were described. These novel polyketide product holds promise to develop new generation drug candidates for use against the multiresistant microbial pathogens. The evidence for a biosynthetic route of macrolactin has been provided, and this may lead to the identification of a new target for antimicrobial lead molecule discovery programs. The results of this screening led to the conclusion that these polyene antibiotics are widespread metabolites of seaweed-associated bacterial populace particularly belonging to *Bacillus* species.

Bacillus amyloliquefaciens MTCC10456 isolated from the seaweed *Laurenciae papillosa* demonstrated a promising antibacterial spectrum. *B. amyloliquefaciens* MTCC10456 demonstrated a positive hit for polyketide synthase gene with an accession number of KC607821. This showed the conceivable vicinity of antimicrobial activity of the seaweed associated bacterial isolate with the polyketide metabolite pathway. Two novel substituted carboxylate analogues, 3- (octahydro-9-isopropyl-2H- benzo [h] chromen-4-yl) - 2-methylpropyl benzoate (**7**) and 3- (octahydro-9-isopropyl-2H- benzo [h] chromen-4-yl) - 2- methylpropyl benzoate (**8**) were isolated upon repeated bioassay guided chromatography over silica columns. The compound **7** exhibited significantly greater activity against the test pathogens (at a concentration of 20 µg per disc) than **8**.

Bioprospecting of antibacterial metabolites in bacteria *B. subtilis* MTCC 10407 associated with seaweed *Sargassum myriocystum* yielded two novel *O*-heterocycle pyrans, 2-(7-(2-ethylbutyl)-2,3,4,4a,6,7-hexahydro-2-oxopyrano[3,2-b]pyran-3-yl)ethyl benzoate (**9**) and 2-((4Z)-2-ethyl-octahydro-6-oxo-3-((E)-pent-3-enylidene)pyrano[3,2-b]pyran-7-yl)ethyl benzoate (**10**). Similarly bioprospecting of antibacterial metabolites in antagonistic bacteria *B. amyloliquefacens* MTCC 10456, which is a biochemically identical strain associated with seaweed *Padina gymnospora* demonstrated the presence of multiple antibacterial compounds. The bacterium was similar in biochemical activities to MTCC 10456, with a different antibacterial spectrum to the pathogens tested. Hence the strain is designated in the

study as *B. amyloliquefacens* MTCC 10456^B. The crude ethyl acetate extract of *B. amyloliquefacens* yielded four antibacterial compounds, namely, 10-(15-butyl-13-ethyl-2-oxotetrahydro-2H-pyranyl)propyl-2-methylbenzoate (**11**), 7,8-dihydro-7-(15-hydroxypropan-14-yl)-8-isobutylbenzo[c]oxepin-1(9H)-one (**12**), 13-(amino methyl)-11-hydroxyoctanyl 10-phenylpropanoate (**13**) and 9-(tetrahydro-12-isopropyl-11-oxofuran-10-yl) ethyl 4-ethoxy-2-hydroxybenzoate (**14**). The recognition of antimicrobial metabolites from seaweed-associated marine bacteria, further reinforces the theory that microbial metabolites of the symbiotic microorganisms helps in chemical defences of the host species against the pathogenic and fouling microorganisms, indicating an ecological role of microbial metabolites in host bacterial interaction in these marine organisms.

Chemically driven interactions are important in the establishment of cross relationships between marine surface-associated microorganisms and their eukaryotic host. It is therefore, that the seaweed–bacterial ecological interactions were studied by comparing the antibacterial metabolites of colonizing bacteria with its host derived seaweed secondary metabolites. Two homologous compounds, namely, 3-(methoxycarbonyl)-4-(5-(2-ethylbutyl)-5, 6-dihydro-3-methyl-2H-pyran-2-yl)butyl benzoate (**15**) and 2-(8-butyl-3-ethyl-3,4,4a,5,6,8a-hexahydro-2H-chromen-6-yl)ethyl benzoate (**16**) have been isolated from the ethyl acetate extract of host seaweed *Sargassum myriocystum*. It is interesting to note that the tetrahydropyran-2-one moiety of the tetrahydropyrano[3,2-b]pyran-2(3H)-one system of compound **9** might be cleaved by the metabolic pool of seaweeds to afford methyl 3-(dihydro-3-methyl-2H-pyranyl) propanoate moiety of compound **15**, which was found to have no significant antibacterial activity. It is therefore imperative that the presence of dihydro-methyl-2H-pyran-2-yl propanoate system is essentially required to impart the greater antibacterial activity. The biotransformation of the bacterial metabolite 3-(methoxycarbonyl)-4-(5-(2-ethylbutyl)-5, 6-dihydro-3-methyl-2H-pyran-2-yl) butyl benzoate (**15**) in seaweed might contribute to the adaptive mechanism of the seaweed to form a tougher cell wall to resist the pathogenic bacterial flora in the oceanic ecosystem. Thus, there exists an interesting chemical ecological interaction between the secondary metabolites produced by the seaweed bacteria and the seaweed host organism. The

antibacterial compound **10** isolated from the ethyl acetate extract of from *B. subtilis* MTCC 10407 and **16** from seaweed *Sargassum myriocystum* shared similar structures, and therefore, might be the result of the identical metabolic pool of seaweed and bacteria. In particular the presence of ethyl benzoate moiety in **10** and **16** from seaweed-associated bacteria and seaweed strongly suggested the ecological and metabolic relationship between these compounds. The seaweed derived metabolite **16** did not show an appealing antibacterial property, and therefore, it can be concluded that the compound has a different role, probably related to structural functionality of seaweed. The fact that polyketides of this type are unprecedented from seaweed and the structural similarity of the seaweed derived homologous compounds to the microbial metabolites suggested that these could be the products of symbiont, and it is biotransformed by the seaweed metabolic pool.

The bioactivity of bacterial species grown under symbiotic condition depends on several abiotic and biotic factors, among which the growth environment plays a major role. The fatty acid profiles of the seaweed associated antagonistic bacilli are found to have an increased amount of *iso* and *anteiso* fatty acids. The *pks* gene is the functional gene determining the bacterial active metabolite, and also there were reports that the seaweed derived polyketide metabolites are related to the bacterial metabolites. Polyketide biosynthesis has much in common with fatty acid biosynthesis, and was reported to have multiple role determining the bioactivity and growth in artificial culture media. Not only are they alike in the chemical mechanisms involved in chain extension but also in the common pool of simple precursors employed, such as, acetyl coenzyme A (CoA) and malonyl-CoA (MCoA) units. It was hypothesized that there might be a relation in the presence of fatty acids, antibacterial activity, and the presence of functional *pks* genes responsible for the antibacterial activity of the seaweed-associated bacterial flora. It is therefore the analysis of bioactive cultivable antagonistic heterotrophic bacterial communities associated with the intertidal seaweeds was carried out to understand the effect of seaweed extract and the metabolic precursors of the seaweed extract on the growth and fatty acid profile of the bacterial species, and to understand the chemical ecological relationship between

the host seaweed and their associated bacterial flora. Fatty acid methyl ester derivatives were examined as a means of characterizing seaweed-associated bacterial isolates and studying the differential composition of branched chain *iso* and *anteiso* fatty acids to understand their effects on the bioactivity. The addition of seaweed extract containing dodecahydro-3-methoxy-4a-methyl-2-vinylphenanthren-7-yl 2-methylbutanoate, to the culture medium caused the increased formation of *anteiso* fatty acids (*anteiso*_{C15:0}) related to these fatty acid substrates. The present study demonstrated how the seaweed associated epiphytic bacterial flora utilize the precursors from the host seaweeds to biosynthesize greater contents of the branched chain fatty acids, which provide greater stability and antibacterial activity of the bacterial flora under the laboratory culture conditions.

With the expanding requirement for novel medication revelation, seaweed-associated marine epibiotic bacteria with potential antimicrobial activity proposes the seaweed species as an ideal ecological niche harboring specific bacterial diversity representing a largely underexplored source of novel antimicrobial secondary metabolites. These epibionts might be beneficial to the seaweeds by limiting or preventing the development of competing, pathogenic and fouling bacteria. The recently advancing antibacterials bearing the polyketide backbone will be progressively vital remembering the development of multi-drug resistant bacteria and pathogenic microorganisms against the existing antibiotics and related molecules. The fact that polyketides of this type are unprecedented from seaweeds and the structural similarity of the seaweed derived homologous compounds to the microbial metabolites suggested that these could be the products of symbiont, and it is biotransformed by the seaweed metabolic pool. The present study also strengthened the hypothesis that seaweed associated epiphytic bacterial flora utilize the precursors from the host seaweeds. The present work may have an impact on the exploitation of antibacterial lead molecules from seaweed-associated bacterial flora for food, pharmaceutical and biotechnological applications.

- Aassila, H., Bourguet-Kondracki, M.L., Rifai, S., Fassouane, A., and Guyot, M. 2003. Identification of Harman as the Antibiotic Compound Produced by a Tunicate-Associated Bacterium. *Marine Biotechnology*, 5:163–166.
- Acebal, C., Canedo, L. M., Puentes, J.L.F., Baz, J.P., Romero, F., de la Calle, F., Gravalos, M.D.G., and Rodriguez, P. 1999. Agrochelin, a new cytotoxic antibiotic from a marine Agrobacterium - Taxonomy, fermentation, isolation, physico-chemical properties and biological activity. *The Journal of Antibiotics*, 52 (11): 983-987.
- Aggarwal, D., Fernandez, M. L., and Soliman, G. A. 2006. Rapamycin, an mTOR inhibitor, disrupts triglyceride metabolism in guinea pigs. *Metabolism*, 55(6): 794-802.
- Alanis, A. J. 2005. Resistance to antibiotics: are we in the post-antibiotic era? *Archives of Medical Research*, 36 (6): 697-705.
- Alavandi, S.V., Vijayan, K.K., Santiago, T.C., Poornima, M., Jithendran, K.P., Ali, S.A., and Rajan, J.J.S. 2004. *Fish and Shellfish Immunology*, 17:115-120.
- Ali, A.I.B., Bour, M.E., Ktari, L., Bolhuis, H., Ahmed, M., Boudabbous, A., and Stal, L.J. 2012. *Jania rubens*-associated bacteria: molecular identification and antimicrobial activity. *Journal of Applied Phycology*, 24 (3): 525–534.
- Anand, T. P., Bhat, A. W., Shouche, Y. S., Roy, U., Siddharth, J., and Sarma, S. P. 2006. Antimicrobial activity of marine bacteria associated with sponges from the waters off the coast of South East India. *Microbiological Research*, 161: 252–262.
- Annous, B.A., Becker, L.A., Bayles, D.O., Labeda, D.P., and Wilkinson, B.J. 1997. Critical role of anteiso-C_{15:0} fatty acid in the growth of *Listeria monocytogenes* at low temperatures. *Applied and Environmental Microbiology*, 63: 3887-3894.
- Arguelles-Arias, A., Ongena, M., Halimi, B., Lara, Y., Brans, A., Joris, B., and Fickers, P. 2009. *Bacillus amyloliquefaciens* GA1 as a source of potent antibiotics and other secondary metabolites for biocontrol of plant pathogens. *Microbial Cell Factories*, 8: 2859-2863.

- Armstrong, E., Yan, L., Boyd, K.G., Wright, C.P., and Burgess, J.G. 2001. The symbiotic role of marine microbes on living surfaces. *Hydrobiologia*, 461: 37–40.
- Austin, B. 1989. Novel pharmaceutical compounds from marine bacteria. *Journal of Applied Bacteriology*, 67: 461–470.
- Ayuso-Sacido, A., and Genilloud, O. 2005. New PCR primers for the screening of NRPS and PKS-I systems in actinomycetes: detection and distribution of these biosynthetic gene sequences in major taxonomic groups. *Microbial Ecology*, 49(1): 10–24.
- Bacque, E., Barriere, J.C., and Berthaud, N. 2005. Recent progress in the field of antibacterial pristnamycins. *Current Medicinal Chemistry -Anti-Infective Agents*, 4:185–217.
- Baharum, H., Schlinglo, A., Morita, H., Omitsuka, A., Lee, F.C., Kim-Yong, N.G., Rahim, R.A., Abe, I., and Ho, C.L. 2011. Molecular cloning, modeling, and site-directed mutagenesis of type III polyketide synthase from *Sargassum binderi* (Phaeophyta). *Marine Biotechnology*, 13 (5): 845–856.
- Barber, M. S. 2001. The future of cephalosporins business. *Chimica Oggi*, 19:9–13
- Barja, J.L., Lemos, M.L., and Toranzo, A.E. 1989. Purification and characterization of an antibacterial substance produced by a marine *Alteromonas* species. *Antimicrobial Agents and Chemotherapy*, 33:1674–1679
- Bauer, A.W., Kirby, W.M., Sherris, J.C., and Turck, M. 1966. Antibiotic susceptibility testing by a standardized single disk method. *Am J Clin Pathol*, 45 (4): 493–496
- Berdy, J. 2005. Bioactive microbial metabolites, A personal view. *The Journal of Antibiotics*, 58:1–26.
- Bernan, V.S., Greenstein, M. and Maiese, W.M. 1997. Marine microorganisms as a source of new natural products. *Advances in Applied Microbiology*, 43:57–90.
- Bhatt, C. B., Stark, W., Harvey, B. M., Gallimore, A. R., Demydchuk, Y. A., Spencer, J. B., Staunton, J., and Leadlay, P.F. 2005. Accumulation of an *E,E,E*-triene by the monensin producing polyketide synthase when

- oxidative cyclization is blocked. *Angewandte Chemie International Edition*, 117: 7237-7240.
- Blunt, J.W., Copp, B.R., Hu, W.P., Munro, M.H.G., Northcote, P.T., and Prinsep, M.R. 2009. Marine natural products. *Natural Products Reports*. 26: 170–244.
- Borel, J.F. 2002. History of the discovery of cyclosporin and of its early pharmacological development. *Wiener klinische Wochenschrift*, 114 (12): 433-437.
- Boyd, K.G., Adams, D.R., and Burgess, J.G. 1999. Antibacterial and repellent activities of marine bacteria associated with algal surfaces. *Biofouling*, 14 (3): 227-236.
- Brock, D.J.H., Kass, L.R., and Bloch, K. 1967. Beta-hydroxy decanoyl thioester dehydrase. II. Mode of action. *The Journal of Biological Chemistry*, 242 (19): 4432-4440.
- Burgess, J.G., Boyd, K.G., Amstrong, E., Jiang, Z., Yan, L., Berggren, M., May, U., Pisacane, T., Granmo, A., and Adama, D.R. 2003 .The development of a marine natural product-based antifouling paint. *Biofouling*, 19: 197-205.
- Burgess, J.G., Jordan, E.M., Bregu, M., Mearns-Spragg, A., and Boyd, K.G. 1999. Microbial antagonism: a neglected avenue of natural products research. *Journal of Biotechnology*, 70 (1-3): 27–32.
- Burkhold, P.R., Pfister, R.M., and Leitz, F.H. 1966. Production of a pyrrole antibiotic by a marine bacterium. *Applied Microbiology*, 14: 649–653.
- Calderone, C. T., Kowtoniuk, W. E., Kelleher, N. L., Walsh, C. T., and Dorrestein, P. C. 2006. Convergence of isoprene and polyketide biosynthetic machinery: isoprenyl-S-carrier proteins in the *pksX* pathway of *Bacillus subtilis*. *Proceedings of the National Academy of Sciences of United States of America*, 103:8977-8982.
- Cao, H., He, S., Wei, R., Diong, R.M., and Lu, L. 2011. *Bacillus amyloliquefaciens* G1: A potential antagonistic bacterium against eel-pathogenic *Aeromonas hydrophila*. *Evidence-Based Complementary and Alternative Medicine*, 2011(7Article ID 824104): 1-7.

- Cardozo, K.H.M., Guaratini, T., Barros, M.P., Falcao, V.R., Tonon, A.P., Lopes, N.P., Campos, S., Torres, M.A., Souza, A.O., Colepicolo, P., and Pinto, E. 2007. Metabolites from algae with economical impact. *Comparative Biochemistry and physiology, Toxicology and Pharmacology: CBP*, 146 (1-2): 60-78.
- Castoe, T. A., Stephens, T., Noonan, B.P., and Calestani, C. 2007. A novel group of type I polyketide synthases (PKS) in animals and the complex phylogenomics of PKSs. *Gene*, 392: 47–58.
- Chakraborty, K., Lipton, A.P., Paulraj, R. 2008. Antibacterial constituents of seaweed *Ulva fasciata*. *Marine Fish Information Service*, 36: 3-4.
- Chakraborty, K., Lipton, A.P., Paulraj, R., Vijayan, K.K. 2010. Antibacterial labdane diterpenoids of *Ulva fasciata* Delile from the southwestern coast of Indian Peninsula. *Food Chemistry*, 119 (4) :1399-1408.
- Chakraborty, K., Vijayagopal, P., Chakraborty, R.D., and Vijayan, K. K. 2010. Preparation of eicosapentaenoic acid concentrates from sardine oil by *Bacillus circulans* lipase. *Food Chemistry*, 120: 433-442.
- Chakraborty, K., and Paulraj, R. 2008. Enrichment of Eicosapentaenoic Acid from Sardine Oil with Δ^5 -Olefinic Bond Specific Lipase from *Bacillus licheniformis* MTCC 6824. *Journal of Agricultural and Food Chemistry*, 55:1428-1433.
- Chakraborty, K., and Paulraj, R. 2009. Selective enrichment of n-3 polyunsaturated fatty acids with C18–C20 acyl chain length from sardine oil using *Pseudomonas fluorescens* MTCC 2421 lipase. *Food Chemistry*, 114: 142-150.
- Chen, X., Vater, J., Piel, J., Franke, P., Scholz, R., Schneider, K., Koumoutsis, A., Hitzeroth, G., Grammel, N., Strittmatter, A., Gottschalk, G., Sussmuth, R., and Borriss, R. 2006. Structural and functional characterization of three polyketide synthase gene clusters in *Bacillus amyloliquefaciens* FZB42. *Journal of bacteriology*, 188:4024-4036.

- Chen, X.H., Scholz, R., Borriss, M., Junge, H., Moegel, G., Kunz, S., and Borriss, R. 2009. Difficidin and bacilysin produced by plant-associated *Bacillus amyloliquefaciens* are efficient in controlling fire blight disease. *Journal of Biotechnology*, 140: 38–44.
- Cinq-Mars, C.D., Hu, C., Kitts, D.D., and Li-Chan, E.C.Y. 2008. Investigations into inhibitor type and mode, simulated gastrointestinal digestion, and cell transport of angiotensin I converting enzyme-inhibitory peptides in pacific hake (*Merluccius productus*) fillet hydrolysate. *Journal of Agricultural and Food Chemistry*, 56 (2): 410-419.
- Cragg, G. M., and Newman, D. J. 2001. Medicinals for the millennia. The historical record. *Annals of the New York Academy of Sciences*, 953a: 3–25.
- Dancey, J. E. 2006. Therapeutic targets: mTOR and related pathways. *Cancer Biology and Therapy*, 5:1065–1073.
- Dart, R. K., and Kaneda, T. 1970. The production of A10-monounsaturated fatty acids by *Bacillus cereus*. *Biochimica et Biophysica Acta(BBA)*, 218:189-194.
- Dedicated website http://en.wikipedia.org/wiki/Vibrio_harveyi
- Dedicated website: http://en.wikipedia.org/wiki/Vibrio_alginolyticus
- Dedicated website: <http://www.drcarman.info/bio251lb/09lab251.pdf>
- Dedicated website: [www.foodsafety.govt.nz/.../Vibrio_Vulnificus Science_Research.pdf](http://www.foodsafety.govt.nz/.../Vibrio_Vulnificus_Science_Research.pdf)
- Dedicated website: www.publichealth.gc.ca
- Dedicated website: http://blast.ncbi.nlm.nih.gov/Blast.cgi?PROGRAM=blast_n&PAGE_TYPE=BlastSearch&LINK_LOC=blasthome
- Dedicated website: <http://www.fda.gov/food/foodborneillnesscontaminants/causesofillnessbadbugbook/ucm070523.htm>, Food and Drug Administration. Accessed on 9-8-2014.
- Desmons, S., Krhouz, H., Evrard, P., and Thonart, P. 1998. Improvement of lactic cell production. *Applied Biochemistry and Biotechnology*, 70: 513 -526.

- Devi, R., Surendran, P.K., and Chakraborty, K. 2009. Antibiotic resistance and plasmid profiling of *Vibrio parahaemolyticus* isolated from shrimp farms along the southwest coast of India. *World Journal of Microbiology and Biotechnology*, 25:2005–2012.
- Donadio, S., Monciardini, P., and Sosio, M. 2007. Polyketide synthases and nonribosomal peptide synthetases: the emerging view from bacterial genomics. *Natural Products Reports*, 24: 1073–1109.
- Dopazo C.P., Lemose, M., odeirojs,L., olinchejs, B., Barja L., Liciae, and Toranz, A .1988. Inhibitory activity of antibiotic-producing marine bacteria against fish pathogens. *Journal of applied bacteriology*, 65:97-101.
- Drucker, D.B. 1976. Gas liquid chromatographic chemotaxonomy. *Methods in Microbiology*, 9:51-125.
- Ecker, D.J., Sampath, R., Willett, P., Wyatt, J.R., Samant, V., Massire, C., Hall, T.A., Hari, K., McNeil, J.A., Büchen-Osmond, C., and Budowle, B. 2005. The Microbial Rosetta Stone Database: a compilation of global and emerging infectious microorganisms and bioterrorist threat agents. *BMC Microbiology*, 5(19):1-17.
- Egan, S., Harder, T., Burke, C., Steinberg, P., Kjelleberg, S., and Thomas, T. 2013. The seaweed holobiont: understanding seaweed-bacteria interactions. *FEMS Microbiology Reviews*, 37 (3): 462-476.
- Eisen, H.J., Tuzcu, E.M., Dorent, R., Kobashigawa, J., Mancini, D., Valantine-von Kaeppler, H.A., Starling, R.C., Sørensen, K., Hummel, M., Lind, J.M., Abeywickrama, K.H., and Bernhardt, P. 2003. Everolimus for the Prevention of Allograft Rejection and Vasculopathy in Cardiac-Transplant Recipients. *The New England Journal of Medicine*, 349:847–858.
- Farnsworth, N.R., Kinghorn, A.D., Soejarto, D.D., and Waller, D.P. 1985. Siberian ginseng (*Eleutherococcus senticosus*): Current status as an adaptogen. In: WAGNER, H.; HIKINO, H. and FARNSWORTH, N.R. eds. *Economic and Medicinal Plant Research*. London, Academic Press, 155-215.

- Faulkner, D. J. 2001. Marine natural products. *Natural products Reports*, 18:1-49.
- Fenical, W. 2009. Chemical studies of marine bacteria: Developing a new resource. *Chemical Reviews*, 93:1673–1683.
- Fleming, A. 1929. On the antibacterial action of cultures of *Penicillium*, with special reference to their use in the isolation of *B. influenzae*. *The British Journal of Experimental Pathology*, 10:226–236 .
- Frans, I., Michiels, C.W., Bossier, P., Willems, K.A., Lievens, B., Rediers, H. 2011. *Vibrio anguillarum* as a fish pathogen: virulence factors, diagnosis and prevention. *Journal of Fish Diseases*, 34 (9): 643-661.
- Fudou, R., Iizuka, T., Yamanaka, S. 2001. Haliangicin, a Novel Antifungal Metabolite Produced by a Marine Myxobacterium. 1. Fermentation and Biological Characteristics. *The Journal of Antibiotics*, 54 (2):149-152.
- Fujino, T., Miwatani, T., Yasuda, J., Kondo, M., Takeda, Y., Akita, Y., Kotera, K., Okada, M., Nishimune, H., Shimizu, Y., Tamura, T., and Tamura, Y. 1965. Taxonomic studies on the bacterial strains isolated from cases of “Shirasu” food-poisoning (*Pasteurella parahaemolytica*) and related microorganisms. *Biken Journal*, 8: 63–71.
- Galanos, C., Luderitz, O., Rietscheel, T., and Westphaol, O. 1977. Newer aspects of the chemistry and biology of bacterial lipopolysaccharide with special reference to their lipid A component. *International Review of Biochemistry: Biochemistry of Lipids*, 11(14): 239-335. Edited by T. W. Goodwin. Baltimore: University Park Press
- Gallimore, A.R., Stark, C.B., Bhatt, A., Harvey, B.M., Demydchuck, Y., Bolanos-Garcia, V., Fowler, D.J., Staunton, J., Leadlay, P.F., and Spenceer, J.B. 2006. Evidence for the role of the *monB* genes in polyether ring formation during monensin biosynthesis. *Chemistry and Biology*, 13: 453–460.
- Gao, C. H., Tian, X.P., Qi, S.H., Luo, X.M., Wang, P., and Zhang, S. 2010. Antibacterial and antilarval compounds from marine gorgonian-associated bacterium *Bacillus amyloliquefaciens* SCSIO 00856. *The Journal of Antibiotics*, 63: 191–193.

- Gerard, J., Haden, P., Kelly, M.T., and Andersen, R.J. 1996. Loloatin B, a cyclic decapeptide antibiotic produced in culture by a tropical marine bacterium. *Tetrahedron Letters*, 37:7201-7204.
- Gil-Turnes, M. S., Hay, M. E., and Fenical, W. 1989. Symbiotic Marine Bacteria Chemically Defend Crustacean Embryos From A Pathogenic Fungus. *Science* 246:116–118.
- Goecke, F., Labes, A., Wiese, J., and Imhoff, J.F. 2010. Chemical interactions between marine macroalgae and bacteria. *Marine Ecology Progress Series*, 409: 267–300.
- Goldman, E., and Green, L. H. 2008. *Practical Handbook of Microbiology*, Second Edition, *CRC Press*.
- Gomez, L.J.V., Mercado, I. E.S., Rivas, G.G., and Sánchez, N.E.A. 2010. Antibacterial and anticancer activity of seaweeds and bacteria associated with their surface. *Revista de Biología Marina y Oceanografía*, 45: 267-275.
- Gomez-Gil, B., Roque, A., and Turnbull, J.F. 2000. The use and selection of probiotic bacteria for use in the culture of larval aquatic organisms. *Aquaculture*, 191: 259-270.
- Gram, L., Melchiorson, J., and Bruhn, J.B. 2010. Antibacterial activity of marine culturable bacteria collected from a global sampling of ocean surface waters and surface swabs of marine organisms. *Marine Biotechnology*, 12 (4): 439-451.
- Gu, L.C., Jia, J.Y., Liu, H.C., Hakansson, K., Gerwick, W.H., and Sherman, D. H. 2006. Metabolic coupling of dehydration in the curacin A pathway: functional identification of a mechanistically diverse enzyme pair. *Journal of American Chemical Society*, 128: 9014-9015.
- Gustafson, K., Roman, M., Fenical, W. 1989. The macrolactins, a novel class of antiviral and cytotoxic macrolides from a deep-sea marine bacterium. *Journal of American Chemical Society*, 111: 7519–7524.
- Hahn, D. R., Gustafson, G., Waldron, C., Bullard, B., Jackson, J. D., and Mitchell, J. 2006. Butenyl-spinosyns, a natural example of genetic engineering of antibiotic biosynthetic genes. *Journal of Industrial Microbiology and Biotechnology*, 33 (2): 94–104.

- Hasegawa, R. H., Kasuya, M. C. M., and Vanetti, M. C. D. 2005. Growth and antibacterial activity of *Lentinula edodes* in liquid media supplemented with agricultural wastes. *Electronic Journal of Biotechnology*, 8 (2): 212-217.
- Hazel, J.R. 1995. Thermal adaptation in biological membranes: is homeoviscous adaptation the explanation? *Annual Review of Physiology*, 57:19–42.
- Hertweck, C. 2009. The biosynthetic logic of polyketide diversity. *Angewandte Chemie International Edition*, 48: 4688 – 4716.
- Hollants, J., Leliaert, F., Clerck, O.D., and Willems, A. 2012 What we can learn from sushi: a review on seaweed–bacterial associations. *FEMS Microbiology Ecology*, 83 : 1–16.
- Hotchkiss, R. D., and Dubos, R. J.1941. The isolation of bactericidal substances from cultures of *Bacillus brevis*. *The journal of Biological Chemistry*, 141:155-162.
- Hou, C.T., and Forman, R.J. 2000. Growth inhibition of plant pathogenic fungi by hydroxy fatty acids. *Journal of Industrial Microbiology and Biotechnology*, 19:34-38.
- Hu, H.Q., Li, X.S., and He, H. 2010. Characterization of an antimicrobial material from a newly isolated *Bacillus amyloliquefaciens* from mangrove for biocontrol of capsicum bacterial wilt. *Biological Control*, 54 (3): 359 -365.
- Hutchinson, C.R. 2003. Polyketide and non-ribosomal peptide synthases: falling together by coming apart. *Proceedings of the National Academy of Sciences of United States of America*, 100 (6): 3010–3012.
- Imamura, N., Nishijima, M., Takadera, T., Adachi, K., Sakai, M., and Sano, H. 1997. New anticancer antibiotics pelagiomicins, produced by a new marine bacterium *Pelagiobacter variabilis*. *The Journal of Antibiotics* (Tokyo), 50(1):8-12.
- Imhoff, J.F., Labes, A., and Wiese, J. 2011. Bio-mining the microbial treasures of the ocean: new natural products. *Biotechnology Advances*, 29(5):468-482.
- Jaruchoktaweechai, K., Suwanborirux, S., Tanasupawatt, P., Kittakoop, P., and Menasveta, P. 2000. New macrolactins from a marine *Bacillus* sp. SC026. *Journal of Natural Products*, 63:984–986.

- Jez, J.M., Bowman, M.E., and Noel, J.P. 2002. Expanding the biosynthetic repertoire of plant type III polyketide synthases by altering starter molecule specificity. *Proceedings of the National Academy of Sciences of United States of America*, 99 (8): 5319–5324.
- Jha, R. K., and Rong, X. Z. 2004. Biomedical Compounds from Marine organisms. *Marine Drugs*, 2:123-146.
- Kanagasabhapathy, M., Hideaki, S., and Shinichi, N. 2008. Phylogenetic identification of epibiotic bacteria possessing antimicrobial activities isolated from red algal species of Japan. *World Journal of Microbiology and Biotechnology*, 24:2315-2321.
- Kanagasabhapathy, M., Hideaki, S., Haldar, S., Shinji, Y., and Shinichi, N. 2006. Antibacterial activities of marine epibiotic bacteria isolated from brown algae of Japan. *Annals of Microbiology*, 56 (2): 167-173.
- Kaneda, T. 1966. Biosynthesis of branched-chain fatty acids. IV. Factors affecting relative abundance of fatty acids produced by *Bacillus subtilis*. *Canadian Journal of Microbiology*, 12 (3): 501–514.
- Kaneda, T. 1969. Fatty acids in *Bacillus* larvae, *Bacillus lentimorbus*, and *Bacillus popilliae*. *Journal of Bacteriology*, 98 (1): 143–146.
- Kaneda, T. 1991. Iso-fatty and anteiso-fatty acids in bacteria—biosynthesis, function, and taxonomic significance. *Microbiological Reviews*, 55: 288–302.
- Kennedy, J., Baker, P., Piper, C., Cotter, P.D., Walsh, M., Mooij, M.J., Bourke, M.B., Rea, M.C., Connor, P.M.O., Paul Ross, R., Hill, C., and Gara, F.O. 2009. Isolation and analysis of bacteria with antimicrobial activities from the marine sponge *Haliclona simulans* collected from Irish waters. *Marine Biotechnology*, 11 (3): 384-396.
- Kennedy, J., Codling, C.E., Jones, B.V., Dobson, A.D.W., and Marchesi, J. 2008. Diversity of microbes associated with the marine sponge, *Haliclona simulans*, isolated from Irish waters and identification of polyketide synthase genes from the sponge metagenome. *Environmental Microbiology*, 10 (7): 1888-1902.

- Khosla, C., Gokhale, R.S., Jacobsen, J.R., and Cane, D.E. 1999. Tolerance and specificity of polyketide synthases. *Annual Review of Biochemistry*, 68: 219 – 253.
- Kimura, M. 1980. A simple method for estimating evolutionary rate of base substitutions through comparative studies of nucleotide sequences. *Journal of Molecular Evolution*, 16 (2): 111-120.
- Kiran, G.S., Sabarathnam, B., and Elavin, J. 2010. Biofilm disruption potential of a glycolipid biosurfactant from marine *Brevibacterium casei*. *FEMS Immunology and Medical Microbiology*, 59 :432–438.
- Kirst, H. A., Creemer, L. C., Lawrence C., Naylor, S. A., Pugh, P. T., Snyder, D.E., Winkle, J. R., Lowe, L. B., Rothwell, J. T., Sparks, T. C., and Worden, T. V. 2002. Evaluation and development of spinosyns to control ectoparasites on cattle and sheep. *Current Topics in Medicinal Chemistry*, 2: 675–699 .
- Komaki, H., Fudou, R., Iizuka, T., Nakajima, D., Okazaki, K., Shibata, D., Ojika, M., and Harayama, S. 2008. PCR Detection of Type I Polyketide Synthase Genes in Myxobacteria. *Applied and environmental microbiology*, 74(17): 5571–5574.
- Kondo, E., and Ueta, N. 1972. Composition of fatty acids and carbohydrates in *Leptospira*. *Journal of Bacteriology*, 110: 459-467.
- Kozubek, A.R., Zarnowski, M.S., and Gubernator, J. 2001. Natural amphiphilic phenols as bioactive compounds. *Cellular and Molecular Biology Letters*, 53:50-75.
- Kubanek, J., Jensen, P.R., Keifer, P.A., Sullards, M.C., Collins, D.O., and Fenical, W. 2003. Seaweed resistance to microbial attack: a targeted chemical defense against marine fungi. *Proceedings of the National Academy of Sciences of United States of America*, 100(12): 6916–6921.
- Kumar, V., Rao, D., Thomas, T., Kjelleberg, S., Egan, S. 2011. Antidiatom and antibacterial activity of epiphytic bacteria isolated from *Ulva lactuca* in tropical waters. *World Journal of Microbiology and Biotechnology*, 27: 1543–1549.

- Laatsch, H. 2006. *Marine bacterial metabolites*. In: *Front. Mar. Biotechnol.* (eds Proksch, P. and Müller, W.E.G.).225–288. Horizon Bioscience, Norfolk, UK. ISBN 1-904933-18-1
- LaPlante, K. L., and Rybak, M. J. 2004b. Daptomycin- anovel antibiotic against Gram- positive pathogens. *Expert Opinion on Pharmacotherapy*, 5:2321–2331 .
- Leclercq, R. 2001. Overcoming antimicrobial resistance: profile of a new ketolide antibacterial, telithromycin. *Journal of Antimicrobial Agents and Chemotherapy*, 48 Suppl T1:9-23.
- Lemos, M.L., Toranzo, A.E., and Barja, J.L. 1985. Antibiotic activity of epiphytic bacteria isolated from intertidal seaweeds. *Microbiology Ecology*, 11 (2): 149-163.
- Li, Z. 2009. Advances in marine microbial symbionts in the China Sea and related pharmaceutical metabolites. *Marine Drugs*, 7 (2): 113-129.
- Lovell, F.M. 1966. The Structure of a Bromine-Rich Marine Antibiotic. *Journal of American Chemical Society*, 88 (19): 4510–4511.
- Marino, J.P., McClure, M.S., Holub, D.P., Comasseto, J.V., Tucci, F.C. 2002. Stereocontrolled synthesis of (-)-macrolactin A. *Journal of American Chemical Society*, 124:1664–1668.
- Mearns-Spragg, A., Boyd, K.G., Hubble, M.O., and Burgess, J.G. 1997. Isolation of antibiotic producing epiphytic marine bacteria from marine algae. Presented at the 4th Underwater Science Symposium, Society for Underwater Technology, Newcastle upon Tyne, Nov. 19/20, 1997.
- Meklat, A., Sabaou, N., Zitouni, A., Mathieu, F., and Lebrihi, A. 2011. Isolation, taxonomy, and antagonistic properties of halophilic actinomycetes in Saharan soils of Algeria. *Applied and environmental microbiology*, 77 (18): 6710-6714.
- Milanovic, N., Kodzic, A., Baras, J., and Brankovic, S. D. 2001. The influence of a cryoprotective medium containing glycerol on the lyophilization of lactic acid bacteria. *Journal of the Serbian Chemical Society*, 66 (7): 435–441

- Moldenhauer, J., Chen, X. H., Borriss, R., and Piel, J. 2007. Biosynthesis of the antibiotic bacillaene, the product of a giant polyketide synthase complex of the trans-AT family, *Angewandte Chemie International Edition*, 119: 1–4.
- Mondol, M.A.M., Shin, H.J., and Islam, M.T. 2013. Diversity of Secondary Metabolites from Marine *Bacillus* Species: Chemistry and Biological Activity. *Marine Drugs*, 11 (8): 2846-2872.
- Moriarty, D.J.W. 1997. The role of microorganisms in aquaculture ponds. *Aquaculture*, 151: 333- 349.
- Moss, C.W., Dowell, V.R. Jr., Farshtchi, D., Raines, I.J., and Cherry, W. B. 1969. Cultural characteristics and fatty acid composition of *propionibacteria*. *Journal of Bacteriology*, 97: 561-570.
- Mukwaya, G.M., and Welch, D.F. 1989. Subgrouping of *Pseudomonas cepacia* by cellular fatty acid composition. *Journal of Clinical Microbiology*, 27: 2646–2649.
- Nagao, T., Adachi, K., Sakai, M., Nishijima, M., and Sano, H. 2001. Novel macrolactins as antibiotic lactones from a marine bacterium. *The Journal of Antibiotics* (Tokyo), 54:333–339.
- Nunez, R., Garateix, A., Laguna, A., Fernández, M. D., Ortiz, E., Llanio, M., Valdés, O., Rodríguez, A., and Menéndez, R. 2006. Caribbean marine biodiversity as a source of new compounds Of biomedical interest and others industrial applications *Pharmacologyonline*, 3: 111-119.
- Okami, Y. 1986. Marine microorganisms as a source of bioactive agents. *Microbiology Ecology*, 12:65-78.
- Ongena, M., Jacques, P., Toure, Y., Destain, J., Jabrane, A., and Thonart, P. 2005. Involvement of fengycin-type lipopeptides in the multifaceted biocontrol potential of *Bacillus subtilis* . *Applied Microbiology and Biotechnology*, 69: 29–38.
- Patel, P.S., Huang, S., Fisher, S., Pirnik, D., Aklonis, C., Dean, L., Meyers, E., Fernandes, P., and Mayerl, F. 1995. Bacillaene, a novel inhibitor of

- prokaryotic protein synthesis produced by *Bacillus subtilis*: production, taxonomy, isolation, physico-chemical characterization and biological activity. *The Journal of Antibiotics* (Tokyo), 48: 997– 1103.
- Patrick, F. 2012. Antibiotic compounds from *Bacillus*: why are they so amazing? *American Journal of Biochemistry and Biotechnology*, 8 (1): 40-46.
- Pelczar, M. J., Reid, R. D., and Chan E. C. S. 1977. *Microbiology*. T.M.H. Edition, Tata McGraw-Hill Publishing Company Ltd., Noida.
- Pelczar, M., Reid, R., and Chan, E. 1957. *Microbiology*. T.M.H. Edition, Tata McGraw-Hill Publishing Company Ltd., Noida.
- Penesyanyan, A., Kjelleberg, S., and Egan, S. 2010. Development of novel drugs from marine surface associated microorganisms. *Marine Drugs*, 8: 438–459.
- Penesyanyan, A., Marshall-Jones, Z., Holmstrom, C., Kjelleberg, S., and Egan, S. 2009. Antimicrobial activity observed among cultured marine epiphytic bacteria reflects their potential as a source of new drugs. *FEMS Microbiology Ecology*, 69 (1): 113-24.
- Peng, Z., Zheng, Y.L., You, Y., Yan, X., and Shao, J. 2009. Molecular phylogeny and modular structure of hybrid NRPS/PKS gene fragment of *Pseudoalteromonas* sp NJ6-3-2 isolated from marine sponge *Hymeniacidon perleve*. *Journal of Microbiology and Biotechnology*, 19 (3): 229-237.
- Pereira, C. R., and Costa- Lotufo, L.V. 2011. Bioprospecting for bioactives from seaweeds: potential, obstacles and alternatives. *Brazilian Journal of Pharmacognosy*, 22(4):894-905.
- Piel, J., Hui, D., Fusetani, N and Matsunaga, S. 2004. Targeting modular polyketide synthases with iteratively acting acyltransferases from metagenomes of uncultured bacterial consortia. *Environmental Microbiology*, 6: 921-927.
- Pietra, F. 1997. Secondary metabolites from marine microorganisms: bacteria, protozoa, algae and fungi. Achievements and prospects. *Natural Product Reports*, 14(5):453-464.

- Quevrain, E., Roue, M., and Bourguet-Kondracki, I. M. 2014. Assessing the potential bacterial Origin of the chemical diversity in calcareous sponges. *Journal of Marine Science and Technology*, 22: 36-49.
- Raaijmakers, J.M., Weller, D.M., and Thomashow, L.S. 1997. *Applied and environmental microbiology*, 63: 881–887.
- Radjasa, O.K., Martens, T., Grossart, H., Brinkhoff, T., Sabdono, A., and Simon, M. 2007. Antagonistic activity of a marine bacterium *Pseudoalteromonas luteoviolacea* TAB 4.2 associated with coral *Acropora* sp. *International Journal of Biological Sciences*, 7: 239–246.
- Ramalingam, K., and Shyamala, D.R. 2006. Influence of *Vibrio parahaemolyticus* MTCC 451 on the levels of ascorbic acid and histamine in *Penaeus monodon* (Fabricius). *Journal of Environmental Biology*, 27 (1): 67-70.
- Rao, D., Webb, J.S., and Kjelleberg, S. 2005. Competitive interactions in mixed-species biofilms containing the marine bacterium *Pseudoalteromonas tunicata*. *Applied and environmental microbiology*, 71 (4): 1729-1736.
- Rapp, C., Jung, G., Katzer, W., and Loeffler, W. 1988. Chlorotetain from *Bacillus subtilis*, an antifungal dipeptide with an unusual chlorine containing amino acid. *Angewandte chemie interationnal edition*, 12: 1733-1734
- Rayl, A. J. S. 1999. Oceans: medicine chests of the future? *Scientist*, 13:1–5
- Rengpipat, S., Phianphak, W., Piyatiratitivorakul, S., and Menasveta, P.2000. Immunity enhancement in black tiger shrimp (*Penaeus monodon*) by a probiont bacterium (*Bacillus* S11). *Aquaculture*, 191:271–288.
- Riesenfeld, C.S., Schloss, P.D., and Handelsman, J.2004. Metagenomics: genomic analysis of microbial communities. *Annual Review of Genetics*, 38: 525–552.
- Robinson, W. E., Reinecke, M. G., Abdel-Malek, S., Jia, O. and Chow, A. 1996. *Proceedings of the National Academy of Sciences of United States of America*, 93: 6326–6331.
- Romero-Tabarez, M., Jansen, R., Sylla, M., Lunsdorf, H., Haubler, S., Santosa, D. A., Timmis, K. N., and Molinari, G. 2006. 7-O-Malonyl Macrolactin A, a New Macrolactin Antibiotic from *Bacillus subtilis* Active against Methicillin-Resistant *Staphylococcus aureus*, Vancomycin-Resistant

- Enterococci, and a Small-Colony Variant of *Burkholderia cepacia*. 50(5):1701-1709.
- Rungprom, W., Siwu, E. R. O., Lambert, D. L. K., Dechsakulwatana, C., Barden, M. C., Kokpol, U., Blanchfield, J. T., Kita, M., and Garson, M. J. Cyclic tetrapeptides from marine bacteria associated with the seaweed *Digenea sp.* and the sponge *Halisarca ectofibrosa*. *Tetrahedron*, 64 : 3147-3152
- Sambrook, J., and Russell, D.W. 2001. *Molecular cloning A Laboratory Manual*. (3rd ed.). New York: Cold Spring Harbor ISBN 0879695773, 2011, pp 999.
- Sambrook, J., Fritsch, E.F., and Maniatis, T. 1989. *Molecular cloning: a laboratory manual*, 2nd edn. Cold Spring Harbor Laboratory Press, Cold Spring Harbor, New York.
- Schirmer, A., Sabaou, N., Gadkari, R., Reeves, C.D., Ibrahim, F., Delong, E.F., and Hutchinson, C.R. 2005. Metgenomic analysis reveals diverse polyketide synthase gene clusters in microorganisms associated with the marine sponge *Discodermia dissoluta*. *Applied Environmental Microbiology*, 71 (8): 4840-4849.
- Schneider, K., Chen, X., Vater, J., Franke, P., Nicholson, G., Borriss, R., and Sussmuth, R. 2008. Macrolactin is the polyketide biosynthesis product of the pks2 cluster of *Bacillus amyloliquefaciens* FZB42. *Journal of for plant disease biocontrol, Trends in microbiology*. 70(9):1417-1423.
- Scotti, C., Piatti, Cuzzoni, A., Perani, P., Tognoni, A., Grandi, G., Galizzi, A., and Albertini, A.M.A. *Bacillus subtilis* large ORF coding for a polypeptide highly similar to polyketide synthases, *Gene*, 130 (1): 65-71.
- Sfanos, K.A., Peterson, C.L., Harmody, D.K., McCarthy, P.J., Pomponi, S.A and Lopez, J.V. 2005. A molecular systematic survey of sponge-derived marine microbes. *Systematic and Applied. Microbiology*, 28:242-264.
- Shiozawa, H., Kagasaki, T., Kinoshita, T., Haruyama, H., Domon, H., Utsui, Y., Kodama, K., and Takahashi, S. 1993. Thiomarinol, a new hybrid antimicrobial antibiotic produced by a marine bacterium: fermentation, isolation, structure, and antimicrobial activity. *The Journal of Antibiotics* (Tokyo), 46: 1834–1842.

- Showalter, H.D., Bunge, R.H., French, J.C., Hurley, T.R., Leeds, R.L., Leja, B., McDonnell, P.D., and Edmunds, C.R. 1992. Improved production of pentostatin and identification of fermentation cometabolites. *The Journal of Antibiotics* (Tokyo), 45(12):1914-8.
- Simmons, T.L., Coates, R.C., Clark, B.R., Engene, N., and Gonzalez D. 2008. Biosynthetic origin of natural products isolated from marine microorganism-invertebrate assemblages. *Proceedings of the National Academy of Sciences of United States of America*, 105: 4587–4594.
- Singh, M.P., Kong, J. E. F., Janso, D. A., Arias, P. J., Petersen, P., Suarez, V.S., Bernan, G., Carter, M., and Greenstein. 2003. Novel Pyrones Produced by a Marine *Pseudomonas* sp. F92S91: Taxonomy and Biological Activities. *The Journal of Antibiotics* (Tokyo), 56 (12): 1033 - 1044.
- Singh, R.P., and Reddy, C.R. 2014. Seaweed-microbial interactions: key functions of seaweed-associated bacteria. *FEMS Microbiology Ecology*, 88 (2): 213-230.
- Sjogren, J., Magnusson, J., Broberg, A., Schnürer, J., and Kenne, L. 2003. Antifungal 3-Hydroxy fatty acids from *Lactobacillus plantarum* MiLAB 14. *Applied Environmental Microbiology*, 69:7554-7557.
- Sohn, M.J., Zheng, C.J., Kim, W.G. 2008. Macrolactin S, a new antibacterial agent with FabG-inhibitory activity from *Bacillus* sp. AT28. *The Journal of Antibiotics*, (Tokyo), 61:687–691.
- Stead, D.E., Sellwood, J.E., Wilson, J., and Viney, I. 1992. Evaluation of a commercial microbial identification system based on fatty acid profiles for rapid, accurate identification of plant pathogenic bacteria. *Journal of Applied Bacteriology*, 72(4): 315-321.
- Stein, T. 2005. *Bacillus subtilis* antibiotics: Structures, syntheses and specific functions. *Molecular Microbiology*, 56: 845–857.

- Strobel, G., and Daisy, B. 2003. Bioprospecting for microbial endophytes and their natural products. *Microbiology and Molecular Biology Reviews*, 67 (4): 491–502.
- Sum, P. E. 2006. Case studies in current drug development: ‘glycylcyclines’. *Current Opinion in Chemical Biology*, 10: 374–379.
- Suutari, M., and Laakso, S. 1992. Unsaturated and branched-chain fatty-acids in temperature adaptation of *Bacillus subtilis* and *Bacillus megaterium*. *Biochimica et Biophysica Acta(BBA)*,1126:119–124
- Suutari, M., and Laakso, S. 1994. Microbial fatty acids and thermal adaptation. *Critical Reviews in Microbiology*. 20: 285–328.
- Tamura, K., Peterson, D., Peterson, N., Stecher, G., Nei, M., and Kumar, S. 2011. MEGA5: Molecular evolutionary genetics analysis using maximum likelihood, evolutionary distance, and maximum parsimony methods. *Molecular Biology and Evolution*, 28: 2731-2739.
- Topliss, J. G., Clark, A. M., Ernst, E., Hufford., Johnston, G.A.R., Rimoldi, J.M., and Weimann, B.J. 2002. Natural and synthetic substances related to human health. *Pure and Applied Chemistry*, 74:1957–1985.
- Torrento, M., and Torres, J. 1996. *In vitro* inhibition of *Vibrio harveyi* by *Pseudomonas* sp. isolated from aquatic environment. *UPV Journal of Natural Sciences*, 130–138.
- Uzair, B., Ahmed, N., Ahmad, V.U., and Kousar, F. 2006. A new antibacterial compound produced by an indigenous marine bacteria — fermentation, isolation, and Biological activity. *Natural product research*, 20 (14): 1326–1331.
- Waksman, S. A., and Woodruff, H. B. 1941. *Actinomyces antibioticus*, a new soil organism antagonistic to pathogenic and non-pathogenic bacteria. *Journal of Bacteriology*, 42, 231-249.
- Weerkamp, A., and Heinen, W. 1972 . Effect of temperature on the fatty acid composition of the extreme thermophiles, *Bacillus caldolytieus* and *Bacillus caldotenax*. *Journal of Bacteriology*, 109:443-446.

- Weinberger, F., and Friedlander, M. 2000. Response of *Gracilaria conferrata* (Rodophyta) to oligogaes results in defence against agar degrading epiphytes. *Journal of Phycology*, 36:1079–1086.
- Weisburg, W.G., Barns, S.M., Pelletier, D.A., and Lane, D.J. 1991. 16S ribosomal DNA amplification for phylogenetic study. *Journal of Bacteriology*, 173(2):697-703.
- Weissman, K., and Leadlay, P.F. 2005. Combinatorial biosynthesis of reduced polyketides. *Nature Reviews. Microbiology*, 3: 925-936.
- Welch, D. 1991. Applications of cellular fatty acid analysis. *Clinical Microbiology Reviews*, 4:422-438
- Whelan, S., and Goldman, N. 2001. A general empirical model of protein evolution derived from multiple protein families using a maximum-likelihood approach. *Molecular Biology and Evolution*, 18 (5): 691-699.
- Wiese, J., Thiel, V., Nagel, K., Staufenberg, T., and Imhoff, F.J. 2009. Diversity of antibiotic-active bacteria associated with the brown alga *Laminaria saccharina* from the Baltic Sea. *Marine Biotechnology*, 11 (2): 287-300.
- Wilson, G.S., Raftos, D.A., Corrigan, S.L., and Nair, S.V. 2010. Diversity and antimicrobial activities of surface-attached marine bacteria from Sydney Harbour, Australia. *Microbiological Research*, 165 (4): 300-311.
- Wright, L.F., and Hopwood, D. A. 1976. Identification of the Antibiotic Determined by the SCPI Plasmid of *Streptomyces coekolor* A3 (2). *Journal of General Microbiology*, 95:96-106.
- Wu, J., Cooper, S. M., Cox, R. J., Crosby, J., Crump, M. P., Hothersall, J., Simpson, T.J., Thomas, C.M., and Willis, C.L. 2007. Mupirocin H, a novel metabolite resulting from mutation of the HMG-CoA synthase analogue, *mupH* in *Pseudomonas fluorescens*. *Chemical Communications*, 28 (20): 2040-2042.
- Xi, L., Ruan, J., and Huang, Y. 2012. Diversity and Biosynthetic Potential of Culturable Actinomycetes Associated with Marine Sponges in the China Seas. *International Journal of Molecular Sciences*, 13: 5917-5932.
- Yang, R.Y., Li, C.Y., Lin, Y.C., Peng, G.T., She, Z.G., and Zhou, S.N. 2006. Lactones from a brown alga endophytic fungus (No. ZZF36) from the South

-
- China Sea and their antimicrobial activities. *Bioorganic and Medicinal Chemistry Letters*, 16 (16): 4205-4208.
- Yoshikawa, K., Takadera, T., Adachi, K., Nishijima, M., and Sano, H. 1997. Korormicin, a Novel Antibiotic Specifically Active against Marine Gram-negative Bacteria, Produced by a Marine Bacterium. *The Journal Of Antibiotics*, 50 (11): 949-953.
- Zeng, L., Han, X., Chen, H., Lin, W., and Yan, X. 2005. Marine bacteria associated with marine macro organisms: the potential resource for antimicrobial agents. *Annals of Microbiology*, 55 (2): 119-124.
- Zhang, Q., Pang, B., Ding, W., and Liu, W. 2013. Aromatic Polyketides Produced by Bacterial Iterative Type I Polyketide Synthases. *ACS Catalysis*, 3 (7): 1439–1447.
- Zhang, W., Li, Z.F., Miao, X., Meng, Q., and Zang, X. 2009. Investigation of bacteria with polyketide synthase genes and antimicrobial activity isolated from South China Sea sponges. *Journal of Applied Microbiology*, 107 (2): 567-575.
- Zhao, K., Zheng, Y., Penttinen, P., Guan, T., Xiao, J., Chen, Q., Xu, J., Lindstrom, K., Zhang, L., Zhang, X., and Strobel, G.A. 2011. The diversity and antimicrobial activity of endophytic actinomycetes from medicinal plants in Panxi Plateau, China. *Current Microbiology*, 62 (1): 182-190.
- Zheng, L., Han, X., Chen, H., Lin, W., and Yan, X. 2005. Marine bacteria associated with marine macroorganisms: the potential antimicrobial resources. *Annals of microbiology*, 55 (2):119-124.
- Zhou, K., Zhang, X., Zhang, F., and Li, Z. 2011. Phylogenetically diverse cultivable fungal community and polyketide synthase (PKS), non-ribosomal peptide synthase (NRPS) genes associated with the South China Sea sponges. *Microbial Ecology*, 62 (3): 644-654.
- Zhu, K., Bayles, D.O., Xiong, A., Jayaswal, R.K., and Wilkinson, B.J. 2005. Precursor and temperature modulation of fatty acid composition and growth of *Listeria monocytogenes* cold-sensitive mutants with transposon-interrupted branched-chain alpha-keto acid dehydrogenase. *Microbiology*, 151 (2): 615-623.

- Zhu, K., Ding, X., Julotok, M., and Wilkinson, B.J. 2005. Exogenous isoleucine and fatty acid shortening ensure the high content of anteiso-C15:0 fatty acid required for low-temperature growth of *Listeria monocytogenes*. *Applied Environmental Microbiology*, 71(12): 8002-8007.
- Zhu, P., Zheng, Y., You, Y., Yan, X., and Shao, J. 2009. Molecular phylogeny and modular structure of hybrid NRPS/PKS gene fragment of *Pseudoalteromonas* sp NJ6-3-2 isolated from marine sponge *Hymeniacidon perleve*. *Journal of Microbiology and Biotechnology*, 19(3): 229-237.
- Zimmerman, S.B., Schwartz, C.D., Monaghan, R.L., Pelak, B.A., Weissberger, B., Gilfillan, E.C., Mochales, S., Hernandez, S., Currie, S.A., and Tejera, E. 1987. Difficidin and oxydifficidin: Novel broad spectrum antibacterial antibiotics produced by *Bacillus subtilis*. I. Production, taxonomy and antibacterial activity. *The Journal Of Antibiotics*, 40: 1677–1681.

PUBLICATIONS

Sl no	Title	Status
Journal Articles		
1	Polyketide family of novel antibacterial 7-O-methyl-5'-hydroxy-3'-heptenoate macrolactin from seaweed-associated <i>Bacillus subtilis</i> MTCC 10403. Chakraborty K, Thilakan B & Raola VK (2014). <i>J Agric Food Chem</i> 62: 12194–12208.	Published
2	Diversity and Antagonistic Properties of Cultivable Bacteria Associated with Seaweeds in Gulf of Mannar of South East Coast of India. Thilakan B , Chakraborty K, & Chakraborty RD . <i>Canadian Journal of Microbiology</i> .	Under review
3	Antibacterial secondary metabolites from seaweed associated marine bacterium <i>Bacillus subtilis</i> MTCC 10407 . Chakraborty K, Thilakan B & Raola VK. <i>J Agric Food Chem</i>	Under review
4	Antibacterial Secondary Metabolites from Heterotrophic <i>Bacillus amyloliquefaciens</i> MTCC 10456 Associated with Marine Macroalga <i>Laurenciae papillosa</i> . Chakraborty K, Thilakan B & Raola VK .European Journal of Biochemistry	Under review
5	Antibacterial compounds and host interactions of antagonistic <i>Bacillus</i> sp associated with seaweed based on differential membrane fatty acid composition . Chakraborty K, Thilakan B & Raola VK (2014). <i>Journal of Applied Phycology</i>	Under review
Papers in International Conferences		
6	<i>Bacillus subtilis</i> MTCC 10403 isolated from seaweed <i>Sargassam longifolium</i> as a potential source to isolate antibacterial metabolites Chakraborty K, Thilakan B & Vijayan K K (2011) ASIA PACIFIC AQUA CULTURE	Presented